[redacted]

ARCTEC CANADA LIMITED

mm

ARCTEC CANADA LIMITED

FR 1364C-2

CA1
DTC820
84
M811F
c.2

MV ARCTIC
ICE TRANSITING PERFORMANCE IN THE RAMMING MODE

FINAL REPORT
TP 5320 E

BY

A.M. NAWWAR
L. GOOSSENS
M. STEELE

FEB 26 1986

OCTOBER 1984

Submitted to:

Transportation Development Centre,
1000 Sherbrooke St. West, Suite 2421,
Montreal, Quebec.
H3A 2R3

Submitted by:

Arctec Canada Limited,
311 Leggett Drive,
Kanata, Ontario.
K2K 1Z8

3/23/3

PROJECT TEAM

The project team for Arctec Canada Limited was composed of:

Dr. A.M. Nawwar,
Mr. L. Goossens,
Mr. B. Menon,
Mr. H. Blount,
Mr. M. Steele,

and others.

DISCLAIMER:

The contents of this report reflect the views of the contractor and not necessarily the official view or policies of the Transportation Development Centre.

APPROVED BY: ______________________

REPORT DOCUMENTATION FORM

1. Transport Canada Report No.
TP 5320E

2. TDC Project No.
4825

3. Recipient's Catalogue No.

4. Title and Subtitle
MV ARCTIC Ice Transiting Performance
in the Ramming Mode
FINAL REPORT

5. Report Date
October 1984

6. Performing Organization Report No.
FR 1364C-2

7. Author(s)
A.M. Nawwar and L. Goossens

8. Transport Canada File No.
D 1460-166-34

9. Performing Organization Name and Address
Arctec Canada Limited
311 Leggett Drive
Kanata, Ontario
K2K 1Z8

10. DSS File No.
11SD. T8200-2-2593

11. DSS or Transport Canada Contract No.
0SD83-00080

12. Sponsoring Agency Name and Address
Transportation Development Centre
1000 Sherbrooke St. W.
Suite 2421
Montreal, Quebec H3A 2R3

13. Type of Report and Period Covered
Final 1979-1981

14. Sponsoring Agency Code

15. Supplementary Notes

16. TDC Project Officer
Richard Bertrand

17. Abstract

This report presents the methodology and results of a study of the MV ARCTIC ice transiting performance in the ramming mode. The report provides an account of ramming mode formulations which include resistance models, performance formulation and ship motions and accelerations. It describes the methods and instruments used in data scanning, categorization and quality assessment. A core database comprising dedicated trials of the Admiralty Inlet trials, 1981 was used as a basis for the analysis because of its higher quality. Data reduction and primary analysis were conducted on an HP9816 computer-based system. The data reduction algorithms are described including a comprehensive speed correction methodology. Results are presented in a standardized graphical format. The MV ARCTIC performance is analyzed and simulated. The analysis includes the effects of acceleration distance, speed of impact, thrust cut off, ice thickness, bubbler operation, trim condition and power level on performance. The latter is measured by average speed of advance and fuel consumption. The analysis also includes cycle time diagnosis. Performance simulation is presented for one model ram to demonstrate the applicability of simulation to analysis and optimization of the MV ARCTIC performance. The CASPPR power requirements, ship design features and instrumentation system has been evaluated. The report is concluded by recommendations for designers and operators of ARCTIC class cargo vessels, and for supplementary evaluation.

18. Key Words
MV ARCTIC
Ice Transiting
Ramming
Pressure Ridges

19. Distribution Statement

20. Security Classification (of this report)
Restricted

21. Security Classification (of this page)
Unclassified

22. No. of Pages
480

23. Price
Nil

TDC CDT 79-005

FORMULE DE DOCUMENTATION POUR RAPPORT

1. N° du rapport Transports Canada
TP 5320E

2. N° de l'étude — CDT
4825

3. N° de catalogue du destinataire

4. Titre et sous-titre
MV ARCTIC Ice Transiting Performance
in the Ramming Mode
FINAL REPORT

5. Date du rapport
Octobre 1984

6. N° du rapport de l'organisme exécutant
FR 1364C-2

7. Auteur(s)
A.M. Nawwar et L. Goossens

8. N° de dossier Transports Canada
D 1460-166-34

9. Nom et adresse de l'organisme exécutant
Arctec Canada Limitée
311 Leggett Drive
Kanata, Ontario
K2K 1Z8

10. N° de dossier — ASC
11SD. T8200-2-2593

11. N° de contrat — ASC ou Transports Canada
OSD83-00080

12. Nom et adresse de l'organisme parrain
Centre de développement des transports
1000 o., rue Sherbrooke
Suite 2421
Montréal, Québec H3A 2R3

13. Genre de rapport et période visée
Final 1979-1981

14. Code de l'organisme parrain

15. Remarques additionnelles

16. Agent de projet — CDT
Richard Bertrand

17. Résumé

Ce rapport présente les méthodes et résultats de l'étude concernant le comportement dynamique et l'efficacité de l'Arctic lors de la charge des glaces. Il donne les équations élaborées concernant: la résistance à l'avancement, les performances, les mouvements et les accélérations. Il décrit les méthodes et instruments utilisés pour la scrutation des capteurs ainsi que le classement et l'appréciation qualitative des données obtenues. La base de données utilisée était formée essentiellement des résultats obtenus en 1981 lors des essais spécialisés dans l'Inlet de l'Amirauté, et retenus à cause de leur haute qualité. Le rapport décrit les algorithmes qui ont servi à la réduction des données ainsi que la méthode utilisée pour la correction automatique des vitesses. Le comportement dynamique et l'efficacité en marche alternée de l'Arctic sont analysés et simulés, les paramètres pris en compte pour évaluer l'efficacité du navire étant: la distance d'accélération, la vitesse à l'impact, le moment de coupure de la poussée, l'épaisseur des glaces, le fonctionnement ou non du système à bulles d'air, l'assiette du navire et la puissance effective développée. L'efficacité du navire est mesurée par la vitesse moyenne d'avancement et la consommation correspondante. Les dispositions de la loi canadienne sur la prévention de la pollution des eaux arctiques ont été évaluées, notamment en ce qui concerne la puissance, la conception de la coque et l'instrumentation. Enfin, le rapport adresse des recommendations aux constructeurs et aux armateurs de navires marchands de cote arctique et suggère une évaluation plus approfondie.

18. Mots-clés
Arctic
Déplacement dans les glaces
Charge des glaces
Crêtes de pression

19. Diffusion

20. Classification de sécurité (de ce rapport)
restreinte

21. Classification de sécurité (de cette page)
non classifiée

22. Nombre de pages
480

23. Prix
néant

CDT/TDC 79-005

TABLE OF CONTENTS

PAGE NOS.

1. INTRODUCTION.. 1

2. RAMMING MODE FORMULATIONS... 7

   2.1 Ramming Performance Model....................................... 8
   2.2 Resistance Models... 12
   2.3 Ship Motions and Accelerations.................................. 18

3. DATA SCANNING, CATEGORIZATION AND QUALITY ASSESSMENT................ 21

   3.1 Data Scanning: Methods and Results.............................. 22
   3.2 Core Database and Validation.................................... 26
   3.3 Categorization.. 28
   3.4 Quality Assessment.. 30

4. DATA REDUCTION PROCEDURES... 37

   4.1 Data Reduction/Instrumentation.................................. 38
   4.2 General Procedures.. 40
   4.3 Data Reduction Algorithms....................................... 44

5. RESULTS OF STANDARD ANALYSIS.. 65

   5.1 Scope of Standard Analysis...................................... 66
   5.2 Typical Case.. 66
   5.3 Results... 73

6. PERFORMANCE FORMULATIONS.. 75

   6.1 General... 76
   6.2 Analysis of Performance under Trial Conditions.................. 78
   6.3 Performance Simulation.. 106
   6.4 MV ARCTIC Capabilities.. 114

7. EVALUATION OF OPERATIONAL ASPECTS................................... 121

   7.1 Power Requirements.. 122
   7.2 Design Features of the MV ARCTIC................................ 124
   7.3 Instrumentation System and Data Acquisition System.............. 125
   7.4 Ramming Strategy.. 128

8. CONCLUSIONS AND RECOMMENDATIONS..................................... 131

   8.1 Conclusions... 132
   8.2 Recommendations for Designers and Operators..................... 134
   8.3 Recommendations for Supplementary Evaluation.................... 136

REFERENCES... 139

TABLE OF CONTENTS
(CONTINUED)

PAGE NOS.

APPENDIX A - DETAILED RAMMING MODE FORMULATIONS.................... A1 - A32

APPENDIX B - DEVELOPMENT OF QUALITY ASSESSMENT - METHOD........... B1 - B6

APPENDIX C - RESULTS OF DEDICATED TRIALS - ADMIRALTY INLET, 1981.. C1 - C242

APPENDIX D - SPEED LOG CORRECTIONS................................ D1 - D13

APPENDIX E - TREND ANALYSIS AND PERFORMANCE PREDICTIONS............ E1 - E31

LIST OF FIGURES

1.1 LINES PLANS OF THE MV ARCTIC....................................3
2.1 RAMMING MODE FUNCTIONS AND MODELS...............................9
2.2 SCHEMATIC REPRESENTATION OF RAMMING CYCLE......................11
2.3 COMPARISON OF LEVEL ICE RESISTANCE.............................15
2.4 COMPARISON OF LEVEL ICE RESISTANCE MODELS......................17
3.1 DATA SCANNING INSTRUMENTATION...................................25
3.2 SHIP ROUTE DURING ADMIRALTY INLET TRIALS JULY 1981 [21].......27
4.1 DATA REDUCTION AND ANALYSIS INSTRUMENTATION.....................39
4.2 CHART RECORDER PLOT RAM NO. C6..................................41
4.3 IDEALIZED RAMMING CYCLE AND COMPONENTS..........................45
4.4 DATA REDUCTION PROGRAM SEGMENTS.................................49
4.5 VARIATION OF NET EXTERNAL FORCE DURING VARIOUS STAGES OF RAMMING CYCLE...53
4.6 COMPARISON OF EFFECTIVE THRUST CALCULATED FROM MODEL TEST DATA AND EQUATIONS DEVELOPED...................................57
4.7 DETERMINATION OF RESISTANCE PROFILES............................61
6.1 EFFECT OF ACCELERATION DISTANCE ON SPEED OF IMPACT..............79
6.2 EFFECT OF ICE THICKNESS ON ACCELERATION VARIABLES...............81
6.3 RIDGE PROFILE AND RAMMING SERIES................................83
6.4 EFFECT OF SPEED OF IMPACT ON SPEED OF ADVANCE...................85
6.5 PENETRATION DISTANCE VERSUS Vo..................................87
6.6 EFFECT OF THRUST CUT-OFF ON PENETRATION.........................89
6.7 EFFECT OF Xa ON AVERAGE FUEL USED PER RAM.......................91
6.8 FUEL USE AS A FUNCTION OF ICE CONDITIONS........................93
6.9 MV ARCTIC PERFORMANCE MODEL IN RAMMING MODE......................95
6.10 TYPICAL EXAMPLES OF EXTENDED REVERSAL DURATION.................101
6.11 RESPONSE CYCLE COMPONENTS......................................103
6.12 EFFECT OF IMPACT SPEED ON CYCLE COMPONENTS.....................104
6.13 PREDICTED VERSUS MEASURED ACCELERATION DISTANCE...............109
6.14 REGENERATED SPEED-PENETRATION PLOT FOR RAM NO C-6.............113
6.15 SPEED OF ADVANCE AND FUEL MILEAGE VERSUS IMPACT SPEED.........116
6.16 OPTIMUM SPEED OF ADVANCE AND FUEL MILEAGE VERSUS ICE THICKNESS...116
6.17 EFFECT OF ASTERN POWER ON SPEED OF ADVANCE AND FUEL MILEAGE..117
6.18 TRANSITION CONTINUOUS RAMMING MODE............................119
6.19 RIDGE BREACHING CAPABILITIES..................................119
7.1 COMPARISON OF THE EFFECTS OF INSTALLED VS CASPPR LEVELS......123
7.2 SAMPLE PRESSURE RIDGE PROFILE..................................127
7.3 RAMMING STRATEGY...129

LIST OF TABLES

1.1 CHARACTERISTICS OF MV ARCTIC SHIP HULL DATA SHEET..............5
2.1 REVIEW OF FEATURES IN RESISTANCE MODELS.......................13
2.2 SUMMARY OF GENERAL EQUATIONS OF MOTION........................19
3.1 SUMMARY OF LENGTH OF RECORDS.................................23
3.2 OVERVIEW OF CORE DATABASE....................................29
3.3 OVERVIEW OF CATEGORIES.......................................31
3.4 OVERVIEW SERIES A RAMS.......................................32
3.5 OVERVIEW SERIES B RAMS.......................................33
3.6 OVERVIEW SERIES C RAMS.......................................34
4.1 CONVERSION EQUATIONS FOR 1981 TRIALS AND VOYAGES.............43
4.2 CYCLE TIME COMPONENTS..47
4.3 A LIST OF GRAPHICAL ILLUSTRATIONS FOR EACH RAM...............51
4.4 COMPARISON OF EFFECTIVE THRUST CALCULATION METHODS...........59
4.5 COMPARISON OF TAPE AND VIDEO ANALYSIS RESULTS................63
6.1 ACTION CYCLE TIME COMPONENTS.................................99
6.2 TYPICAL RAMMING CYCLE PROFILES FOR MV ARCTIC.................105
6.3 SUMMARY OF MV ARCTIC THRUST AND RESISTANCE FORMULATIONS......107
6.4 SIMULATION OF RAM NO. C6.....................................111

1. INTRODUCTION

1. INTRODUCTION

The MV ARCTIC is the first Arctic Class 2 bulk carrier to be designed and built in accordance with the Canadian Arctic Shipping Pollution Prevention Regulations (CASPPR). The hull lines plans and major characteristics of the vessel are given in Figure 1.1 and Table 1.1 for reference purposes.

Since its delivery in 1978, the MV ARCTIC has been primarily operating to and from Nanisivik Harbour in the Canadian Arctic. The ship was fitted with a computerized data acquisition system which has been described in several Transport Canada publications [1]. Data have been collected during three Arctic operating seasons from 1979 through 1981. The data have been documented in various project reports each season and summarized in a Master Data Package in 1982 [2] which represents a comprehensive record of four dedicated trials and several Arctic voyages.

Transport Canada has recently commissioned five independent studies to analyze and evaluate various aspects of the performance and capabilities of the ship. This study is only concerned with the ice transiting performance in the ramming mode of operation.

The overall objective of this study is to establish the ramming mode and ridge penetration capabilities of the MV ARCTIC and its design features including the bubbler system and to provide and demonstrate some means of performance formulation which permits the utilization of the findings of this study into the operation of the MV ARCTIC and the design of other Arctic Class cargo ships.

The statement of work covered the following items:

a) Review of ramming mode formulations.
b) Data scanning and categorization.
c) Data reduction, performance analysis and development of algorithm for the classification of ridges.
d) Development of ramming mode ice-transiting performance formulations.
e) Graphical presentation of the MV ARCTIC's ramming mode ice-transiting capability.
f) Identification of the transition zone between continuous and ramming modes, the maximum ramming mode capability and ridge breaching capability.
g) Interpolation and extrapolation of performance to vessels of lower and higher ice class.
h) Evaluation of CASPPR power provisions.
i) Determination of the techno-economic significance of the "as fitted" power level and identify the optimum energy related tactics for ramming mode icebreaking.
j) Evaluation of the techno-economic significance of the bubbler system.
k) Determination of the extent and probabilities of any ice-transiting delays/restraints as per CASPPR.
l) Evaluation of the main features of the MV ARCTIC hull and ice milling with regards to the vessel's ramming mode performance.

FIGURE 1.1 LINES PLANS OF THE MV ARCTIC

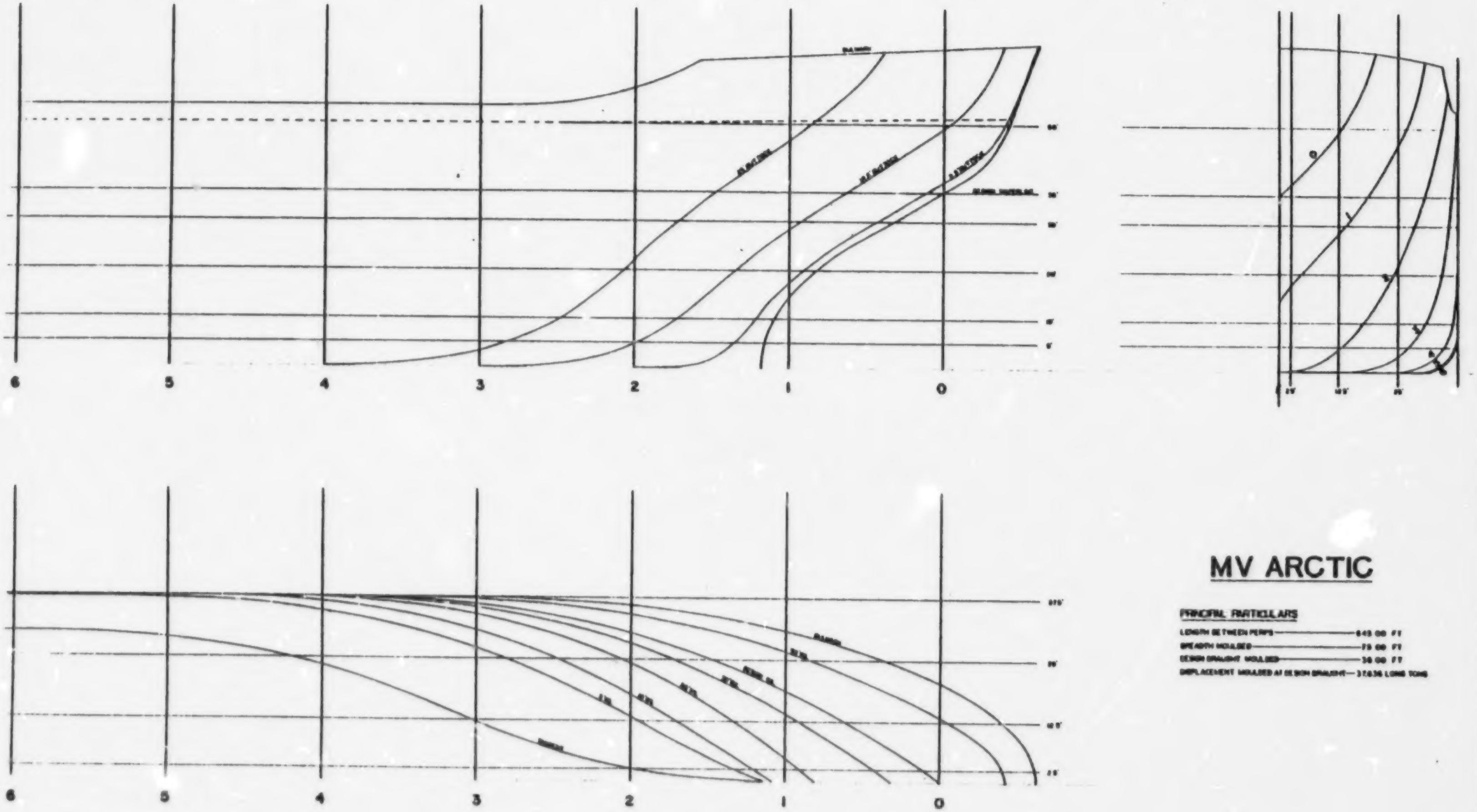
6
5
4
3
2
1
0
MV ARCTIC
PRINCIPAL PARTICULARS
LENGTH BETWEEN PERPS — 643.00 FT
BREADTH MOULDED — 75.00 FT
DESIGN DRAUGHT MOULDED — 36.00 FT
DISPLACEMENT MOULDED AT DESIGN DRAUGHT — 37,636 LONG TONS

m) Evaluation of the rigid body motions.
n) Evaluation of the instrumentation system, the data acquisition procedure and acquired data bank.

This report presents the results of this study and covers the various aspects of MV ARCTIC performance in the ramming mode. The interim report [3] (Transport Canada Publication TP 5169E) has been incorporated in the present report to ensure a minimum of cross referencing to the said document.

The following seven chapters address the various requirements of the project. Chapter 2 summarizes the ramming mode formulations. Chapter 3 deals with data scanning, categorization and quality assessment. Data reduction procedures and algorithms are discussed in Chapter 4 while the results are presented and summarized in Chapter 5. Performance formulations may be found in Chapter 6 which includes the reconstruction of a typical case using the developed techniques. Chapter 7 covers the various aspects of evaluation of CASPPR power requirements, bubbler system efficiency, instrumentation system and data acquisition strategies, conclusions and recommendations for designers and operators, supplementary evaluation and further R&D work.

The data on ice conditions that should complement the ramming data in order to successfully carry out the performance analysis, were not complete and had to be supplemented with data from nearby locations. Especially the information on ridges was insufficient to fully investigate the performance under these conditions. The available information, however, indicate that those ice conditions may be interpreted as thick level ice. Therefore the analysis of the data was basically directed at ramming mode performance in level ice.

The total number of runs in the dedicated trials under consideration was 57, of which 39 runs were suitable for further analysis. Not all parameters that were anticipated to form part of the performance evaluation have been covered in the trials, while for some other parameters only a few single data points are available. For that reason the study cannot be conclusive in all areas, as detailed in the statement of work. However, the results of the data reduction and analysis provide an excellent insight in the factors and parameters that affect the performance in the ramming mode as deduced from the available data base. The graphical presentations of the ramming incidents show the ship responses to a variety of propulsion system actions, from which after evaluation with reference to the reduced data the better ramming operation procedures have been identified.

Interpretation of the data obtained through analysis has been carried out for as far as the original data base permitted. The methodology of dividing the ramming process into cycle components provides useful information which can be used for the development of extended and more detailed performance formulation based on regression analysis followed by computations conducting a sensitivity analysis. This work is beyond the scope of this study and is therefore strongly recommended for further work in order to fully exploit the outcome of the study as presented in this report.

TABLE 1.1

SERIAL #	CHARACTERISTICS OF MV ARCTIC SHIP HULL DATA SHEET	**DESIGNATION**
VESSEL NAME & HULL FORM	MV ARCTIC (14,770 BHP) (28,094 ton DWT)	**SCALE** FS

***DIMENSIONAL PARAMETERS**

L_o = 209.55 m

L_{BP} = 196.59 m

B = 22.93 m

T = 10.93 m

Δ = 38,104 ton metric

****NONDIMENSIONAL PARAMETERS**

L/B = 8.60

B/T = 2.084

C_b = 0.759

C_{bf} = 0.798

C_p = 0.764

C_w = 0.876

C_{wf} =

C_m = 0.991

γ_0 = 30°

β_5 = 0°

μ_0 = 1.669

η_2 = 2.473

FRICTION FACTORS, *f*:

f = 0.2

GEOMETRY-FRICTION COEFFICIENTS

f	μ_1	μ_2
0.000	0.669	0.404
0.1	0.861	0.548
0.2	1.054	0.707
0.3	1.246	0.884
0.4	1.439	1.084
0.5	1.631	1.309

FOREBODY WATERPLANE ANGLES

STATION	10 (FP)	$9\frac{3}{4}$	$9\frac{1}{2}$	$9\frac{1}{4}$	9	$8\frac{3}{4}$	$8\frac{1}{2}$	$8\frac{1}{4}$	8	$7\frac{3}{4}$	$7\frac{1}{2}$
α °	32.8	30.8	27.2	21.8	15.2	10.3	6.3	2.9	0	0	0
β °	55.4	44.1	35.0	27.2	19.6	12.3	6.3	2.4	0	0	0

2. RAMMING MODE FORMULATIONS

2. RAMMING MODE FORMULATIONS

2.1 Ramming Performance Model

A comprehensive review of the ramming mode operation and formulations is presented in Appendix A. The various functions and models covered are schematically illustrated in Figure 2.1.

When considering the ramming mode it is useful to refer to the transition mode of operation. The latter represents the slow unstable continuous progress which is interrupted from time to time. Ship motion in this range is difficult to express in mathematical terms and usually involves probabilistic methods. This problem was analyzed by Kheysin in 1973 [4] and his solution may be adopted and expanded to "the transition point" concept. The solution simply indicates that as the ice thickness increases the continuous progress slows down and the frequency of stopping increases. At some point it becomes more logical to switch to the ramming mode and this point is usually left up to the discretion of ship pilots. Nonetheless, a successful selection of the "transition point" can lead to faster overall progress and lower fuel costs.

During the ramming mode of operation, the ship rides up on the ice until it develops sufficient vertical force to break the ice. The maximum force a given ship can generate depends on the ship displacement, hull geometry, bow geometry, friction between the bow and ice, and installed power which essentially determines how fast the ship can accelerate in the broken channel before impacting the ice. In [4] the theoretical method of determining the ice navigating capability is briefly discussed. A formula for estimating the icebreaking capability of a ship in continuous motion in solid ice was first proposed by Runeberg in 1890. Later in 1946 Vinogradov used this formula in the theoretical method of estimating the ice navigating capability in operating by short runs. Solving the equation of the energy balance an expression was obtained for the vertical force on the stem. In 1965, White [5] developed expressions for the maximum ice thickness which can be broken by a ship and the penetration distance as a function of impact speed. This relationship was recently used by Gill et al [6] in their transit model. White's model (which was adopted by Gill and others) is rather simple and it may deviate significantly from actual observations if strength and friction values as well as the failure load of the ice cover are not properly determined. However, from our examination of White's model we find that it produces an acceptable trend of variation of penetration distance versus speed of impact.

In 1978, Peirce [7] reviews an approach using a kinetic energy concept to evaluate initial ice encounter of ships moving through open water. From a work diagram, visualizing the penetration process, an equation was derived from which the penetration distance was obtained. In the analysis method thrust and resistance relation versus ship speed were assumed to be known. The same technique was used for the conditions of steady speed in level ice when encountering a ridge. Simple ridge parameters were defined to alter the given resistance expression and an expression was derived to estimate the minimum approach speed required to breach a ridge. The comparison of some computations with full scale observations were reported to be encouraging. The presently

FIGURE 2.1

RAMMING MODE FUNCTIONS and MODELS

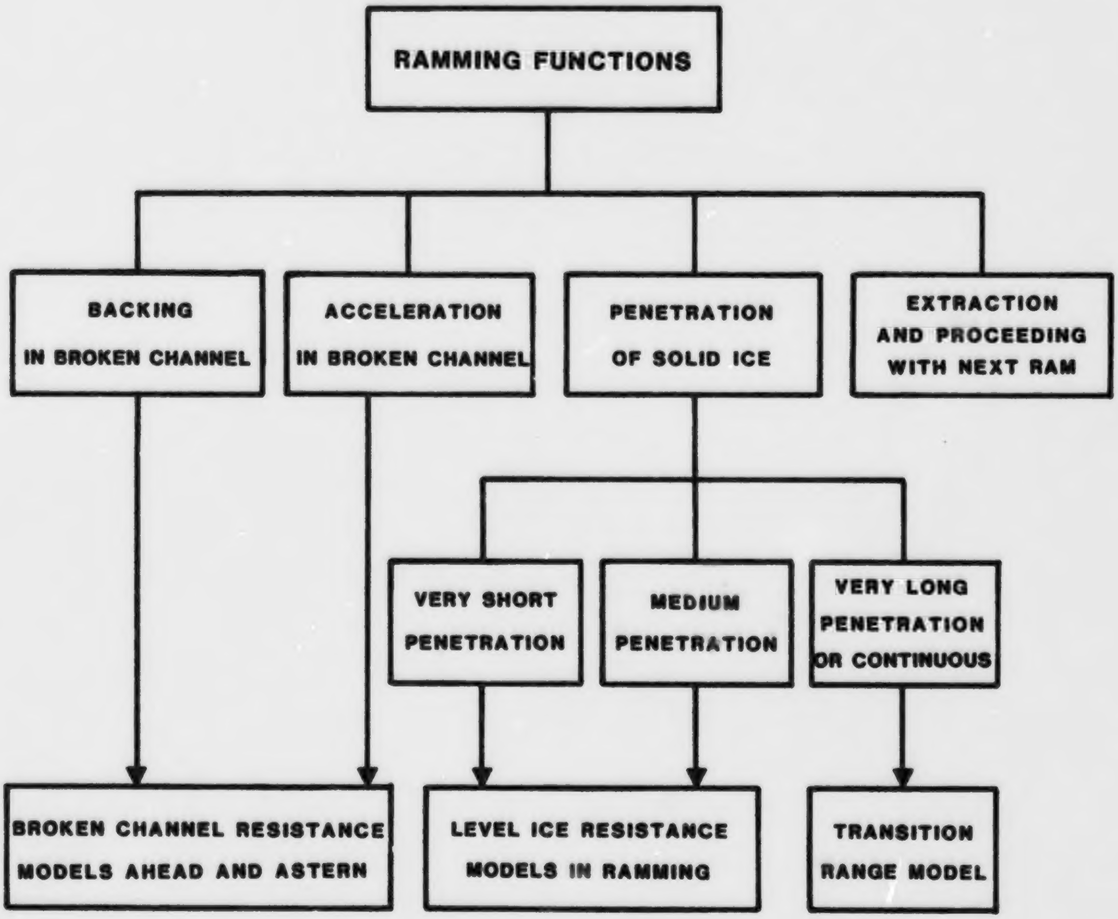
RAMMING FUNCTIONS
BACKING IN BROKEN CHANNEL
ACCELERATION IN BROKEN CHANNEL
PENETRATION OF SOLID ICE
EXTRACTION AND PROCEEDING WITH NEXT RAM
VERY SHORT PENETRATION
MEDIUM PENETRATION
VERY LONG PENETRATION OR CONTINUOUS
BROKEN CHANNEL RESISTANCE MODELS AHEAD AND ASTERN
LEVEL ICE RESISTANCE MODELS IN RAMMING
TRANSITION RANGE MODEL

used simplifications however, may be a drawback at this point in time.

A mechanics approach is that proposed by Lewis and Edwards [8], Petrov and Kheysin [9] and Ryvlin and Tegkayeva [10] and other Russian investigators. We have furthered this approach as detailed by Nawwar [11] and developed a general solution for the ramming operation which can be used for:

- acceleration or deceleration in level or broken ice.
- engine reversal interval and stopping in ice with no thrust.
- braking in ice.

This model is capable of mathematically describing all segments of the ramming cycle, as shown in Figure 2.2. The figure represents the ramming cycle in the speed-penetration space and describes the various stages of the cycle.

In general, the average speed of advance of a ship during ramming is determined by dividing the total distance of penetration (forward progress) by the total time of penetration. Meanwhile, the fuel consumption is a function of the total distance travelled (ahead and astern) or the path traced. For a single cycle; the total cycle time, t, may be written:

$$t = t_b + t_a + t_p + t_l \qquad (2.1)$$

where t_b = backing time from the broken channel

t_a = acceleration time in the broken channel

t_p = penetration time

t_l = the share of time losses when the ship gets lodged at any part of the cycle particularly at the end of a ram or under ice pressure conditions. It also includes indirect time losses associated with thrust reversal (or engine reversal).

The ramming mode formulation [11], used in this study requires relationships between ice resistance and ship speed for the various stages of the ramming cycle. Descriptions of candidate ice resistance models are included in Appendix A.

The selection of models suitable for application to the MV ARCTIC will be discussed in the following section.

FIGURE 2.2

SCHEMATIC REPRESENTATION OF RAMMING CYCLE

v = speed, x = penetration

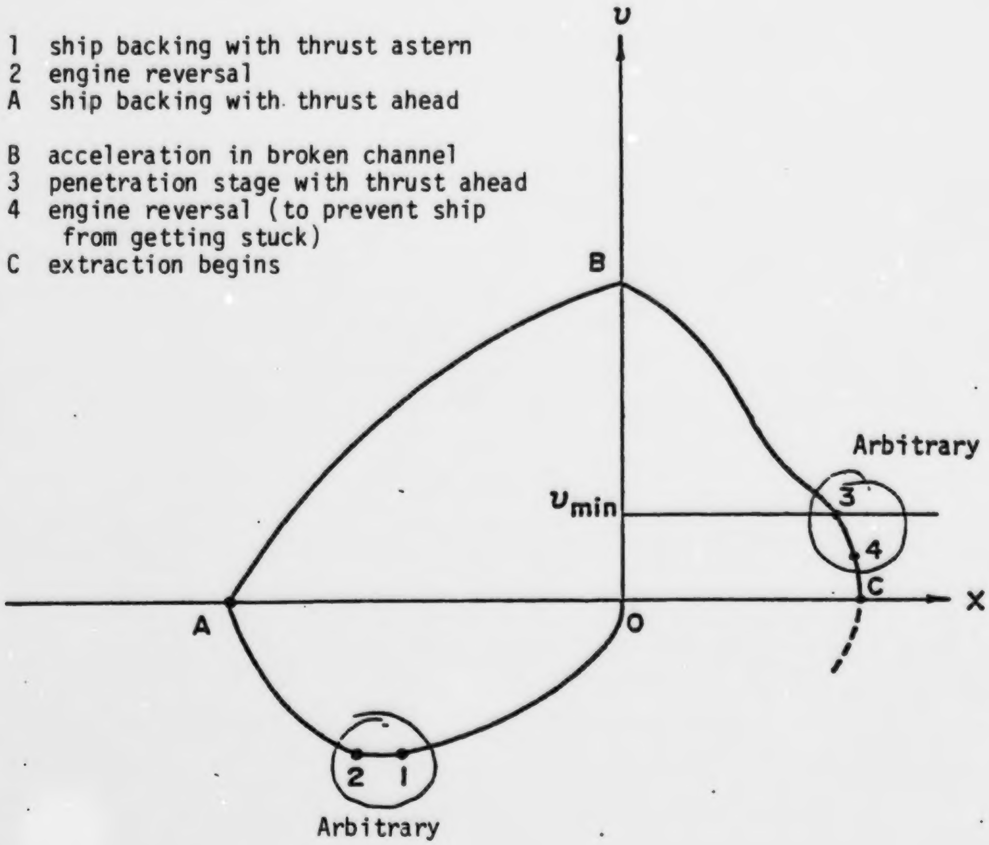

0 - 1 ship backing with thrust astern
1 - 2 engine reversal
2 - A ship backing with thrust ahead

A - B acceleration in broken channel
B - 3 penetration stage with thrust ahead
3 - 4 engine reversal (to prevent ship from getting stuck)
4 - C extraction begins

Summary of Formulations:

$$M \frac{dv}{dt} = X(v) \qquad (2.2)\ a$$

$$\therefore \quad \text{duration or time} = t = M \frac{dv}{X(v)} \qquad (2.2)\ b$$

$$M.v.\frac{dv}{dx} = X(v) \qquad (2.3)\ a$$

$$\therefore \quad \text{Penetration distance} = X = M\ v.\frac{dv}{X(v)} \qquad (2.3)\ b$$

$$X(v) = T(v) - R(v) \qquad (2.4)$$

= the net force; the difference between thrust, T(v), and resistance R(v).

v = ship speed

2.2 Resistance Models

The selection of resistance models to be used in conjunction with the ramming mode formulation as outlined in 2.1 and detailed in Appendix A, will depend on the applicability to ice-capable cargo vessels such as the MV ARCTIC. Therefore the following selection criteria have been generated.

a) shall be corroborated by full scale data under different operating conditions.

b) shall be valid and account for the following hull parameters:

   - slenderness, L/B high (6-10)
   - block coefficient high (0.7 - 0.8)
   - displacement, L, B
   - hull and bow geometry

c) shall make proper consideration of hull-ice friction factor.

d) shall be a closed form formulation such as a quadratic function of ship speed for application in a ramming optimization model.

e) shall provide a means to include snow effect and to account for ice pressure.

The last condition can be met by introducing additional terms to a basic equation and are excluded from further consideration at this point in time.

The candidate models given in Table 2.1 along with a review of the various parameters which were considered in each model. The review covers the following conditions of level ice, broken channel and pressure ridges.

For the level ice models, the findings can be summarized as follows:

- Kashteljan et al [12]: no account for friction.

- Enkvist [13]: lengthy formulation, based on specific ship types, model development subject to criticism.

- Wartsila [14 & 15]: specifically for large sized bulk carriers, no flexibility for application to similar ships, no detailed hull and bow geometry included.

- Edwards et al [16]: model based on icebreaker forms, coefficients for limited range of block coefficients and relative ice thickness, no detailed bow geometry included.

- Nawwar & Edwards [17]: two models developed from large model scale data base, offers wide range of many variables, may not provide the desired accuracy for particular ship type, non-dimensional model contains more specific form variables, some

TABLE 2.1 REVIEW OF FEATURES IN RESISTANCE MODELS

MODEL	HULL PARAMETERS												Friction	ICE PARAMETERS			RIDGE PARAMETERS						DATA M&F*	REMARKS
LEVEL ICE	L	B	T	C_b	C_{bf}	C_w	C_{wf}	α_0	B_5	ϕ	L_e	Bow		σ	h	r	Area	l_r	h_r	s	m	shape		
Kashteljan et al [1968]		x									x	x		x	x								M&F	No friction
Enkvist [1972]		x	x				x			x		x	x	x	x								M	Specific Ship Types
Wartsila [1975]		x	x										x	x	x								M	Bulkcarriers
Edwards et al [1976]		x	x	x									x	x	x								M	$0.50<C_b<0.625$; $10<\frac{T}{h}<73$
Nawwar & Edwards [1978]	x	x		x								x	x	x	x								M	See footnote (1)
Nawwar & Edwards [1978]	x	x			x			x	x			x	x	x	x								M	See footnote (2)
Poznyak & Ionov [1981]	x	x						x				x	x	x	x								M&F	icebreakers
BROKEN CHANNEL																								
Ryvlin [1968]	x	x				x	x	x							x	x								only available
PRESSURE RIDGES																								
General Approach											x						x					x		incomplete
Peirce [1979]											x							x	x	x	x			symplified
Makinen [1976]											x						x					x		complex

* M = Model Scale
F = Full Scale
L = Ship Length
B = Ship Beam
T = Ship Draught
L_e = Length of Entrance

C_b = Block Coefficient
C_{bf} = Block Coefficient Forward
C_w = Waterplane Coefficient
C_{wf} = Waterplane Coefficient Forward
α_0 = waterline angle of entrance

B_5 = flare angle midship
ϕ = stem angle
σ = flexural strength
h = thickness
r = floe size
l_r = effective length

h_r = effective height
s = strength factor
m = density factor

Footnotes: (1) dimensional model based on statistical analysis of world wide data base of more than 1200 data points.
(2) dimensionless analysis based on same data as in footnote (1). Both models account for hull angles at waterline α and β, as well as the coefficient of friction.

difficulty in expanding to full scale.

- Poznyak and Ionov [18]: specific for icebreakers, hull and bow geometry included in a reasonable form which accounts for geometry and friction.

From this evaluation the following models were selected for a more detailed analysis:

- Edwards et al [16]
- Nawwar and Edwards [17]
  a) Dimensional Model
  b) Non-Dimensional Model

These models were applied to the MV ARCTIC and compared with predictions from model test data. The computations were carried out for two ice strengths. It appeared that the non-dimensional model of Nawwar and Edwards predicted resistance values significantly higher than the others and was therefore eliminated from further considerations. The dimensional model was corrected to permit its use for full scale predictions.

The results of the computations are shown in Figures 2.3 and 2.4. It can be seen that the model of Nawwar and Edwards consistently overpredicts but with a correct trend, while the model of Edwards et al generally shows the same level of resistance at low speeds but a different trend with increasing speed. In other words the first is considered more in line with the prediction from model test data. Also plotted are the results of computations using the resistance equation developed from full scale trials as reported in TDC TP3646E (MV ARCTIC Experimental Voyage to Lake Melville, Labrador, in February/March 1981). The agreement with the model of Nawwar and Edwards is rather good, especially around the ice strength of 150 kPa and ice thickness of 1.0m, which approximates the ice conditions observed during the ramming trials that will be analyzed in this study.

Therefore it was concluded that at this stage the dimensional model by Nawwar and Edwards would be the best suited model for the following reasons:

- developed from large model scale data base,
- shows similar trend as results of model tests and full scale observations,
- universality,
- expandability,

Refinement of the selection of a level ice resistance model for ice-capable cargo vessels such as the MV ARCTIC and consequently the development of such a model can only be undertaken on the basis of analysis of available data for the continuous mode of operation.

A recent model developed by Carter [20] has also been considered. It is formulated in closed form and has the merits of including geometric description of the bow in terms of waterline angle, stem

FIGURE 2.3 COMPARISON OF LEVEL ICE RESISTANCE

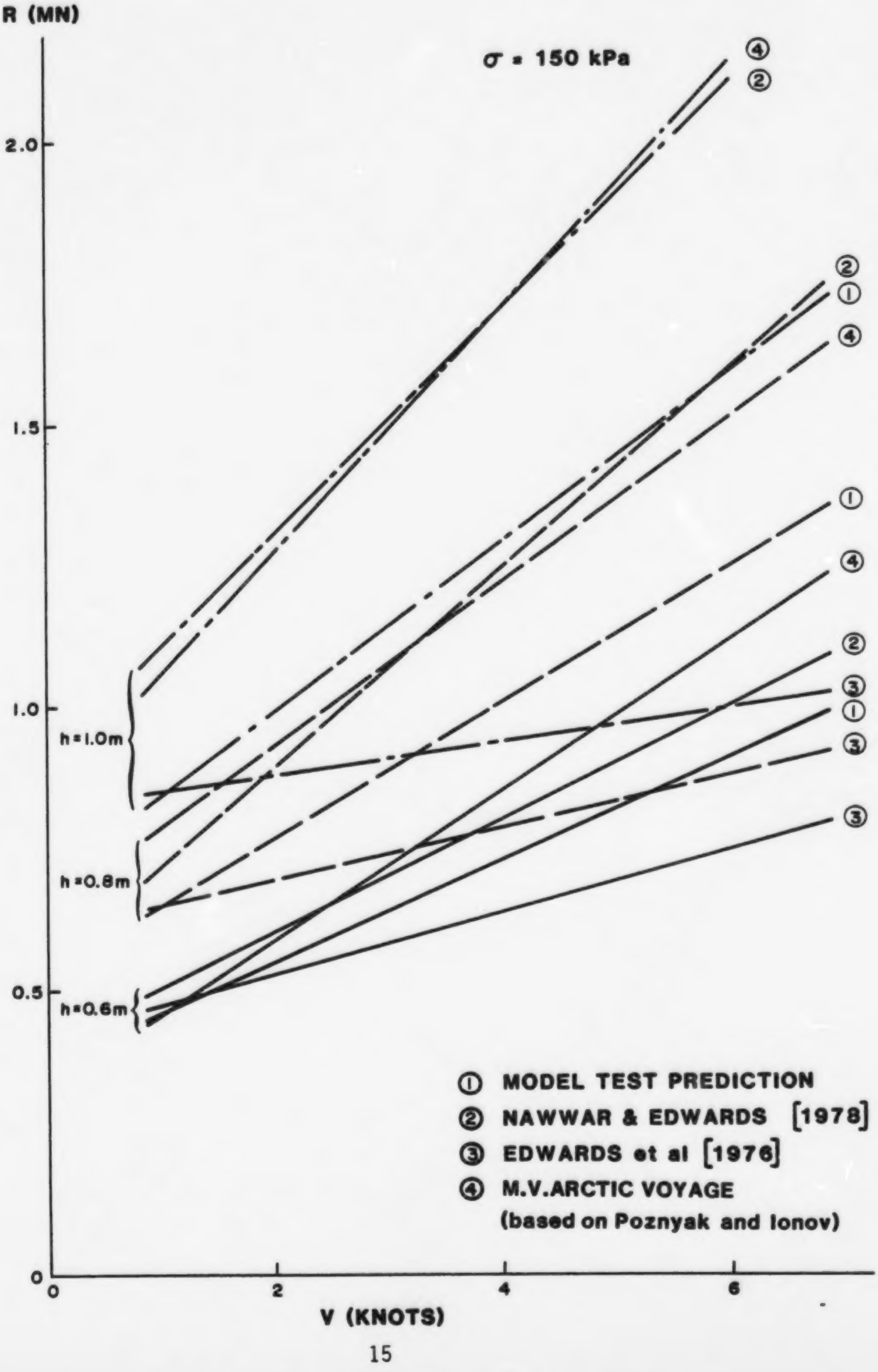

angle, flare angle at midship, length of entrance, and beam. Carter makes some strong assumptions in the development of this model regarding the dynamic behaviour of the ice cover and solves the wedge equation accordingly. Because this is a simplistic approach and must be validated as to the resulting approximations and limits of application it has been excluded from evaluation in this study.

The model given by Ryvlin [12] for resistance in a broken channel is the only model available. The model contains sufficient hull form parameters for use in the ahead and astern modes and is suitable for application to the proposed ramming mode formulation.

A resistance model in ridges is not readily available. The general approach outlined in Appendix A would be the ultimate, but has not been fully developed and requires input data from penetration characteristics of an ice edge. The method adopted by Peirce [7] is oversimplified for the purpose of analysis in this study. The method proposed by Makinen [19] seems to be the best suited and most practical approach in preparing a model for which, however, a rather detailed description of the ridge must be known.

Since ramming involves thicker ice, the ice resistance models used in the ramming mode formulation may not adequately predict the ice resistance. However, based on Figures 2.3 and 2.4 it can be seen that the agreement is acceptable for this stage of the study. For the broken channel no material for comparison is available. This would require the adjustments of the empirical constants of the resistance predictor equations to fit the actual data to be collected in this study. Since data available for analysis can be used to calculate the instantaneous resistance profile during all stages of the ramming cycle, sufficient information on resistance ahead and astern in broken channels as well as ahead in level unbroken ice may be available for comparison with and adjustment of selected models. It should be noted that the major difference is that while the models have been developed for steady progress, i.e. at constant speed, the ramming operation involves dynamically changing speeds, the effect of which on the resistance of ice has not been identified in previous investigations.

FIGURE 2.4 COMPARISON OF LEVEL ICE RESISTANCE MODELS

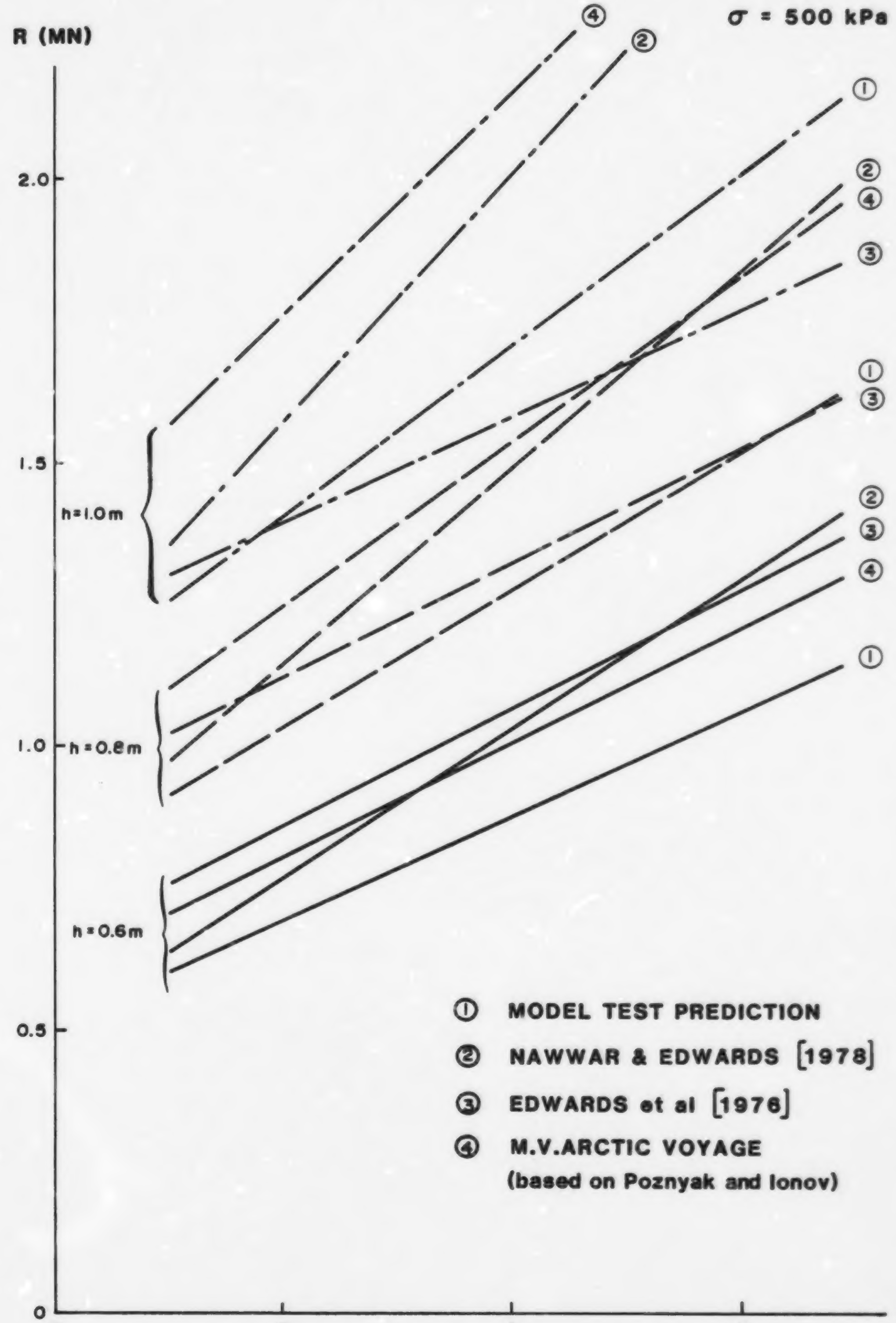

2.3 Ship Motions and Accelerations

It was initially intended to evaluate the rigid body motions (heave, surge, sway, yaw, pitch and roll) under the various conditions of ramming mode ice-transiting performance and develop appropriate equations of motion/acceleration in respect of the six degrees of freedom. This was required at a later phase of the study. However, it was felt advantageous to study this aspect earlier on in the work in order to explore possible extensions to data reduction.

The main reason behind this was the generally poor accuracy of the doppler log speed record particularly at lower speeds. It was felt that an alternate approach to the determination and validation of the speed from measured rigid body motions may be possible. However, due to limited resources we have only been able to develop the formulations and explore some of the possible applications. We have not been able to investigate the actual application of the developed algorithms to data reduction or provide typical examples. Nonetheless, it should be mentioned that the 1981 database contains substantial records of translational and rotational motion measurement of the MV ARCTIC. Reference is made to Transport Canada's publication TP 3632, [21] which provides some extracts and plots of such records. This data could be used for the analysis of rigid body motions to determine ship speed of advance and other parameters.

The equations of motion have been derived for the pertinent conditions of operation and are summarized below. Detailed mathematical derivations have been reported by Nawwar et al [3]. Such details have not been included in this document for reasons of brevity and relevance to the type of analysis reported in the following chapters. However, it should be noted that methods of coordinate transformation of motion variables and methods of determining hydrodynamic coefficients as applicable to the MV ARCTIC have been outlined in Reference [3].

A summary of the governing equations of motion in the three modes of translation as well as the three modes of rotation in general form is given in Table 2.2 along with definitions of the terms of the equations. It should be noted that the ship motions and accelerations given in these equations refer to the ship-fixed coordinate system. During the ship motion the ship-fixed coordinate system moves (translates and rotates) relative to the Newtonian frame of reference (space-fixed coordinate system). Nonetheless, in the MV ARCTIC case the accelerometers were ship fixed and no transformation will be required for such motion variables.

TABLE 2.2

SUMMARY OF GENERAL EQUATIONS OF MOTION

$$m\,[\dot{u} + qw - rv - x_G(q^2 + r^2) + y_G(pq - \dot{r}) + z_G(pr + \dot{q})] = X$$

$$m\,[\dot{v} + ru - pw - y_G(r^2 + p^2) + z_G(qr - \dot{p}) + x_G(qp + \dot{r})] = Y$$

$$m\,[\dot{w} + pv - qu - z_G(p^2 + q^2) + x_G(rp - \dot{q}) + y_G(rq + \dot{p})] = Z$$

$$I_x\dot{p} + (I_z - I_y)qr + m\,[y_G(\dot{w} + pv - qu) - z_G(\dot{v} + ru - pw)] = K$$

$$I_y\dot{q} + (I_x - I_z)rp + m\,[z_G(\dot{u} + qw - rv) - x_G(\dot{w} + pv - qu)] = M$$

$$I_z\dot{r} + (I_y - I_x)pq + m\,[x_G(\dot{v} + ru - pw) - y_G(\dot{u} + qw - rv)] = N$$

where

m, I_x, I_y, I_z = Ship mass, moments of inertia in roll, pitch and yaw respectively

u, v, w = Surge, heave and sway velocities (in ship-fixed coordinate system)

$\dot{u}, \dot{v}, \dot{w}$ = Accelerations (ship-fixed coordinate system)

p, q, r = Angular velocities (ship-fixed coordinate system)

$\dot{p}, \dot{q}, \dot{r}$ = Angular accelerations

x_G, y_G, z_G = Coordinates of position of center of gravity relative to the point where motions are measured

X, Y, Z = Components of the total external force acting on the hull

K, M, N = Components of the total external moment acting on the hull

One special case of interest is that of head-on ramming. In this case, we assume that the centre of gravity of the vessel falls in the longitudinal midship plane so that the vessel has zero heel angle. We take the origin of the ship-fixed coordinate system so that $y_G = 0$, and consider only surge, heave and pitch motions. The resulting equations of motion are:

$$m\,[\dot{u} + qw - x_G q^2 + z_G \dot{q}] = X$$

$$m\,[\dot{w} - qu - z_G q^2 - x_G \dot{q}] = Z$$

$$I_y \dot{q} + m\,[z_G(\dot{u} + qw) - x_G(\dot{w} - qu)] = M$$

In the above equations,

m, I_y = Ship mass and ship moment of inertia in pitch

u, w = Surge, heave velocities (in ship-fixed coordinate system)

$\dot{u}, \dot{w}$ = Surge, heave accelerations (ship-fixed)

$q, \dot{q}$ = Pitch velocity, Pitch acceleration

x_G, z_G = Coordinate of origin of ship-fixed axis relation to centre of gravity

X, Z = Total external forces in surge and heave modes

M = Total external moment in pitch

The above form of the equations of motion is preferred if the aim is determination of forces.

Among the motion parameters, $\dot{u}$ and $\dot{v}$ are measured, u and v have to be determined by integrating the accelerations after transforming them to earth-fixed coordinates and then transforming back to the ship-fixed system, $\dot{p}$ and $\dot{q}$ are derived quantities and p and q are obtained by tranformation, integration and transformation. On the other hand, if the aim is analysis of ship motions to specific forcing functions, it is preferred that the above equations of motion be transformed to the earth-fixed system and then integrations performed.

3. DATA SCANNING, CATEGORIZATION AND QUALITY ASSESSMENT

3. DATA SCANNING, CATEGORIZATION AND QUALITY ASSESSMENT

3.1 Data Scanning: Methods and Results

The first step in data scanning was accomplished by reviewing the master data bank [2] for both dedicated trials and voyage monitoring. Based on this review we have determined the approximate lengths of records as summarized in Table 3.1. It was clear that the majority of ramming incidents occurred during the 1981 season either during dedicated trials or voyage monitoring routines. The portion of data collected in the 1979 season during voyage monitoring represents less than 8% of all available data and it was agreed with TDC to look first into 1981 data. For this reason only tapes for the 1981 Season were supplied at the beginning of the program.

According to this preliminary survey only 32 tapes were required for the data scanning, reduction and analysis.

One of the objectives of the present study was to provide a quality assessment and validation of the data. This was best accomplished by scanning the tapes identified containing useful data and displaying the information contained in them on ramming of level ice, pressure ridge or other ice features. This display of the available information permitted the assessment of the quality of the records, as well as the verification of the existence of such information. For this reason the data scanning instrumentation was designed.

The data scanning instrumentation consisted of the following:

a) Perkin-Elmer, 9-track magnetic tape drive with controller

b) Apple II plus computer (6502 microprocessor)

c) Apple Floppy Disc Drive

d) Epson Printer

e) Gould Brush 260 - 6 channel chart recorder

Figure 3.1 is a line diagram describing the data scanning instrumentation system.

A special software program was written in Assembly Language to command the tape drive. Programming in Assembler provides a much faster method for data scanning and reduction than other techniques using Basic or Fortran. In this stage of data reduction, the primary focus was made on graphical presentation of data to identify the events of interest. Therefore, each tape which was identified as containing relevant data was played back in its entirety to identify the events.

TABLE 3.1

SUMMARY OF LENGTH OF RECORDS

	ESTIMATED TIME OF DATA IN MINUTES		
	LEVEL ICE	RIDGES	MULTI-YEAR, PACK ICE,ETC.
1. Dedicated Trials			
Lake Melville - 1981	14	2	-
Admiralty Inlet - 1981	296.10	35.57	-
Totals	310.10	37.57	-
Total No. of Tape Hours	5.17	0.63	0
2. Arctic Voyages			
1979 Season	-	-	146.83
1981 Season	68.97	129.40	1191.08
Totals	68.97	129.40	1337.91
Total No. of Tape Hours	1.15	2.16	22.30

Not all the recorded channels were of interest to the present objectives. Therefore, the program was designed to identify the headers/file marks, and scan only the channels of interest. Using header information the sampling rates were used to determine the selection of recorded information.

Each signal was then processed to obtain the following:

a) Interval statistics for every channel which included the maximum, minimum and average. In addition to digital counts the information was transformed into engineering units and printed. The interval was arbitrary with a default value of 15 minutes.

b) The signals were converted into analogue form using D/A converters (Apple), and displayed graphically using the chart recorder. Due to the limit of the number of channels for display only the following data signals have been plotted:

1. ship speed as recorded by doppler log (Ch. 236)
2. fuel rack position (Ch.199)
3. propeller pitch (Ch.201)
4. shaft torque (Ch.208)
5. shaft thrust (Ch.198)
6. event marker signal (Ch.255)

The last signal was displayed to identify the events. Its consistent use would greatly simplify the definition of significant ramming events. However, it was observed that in most cases this marker was not used to identify ramming incidents. Therefore, the absence of this signal from the graphical display of data should not be interpreted as a problem with the data reduction procedures.

The interval statistics for all channels were collected and stored on floppy disc for later mass retrieval. This was done to speed up the data scanning, since the printer was the slowest of all elements of the system. However, to provide an update of the plotted channels which would assist in interpretation of data, a limited printout was provided for headers as well as 15-minute data summary.

The results of data scanning were obtained in a standard format. Each tape was essentially reduced into a short roll of chart paper and statistical summaries. These were used as working papers to identify and verify data, examine the quality, define specific problems, and conduct sample calculations on typical examples. Since all such data was later presented in a better format with the proper analysis, its reproduction for this report was unnecessary. All data resulting from the scanning have been compiled in an annex to this report and one complete copy is provided for TDC reference (as working papers).

FIGURE 3.1

DATA SCANNING INSTRUMENTATION

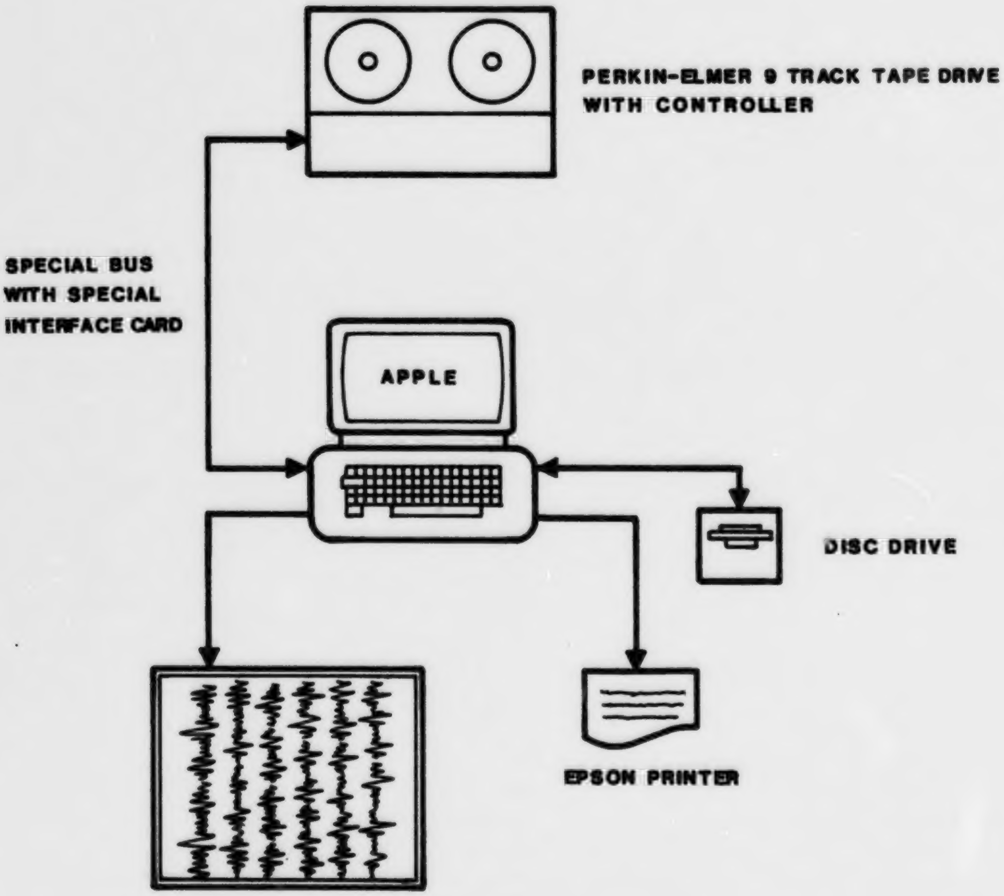
PERKIN-ELMER 9 TRACK TAPE DRIVE
WITH CONTROLLER
SPECIAL BUS
WITH SPECIAL
INTERFACE CARD
APPLE
DISC DRIVE
EPSON PRINTER
6 CHANNEL CHART RECORDER

3.2 Core Database and Validation

Following the data scanning, it was possible to distinguish two major categories of data from the 1981 trials:

a) The dedicated trials of Admiralty Inlet which contained most of the better documented ramming incidents.

b) The Arctic voyages which contained a large number of ramming incidents but with much less known about the ice conditions encountered.

Data from Lake Melville trials were incompletely recorded and due to the little information it offered, these rams were excluded from the first category.

The two major categories identified above required two different approaches to data interpretation. The first category can be used to conduct detailed analysis of the variables associated with ramming while the latter offers a broader statistical database which can be analyzed to assess transit capabilities with little certainty of ice conditions. It was felt that, while data from the first category lends itself to the conduct of rigorous analysis and interpretation, the second category of data complements this analysis and broadens its applicability under realistically variable but incompletely defined ice conditions.

For the above mentioned reasons, data from the Admiralty Inlet dedicated trials were used as a "core data base" to develop, test and validate data reduction and analysis methodology and to establish formulations for the performance of the MV ARCTIC. It was anticipated that data from 1981 Arctic voyages could be used in a future stage to develop a broader statistical validation of the results reported in the present document.

Therefore, the dedicated trials data have been used to establish the primary data and performance categories and prepare a quality assessment system. Data from other trials or voyages could easily be classified according to the categories established herein. Some special cases may be expected and may be dealt with individually.

Figure 3.2 illustrates the ship route during ramming tests which formed the core data base.

The rams identifiable from the charts have been checked for the ram number or impact number using reports MV ARCTIC Master Data Package 1979-1980-1981 Seasons (TP 3821E) [2] and MV ARCTIC 1981 (Early Season) Data Collection and Instrumentation (TP 3632) [21]. From these documents, the following types of information have been extracted and tabulated in Table 3.2:

- test number
- tape identification
- start and stop time of tape
- date
- ice characteristics

FIGURE 3.2

SHIP ROUTE DURING ADMIRALTY INLET TRIALS
JULY 1981 [21]

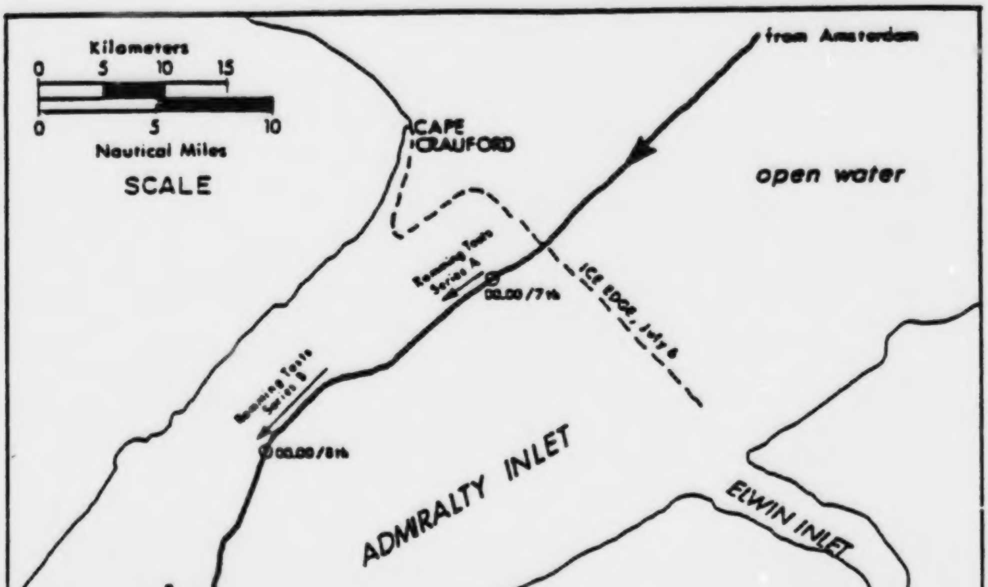
Kilometers
0
5
10
15
0
5
10
Nautical Miles
SCALE
from Amsterdam
CAPE CRAUFORD
open water
Ramming Tests Series A
00.00/7th
ICE EDGE, July 6
Ramming Tests Series B
00.00/8th
ADMIRALTY INLET
ELWIN INLET
BAILLARGE BAY
Ramming Tests Series C
00.00/9th
10/10 ICE
ICE EDGE July 9
STRATHCONA SOUND
NANISIVIK
ARCTIC BAY

- bubbler status
- trim and loading condition
- speed of impact
- ram number

Possibly due to difficulties with the recording instrumentation during the execution of the trials, not all recordings were found complete. This made the identification of the rams in a number of cases uncertain and a validation check using analysis of the series presented in [21] was carried out to identify these rams on the basis of impact speed, cycle time components and penetration. Finally, the rams identified on the charts were included in Table 3.2.

The following comments may be made:

a) Ramming tests No. A11 and A12 were previously reported [21] as aborted. However, on reviewing the tapes for Series A we found no evidence of aborted rams and also identified 18 complete rams. While we can offer no explanation of this discrepancy, we have included rams A11 and A12 particularly since penetration records were available in reference [21].

b) Ram No. B3 was identified as a small ridge, however the difference in ice thickness from level ice was small. Therefore, classification of this ram may be debated and while it is classed in level ice category the consideration of reclassification as a small ridge may be explored if the data is shown to deviate from the general trend of level ice.

c) Ram Nos. B13 to B15 were not found on tape, while B14 was aborted, there was no explanation for the absence of data of B13 and B15.

d) No record for test No. 7 was found on tape and hence, no data was available for rams B25 to the end of the Series B tests.

e) The same argument for B3 applies to C32 and C33 where a small ridge was indicated.

f) No records were found for ram Nos. C1-5, C11-17, C19-23, C28, C37-38.

3.3 Categorization

The categorization of the data has been performed on the basis of ice conditions, trim and bubbler status. Table 3.3 gives an overview of the data categories and the rams previously identified are grouped accordingly.

It is shown that most data exists in two categories for level ice and two others for ridges. In combination, the largest set of data exists in level ice or ridges for level keel (zero trim) and with the bubbler system operative. Based on data from dedicated trials in level ice it is possible to provide an assessment of trim condition on ramming performance only when the bubblers are on. Meanwhile, the lack of data

TABLE 3.2 Overview of Core Database

TEST	TAPE	RUN NO.	START	STOP	DATE	ICE TYPE	BUBBLER STATUS	TRIM	IMPACT SPEED(kts)	RAM	REMARKS
1	D2	81-T2-2.1	2:28:00	2:57:38	July	R	off	LK	4	A1-4	
2			3:04:38	4:02:40	7	R	off	LK	5	A5-10	
						R	off	LK		A11-12	
3			4:07:30	4:46:20		R	on	LK	5	A13-18	
4	D3	81-T2-3.1	14:04:03	15:04:00		L	on	LK	6	B1-7	B3 small ridge
5			15:08:50	15:41:23		R	on	LK	6	B8-12	
		81-T2-3.2	15:47:45	15:50:46							Not useful
6	D4	81-T2-4.1	17:55:45	17:57:22		L	on	LK	6		Not useful
		81-T2-4.2	18:04:25	18:35:30		L	on	LK	6	B16-19	
		81-T2-4.3	18:39:40	18:51:10		L	on	LK	6	B20-21	
		81-T2-4.4	18:58:40	19:30:00		L	on	LK	6	B22-24	
7											No recording
8	D5	81-T2-5.1	14:12:38	14:22:41	July	L	off	BU	6	C6	
9			14:26:30	14:56:53	8	L	on	BU	6	C7-10	
10		81-T2-5.2	15:27:25	15:27:25		L	on	BU	2		Not useful
		81-T2-5.3	15:35:50	15:37:10		L	on	BU	2		Not useful
		81-T2-5.5	15:43:48			L	on	BU	2		Not useful
		81-T2-5.7	15:54:50			L	on	BU	2	C18	
11											No recording
12	D6	81-T2-6.1	19:07:30			L	off	BU	2	C24	
		81-T2-6.3	19:17:55			L	off	BU	2	C25	
		81-T2-6.4	19:24:38			L	off	BU	2	C26	
		81-T2-6.5	19:28:28			L	off	BU	2	C27	
13		81-T2-6.9	19:44:20			L	off	BU	4	C29	
		81-T2-6.10	19:50:54			L	off	BU	4	C30-32	C32 small ridge
		81-T2-6.11	20:16:30			R	off	BU	4	C33	C33 small ridge
		81-T2-6.12	20:25:11			L	off	BU	4	C34	
		81-T2-6.13	20:35:26			L	off	BU	4	C35	
		81-T2-6.14	20:36:35			L	off	BU	4		Not useful
14	D7	81-T2-7.9	23:25:53	23:38:50		L	on	BU	4		Not useful

NOTES: 1. All tests conducted at ballast condition.
2. Measurements of ice thickness and salinity in vicinity of all locations of rams.

LEGEND: L = level ice, R = ridges, LK = level keel, BU = bow up makes it difficult to provide any direct assessment of the effect of bubbling on performance in level keel condition. On the otherhand in ridges the small data base of categories R2 and R4 makes the only credible evaluation that of the effect of bubblers with level keel.

An overview of the ramming Series A, B and C is provided in Tables 3.4, 3.5 and 3.6. The tables include, in addition to previously tabulated information, the category of the ram, more details on ice characteristics and the quality of the set of information available for each ram.

The ice characteristics were taken from [21]. Not all combinations of ram number and reported ice characteristics were found consistent through the various tables and plots. From a closer look at the available data, it was found that for ice thickness values, the data plots showing all rams consecutively seemed most reliable. When ice thickness measurement was available at the location of the ram, this value was marked M and marked MC when confirmation of this value was found elsewhere in the report. Estimated values marked E were obtained through interpolation from surrounding measurements. Other available ice characteristics and corresponding locations as reported in [21] are included in the tables and the assumed sets of ice properties are given for each series of rams. For Series A, the properties were taken from Site 6/2 which was about 3 km away from the Series A location since no measurements were carried out on location. The flexural strength was calculated from the brine volume, which was determined from temperature and salinity measurements.

3.4 Quality Assessment

Due to the many variables involved the quality assessment system was developed in such a way to account for all significant parameters to the ramming mode of operation. It should be indicated that while the quality numbers were not intended as means of exclusion of data points from the analysis, their primary function was to identify and quantify to some extent the limits of any given data set so that such data can be utilized with confidence to the fullest extent. The quality numbers can also serve to explain large scatter in data or the presence of outliers. Such events may not be possible to explain using the data base. For instance, a speed record containing a partly erroneous signal can result in miscalculation and, hence, misinterpretation of penetration (thus the average speed of advance) or the acceleration (thus the inertial component and the calculated resistance). Therefore, if the data analysis is conducted with the quality numbers in mind, a better understanding and interpretation of the entire data base can result.

Eventually, this system replaces the confidence intervals which are commonly used to define the possible range of validity of a measurement at a given confidence level. However, due to the complexity of the system of measurements and lack of qualitative data on repeatability and reliability of individual measurements, we have elected to follow the approach described herein.

TABLE 3.3

OVERVIEW OF CATEGORIES

CATEGORY	L1	L2	L3	L4	R1	R2	R3	R4
NO.OF RAMS	16	5	0	10	11		12	2
RAMS NO.	B1 B2 B3 B4 B5 B6 B7 B16 B17 B18 B19 B20 B21 B22 B23 B24	C7 C8 C9 C10		C6 C24 C25 C26 C27 C29 C30 C31 C34 C35	A13 A14 A15 A16 A17 B3 B8 B9 B10 B11 B12		A1 A2 A3 A4 A5 A6 A7 A8 A9 A10 A11 A12	C32 C33

TOTAL NO. OF RUNS IN DEDICATED TRIALS = 57

LEGEND OF CATEGORIES	ICE TYPE	TRIM	BUBBLER STATUS
L1	level ice	level keel	on
L2	level ice	bow up	on
L3	level ice	level keel	off
L4	level ice	bow up	off
R1	ridges	level keel	on
R2	ridges	bow up	on
R3	ridges	level keel	off
R4	ridges	bow up	off

TABLE 3.4 OVERVIEW SERIES A RAMS

RAM NO.	ICE TYPE	BUBBLER STATUS	TRIM	CATEGORY	ICE THICKNESS (m)	QUALITY	
						NO.	ID
A1	R	off	LK	R3	2.00 MC	80	AB2
A2	R	off	LK	R3	2.36 E	61	AD
A3	R	off	LK	R3	2.52 E	62	AD
A4	R	off	LK	R3	2.60 E	67	BD
A5	R	off	LK	R3	2.68 E	64	AD
A6	R	off	LK	R3	2.75 M	41	AC
A7	R	off	LK	R3	2.74 E	61	AD
A8	R	off	LK	R3	2.71 E	61	AD
A9	R	off	LK	R3	2.67 MC	21	AB
A10	R	off	LK	R3	2.64 E	63	AD
A11	R	off	LK	R3	2.61 E	62	AD
A12	R	off	LK	R3	2.56 E	67	BD
A13	R	on	LK	R1	2.52 E	71	BD
A14	R	on	LK	R1	2.49 E	68	BD
A15	R	on	LK	R1	2.45 E	67	BD
A16	R	on	LK	R1	2.40 MC	30	BB
A17	R	on	LK	R1	2.11 E	72	BD
A18	R	on	LK	R1	1.82 E	65	AD

TOTAL NO. OF RAMS 18

AVAILABLE ICE CHARACTERISTICS:

LOCATION	SITE 6/2	ASSUMED SERIES A
Ice Temperature (° C)	-2.7	-2.7
Salinity ($^0/_{00}$)	3.4	3.4
Brine Volume ($^0/_{00}$)	64	64
Cont. Compr. Strength (MPa)	6.2	6.2
Flexural Strength (kPa)	407	407

NOTES: a. Air Temperature 1°C from Ship Log
b. Calculated Flexural Strength

LEGEND: L = level ice
R = ridges
LK = level keel
BU = bow up
MC = measured and confirmed
M = measured
E = estimated from measurements

TABLE 3.5 OVERVIEW SERIES B RAMS

RAM NO.	ICE TYPE	BUBBLER STATUS	TRIM	CATEGORY	ICE THICKNESS (m)	QUALITY	
						NO.	ID
B1	L	on	LK	L1	1.51 MC	26	AB
B2	L	on	LK	L1	1.60 MC	30	BB
B3	L	on	LK	L1	2.00 MC	29	BB
B4	L	on	LK	L1	1.40 M	45	AC
B5	L	on	LK	L1	1.62 MC	28	BB
B6	L	on	LK	L1	1.66 MC	31	BB
B7	L	on	LK	L1	1.56 MC	31	BB
B8	R	on	LK	R1	1.67 M	47	BC
B9	R	on	LK	R1	4.90 M	48	BC
B10	R	on	LK	R1	1.67 M	87	BC1
B11	R	on	LK	R1	1.60 M	104	CC2
B12	R	on	LK	R1	1.56 M	104	CC3
B16	L	on	LK	L1	1.62 MC	57	BB1
B17	L	on	LK	L1	1.70 MC	15	BA
B18	L	on	LK	L1	1.55 E	54	BD
B19	L	on	LK	L1	1.40 MC	31	BB
B20	L	on	LK	L1	1.50 E	68	BD
B21	L	on	LK	L1	1.65 M	47	BC
B22	L	on	LK	L1	1.45 M	51	BC
B23	L	on	LK	L1	1.40 MC	32	BB
B24	L	on	LK	L1	1.48 MC	30	BB

TOTAL NO. OF RAMS 21

AVAILABLE ICE CHARACTERISTICS:

LOCATION	B8	B17	B18	ASSUMED SERIES B
Ice Temperature (°C)		-0.41	-0.41	-0.41
Salinity (°/oo)		2.15	2.46	2.31
Brine Volume (°/oo)		259	296	278
Conf. Compr. Strength (MPa)	6.7			6.7
Flexural Strength (kPa)		176	151	163

NOTES: a. Air Temperature 2°C from Ship Log.
b. Calculated Flexural Strength

LEGEND:
L = level ice
R = ridges
LK = level keel
BU = bow up
MC = measured and confirmed
M = measured
E = estimated from measurement

TABLE 3.6 OVERVIEW SERIES C RAMS

RAM NO.	ICE TYPE	BUBBLER STATUS	TRIM	CATEGORY	ICE THICKNESS (m)		QUALITY	
							NO.	ID
C6	L	off	BU	L4	1.56	MC	26	AB
C7	L	on	BU	L2	1.80	M	55	CC
C8	L	on	BU	L2	1.60	M	47	BC
C9	L	on	BU	L2	1.35	M	27	BB
C10	L	on	BU	L2	1.82	MC	24	AB
C18	R	on	BU	R2	1.68	M	76	AC1
C24	L	off	BU	L4	1.65	E	61	AD
C25	L	off	BU	L4	1.60	MC	21	AB
C26	L	off	BU	L4	1.65	MC	20	AB
C27	L	off	BU	L4	1.68	MC	53	AB1
C29	L	off	BU	L4	1.52	MC	26	AB
C30	L	off	BU	L4	1.68	MC	23	AB
C31	L	off	BU	L4	1.42	MC	23	AB
C32	R	off	BU	L4	1.75	M	32	BC
C33	R	off	BU	L4	1.84	MC	77	AB2
C34	L	off	BU	L4	1.65	MC	61	AB1
C35	L	off	BU	L4	1.50	MC	97	AB3

TOTAL NO. OF RAMS 17

AVAILABLE ICE CHARACTERISTICS:

LOCATION	C8	C32	ASSUMED SERIES C
Ice Temperature (°C)		-0.45	-0.45
Salinity (°/₀₀)		3.53	3.53
Brine Volume (°/₀₀)		388	388
Conf. Compr. Strength (MPa)	6.7	6.5	6.6
Flexural Strength (kPa)		104	104

NOTES; a. Air Temperature 4°C from Ship Log
b. Calculated Flexural Strength

LEGEND:
L = Level ice
R = ridges
LK = level keel
BU = bow up
MC = measured and confirmed
M = measured
E = estimated from measurement

The quality indicated for each ram consists of a set of number and letter identifications. The quality assessment was set up to identify the usefulness of analyzing and evaluating a set of data for a particular ram and assess the quantity and quality of the output to be expected in order to set priorities in the data processing.

A penalty-point system was used to classify each ram, which means a low number would indicate a high expectation in terms of combined quantity and quality. The letter identification firstly indicates the quality level of the data on tape, and secondly the quality of the set of ice characteristics, where A represents high quality. Thirdly a figure, if present, indicates the level of tape data incompleteness, which will result in less output from analysis of the data. A more detailed description of the quality assessment is given in Appendix B.

The quality of the ice characteristics basically relates to the availability of ice thickness and other properties which become relevant when evaluating ramming performance. The quality of the data on tape is almost completely governed by the quality of the speed recording and by the completeness of recording a ram cycle. The reason for this is that in the procedure of data analysis the speed signal is crucial, having no other sources for validation. The doppler-log speed measurements frequently show strongly fluctuating readings, possibly caused by passing ice floes or ship motions, which will cause inaccuracies and difficulties in the analysis.

The other channels of information that will be used in the analysis produced reliable output and did not require any qualitative evaluation. The shaft speed signal can only be reviewed when processing of this signal has been carried out in conjunction with the overall analysis of the data. The propeller pitch signal is good, however, there was some doubt about the absolute level when the signal was expressed in engineering units. It seemed that the design pitch was not being reached.

In general the quality of the data of the dedicated trials performed in Admiralty Inlet was good except for the speed log. From preliminary evaluations of the remaining data, trials at Lake Melville were of lower quality, and the results from voyage monitoring appeared to be good with some limitation on their usefulness due to the lack of properly measured and defined ice conditions. Their quality ranking will be in second place following dedicated trials.

4. DATA REDUCTION PROCEDURES

4. DATA REDUCTION PROCEDURES

4.1 Data Reduction/Instrumentation

Following the first stage of data scanning and graphical display, the instrumentation system was redesigned for data reduction and analysis. Figure 4.1 provides a description of system components:

- Perkin-Elmer Tape Drive
- Apple II Plus Computer with disc drive
- HP9816 microcomputer with two built-in disc drives
- Epson printer
- HP7470A graphics plotter

The Apple 6065 microprocessor was used to control the tape drive and transfer selected segments of the tape to the HP9816 which is a more capable and user friendly machine. The HP9816 received the data and processed the information according to the procedures outlined in the following sections of this chapter.

The instrumentation system used Assembly language to communicate between the tape drive and the HP9816 computer while the latter was programmed in Basic. Once the data was transferred to the HP computer it was stored on micro discs for fast retrieval and processing. It should be noted that the data transfer was the weakest link in the chain in terms of speed and efficiency. For this reason the transfer function was separated from the actual data analysis phase.

The system was designed for interactive use and direct production of report-quality drafts.

FIGURE 4.1

DATA REDUCTION and ANALYSIS INSTRUMENTATION

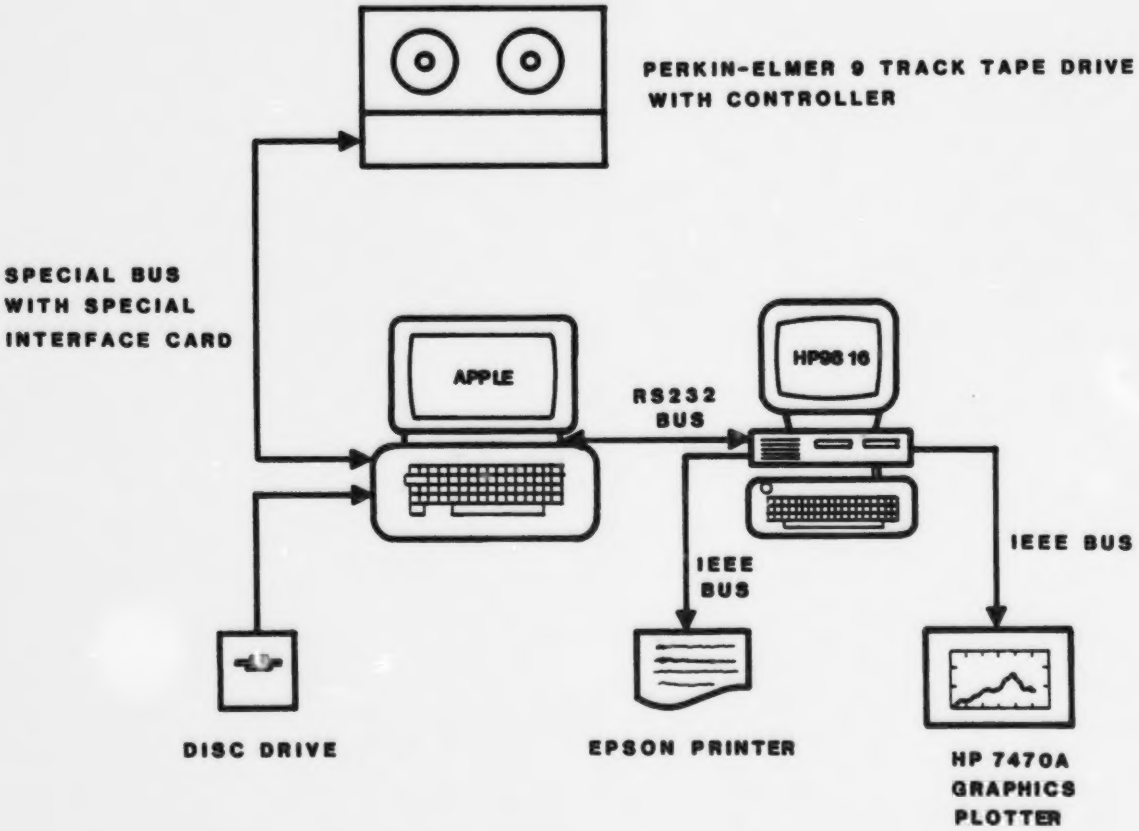
PERKIN-ELMER 9 TRACK TAPE DRIVE WITH CONTROLLER
SPECIAL BUS WITH SPECIAL INTERFACE CARD
APPLE
RS232 BUS
HP98 16
IEEE BUS
IEEE BUS
DISC DRIVE
EPSON PRINTER
HP 7470A GRAPHICS PLOTTER

4.2 General Procedures

Using the work charts obtained from the data scanning task, it was possible to examine each ram for further analysis. A complete ram such as that shown in Figure 4.2 for Ram No. C-6, was easy to define with all functions, e.g. backing, acceleration, penetration and extraction. It was necessary to examine the records of propeller pitch response and thrust in conjunction with the ship speed for validation and confirmation. Some discrepancies could occur because of the sense of the speed which was always positive during all stages of the ramming cycle.

This particular ram will be used as a demonstration case throughout this report. It has a relatively low quality number (26AB) which indicates a good overall record, an excellent tape quality relative to other available data and the highest available quality of ice characteristics. No data was missing from the records nor was there any file mark or header interruptions during the ram.

For each ram, once defined on the charts, a sufficiently long time span which covered the entire cycle was defined. The cycle by definition starts on the beginning of the backing stage and ends at the moment of start of the following cycle. This definition is the best possible one since it accommodates any time losses due to extraction or wedging at the end of the ram which causes such loss of time. Other definitions which include the time loss due to the previous ram have been used by others and can usually result in error when the impact speed varies from ram to ram. Each block of data was then transferred from tape to the processing computer where immediate conversion to engineering units was performed and the data reduced to average values calculated over one second time intervals. Smaller time intervals were not necessary since the ship speed was recorded at a rate of 1 Hz. The averaging of all other recorded parameters was reasonably justified due to the absence of sharp changes in the recorded data. This procedure allowed us to display a complete ramming cycle on the CRT screen and for an average cycle time of 500 seconds a total of 500 data points per channel was reasonable from the data storage capacity point of view.

Figure 4.2 shows the channels that were initially required for identification of ramming incidents. The ship speed, being the most important data signal, reflects the behaviour of the ship during the ram. The event marker was used to assist in identifying the ram and its phases where the speed information was not conclusive. In combination with the thrust, backing and acceleration during the ram could be identified. The propeller pitch response indicates the action directed from the bridge of the ship. With the combination of speed, thrust and pitch it was possible to determine the effective thrust developed by the propeller/nozzle/hull configuration as detailed in Section 4.3.2. The shaft torque in combination with the shaft speed that was added on to the data for the detailed computer analysis, provided the shaft power. Finally the fuel rack settings as recorded were included in the data analysis for the purpose of calculating the fuel consumption.

FIGURE 4.2

CHART RECORDER PLOT RAM NO. C6

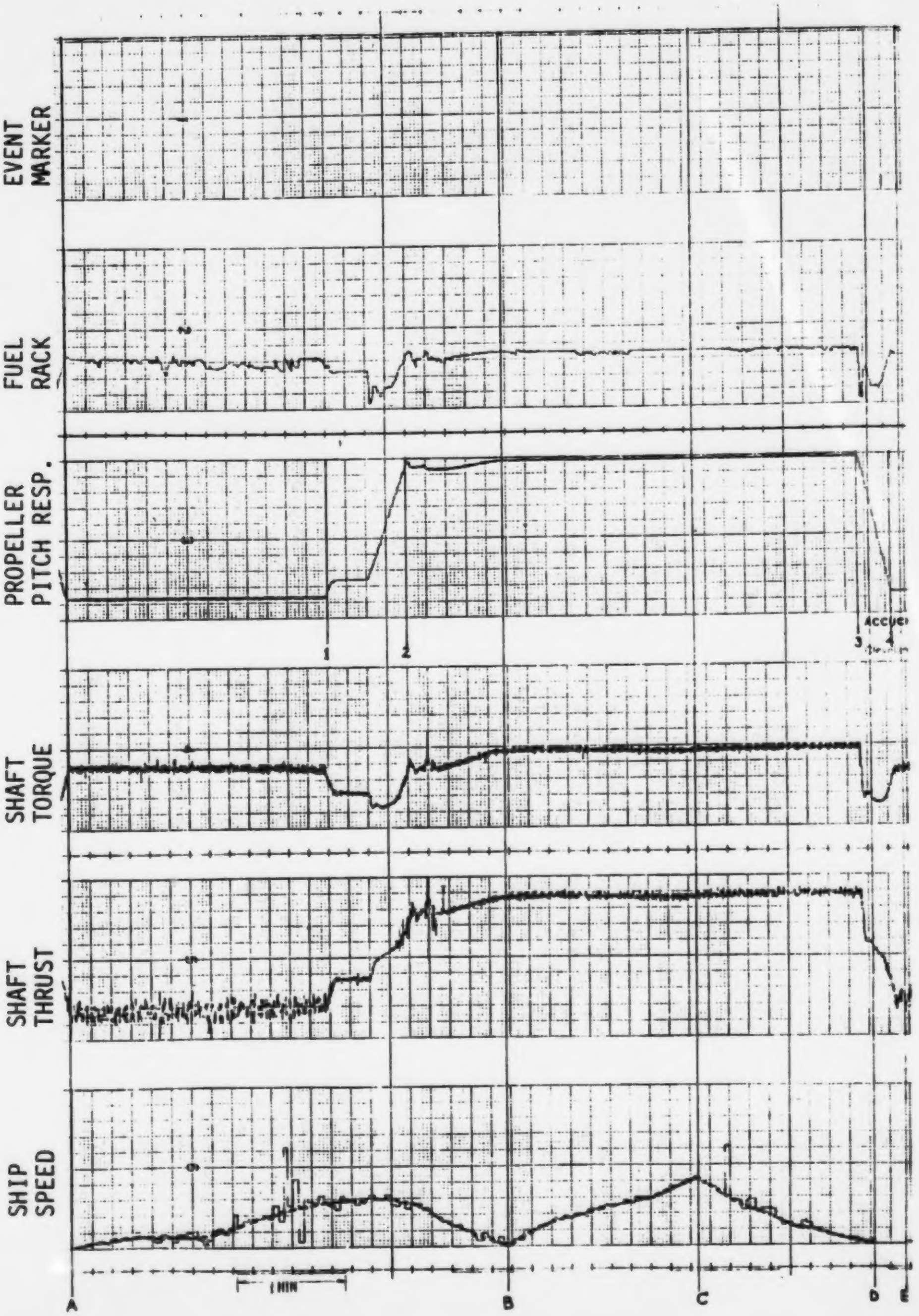

The conversion equations used in data reduction for the selected channels which have been scanned were taken in accordance with Attachment 4 of the minutes of the progress meeting held on November 18, 1983. These conversion equations are given in Table 4.1. During the data analysis it was noted that the fuel consumption rates determined from the fuel rack data indicated rather low values as demonstrated in Section 5.2. Therefore the data conversion for fuel rate was only carried out to obtain the fuel rack setting in mm.

Once the data was transferred, averaged, converted and stored on micro-disc it was easily accessible at any time. The analyst would conduct the analysis interactively for any ram he selects, and at the end of each run he would have a complete set of graphs and a table summarizing the data and analysis. The following standard types of analysis were conducted for each ram:

- Time cycle analysis, to determine the length of time and proportions of cycle components. The penetration distance was also calculated for each stage of the ramming cycle.
- Propulsion force and resistance profiles were calculated for each ram using the unsteady motion formulations and accounting for inertial effects. The effective thrust was also calculated on the basis of experimental data.
- Fuel consumption in terms of fuel rate and total consumption during each ram.

The above sequence presents the general procedures used to reduce and analyze the data. Before we present the results, it is worthwhile to discuss the underlying assumptions and methods developed to produce these results.

TABLE 4.1

CONVERSION EQUATIONS FOR 1981 TRIALS AND VOYAGES

PARAMETERS	UNIT	CHANNEL	1981
Shaft Thrust	kN	198	2.29N -1177.2
Fuel Rack	%	199	0.2201N-9.97
Propeller Pitch (Response)	deg.	201	0.037N-15
Propeller Pitch O.D.B. Diff. Press.	MPa	203	0.0009766N
Shaft Torque	kN.m	208	1.803N-185
Shaft RPM	rpm	211 (1)	61440/[N+18.4]
Surge (AFT) Sway (AFT)	$m.s.^2$	212	0.048N-24.5
Ship's Speed	knot	236	0.0293N
Engine RPM	rpm	241	-
Propeller Pitch (Command)	units	244	0.01953N-10

(1) For Lake Melville Trials the Conversion Equation is:
1203.6 / [0.01963 N + 0.09]

4.3 Data Reduction Algorithms

4.3.1 Ramming Cycle Analysis

A part of the data reduction procedure was the determination of the ramming cycle components. From a review of the available ramming incidents it was concluded that the development of an algorithm that would scan and interpret the data properly was not considered time nor cost effective. Due to the irregular patterns in the ship operation commands (pitch) and due to the accuracy and quality of the response (the speed recorded from the doppler-log) with its unpredictable eruptions caused by external disturbances, the cycle components could be defined best by means of human interaction.

The user would set the breakpoints in the ramming cycle to distinguish the various components. A ramming incident is composed of two cycles in one: the action cycle, being the ship operation command which is reflected in the pitch signal and the response cycle, which is given by the course of the speed obtained from the doppler-log. By definition the ramming cycle starts with backing at zero speed and ends when extraction appears successful, before the backing of the next ramming cycle starts and also at zero speed. In other words, the total ramming cycle is determined by the start of subsequent backing periods. The action cycle, the pitch response of the operation commands, is considered only for the duration of the response cycle. Any action not within the time frame determined by the response cycle is not considered part of the ramming incident. Figure 4.3 shows the principle of the cycles and the breakpoints that define the various components in the ramming cycle. The pitch and speed used in setting the breakpoints result from the preprocessing of the original data for the purposes of graphical representation and analysis. The speed profile shown will be the result of the curve fitting to be discussed later in this section.

The response cycle is divided into the following components:

- backing	(A - B)
- acceleration	(B - C)
- penetration	(C - D)
- extraction	(D - E)

The action cycle consists of:

- astern pitch during backing (A - 1)
- pitch reversal from astern pitch to ahead pitch during backing (1 - 2)
- ahead pitch during backing while stopping followed by acceleration ahead into the penetration stage (2 - 3)
- pitch reversal from ahead pitch to astern pitch after impact into the extraction (3 - 4)
- astern pitch during extraction till the end of the cycle (4 - E)

FIGURE 4.3

IDEALIZED RAMMING CYCLE AND COMPONENTS

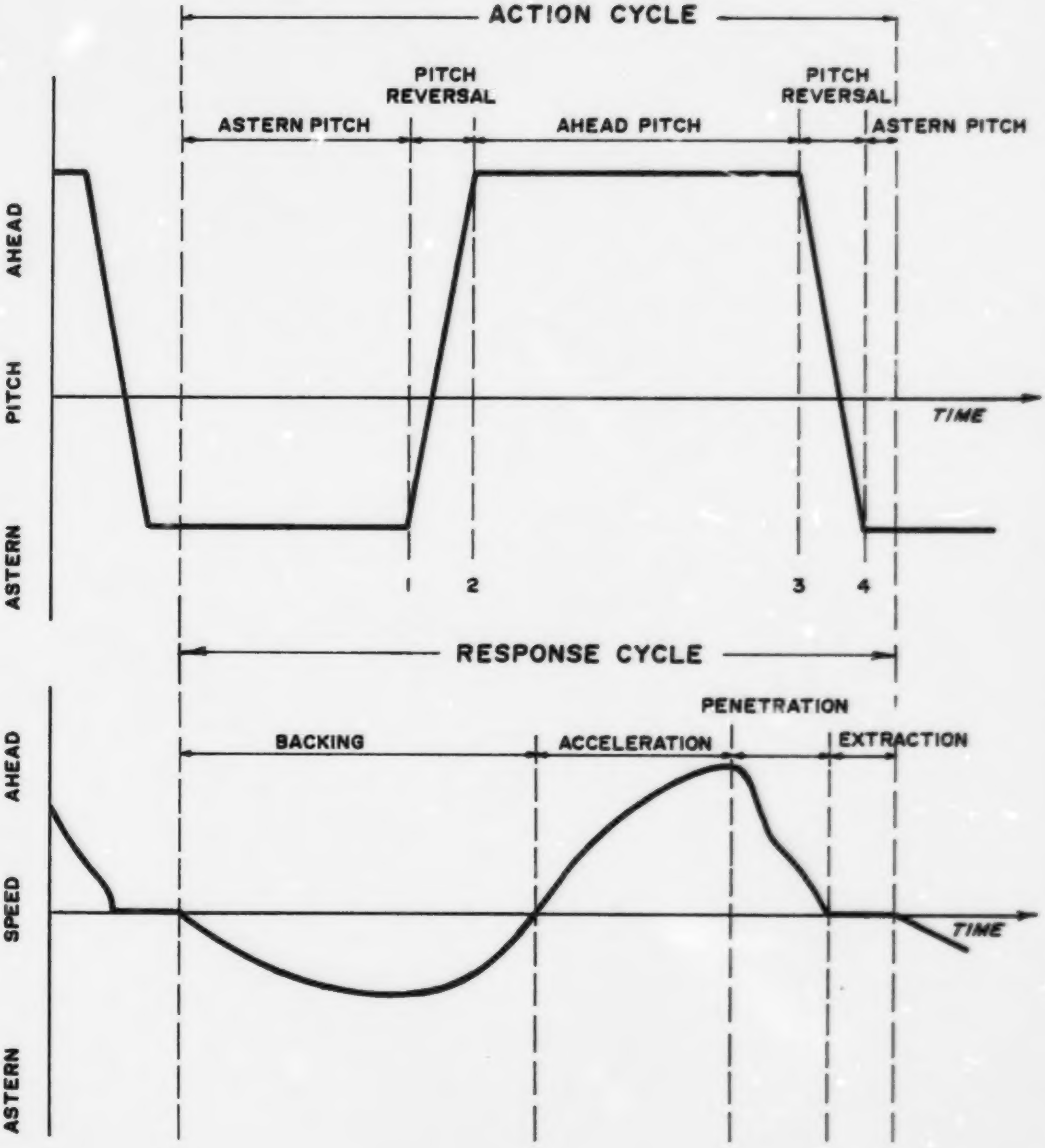
ACTION CYCLE
PITCH REVERSAL
PITCH REVERSAL
ASTERN PITCH
AHEAD PITCH
ASTERN PITCH
AHEAD
PITCH
ASTERN
TIME
1
2
3
4
RESPONSE CYCLE
PENETRATION
BACKING
ACCELERATION
EXTRACTION
AHEAD
SPEED
ASTERN
TIME
A
B
C
D
E

The software written for the analysis sorts the various breakpoints in chronological order required for continuation of the analysis and allows the user to define invalid portions of the speed data. Often there are large excursions or erroneous shifts in the speed log which, if left uncorrected, would adversely affect the analysis and interpretation of data. Most ramming incidents have the principal configuration as shown in Figure 4.3. However, the doppler speed log is unidirectional and, hence, reversal of the backing portion is necessary to correct the shape of the speed record.

Due to the nature of the response cycle curve fitting was necessary to smooth out the erroneous excursions of speed. A seventh degree polynomial was used to describe the speed record during backing and acceleration stages (A to C) and a fourth degree polynomial expression was used to describe the penetration stage (C to D). The selection of the degrees of the polynomial was done by examination and comparison to the original data to select the most appropriate expressions.

The various characteristics of the ramming cycle were mostly straight forward calculations and statistics. The ship's progress in terms of distance was obtained from integration of the fitted speed curves versus elapsed time for the three applicable stages, backing, acceleration and penetration.

Table 4.2 lists the cycle time components which were evaluated directly from both the action and response cycles.

It should be noted that the sum of durations of the action cycle is not necessarily equal to the total cycle time. Also in situations where extended delay at the end of a cycle was not due to extraction, the last component of the cycle time would be meaningless. In some cases, a long pause would follow a ram where no thrust or very little thrust would be exerted on the ship. While no reason may be obtained from data tapes, it is reasonable to suggest operational considerations, course review or others. In such cases, the extraction component could be ignored, and averaged over a block of rams. Fortunately, this was not the case during dedicated trials, and hence, no special attention was given during the reduction and analysis of the core database.

TABLE 4.2

CYCLE TIME COMPONENTS

CYCLE	COMPONENT	DURATION	COMMENTS
Response	Backing Time	A-B	(Also calculate percentage of various components of response cycle to the total cycle time).
	Acceleration Time	B-C	
	Penetration Time	C-D	
	Extraction Time	D-E	
	Total Cycle Time	A-E	By definition = T_c
Action	Astern mode	A-1	Less than backing time
	Reversal to ahead	1-2	
	Ahead mode	2-3	greater than acceleration time
	Reversal to astern	3-4	

It may be advantageous at this point to give a brief description of the data reduction program structure. It is basically structured into 5 program segments as illustrated in Figure 4.4. The first program segment allows a specific ram to be chosen for further analysis. Any ram specific housekeeping information may also be input in this section. This information consists of: ram category, data quality assessment, ship trim, bubbler status, ice thickness and ice strength.

The second program segment allows the user to identify various events (breakpoints) within the ramming cycle as defined earlier in this section. These breakpoints determine the type of processing which is applied to the data (particularly speed) and set intervals for output of results. They also serve to define the various portions of the ramming cycle. It also allows the user to define invalid portions of the speed data.

The third program segment performs a number of operations dealing with the breakpoints that have been set, all of which are associated with ship speed as described in Figure 4.4.

The fourth program segment creates additional data files associated with resistance and propulsion. Effective thrust throughout the ram is calculated as a function of corrected speed, measured pitch and measured thrust. Resistance is calculated as a function of ship mass, added mass, calculated acceleration, and effective thrust. Power is calculated as a function of shaft torque and RPM. The created data files are stored for use in the output segment.

The final segment generates report quality output of one summary page and five graph pages. The contents of the graph pages are detailed in Table 4.3. All data files are plotted as a function of time on three graph pages. A fourth graph plots corrected speed and resistance as functions of distance travelled, and the fifth graph page illustrates the relationship between resistance and speed. For the fourth and fifth plotted pages, rather than drawing a line between data points, each data point is represented as a dot on the plot. Dots are spaced by one-second intervals. This technique was used to better illustrate the relationship between two sets of data and results in a continuous line for closely spaced data pairs to a widely spaced dotted line when data pairs change at a faster rate with time. A printed summary of the results for the particular ram is then output, and the results are also stored for any further analysis.

The data reduction program was written in BASIC on an HP9816 microcomputer and was operated interactively. The interactive operation was menu driven which permitted the user to conduct the analysis in a flexible manner.

FIGURE 4.4 DATA REDUCTION PROGRAM SEGMENTS

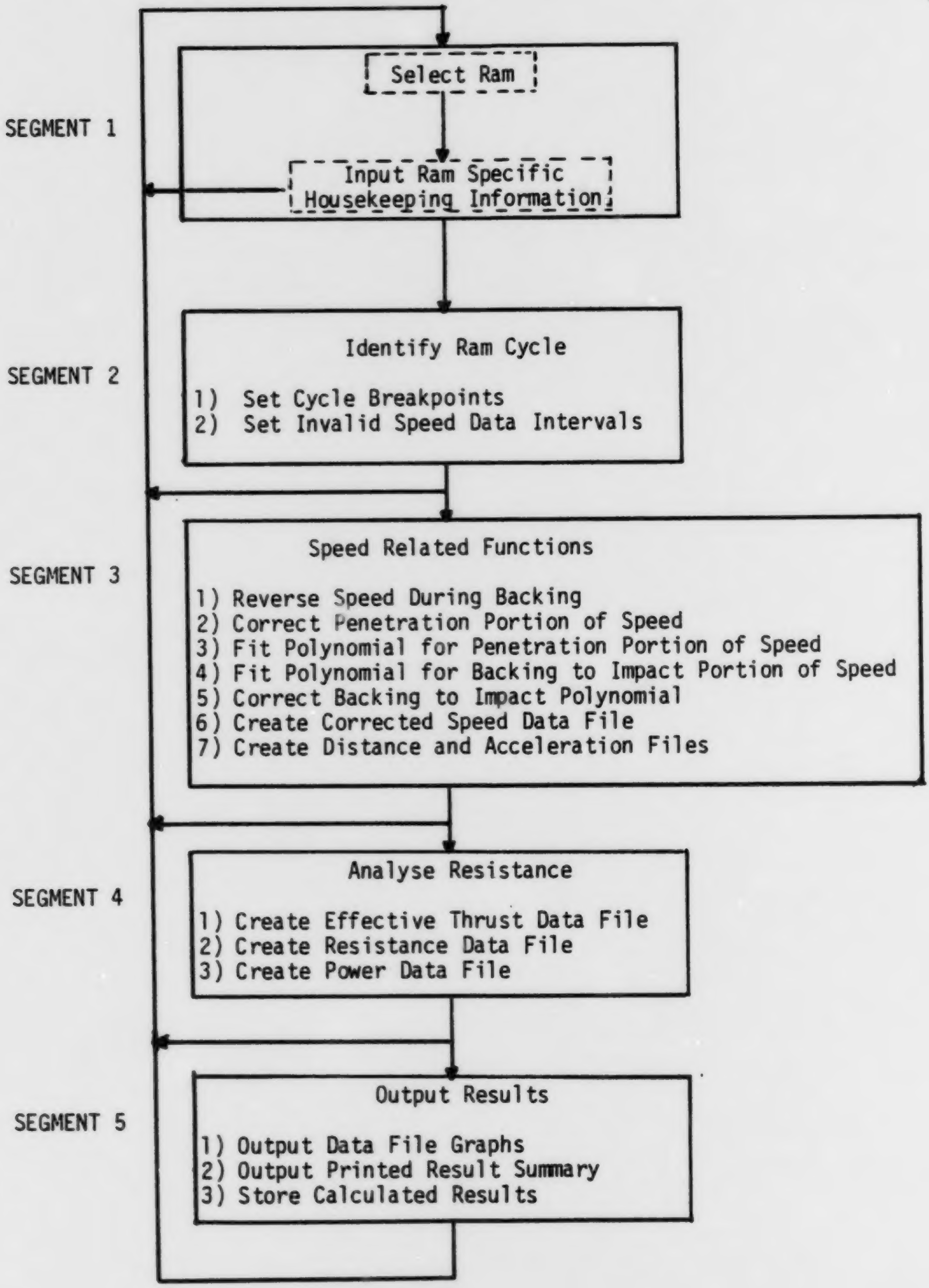

SEGMENT 1
Select Ram
Input Ram Specific Housekeeping Information
SEGMENT 2
Identify Ram Cycle
1) Set Cycle Breakpoints
2) Set Invalid Speed Data Intervals
SEGMENT 3
Speed Related Functions
1) Reverse Speed During Backing
2) Correct Penetration Portion of Speed
3) Fit Polynomial for Penetration Portion of Speed
4) Fit Polynomial for Backing to Impact Portion of Speed
5) Correct Backing to Impact Polynomial
6) Create Corrected Speed Data File
7) Create Distance and Acceleration Files
SEGMENT 4
Analyse Resistance
1) Create Effective Thrust Data File
2) Create Resistance Data File
3) Create Power Data File
SEGMENT 5
Output Results
1) Output Data File Graphs
2) Output Printed Result Summary
3) Store Calculated Results

The fourth program segment creates additional data files associated with resistance and propulsion. Effective thrust throughout the ram is calculated as a function of corrected speed, measured pitch and measured thrust. Resistance is calculated as a function of ship mass, added mass, calculated acceleration, and effective thrust. Power is calculated as a function of shaft torque and RPM. The created data files are stored for use in the output segment.

The final segment generates report quality output of one summary page and five graph pages. The contents of the graph pages are detailed in Table 4.3. All data files are plotted as a function of time on three graph pages. A fourth graph shows corrected speed and resistance as functions of distance travelled, and the fifth graph page illustrates the relationship between resistance and speed. For the fourth and fifth plotted pages, rather than drawing a line between data points, each data point is represented as a dot on the plot. Dots are spaced by one-second intervals. This technique was used to better illustrate the relationship between two sets of data and results in a continuous line for closely spaced data pairs to a widely spaced dotted line when data pairs change at a faster rate with time. A printed summary of the results for the particular ram is then output, and the results are also stored for any further analysis.

TABLE 4.3

A LIST OF GRAPHICAL ILLUSTRATIONS FOR EACH RAM

A. FIGURE 1 - PERFORMANCE AND PROPULSION PLOTS:

1. Power vs. time
2. Fuel consumption vs. time
3. Shaft torque vs. time
4. Propeller pitch vs. time
5. Shaft RPM vs. time

B. FIGURE 2 - MOTION CHARACTERISTICS

1. Ship speed vs. time (including original and corrected records)
2. Distance vs. time
3. Acceleration vs. time

C. FIGURE 3 - TIME SERIES PLOTS:

1. Ship speed vs. time
2. Ship acceleration vs. time
3. Shaft thrust vs. time
4. Total (effective) thrust vs. time
5. Total resistance vs. time

D. FIGURE 4 - SPATIAL PLOTS:

1. Ship speed vs. penetration (distance)
2. Total resistance vs. penetration

E. FIGURE 5 - RESISTANCE VS. VELOCITY:

1. In broken channel astern (backing)
2. In broken channel ahead (acceleration)
3. In level ice ahead (penetration)

4.3.2 Thrust and Resistance Analysis

During the entire ramming cycle the sum of all forces acting on the ship in longitudinal direction, $X(v)$, can be expressed by:

$$X(v) = T(v) - R(v) \qquad (4.1)$$

where T = total effective thrust force
R = total resistance force

Figure 4.5 illustrates the direction of $X(v)$ during various stages of the ramming cycle.

The total resistance force can be written as:

$$R = R_{Water} + R_{Ice} + R_{Wind} + R_{Motions} \qquad (4.2)$$

This resistance is further referred to as the total resistance in ice or broken channel, including the effect of water resistance. The wind resistance and the added resistance due to ship motions are not considered in detail but their effects are included in the measured data, so they will also form part of the resistance obtained from the analysis.

It is recognized that the wind in particular may exert additional forces which may add or subtract from the total resistance in ice. The wind loads are dependent on the relative wind speed, direction and the shape factors of the ship freeboard and superstructure. Due to the relatively lower speeds and greater forces associated with ramming operation, and the inaccuracies associated with speed measurement, it was felt that inclusion of wind loads from the total measured resistance of the ship is of secondary importance and may be dealt with at a later stage. However, it is conceivable that the wind forces would place their effect within the band of experimental scatter[1] and hence render a more detailed account undesirable at this time.

The net external force is also equal to the inertia force, I, given by:

$$I = (M + M_A)\, a \qquad (4.3)$$

where I = inertia force
M = ship mass
M_A = added mass of entrained water
a = acceleration

---

[1] For the CCGS LOUIS S.ST.LAURENT moving at 8 kts in ice covered water we estimated the wind resistance to be:
+0.21 MN, for 30 kts head wind, - 0.08 MN, for 30 kts tail wind (assistance) and + 0.07 MN, for 30 kts cross wind.

FIGURE 4.5

VARIATION OF NET EXTERNAL FORCE
DURING VARIOUS STAGES OF RAMMING CYCLE

A → 1
Backing
Thrust Astern

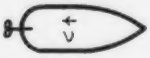

$X(v)$
$R(v) \rightarrow \quad \leftarrow T(v)$

$T(v) > R(v)$
$X(v) = T(v) - R(v) < 0$
$v < 0$

1 → 2
Backing
During Thrust
Reversal

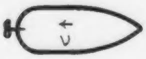

$X(v) \leftrightarrow$

$X(v)$: varies from < 0
to > 0
$v < 0$

2 → B
Backing
Thrust Ahead

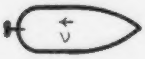

$X(v) \rightarrow$
$T(v) \rightarrow \quad \leftarrow R(v)$

$T(v) > R(v)$
$X(v) = T(v) - R(v) > 0$
$v < 0$

B → C
Acceleration
Thrust Ahead

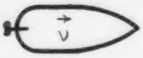

$X(v) \rightarrow$
$T(v) \rightarrow \quad \leftarrow R(v)$

$T(v) > R(v)$
$X(v) = T(v) - R(v) > 0$
$v > 0$

C → D .
Penetration
Thrust Ahead

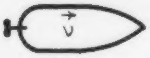

$X(v) \leftarrow$
$T(v) \rightarrow \quad \leftarrow R(v)$

$R(v) > T(v)$
$X(v) = T(v) - R(v) < 0$
$v > 0$

C → D
Penetration
Thrust
Cut off

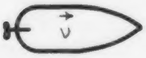

$X(v) \leftarrow$
$T(v) = 0 \leftarrow R(v)$

$X(v) = -R(v) < 0$
$v > 0$

The added mass is estimated at 5% of the ship's mass on the basis of values obtained for other ships (e.g. LOUIS ST. LAURENT 6%). The ship displacement is 38,250 tonnes for operations at deep draft. All forces are assumed positive in the case of forward velocity and acceleration. The total resistance during the ram cycle may now be determined from:

$$R = T - (M + M_A)a \qquad (4.4)$$

The acceleration "a" can be obtained from differentiation of the curve fitted speed data at any moment during the ramming cycle. After determination of the total effective thrust for the momentary propulsion characteristics, the resistance can be calculated at one second time intervals throughout the ramming cycle.

The total effective thrust force is the net force on the ship that is developed by the propulsor, including effects of nozzle thrust augmentation and hull interaction. The effective thrust may be given by:

$$T = (T_P + T_A)(1 - t) \qquad (4.5)$$

where T = total effective thrust force

T_P = measured propeller thrust

T_A = thrust augmentation by the nozzle

t = thrust deduction factor

The thrust measured and recorded during the trials only represents the thrust developed by the propeller, T_P. The propeller arrangement of the MV ARCTIC includes a nozzle or duct around the propeller. The effects of the nozzle and the interaction of propeller and nozzle with the hull have to be included in the estimation of the effective thrust that must be known in order to determine ship resistance. Because of these effects the effective thrust can be considerably different from the measured propeller thrust, and unreliable resistance estimations could be made if these effects are not sufficiently examined.

It was therefore considered important to this study to investigate the hydrodynamic propulsion characteristics in more detail, however, only to the extent required for the analysis of the data from a view point of ramming performance evaluation. A thorough evaluation of the hydrodynamic performance of the propulsor is beyond the scope of the present work, so a limited and practical evaluation was desirable.

In consultation with TDC it was decided to search for supporting information from other work carried out in connection with the MV ARCTIC. In connection with the continuous mode of operation of the MV ARCTIC it was indicated [22] that good correlation between the hydrodynamic propulsion characteristics at full scale in ice and results obtained from propulsion and overload model experiments in water conducted at NRC [23] exists. It was therefore decided to use these experimental results in this study for the determination of resistance in ice.

A series of diagrams prepared by Coldstream Inc. [22] on the basis of the NRC test results were made available for the purpose of this study. The diagrams showed the relationship between the usual propeller torque and thrust coefficients, the duct-thrust coefficient and the tow force coefficient versus propeller pitch angle (from 16.5 degrees to 22.5 degrees) for ship speeds of 0, 2, 4 and 6 knots. The use of these diagrams in this study for computation of the resistance would require the following input data:

- ship speed
- shaft speed
- propeller pitch
- propeller thrust

The tow force obtained from the diagrams still needed the addition of the open water resistance to determine the total effective thrust.

Although this procedure may give a reasonable approximation of the effective thrust, a closer examination of the results in the NRC report showed variation of characteristics depending on the thrust level, which would not be covered by the above mentioned diagrams.

A more direct approach was used to simplify the procedure and to obtain higher accuracy in the approximation of the effective thrust using the results of the overload experiments. The effective thrust was calculated for the various ship speeds, power levels and propeller pitch settings given in the NRC report and plotted against propeller thrust. Ship speed was varied from 0 to 6 knots and propeller pitch from 16.5 to 22.5 degrees over a range of power levels from 2500 kW to 15000 kW. In the astern mode only the bollard condition at a propeller pitch of -16.5 degrees was available.

A set of equations was derived that fit the data very well, as shown in Figure 4.6, for a number of data points. Therefore the effective thrust was expressed by the linear equations given as follows:

$$T_{eff} = -20V + T_p \times \tan(55.4 - 0.65V + 0.25P) \text{ for } T_p > 0 \qquad (4.6)$$

and

$$T_{eff} = -20V + T_p \times \tan(25.4 + 0.40V - 0.25P) \text{ for } T_p < 0 \qquad (4.7)$$

where T_{eff} = total effective thrust (kN)
T_p = propeller thrust (kN)
V = ship speed (kt)
P = propeller pitch (deg)

From the above equations it can be seen that the shaft speed has been eliminated because of the direct approach of selecting the effective thrust as a function of thrust speed and pitch. It can also be seen that the effective thrust calculated with the equations shows little sensitivity to changes in propeller pitch. A change of 4 degrees in pitch results in only 5 percent change in thrust. Therefore the pitch accuracy becomes of secondary importance. Furthermore the propeller/ship interaction factors (wake fraction and thrust deduction) were already included in the effective thrust calculated with the equations and did not need to be determined separately for each propulsion condition.

Although these equations are unusual for the description of propulsion characteristics, they are simple and practical for the purposes of this study. The ship speed observed in the ramming data varies from approximately 4 knots astern to 6 knots ahead, which means that extrapolation will be necessary, especially in the astern mode. Also the range of propeller pitch covered by the model test data in the NRC report is not sufficient to avoid extrapolation. From examination of nozzle/propeller characteristics available from literature it is felt that the above equations give a realistic estimate of the effective thrust calculated on the basis of the available information.

FIGURE 4.6

COMPARISON OF EFFECTIVE THRUST CALCULATED FROM MODEL TEST DATA AND EQUATIONS DEVELOPED

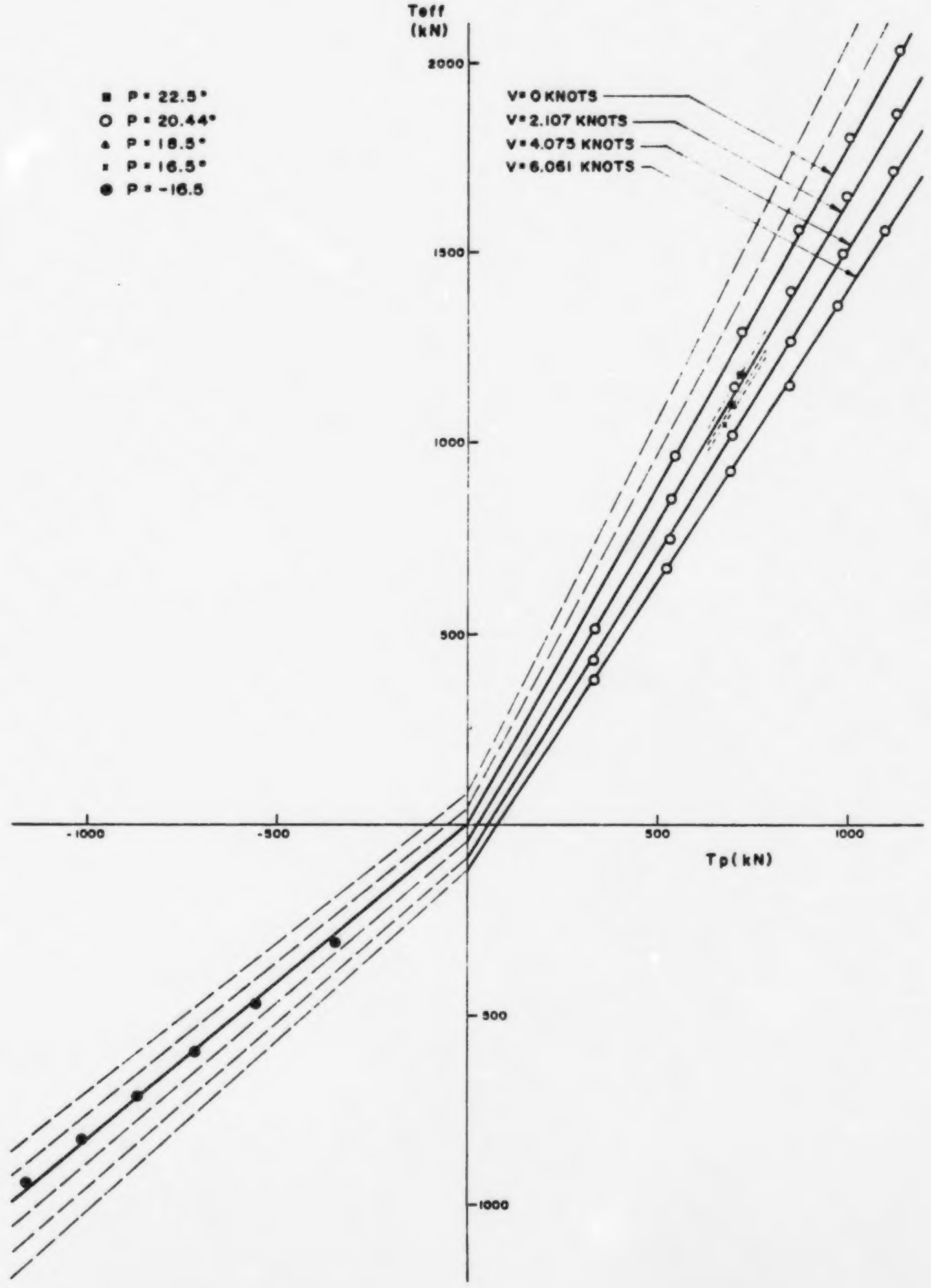

The results of calculating the effective thrust using equation 4.6 for a number of cases have been compared with the results of calculations using the diagrams prepared by Coldstream Maritime Inc. These diagrams show various propeller coefficients versus propeller pitch for ship speeds 0, 2, 4 and 6 knots.

Using the diagrams the pull force was calculated by:

$$\text{Pull Force} = \text{Shaft Thrust} \times \frac{K_F}{K_{TP}} \qquad (4.8)$$

where K_F and K_{TP} were read from the diagrams for the given speed and pitch. The effective thrust was then calculated by adding the open water resistance, given in the NRC Model Test Report, to the pull force. The results are compiled in Table 4.4.

The comparison clearly shows that in the low speed range the agreement between thrust obtained by both methods is good. As the speed increases there appears to be a trend of deviation which depends on the speed, pitch and shaft thrust. The differences may be attributed to several reasons including the level of detail of the methodology.

TABLE 4.4

COMPARISON OF EFFECTIVE THRUST CALCULATION METHODS

SPEED (Kts)	PITCH (deg)	SHAFT THRUST (kN)	COLDSTREAM MARITIME INC. DIAGRAMS					ARCTEC FORMULATION	THRUST RATIO
			K_{TP}	K_F	PULL FORCE (kN)	OPEN WATER RESISTANCE (kN)	EFFECTIVE THRUST (kN)	EFFECTIVE THRUST (kN)	COLD STREAM METHOD ARCTEC METHOD
0	16.5	200	0.143	0.247	345	0	345	340	1.015
		400			691		691	680	1.016
		600			1036		1036	1020	1.016
	20.44	400	0.206	0.365	709		709	707	1.002
		600			1063		1063	1061	1.002
		800			1417		1417	1415	1.001
4	16.5	400	0.133	0.164	493	47	540	534	1.011
		600			740		787	841	0.936
	20.44	400	0.192	0.272	567		614	558	1.100
		600			850		897	877	1.023
		800			1133		1180	1196	0.987
6	16.5	400	0.126	0.116	368	86	454	465	0.976
		600			552		638	757	0.843
	20.44	400	0.186	0.227	488		574	487	1.179
		600			732		818	790	1.035
		800			976		1062	1094	0.971

The resistance can be calculated following the foregoing procedures after the total effective thrust and the inertia force have been determined. Figure 4.7 illustrates the results of manual calculations. As can be seen from the figure, the resistance in the acceleration and backing stage shows an unrealistic characteristic.

For instance, during the backing and while the MV ARCTIC is moving at an indicated speed of 3 knots, the total resistance is a positive 900 kn, i.e. the ship is being assisted by the ice. (It was noted that the astern acceleration limit was exceeded). Similarly during acceleration the total calculated resistance at both ends of the acceleration stage show reversed values rather than values consistent with the physical behaviour of the ship. This is mainly caused by the profile of the accelerations, obtained from the speed profile. The limits of possible ship accelerations are calculated from the effective thrust and ship mass. These limits are plotted in the figure. Considering this observation and others, the only conclusion that could be made was that the measured speeds were not accurate and that their indicated values were higher than the actual values particularly at lower ship speeds. This reflects very strongly on the calculated total resistance which appears to be incorrect in some parts of the cycle.

There were no means available to us to determine what kind of correction should be applied on the basis of experimental calibration. This was not done in connection with Admiralty Inlet trials or at fixed intervals during the Arctic voyages. As a result we had to explore other possible means of corroborating and correcting the speed signals as recorded on tape. This subject will be discussed in the following section.

FIGURE 4.7

DETERMINATION OF RESISTANCE PROFILES

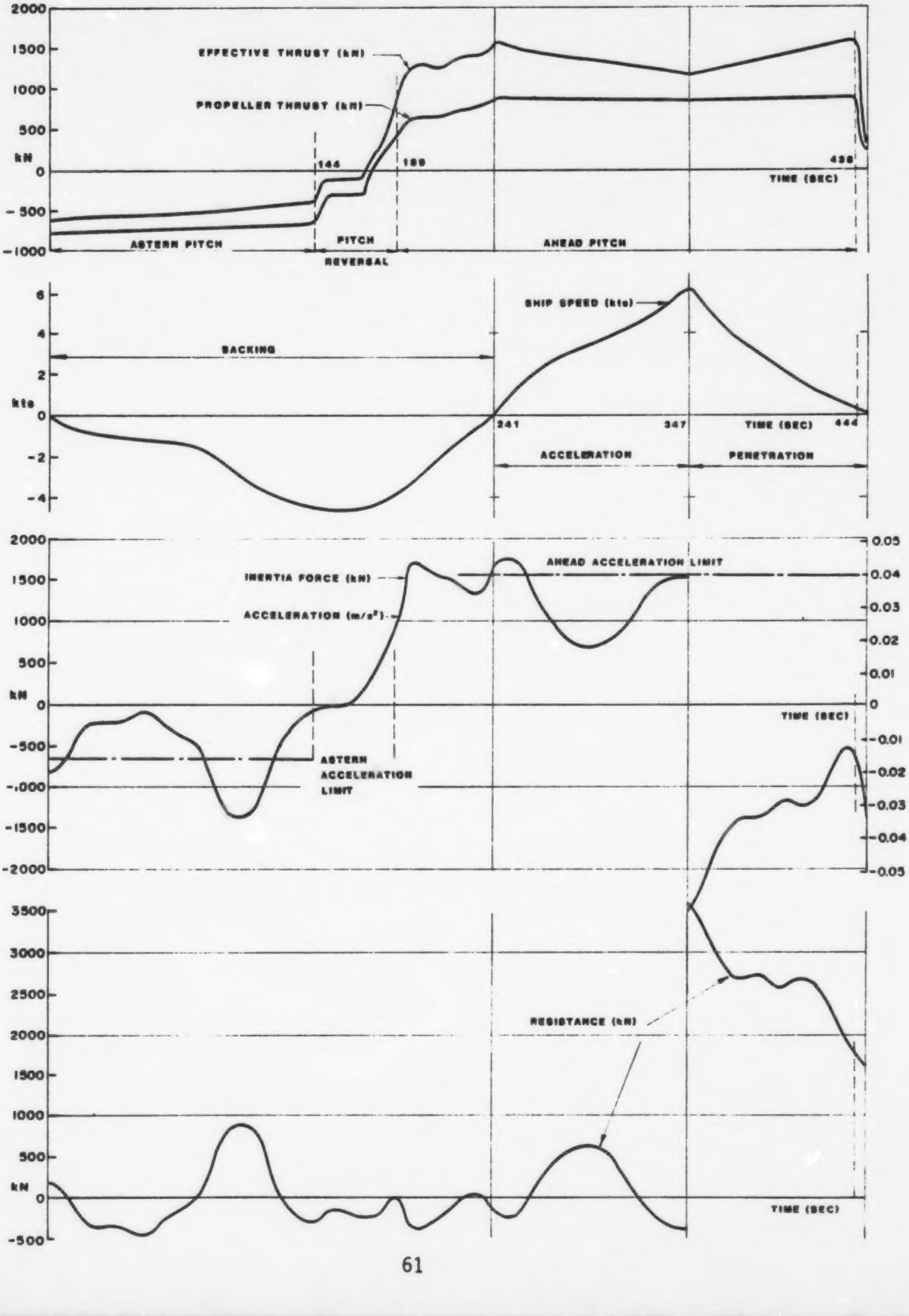

4.3.3 Speed Corrections

The speed profile described earlier in the data reduction and analysis procedures has been derived from the speed recorded by the doppler-log. This doppler-log speed profile was not suitable for direct use in the analysis procedure because of the noise-type of irregularities in the records and the occasional large excursions. Therefore a polynomial curve fitting procedure was adopted to smooth the speed profile. The large excursions were eliminated from the profile prior to curve fitting.

From preliminary analysis it was found that even after clean-up of the speed profile, inconsistencies still existed. For example, the rate of acceleration of the ship ahead or astern, as deduced from the fitted curve, were found to be higher than the acceleration levels the ship was capable of developing with its propulsion system. Furthermore, the backing and acceleration distances would normally be expected to be equal. However, such distances as calculated by integration of the speed profile were mostly different. The impact speed and the penetration time and distance have been compared for a number of rams with those reported in the trials report [21] and were generally greater than reported as shown in Table 4.5. The various time cycle components and the breakpoints in the ramming cycle were generally in good agreement with the reported values.

It became clear that a speed correction was necessary to eliminate the fore-mentioned discrepancies. In close consultation with TDC, a suitable speed self-correction algorithm was developed which through the velocity/time relationship approximated the measured penetration distances well. A comparable basis was used for the backing and acceleration phase adjustments. Full details of the correction algorithms are included in Appendix D.

TABLE 4.5

COMPARISON OF TAPE AND VIDEO ANALYSIS RESULTS

RAM NO.	IMPACT SPEED (knots)		PENETRATION TIME (sec)		PENETRATION DISTANCE (m)	
	TAPE	VIDEO	TAPE	VIDEO	TAPE	VIDEO
C6	6.3	6.0	97	100	133	97
C9	6.7	5.5	179	175	216	176
B1	5.0	5.0	216	210	220	179
B4	5.6	5.5	174	165	174	114
B5	5.6	5.5	176	170	176	136
B6	6.0	5.5	134	140	165	121
B7	5.7	5.5	143	135	168	129
MEAN RATIO TAPE/VIDEO	1.062		1.018		1.331	
STANDARD DEVIATION AS % OF MEAN	7.06%		3.90%		7.77%	

5. RESULTS OF STANDARD ANALYSIS

5. RESULTS OF STANDARD ANALYSIS

5.1 Scope of Standard Analysis

Standard analysis refers to the application of the data reduction program to a standard case of ramming. A standard case is necessarily complete with backing, acceleration and penetration. Incomplete data with minor truncation at the beginning or the end of the ram may be tolerated but rams without a nearly complete cycle cannot be analyzed using the present software. These incomplete rams had to be analyzed manually for incorporation into the performance analysis. However, these cases will only provide limited information.

The standard analysis provides complete speed correction, thrust and resistance analysis, cycle time analysis, and fuel calculations. It produces a standardized set of results consisting of one summary data sheet and five pages of graphical output as explained earlier in Section 4.3.

5.2 Typical Case

As an illustration of a typical result of the data reduction and analysis program, Ram No. C-6 was used for this purpose. In the following pages a typical output is presented. The format of the presented results is self-explanatory except for the following clarifications:

a) The speed of impact is listed as follows:

"Speed of Impact (knots) 6 (6.25)"

The first number 6 is the speed in knots as measured from the video. The number in parenthesis is the speed as determined after correction and after applying the curve fitting routines to obtain the best fit of the data.

b) The penetration distance is also listed as follows:

97 (93.55)

The first number corresponds to 6 knots (is an input value of the measured penetration) and the second number in parenthesis is the best estimate after correction and curve fitting of the speed data.

c) The fuel rate and total fuel used are reported in mm and mm.hr, respectively. Furthermore, the conversion to kg and hr was done in accordance with the following conversion equations:

$$\text{Fuel Rate (FR)mm} = 0.187 \,.\, n - 8.47 \qquad (5.1)$$

$$\text{Fuel Rate, kg/hr} = 72.08 \,.\, FR - 2780.83 \qquad (5.2)$$

$$\therefore \text{Fuel Rate, kg/hr} = 13.48 \,.\, n - 3391.35 \qquad (5.3)$$

RESULTS OF RAMMING CYCLE ANALYSIS

RAM No. __C6

TAPE:	81-T2-5.1	ICE CONDITIONS:	LEVEL ICE
CATEGORY:	L4	ICE THICKNESS:	1.56 m
QUALITY:	26AB	FLEXURAL STRENGTH:	104 kPA
TRIM:	BOW UP	BUBBLER STATUS:	OFF

RAMMING CYCLE CHARACTERISTICS:

Speed of Advance	(knots)	.389	
Speed of Impact	(knots)	6	(6.25)

	Duration (sec)	% Cycle Time	Distance (m)
Backing	246	52.6	-158
Acceleration	102	21.8	158
Penetration	102	21.8	97 (93.55)
Extraction	18	3.85	
Total Cycle	468		

Duration of Astern Mode	(sec)	146
Duration of Reversal to Ahead	(sec)	47
Duration of Ahead Mode	(sec)	247
Duration of Reversal to Astern	(sec)	21
Start of Reversal after Impact	(sec)	92

Total Fuel Used	(mm*hr)	6.52	Est. kg:	108.1
Average Fuel Rate	(mm)	50.12	Est. kg/hr:	831.76

Backing Power	(kW)	7163.9
[Est Fuel Rate	(kg/hr)]	1520.7
Acceleration Power	(kW)	9680.6
[Est Fuel Rate	(kg/hr)]	2022.6

RAM # __C6 TAPE: 81-T2-5.1 08 JUL 1981 14:12:39 **FIG. #1**

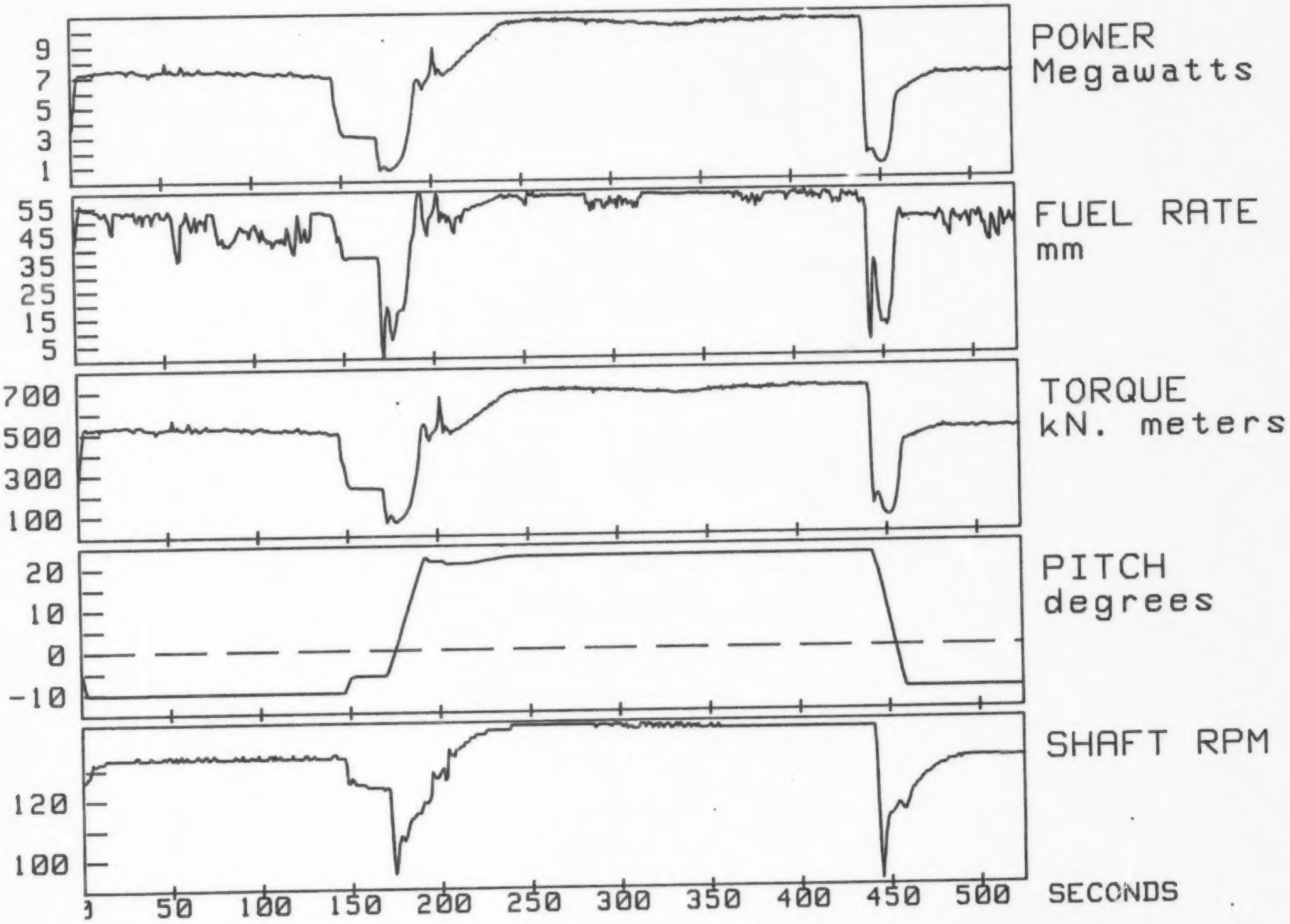

RAM # __C6   TAPE: 81-T2-5.1   08 JUL 1981 14:12:39   **FIG. #2**

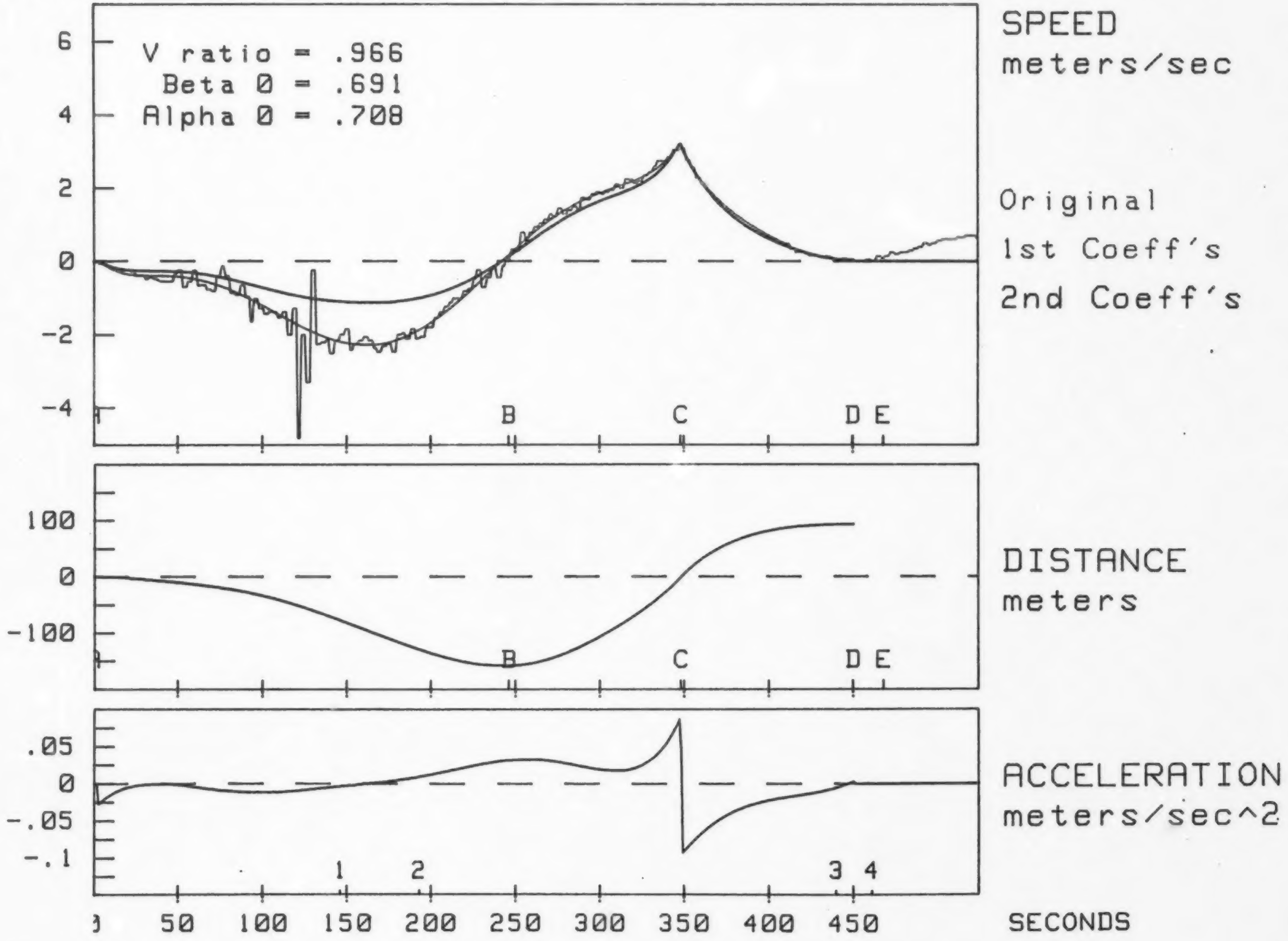

FIG. #3

RAM # __C6 TAPE: 81-T2-5.1 08 JUL 1981 14:12:39

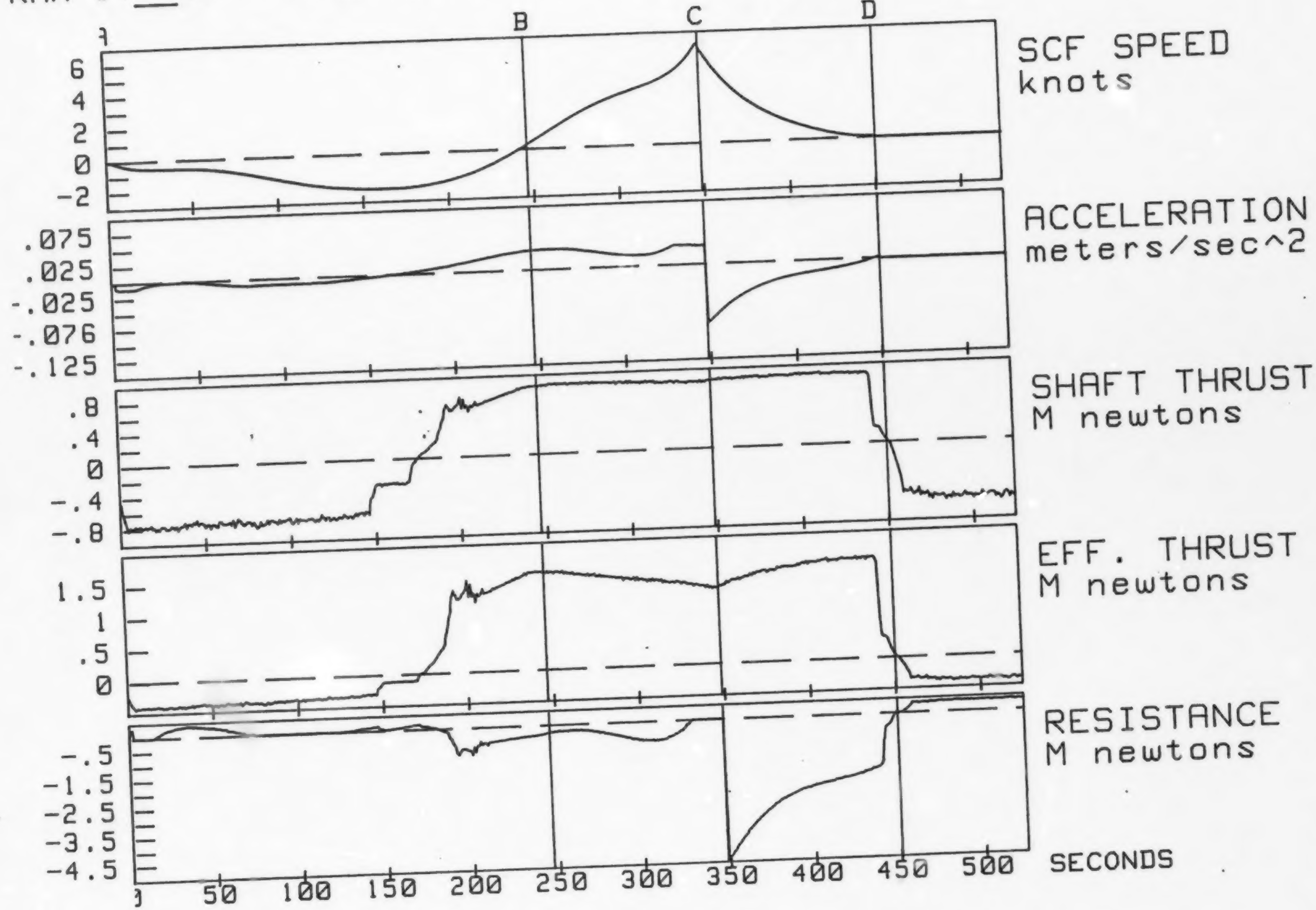

RAM # __C6   TAPE: 81-T2-5.1   08 JUL 1981 14:12:39   Fig.# 4

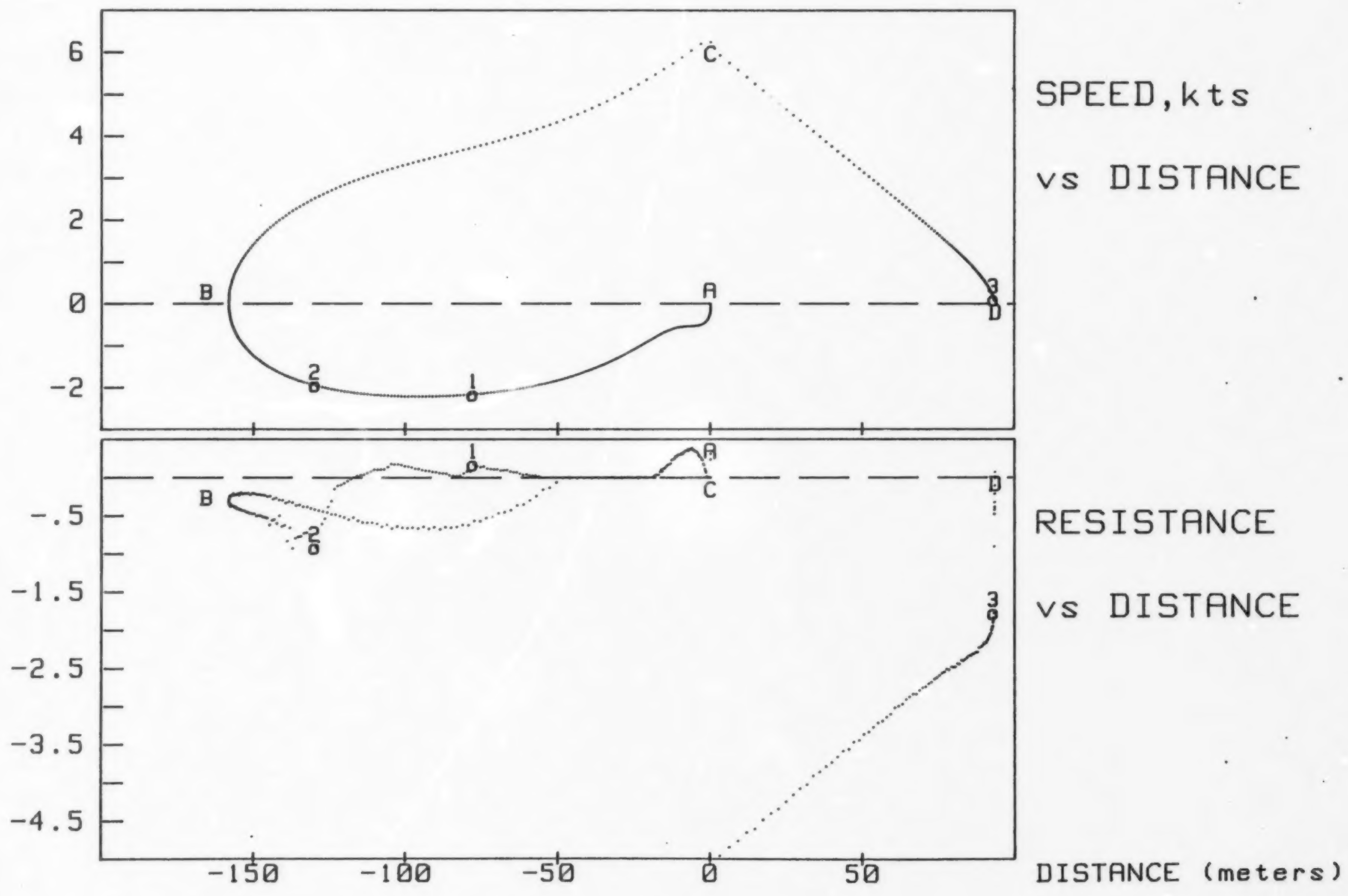

RAM # __C6   TAPE: 81-T2-5.1   08 JUL 1981 14:12:39   Fig.# 5

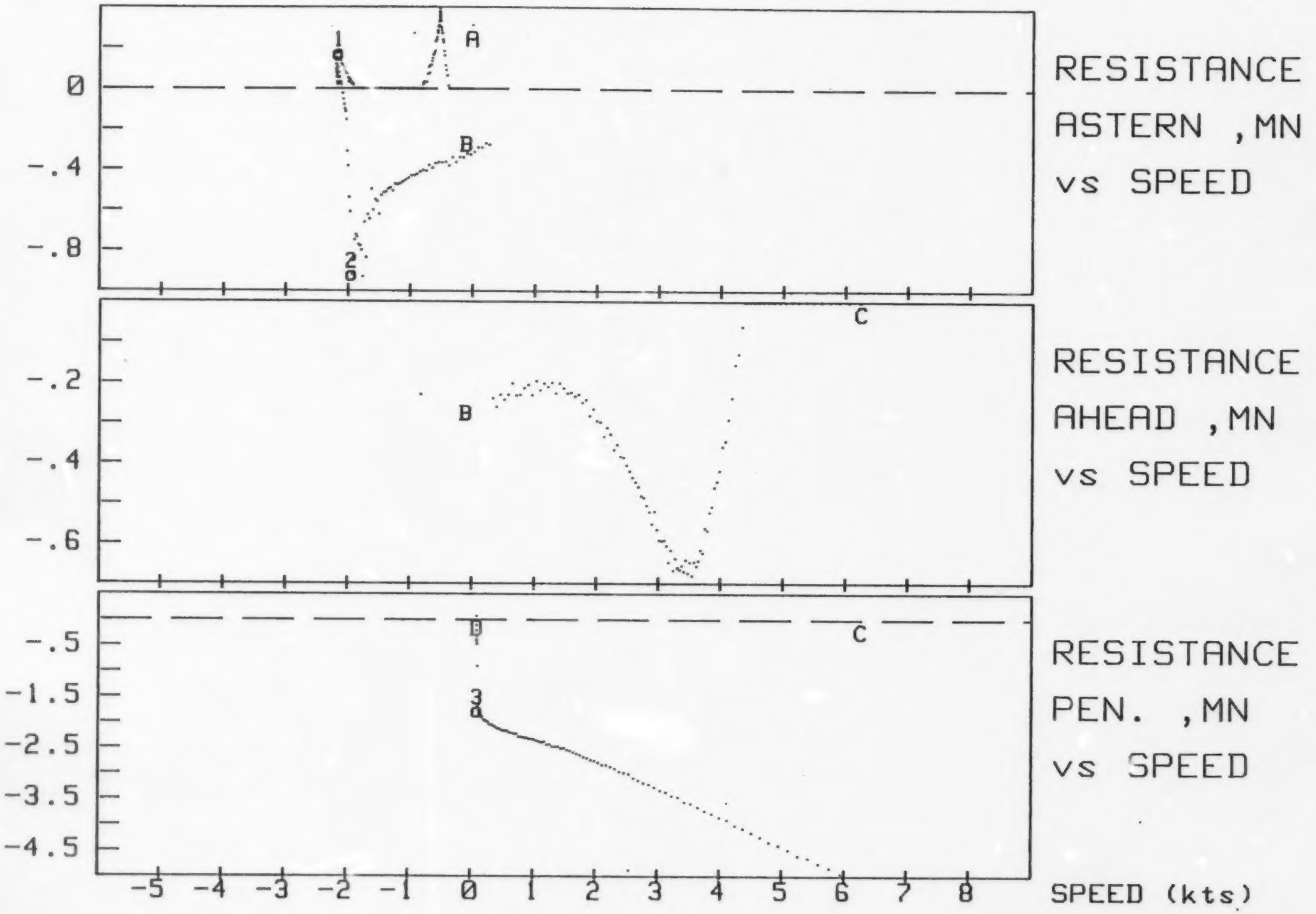

Equation (5.3) was used to calculate the average fuel rate and, hence, total fuel used. These values are reported as:

Est. kg: 108.1
Est. kg/hr: 831.76

However, the above numbers on fuel rate could not be validated for the MV ARCTIC and seemed to be in error. There was no other source for validation or calibration of Equation (5.2). Therefore, another method was used to calculate the fuel rate from power levels. Since power levels were averaged over the backing and acceleration/penetration (excluding reversals) the fuel rates were calculated for both durations from the following empirical relationship:

$$\text{Fuel Rate, kg/hr} = 199.4 \times \text{Power Level (MW)} + 92.25 \qquad (5.4)$$

Equation (5.4) was based on a linear interpolation between the following two points:

- Fuel Rate of 180 gm/hp.hr at 20% of full power
- Fuel Rate of 155 gm/hp.hr at 100% of full power

The full power was 11 MW. These estimates were the best which could be obtained for the MV ARCTIC during the course of this study. The two estimates for fuel rates in the backing and acceleration modes are reported following average power estimates and should be regarded as better estimates of fuel consumption. They may be used to define fuel used as described below.

Based on cycle durations of the astern and ahead modes one could estimate the total fuel used in a cycle as follows:

146 sec x 1520.7 ÷ 3600 = 61.7 kg
+ 47 sec x ½ x 1520.7 ÷ 3600 = 9.9 kg
+ 247 sec x 2022.6 ÷ 3600 = 138.8 kg
+ 28 sec x ½ x 2022.6 ÷ 3600 = 7.9 kg
= 468 sec and total fuel = 218.2 kg
Average fuel rate =1678.8 kg/hr

These are greater than the estimates obtained from Equation (5.3) by a factor of 2, which suggests a basic calibration error in Equation (5.2). It should be indicated that when the fuel rate FR drops below 38.6 mm the calculated fuel rate becomes negative. This happens frequently during the ramming cycle reversal intervals. For any further analysis the fuel rate in mm or the total fuel in mm.hr will be used.

5.3 Results

The results of standard analysis as exemplified by Ram No.C6 are included in Appendix C.

6. PERFORMANCE FORMULATIONS

6. PERFORMANCE FORMULATIONS

6.1 General

In Section 3.3, we have identified eight (8) data categories for level ice and pressure ridges which take into account combinations of bubbler status and trim conditions. The core data base, however, does not cover all eight categories but it provides sufficient information in form of the categories to enable a study of the effect of variables such as ice thickness, strength, ship speed, and power to be made. Therefore, within each major category - namely level ice and pressure ridges - the various trends and effects as well as possible means for formulating the performance of the MV ARCTIC can be determined.

In the ramming mode, the cycle variables are important within each category. That is, the variability in performance during backing, acceleration, penetration and extraction play a direct role in affecting the overall performance under any set of conditions. Therefore, the impact of any variable on the overall performance will be determined by its impact on the various stages of a ramming cycle. For instance, the ship trim may affect the ship performance in the broken ice channel ahead and astern in different ways so that the influence of the trim level on the overall performance may not be obvious. Therefore, unless such effects can be modelled and incorporated in a performance prediction model, it would be extremely difficult to quantify their effects on the overall performance due to the relatively small size of the data base and the usually high scatter in full scale tests.

Therefore, we have chosen a realistic approach by dividing the performance formulation task into three major subtasks:

(a) Analysis of Performance Under Trial Conditions:
Effects of several variables have been examined for level ice and pressure ridge penetration under the conditions in which the trials have been executed. The results of the analysis are reported in Section 6.2.

(b) Performance Simulation:
The techniques which can be used for ramming simulation and which would permit the future study of effects of variables on the various stages of the ramming cycle as well as permit optimization of ramming operations in thick ice conditions or pressure ridges is demonstrated. - The results of the simulation may be found in Section 6.3.

(c) Determination of Ultimate Performance:
Breakdown of ramming cycle into components that individually affect the performance, followed by separate analysis of these components and finally synthesis of the components to determine the ultimate ramming performance for given strategies of ship operation are described in Section 6.4.

ILLUSTRATION OF PERFORMANCE MEASUREMENT

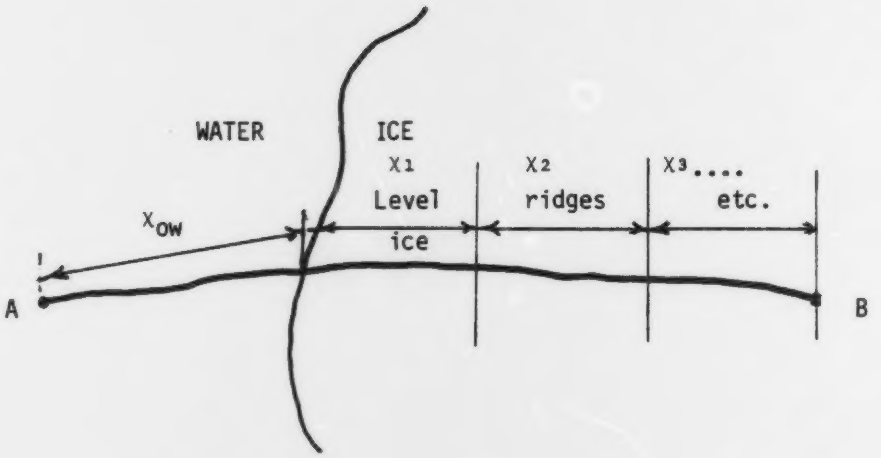
WATER
ICE
χ_1
Level
ice
χ_2
ridges
χ_3....
etc.
χ_{ow}
A
B

- ° Total transit time (t) = $\chi_{ow}/\nu_{ow} + \Sigma\ \chi_{ice}/\nu_{ice}$
- ° Overall average speed of advance $\bar{\bar{\nu}}_a = \Sigma\chi/t$
- ° Total fuel consumed = $(FR)_{ow}\ (\frac{\chi_{ow}}{\nu_{ow}}) + \Sigma\ (FR)_{ice} \cdot (\frac{\chi_{ice}}{\nu_{ice}})$

χ = distance

ν_{ow} = average speed of progress in open water

ν_{ice} = average speed of progress in any leg of ice transit
= $\bar{\nu}_a$ in given ice conditions

t = time

FR = average fuel rate, kg/hr

It should be noted that, the MV ARCTIC performance can be measured by two aspects:

- the time it takes to travel from Point A to Point B.
- the fuel it consumes to complete the transit.

The first aspect is measured by the average speed of advance while the second aspect may be measured by the average fuel rate during a given leg of the transit.

The formulation of the performance of the MV ARCTIC should permit the determination of limits and capabilities. Usually an empirical formulation is limited to the range of determination, i.e. when extrapolation is attempted outside this range it should be done with caution. To explain this we may consider a parabollic relationship which extends over a given range. When only part of the range is considered, a linear relationship may closely describe the data within their range. However, when extrapolation is attempted it is obvious that the farther the linear extrapolation goes the greater the divergence from the true data will be. Therefore, there is a risk factor or a reliability factor in extrapolation. This has to be borne in mind when considering extrapolation to determine the capability limits of the MV ARCTIC.

6.2 Analysis of Performance under Trial Conditions

6.2.1 Effect of Acceleration Distance on Speed of Impact:

The acceleration distance and power level during acceleration affect the speed of impact at the end of the broken channel. For all test series (A, B and C) the measured speed of impact has been plotted vs. the acceleration distance in meters. The results are shown in Figure 6.1. Examination of the results suggests the following:

a) There are two distinct sets of data. The first represents Series A and the second combines Series B and C. Series A involved mainly ridge penetration while the other series were mainly performed in level ice. Examination of the ice thickness and its variation expressed in terms of the standard deviation (*alias* s.d.) revealed that Series B and C were conducted under similar ice conditions. Listed below are the ice thickness summaries:

Series A: $\bar{h}$ = 2.55 m, s.d. = 0.17 m, n = 16

Series B: $\bar{h}$ = 1.56 m, s.d. = 0.17 m, n = 12

Series C: $\bar{h}$ = 1.59 m, s.d. = 0.15 m, n = 9

where $\bar{h}$ = mean ice thickness, s.d. = standard deviation, and n = number of data points used. Therefore, series B and C may be considered as one set of data with an average ice thickness of 1.57 m.

FIGURE 6.1

EFFECT OF ACCELERATION DISTANCE ON SPEED OF IMPACT

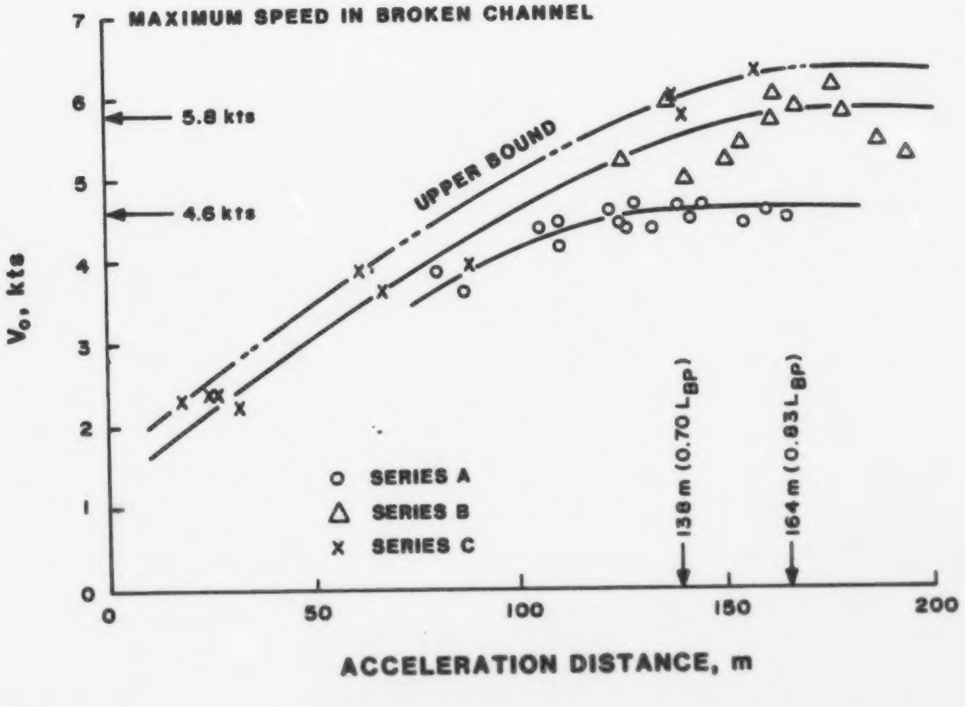

b) Each data set may be represented by a mean line which indicates that the speed gradually decreases and converges to a maximum value. This conforms to what may be expected in ship acceleration in broken channels where the maximum speed is determined by the ice thickness, floe size, and channel coverage (or concentration of broken floes). Usually a ship breaks the ice in a characteristic pattern which varies with speed and ice properties. Therefore, some estimates of these variables will be made in due course. This trend of variation of impact speed suggests that any attempt to increase the acceleration distance beyond a maximum value will not result in a corresponding increase in impact velocity and hence would result only in loss of time and unnecessary increase in fuel consumption.

c) The maximum achievable impact speed and the corresponding acceleration distance vary with ice thickness. For the two ice thickness levels available, these variables are plotted vs. thickness in Figure 6.2. The acceleration distance is expressed in terms of the ship length, L_{BP}. It is known that the ice resistance in broken channels is mostly linearly dependent on ice thickness except for higher concentrations 60%. Therefore, a linear relationship may be proposed to relate the acceleration variables to the mean ice thickness. It should be noted that extrapolations are represented by dotted lines. It is also worthy of note, that the maximum conditions are not necessarily optimum. This concurs with the reversed effect of thickness on acceleration variables. For thicker ice a longer acceleration distance will be necessary to accelerate the ship to a lower speed of impact. As ice conditions get worse, the ice concentration in the broken channel will increase and the ship may have to resort to ramming in the broken channel. Under such conditions the effectiveness of ramming mode progress will be very low and operation may be stopped until conditions improve.

As stated earlier, the power level during acceleration in a broken channel is an important parameter which affects the speed of impact. However, this effect was not evaluated because of the fact that in all dedicated trials acceleration was done at full power ahead. Therefore, the effect of power was not pursued any further.

It should be mentioned that acceleration in broken ice channel does not appear to be strongly affected by the type of ice. That is, in the pressure ridge, Series A, we have not observed any drastic reduction in speed except for what may be attributed to ice thickness effects. The ice thickness for the pressure ridge, Series A, appears to have the same variability as in level ice; and even less variability in relative terms:

Series A: s.d. = 6.7% of mean thickness
Series B: s.d. = 10.9% of mean thickness
Series C: s.d. = 9.4% of mean thickness

FIGURE 6.2

EFFECT OF ICE THICKNESS ON ACCELERATION VARIABLES

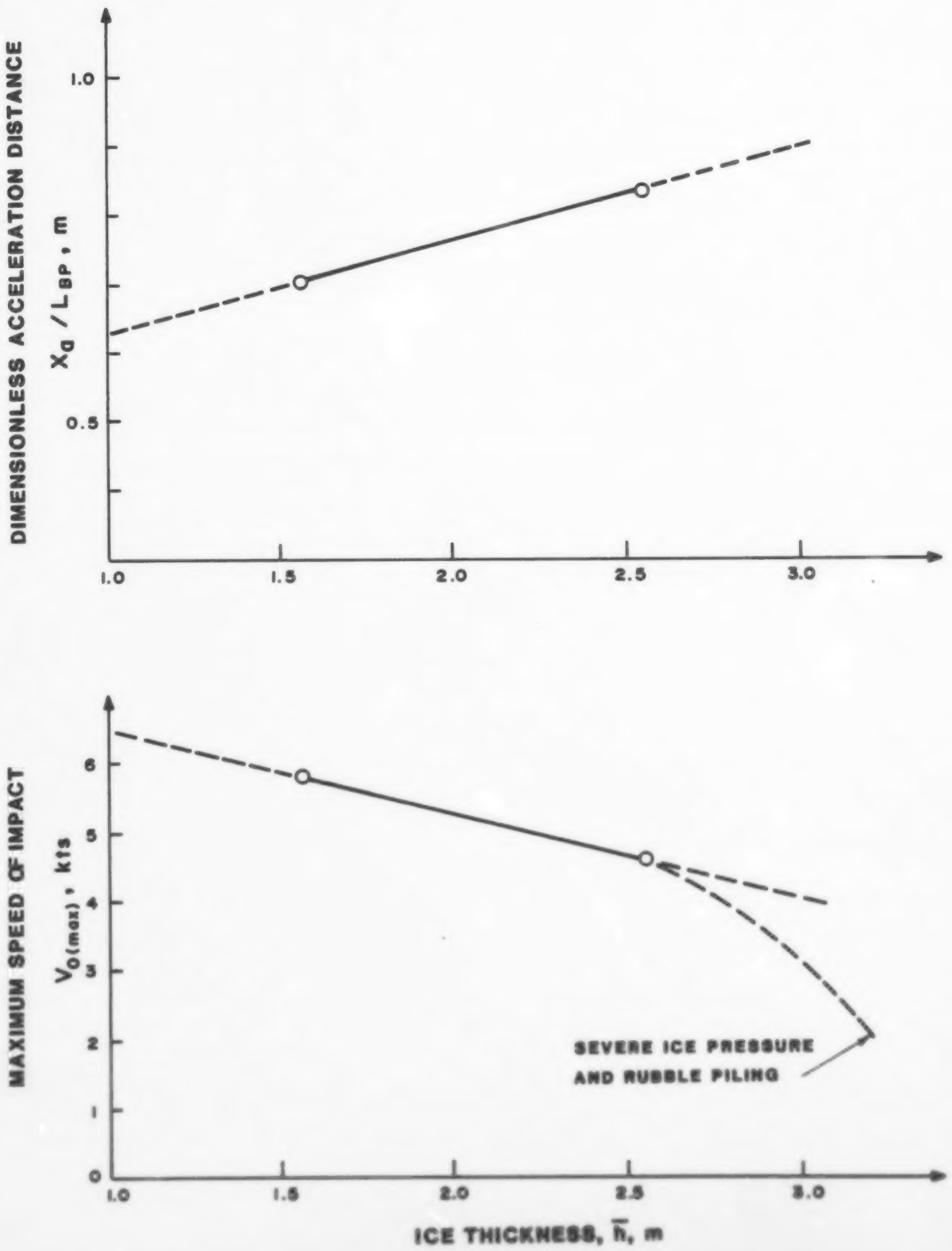

Therefore, one may suggest that the Pressure Ridge of Series A was almost as flat as level ice. A review of the measured profile of the ridge had a flat keel which extended for about 30 meters. Having a total width of about 290 meters and a maximum thickness of about 2.8 m. These dimensions suggest a sail width of the order of 53 m and knowing that the sail height was 0.25 m, we may conclude that this was not a first year pressure ridge. The ridge proportions are not consistent with any full scale data we have in hand. Therefore, it is possible that due to the small number of holes drilled to measure the ridge thickness (only 3) (See Figure 6.3), that the ridge profile was not properly defined or that a ridge cluster was mistaken for a single first year pressure ridge. In the forthcoming analysis, however, Series A will be designated as a ridge series but for the purposes of characterization of performance it will be dealt with as thick level ice or a two ridge cluster as may be found appropriate. The two ridge cluster profile is illustrated in Figure 6.3.

6.2.2 Effect of Speed of Impact on Speed of Advance

The ship progress rate in the ramming mode can be measured by its average speed of advance. For a single ram it is the net penetration divided by the cycle time and for a series of successive rams it is the total distance travelled, divided by the total time of travel. The latter is not equal to the average of the former except when ice conditions are uniform such that the variation in cycle duration from ram to ram is negligible.

The average speed of advance is influenced by two groups of variables:

a) Those variables affecting the penetration distance which, for given ice conditions include the speed of impact and power level maintained during penetration.

b) These variables affecting the total cycle time which include backing and acceleration power levels, broken channel characteristics, operational aspects of thrust reversal, and time losses.

Due to the large number of variables involved one would expect some scatter in the measurements.

Figure 6.4 is a plot of average speed of advance per ram, $\bar{v}_a$ versus the impact speed, v_o. It is shown that the data suggests an optimum impact speed for which the ship progress is fastest. The optimum speed of advance is estimated to be:

° For pressure ridges Series A: $\bar{v}_a = 0.084$ kts @ $v_o = 4.0$ kts
° For level ice Series B and C: $\bar{v}_a = 0.52$ kts @ $v_o = 4.8$ kts

These optimum impact speeds are, on the average, 15% lower than the maximum speed in broken channels.

FIGURE 6.3

RIDGE PROFILE and RAMMING SERIES

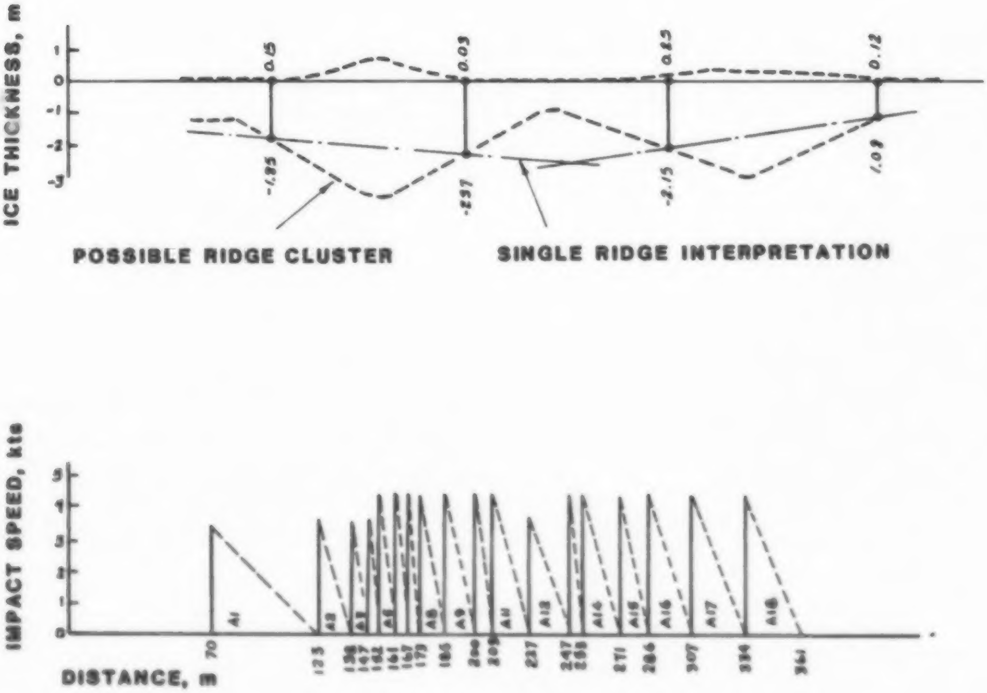

Some effects of the bubbler operation have been noticed in thick ice, Series A, and it is estimated that:

with bubbler ON: v_a = 0.098 kts [h = 2.39 m, s.d. = 0.17 m]

with bubbler OFF: v_a = 0.063 kts [h = 2.62 m, s.d. = 0.17 m]

It should be noted, however, that this improvement cannot be entirely attributed to bubbler system. Examination of the ice conditions in the given cases shows that when the bubbler was operated the ice was thinner. However, we estimate that the ice thickness difference cannot entirely account for the observed improvement. There was no discernible difference in performance in Series B and C which could be attributed to the bubbler effect.

Figure 6.4 illustrates that two samples, C7 and C9, exhibit a much improved performance compared to the rest of the samples in Series B and C. These two runs belong to category L2: bubbler on and bow up. Compared to other results in the same impact speed range and of comparable ice thickness we find that around v_o = 5.8 kts:

° runs C7 and C9 with average v_a = 0.59 kts belong to category L2
° runs B6, B7, B20, B23,
and B3 with (fitted) v_a = 0.38 kts belong to category L1

Both categories had similar bubbler ON status with the only difference being the trim condition. Therefore, the immediate conclusion which follows from this is that the bow up position significantly improves the performance over the zero trim position. Further analysis is needed to corroborate this conclusion.

It should be noted that categories L1 and L4 appear to produce the same performance. In the former category the bubbler was on with no trim while in the latter category the bubbler was off with the bow up. Therefore, it may be suggested that the effect of the bubbler system operation was comparable to the trim effect under the conditions investigated. It is therefore, possible to suggest that significant improvements in performance may be gained by either means. The present data indicates a gain in speed of advance of the order of 50 percent.

FIGURE 8.4

EFFECT OF SPEED OF IMPACT ON SPEED OF ADVANCE

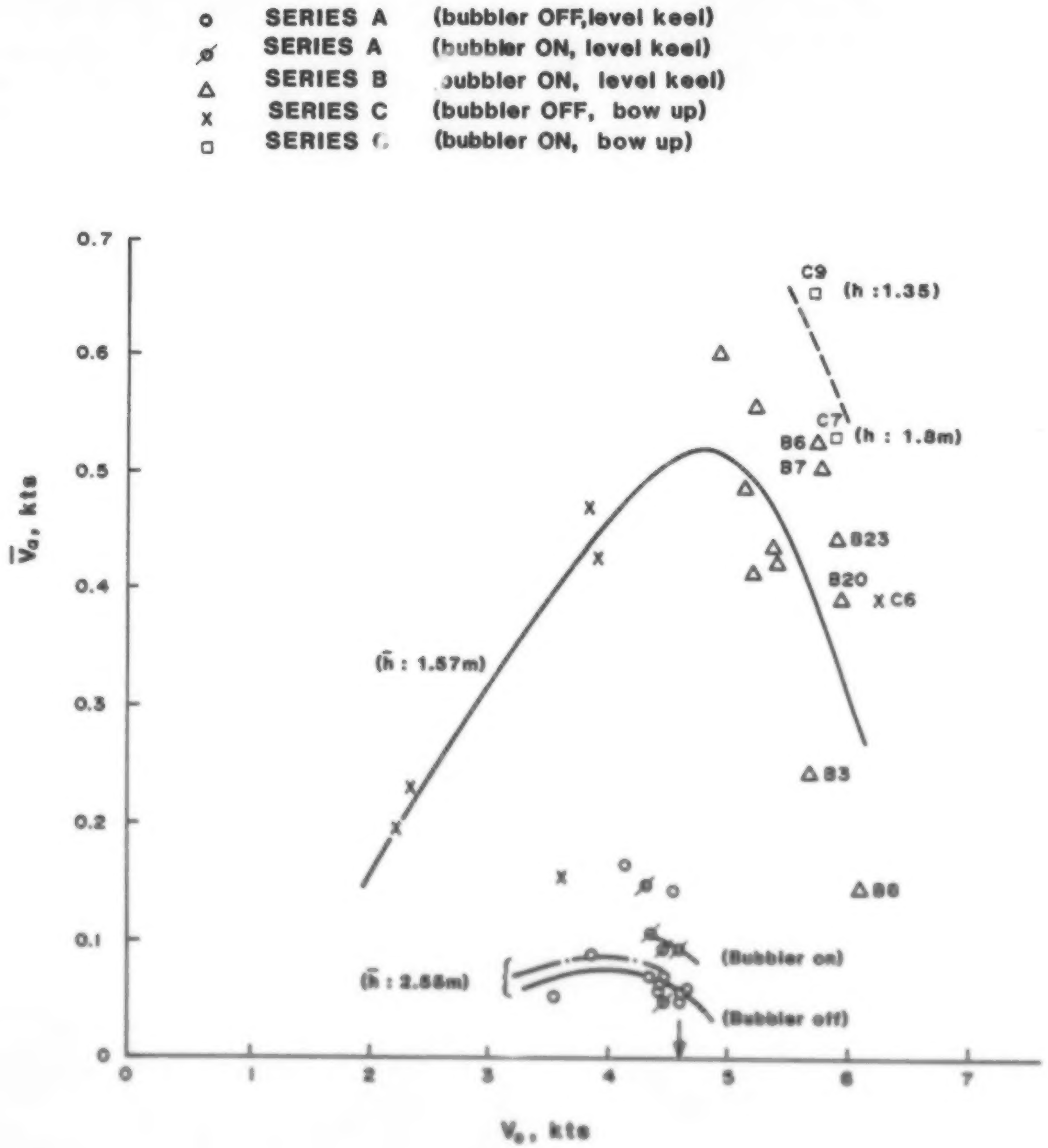

6.2.3 Effect of Thrust Cut-off

The effect of thrust cut-off on impact was investigated during the trials of the MV ARCTIC. It is obvious that the thrust application during the penetration stage would provide more energy and hence allow a longer penetration distance per ram. The question is how much does the thrust contribute to the ship performance and whether it would be advantageous to cut-off the thrust during penetration to facilitate extraction.

Based on the total available energy, it is easy to show by simple calculation that:

a) When the ice is thin or medium, its resistance is low and the penetration would be long. In this case the thrust contributes a large share of the total penetration energy and thrust cut-off is a definite disadvantage. Consider, for instance the following case of medium ice thickness of:

- $h = 1.56$ m
- $v_o = 5.4$ kts
- Kinetic Energy = 147.3 MJ (43.4%)
- Thrust Energy = 192.0 MJ (56.6%) (full thrust)
- Total Energy = 339.3 MJ
- Actual penetration = 128 m with thrust
- Est. penetration = 66 m without thrust

This compares with 80 m penetration in a similar test with thrust cut off considering ice thickness variability.

b) For thick ice (2.55 m) the above method indicates the following:

- $v_o = 3.5$ kts
- Kinetic Energy = 61.9 MJ (83.4%)
- Thrust Energy = 12.0 MJ (16.2%) (Thrust = 1.2 MN)
- Total Energy = 73.9 MJ
- Actual Penetration = 10.0 m with thrust
- Est. Penetration = 8.3 m without thrust

Figure 6.5 is a plot of penetration distance as a function of impact speed, in which the solid symbols indicate thrust cut off cases. It is clear that in thick ice (Series A) there is no evidence that thrust cut off has an effect on penetration distance. Probably the differences were within the scatter range of ice thickness, strength, and ship penetration. In thinner ice, it is shown that there is a more discernible effect of thrust cut off (Series B and C). For the impact speed range of 5 to 6 knots the average penetration drops from 128 to 80 meters. This is consistent with energy considerations.

FIGURE 6.5

PENETRATION DISTANCE VERSUS V_0

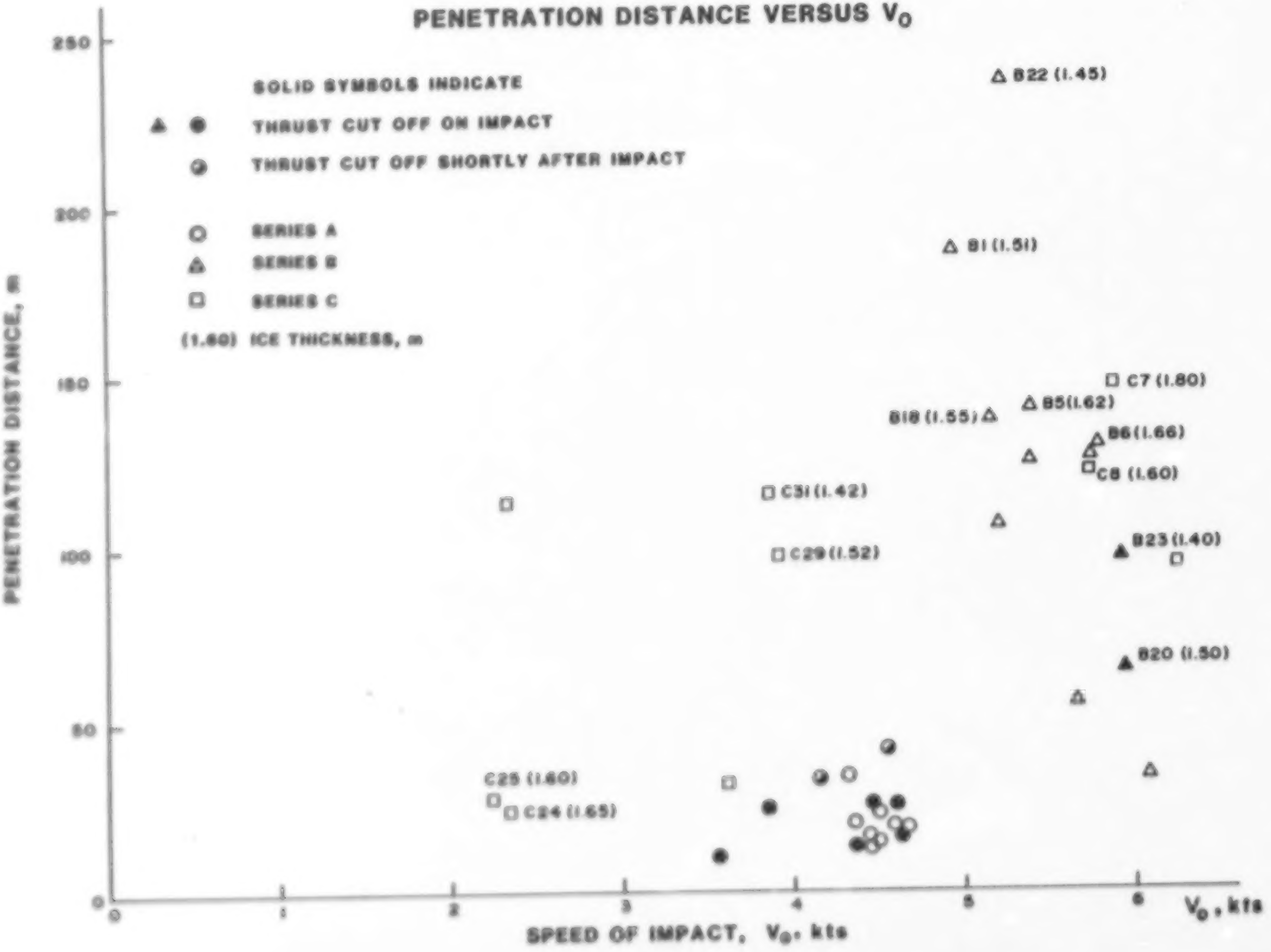

Two ramming incidents under comparable ice conditions are shown in Figure 6.6 to illustrate the effect of thrust cut-off on the penetration profile.

Ram B22, in 1.45 m ice thickness was executed at an impact speed of 5.3 kt while maintaining the thrust throughout the penetration phase, which resulted in a penetration distance of 235 m.

During ram B23, 1.40 m ice thickness, the thrust was cut off on impact at a speed of 5.9 kt. The penetration distance in this case was 97 m.

It can be seen that maintaining the thrust or power during the penetration phase is extremely beneficial under the conditions as per ram B22 and B23. As explained above, the benefit of increased penetration distance reduces when thicker ice is encountered, in fact, when the penetration distance is shorter.

FIGURE 6.6

EFFECT OF THRUST CUT-OFF ON PENETRATION

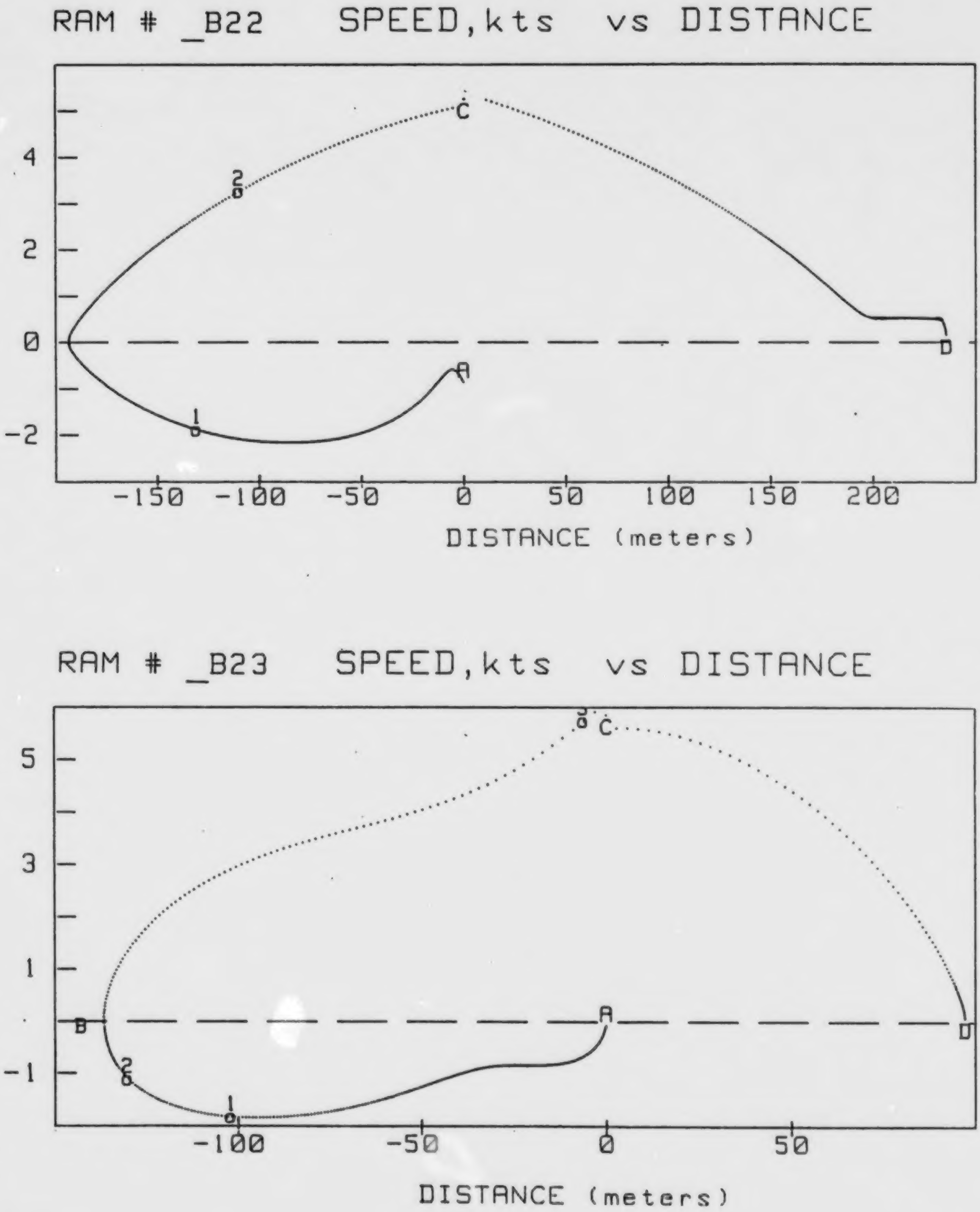

6.2.4 Effect of Ice Thickness on Fuel Consumption

The fuel consumed during a single ram varies depending on the control of power levels and the control exercised over the ramming cycle components. An attempt to correlate the total fuel used per ram with the acceleration distance, x_a resulted in the plot of Figure 6.7. It is shown that there is a trend of increasing the total fuel used per ram as the penetration distance increased. However, to quantify this type of relationship is difficult because of the many other variables associated with the ramming cycle. As a result ice thickness was sought as an independent variable which controls the overall ramming behaviour. A dependent variable for fuel consumption was developed to accommodate the differences in a ramming cycle. For instance, when ramming at a slow speed of impact the cycle is usually short and the total fuel consumed would be lower than that of ramming at a higher speed. Also ramming at a lower speed would produce shorter penetrations and slower speeds of advance. In order to neutralize the cycle variability the following variable was used:

$$F/v_a = \frac{\text{average fuel rate}}{\text{average speed of advance}}$$

The units of average fuel rate per ram, F, is kg/hr and that of v_a, is knots, i.e. the variable may be expressed in terms of kilograms of fuel used for every kilometer of distance travelled; kg/km. Since the conversion from fuel rate in millimeters to kg/hr was not realistic, a variable was developed based on actual measurements in mms and is given by:

$$\alpha_f = \frac{F(\text{mm})}{v_a(\text{knots})}$$

This variable will be directly proportional to the fuel consumed per km of travel. Figure 6.8 is a plot of α_f vs ice thickness in semilogarithmic space. It is shown that much of the scatter observed in Figure 6.7 has been reduced. An attempt to include the effect of ice strength did not result in improving the data scatter.

The relationship between ice thickness and the fuel used to travel a given distance is quite strong. It is realized that when operating close to optimum conditions better fuel economy may be realized, and this may explain some of the scatter which still remains.

The bubbler operation/trim condition seems to have a slight economic advantage in medium thickness ice and little advantage in the thick ice range. The fuel consumption, however, appears to increase considerably with increased ice thickness. For 2.7 m thick ice the fuel used per kilometer is almost six times that used in ice 1.6 m thick. This sensitivity of fuel consumption to ice conditions should be underlined for the benefit of commercial transit.

FIGURE 6.7

EFFECT of X_a on AVERAGE FUEL USED PER RAM

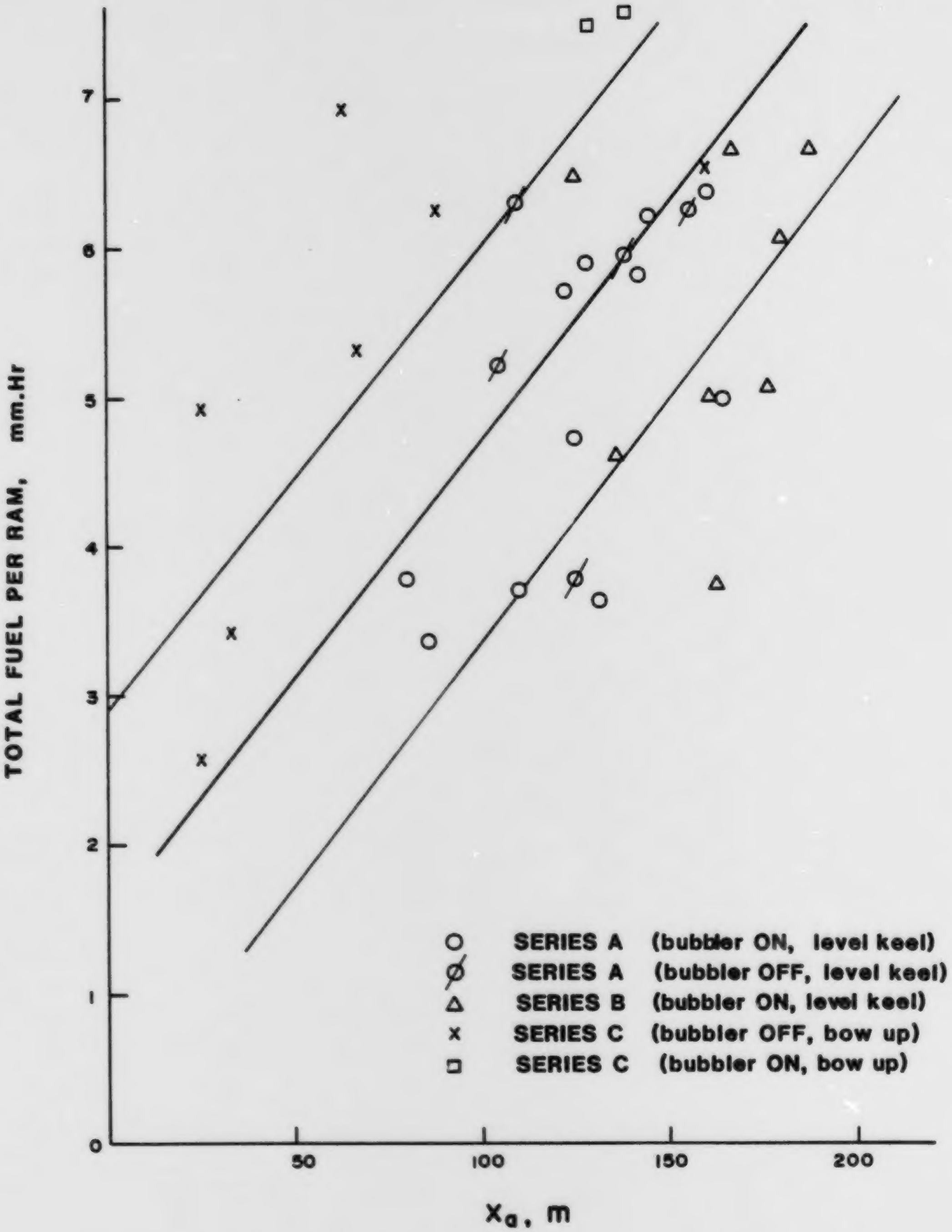

Figure 6.8 shows that a linear relationship is possible and it may be expressed by:

$$\boxed{\alpha = \dot{\bar{F}}/\bar{v}_a = e^{(2.282 + 1.521\ h)}} \qquad (6.1)$$

This relationship is a simple and powerful model for the MV ARCTIC. It includes:

a) The ice thickness which is the dominant parameter in characterization of an ice field.

b) The fuel rate which is an indication of the mean operating power level during ramming. It also accounts for the cycle proportions.

c) The average speed of advance of the MV ARCTIC under such conditions.

Therefore, to use this model for performance prediction we may rewrite Equation (6.1) in the form:

$$\boxed{\bar{v}_a(\text{kts}) = \dot{\bar{F}}(\text{mm}).e^{-(2.282 + 1.521\ h)}} \qquad (6.2)$$

This equation is a description of the average as-is performance of the MV ARCTIC without optimization of the speed of advance. The optimum operating condition would probably be represented by a line close to the lower bound to the data plotted in Figure 6.8. Obviously the upper bound represents worse than average operating tactics. To demonstrate the benefit of this diagram let us make two comparisons:

a) A comparison of the effect of ramming tactics under identical ice conditions. Consider transit of the MV ARCTIC in 1.5 m thick ice and that the average ramming tactics can be used as a reference.

By the adoption of: °average ramming tactics will burn 100% fuel per km travelled.
°poor ramming tactics will burn 139% more fuel than average.

FIGURE 6.8

FUEL USE AS A FUNCTION OF ICE CONDITIONS

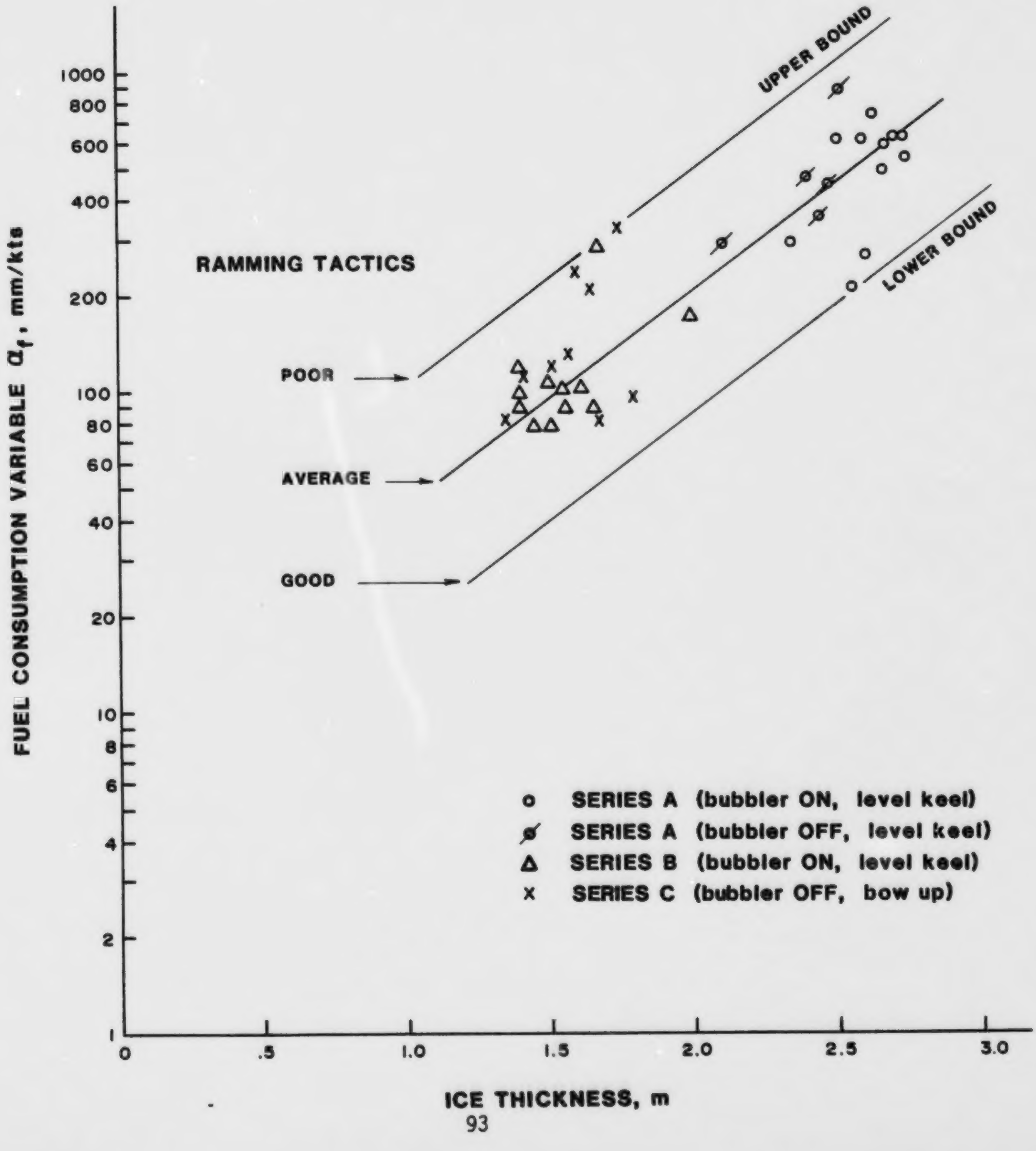

- good ramming tactics will burn 56% less fuel than average.
- best (optimum) ramming tactics will burn 68% less fuel than average.

It is obvious that the differences are significant.

b) Same ice thickness range for a given fuel use.

Now Equation (6.2) may be used to derive the performance curves for the MV ARCTIC in the ramming mode of operation. This is presented in Figure 6.9 in which the average speed of advance is plotted against the ice thickness for different operating fuel rates.

The actual core database is laid over the performance curves in Figure 6.9. It is shown that in Series A, the cautious attitude towards pressure ridge penetration resulted in slow progress at a mean rate of 0.066 kts at a mean fuel rate of about 30 mms. A more liberal use of available power could easily increase the progress rate by 70 - 75 percent.

To demonstrate the applicability of this general model take for instance Ram No. C6. With $h = 1.56$ m and $\bar{F} = 50.12$ mm the predicted progress is $v_a = 0.477$ kts which is 22 percent higher than that reported in Appendix C, and 16 percent higher than the speed calculated from field data.

It should be noted that this model is most suitable for predicting the average rate of progress in ice for MV ARCTIC using current operational strategies.

FIGURE 6.9

MV ARCTIC PERFORMANCE MODEL IN RAMMING MODE

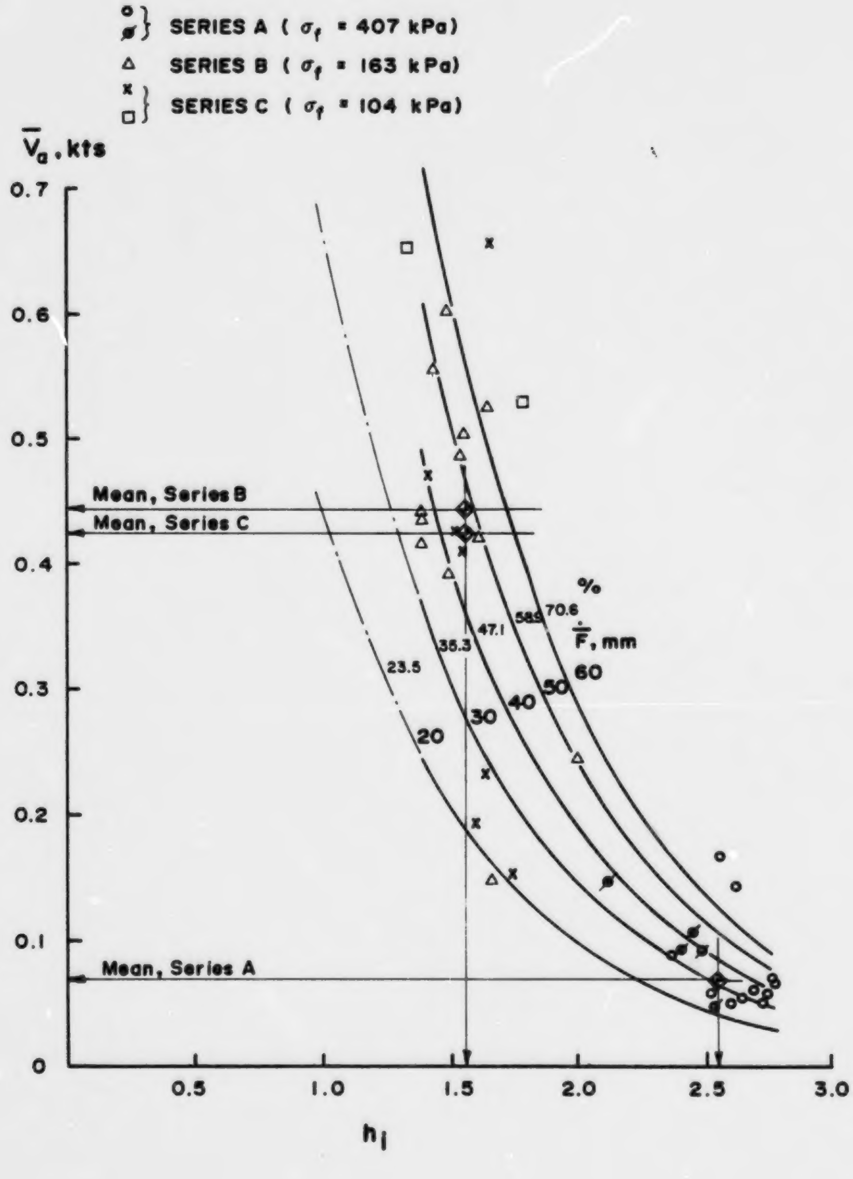

6.2.5 Effect of Bubbler System and Trim

The effect of the bubbler system and the trim of the ship on the ramming performance has been investigated using data points of the Series B and C. As further detailed in Section 6.4, the bubbler system and trim have no detectable effect on the backing and acceleration characteristics. Therefore, any effect on the speed of advance should show up in the penetration phase of the ram. The available data points were from three categories:

- bubbler on, level keel (L1)
- bubbler on, bow up (L2)
- bubbler off, bow up (L4)

The first category is found in Series B, of which a number of data points have been identified with their ice thickness in Figure 6.5. They seem to be in line with each other, considering the variation in ice thickness as discussed in Section 6.4. The third category are data points from Series C while the second category is represented by rams C7 and C8.

Detailed observation and comparison of the penetration versus impact speed of the categories L1 and L4 learned that both categories can be considered in line with each other and no systematic difference could be found. This would indicate that the effect of the bubbler system equals the effect of trim. The effect of trim was examined by comparing the categories L1 and L2 and the effect of the bubbler by comparing L2 and L4.

For the comparison between the second category and one of the other two, only ram C7 and C8 are available. Ram C8 resulted in a penetration about 15 percent lower than would have been expected from the trend of the other categories. Ram C7 on the other hand, resulted in a penetration about 15 percent higher than the expectation. Therefore this part of the data base does not permit a conclusive statement on the effect of the bubbler system and trim on penetration.

A similar examination was performed on the data points of Series A to determine the effect of the bubbler system for a level keel trim. However, due to the scatter it was not possible to come to a conclusion. The scatter is attributed to the lack of accurate information on ice characteristics.

It should be noted that a direct comparison of the speed of advance as achieved during the trials is insufficient since the backing and acceleration phases have mostly not been executed in a comparable manner. Therefore a conclusive analysis can only be performed on the basis of more data points with reliable information on ice conditions, followed by a type of analysis as detailed in Section 6.4. Nevertheless, it has been observed from the trial data that bubbler on and bow up seem to have a positive effect on the speed of advance. However, the number of data points is not sufficient to perform a quantative analysis.

6.2.6 Effect of Operating Power Level

Throughout the trials the target for power level ahead was full power (10.5 MW). However, full power ahead was not applied consistently, resulting in less efficient stopping and acceleration maneuvers, reducing the speed of advance. Other power levels were not used in the trials, so that the effect of operating power ahead cannot be determined directly from the data base. In Section 6.4 the data base has been analysed more in detail, from which it has been estimated that a 10 percent power reduction would lower the speed of advance by 10 percent and reduce the fuel mileage by 3 to 8 percent. Therefore, operation at reduced power level ahead is not beneficial.

It should be noted that during most rams the power level was fluctuating below full power by 5 to 10 percent. This may be caused by the machinery control system. A few rams don't show this phenomena (B6, B23, C6, C7). Based on the earlier mentioned effect of power reduction, this could cause up to 5 percent lower speed of advance and up to 4 percent increased fuel consumption.

The power levels used in the astern mode during the backing phase have been varied between 3 MW and 8 MW. A direct evaluation of the effect of astern power level on the speed of advance would not be correct. The results of the analysis presented in Section 6.4 have learned that the astern power level is the parameter for trade-off between speed and fuel economy. In a practical range of astern power, a reduction from 7.5 MW to 5.0 MW power in 1.6 m level ice will give about 9 percent lower speed of advance and about 5 percent increased fuel mileage. In 2.5 m level ice these percentages are respectively 6 and 9. This means that high astern power can be used to increase the speed of advance without great penalty on fuel in relatively thin ice, while reduced astern power can be used to save fuel without great loss of progress speed in thick ice.

6.2.7 Cycle Time Analysis

The ship performance (expressed in terms of rate of progress, $\bar{v}_a$, and fuel consumption, α_f), is directly influenced by the cycle time and its components. The ideal condition would maintain the maximum penetration in the shortest possible time. Therefore, the understanding of the cycle time proportions for the MV ARCTIC may assist in developing better ramming strategies. The analysis of cycle time may be performed on either (or both) the action cycle or the response cycle.

Table 6.1 provides a statistical summary of the action cycle components for the core database. The following is noted:

a) Duration of the astern mode depends on the backing distance and speed. In Series A, the backing speed was generally lower and the backing distance shorter, while in Series B and C these variables were relatively higher, thus the duration of astern mode is comparable.

b) Similar argument applies to the ahead mode. While the penetration in thick ice was shorter and impact speeds were generally lower, the time duration of the ahead mode was shorter, (100.2 secs for Series A compared to 231 to 236 seconds in other series). However, we must note that Series B and C were very comparable in the ahead mode duration.

c) The reversal time is a critical part of the cycle. It does not appear directly as part of the response cycle time components but it influences them indirectly because it is non-productive duration where the average thrust is zero.

   It should be noted that the reversal time from ahead to astern was normally done quickly within 24.1, 20.4, 17.5 secs. on average for series A, B, C, respectively. The shortest reversal duration was observed to be 7 seconds. The standard deviation was reasonably low and ranged between 14.9 to 27.3% of the mean. On the contrary, reversal from astern to ahead took longer; 159.9, 78.6 and 47.1 for series A, B and C; respectively. The standard deviation was also high and ranged from 45.8 and 92.9 percent of the mean. This long reversal time was high in thick ice, we think because the master was trying to avoid propeller ingestion with broken ice.

   This area is where most benefit can be gained. The lowest observed reversal duration to ahead was 23 seconds in Ram B19 and it should be a target for improving responsiveness of the ship and performance in ramming to reduce reversal times to a level below 20 seconds in either ahead or astern reversal.

TABLE 6.1

ACTION CYCLE TIME COMPONENTS

	SERIES A		SERIES B		SERIES C	
	mean	s.d.	mean	s.d.	mean	s.d.
T_c	516.6	106.2(20.6%)	522.3	128.8(24.7%)	397.7	112.2(28.2%)
ΔT_{AST}	158.7	54.5(34.3%)	173.0	39.8(23%)	108.1	56.6(52.3%)
ΔT_{Rhd}	159.9	87.7(54.9%)	78.6	73.0(92.9%)	47.1	21.6(45.8%)
ΔT_{AHD}	100.2	43.5(43.4%)	236.2	81.0(34.3%)	230.6	82.2(35.7%)
ΔT_{RSt}	24.1	3.9(16.1%)	20.4	3.0(14.9%)	17.5	4.8(27.3%)

Legend: T_c = cycle time, seconds
ΔT_{AST} = duration of astern thrust
ΔT_{Rhd} = duration of reversal to ahead thrust
ΔT_{AHD} = duration of ahead thrust
ΔT_{RSt} = duration of reversal to astern thrust

(1) High scatter due to variability of backing distance with speed of impact.

(2) In cases with thrust cut off on impact ΔT_{RS} will be longer by definition.

In many cases the reversal duration was long because of the indecision of the vessel master on whether to reverse the thrust or continue. This is typically illustrated in Figure 6.10. Part of this is caused by cautious operation and reaction to the least vibrations caused by propeller milling.

All these can be avoided if clearer understanding of the MV ARCTIC capabilities and the operational limits are developed.

d) The total ramming cycle time appears to be independent of the ice thickness, and typically was 8-9 minutes in Series A and B with comparable standard deviation of 21 - 25% of the mean. In Series C, the impact speed was generally lower on the average and that decreased the total cycle time.

e) During the Admiralty Inlet dedicated trials the following cycle time breakdown may be given:

- 27.2 to 30.7% of cycle time was spent in astern mode.
- 31.0% of cycle time was used to reverse from astern to ahead in very thick level ice (pressure ridge) compared to:
  11.8 - 15.0% in thick level ice 1.57 m thick.
- 19.4% of cycle time in ahead mode in very thick level ice (2.55 m) compared to:
  45.2 - 58.0% of cycle time in 1.57 m thick ice.
- 3.9 - 4.7% of cycle time spent in reversal to astern mode at the end of the ram.

This breakdown identifies the following pay-off areas for improving ramming strategies:

- reduce the astern mode duration (by increasing power levels)
- reduce the reversal time from astern to ahead particularly in very thick ice conditions.

If the response cycle components are plotted against the average speed of advance, Figure 6.11, some information may be obtained on which is the most influencial component. The figure shows that:

a) Higher speeds of advance are generally associated with shorter backing, acceleration and extraction durations and longer duration for the penetration stage.

FIGURE 6.10

TYPICAL EXAMPLES of EXTENDED REVERSAL DURATION

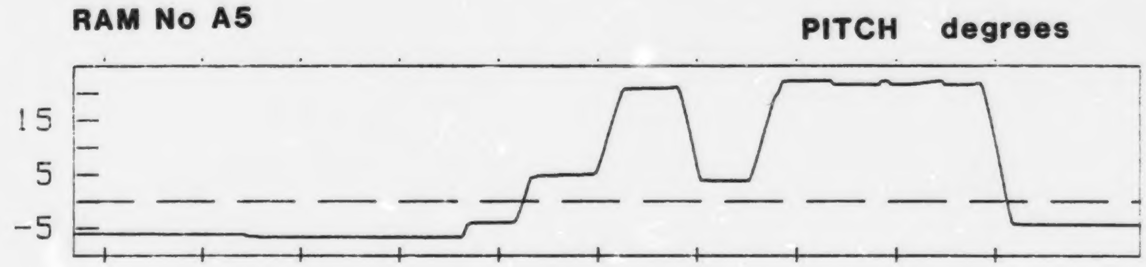

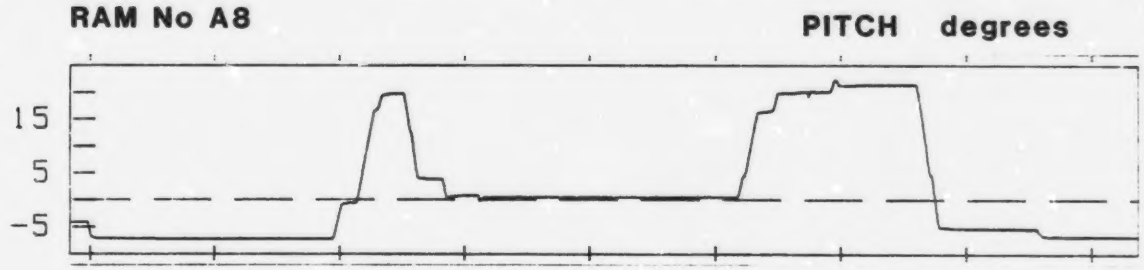

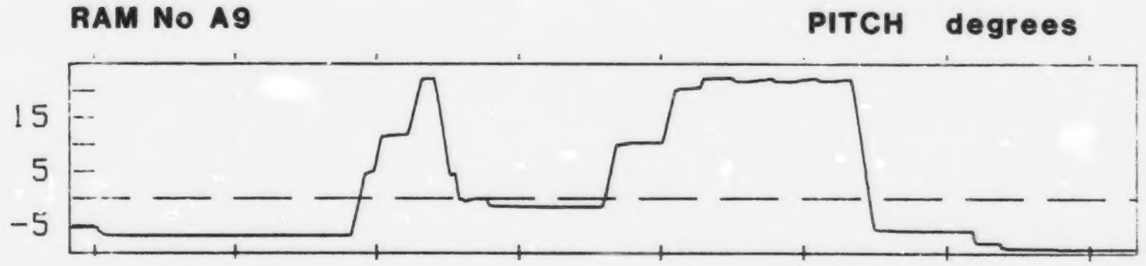

b) Time losses at the end of the ram (extraction) may be reduced significantly from up to 29% to levels close to zero.

c) The penetration time percentage appears to vary linearly with $\bar{v}_a$.

d) The acceleration time varies within a narrow band and ranges between 14 - 31% of the cycle time, and is 20% on the average at higher rates of programs.

e) The backing time varies in a wide range from 35 to 68% and this appears to be an area of possible optimization as it represents the largest part of the ramming cycle time.

The above trends are corroborated by plotting the effect of speed of impact on cycle time components as shown in Figure 6.12. From the mean lines defined on the plots of Figure 6.11 and Figure 6.12 it is possible to identify typical profiles and possible optimum profiles as shown in Table 6.2. Let us select an average speed of advance of 0.05 and 0.5 knots and from Figure 6.11 we can determine typical cycle time proportions as listed in the table. Now let us recall the optimum speeds of impact from Section 6.2.2 being 4.85 and 4.0 kts for both cases respectively. The acceleration distances from Figure 6.1 are 109 and 94 meters and the penetration distances, from Figure 6.5 are of the order of 115 m and 15 m respectively. Now refer to Figure 6.12 and determine the cycle time components and their percentages. Two optimum cases have been derived:

° Optimum (1): for optimum v_0 without optimization of power levels, etc. but with time losses eliminated.

° Optimum (2): same as optimum (1) except that as typical time loss is added.

Based on these results we may observe the following:

a) Optimizing for v_0 only can improve the speed of advance by:

12% in thick ice, $h = 1.57$ m
34% in very thick ice, $h = 2.55$ m

b) Optimizing for v_0 and eliminating extraction time loss, the improvements become: 18% and 70% respectively.

Proper optimization of the ramming strategies by eliminating unnecessary time losses and operating at the optimum speed levels in backing, acceleration and penetration can be much more effective than the levels defined above. Still improvements ranging between 12 to 70% can have a significant impact on the overall economics of operation of a ship like the MV ARCTIC. It should be noted that the total cycle time, and hence fuel consumption would be reduced through optimization.

FIGURE 6.11 RESPONSE CYCLE COMPONENTS

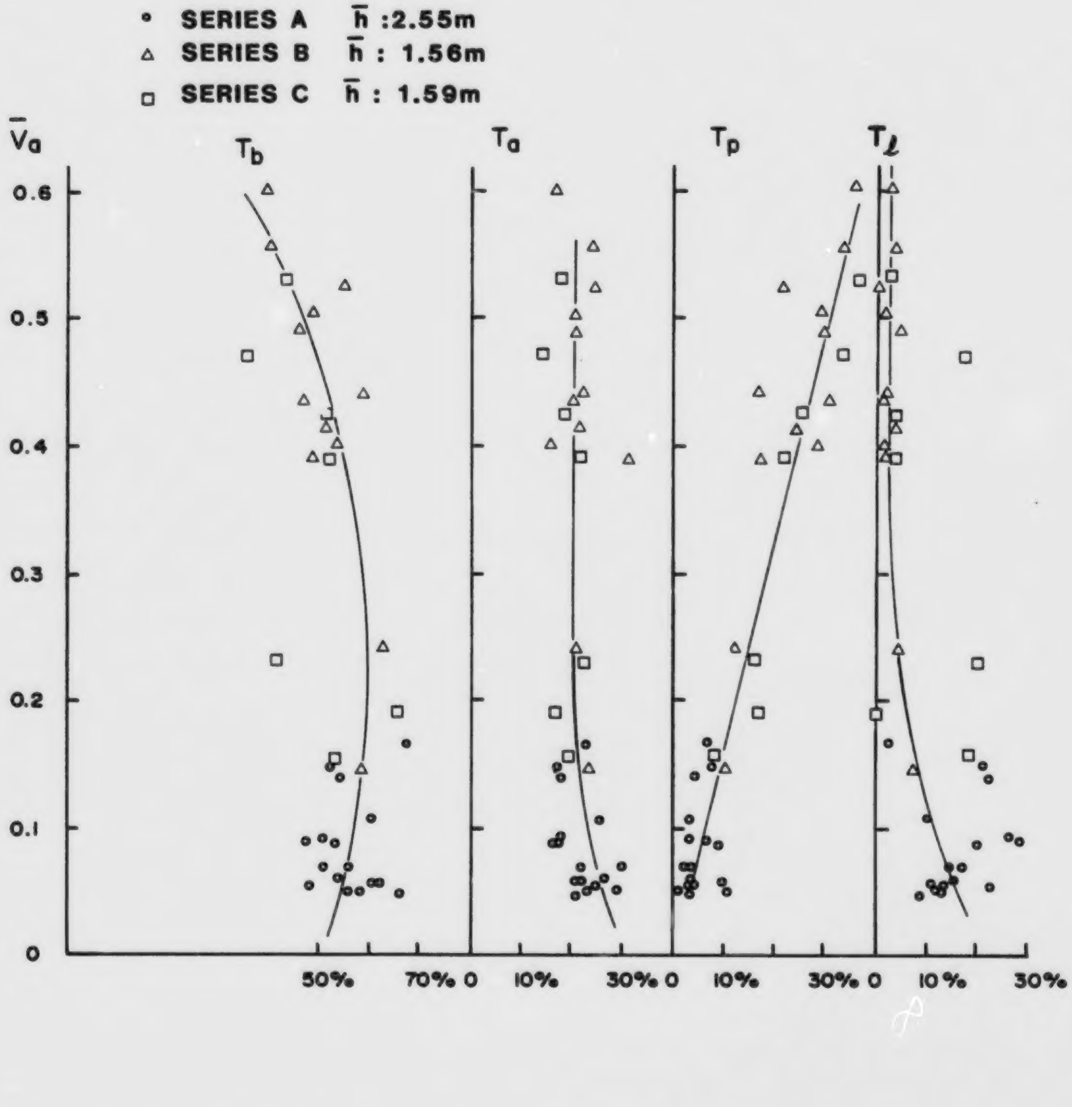

FIGURE 6.12

EFFECT OF IMPACT SPEED ON CYCLE COMPONENTS

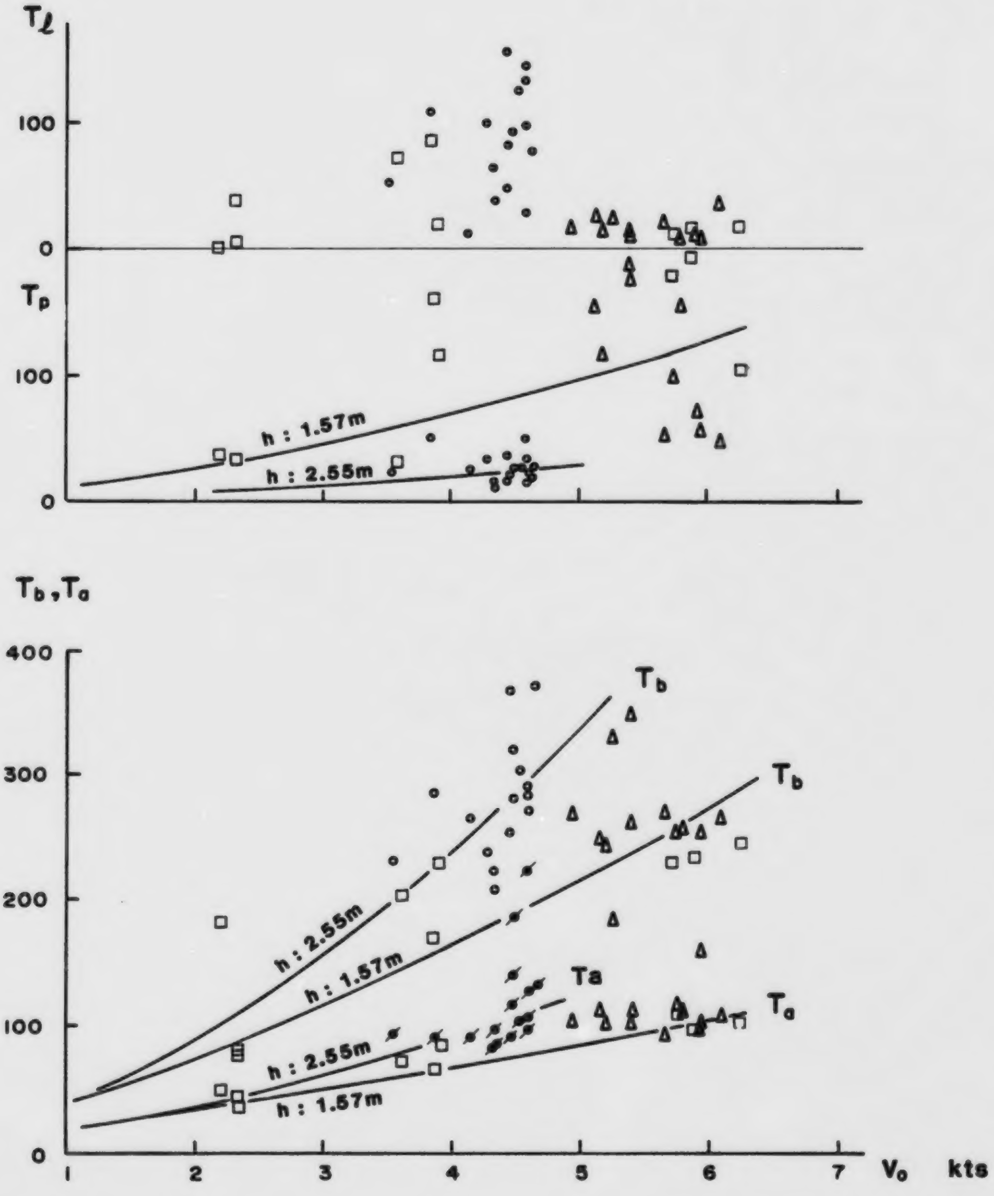

TABLE 6.2

TYPICAL RAMMING CYCLE PROFILES FOR MV ARCTIC

CASE	THICK LEVEL ICE h = 1.57 m			VERY THICK LEVEL ICE h = 2.55 m		
	TYPICAL	OPTIMUM (1)	OPTIMUM (2)	TYPICAL	OPTIMUM (1)	OPTIMUM (2)
$\bar{v}_a$ kts	0.5	0.59	0.56	0.05	0.085	0.067
T_b	46%	(208) 55%	(208) 52%	54%	(235) 69%	(235) 54%
T_a	20%	(82) 22%	(82) 21%	26%	(90) 26%	(90) 21%
T_p.	30%	(90) 23%	(90) 22%	3%	(18) 5%	(18) 4%
T_1	4%	(0) 0%	(20) 5%	15%	(0) 0%	(90) 21%
Total	100%	(380)seconds 100%	(400)seconds 100%	100%	(343)seconds 100%	(433)seconds 100%

6.3 Performance Simulation

Simulation of ship performance may be accomplished by using the model developed by Nawwar [11]. The model uses closed form formulations applicable to any stage within the ramming cycle. The model requires the following formulations as input:

- Equations for total thrust as a function of ship speed at any given power level in the range of interest or a single formulation of thrust as a function of power level and ship speed.
- Expressions for the resistance of ice to ship motion ahead and astern in broken channel and ahead in unbroken ice.
- Ship mass (at operating draft).
- Definitions of the ramming cycle breakpoints which may be defined in several ways such as durations or speed limits. In the present study, the durations of the various cycle components may be used as a basis for the break points, i.e. the action cycle is used as input to obtain the response of the ship.

To demonstrate the application of this powerful method, we will regenerate Ram No.C6 and compare it with the actual measurements. In order to accomplish this we developed formulations, specific to the MV ARCTIC, for thrust and resistance. These are presented in the following subsections.

Table 6.3 gives a summary of the MV ARCTIC thrust and resistance formulations which are described below. It should be indicated that these formulations are based on the MV ARCTIC characteristics as observed in the previous analysis. For instance, the resistance in broken channel was based on empirical formulation and observed acceleration performance in broken channel. Therefore, minor inefficiencies are inherent in the present formulations. However, the same methods can indeed be used to simulate the optimised performance of the MV ARCTIC by using the relevant resistance formulations.

TABLE 6.3

SUMMARY OF MV ARCTIC THRUST AND RESISTANCE FORMULATIONS

a) Thrust at full power ahead:

$$T(v) = 1.558 - 0.1520\ v + 0.006455\ v^2 \qquad (6.3)$$

b) Thrust astern at different power levels:

$$T_{AST}(v) = 0.473 - 0.04594\ v, \text{ at 5 MW} \qquad (6.4)$$

$$T_{AST}(v) = 0.597 - 0.03866\ v, \text{ at 7.5 MW} \qquad (6.5)$$

c) Broken Channel Resistance Astern:

$$R_{BI}(\text{ASTERN}) = 0.036276\ h^2v + 0.011251\ h^2v^2 \qquad (6.6)$$

d) Broken Channel Resistance Ahead:

$$R_{BI}(\text{AHEAD}) = 0.035714\ h^2v + 0.011251\ h^2v^2 \qquad (6.7)$$

e) Level Ice Resistance (Ram C6 only)

$$R_{LI} = 1.80 + 1.0356\ v \qquad (6.8)$$

where: v = ship speed, m/s

h = ice thickness, m

6.3.1 Thrust Formulation

The total or effective thrust of the MV ARCTIC has been determined in Chapter 4 based on model scale experiments. Equations (4.6) and (4.7) are not suitable for the purposes of the ramming simulation since they are not expressed quadratic functions of ship speed. Therefore, we used the model data at 10.97 m draft to determine Equation (6.3), Table 6.3,for total thrust at full power ahead in MN.

In the astern mode we considered ship backing at two different power levels and due to the lack of data points we had to assume that the thrust is reduced by 30% and 20% for power levels 5 MW and 7.5 MW at an astern speed of 6 kts. Equations (6.4) or (6.5) may be used at the proper power level.

6.3.2 Resistance Formulations

Ryvlin's equation for resistance in broken channel has been specialized for the MV ARCTIC and the actual data was used to determine the closest estimates of ice concentration in the broken channel as well as the size of the broken floes.

It was found using measurements of impact speed vs acceleration distance that:

a) The concentration of ice in the broken channel behind the MV ARCTIC was likely less than 60 percent.

b) The average value of the parameter (rh) is equal to $7h^2$.

c) The friction factor used to develop the coefficients was 0.2.

After a series of trial and error runs, it was possible to develop a general formula for the MV ARCTIC resistance (in MN) in broken channel given by Equations (6.6) and (6.7) in Table 6.3.

The difference between ahead and astern resistance is small and is primarily caused by the small difference in forebody and aftbody waterplane coefficients. However, these resistance estimates should be verifiable from steady speed resistance test runs (continuous mode) in broken channels of ice of different thicknesses.

Figure 6.13 illustrates the prediction line of acceleration distance based on full thrust and equation (6.7) and its good fit with actual data is shown.

The level ice resistance during the penetration stage was established from linear regression of actual estimates during the ram C6 and is given by Equation (6.8). No generalized level ice formulation was developed during this study.

FIGURE 6.13

PREDICTED VERSUS MEASURED ACCELERATION DISTANCE

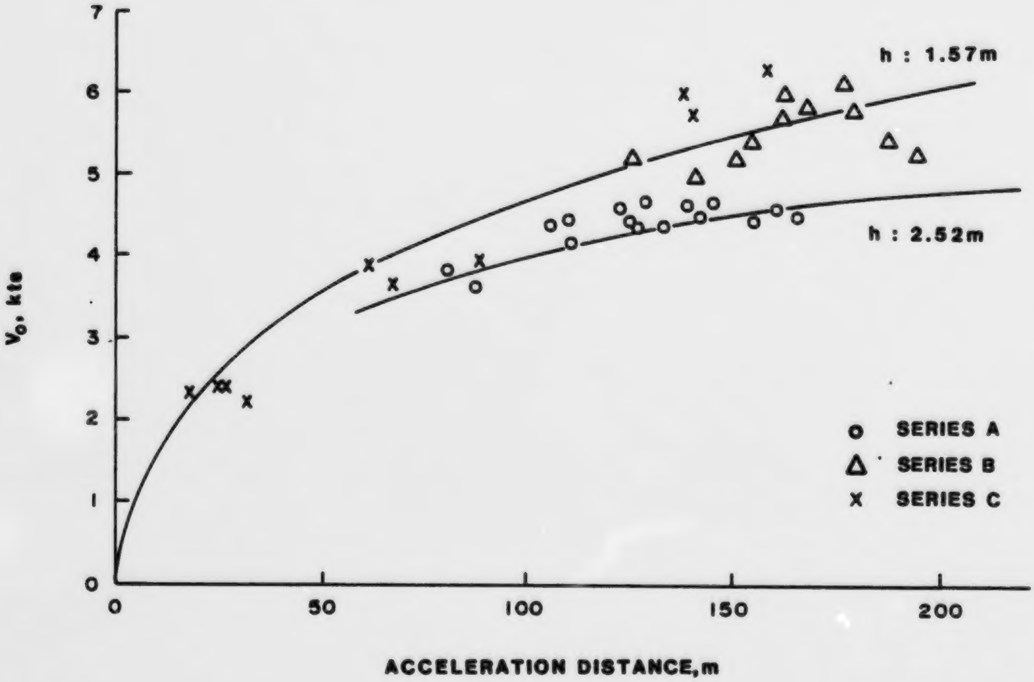

6.3.3 Ramming Cycle Simulation

Using the ramming model [11] with input from thrust and resistance equations given in Sections 6.3.1 and 6.3.2 it is possible to regenerate the velocity and penetration histories of the MV ARCTIC. In this section, this will be demonstrated using Ram C6 as an example. The following particulars may be given:

- ice thickness = 1.56 m
- flexural strength = 104 kPa
- speed of impact = 6 kts as reported in [21]
  = 6.25 kts as determined in the present study
- Average speed of advance = 0.40 kts as reported in [21]
  = 0.389 kts as determined here

The ramming "action" cycle was controlled from the bridge by changing the pitch, and hence total thrust. Table 6.4 (a) is a summary of the sequence of events which will be used to run the simulation.

The backing stage involves acceleration astern in broken channel under 7.5 MW power level. From A to 1 at point 1 the reversal of the thrust starts and lasts approximately 47 seconds. During this time interval the thrust drops from maximum astern to zero at an intermediate breakpoint BP, then it increases from zero to maximum over a short interval followed by braking to zero speed at Point B when the backing progress ends and the ship reverses direction to accelerate in the broken channel. Therefore, during backing the speed is constantly negative while the thrust changes direction. The durations of the various segments of backing were established as measured in this study. From the action cycle the time intervals for A-1, 1-BP and BP-2 have been established. The limit control parameter for the remainder of the backing stage was not time but a zero terminal speed at point B.

TABLE 6.4

SIMULATION OF RAM NO. C6

(a) RAMMING CYCLE LIMITS

STAGE	POWER (MW)	DESCRIPTION	THRUST	RESISTANCE	DURATION (sec)
Backing (A-1)	7.5	V $R_{BI}(AST) \rightarrow$ 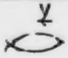 $\leftarrow T_{AST}$	Eq.(6.5)	Eq.(6.6)	145
(1-BP)	Transient	$R_{BI}(AST) \rightarrow$ $\leftarrow \frac{1}{2} T_{AST}$	$\frac{1}{2}$ x Eq.(6.5)	Eq.(6.6)	29
(BP-2)	Transient	$R_{BI}(AST) \rightarrow$ $\rightarrow \frac{1}{3} T_{AHD}$	$\frac{1}{3}$ x Eq.(6.3)	Eq.(6.6)	18
(2-B)	10.0	$R_{BI}(AST) \rightarrow$ $\rightarrow T_{AHD}$	Eq.(6.3)	Eq.(6.6)	(1)
Acceleration (B-C)	10.0	$T_{AHD} \rightarrow$ $\leftarrow R_{BI}(AHD)$	Eq.(6.3)	Eq.(6.7)	(2)
Penetration (C-A)	10.0	$T_{AHD} \rightarrow$ 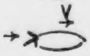 $\leftarrow R_{LI}$	Eq.(6.3)	Eq.(6.8)	(1)

Footnotes:
(1) Speed control. Final Speed = 0 at end of interval.

(2) Distance control. Acceleration Distance = backing distance

(b) COMPARISON OF RESULTS BY VARIOUS METHODS

STAGE		SIMULATION (sec)	TAPE (sec)	VIDEO [21]	SIMULATION WITH THRUST CUT OFF
Backing A-1	Duration	145	145	-	145
1-BP		30	29	-	30
BP-2		18	18	-	18
2-B		36	53	-	36
Backing total		229	246	235	229
Acceleration		124	102	120	124
Penetration		91	102	100	39
Extraction (losses)		18	18	-	18
Total Cycle duration, sec		462	468	455	410
Acceleration Distance, meters		239	158	-	239
Penetration Distance, m		87.1	93.55	97	52.6
Average speed of advance, kts		0.366	0.389	0.40	0.249
Speed of Impact, kts		6.35	6.25	6.0	6.35

The simulation was than conducted for the ramming cycle, and the results are shown in Figure 6.14. It is shown that in general it compares well with the overall performance as presented in Section 5.2. In fact Figure 6.14 is a better representation of the ram since it excludes the anomalies observed at the beginning of backing and end of acceleration. Such anomalies were primarily created by the errors in the doppler speed record.

Now we will compare some of the results of the simulated ram with the results of this study and the field measurements reported in [21]. Table 6.4.(b) gives such comparison. It is shown that the overall prediction of the cycle time is very good while the prediction of the penetration distance, which is very sensitive to level ice resistance, is approximately 10 percent less than the video distance and 7 percent less than the tape estimates. This reflects on the average speed of advance. Therefore, it may be suggested that the resistance of level ice be revised downward or an acceptable level ice resistance equation be utilized instead of Equation (6.8). The impact speed, according to MV ARCTIC performance in level ice, is consistant with tape estimates and suggest that the speed of impact is higher than what is reported in [21] for Ram C6.

Using this simulation technique it is also possible to study the effect of thrust cut-off on impact as shown in Figure 6.14 and Table 6.4.(b). This predicts a reduction of 32 percent in the speed of advance due to thrust cut-off on impact.

It should be noted that a more precise simulation may be achieved by better simulation of the reversal characteristics of the MV ARCTIC. It also provides a powerful means of investigating the effect of improved ramming strategies in quantitative manner. For instance, the effect of reversal time, backing power, backing distance, etc.

FIGURE 6.14 REGENERATED SPEED-PENETRATION PLOT FOR RAM No C-6

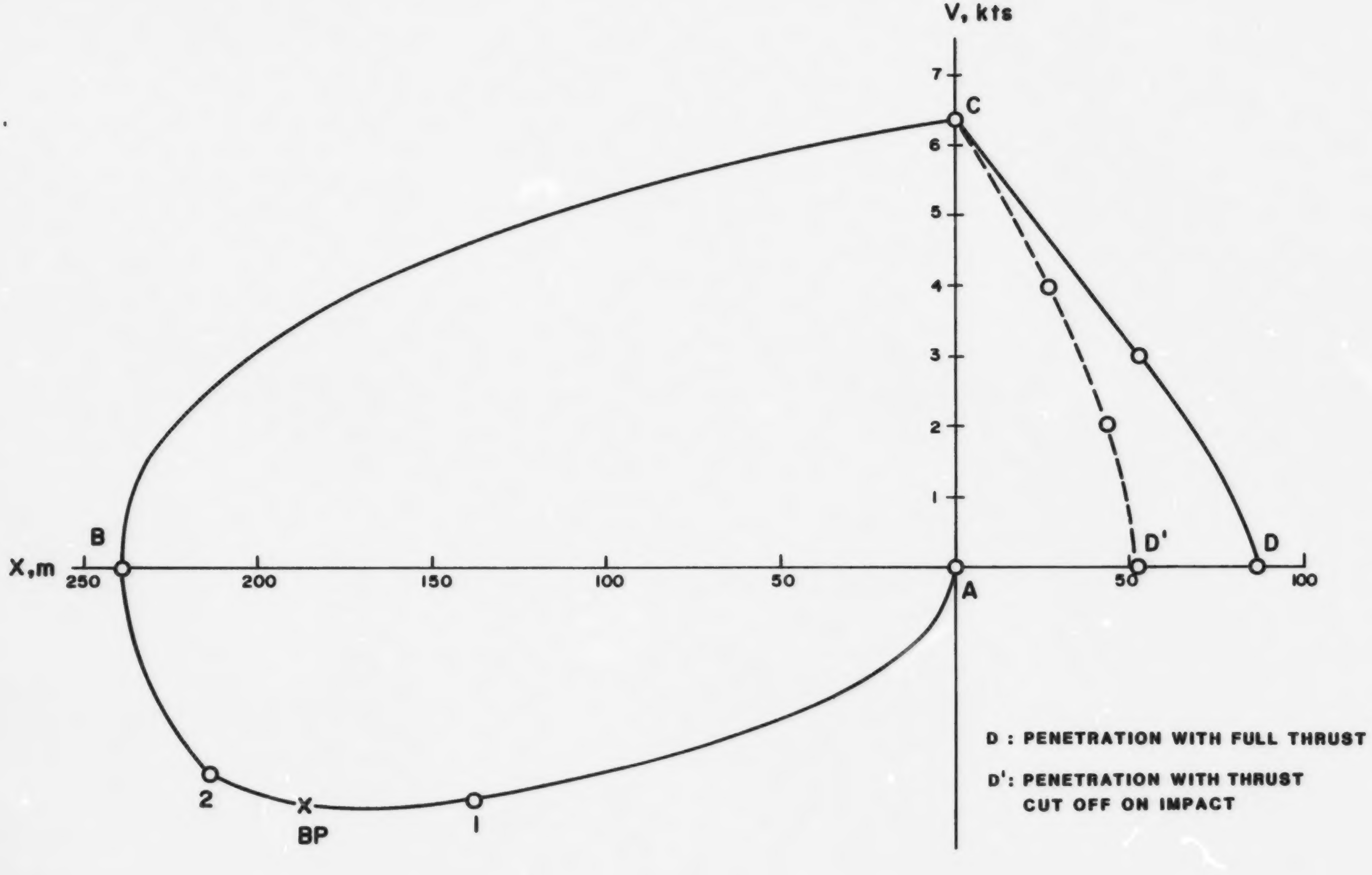

6.4 MV ARCTIC Capabilities

6.4.1 Ramming Cycle Components Analysis

Review of the results of the preceeding analysis and the graphical output in Appendix C has indicated that the ship has not been operated to demonstrate the maximum capabilities in the ramming mode under the trial conditions. Referring to the concept of action cycle and response cycle, it is the action cycle that needs optimization, while the maximized response to the optimized action has to be established. Therefore the ramming process was divided into the following components, which after idealizing could be used to compose an idealized ram:

Component	Action	Response
astern mode	astern power astern mode time	astern mode distance backing speed
stopping	pitch reversal ahead power	stopping distance stopping time
acceleration	ahead power	impact speed
penetration	ahead power pitch reversal	penetration distance penetration time

A relationship between the action components and the response components that was considered achievable and would maximize the ramming performance, has been determined from the results of the data analysis for each stage separately. All ramming incidents that were included in this evaluation have been reviewed for the following items:

- distance and time for penetration, acceleration, astern mode, stopping,
- impact and backing speed,
- ahead and astern power and operation effectiveness, including thrust cut-off
- pitch reversal operation and duration,
- extraction time and other time losses,
- ice thickness,
- bubbler operation and trim.

The evaluation was carried out using the graphical presentation of the data for each stage. The graphs are included in Appendix E and show the trends of the relationships between the various parameters. The trends have been developed on the basis of a combination of practical and theoretical considerations for the following conditions:

- full power (10.5 MW) in ahead mode,
- 5 MW and 7.5 MW in astern mode,
- fast and efficient pitch reversals,
- ice thickness 1.6 m and 2.5 m,
- mainly based on data for bubbler on with level keel and bubbler off with bow up

From evaluation of each ram individually it was found that a number of rams appear to be well executed. They have been identified in Appendix E. Generally speaking, Series B and C have been reasonably executed, but the ship operation during the Series A was poor from a viewpoint of performance with reference to progress speed. Mostly the indecisive behaviour from the time of pitch reversal during the backing phase to the actual start of the acceleration phase accounts for most losses in time. Comparing the speed of advance of the trial performance in Figure 6.4 with the speeds achieved through optimized ship operation in Figure 6.15 may illustrate the difference in performance.

6.4.2 Ramming Optimization

Using the trends obtained for each stage of the ramming cycle, Figure 6.15 was obtained by creating a composite of the four stages which in the end would give a speed of advance and fuel mileage for every selected impact speed. This procedure is illustrated in Appendix E and consists of the following steps:

- select impact speed,
- determine penetration distance and time,
- determine required acceleration distance and corresponding duration,
- determine combination of astern mode and stopping distance to match the required acceleration distance,
- determine time components for astern mode and stopping,
- determine total cycle time, including minimum standard losses as a result of pitch reversal at the end of the penetration phase,
- compute speed of advance in meter per hour and the fuel mileage in nautical miles per tonne fuel.

Two power combinations and two ice thicknesses were used in producing Figure 6.15. The figure shows that the optimum for speed of advance and for fuel mileage essentially coincide at about 6.3 kts in 1.6 m ice and about 4.0 kt in 2.5 m ice, irrespective of the astern power level. The trends have been expanded to other ice thicknesses which resulted in Figure 6.16, showing the optimum speed of advance and fuel usage versus ice thickness.

6.4.3 Power Level Variation

In addition to the power levels mentioned in Section 6.4.1, three more power level combinations were considered: two combinations with a higher and lower astern power and one combination with a lower ahead power level. They are included in Figure 6.16. This shows that high astern power gives higher speed of advance while lower astern power results in better fuel mileage. A reduction of power level in the ahead mode during a ram is detrimental to both progress speed and fuel economy and should therefore not be adopted.

As Figure 6.17 illustrates, the power level applied in the astern mode can be used for trade-off between fuel mileage and speed of advance. It seems that the practical range of power level is around 5 MW to 7.5 MW. In less thick ice the speed of advance can be increased

FIGURE 6.15 SPEED OF ADVANCE AND FUEL MILEAGE VERSUS IMPACT SPEED

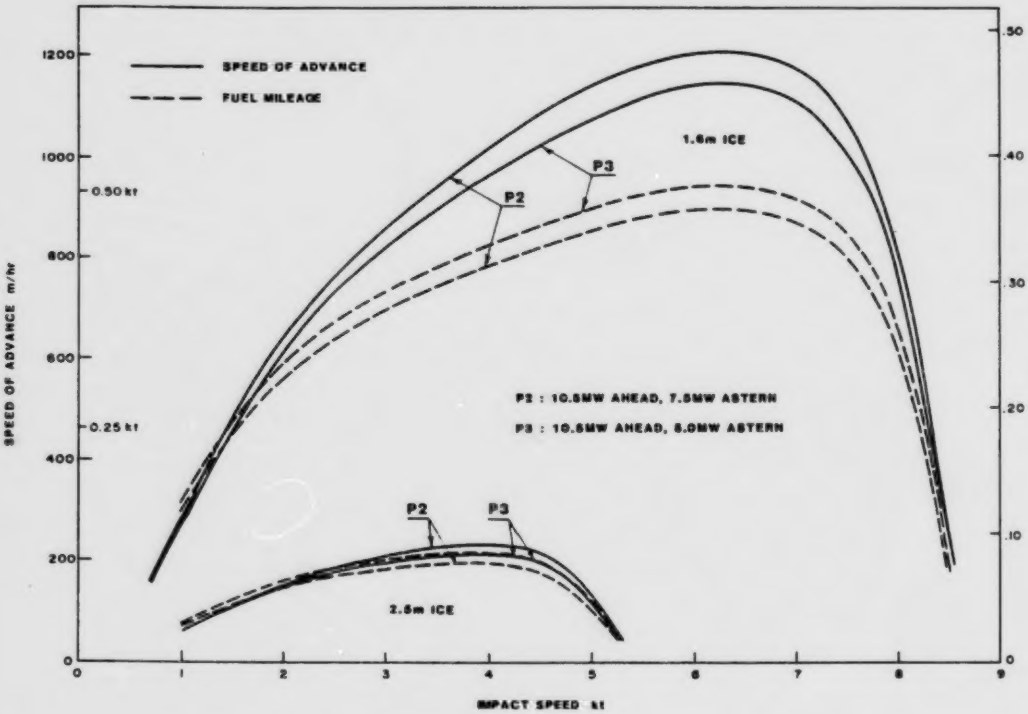

FIGURE 6.16 OPTIMUM SPEED OF ADVANCE AND FUEL MILEAGE VERSUS ICE THICKNESS

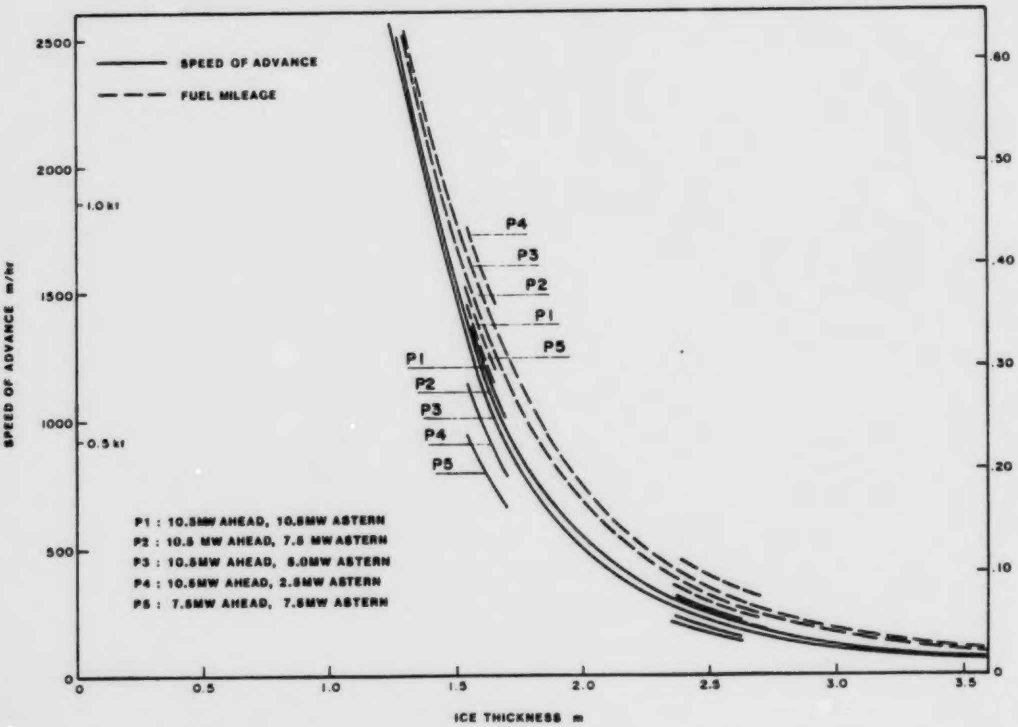

FIGURE 6.17

EFFECT OF ASTERN POWER ON SPEED OF ADVANCE AND FUEL MILEAGE

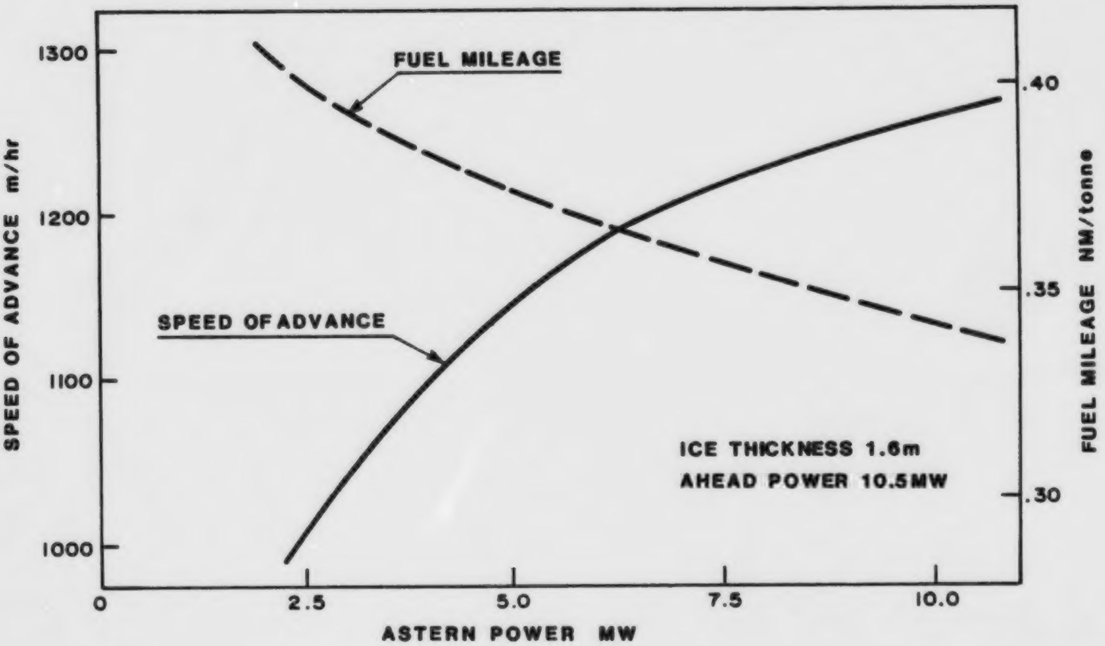

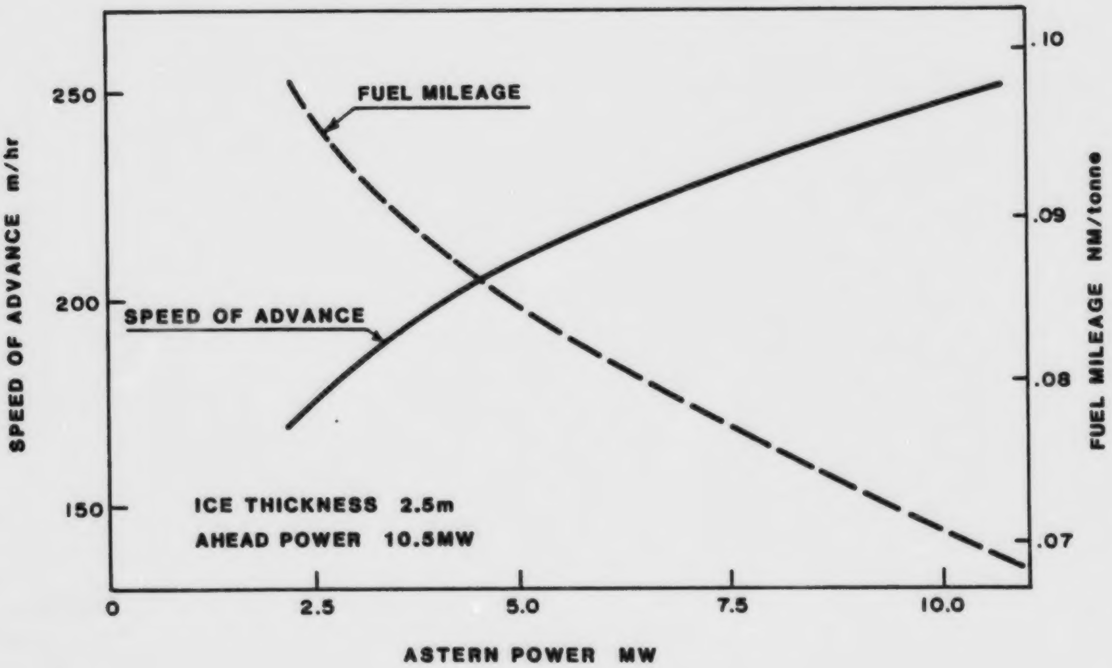

by increasing power with a relatively smaller penalty than in thick ice, in which fuel can be saved by reducing power with a relatively small loss in progress speed.

A good combination of power levels is full power ahead (10.5 MW) and 7.5 MW astern. This combination is used in further evaluation of the performance of the MV ARCTIC in the ramming mode.

6.4.4 Transition Zone

Through extrapolation of the trends to smaller ice thicknesses, Figure 6.18 was reconstructed. The trends indicated that the MV ARCTIC might be operating continuously at very low speeds in ice thinner than about 1.28 m. The continuous mode line in Figure 6.18 was obtained from the mean of the level ice resistance as per Nawwar and Edwards and as per MV ARCTIC Voyage (based on Poznyak and Ionov) illustrated in Figure 2.3 of Section 2. Both speed of advance and fuel mileage have been plotted in Figure 6.18, which indicates that the transition point is at an ice thickness of about 1.08 m.

6.4.5 Ridge Breaching

The results of trend development were used to estimate the ridge penetration capabilities of the MV ARCTIC. Although the penetration characteristics were essentially determined for level ice conditions, it is assumed that the ridge can be approximated by an effective thickness and width.

Figure 6.19 illustrates the ridge breaching capabilities under four ice conditions. Two of those are in 0.8 m and 1.0 m ice thickness when the ship is operating in the continuous mode. The other two represent the ship operating in the ramming mode in 1.6 m and 2.5 m ice broken channel, where the impact speed is taken at 85 percent of the maximum speed in the broken channels. The requirements for ship operation are indicated in the Figure.

The range of first year pressure ridge proportion as they may be found in nature is indicated on the figure by the hatched zone. It is shown that in 2.5 m thick ice, while the MV ARCTIC will be operating in the ramming mode it will not be capable of breaching the smallest possible ridge in a single ram and it will require several rams, to accomplish this depending on the ridge size. In 1.6 m thick ice, the MV ARCTIC can breach smaller ridges having an effective thickness in the range from 2.8 m to 4.1 m in a single ram only if it backs up a distance well in excess of twice ship length and accelerate to an impact speed of 7.5 kts.

FIGURE 6.18 TRANSITION CONTINUOUS RAMMING MODE

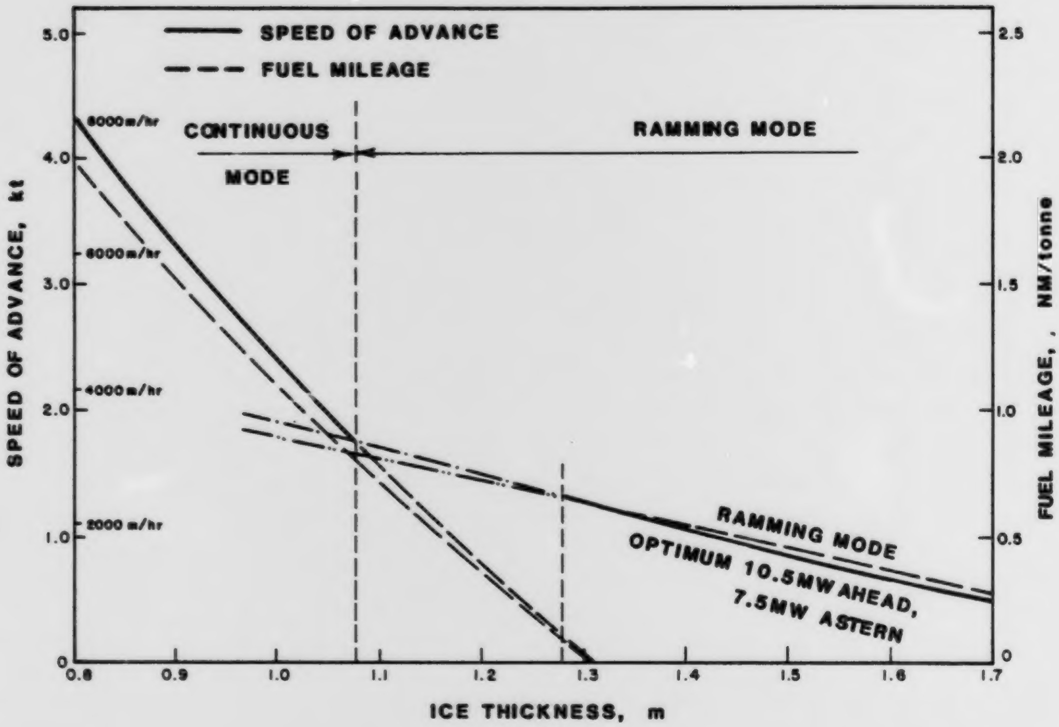

FIGURE 6.19 RIDGE BREACHING CAPABILITIES

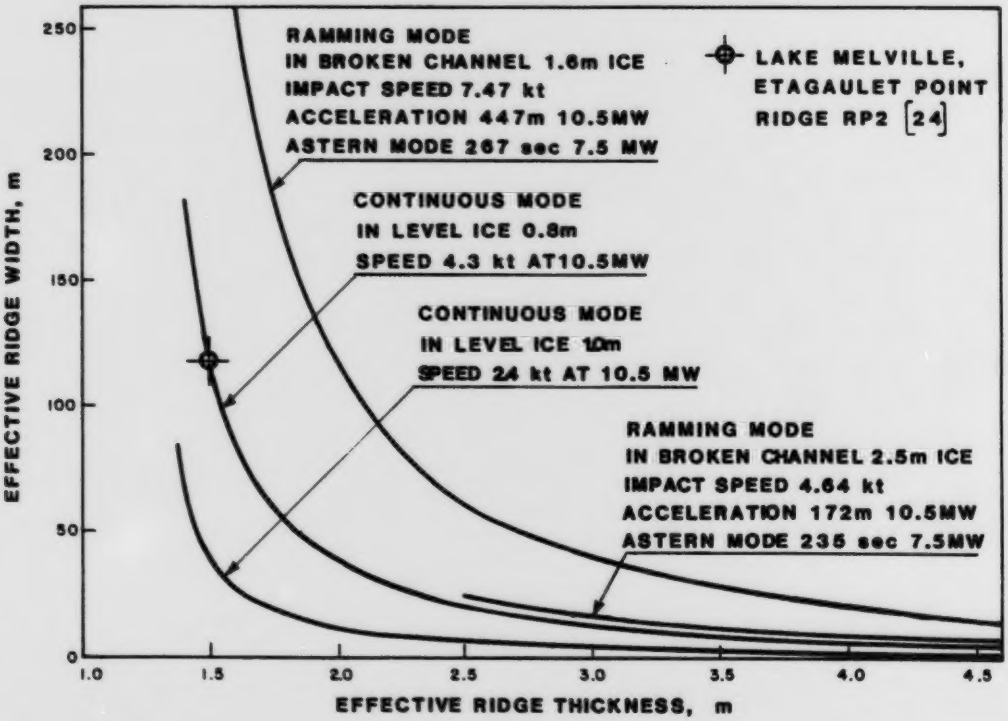

During Lake Melville Trials [24] it was observed that the ship could penetrate a pressure ridge by ramming once. The MV ARCTIC would penetrate into the ridge at an approach speed of 2 knots, then a single ram was necessary at an impact speed of 3.0 - 4.0 knots to completely clear the ridge and begin to accelerate to its operating speed in level ice. On one occasion the ridge was 120 m wide and had a consolidated depth of 1.5 meters. The surrounding ice thickness was less than 1.0 meter on both sides of the ridge. The effective ridge thickness was estimated to be 1.5 meters including the unconsolidated keel. This ridge is marked on Figure 6.19. Based on the figure the MV ARCTIC would be capable of breaching the ridge without stopping if it was proceeding continuously at a speed of 4.3 knots. From experimental observations [24] the ship speed on contact with the ridge was 4.3 knots and on exit at 115 meters it was 1.40 knots (without stopping).

This example demonstrates the applicability of this figure to verify actual experimental observations.

7. EVALUATION OF OPERATIONAL ASPECTS

7. EVALUATION OF OPERATIONAL ASPECTS

7.1 Power Requirements

Schedule G of the Arctic Shipping Pollution Prevention Regulation deals with the power requirements for Arctic class ships. The schedule has been amended in 1977 and this amended version will be used as a basis for this analysis.

According to the procedures of Schedule G, the minimum power requirement is 4.2 MW. The installed power is 11 MW which means that the MV ARCTIC is 162% overpowered. The ship is Class 2, therefore the minimum power would be necessary to propel the ship through 0.61 m thick ice.

With the over power the ship is capable of proceeding continuously through thicker ice. The maximum continuous ice thickness the ship can progress through with its installed power may be estimated from Schedule G as follows.

$$P_r = (579.4 - 2.6\sqrt[3]{W})\, BA^2 \qquad (7.1)$$

where

P_r = SHP
W = Ship displacement in tons at operating water line
B = maximum breadth at operational water line
A = ice thickness index = ice thickness in ft.

Therefore, the ice thickness is proportional to the square root of the power, and hence

$$\sqrt{\left(\frac{11.0}{4.2}\right)} = \frac{A_{max}}{2} = \frac{h_{max\ (meters)}}{0.61}$$

Therefore, the maximum ice thickness the MV ARCTIC can progress through in the continuous mode is 0.987 m, say 1 meter.

This shifts the transition to the ramming mode upwards and indeed the MV ARCTIC has been observed to break ice 1.07 m thick continuously.

The installed power level gives the MV ARCTIC greater ramming mode capabilities. An estimate of the effect of over power is presented in Figure 7.1 which is based on Equation (6.2). The installed power was considered to be equivalent to 50 mm average fuel rate in the ramming mode of operation while the CASPPR power was considered 38.2% of the installed power which is equivalent to 19.1 mm. It is shown that the installed power permits an improvement in advance speeds of about 162%. It is interesting to note that for given rates of progress the thickness of ice varies significantly depending on the available power as given

FIGURE 7.1

COMPARISON OF THE EFFECTS OF INSTALLED VERSUS CASPPR LEVELS

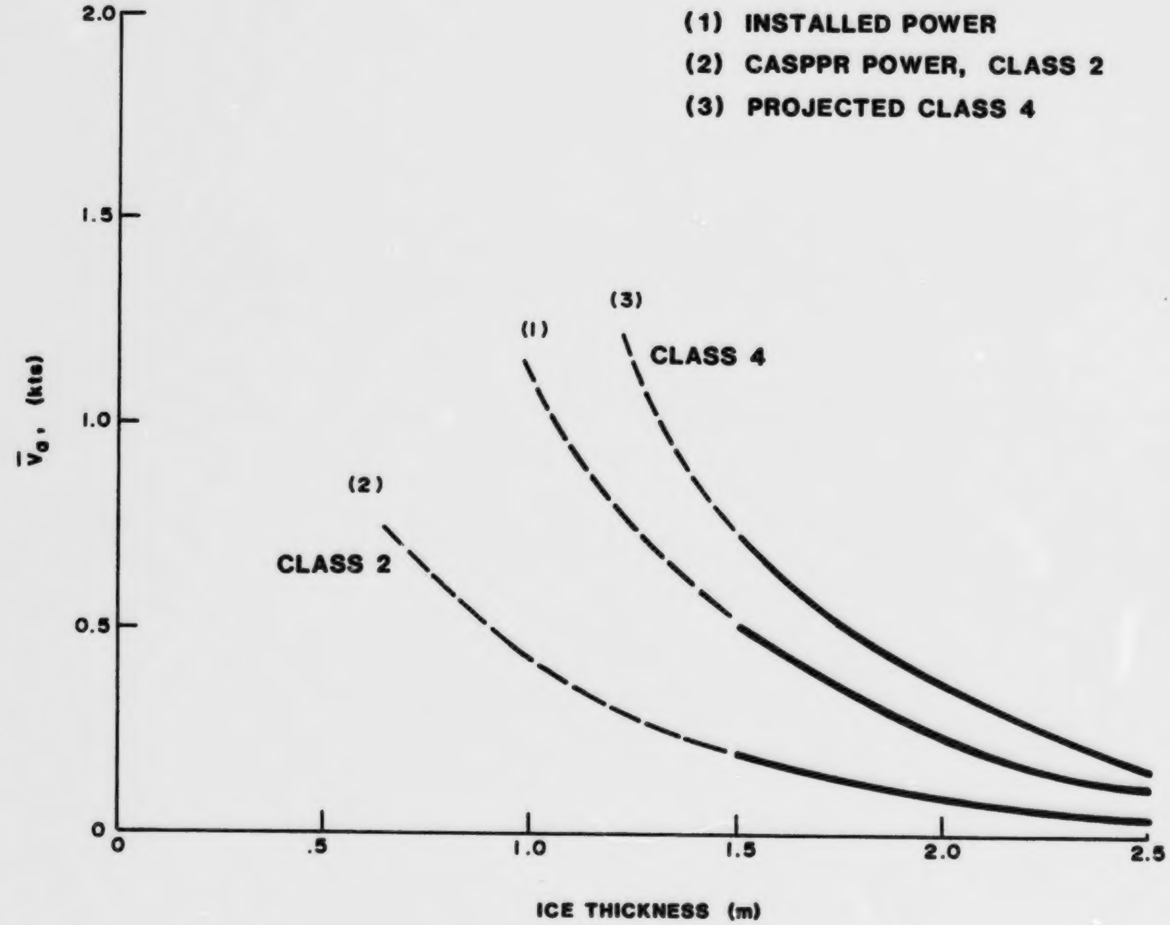

in Table 7.1.

TABLE 7.1

v_a, kts	h_{max}(installed Power)	h_{max}(CASPPR Power)	Ratio
0.05	3.06	2.43	1.26
0.1	2.60	1.97	1.32
0.2	2.15	1.51	1.42
0.4	1.69	1.05	1.61

The improvement is quite obvious in the range closer to transition but the advantage of higher power continues to decline as the ice gets thicker. However, there is an extension of the ship capability by about 25% due to over power.

7.2 Design Features of the MV ARCTIC

The MV ARCTIC has been designed with some unique features for an ice class ship. These include the bubbler system, the propeller nozzle and others.

From the point of view of ramming operations efficiency, we have been able to conduct a limited evaluation based on the core database for the bubbler system and bow trimming. These evaluations, which may be found in Chapter 6, have shown that both bubbler and trim affect the MV ARCTIC performance to varying degrees. However, due to the limited database no rigorous quantitative assessment could be made.

However, it is interesting to note that while trimming the bow upwards would increase the stem angle, it would also change all the angles along the waterline. The flare angle would generally increase and this promotes bending failure of the ice along the hull. Therefore, despite the increase in stem angle which is generally detrimental to ice resistance the refinement of the waterline and flare angles would produce a combined benefit.

A better understanding of the influence of design features in the ramming mode could be achieved by using the MV ARCTIC ramming simulation method described in Chapter 6.2. Once a resistance formulation in level ice could be developed, which includes important features such as hull geometric parameters, an assessment of their influence can be made. For instance, using Nawwar and Edwards level ice resistance equation (See Chapter 2) one would account for the waterline geometry through the coefficients μ_1 and μ_2 as well as the forebody block coefficient. Changing the trim, draft or friction factor can be expressed in terms of the geometry friction coefficients (given in Chapter 1 for the base operating condition). Hence the effect of various trim levels. It should be noted that the resistance in broken ice astern is likely to increase due to increased trim level (bow up) and, hence, the overall performance in ramming could be predicted through simulation and without the effects of scatter associated with full scale results.

7.3 Instrumentation System and Data Acquisition System

The instrumentation and data acquisition system was designed for use over a wide range of ship operations. With regards to the specific operating condition of backing and ramming, the system was deemed to have performed quite well with respect to a number of measured parameters. Unfortunately, the few areas where the system's performance was felt to be lacking, were coincidentally, the most important ones for the analysis of backing and ramming.

Data acquired on shaft torque, shaft thrust, shaft rpm and propeller pitch were found to be of high quality and reliability. Throughout the three shipping seasons shaft RPM was not operational the entire time, but when operating gave quite acceptable results.

Probably the single most important parameter for ramming cycle analysis is ship speed from which distance, acceleration and resistance are derived. Inaccuracies in the ship speed record therefore, have a crucial impact upon data analysis. The problems posed to this study by an inadequate speed record have been quite challenging.

Portions of the speed records were found to be unreliable and these were evidenced by large excursions which could not be rationalized and had to be deleted from the data base.

With respect to the overall quality of the speed record; resolution and overall accuracy were not good enough to directly calculate distance, acceleration and resistance. This made a number of data smoothing and correction techniques necessary. The accuracy of the speed record when the ship is travelling astern is questionable as no calibrations were performed. This astern inaccuracy is substantiated by the finding that the calculated distance in backing rarely equates to the ahead distance to ice impact.

The measuring range of the speed data was set to 0 to 30 knots. This resulted in a loss of accuracy and resolution at the low speeds primarily of interest to this study. The sampling rate used throughout dedicated tests was either 1/10 sec or 1/sec. This rate presented problems in defining speed during short penetration rams. A doppler radar unit with faster update capabilities and digital filtering techniques would probably be better suited for this type of study.

A number of recommendations can be made as to improving the accuracy of the speed data. A second doppler radar unit should be employed to serve as a check for the primary unit. This second unit should have an operational range of 0 to 16 knots for improved low speed accuracy, and be aimed astern (the primary unit is aimed ahead). With proper calibration techniques both ahead and astern, the two units should combine to give reliable results. It is also suggested that a fixed view video camera be employed to provide very accurate speed and distance measurements at speeds below 3 knots.

Additional problem areas in the data record include fuel rack, bubbler status, and ship trim. Fuel rack position is not a direct measurement of fuel rate and when used to determine rate, produces unreliable results. A better solution is to incoporate a flow meter in the fuel line for direct measurement. Uncertainties as to the true bubbler status and ship trim arise from the fact that these are manually recorded data. Direct measurement of the two would provide one with a more positive feel of those data.

To summarize the above discussion on instrumentation system deficiencies:

(a) Method of speed measurement was inadequate for the purposes of monitoring transient speeds during ramming.

(b) Sampling rates for speed was inadequate and in the future a sampling rate of at least 10 Hz is recommended particularly for short rams in thick ice. Other channel sampling rates were acceptable.

(c) Channels which require manual input should be eliminated and data acquisition be accomplished automatically through logic circuits.

(d) Fuel measurement was inadequate and resulted in interpretation problems.

In addition to the above diagnosis, it is extremely useful to the analyzer as well as the designer to have proper documentation of the ice characteristics. Time must be allowed during the trials for complete documentation of the ice characteristics. While this cannot be attributed to lack of equipment or appreciation, the test plan and test director must pay proper attention to documentation of ice characteristics. An excellent example of comprehensive documentation of ice may be demonstrated by the POLAR CLASS test program, which is co-sponsored by Transport Canada. An example of pressure ridge documentation is illustrated in Figure 7.2. In fact, ice documentation during Lake Melville trials was better than Admiralty Inlet trials.

FIGURE 7.2

SAMPLE PRESSURE RIDGE PROFILE

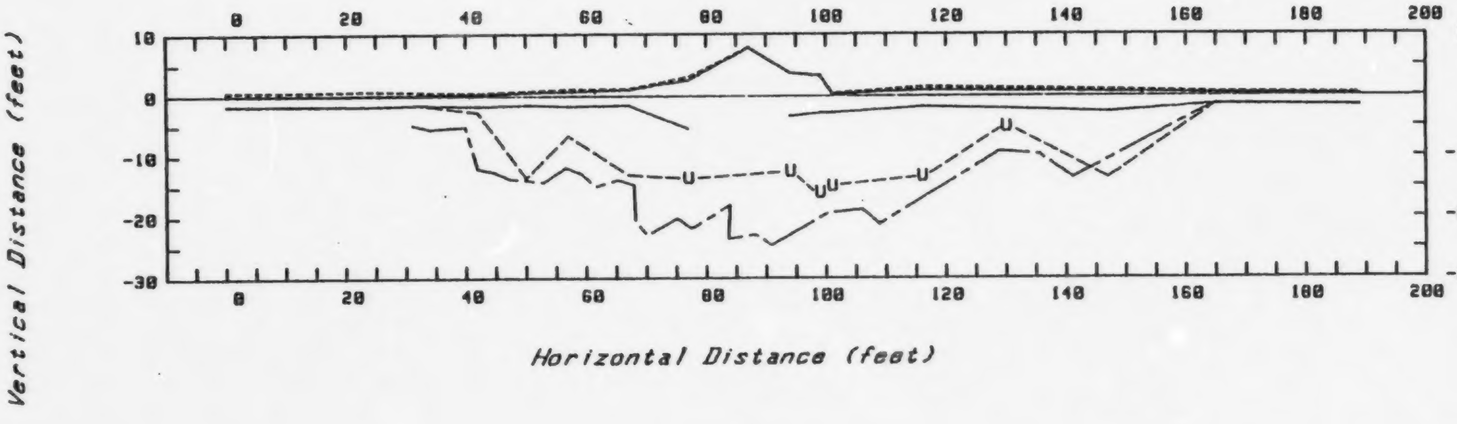

PRESSURE RIDGE NO. 20
(First-Year)
Position: Lat. 64° 16.8′ N
Long. 169° 6.9′ W
4/25/82
Floe Drift: Spd. .4 kts.
Course 120° True

Snow Cover: ----------------------------
Solid Ice Surfaces: ____________________
Total Depth By Drilling: — — — — — — — —
Sonar Depth: ___ - ___ - ___ - ___
C: Consolidated Depth, Ice Below
U: Unconsolidated Depth, Ice Below

7.4 Ramming Strategy

The capabilties of the MV ARCTIC as presented in Section 6.4 can be approached if not achieved only under strict operational procedures, which summarized are:

- prompt and decisive operation,
- proper selection of intended procedure of ship operation, based on ice conditions,
- application of full power ahead,
- fast and efficient pitch reversal,
- maintaining full power during the penetration, with start of pitch reversal to astern pitch just before the ship comes to a halt.

The selection of the ship operation procedure can be made using Figure 7.3, which is drawn for only one power combination. The figure shows the various ship operation parameters, of which only the astern mode time depends on the astern power. The other parameters are fixed by the ahead power. The required astern mode time (time from start of backing of ship to start of fast pitch reversal to ahead pitch) and the acceleration distance (obtained at the end of the backing phase and required to achieve the optimum impact speed) can be read from the Figure for the ice thickness.

For example for ramming with full power ahead and a power level of 7.5 MW astern in ice thicknesses of 1.6 m and 2.5 m, the following procedures should be adopted:

- ice thickness (m)	1.6	2.5
- required optimum impact (kt)	6.35	4.0
- required acceleration distance (m)	192	75
- duration of 7.5 MW power astern (sec)	162	130
- fast pitch reversal to full power ahead for stopping and direct start of acceleration		
- speed of advance (Figure 6.16) (m/hr)	1120	230
- fuel mileage (Figure 6.16) (NM/tonne)	0.358	0.077

This procedure may be used for ramming in the transition zone for ice thicknesses between 1.0 m and 1.3 m when the speed of advance in the continuous mode is low or the probability of stoppage is high. When the operational cut-off point for ramming is set at a speed of advance of 0.03 knots, which is about 60 meters per hour or one third of the ship length per hour, then the upper limit for ice thickness is estimated about 3.6 m.

The fuel mileage can be increased by reducing the astern power at the expense of speed of advance (see Figure 6.17). In that case only the astern mode time will have to be adjusted to match the required acceleration distance.

It should be noted that efficient execution and good timing of the astern mode followed by the stopping maneuver, are crucial in reaching the desired acceleration distance without unnecessary time losses. Then full power should be applied during the entire acceleration phase to

FIGURE 7.3 RAMMING STRATEGY

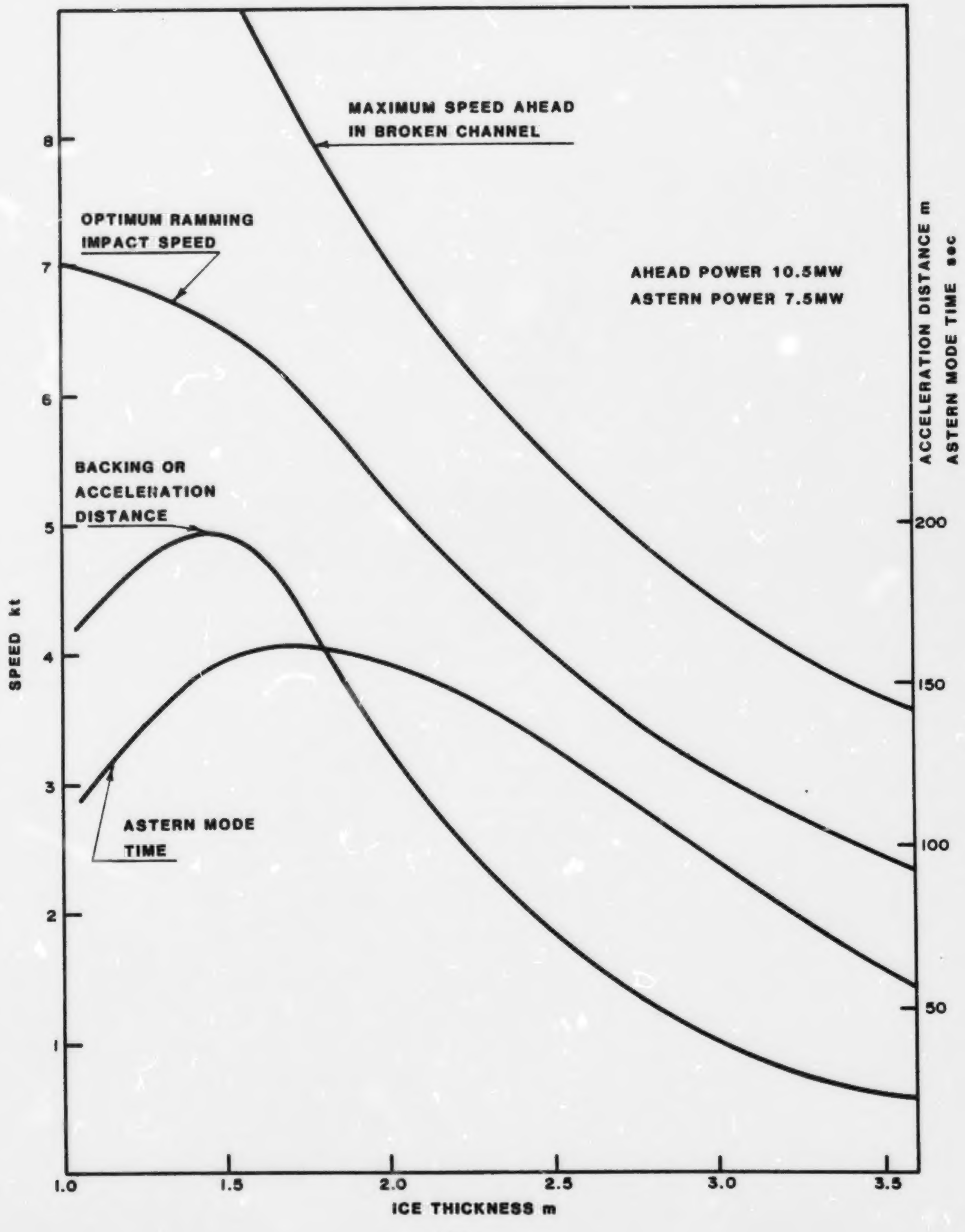

achieve the optimum impact speed within the acceleration distance. Also during the penetration phase, full power operation is effective as long as the ship makes penetration progress. Towards the end of the penetration phase the progress is slow. Therefore, this time can be better used for pitch reversal in preparation for the start of the next ramming cycle.

Losses could be built up of small seemingly innocent relaxations of the above mentioned procedure. A typical case for the earlier given examples may be, estimating the losses as a percentage of the speed of advance:

- ice thickness (m)	1.6	2.5
- 5 percent lower power ahead	9%	11%
- 10 seconds extra extraction time	2%	3%
- 15 seconds during stopping maneuver	3%	4%
- 5 percent extra acceleration distance	1%	1%
- delayed power-up during acceleration	3%	4%
- total loss in speed of advance	18%	23%

The astern power level is not considered since this involves a trade-off between speed and fuel mileage. Under the reasonable assumption that the amount of fuel used remains unchanged, the above percentages may also give an indication of the losses in fuel mileage.

The ridge breaching capabilities of the MV ARCTIC without being stopped while the ship is in the continuous mode are given in Figure 6.19 of section 6.4.5, where effective ridge thickness is plotted against effective ridge width. In addition, the breaching capabilities of the ship when operating in the ramming mode are shown. The approach speed through the broken channel is taken at 85 percent of the maximum attainable speed shown in Figure 7.2. Figure 6.19 also provides the requirements for operational procedures in terms of acceleration distance and astern mode time.

As far as the bubbler status and trim of the ship is concerned, the evaluation of the results of the data analysis did not lead to a conclusion as to what effect these factors may have on the performance. The trends that were used to estimate MV ARCTIC's ramming capabilities, have been developed on the basis of data points for bubbler on, level keel, and for bubbler off, bow up. Both conditions appeared to show no detectable difference in performance. Evaluations of data points for other conditions, bubbler on with bow up and bubbler off with level keel, were not conclusive due to scatter or insufficient number of data points. However, direct comparison of the trial results indicate a positive effect of the bubbler on and bow up on the speed of advance, which cannot be quantified.

8. CONCLUSIONS AND RECOMMENDATIONS

8.1 Conclusions

Based on the methods developed during this study and the analysis of a limited number of ramming cases obtained during dedicated trials in the Admiralty Inlet, 1980, the following conclusions may be made:

a) The overall quality of the data was generally good. The data base has proven to be very suitable for analysis, the results of which provide a better understanding of the ramming process as well as an indication of the potential for improvement of performance.

b) Data reduction instrumentation and methodology were developed and applied successfully to most cases. However, two major shortcomings were encountered and were related to:

   i) Poor accuracy and reliability of the doppler log records particularly during backing and at low speeds.

   ii) Insufficient data on ice conditions and particularly on pressure ridge characteristics.

c) The speed of impact significantly influences the average speed of advance. There exists an optimum impact speed for every ice thickness. When adopting optimum ramming strategy, a speed of advance of 0.65 knots or 1210 m/hr can be achieved in 1.6 m level ice with an impact speed of 6.35 knots. In level ice with a thickness of 2.5 m, an optimum impact speed of 4.0 knots can result in a speed of advance of 0.124 knots or 230 m/hr. The values are for full power ahead and 7.5 MW astern.

d) The bubbler system appears to have an influence on the MV ARCTIC performance in the ramming mode. However, it does not appear to offer a distinctive economic advantage. The assessment was necessarily qualitative due to the size and distribution of the core database during dedicated trials.

e) The ship trim was tested in two conditions; bow up and level trim. The former case was notably advantageous in very thick ice (or pressure ridges). Insufficient data was available for evaluation under different conditions. However, the bow up position appears to have an equal effect as the bubbler but it is more economical to use.

f) Thrust cut-off during ramming is a detrimental practice in ramming. Based on analysis and results of the present study, thrust cut-off adversely affects the speed of advance without offering a corresponding economic advantage (in terms of proportionally lesser fuel consumption).

g) The fuel mileage (NM/tonne) is directly related to the ice thickness in an exponential form. It is also shown that the fuel mileage is directly proportional to the speed of advance.

h) Performance components were optimized to determine the maximum capability of the MV ARCTIC. The following has been found:

  i) In level ice ramming the maximum ice thickness is of the order of 3.6 m.

  ii) In first-year pressure ridges in 1.6 m thick ice, the MV ARCTIC can breach ridges having an effective thickness of 2.8 to 4.1 m. In thick ice cover any first year ridge will slow the progress to unacceptable levels.

i) Performance predictions based on trend analysis have indicated that the performance of the MV ARCTIC in the ramming mode of operation would be better in both speed of advance and fuel mileage with a higher installed power. A power increase of 10 percent would improve the speed of advance by 10 percent and the fuel mileage by about 5 percent. The use of reduced power in ramming operations would reduce the performance with approximately the same percentages.

j) The transition point for continuous to ramming mode is estimated at an ice thickness of 1.08 m.

k) Based on cycle time analysis it is concluded that the MV ARCTIC performance in ramming can be improved significantly by: optimization of impact speed, increasing the power level during backing in broken channel, minimization of thrust reversal intervals (a major source of hidden time losses) and elimination of time loss at the end of a ram. These measures DO NOT require any expensive refitting or improved hull geometry, they only require the proper application of the best ramming strategy.

l) Performance simulation of the MV ARCTIC ramming performance has been successfully demonstrated. Proper performance simulation is instrumental in developing proper understanding of the key elements of a successful ramming strategy.

m) Models for the MV ARCTIC broken channel ahead and astern have been developed.

n) The installed power of the MV ARCTIC is greater than CASPPR minimum requirements. It first extends level ice continuous mode capability to 1.0 m and at this thickness it improves the ramming performance by 162 percent. The effect of over power decreases to 126 percent at a speed of advance of 0.05 knots.

8.2 Recommendations for Designers and Operators

Based on the results of this study, a few recommendations may be made to aid in design and operation of similar ships in the future.

From a design point of view it may be recommended that:

a) The stern design should be modified to minimize ice resistance to ship motion astern. While this does not impose a penalty on icebreaking efficiency ahead, it can significantly influence the ship performance in ramming.

b) A hull design which leaves lesser ice in the channel is more desirable if the ship is to operate in the ramming mode for a significant length of time. Basically a lower broken channel resistance should be sought and a compromise design may be necessary.

c) Measures should be taken in the bow design to prevent wedging at the end of a ram. Particular attention should be paid to ice under lateral pressure. Low friction coatings may be used to minimize the possibilities of wedging under normal conditions of operation thus minimizing the time losses.

d) The propeller design requires a balance between service speed in open water and ice going conditions which depends on the operational profile. In the case of the MV ARCTIC, the nozzle design is important. The nozzle is a good feature for highly loaded propellers and provides additional thrust which is extremely beneficial in the ramming mode. It usually means a small disadvantage at service speed in open water. The MV ARCTIC nozzle apparently optimized for ahead mode, is a compromise of low and high speed while the performance is sacrificed in the astern mode. This is reflected in the relatively low effective thrust developed while going astern, which degrades the ramming performance. A nozzle also reduces propeller ice milling although the nozzle propeller is more expensive than an open propeller, it has to be considered in the overall ship design especially when the ship is required to operate under ice conditions. When the ramming mode of operation forms an important aspect of the operational profile of the ship, it may be worthwhile to consider a propeller/nozzle design that is optimized for low speeds ahead and astern, to improve the ramming capabilities.

From an operations point of view we may recommend:

a) Successful ramming strategy can be adopted through proper selection of optimum impact speed, based on ice conditions, determination of the required procedure of ship operation based on power and fuel constraints, and accurate and decisive execution of the procedure with fast pitch reversals, avoiding time losses between backing and acceleration phase or at the end of the ram prior to the start of the next ram.

b) Utilization of full power ahead without hesitation or interruption is essential, since otherwise both speed of advance and fuel mileage will be lower.

c) Utilization of astern power is a matter of trade-off between speed and fuel economy. A power of 7.5 MW seems a good compromise.

d) Routing optimization can easily be accomplished onboard and in real time provided that the ship performance under various ice and environmental conditions are well understood and that ice and weather conditions can be made available to the ship as they become available. This is now possible via satellite communications and its usefulness is obvious.

e) If the vibration level in the astern operation imposes a restriction on the power level which can be applied in the backing mode, it may be worthwhile to investigate the causes of such vibrations and eliminate them. The only limitation is vibration caused by external sources such as propeller ice milling which can only be dealt with through design modification.

f) A test program in case of future trials should be set up with the results of this study in mind to confirm the MV ARCTIC performance predictions and to expand the present data base.

8.3 Recommendations for Supplementary Evaluation

The present study has addressed several key aspects of the MV ARCTIC ramming mode performance. However, there are some areas which may be recommended for supplementary evaluation of the vessel's performance which either were not directly addressed in the present work or were found to require better understanding and assessment. These areas are listed below:

a) Expansion of the database is recommended to include a wider range of variation of ice thickness, ice conditions, speed of impact, speed of advance, etc. The data available from the arctic voyages is not well documented in terms of ice conditions. Therefore, an alternative source of ice characteristics should be consulted to identify such conditions. It should be noted that the most influential ice quality appears to be the ice thickness. Hence, ice thickness could be estimated using ice growth calculations, side looking TV camera, occasional estimates made during the vogages. The quality numbers for such data may be lesser than those for dedicted trials but the size of the database can offset the quality problem of ice characterization particularly since we have a sufficient core database with better quality (of ice measurements).

b) Conduct a more detailed analysis of level ice ramming. Should the ice thickness database be increased, the formulations of the MV ARCTIC resistance in broken channel ahead and astern should be corroborated by the additional data. Level ice resistance formulations from the continuous mode study may be examined for incorporation in ramming simulation. The larger database should incorporate nontypical penetration cases in ice thickness in the vicinity of the maximum continuous mode limit.

c) In the analysis of ramming performance, the resistance has been determined from the net forces acting on the ship. The inertia forces were determined from the accelerations of the ship. The effective thrust was calculated from the results of model tests conducted in open water. Here, the effective thrust was defined as being the net force acting on the ship developed by the propulsion system. The relation between the propeller shaft thrust and the effective thrust is determined by the propeller/hull interaction which in general is expressed in terms of wake fraction, thrust deduction and relative rotative coefficient. In case of the MV ARCTIC which has a ducted propeller, this relationship has become more complex due to the effects of the nozzle on the thrust characteristics. Usually the propeller/hull interaction is determined from model test results often on a basis of ship speed. Although the propeller loading normally has a small effect on the interaction, it is not always being investigated because of the limited practical use of this information. However, in the case of ship operation in ice covered waters, the propeller loading is significantly higher than for normal open water conditions. The overload model experiments conducted for the MV ARCTIC have proven to be essential for performance analysis under ice going conditions. The results of the experiments showed that the usual method of assessment of effective thrust was not adequate for all power levels at low speeds. Therefore it would be desirable to conduct such experiments for all ships concerning the assessment of the effective thrust in determining the ice resistance.

It would further be desirable to validate the performance predictions from the model tests by correlation with full scale trials. Especially at low speeds the scale effects have to be evaluated. Furthermore, the effect of ice on the propulsion parameter needs consideration, since the overload experiments have been conducted in open water.

For evaluation of ship performance in the ramming mode of operation, the astern propulsion performance is an important aspect. The overload experiments for the MV ARCTIC basically concerned the ahead direction. In the astern mode, only the bollard condition was tested. The results of more tests going astern would have been useful in completing the ramming performance evaluation.

Summarizing, on the propulsion aspect the following work would be valuable to the MV ARCTIC.

1. Additional overload experiments in astern mode.

2. Development of procedure to assess the effective thrust from shaft thrust measurements.

3. Correlation of model test results with full scale trials.

4. Investigation on scale effects and effects of ice on propeller/hull interaction.

d) The optimization of the ramming tactics presented here are based on trends developed from the available data. It is felt however that further corroboration of the results is needed. More specifically, astern thrust data, accurate fuel consumption figures and an expanded data base with reliable information on ice conditions are required to confirm the outcome of the initial trend analysis.

e) The analysis and prediction techniques demonstrated in this study have shown the value of the ramming data for the prediction and optimization of the MV ARCTIC's performance in the ramming mode. The techniques have the potential to be further developed on a wider basis which may lead to more general performance formulations that can be used to optimize the ramming procedures or to predict the performance of other existing or future design vessels (e.g. icebreakers, tankers.)

f) Pressure ridges are a major impedement for icebreaking ships, in general. In thinner ice, the ship may be capable of breaching smaller ridges without stopping but in thicker ice, the ship will likely resort to ramming to clear a ridge. Every ship has its own sensitivity to pressure ridges which is determined by bow length and geometry. Therefore, a ship with a long bow and high kinetic energy may not sense the difference between a large ridge and a cluster of smaller ridges or a hummock field. This is true despite the fact that the vertical force required to break the ridge probably remains the same. Therefore, in order to characterize the ridge penetration capabilities of the MV ARCTIC knowledge the specific ship performance should be related to known ridge characteristics. A sufficient description of the ridge may be given by sail height and width, provided that the data be analyzed by statistical means. That is to relate penetration requirements such as energy and maximum resistance to ridge characteristics which can be defined on the surface and without profiling. This approach was used successfully in previous studies, and can be complemented by detailed case studies as noted in the dedicated trials (particularly Ridge A). Such characteristics can be defined from calibrated masthead video camera, or by remote sensing data such as laser profilometer data (which may be readily available on the area of interest from AES files).

Therefore, it is recommended that a detailed study of cargo ship (MV ARCTIC) capability in penetration of pressure ridges be conducted. A comparison with icebreakers performance (CCGS LOUIS S.ST.LAURENT - available data and possibly U.S. Polar Class) may be possible.

REFERENCES

REFERENCES

[1] Boteler, D.J., Benjamin, A., and German, J.G., "MV ARCTIC Instrumentation and Data Collection System for Ship Operations in Ice - System Operating and Users Manual", 3 volumes, Transport Canada Report Nos. TP3097, May 1981.

[2] German, J.G., Benjamin, A., Stirling, J.F., and Quart, B.G., "MV ARCTIC - Master Data Package, Seasons 1979, 1980, 1981", Transport Canada Report No. TP3821, October 1981.

[3] Nawwar, A.M., Goossens, L., et al, "MV ARCTIC Ice Transitting Performance in the Ramming Mode", Interim Report 1364C-1, Transport Canada Report No. TP 5169E, January 1984.

[4] Kheysin, D.Ye., "On the Ice Navigation Speed of Ships in Extremely Solid Ice", Ice Navigation Qualities of Ships, ed. by Kheysin, D.Ie., and Popov, Iu.N., Translation, CRREL TL 417, August 1973, pp.19-30.

[5] White, R.M., "Dynamically Developed Force at the Bow of an Icebreaker", Ph.D. Thesis, MIT, 1965.

[6] Gill, R.J., Aboul-Azm, A., Terry, B.F., and Russel, W.E., "A Ship Transit Model for Passage through Ice and Its Application to the Labrador Area", SNAME Paper 8, STAR Symposium, Ottawa, June 1981.

[7] Peirce, T.H., "Arctic Marine Technology: A Review of Ship Resistance in Ice", RINA, October 10, 1978.

[8] Lewis, J.W., & Edwards,R.Y.Jr., "Methods of Predicting Icebreaking and Ice Resistance Characteristics of Icebreakers", Paper #5, SNAME Annual Meeting, New York, November 1970.

[9] Petrov, Ye Yu, and Kheysin, D.Ye., "Calculation of the Inertial Characteristics of Ships Floating in Ice", Proc. of the 14th Scientific and Engineering Con. of Gor'kiy Poly.Inst. Immeni Zhdanov (Shipbuilding Inst.)

[10] Rylin, A.Ya., and Tegkayeva, T.Kh., "Investigation of the Inertial Characteristics of Unsteady-State Motion of an Icebreaker in Ice", Ice Navigation Qualities of Ships, ed. by Kheysin, D.Ye. and Popov, Yu.N., Translation, CRREL 417, August 1973, pp.59-65.

[11] Nawwar, A.M. "On the Optimization of Ship Motion in Heavy Ice Conditions", Proc. 3rd Intl. Offshore Mechanics and Arctic Eng. Symposium, Energy-Sources Technology Conference & Exhibition, New Orleans, Louisiana, February 1984, Vol. II, pp.267-274. Also accepted for publication in ASME Transactions, Journal of Energy Resources in Technology in 1984.

[12] Kashteljan, V.I., Poznjak, I.I., & Ryvlin, A.Ja., "Ice Resistance to motion of a Ship", Sudostroenie, Leningrad, 1968 (translation).

[13] Enkvist, E., "On the Ice Resistance Encountered by Ships Operating in the Continuous Mode of Icebreaking", The Swedish Academy of Engineering Sciences in Finland, Report No.24, Helsinky, 1972.

[14] Laini, A., et al "Great Lakes Ore Carrier Series Ice Resistance Model Tests in Ballast Conditions",WIMB Report No.24, Sept.25,1975.

[15] Virtamen, J., et al, "Great Lakes Ore Carrier Series - Ice Resistance Model Tests Draft Variations", WIMB Report No.34, April 15, 1975.

[16] Edwards, R.Y.Jr., Major, R.A., Kim, J.K., German, J.G., Lewis, J.W., & Miller, D.M., "Influence of Major Characteristics of Icebreaker Hulls on Their Powering Requirements and Maneuverability in Ice", Paper No.12, SNAME Annual Meeting, New York, Nov.'76.

[17] Nawwar, A.M., & Edwards, R.Y.Jr., "Compilation and Analysis of Recent Icebreaking Model Test Data of a World-Wide Variety of Hull Forms", three volumes, FR211C, by ARCTEC CANADA LIMITED, submitted to Transport Canada R&D Centre, Montreal, January 1978.

[18] Poznyak, I.I., and Ionov, B.P., "The Division of Icebreaker Resistance into Components", SNAME Paper 19, STAR Symposium, Ottawa, June 81.

[19] Makinen, E., "Ice Resistance Measurements in Ridges with I/B APU in the Baltic Sea", Paper presented at the 3rd Int. Conf. on Port & Ocean Engineering Under Arctic Conditions, Univ.of Alaska, 1976.

[20] Carter, D., "Ship Resistance to Continuous Motion in Level Ice", Transport Canada, Transportation Development Centre Publication No. TP3679E, March 1983.

[21] MV ARCTIC 1981 (Early Season) Data Collection and Instrumentation, TP3632, prepared for TDC by Fenco Consultants Ltd. and Melville Shipping Ltd., September 1982.

[22] Mathews, S., Coldstream Maritime Inc., Private Communication, December 1983.

[23] MV ARCTIC, Results of Resistance, Propulsion and Overload Experiments Including Measured Duct Forces Model Hull 326, Model Propeller 68, National Research Council Ottawa, Report No. LTR-SH-349, May 1983.

[24] Dick, R.A., Thompson, E.W., Cheung, H., and Dixit, B., "MV ARCTIC Experimental Voyage to Lake Melville, Labrador, in February/March 1981", TP 3646, October 1981.

APPENDIX A

DETAILED RAMMING MODE FORMULATIONS

A.1 Ramming Mode Formulations

A.1.1 General

In Appendix A.1.2 the transition point concept based on Kheysin's analysis on 1973 [2][1] has been reviewed in conjunction with the development of a general solution for the ramming operation from a mechanics approach as proposed by Lewis and Edwards [6], Petrov and Kheysin [7], and Ryvlin and Tegkayeva [8] and other Russian investigators.

The theoretical method of determining the ice navigating capability, based on a single-contact scheme of the breaking of ice by an icebreaker, is briefly discussed in [2] by Kheysin and Popov. A formula for estimating the icebreaking capability of a ship in continuous motion in solid ice, was proposed by Runeberg in 1890. In analyzing the forces acting on an icebreaker in its static pressure against the ice, an analytical dependence was established between the magnitude of the vertical force on the stem and the propeller thrust:

$$P_{ZF} = T \frac{\cos\phi \cos\beta - f \sin\phi}{\sin\phi \cos\beta - f \cos\phi}$$

where ϕ = stem angle
β = flare angle in the vicinity of the stem (vertical is 90°)
f = ice-hull friction coefficient
P_{ZF} = vertical force on the stem

Later in 1946, Vinogradov used this formula in the theoretical method of estimating the ice navigating capability in the ramming mode. In solving the equation of the energy balance, when the breaking of ice by the stem occurs from acceleration due to the work of the propeller thrust and the kinetic energy of the moving ship, an expression was obtained for the vertical force on the stem:

$$P = a\,T + \{a^2T^2 + \frac{b}{C}\,\frac{D^2}{gH}\,v^2\,[1-(1-e^2)\sin^2\phi - v_1{}^2]\}^{\frac{1}{2}}$$

where $a = \dfrac{\cos\phi \cos\beta - f \sin\phi}{\sin\phi \cos\beta - f \cos\phi}$

$b = F_1\,(\phi, B, f)$

$e = F_2\,(\delta, \alpha)$

D = displacement
H = longitudinal metacentric height
v = speed of impact
v_1 = speed at the moment that the stem breaks the ice
e = righting factor during impact
α = waterplane coefficient
δ = block coefficient

---

[1] Reference numbers pertain to the list at the end of this appendix.

The various assumptions made in the derivation of the theoretical formulation reduce the practical value of this method. Other authors elaborated the above approach to more practical formulations.

The ramming mode of operation exists in the range of ice thicknesses from the transition point up to the ultimate capability of the ship which may be evaluated from the expression developed by White in 1965 [3]:

$$h_u = [F/c_1 . \sigma]^{0.5}$$

where c_1 is a geometric factor which depends on the cracking geometry and is approximately equal to 0.891, σ is the flexural strength of ice, and F is the maximum vertical force which can be generated by the impacting ship at the stem. The latter is given by:

$$F = 4450 \, v_i \, (WR.\Delta)^{0.845} \quad \text{, lbs}$$

where v_i is the impact speed in fps

Δ is the ship displacement in long tons

WR is a hull dimensionless coefficient known as White Ratio and is given by:

$$WR = 0.000234 \, (10.72 + \frac{B}{T}) \, (0.1833 + C_{wp}) \, (1.652 - C_B)$$
$$\times \, (6.14 - SAC^2) \, (0.725 - \mu) \, (1.718 - BA)$$

where B = ship beam

T = ship draught

C_{wp} = waterplane coefficient

C_B = block coefficient

SAC = spread angle complement in radians (in section between horizontal and shell)

BA = bow angle in radians (in elevation between horizontal and stem)

μ = coefficient of kinetic friction

In SI units, the maximum thickness h_u may be rewritten:

$$h_u = 8.600 \left[\frac{v_i(WR.\Delta)^{0.845}}{\sigma}\right]^{0.5} \quad , \text{m}$$

where v_i is given in m/s, Δ in metric tonnes and σ in KPa.

It can be seen that the maximum capability of the ship in ramming may be extended by increasing one of the following variables:

- ° Ship displacement
- ° The impact speed
- ° White's ratio through hull improvement which may involve one or more of the following approaches:
  - increasing the beam-draft ratio or the waterplane area
  - decreasing the block coefficient, spread and bow angles or hull-ice friction coefficient.

It is obvious that for operation in Arctic waters, a sizable ship will be required to cope with severe environmental conditions. Therefore, a ship with large displacment, say 125000 tons, will have an extended capability of 250% as compared to a 15000 ton ship provided that other variables remain unchanged. Increasing the speed of impact is a potential factor which can significantly improve the ultimate capability of an icebreaking ship. The speed can be increased by increasing engine power and improving the hull geometry and strength. White's ratio can be increased with some restriction. The best improvement can generally be achieved through lower friction factors.

A formulation using a "kinetic energy" concept was presented by Peirce in 1978 [5]. The reviewed resistance formulations in level ice were divided into two components, which led to a simplified equation for the steady-state icebreaking conditions:

$$\underset{\text{(TOTAL)}}{R_i} = \underset{\text{(YIELD)}}{R_y} + \underset{\text{(VELOCITY)}}{R_v} = \underset{\text{(THRUST)}}{T}$$

where the yield component represents the breaking and turning components in the ice resistance.

The process of ice sheet penetration during initial ice encounter was analyzed using a visual presentation in the form of a work diagram. Introducing the ice-resistance length, being the entrance length of the ship, the penetration of a ship in the ramming mode may be estimated by solving the equation:

$$T . l + KE . l/x = R_y.x$$

where T = the given propeller thrust
l = resistance length
KE = kinetic energy based on initial speed
x = penetration distance
R_y = yield component of ice resistance

The estimated penetrations are reported to show a reasonable degree of approximation to the observed full scale values, despite some uncertainties about ice-characteristics and ship displacement.

A similar technique of analysis was used to determine an expression for the minimum approach speed, required to breach a significant ridge. The effective width and depth, as well as ice properties were used in the level ice resistance expression in order to obtain the icebreaking resistance in the ridge.

A.1.2 Transition Point Concept and Ramming Optimization

In this section the transition point concept and generalized closed form formulations for the ramming mode of operation are described and discussed.

Reference: Nawwar, A.M., "On the Optimization of Ship Motion in Heavy Ice Conditions", Proc. of the 3rd OMAE (Offshore Mechanics and Arctic Engineering) Symposium, Paper No.61, New Orleans, L.A., Feb. 12-16, 1984. Also accepted for publication in ASME Transactions, JERT (Journal of Energy Resources Technology) in 1984.

ON THE OPTIMIZATION OF SHIP MOTION IN HEAVY ICE CONDITIONS

A.M. NAWWAR, Ph.D.
VICE PRESIDENT
ARCTEC CANADA LIMITED
KANATA, ONTARIO.

ABSTRACT

For a given ship, its speed in ice decreases as ice conditions become more severe until it can no longer move continuously. The transition speed concept provides a valid cut-off point below which a ship has to switch to the discontinuous or ramming mode of operation. Solutions for the continuous and ramming mode ship motions and an analysis of a typical ramming cycle are presented. A general solution valid for all stages of ramming is given. It provides a closed form equation which can be used both to study the influence of ship characteristics and operational tactics upon ship performance and to optimize ship motion in heavy ice conditions decreasing fuel consumption and transit time.

NOMENCLATURE

A_t, B_t and C_t = regression coefficients for thrust

B = ship beam

c_0, c_1 and c_2 = regression coefficients for resistance

F = force required to break ice cover
F_n = Froude number

g = acceleration due to gravity
h = ice thickness
K = coefficient (= $C_t \rho \xi b h$)
kN = kiloNewton
k_σ = stability coefficient

ℓ_0 = an arbitrary travel in terms of L (n.L)

L = ship length
M = moment per unit width of wedge
n = a proportionality constant ($n = \ell_0/L$)
P = probability; penetration
p = penetration
R = resistance
t = time
T = thrust
V = velocity
$\hat{v}_s$ = transition speed (at probability of stoppage = 0.5)
v_s = ship speed

X(v) = net external force

α = coefficient of linear dependence of resistance on speed
β = $\alpha . g/\Delta$
Δ = ship displacement
δ = 1, 0 or -1 depending on position within the ramming cycle
λ = average distribution density of impact pulses per unit time determined experimentally; added mass coefficient
ξ = penetration relative to ship length (=P/L)
σ_R = dispersion of the distributing force
ρ = mass density of ice

INTRODUCTION

Continuous motion of a ship in ice-covered water depends on the ice effect, ship size and available power. The presence of level or broken ice, will impede the ship motion, and require additional force for penetration and power to be expended to maintain ship progress at a specified speed. The ice thickness is a major parameter which governs the ship speed. Other parameters include ice type and strength, temperature, hull-ice friction, presence and depth of snow cover, lateral pressure in ice in addition to the extent of unevenness of the ice. This unevenness is caused by many features such as ridges, raftings, rubble fields or uneven growth which may be a result of snow drifts and accumulation, refrozen leads and other factors.

Usually the ability of a ship to proceed in ice is expressed in terms of a relationship between ship speed of advance and the thickness of level ice cover. A typical relationship is illustrated in Figure 1 in which three regions signifying three modes of icebreaking operations may be identified. In region I the continuous progress of the ship in level ice is possible assuming full power is always employed. The

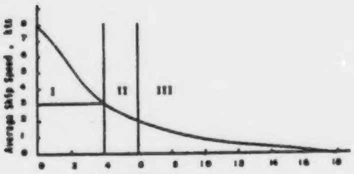

FIGURE 1

TYPICAL RELATIONSHIP BETWEEN THE SPEED OF ADVANCE AND ICE THICKNESS

speed of advance drops as the thickness increases until at some speed continuous progress at a reasonable speed may no longer be possible and this marks the transition to region II. Melberg et al (1) explain that this region, the transition region, extends possibly over a couple of feet of ice thickness. It is possible that the ship can maintain a constant, but low speed of advance in ice close to its limiting capability of continuous progress. However, this continuous progress is likely to be halted frequently. Upon backing, accelerating and impacting the ice, the ship may again be capable of maintaining continuous progress at low speed for a considerable length of time. As the thickness increases, the probability of the ship being stopped and forced to ram the ice increases until this mechanism ceases and region III is realized.

Region III is the ramming or discontinuous mode region in which the rate of progress is considerably low. This region extends up to the limit of the icebreaking capability of the ship at which most of the kinetic energy is transformed to potential energy and no significant progress is made.

Both the continuous and ramming modes of icebreaking are well defined. In the continuous mode, hull interaction with ice occurs all along the waterline from the stem to the section of maximum beam and trim angles and accelerations are usually small. Interaction models may be obtained for each ice type as a function of the hull geometry and environmental conditions. In the ramming mode of operation, the action of penetration occurs in the vicinity of the stem and forward bow sections and trim angles and accelerations are usually large which prompts a different formulation of the problem.

However, the process of icebreaking in the transition mode (in the vicinity of the limiting ice thickness) is difficult to express in mathematical terms. It is unstable continuous motion which is interrupted from time to time. Kheysin (2) studied the stability of motion in the transition range by employing analytical techniques which involve probability methods. His solution may be used to show that in region II the probability of ship stoppage in a given period of time or length of track is very small adjacent to region I, while very large when region III is reached. This implies that the frequency of stopping and ramming increases as the thickness increases.

For purposes of evaluating or comparing ship performance in ice, a relationship may be developed for the dependence of speed of advance on ice thickness, as exemplified by Figure 1. While the derivations in regions I and II are straight forward, there are two possible methods for developing this relationship in the vicinity of the transition region. The first method determines the most probable speed of advance based on a weighted average for different probable frequencies of stopping. The weighting factor is the probability of the ship stopping in a specified base time or distance. The second method introduces the concept of transition speed to provide a valid cut-off point between the continuous and ramming modes of operation. Effectively this method eliminates the second region and replaces it by a single point which marks the switching from continuous to discontinuous operation.

The first method is a statistical representation of physical occurrences and it represents a smooth transition between the two major modes. On the other hand, the second method represents no physical occurrence, and implies that the probability of stopping the ship is either zero or 1 at either side of the transition point.

In this paper the second method is adopted and the justification is provided. This is followed by solutions for the continuous and ramming mode transit and optimization.

TRANSITION POINT CONCEPT

On the basis of Kheysin's analysis (2) the transition point may be evaluated as follows:

The probability of stoppage of a ship moving steadily at a speed of v in a time t is given by:

$$P(v_s/o,t) = \exp\left[-\frac{2\alpha\Delta(\beta+\lambda)v_s^2}{gt\,\sigma_R^2}\right] \quad (1)$$

where
Δ = ship displacement
α = coefficient of linear dependence of resistance on speed
$\beta = \alpha.g/\Delta$
λ = average distribution density of impact pulses per unit time determined experimentally
σ_R = dispersion of the disturbing force.

This equation describes the probability of stoppage of a ship during operation in the transition zone. The transition from the continuous mode is realized when, if the ship is stopped and operated in the ramming mode, the penetration per ram is quite long and may be of the order of say five ship lengths. Under these circumstances the ship may continue to progress continuously for an extended period of time at low speed and the frequency of stopping is low. As the ice thickness increases the steady speed decreases and frequency of stopping also increases. This continues until the limiting thickness for continuous icebreaking is reached and ramming operation predominates. As the ship approaches this limit the probability of stoppage approaches 100%.

The transition point, by definition, is that speed at which P equals 0.5 (equal probability point). Substituting in equation (1) gives:

$$-\frac{2\alpha\Delta(\beta+\lambda)\,v_s^2}{gt\,\sigma_R^2} = \ln 0.5 = -0.693$$

But the time interval t is equal to $\ell o/v$ where ℓo is an arbitrary base length of travel and in terms of the ship length, L; $\ell o = nL$ and hence $t = nL/\bar{v}_s$.

Therefore, $\hat{v}_s$ may be written:

$$\hat{v}_s = \left[\frac{3.40\ nL\sigma_R{}^2}{\alpha\Delta(\beta+\lambda)}\right]^{1/3} \qquad (2)$$

For a given ship, hull characteristics and ice conditions, equation (2) represents the locus of transition speed as an implicit function of ice thickness by using the following expression for the dispersion of disturbing force:

$$\sigma_R = k_\sigma \cdot (1.04\sigma h^2)$$

where k_σ is a stability coefficient which depends on the hull geometry and σ is the ice flexural strength. From experimental observations (2), it was found that for icebreakers, $k_\sigma = 8 - 10\%$, while for icebreaking cargo vessels $k_\sigma = 19 - 20\%$. It should be noted that k_σ is never equal to zero even in ideally homogeneous solid ice, since icebreaking still occurs randomly at sections having different angular orientations.

From equation (2) it is obvious that as the ship displacement increases the stability improves and transition speed decreases, which is the case for large displacement vessels envisaged for Arctic navigation routes. It also appears that ice thickness and strength are most significant in determining the transition point.

For demonstration purposes, let the resistance of the ice be given in the simple and sufficiently descriptive form:

$$R = c_s + c_1' vh$$

Therefore, $\alpha = c_1' h$ and $\beta = c_1' gh/\Delta$

Substituting into Equation (2) a solution may be obtained.

A typical example is given below for a hypothetical icebreaker with the following particulars:

Δ = 15000 tons,
L = 100 m,
$\alpha = 4.09 \times 10^5\ h$, N.s/m,
$\beta = 0.0273\ h,\ s^{-1}$,
λ = 1.0 per second (assumed),
$\sigma = 5 \times 10^5\ N/m^2$,
k_σ = 0.08, and

$$\sigma_R{}^2 = 1.731 \times 10^9\ h^4$$

and the transition speed is given by:

$$\bar{v}_s = 0.124\ h\ .\ \sqrt[3]{n/(1 + 0.0273h)}$$

The possible solutions are given in Figure 2 for different values of n.

According to the foregoing analysis, the transition speed and ice thickness (arbitrarily based on n = 5) are 0.4 m/s (approx. 0.8 knots) and 1.25 m; respectively. These limits are sensitive to the parameter λ which has to be evaluated experimentally. However, at the low speeds in the transition region the assumed value is not unreasonable. Also, the values of α, β and $\sigma_R{}^2$ are significant and depend primarily on the hull design.

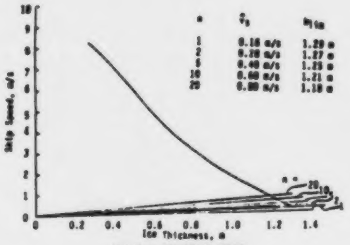

FIGURE 2 TRANSITION POINT

This concept permits a simpler mathematical representation and bears some practicality. It is always desirable to prevent ship wedging when operating in the ramming mode. One of the techniques used to achieve this goal is by reversing the engines as the ship approaches the end of the penetration. This may be simulated by setting a minimum speed at which the ship is to be stopped. This reduces the total penetration but prevents wedging and results in considerable saving of cycle time by eliminating extraction loss. Furthermore, for large displacement Arctic ships, the transition range is likely to be narrow enough to ignore.

Therefore, the concept of transition point or transition speed may serve two purposes. Firstly, it eliminates the transition mode simulation and associated complexities, and secondly, it provides a valid "cut-off" speed below which the ship will not be permitted to continue penetration. Thus, the transition point (or speed) may also be referred to as "minimum permissible speed" in simulated operation, or briefly, "minimum speed".

It should be indicated that the concept, of transition point and related probabilistic estimates are provided for level ice transit. The estimate may be arbitrarily extended to cover all types of ice transit, particularly ridged ice, where the avoidance of an immobile situation (wedging) is of prime significance in reducing the overall transit time.

CONTINUOUS MODE

The solution for the continuous mode of icebreaking is obtained by simply equating the thrust, developed by the propellers, to the ice resistance. In general the ice resistance may be given in the form:

$$R(v) = c_s + c_1.v + c_2.v^2 \qquad (3)$$

where c_s, c_1 and c_2 are coefficients to be determined from ice properties and hull characteristics. The resistance expression includes all resistance components which impede the progress of the ship. The ship thrust may also be expressed in terms of a polynomial

$$T(v) = C_t + B_t.v + A_t.v^2 \qquad (4)$$

where C_t, B_t, and A_t are coefficients to be determined for the operating power level.

Continuous motion at a speed, v_s, is achieved if the following conditions are satisfied:

$$T\ (v_s) = R(v_s)$$

and

$$v_s > \hat{v}_s$$

Apparently if c_0 is greater than C_t continuous motion is not possible. Applying the first condition, rearranging terms, and solving a quadratic equation with v_s as a variable gives the general solution in the form:

$$v_s = -\frac{b}{2} \pm \sqrt{(\frac{b}{2})^2 - c} \qquad (5)$$

where $b = (B_t - c_0)/(A_t - c_2)$

$c = (C_t - c_0)/(A_t - c_2)$

Only the positive answer is accepted. Therefore, a solution is obtained for the given ice conditions and operating power level by using Equation (5). Notice that if $A_t = c_2$ the solution is simply $v_s = -c/b$. Apparently, the maximum speed can be obtained at maximum power operation. However, it is possible, in view of other operating requirements, that the optimum speed will be lower than the maximum value.

RAMMING MODE

The ramming mode of operation exists in the range of ice thicknesses from the transition point up to the ultimate capability of the ship.

It can be seen that the maximum capability of the ship in ramming may be extended by increasing one of either ship displacement, impact speed or White's ratio through hull improvement. To increase White's ratio, one of two approaches may be involved: to increase the beam draft ratio or the water plane area; or decreasing the block coefficient spread and bow angles or hull-ice friction coefficient.

It is obvious that for operation in Arctic waters, a sizeable ship will be required to cope with severe environmental conditions. Therefore, a ship with large displacment, say 125000 tons, will have an extended capability of 250% as compared to a 15000 ton ship provided that other variables remain unchanged. Increasing the speed of impact is a potential factor which can significantly improve the ultimate capability of an icebreaking ship. The speed can be increased by increasing engine power and improving the hull geometry and strength. The best improvement can generally be achieved through lower friction factors.

A typical ramming cycle is illustrated in Figure 3. The cycle consists of the following stages starting from a halt position:

a) Stage 0 - A is the backing stage in which the ship backs down the required ramming distance before reversing the direction of motion. In fact, the engines may be reversed before the end of the stroke to decelerate the ship. From 0 to 1 the ship backs with thrust acting astern. From 1 to 2 the engines are being reversed and the ship moves for a short period of time under the effect of resistance forces and from 2 to A the thrust acts ahead and the ship decelerates until point A where the speed drops to zero and the next stage begins.

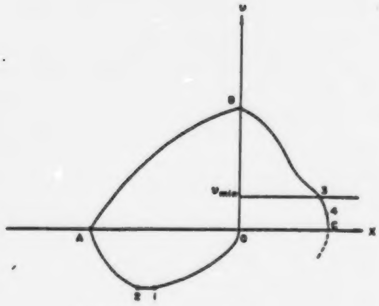

v = speed, x = penetration

FIGURE 3
SCHEMATIC REPRESENTATION OF RAMMING CYCLE

b) Stage A - B is the acceleration stage where the ship moves at full power ahead in the broken channel until it impacts with the ice edge.

c) Stage B - C is the penetration stage in which the ice resistance causes the ship to decelerate to a complete stop where another cycle begins. This penetration stage may be divided into three steps: from B to 3 where the thrust aids the penetration, from 3 to 4 the thrust is neutralized during engine reversal and from 4 to C the deceleration continues under the action of reversed thrust added to the ice resistance. The thrust is reversed at an arbitrary speed, v_{min}, to prevent wedging in ice. This speed may be set equal to $\hat{v}_s$ determined by Equation (2).

In mathematical terms the ramming process may be represented by the following differential equation:

$$\frac{\Delta}{g}\,(1+\lambda)\,\frac{dv}{dt} = T(v) - R(v) \qquad (6)$$

where λ is the added mass coefficient.

Lewis and Edwards (3) solved the above equation for bollard thrust condition and resistance dependence on the square of the ship speed using Riccati's method. Petrov and Kheysin (4) used the resistance as a function of v and v^2 and obtained a solution by Euler's graphic method.

Lewis and Edwards' solution may be summarized as the following:

- the speed at any time t during deceleration period BC:

$$v = \sqrt{\frac{F}{K}} \cdot \left(\frac{\sqrt{\frac{K}{F}}\, v_o \cos\sqrt{\frac{KF}{M^2}} \,.\, t - \sin\sqrt{\frac{KF}{M^2}} \,.\, t}{\cos\sqrt{\frac{KF}{M^2}} \,.\, t + \sqrt{\frac{K}{F}} \,.\, v_o \,.\, \sin\sqrt{\frac{KF}{M^2}} \,.\, t} \right) \quad (7)$$

where $v_o = v)_{t=o}$

- the time to complete stop:

$$t\ (v_o/o) = \sqrt{\frac{M^2}{KF}} \quad \tan^{-1}\sqrt{\frac{K}{F}} \cdot v_o \quad (8)$$

- the maximum penetration during the ram:

$$P = \frac{M}{2K} \ln \left(1 + \frac{K}{F} \cdot v_o^2\right) \quad (9)$$

where $M = \frac{\Delta}{g}(1 + \lambda)$, $F = C_o - T_o$

and $T(v) = T_o$

$R(v) = C_o + Kv^2$

This expression relates the penetration to the speed of impact and coefficients of resistance equation. The authors regressed the above formula to full scale observation and found that the penetration ranges from 0.2 to 200 times the ice thickness depending on the speed of impact, thickness and thrust.

Ryvlin and Tegkayeva (5) used the following dimensionless form of Equation (6).

$$\frac{dF_n}{d\xi} = \frac{T(F_n) - R(F_n)}{\Delta(1+\lambda)F_n}$$

where $F_n = v/\sqrt{gl}$ = length Froude number, and

$\xi = P/L$ + penetration relative to ship length.

Assuming bollard thrust and using a quadratic expression for the resistance, they examined the factors which influence the ship performance in ramming, stopping or braking. Two major terms were identified.

a) bollard thrust per ton displacement which was found to greatly influence the ship capability to accelerate and brake. If the displacement alone is increased the maneuvering capabilities of the ship will be affected. Thus the thrust-displacement ratio appears as an important factor to be optimized to avoid the situation of an overpowered or underpowered ship.

b) the impact speed which is also shown to significantly influence the pentration.

Severe Arctic environment may require the ship to operate in the ramming mode for extended periods, particularly when thick ice and ridge systems are involved. Therefore, the next section is devoted to an analysis of the ramming mode in an effort to expose the relative significance of the variables involved and to assess the impact of optimization on the performance.

ANALYSIS OF RAMMING - GENERAL SOLUTION

A general solution for Equation (6) may be obtained. The solution will cover all phases of the ramming cycle as depicted in Figure 3 by considering the net external force X(v) which is the resultant of the thrust and resistance. Equation (5) may be rewritten:

$$M \frac{dv}{dt} = X(V) \quad (10)$$

where $M = \frac{\Delta}{g}(1+\lambda)$

Another alternate form is: $M\, v \frac{dv}{dx} = X(v)$ (11)

By separation of variables and integration of Equations (10) and (11), expressions for the penetration, p, and elapsed time, t, as functions of the speed limits can be obtained:

$$p = \int dx = \int_{v_1}^{v} M \frac{v}{X(v)}\, dv \quad (12\text{-a})$$

$$t = \int dt = \int_{v_1}^{v} M \frac{dv}{X(v)} \quad (12\text{-b})$$

where v_1 is the initial speed. These integrals may be evaluated for a given function X(v) and speed limits. Inversely if the time or penetration are known the speed at the end of the stage can be determined.

Using these two expressions it will not be necessary to derive a general solution for the speed as a function of time which has proven to be a tedious mathematical exercise. The speed variation will generally follow a pattern connecting the terminal points.

It has been suggested that both thrust and resistance can be expressed in terms of a simple polynomial of the second degree in speed. Therefore, for a variety of conditions the external force X(v) which is the algebraic sum of T(v) and R(v) is determined in the following format:

$$X(v) = a + bv + cv^2 \quad (13)$$

Let $q = 4ac - b^2$

Therefore, the general solution of (12) may be given by:

$$\text{If } q > 0; \quad p = \frac{M}{2c}\Big\{\ln X(v) - \frac{2b}{\sqrt{q}} \arctan\Big(\frac{2cv+b}{\sqrt{q}}\Big)\Big\}_{v_i}^{v} \qquad (14a)$$

$$t = \frac{2M}{\sqrt{q}}\Big\{\arctan\Big(\frac{2cv+b}{\sqrt{q}}\Big)\Big\}_{v_i}^{v}$$

$$\text{If } q < 0; \quad p = \frac{M}{2c}\Big\{\ln X(v) + \frac{2b}{\sqrt{q}} \operatorname{arctanh}\Big(\frac{2cv+b}{\sqrt{-q}}\Big)\Big\}_{v_i}^{v} \qquad (14b)$$

$$t = \frac{-2M}{\sqrt{-q}}\Big\{\operatorname{arctanh}\Big(\frac{2cv+b}{\sqrt{-q}}\Big)\Big\}_{i}^{v}$$

$$\text{If } q = 0; \quad p = \frac{M}{c}\Big\{\ln\Big(\frac{2cv+b}{2c}\Big) + \Big(\frac{b}{2cv+b}\Big)\Big\}_{v_i}^{v} \qquad (14c)$$

$$t = -2M\Big\{\frac{1}{2cv+b}\Big\}_{v_i}^{v}$$

Table 1 demonstrates how to evaluate the coefficients a, b and c for acceleration and deceleration under thrust action and stopping at no thrust action.

TABLE 1

APPLICATION OF EQUATION (14) TO A RAMMING CYCLE

SERIAL	CASE DESCRIPTION	δ	a	b	c
1	Accelerate or decelerate in ice under normal progress conditions. Thrust may be greater or less than resistance, cases [0-1, A-B, B-3] in Figure 3	1	$C_t - c_0$	$B_t - c_1$	$A_t - c_2$
2	Stop in ice with thrust = 0 (situation during engine reversal, cases [1-2, 3-4].	0	$-c_0$	$-c_1$	$-c_2$
3	Brake in ice with thrust and resistance oppose the motion, cases [2-A, 4-C]	-1	$-C_t - c_0$	$-B_t - c_1$	$-A_t - c_2$

$X(v) = \delta . T(v) - R(v)$ = net external force

$T(v) = C_t + B_t v + A_t v^2$ = net thrust at a given power level

$R(v) = c_0 + c_1 v + c_2 v^2$ = total resistance of ice

Therefore, $X(v) = a + bv + c v^2$

Where, $a = \delta C_t - c_0$, $b = \delta B_t - c_1$, $c = \delta A_t - c_2$, and

$\delta = 1, 0$ or -1 according to tabulated cases.

The general solutions given by Equations (14) will cover all special cases and produce more accurate estimates of penetration and time since they take into consideration variation of thrust with speed. Consider, for instance, Lewis and Edwards's solution for the case of bollard thrust ($A_t = B_t = 0$) and resistance dependence without a linear term ($c_1 = 0$). Following the procedure outlined in Table 1,

$\delta = 1$

$a = C_t - c_0$, usually negative in the ramming mode.

$b = 0$

$c = -c_2$

Therefore, $q = 4ac > 0$ and Equation (14-a) may be used to obtain:

$$P = \frac{M}{2c}\Big\{\ln(a + cv^2)\Big\}_{v_0}^{0} = \frac{M}{2c}\ln\Big(\frac{a}{a + cv_0^{2}}\Big)$$

$$t = \frac{2M}{\sqrt{q}}\Big\{\arctan\Big(\frac{2cv}{\sqrt{q}}\Big)\Big\}_{v_0}^{0} = \frac{-M}{\sqrt{ac}}\arctan\Big(\frac{cv_0}{\sqrt{ac}}\Big)$$

Substituting the symbols used by Lewis and Edwards (3), ($a = -F$, $c = -K$), the solution will be identical to Equations (8) and (9) determined by Ricatti's method.

The proposed general solution provides us with a method, in closed form, for studying the influence of thrust as well as hull characteristics of the ship and ramming tactics upon the ramming performance. The optimization of the ramming process can result in significant savings in transit time and cost. Also, optimized performance in level ice is a prerequisite to assessment of ramming performance in excessive ridge systems which are indeed, the largest impediment to Arctic navigation.

OPTIMIZATION

The purpose of this section is to explore the potential benefits of optimizing the ramming mode and to define some of the parameters and trends to be examined in a future study. It is hypothesized that:

> "For a given ship with specified power capabilities and hull icebreaking properties operating in the ramming mode in given ice conditions there exists an optimum speed of advance. The latter will vary with the ice environment.

It is also feasible to optimize the ship displacement and hull shape for best ramming capability. In fact, it is the combination of mass and thrust, or in more conventional terms the thrust per ton of ship displacement, which can produce a better ship for Arctic navigation. A large displacement ship with low power is analogous to a huge flywheel which is being charged at low speed. Such a vessel will generally require longer time to back down the broken channel and to accelerate to accumulate sufficient energy for comparably large penetration. Therefore, the use of optimization could produce some recommendations regarding the power requirements per ton displacement.

In the following, evidence is provided to consolidate the grounds of the foregoing hypothesis. It is shown that an optimum speed of advance exists and that the conventional ramming procedure of backing an arbitrary ramming distance could produce advance rates well below the ship capability.

Assume that for a medium sized icebreaker (similar to CCGS LOUIS. S. ST. LAURENT) and given ice conditions, the following relations are known in terms of the ship speed, v(m/s),

a) the net thrust ahead at full power,

$$T = 2000 - 50v - 5v^2, \text{ kN}$$

b) the net thrust astern at half power,

$$T_{as} = 882 - 27.8v - 3.5v^2, \text{ kN}$$

c) the resistance in thick level ice (approximately 2m),

$$R = 4000 + 800v, \text{ kN}$$

d) the resistance in the broken channel ahead or astern,

$$R_b = 140 + 100v + 5v^2 \text{ , kN}$$

The above equations are plotted in Figure 4 from a maximum ramming speed of 8.1 m/s (15.7 knots) and a maximum backing speed of 4.5 m/s (8.7 knots).

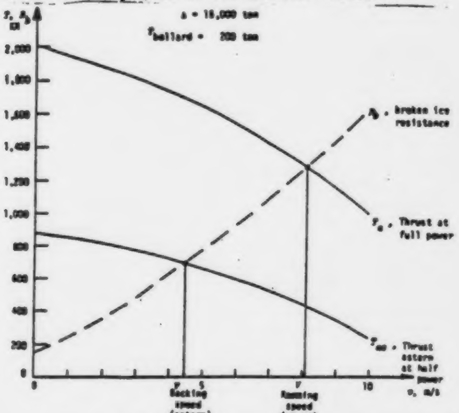

FIGURE 4 RESISTANCE AND THRUST CURVES FOR A HYPOTHETICAL SHIP

For convenience, it is also assumed that the ship backs at half power astern and then accelerates forward at full power until coming to a complete stop at the end of penetration. This approximation will not affect the trends of variation but simplifies the calculations.

The average speed of advance is defined as the total penetration per ram divided by the total cycle time, t, which consists of:

$$t = t_b + t_a + t_p + t_1 \qquad (15)$$

where t_b = the total time required to back down the channel
t_a = the time acceleration in the broken channel
t_p = the time from the moment of impacting the ice until complete rest
t_1 = the share of time losses when the ship gets stuck in ice and maneuvers to free herself.

In this analysis the reversal time is neglected and efficient operation is assumed. This is a general formula which may further be broken down into subcomponents corresponding to the stages described in Figure 3.

The external force during the different stages is obtained with the aid of Table 1 and is given:

for backing: $X(v) = 742 - 127.8\,v - 8.5v^2$

for acceleration: $X(v) = 1860 - 150v - 10v^2$

for penetration: $X(v) = -2000 - 850v - 5v^2$

Equation (14-b) may be used to evaluate the components of the ramming cycle. The results are shown graphically in Figures 5 and 6. Figure 5 demonstrates the relative duration of backing, acceleration and penetration. It appears that almost 50% of the cycle time is used to back down in the broken channel while acceleration takes a third of t and penetration constitutes the least significant portion of the cycle time. Therefore, priority must be given to the consideration of improving the vessel capabilities in broken ice. Unfortunately, the lack of available information in this area does not provide an adequate means of optimizing the ramming performance.

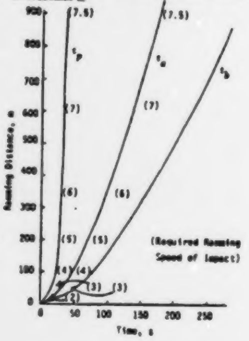

FIGURE 5: COMPONENTS OF RAMMING CYCLE TIME FOR DIFFERENT CONDITIONS

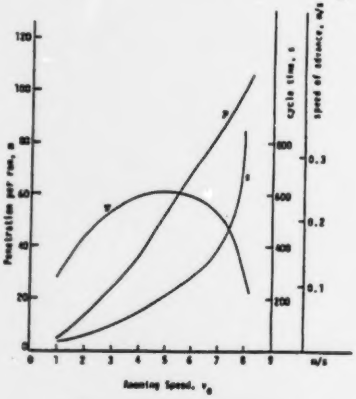

FIGURE 6: PREDICTED PERFORMANCE IN RAMMING

Figure 6 displays the total cycle time, t, the penetration, p, and the average speed of advance, v, versus the ramming (impact) speed. It is evident that an optimum speed exists for this particular situation and corresponds to a ramming speed of approximately 5 m/s (10 knots). This is about 60% of the maximum achievable speed in the broken channel. If ramming is arbitrarily performed at 7.7 m/s (15 knots), progress can be maintined at 0.165 m/s and it takes 50% longer than the optimum transit time. Ramming at 2.6 m/s (5 knots) can result in a 27% increase over the optimum transit duration.

Therefore, it appears that the optimization of the ramming mode can produce significant improvements in transit performance. Overall higher benefits can be realized through thrust and resistance optimization as well. Moreover, improving transit capabilities in broken channels shall prove to be beneficial.

DISCUSSIONS

An interesting observation is that the optimized tactics are valid regardless of the vessel displacement. Further examination of Equation (14) indicates that both the penetration and cycle time are in direct proportion with ship mass or displacement. Therefore, for the same external force X(v), the optimum conditions are independent of displacement, i.e., valid for both large and small ships. Although the penetration and time components may differ, the speed of advance will be identical.

For larger ships, the resistance and thrust scale up differently. Hence, different performance may be expected. A 135,000 ton ship will be 10 times larger than a 13,500 ton ship (e.g. the LOUIS S. ST. LAURENT) but the resistance will only be 2.15 times greater. If the thrust is scaled up by the same ratio, the ship will require some 50,000 HP and, according to Equation (14), could penetrate longer distances (4.65 times) per ram. However, the speed of advance would still be comparable to the smaller ship. Should the same thrust/displacement ratio be maintained improved performance will result.

Optimum powering requirements for ships navigating in ice should be determined from transit considerations to avoid underpowered or overpowered situations.

Finally, a word of caution is in order. As is indicated earlier, trim angles and accelerations in ramming are usually large and a certain amount of energy is dissipated in causing such motions. As the ice thickness increases the ship will ride up on the ice edge until sufficient vertical force to break the ice is developed. In the vicinity of limiting conditions the ship may ride up on the ice without being able to fracture it and the foregoing analysis will entail large errors. It is evident that the error arises from the consideration of motion in the forward direction alone without regard to ship motions in other coordinates. A more complete, and also complex, solution shall take the dynamics of ship motion during ramming into account and designate a "net" or "actual" penetration in ice as that on ice coordinates rather than ship coordinates. Nonetheless, for all practical purposes and convenience of analysis the above solution may be used as a basis for optimization of ramming in the regions well removed from the ultimate capability of the ship.

Optimization of ramming can produce very significant improvements in performance. For a given ship, the speed of advance can be doubled if optimum ramming procedures are followed. Moreover, an improved hull forebody which minimizes resistance, a better stern and appendages arrangements and properly selected powering can at least quadruple the speed of advance of the ship used in the illustrated example.

However, ship wedging during ramming and the associated loss of time in freeing the stuck vessel poses a serious threat to the optimization benefits. This problem should also be given due consideration in future studies of ramming. It should be mentioned that Popov and Kashteljan (6) theoretically studied the problem and analyzed the various methods used in freeing a wedged icebreaker but no experimental verification could be cited. The benefits and efficiency of using low friction coatings should also be addressed.

It is needless to say that ramming tactics can be improved to the limits imposed by other design characteristics such as the structural integrity of the hull and its capability to withstand high impact loads. The most serious impediment is, in fact, the speed limit imposed in backing as a requirement to protect propellers and rudder from damage caused by interaction with broken ice pieces.

ACKNOWLEDGEMENTS

This work was part of a comprehensive study entitled "Development of a Research Program for Improving Arctic Marine Transportation Technology" supported by Transport Canada - Transportation Development Centre (TDC) and reported in TP 2004, March 1979. The author would like to thank M. Brenckmann, Associate Director of TDC for permission to publish this paper, and D. Hearnshaw of CMTA who was the project officer. The author would also like to thank R.Y. Edwards, Jr., President of Offshore Technology Corporation, for his advice and encouragement during the course of this work. Thanks are due to L. Keech, G. Avery, and R. Gardner for their assistance in preparing the manuscript.

REFERENCES

(1) Melberg, L.C., et al "The Design of POLAR Icebreakers", Paper No.2, Presented to SNAME Spring Meeting, Washington, D.C., April 1979, pp. 2-1, 2-26.

(2) Kheysin, D.Ye., "On the Ice Navigation Speed of Ships in Extremely Solid Ice", Ice Navigation Qualities of Ships, ed. Kheysin, D.Ye., and Popov, Yu.N., Translation, CRREL TL 417, August 1973, pp.19-30.

(3) Lewis, J.W. and Edwards, R.Y. Jr., "Methods of Predicting Icebreaking and Ice Resistance Characteristics of Icebreakers", Paper #5, SNAME Annual Meeting, New York, November 1970.

(4) Petrov, Ye Yu, and Kheysin, D.Ye., "Calculation of the Inertial Characteristics of Ships Floating in Ice", Proc. of the 14th Scientific & Engineering Con. of Gor'kiy Poly.Inst. Imeni Zhdanov (Shipbuilding Inst.)

(5) Rylin, A. Ya., and Tegkayeva, T.Kh., "Investigation of the Inertial Characteristics of Unsteady-State Motion of an Icebreaker in Ice", Ice Navigation Qualities of Ships, ed. by Kheysin, D.Ye. and Popov, Yu.N., Translation, CRREL 417, August 1973, pp.59-65.

(6) Popov, Yu. N., and Kashteljan, V.I., "Wedging of Icebreakers in Ice", Ice Navigation Qualities of Ships, ed. by Kheysin, D.Ye., and Popov, Yu. N., Translation, CRREL TL 417, August 1973, pp.66-81.

A.2 Resistance Profiles

The above described method of analysis of the ramming cycle, requires the input from the expressions for thrust T (v) and resistance R (v). The thrust relation can be determined from the ships engine and propeller characteristics and are dictated by power settings and operational procedures. The expression has to be developed for the ahead and astern conditions. In order to cover the various stages of the ramming cycle, the resistance profiles need to be selected for:

- level ice ahead,
- pressure ridge ahead,
- broken channel resistance ahead and astern.

A.2.1 Level Ice Model

Previous work performed by Arctec on the examination of the various models as to their suitability for cargo ships such as the MV ARCTIC has shown that there are a few candidate models which take into account specific geometric features of cargo ship design and permit the variation of hull shape and dimensional ratios within the equations. For the sake of application to the proposed ramming mode formulation, it is suggested to consider closed form formulations only.

Figure A.1 gives a comparison of the candidate models to full scale observations obtained for CCGS LOUIS S. ST. LAURENT in the Canadian Arctic. It can be seen that most models do not give adequate predictions. Each model or equation best describes its particular data base, restricted by ship type and size, hull form parameters, speed range and ice conditions covered by the data base.

Kashteljan et al [9] proposed the following form:

$$R_i = 0.004\ \mu_o\,[\sigma B h] + 3.6\ \mu_o\,[\gamma_i B h^2] + 0.25\ (1/\eta_2)\ [B^{1.65}\ h v]$$

in which the variables related to each component, respectively, are included in square brackets. This equation accounts for ship beam, B, ice thickness, h, flexural strength, σ, weight density, γ_i, and the speed, v. The hull form effect is incorporated in the hull form coefficients μ_o and η_2 usually referred to as Kashteljan-Shimansky coefficients. However, it is not clear how friction effects are taken into account in this equation and it is still difficult to explain the beam exponent in the velocity dependent term. It has been indicated, for instance by Enkvist [10] that this equation does not adequately explain experimental data.

FIGURE A.1

COMPARISON of VARIOUS LEVEL ICE MODELS

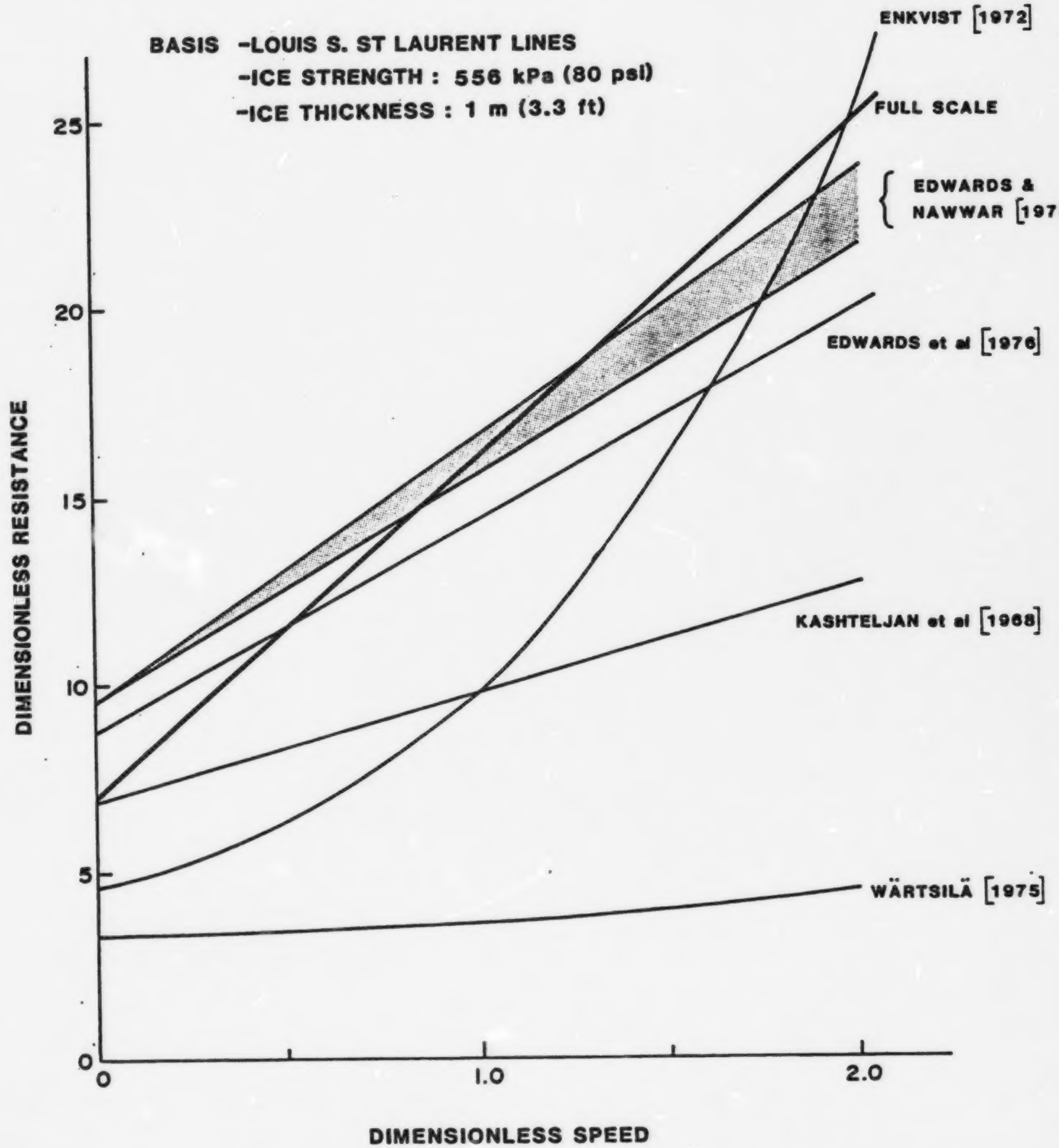

Enkvist [10] reports a comprehensive analysis corroborated by data obtained from model tests on Finncarrier, Moskva icebreaker and small icebreaking tug Jelppari. He proposed a general equation of the form:

$$R_i = C_\sigma (\sigma Bh) + C_s (\gamma_\Delta BhT) + C'_v (\gamma_i Bh^2) + C''_v (\gamma_w Bh^2)$$

where $C_\sigma = 5.8 (\frac{\sigma}{E}) (1 + \eta_{\mu s} \cdot \eta_{\mu c}) \times 2.0$

$$C_s = (\eta_{sp} + \mu \cdot \eta_{s\mu E} \frac{Le}{T}) \times 2.0$$

$$C'_v = (1 + 0.218 \frac{1}{\bar{h}}) (1 + \eta_{\mu s} \cdot \eta_{\mu c}) \overline{\tan^2 \phi}$$

$$C''_v = 1/2 (\frac{1}{\bar{h}})^2 (0.167 \overline{\sin\psi} + \frac{H_{BW}}{1}) (\eta_{\mu\psi} + \eta_{\mu\theta})$$

The C-coefficients are semi-empirical functions of ice properties, hull geometry, friction, and the relative proportions of broken cusps. The bow wave height, H_{BW}, is estimated from:

$$H_{BW} = 0.5\ v^2/2g$$

The hull form and friction coefficients are given by:

$$\eta_\mu = 1/ (\overline{\sin\phi}\ \overline{\cos\phi})$$

$$\eta_\mu = \mu/ (1 - \mu\ \overline{\sin\phi}/\overline{\cos\psi})$$

$$\eta_{\mu\psi} = [\overline{\sin\phi}\ \overline{\cos\psi} + \mu\,\overline{\cos^2\phi}]/[\overline{\cos\psi}\ \overline{\cos\phi} - \mu\,\overline{\sin\phi}\ \overline{\cos\phi}]$$

$$\eta_{\mu\theta} = \overline{\sin\psi}\ \overline{\sin\alpha} + \mu\,\overline{\cos\alpha}$$

$\eta_{sp} = \bar{S}/T$, $\bar{S}$ = mean depth of submersion

$\eta_{s\mu E} = C_{wf}\ \overline{\sin\beta}$, C_{wf} = forebody waterplane coefficient

All trigonometric functions are independently integrated over the entire forebody (or mean values). The angles are defined as:

ϕ = angle between stem or buttock line and horizontal plane

ψ = angle between a horizontal plane and a section perpendicular to the waterline

α = half angle of entrance of a waterline

β = angle between section and vertical plane = (90° $-\psi$).

It is obvious that this method contains significant computation to evaluate all the hull dependent coefficients. However, this could be computerized and systematic evaluation of the coefficients can be comparatively easy. Enkvist's model has an edge over Kashteljan's by accounting for both friction and hull geometry in developing the resistance components. However, the manner in which the incremental forces are integrated is subject to criticism. The use of mean or average values of trigonometric functions is an oversimplification and is not compatible with the degree of involvement in the derivation of the components.

Another parametric study was conducted by Wartsila of Finland and reported in a number of publications [11, 12, 13, 14, 15]. In this parametric study a total of nine models were tested providing considerable variations in ship dimensions and coefficients. However, the fact that the series was concerned with large sized bulk carriers limited the block coefficient variation to a very narrow range which, unfortunately, does not permit us to compare their resistance model directly to that of Edwards et al [16]. Wartsila's model is given in the following general form:

$$R_i = \rho_\Delta gBhT \; C_\mu(k_i C_\sigma + C_s + C_v)$$

where $\rho_\Delta g$ = 884 N/m³ is the weight density differential,

B = beam

T = ship draft at DWL

h = ice thickness

k_i = correction factor to account for differences between model and natural ice and is approximately equal to 0.02.

C_μ = is a friction multiplier to be evaluated for hull-ice friction

$C_\sigma = K_1 \left(\frac{\sigma}{\rho_\Delta gT}\right)^{k_2} \left(\frac{T}{h}\right)^{k_3}$ = specific breaking resistance

$C_s = K_4 \left(\frac{T}{h}\right)^{k_5}$ = specific submerging resistance

$C_v = K_6 \left(\frac{v}{\sqrt{gT}}\right)^{k_7} \left(\frac{T}{h}\right)^{k_8}$ = specific velocity dependent resistance

The values of the eight coefficients can be determined from graphs supplied for each model. Unfortunately, this does not permit any flexibility in applying the above model to similar ships. Only the ship draft is explicit in the terms whereas the effects of other ship variables are included in the coefficients. It should be pointed out that draft was shown to have insignificant influence on resistance in ice.

Edwards et al [16] reported the results of a parametric study of nine different hull forms proposed for the Polar VII icebreaker. The model hulls compromised variations in length, beam, draft, block coefficient and friction factor. The following level ice resistance equation was derived:

$$R^* = C_0 + C_1 \sigma^* + C_2 v^*$$

where $R^* = R/\gamma_w B h^2$ is the dimensionless resistance

$\sigma^* = \sigma/\gamma h$ is the dimensionless ice strength, $104 > \sigma^* > 8$

$v^* = v/\sqrt{gh}$ is the dimensionless speed, $2.5 > v^* > 0.2$

and $C_0 = 5.7 + 0.147 (T/h) - 7.83 C_b^2$

$C_1 = -0.318 + 0.265\mu + 0.394 C_b$

$C_2 = -68.16 + 0.0477\sigma^* + 223.73 C_b - 181.3C_b^2 + 0.249 (T/h)$

The above formula is valid for $0.625 > C_b > 0.50$

$$73.0 > \frac{T}{B} > 10.$$

This equation, in fact, consists of four terms rather than three since the strength appears in the speed term coefficient. This was the first report in which the block coefficient appeared to be an influential parameter. It should be noticed that the ship length is absent, the draft affects two components and, for the range of variables tested, level ice resistance is a linear function of beam.

Edward's equation is statistically valid (0.9914 correlation with 8.8% standard error) but it is difficult to explain the forms of the coefficients; particularly the negative signs and exponent of the block coefficient. Furthermore, the nature of development does not permit physical explanations which may lead to systematic evaluation procedure of resistance in level ice of a ship with different parameters.

It is not known whether this model, or any of the above mentioned, can successfully predict full scale data. Although all of them consider at varying degrees the hull geometry and friction coefficient in a standard solution, none was directly compared with full scale observations except Kashteljan's model which was obtained using model and full scale data.

Figure A.1 gives a comparison of the above mentioned models to full scale observations obtained for CCGS LOUIS S. ST. LAURENT in the Canadian Arctic. Edwards et al [16] presents this data in a concise form and reports a best fitting regression equation in the form:

$$R^* = 4.242 + 0.05033\sigma^* + 8.948 v^*$$

This equation may be used to represent a reference line for full scale data.

It can be seen that Wartsila's equation originally derived for Great Lakes bulk carriers is completely inadequate while Kashteljan's model diverges considerably as the speed increases. Enkvist's equation consistently underestimates the resistance (with the empirically corrected coefficients). The best agreement is that of Edward's model.

An extensive investigation is reported by Nawwar and Edwards [17]. The study presents a compilation of 1275 data points for thirty-five different hulls, assessment of the various hull characteristics which may influence the icebreaking resistance and, through statistical analysis, two models were derived from regression of dimensional and dimensionless data. In dimensional form:

$$R = C_0(\sigma Bh) + C_1(\gamma_i Bhv) + C_2\,(\gamma_i Bh^2)$$

$$C_0 = 0.099\, C_b^{3.6}$$

$$C_1 = 0.328 \sqrt[6]{\Delta}\,(L/B)^{0.48}\,(\mu_1 + 1.17\mu_2)/\sqrt{g}$$

$$C_2 = 3.775\, \mu_1^{0.55}$$

where L = ship length
B = ship beam
h = ice thickness
σ = ice strength
v = ship speed
γ_i = density of ice
C_b = block coefficient
μ_1, μ_2 = geometry-friction coefficients
R = ice resistance

which consists of three basic components representing two functions, ice-fracturing and ice-moving. The latter explains the composite middle term which contains a velocity dependent component associated with the ice-fracturing function and another associated with the ice-moving function. The hull geometry is well represented by the block coefficient and length/beam ratio while μ_1 and μ_2 are geometry-friction coefficients integrated over the entire waterline. The middle term has a dimensional coefficeint which provides some difficulty in expanding the model to full scale predictions.

In dimensionless form the following equation was obtained:

$$R^* = 0.727\,(\mu_1 + 1.17\mu_2)^{0.965}\,\left(\frac{L}{B}\right)^{1.036}\,(\tan\alpha_0)^{0.332}\,(\cos\beta_5)^{-0.678}$$

$$+\, 0.363\, C_{bf}^{2.92}\,(\tan\alpha_0)^{0.841}\,(\cos\beta_5)^{14.54}\,\sigma^* \cdot v^*$$

where $R^* = R/\gamma\ Bh^2$

$\sigma^* = \sigma/\gamma h$

$v^* = v/\sqrt{gh}$

α_0 = stem angle

B_5 = flare angle

C_{bf} = block coefficient of forebody

Notice that it contains a larger number of hull parameters such as the forebody block coefficient, the stern angle and flare angle at midship. It also contains two terms rather than three. The above equations are derived from model data which are valid in a wide range of variables for conventional icebreakers. Therefore, an aspect of universality is present despite the fact that it may not provide the best fit to any particular subgroup of the data base.

To maintain consistency in comparing the models using equations of similar construction, the dimensional equation was non-dimensionalized and the middle term was scaled up using the LOUIS scale models of 36 and 48. The resulting predictions are shown in Figure A.1. It is obvious that the dimensional model provides reasonable predictions over the entire speed range and some of the deviation could probably be attributed to snow effect present in full scale trials.

Poznyak and Ionov [18] present an analytical method for the estimation of icebreaker ice resistance and its components. The method applies to the continuous icebreaking mode at low speeds, between one and four knots. The resistance was broken into six components: icebreaking, ice submerging, velocity and three types of friction. The formula is given by:

$$R = 0.014\sigma_f h^2\ [\alpha_1(\beta)\ B + f_d\alpha_2\ (\beta)\ L\ ]$$

$$+\ 0.1\ \gamma_0 hBL\ \left(\frac{t_g\ \alpha_0}{t_g\ \alpha_0 + B/L}\right)\ [\alpha_1(\beta)\ \sin\alpha_0 + f_d\alpha_0\ (\beta)\ (1 + \cos\alpha_0)]$$

$$+\ 1.5\ \gamma_{ice}\ hB^2\ F_n\left(1 + \frac{1}{\cos\alpha_0}\right)\ \left[\ \frac{(t_g\alpha_0)^2}{(2t_g\alpha_0 - B/L)} + f_d\right]$$

where L = length of the icebreaker on the waterline, m

B = breadth at midships, m

h = ice thickness, m

α_0 = the angle of entrance of the waterline, degrees

σ_f = ice flexural strength, Pa

γ_{ice} = specific gravity of ice, N/m³

γ_0 = difference between the specific gravities of water and ice, N/m³

f_d = dynamic coefficient of friction between the hull and the ice

and F_n = Froude number

$\alpha_1(\beta)$ and $\alpha_2(\beta)$ are non-dimensional coefficients of hull shape which may be derived from the following equations:

$$\alpha_1(\beta) = \frac{1}{n} \sum_{i=0}^{n} \frac{0.57}{\sin\beta} (1.6 \cos\beta + 0.11)$$

$$\alpha_2(\beta) = \frac{1}{n} \sum_{i=0}^{n} \frac{1}{\sin \rho}$$

The method has been developed on the basis of icebreaker data. Its restrictions with regards to the range of hull parameters are not known and therefore application to the M.V. ARCTIC ramming analysis would become questionable.

A.2.2 Pressure Ridge

The before mentioned report prepared by Arctec for TDC in 1979 [13], gives a comprehensive review of factors concerning ice-transitting performance. A general approach is presented in which the resistance is expressed as the integral of forces over the length of entrance, in which the thickness profile as a function of penetration is included. The ridge resistance at a given penetration into a known ridge profile (as shown in Figure A.2) is given by:

$$R(\zeta) = \left(R_0\right)_{L_e} - \int_0^{L_e} f . \frac{\partial R_0}{\partial h_e} . \frac{dH(\zeta-x)}{dx} \; dx$$

FIGURE A.2

SHIP-RIDGE INTERACTION COORDINATES

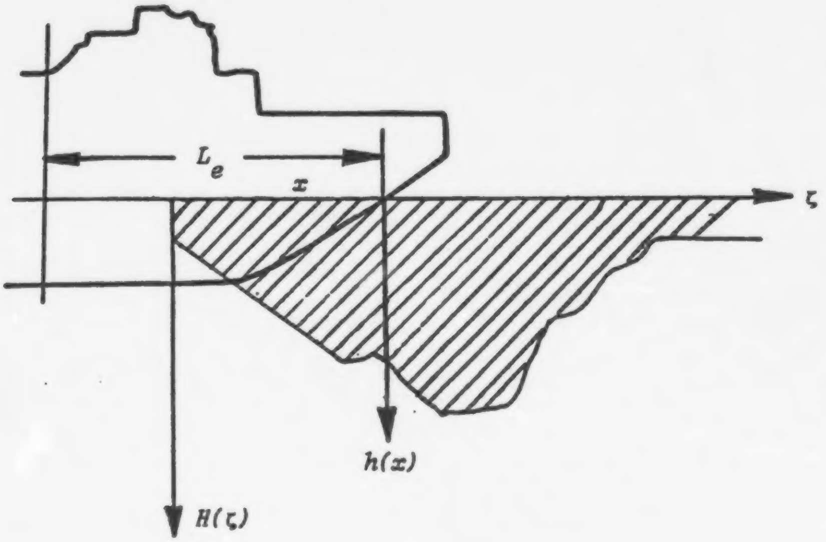

°Ship penetration into the ridge = ζ

°Thickness: $h(x) = H(\zeta - x)$

°$H(\zeta)$ = total ridge thickness including sail height

°If ridge is not fully consolidated the thickness profile represents the effective thickness which is a function of total depth and refrozen crust thickness.

°Point of penetration is defined at the stem.

where $R_0 = R_0(h_e, v, \sigma, \mu, \text{hull geometry})$

$f = f(x)$, 0 at $x = 0$, 1 at $x = L_e$

L_e = length of entrance

h_e = effective thickness of ridge

If the integral term can be solved, the ridge resistance profile will be obtained in terms of the penetration into the ridge, ζ, and other variables. The solution feasibility is determined by the degree of complexity of the functions involved.

The foregoing analysis clarifies several requirements for a useful ridge penetration model and process optimization. The most significant part of ridge resistance is influenced by:

- resistance distribution function of the forebody
- sensitivity of resistance to ice thickness
- ridge thickness gradient along the forebody
- resistance, in general, to ship motion in uniform consolidated or semi-consolidated ice cover
- length of entrance of the forebody (integration interval)

Peirce [5] uses a modification of the breaking and gravitational components to obtain an expression for the ridge resistance in determining the minimum approach speed in field ice of uniform thickness in order to breach a significant ridge:

$$R_r = l_r/l_e\,[C_1 \sigma B(sh_r) + C_2\, \rho g B(mh_r)^2]$$

where R_r = ridge resistance

l_r = effective width of ridge

h_r = effective depth of ridge

l_e = length of entrance

C_1, C_2 = resistance coefficients

σ = ice strength

B = ship beam

ρ = ice mass density

g = gravitational acceleration

s = strength factor of ridge = adhesion x m

m = density factor of ridge = (1 - porosity)

The validity of this simplified expression is unknown, although the approach of using the effective ridge characteristics in the expression for level ice resistance may be most suitable for application in the proposed ramming mode formulation. If the geometry of the ridge is known, the effective ridge thickness can be estimated as proposed by Makinen [19].

Makinen reports a leading study on the mechanics of ship penetration through ridges in the Baltic Sea. Figure A.3 shows a schematic presentation of different modes of penetration through ridged ice fields. It shows, in a manner similar to Bustard [21], the significance of ship displacement. It also shows that a ship having best performance in level ice is not necessarily the best performer in ridges. The design characteristics which influence such performance have not yet been fully examined. For instance, Johansson [22] showed that the predicted mean speed in ridges of varying height can significantly be increased by employing lower hull-ice friction coefficients. But no systematic study was conducted to determine the effect of friction among other variables, on the mechanics of ridge penetration which is a key to an optimal hull design for Arctic going ships.

Full scale ice trials reported by Makinen [19] were conducted using the APU Baltic Icebreaker equipped with bow propellers and 8.8 MW installed power. During these tests, conducted in the Gulf of Bothnia in April 1974, ridge profiles were determined by mapping the sail profile and calculating the keel profile accordingly. The degree of consolidation was ignored as it was regarded insignificant for Baltic conditions. The total ridge thickness, h_r, was calculated from:

$$h_r = h_a + h_b$$

where $h_a = \mu_s \, . \, h_s + \frac{\rho_s}{\rho_i} \quad h_{sc}$ is the equivalent thickness of sail and

and μ_s is the block density $\cong 0.7$,

h_s is the sail height,

h_{sc} is the snow depth,

ρ_s/ρ_i is the snow/ice density ration $\cong 0.33$.

$h_b = h_s \, . \, (\mu_s \rho_i)/(\mu_k \rho_\Delta)$ is the calculated keel depth where the keel density $\mu_k \cong$ the sail density, $\mu_s \cong 0.7$.

According to Makinen, the keel to sail ratio is 7.76 which is higher than the 4.5 value reported for Arctic ridges [23].

Unfortunately, during these experiments, the bow propellers were operated at 50% of the available power which probably resulted in significant differences in the penetration mechanism from smooth bow

FIGURE A.3

DEFINITION OF STAGES OF SHIP PENETRATION INTO A RIDGE

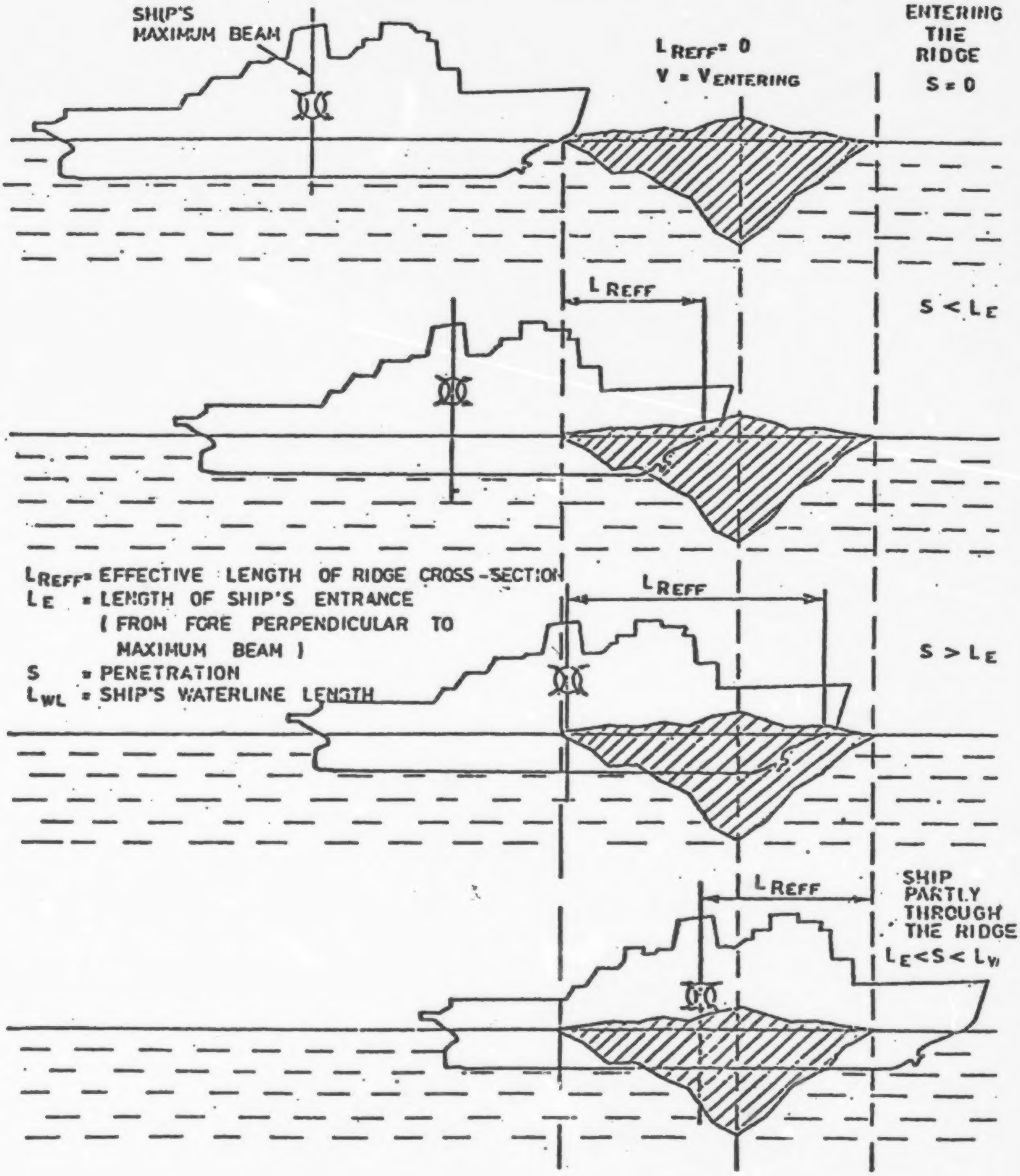
SHIP'S MAXIMUM BEAM
$L_{REFF} = 0$
$V = V_{ENTERING}$
ENTERING THE RIDGE
$S = 0$
L_{REFF}
$S < L_E$
L_{REFF} = EFFECTIVE LENGTH OF RIDGE CROSS-SECTION
L_E = LENGTH OF SHIP'S ENTRANCE (FROM FORE PERPENDICULAR TO MAXIMUM BEAM)
S = PENETRATION
L_{WL} = SHIP'S WATERLINE LENGTH
L_{REFF}
$S > L_E$
L_{REFF}
SHIP PARTLY THROUGH THE RIDGE
$L_E < S < L_{WL}$

shapes. However, Makinen's approach can be generalized without error. The effective ridge thickness or "average ridge thickness for effective length of ridge cross section" is defined as shown in Figures A.3 and A.4. According to this approach, a ridge is subdivided into a series of uniform segments of ice in which the instantaneous resistance may be evaluated. The calculated values depend on both the ridge width and length of entrance of the bow. On the other hand, resistance was measured from thrust and deceleration records. The influence of added ice and water masses was not taken into account. Correlations were made between the evaluated resistance and effective ice thickness. However, no satisfactory correlation was found between ice resistance and ship speed. This was attributed to inaccurate synchronization of measurements of the penetration, speed and thrust or to ignoring added mass effects.

We may observe that the dynamics of penetrating ships have been completely ignored in computing the resistance. It should be noted that part of the kinetic energy of the ship will be converted to potential energy and the rest will be absorbed by the ridge. In a light ship like the APU (approximately 5000 tons) trimming and heaving may be significant - this may explain why Makinen's results were pessimistic.

A.2.3 Broken Channel Resistance Ahead and Astern

Earlier reviews showed that only limited work has been carried out in this field, mainly by Russian authors. The only available satisfactory model is that developed by Ryvlin in 1968 [20] that was later confirmed by Kashteljan in 1973. This model is used extensively by Russians and others to evaluate broken ice resistance and is given by:

$$R_i = \gamma_i \sqrt{rh} \left(\frac{B}{2}\right)^2 [\bar{k}_1 + 2\mu \ C_{wf} L/B) + (\bar{k}_4 \ \mu \ C_{wp} L/B \ S_c^*)] +$$

$$\bar{k}_2 \gamma_i \ rhB \ (\mu + C_{wf} \tan\alpha_0) F_n + \bar{k}_3 \gamma_i \ rhL \tan^2\alpha_0 \ F_n{}^3$$

where R_i = net ice resistance, kg

r = length or radius of ice floes, m

h = average thickness of ice, m

S_c^* = the degree of compression, points

γ_i = ice density, kg/m³

μ = hull-ice friction coefficient

L = ship length, m

FIGURE A.4

DEFINITION OF THE EFFECTIVE RIDGE THICKNESS AT VARIOUS STAGES OF SHIP PENETRATION

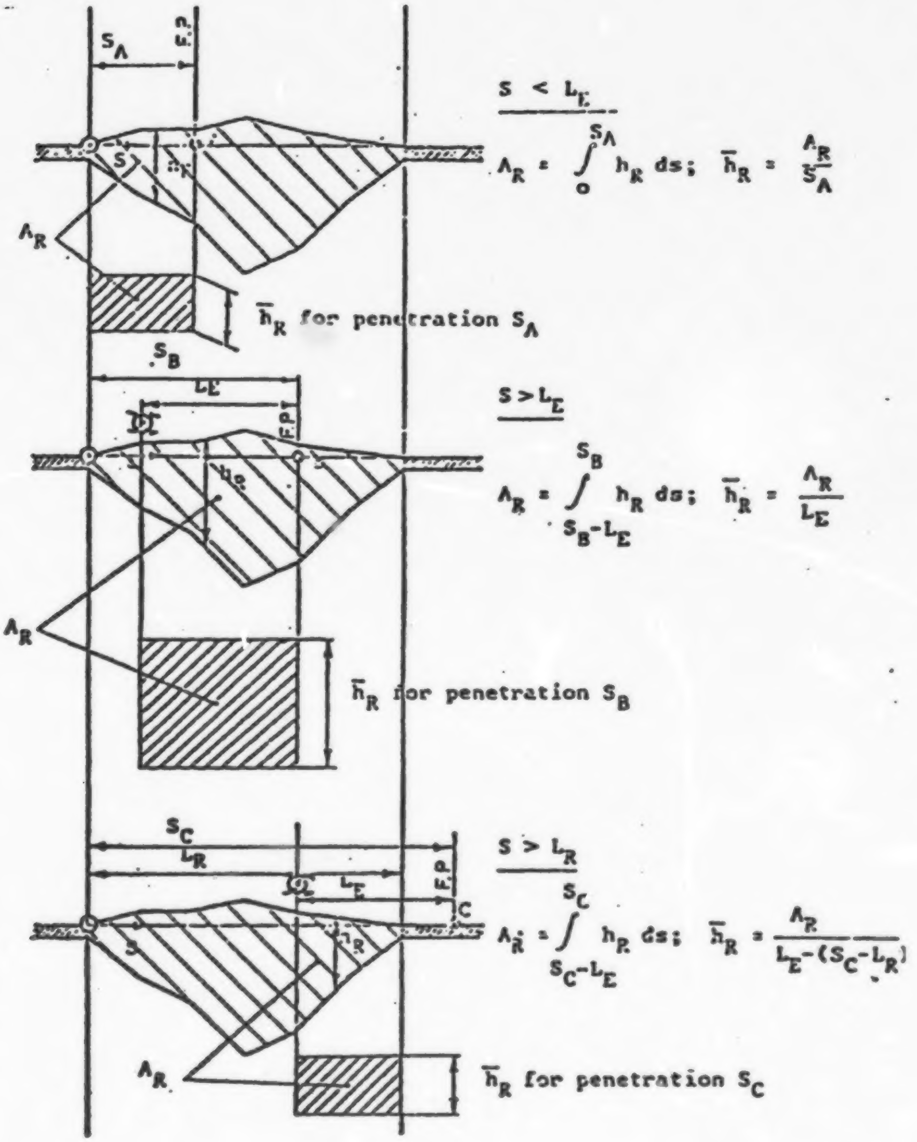
S_A
F.P.
$S < L_E$
$A_R = \int_0^{S_A} h_R \, ds; \quad \bar{h}_R = \frac{A_R}{S_A}$
S
h_R
A_R
$\bar{h}_R$ for penetration S_A
S_B
L_E
F.P.
$S > L_E$
$A_R = \int_{S_B - L_E}^{S_B} h_R \, ds; \quad \bar{h}_R = \frac{A_R}{L_E}$
h_R
A_R
$\bar{h}_R$ for penetration S_B
S_C
L_R
L_E
F.P.
C
$S > L_R$
$A_R = \int_{S_C - L_E}^{S_C} h_R \, ds; \quad \bar{h}_R = \frac{A_R}{L_E - (S_C - L_R)}$
S
h_R
A_R
$\bar{h}_R$ for penetration S_C

S = penetration

L_E = length of ship's entrance (from fore perpendicular to maximum beam)

L_R = total length of ridge cross section

h_R = thickness of ridge

A_R = area of ridge cross section

$\bar{h}_R$ = effective ridge thickness (average ridge thickness for effective length of ridge cross section)

F.P = fore perpendicular of ship

⊠ = midship section (maximum waterline beam) of ship

B = ship beam, m

C_{wp} = waterplane coefficient at DWL

C_{wf} = forebody waterplane coefficient at DWL

α_0 = entrance angle of the bow at DWL, degrees

F_n = length Froude number - $v/\sqrt{gL}$

v = ship speed, m/s

g = gravitational acceleration, m/s²

$\bar{k}_i$, i = 1, 4 are dimensionless coefficients determined from model experiments. Values are given in Figure A.5

This equation is valid for very finely broken ice in the size range from 2 to 20 m which may be found in a channel previously broken by an icebreaker. Sufficient hull form parameters are included in the model to make it not only applicable to the ahead motion, but also to the astern motion. Since there are no separate expressions found for ships, going astern, this resistance model can be used in the ramming mode evaluation. The influence of the appendages usually found in the ships stern configuration, are not considered to have a significant effect on the ice resistance. The broken ice floes will remain near the surface and will not be submerged as in the icebreaking mode. Therefore the waterline form will greatly affect the resistance in broken ice, as can be seen from the set of parameters included in the above model.

FIGURE A.5

NUMERICAL VALUES TO BE USED IN RYVLIN'S EQUATION

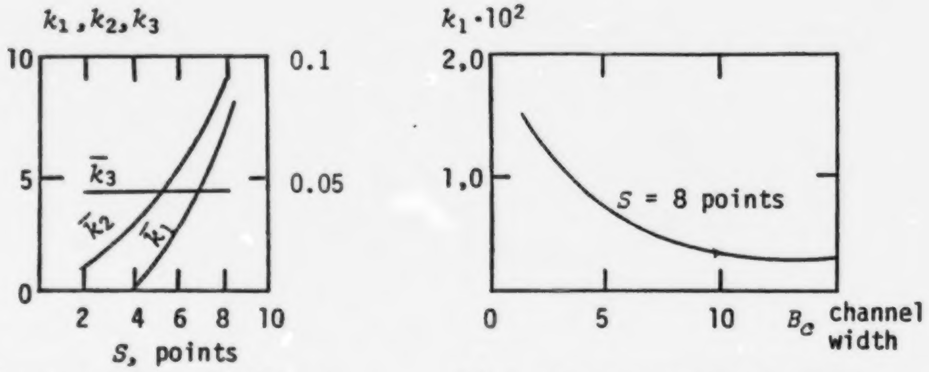

(a) COEFFICIENTS $\bar{k}_1$, $\bar{k}_2$ and $\bar{k}_3$ AS FUNCTIONS OF ICE CONCENTRATION, S IN BALLS (OR TENTHS)

(b) k_1 AS A FUNCTION OF CHANNEL WIDTH FOR S = 8 POINTS

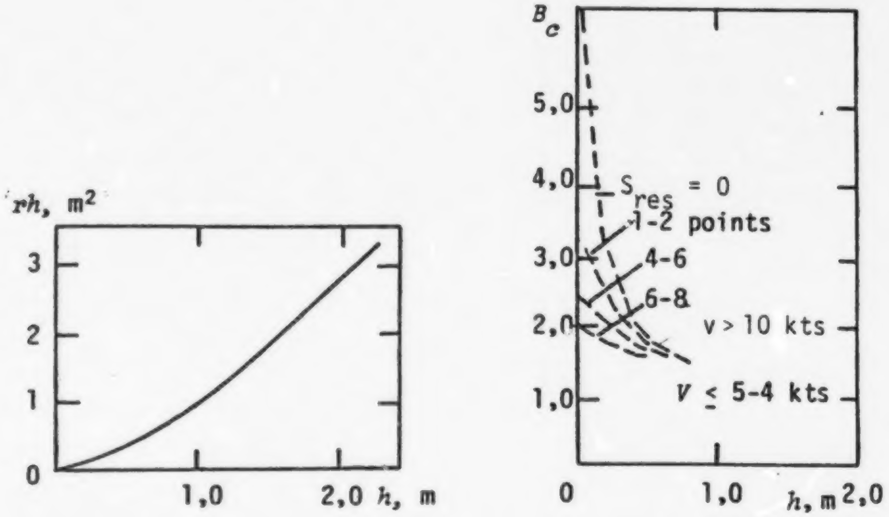

(d) PARAMETER rh AS FUNCTION OF THICKNESS OF CONSOLIDATED ICE

(c) CHANNEL WIDTH AS FUNCTION OF THICKNESS OF CONSOLIDATED ICE (S_{res} IS THE CONCENTRATION OF RESIDUAL ICE). B = 23.5 m

REFERENCES

[1] Nawwar, A.M., Noble, P.G., Edwards, R.Y. and Dunne, M., "Development of a Research Program for Improving Arctic Marine Transportation Technology", Volume II, Situation Reports, for TDC, 1978 also TP2004, 1979. Chapter 3 - Ship Transiting Performance.

[2] Kheysin, D.Ye., "On the Ice Navigation Speed of Ships in Extremely Solid Ice", Ice Navigation Qualities of Ships, ed. by Kheysin, D.Ie., and Popov, Iu.N., Translation, CRREL TL 417, August 1973, pp.19-30.

[3] White, R.M., "Dynamically Developed Force at the Bow of an Icebreaker", Ph.D. Thesis, MIT, 1965.

[4] Vinogradov, I.V. "Suda legovogo plavaniya" (Ships for ice navigation), Moscow, Oborongiz, 1946.

[5] Peirce, T.H., "Arctic Marine Technology: A Review of Ship Resistance in Ice", RINA, October 10, 1978.

[6] Lewis, J.W., & Edwards,R.Y.Jr., "Methods of Predicting Icebreaking and Ice Resistance Characteristics of Icebreakers", Paper #5, SNAME Annual Meeting, New York, November 1970.

[7] Petrov, Ye Yu, and Kheysin, D.Ye., "Calculation of the Inertial Characteristics of Ships Floating in Ice", Proc. of the 14th Scientific and Engineering Con. of Gor'kiy Poly.Inst. Immeni Zhdanov (Shipbuilding Inst.)

[8] Rylin, A.Ya., and Tegkayeva, T.Kh., "Investigation of the Inertial Characteristics of Unsteady-State Motion of an Icebreaker in Ice", Ice Navigation Qualities of Ships, ed. by Kheysin, D.Ye. and Popov, Yu.N., Translation, CRREL 417, August 1973, pp.59-65.

[9] Kashteljan, V.I., Poznjak, I.I., & Ryvlin, A.Ja., "Ice Resistance to motion of a Ship", Sudostroenie, Leningrad, 1968 (translation).

[10] Enkvist, E., "On the Ice Resistance Encountered by Ships Operating in the Continuous Mode of Icebreaking", The Swedish Academy of Engineering Sciences in Finland, Report No.24, Helsinky, 1972.

[11] Johansson, B.M., & Makinen, e., "Great Lakes Ore Carrier Series Ice Resistance Model Test Program", Wartsila Icebreaking Model Basin (WIMB), Test Report No.18, December 29, 1972.

[12] Makinen, E., & Roos, A., "Ice Resistance in Level Ice of Ships with Main Dimensions typical for the Great Lakes Bulk Carriers", Supplement to WIMB Test Report No.A18, September 28, 1973.

[13] Laini, A., et al "Great Lakes Ore Carrier Series Ice Resistance Model Tests in Ballast Conditions",WIMB Report No.24, Sept.25,1975.

[14] Virtamen, J., et al, "Great Lakes Ore Carrier Series - Ice Resistance Model Tests Draft Variations", WIMB Report No.34, April 15, 1975.

[15] Roos, A., et al, "Great Lakes Ore Carrier Series - Ice Resistance Model Test Program", WIMB Report No.A41, November 21, 1974.

[16] Edwards, R.Y.Jr., Major, R.A., Kim, J.K., German, J.G., Lewis, J.W., & MIller, D.M., "Influence of Major Characteristics of Icebreaker Hulls on Their Powering Requirements and Maneuverability in Ice", Paper No.12, SNAME Annual Meeting, New York, Nov.'76.

[17] Nawwar, A.M., & Edwards, R.Y.Jr., "Compilation and Analysis of Recent Icebreaking Model Test Data of a World-Wide Variety of Hull Forms", three volumes, FR211C, by ARCTEC CANADA LIMITED, submitted to Transport Canada R&D Centre, Montreal, January 1978.

[18] Poznyak, I.I., and Ionov, B.P., "The Division of Icebreaker Resistance into Components", SNAME Paper 19, STAR Symposium, Ottawa, June 81.

[19] Makinen, E., "Ice Resistance Measurements in Ridges with I/B APU in the Baltic Sea", Paper presented at the 3rd Int. Conf. on Port & Ocean Engineering Under Arctic Conditions, Univ.of Alaska, 1976.

[20] Carter D., "Ship Resistance to Continuous Motion in Level Ice", Transport Canada, Transportation Development Centre Publication No. TP3679E, March 1983.

[21] Bustard, E.E., "The Importance of Size in an Arctic Ship", Paper No.F., Symposium on Icebreaking and Related Technologies, Ice Tech.'75, Mtl. April 75.

[22] Johansson, B.M., Saarinkangas, J.M., & Waltzer, I., "16.2 MV Baltic Icebreakers", Paper C, Ice Tech '75, Proc. of Symposium on Icebreaking and Related technologies, Montreal, April 1975.

[23] Ackely, S.F., Hibler, W.D., Kovacs, A., Weeks, W.F., Hartwell, A., and Campbell, W.J., "Investigation Performed on the Arctic Ice Dynamics Joint Experiment, March 1971; CRREL, December 1973.

APPENDIX B

DEVELOPMENT OF QUALITY ASSESSMENT - METHOD

The procedure for classification of the quality of each individual set of data that is available for the analysis of each particular ram, was set up to reflect:

- the quality of the data recording,
- the quality and quantity of output expected from the analysis of the data,
- the availability and reliability of the ice characteristics.

The first two items, are linked together in one group and are reviewed for:

- completeness of ram cycle and availability of the components of the ram cycle,
- suitability for and expected accuracy of curve-fitting applied to the speed signal.

In the analysis of the ram data the speed signal is the only available signal from which the ram cycle can be identified and therefore forms the basis of all further analysis.

A penalty-point system was used for the quality assessment. The speed signal was evaluated for completeness of the ram cycle and the level of eruptions due to inadequate doppler-log readings. The classifications used and the penalty-points assigned are:

Speed Signal Classification

Excellent	(E)	0 points
Good	(G)	1 point
Fair	(F)	2 points
Poor	(P)	3 points

The ram cycle was split up into three components with their proportion ratio of the output they affect and with the percentage output lost if the cycle component is incomplete or not available at all:

Backing (B), ratio 1, incomplete: 10%, not available: 5%
Acceleration (A), ratio 2, incomplete: 20%, not available: 10%
Penetration (P), ratio 3, incomplete: 20%, not available: 15%

The ratio was used as a weightfactor in the assessment. If one of the components is not complete, 20% of the output is lost automatically (e.g. cycle time, speed of advance).

The number of penalty-points is then added to the total percentage of output lost and results in the final tape data quality number, which ranges from 0 to 100. Table B.1 shows the results for all rams.

A similar approach was adopted for the classification of the availability and reliability of the ice characteristics taken from [21]. For ice thickness the following rating was used:

Measured and Confirmed (MC): 0 points
Measured (M) : 20 points
Estimated (E) : 40 points
Not Available (N) : 60 points

The classification MC is used for given thickness measurements that were confirmed elsewhere in [21]. In a number of occasions the values of ice thickness were conflicting in which cases the most reliable values were taken and classified as M.

The following ice properties were considered in the quality assessment and classification was assigned when measured (M), estimated from surrounded measurements (E), calculated (flexural strength) from temperature and salinity (C), or not available (N):

Flexural Strength: M = 0, C = 5, N = 10
Conf. Compr. Strength: M = 0, E = 5, N = 10
Ice Temperature: M = 0, E = 5, N = 10
Salinity: M = 0, E = 5, N = 10

The temperature and salinity should only be taken into consideration when the flexural strength is not measured.

The total of points for ice thickness and ice properties represents the quality number for ice characteristics. This total was added to the tape data quality number to obtain the overall quality number, which ranges from 0 to 200. For quick reference and insight in the quality build up, a quality identification was defined by two letters and a figure was added to indicate the incompleteness of the tape data and consequently the output of data analysis as follows:

Tape Data Quality: A: 6 points
B: 12 points
C: 18 points

Ice Data Quality: A: 10 points
B: 20 points
C: 40 points
D: 60 points
E: 60 points

Tape Data Collection: None: no data and output missing
1 : 50% missing
2 : 70% missing
3 : 70% missing

The quality assessment is reviewed in Table B.1, and an example describing the above stated procedure is given in the following.

TABLE B.1

RAM NO.	TAPE DATA		DATA COMPL.	DATA TOTAL	ICE THICKNESS	ICE PROP.	ICE TOTAL	QUALITY	
	COMPONENTS BAP	Q NO.	Q NO.	Q NO.	Q NO.	Q NO.	Q NO.	NO.	ID
A1	-GG	5	55	60	0	20	20	80	AB2
A2	GEE	1		1	40	20	60	61	AD
A3	FEE	2		2	40	20	60	62	AD
A4	FGG	7		7	40	20	60	67	BD
A5	FGE	4		4	40	20	60	64	AD
A6	GEE	1		1	20	20	40	41	AC
A7	GEE	1		1	40	20	60	61	AD
A8	GEE	1		1	40	20	60	61	AD
A9	GEE	1		1	0	20	20	21	AB
A10	GGE	3		3	40	20	60	63	AD
A11	FEE	2		2	40	20	60	62	AD
A12	FGG	7		7	40	20	60	67	BD
A13	FEP	11		11	40	20	60	71	BD
A14	PGG	8		8	40	20	60	68	BD
A15	FGG	7		7	40	20	60	67	BD
A16	FGF	10		10	0	20	20	30	BB
A17	FFF	12		12	40	20	60	72	BD
A18	FEG	5		5	40	20	60	65	AD
B1	GGG	6		6	0	20	20	26	AB
B2	FGF	10		10	0	20	20	30	BB
B3	GGF	9		9	0	20	20	29	BB
B4	FEG	5		5	20	20	40	45	AC
B5	FEF	8		8	0	20	20	28	BB
B6	PGF	11		11	0	20	20	31	BB
B7	PGF	11		11	0	20	20	31	BB
B8	PEP	11		12	20	15	35	47	BC
B9	PGG	8		8	20	20	40	48	BC
B10	GGP	12	35	47	20	20	40	87	BC1
B11	PGP	14	50	64	20	20	40	104	CC2
B12	PGP	14	50	64	20	20	40	104	CC2
B16	GEF	7	30	37	0	20	20	57	BB1
B17	FGF	10		10	0	5	5	15	BA
B18	GGF	9		9	40	5	45	54	BD
B19	PGF	11		11	0	20	20	31	BB
B20	FEF	8		8	40	20	60	68	BD
B21	GEF	7		7	20	20	40	47	BC
B22	PGF	11		11	20	20	40	51	BC
B23	GGP	11		12	0	20	20	32	BB
B24	FGF	10		10	0	20	20	30	BB
C6	GGG	6	30	6	0	20	20	26	AB
C7	FFP	15		15	20	20	40	55	CC
C8	GGP	12		12	20	15	35	47	BC
C9	GEF	7		7	00	20	20	27	BB
C10	GEG	4	30	4	00	20	20	24	AB
C18	PEG	6		36	20	20	40	76	AC1
C24	GEE	1		1	40	20	60	61	AD
C25	GEE	1		1	0	20	20	21	AB
C26	EEE	0		0	0	20	202	20	AB
C27	GGE	3		33	0	20	20	53	AB1
C29	GGG	6		6	0	20	20	26	AB
C30	GGE	3		3	0	20	20	23	AB
C31	GGE	3		3	0	20	20	23	AB
C32	FGG	7		7	20	5	25	32	BC
C33	-GE	2	55	57	0	20	20	77	AB2
C34	-GG	5	35	40	0	20	20	61	AB1
C35	-GE	2	75	77	00	20	20	97	AB3

EXAMPLE OF QUALITY ASSESSMENT

RAM NO. C18

Tape Data

Speed Signal Classification (Figure B.1)

Backing,	Poor (P),	3 points,	ratio 1,	points 3
Acceleration,	Excellent (E),	0 points,	ratio 2,	points 0
Penetration,	Good (G)	1 point,	ratio 3,	points 3

Tape Data Q. No. = 3 + 0 + 3 = 6

Data Completeness

Cycle completeness,	20% of data,	incomplete,	data lost 20%
Backing compl.,	10% of data,	incomplete,	data lost 10%
Backing availability	5% of data,	available,	data lost 0%
Acceleration compl.	20% of data,	complete,	data lost 0%
Acceleration availability,	10% of data,	available,	data lost 0%
Penetration compl.	20% of data,	complete,	data lost 0%
Penetration availability,	15% of data,	available,	data lost 0%
Total	100%	Total data and output lost	30%

Data Compl. Q. No. = 30

Data total Q. No. = 6 + 30 = 36

Ice Characteristics

Ice thickness, measured (M), 20 points

Ice Thickness Q.No. = 20

Flexural Strength, calculated (C), 5 points

Flexural strength not measured, therefore:

Conf. Compr. Strength,	estimated (E), 5 points
Ice Temperature,	estimated (E), 5 points
Salinity,	estimated (E), 5 points

Ice Properties Q.No. = 5 + 5 + 5 + 5 = 20

Ice Total Q. No. = 20 + 20 = 40

Quality

Quality No. = 36 + 40 = 76

Tape Data Quality:	6 < 6	ID = A
Ice Data Quality :	40 < 40	ID = C
Tape Data Collection :	30% missing < 50%	ID = 1

Quality ID = AC1

FIGURE B.1   OUTPUT SIGNALS FOR RAM NO.C18

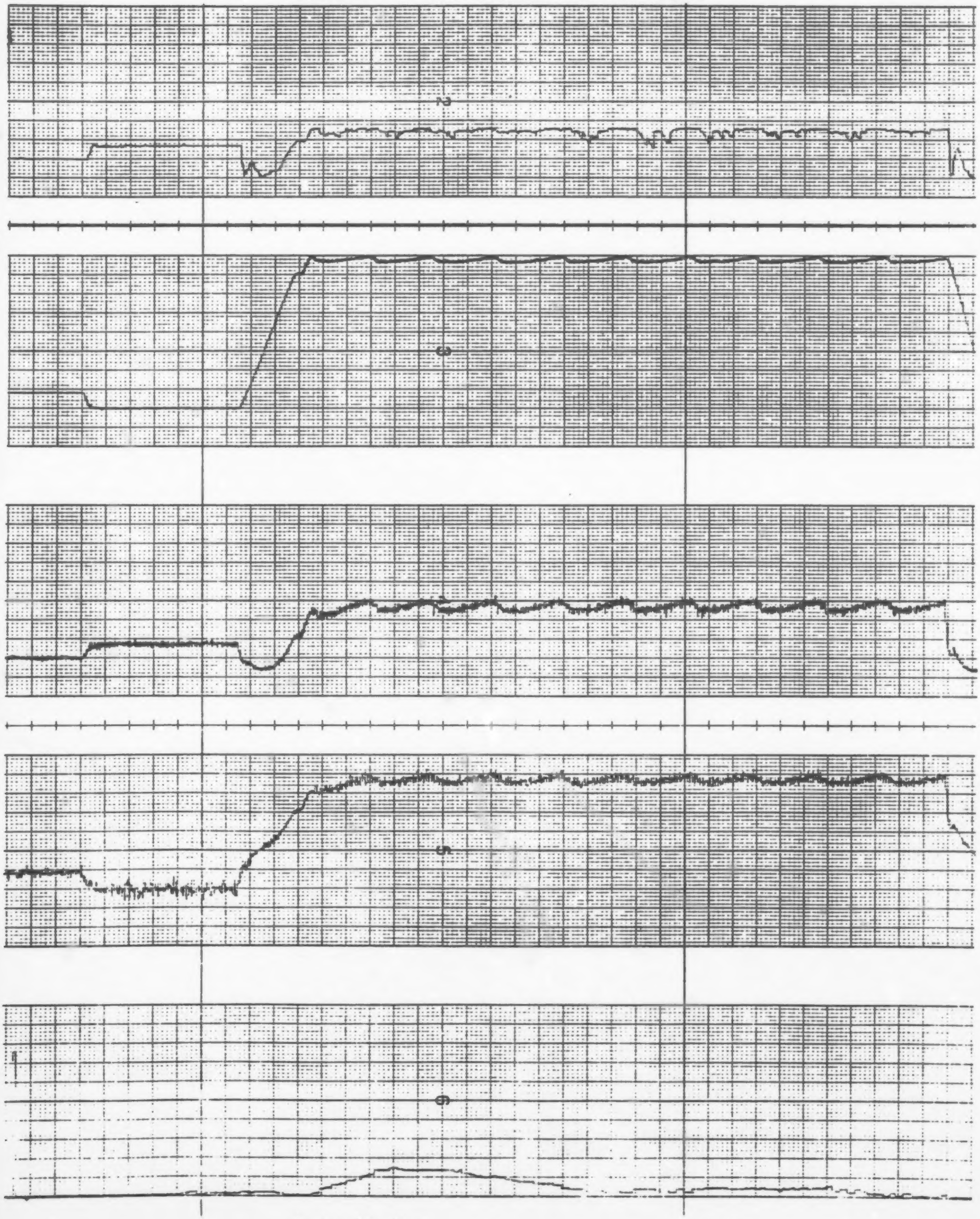

APPENDIX C

RESULTS OF DEDICATED TRIALS

ADMIRALTY INLET, 1981

The following rams have been analyzed and the results of analysis are listed sequentially in the same order in the following pages:

Admiralty Inlet Trials, 1981 Season

Series A: A2 - A18

Series B: B1, B3 - B8, B18 - B23

Series C: C6, C7 - C9, C24, C25, C27, C29, C31, C32

Following are some remarks on the listings and graphical output:

a) In some cases the estimated fuel rate and total fuel used are negative. This is mainly due to the erroneous formulas for conversion from mms to kg/hr. Since we could not correct such formulas nor verify them we have opted to calculate the fuel variables in mms and mm.hr as well as provide estimates of such rates based on operating power levels.

b) In some cases there appears to be a discontinuity at the point of impact. This occurs when the deceleration on impact is high and the curves fit independently for the acceleration and penetration stages do not meet at breakpoint C. Generally, the low accuracy of doppler speed records cause some unexpected trends such as increasing acceleration or deceleration prior to reaching point C. Limited attempt has been made to rectify this because a complete solution would require simultaneous satisfaction of the three conditions of speed correction, namely; impact speed, penetration distance, and equality of backing and acceleration distances. This could not be achieved within the scope of the present work. Therefore, the regions just before and just after impact may be reviewed within this context and low reliability of acceleration and hence resistance estimates in this range may be expected. However, such errors may not significantly affect the distances travelled or cycle time components.

c) In cases of short penetration distances (particularly Series A rams), the duration of penetration is short and the total number of points is small, considering the sampling rate of 1 Hz. Combined with the level of accuracy and reliability of the doppler log, this makes the application of speed correction and curve fitting rather tricky and may cause anomalies such as that observed in Ram A2 where significant correction of the penetration speed history was necessary to match the measured penetration. Further development of the data reduction program will be necessary to remove these effects and discontinuities. This problem was also observed in cases of poor speed record (e.g. Ram B8).

d) In Ram B1, the torque measurement was missing and this affected the estimated power levels and fuel rates. Therefore, the negative readings should be discarded. This error due to missing data does not affect other calculations of speed, penetration, etc. and in fact this was one of the good quality rams except for the above noted error.

e) In some cases, the deceleration at the first part of the penetration stage appears to increase slowly. This causes the resistance to be lower than expected. The physical reason behind this could be the failure and cracking of the ice cover. Case B3 is an example for this phenomenon occuring in a small ridge while Ram B23 is a similar occurance in level ice. In the latter case the poor speed quality during the penetration stage must be noted.

f) In some rams a large discrepancy between measured and calculated penetration exists. For instance, in Ram C27 the difference is so large that the correction procedures could not account for all of it.

ADMIRALTY INLET TRIALS, 1981

SERIES A

```
                    RESULTS OF RAMMING CYCLE ANALYSIS


                              RAM No.  __A2

TAPE:        81-T2-2.1                ICE CONDITIONS:      RIDGES

CATEGORY:    R3                       ICE THICKNESS:       2.36  m

QUALITY:     61AD                     FLEXURAL STRENGTH:   407  kPA

TRIM:        EVEN
                                      BUBBLER STATUS:     OFF


RAMMING CYCLE CHARACTERISTICS:

Speed of Advance  (knots)      .0872

Speed of Impact   (knots)      3.7     ( 3.86 )


                               Duration (sec)   % Cycle Time   Distance  (m)
Backing                        284              53.5          -80.36
Acceleration                   89               16.8           80.36
Penetration                    50               9.42           15.2 (23.81)
Extraction                     108              20.3
Total Cycle                    531


Duration of Astern Mode        (sec)     182
Duration of Reversal to Ahead  (sec)     130
Duration of Ahead Mode         (sec)     61
Duration of Reversal to Astern (sec)     158
Start of Reversal after Impact (sec)     0

Total Fuel Used    (mm*hr)               3.79         Est. kg:     -137.2
Average Fuel Rate  (mm)                  25.67        Est. kg/hr: -930.24

Backing Power      (kW)                  2624.9
[Est Fuel Rate     (kg/hr)]              615.66

Acceleration Power (kW)                  9263.2
[Est Fuel Rate     (kg/hr)]              1939.3
```

RAM # __A2 TAPE: 81-T2-2.1 07 JUL 1981 02:16:12

FIG. #1

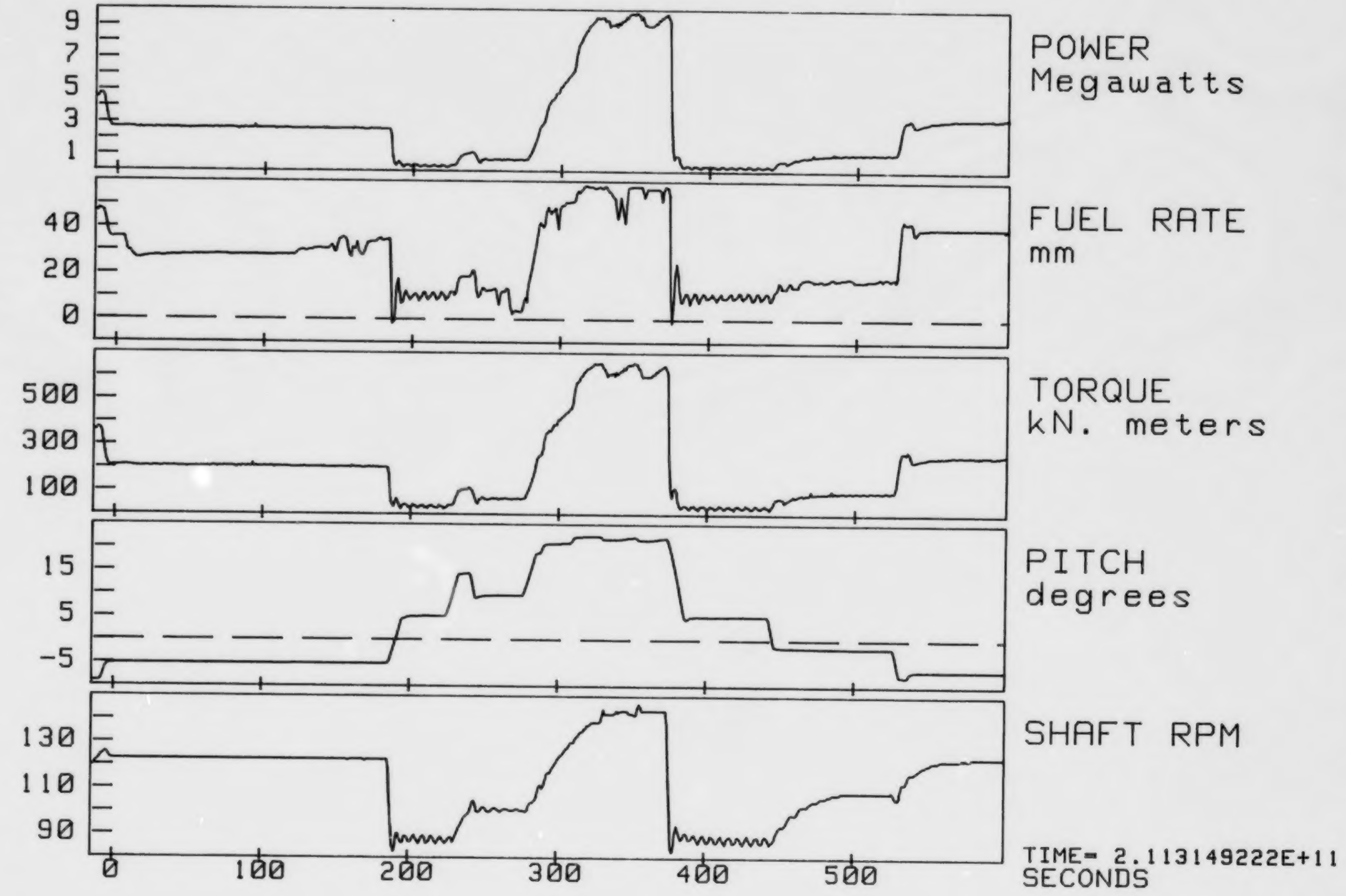

RAM # __A2 TAPE: 81-T2-2.1 07 JUL 1981 02:16:12 **FIG. #2**

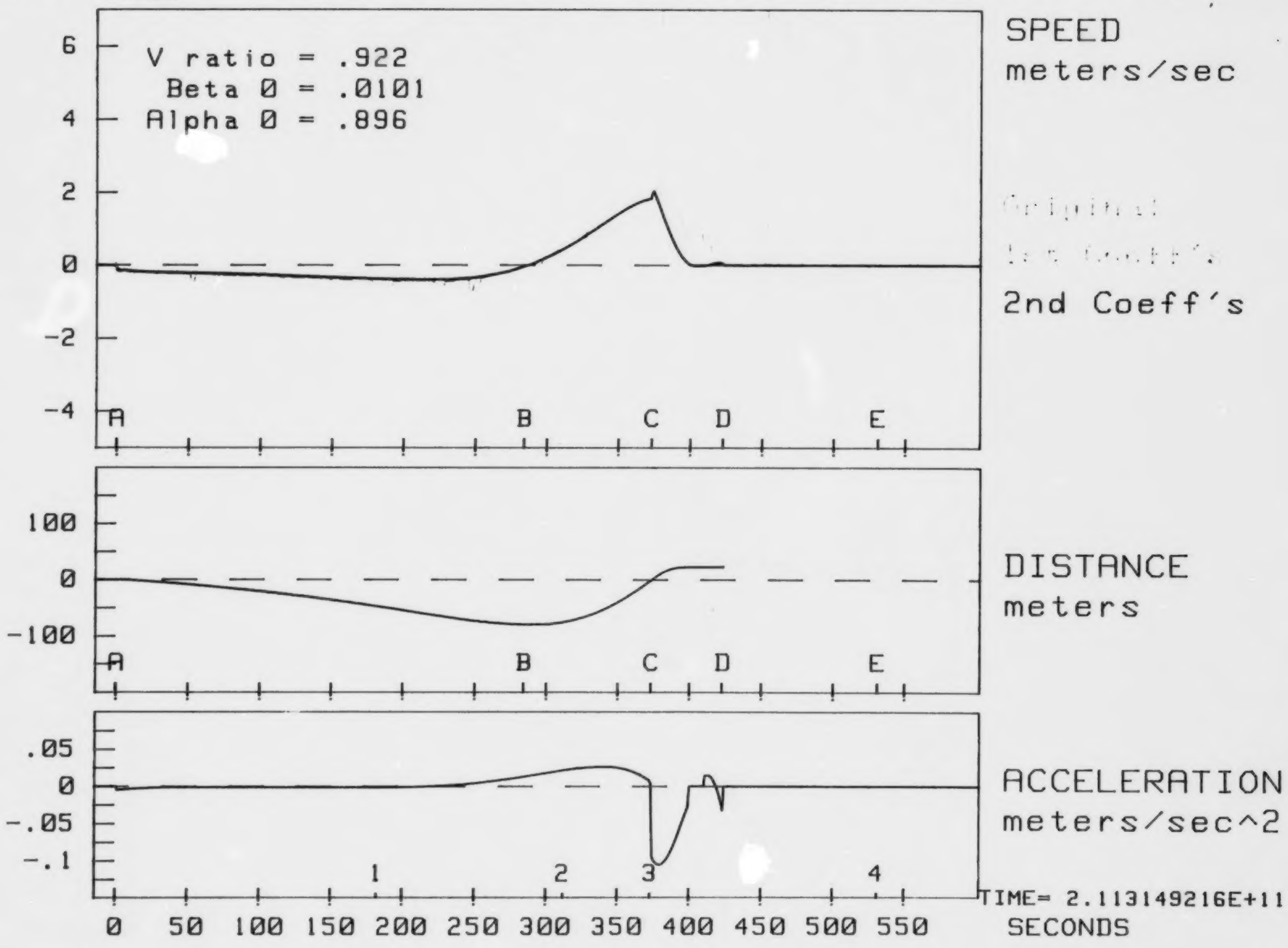

RAM # __A2 TAPE: 81-T2-2.1 07 JUL 1981 02:16:12

FIG. #3

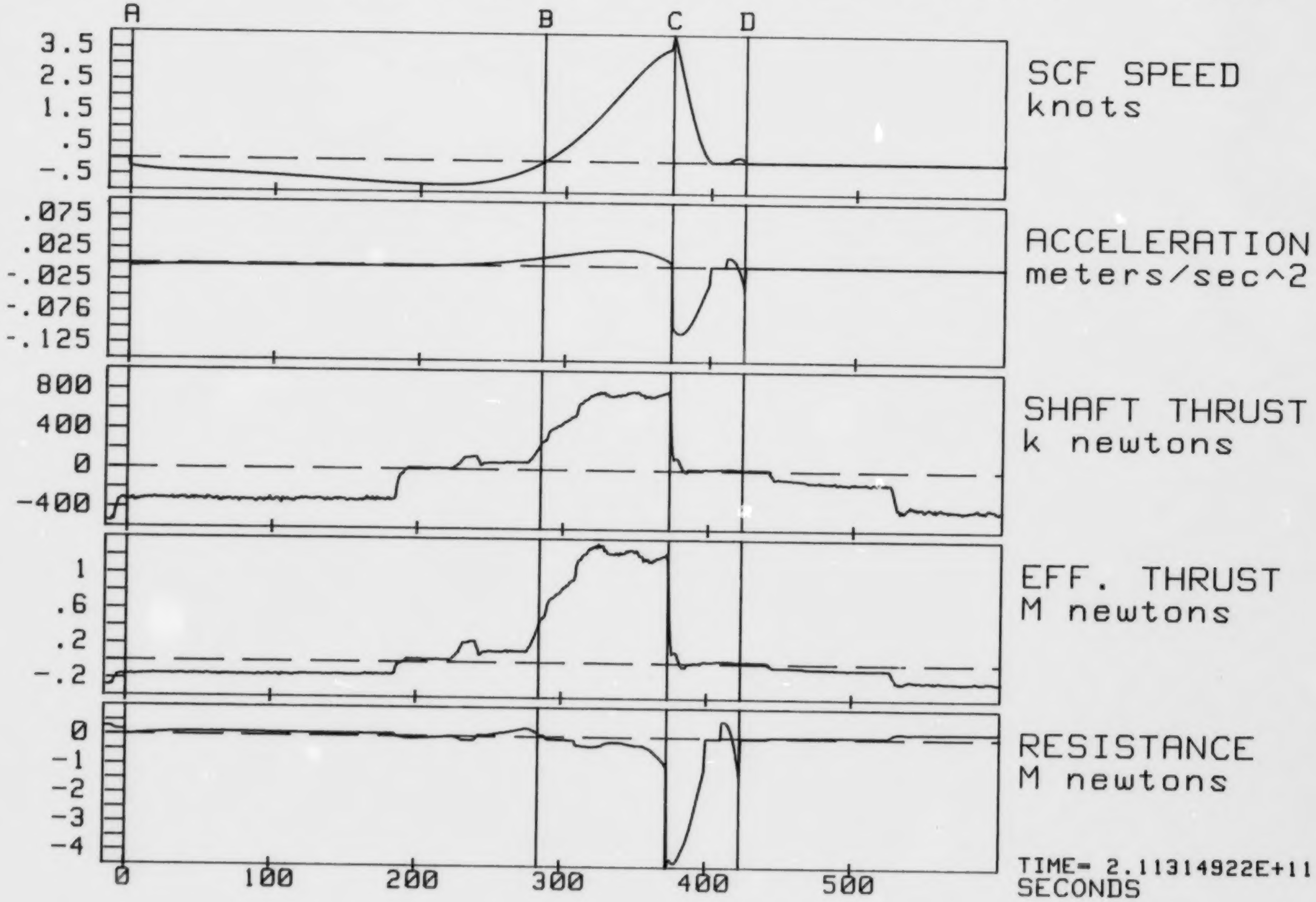

RAM # __A2 TAPE: 81-T2-2.1 07 JUL 1981 02:16:12 Fig.# 4

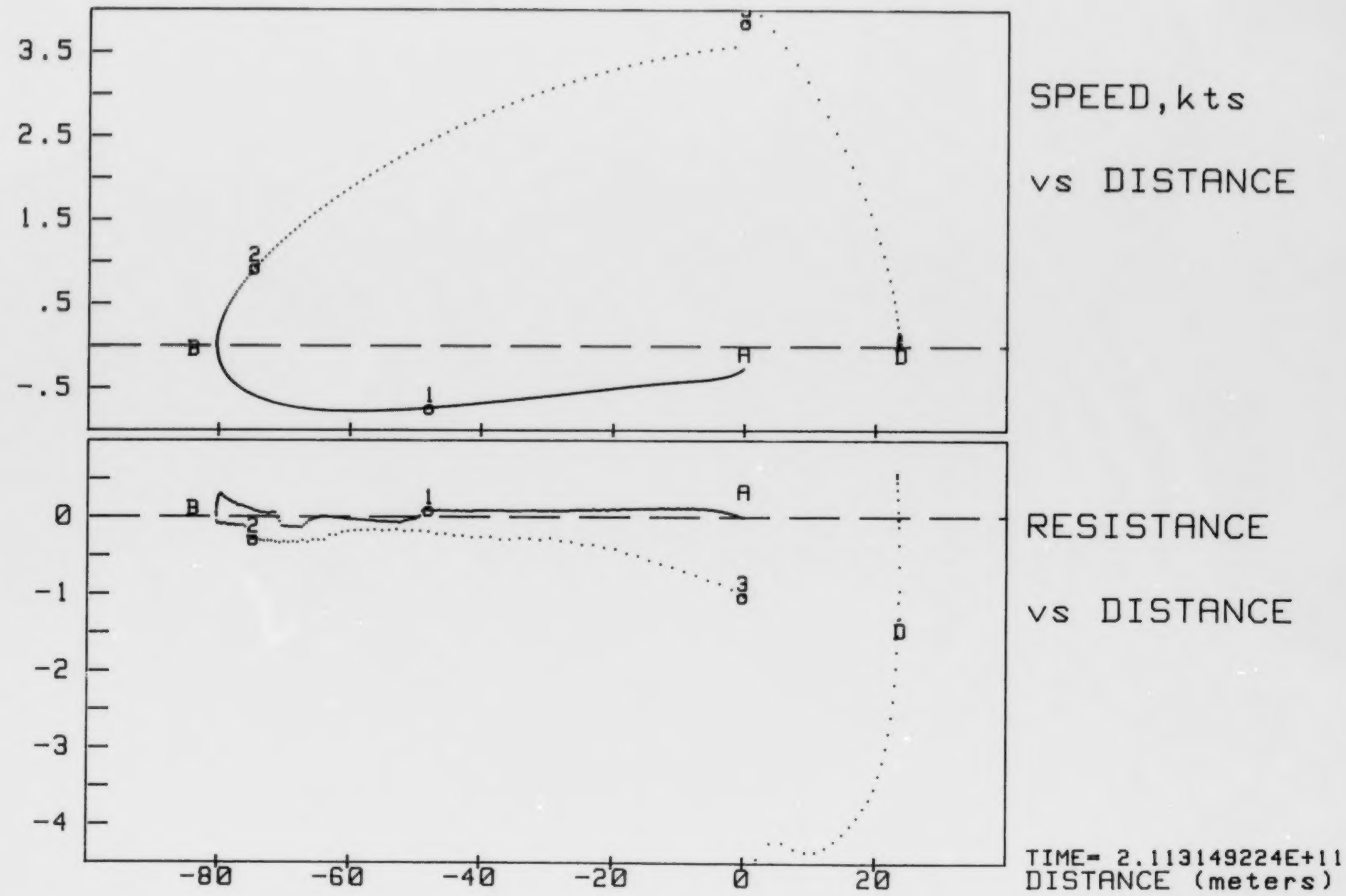

SPEED,kts vs DISTANCE

RESISTANCE vs DISTANCE

TIME= 2.113149224E+11

RAM # __A2 TAPE: 81-T2-2.1 07 JUL 1981 02:16:12 Fig.# 5

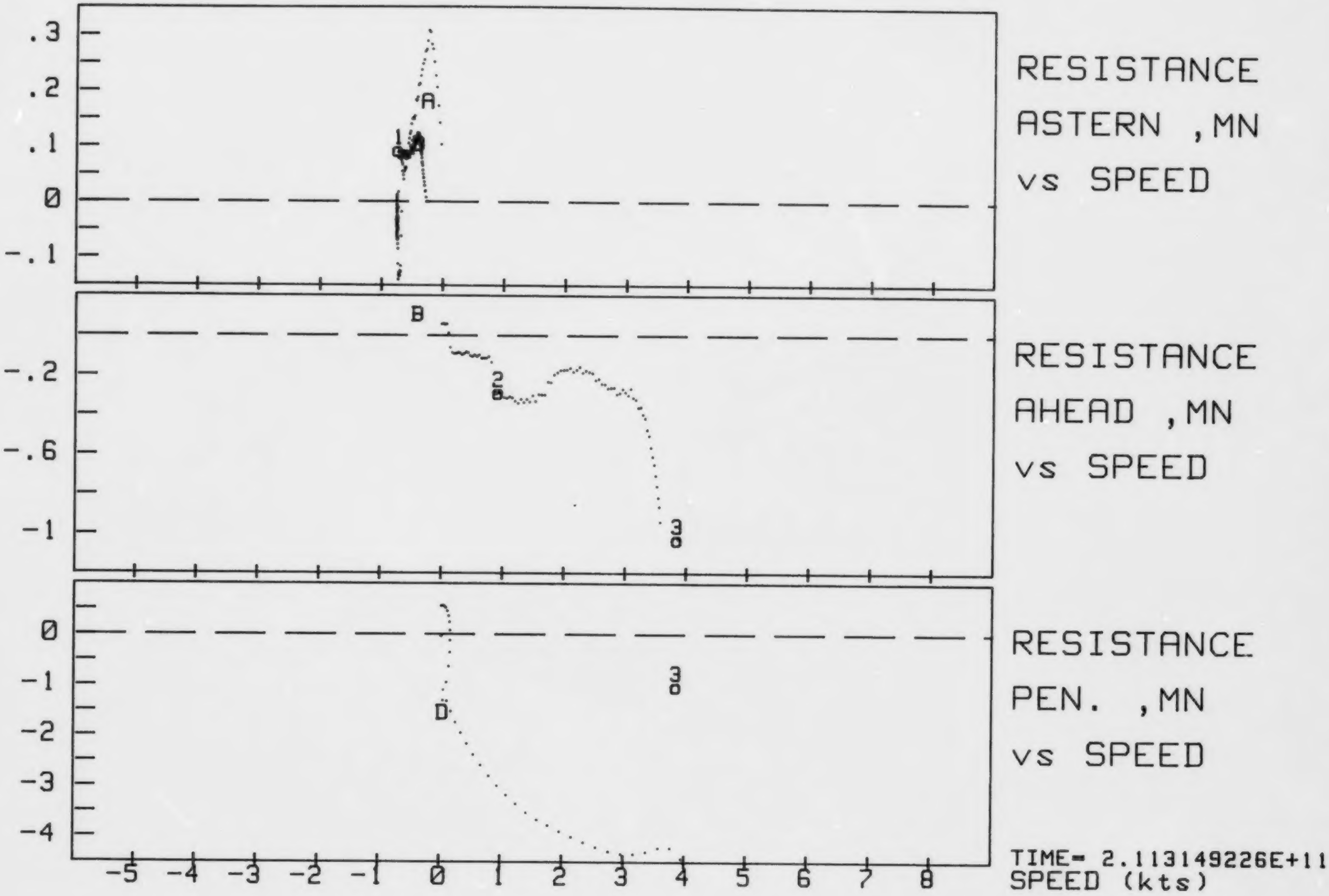

RESULTS OF RAMMING CYCLE ANALYSIS

RAM No. __A3

TAPE:	81-T2-2.1	ICE CONDITIONS:	RIDGES
CATEGORY:	R3	ICE THICKNESS:	2.52 m
QUALITY:	62AD	FLEXURAL STRENGTH:	407 kPA
TRIM:	EVEN	BUBBLER STATUS:	OFF

RAMMING CYCLE CHARACTERISTICS:

Speed of Advance	(knots)	.0576
Speed of Impact	(knots)	3.7 (4.43)

	Duration (sec)	% Cycle Time	Distance (m)
Backing	309	62.7	-124.6
Acceleration	105	21.3	124.6
Penetration	50	10.1	9.1 (14.62)
Extraction	29	5.88	
Total Cycle	493		

Duration of Astern Mode	(sec)	140
Duration of Reversal to Ahead	(sec)	213
Duration of Ahead Mode	(sec)	111
Duration of Reversal to Astern	(sec)	29
Start of Reversal after Impact	(sec)	50

Total Fuel Used	(mm*hr)	4.72	Est. kg:	-40.83
Average Fuel Rate	(mm)	34.44	Est. kg/hr:	-298.14

Backing Power	(kW)	3264
[Est Fuel Rate	(kg/hr)]	743.1

Acceleration Power	(kW)	9332.5
[Est Fuel Rate	(kg/hr)]	1953.1

RAM # __A3   TAPE: 81-T2-2.1   07 JUL 1981 02:25:12

FIG. #1

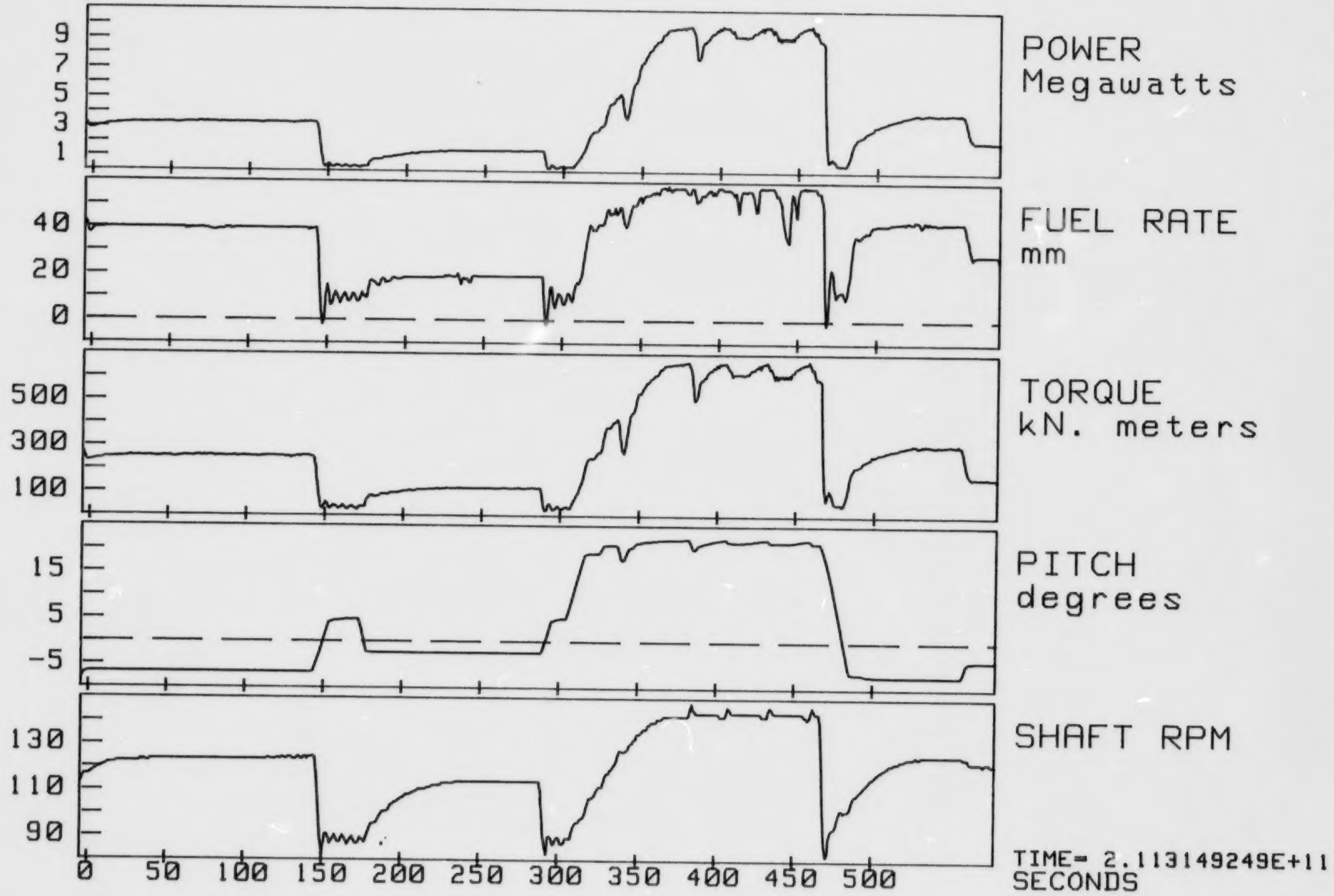

RAM # __A3 TAPE: 81-T2-2.1 07 JUL 1981 02:25:12 **FIG. #2**

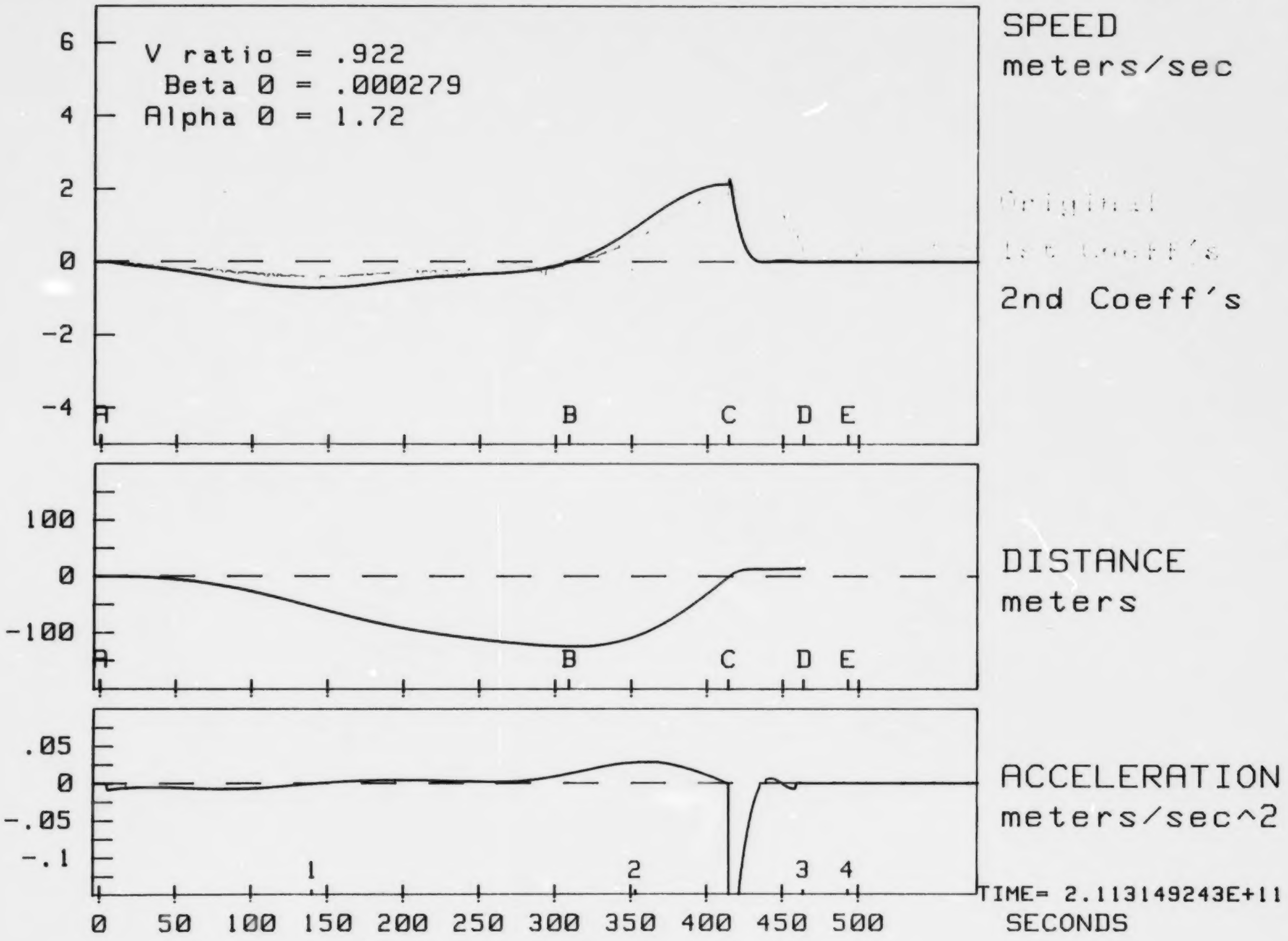

RAM # __A3 TAPE: 81-T2-2.1 07 JUL 1981 02:25:12 **FIG.#3**

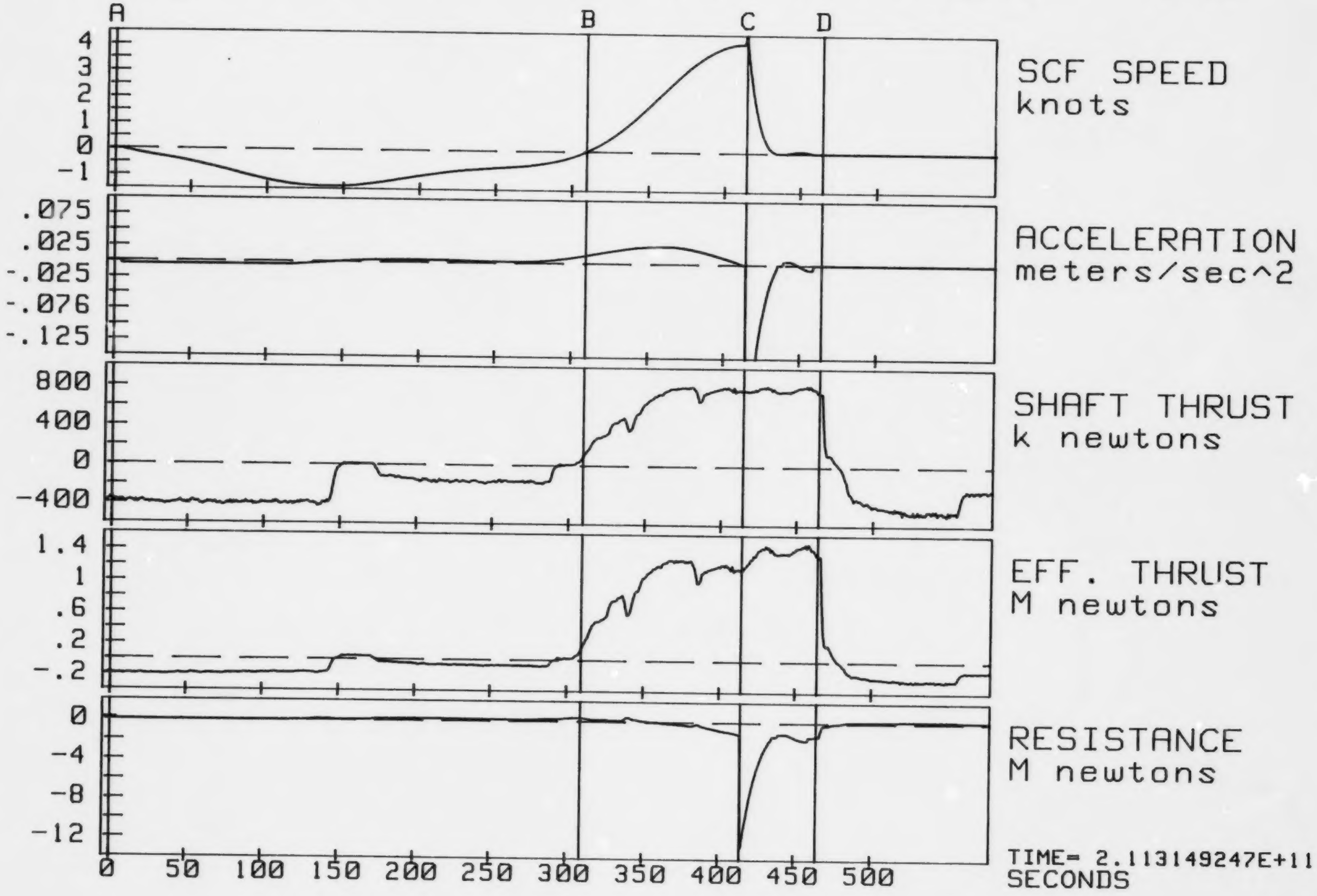

RAM # __A3 TAPE: 81-T2-2.1 07 JUL 1981 02:25:12 Fig.# 4

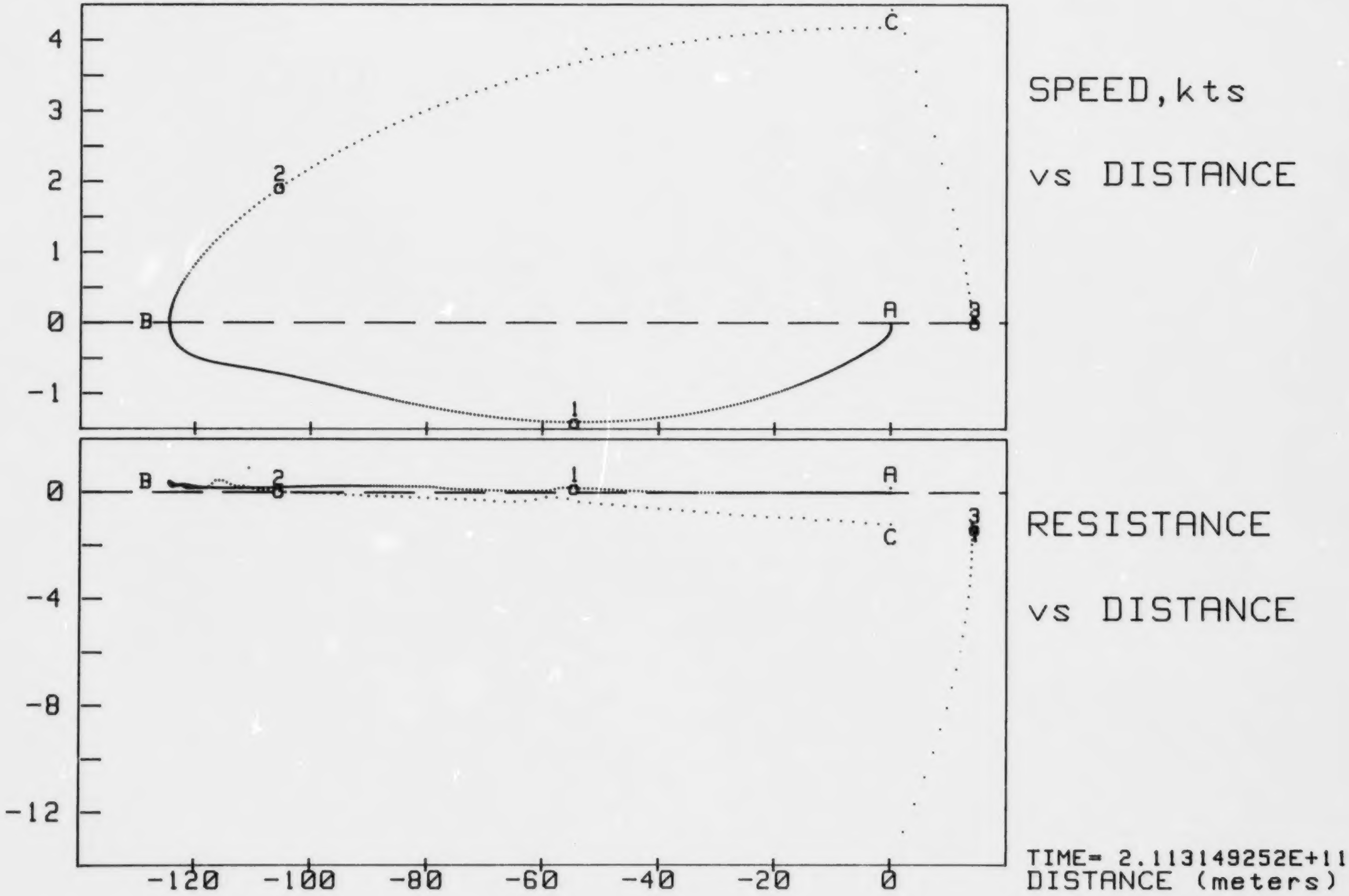

RAM # __A3 TAPE: 81-T2-2.1 07 JUL 1981 02:25:12 Fig.# 5

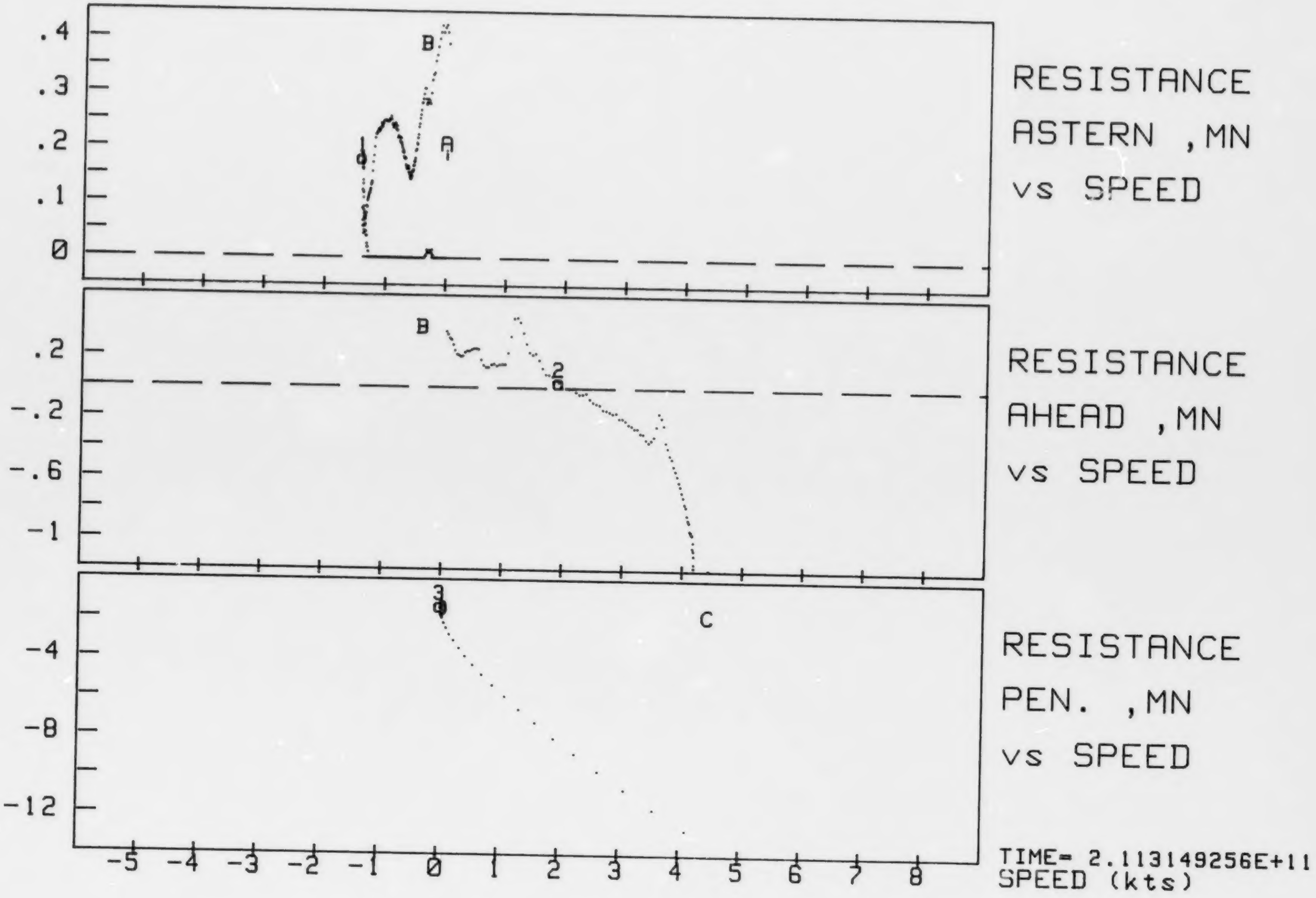

RESULTS OF RAMMING CYCLE ANALYSIS

RAM No. __A4

TAPE:	81-T2-2.1	ICE CONDITIONS:	RIDGES
CATEGORY:	R3	ICE THICKNESS:	2.6 m
QUALITY:	67BD	FLEXURAL STRENGTH:	407 kPA
TRIM:	EVEN	BUBBLER STATUS:	OFF

RAMMING CYCLE CHARACTERISTICS:

Speed of Advance	(knots)	.0502	
Speed of Impact	(knots)	3.7	(3.57)

	Duration (sec)	% Cycle Time	Distance (m)
Backing	232	58.1	-87.23
Acceleration	93	23.3	87.23
Penetration	22	5.51	4.5 (10.3)
Extraction	52	13	
Total Cycle	399		

Duration of Astern Mode	(sec)	40		
Duration of Reversal to Ahead	(sec)	228		
Duration of Ahead Mode	(sec)	55		
Duration of Reversal to Astern	(sec)	76		
Start of Reversal after Impact	(sec)	-2		
Total Fuel Used	(mm*hr)	3.36	Est. kg:	-66.08
Average Fuel Rate	(mm)	30.31	Est. kg/hr:	-596.25
Backing Power	(kW)	3974.7		
[Est Fuel Rate	(kg/hr)]	884.8		
Acceleration Power	(kW)	9655.3		
[Est Fuel Rate	(kg/hr)]	2017.5		

RAM # __A4 TAPE: 81-T2-2.1 07 JUL 1981 02:34:42 **FIG. #1**

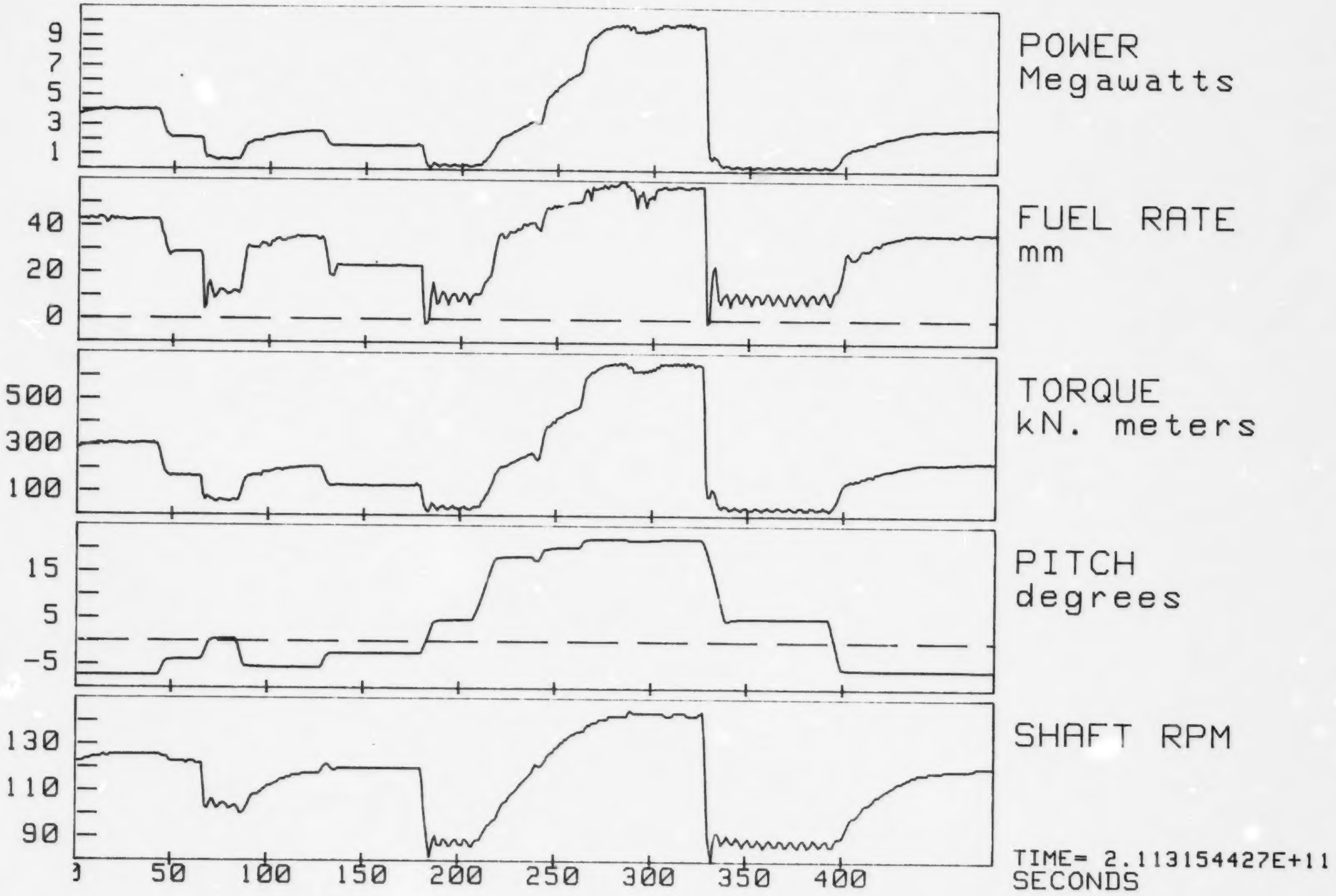

RAM # __A4 TAPE: 81-T2-2.1 07 JUL 1981 02:34:42

FIG.#2

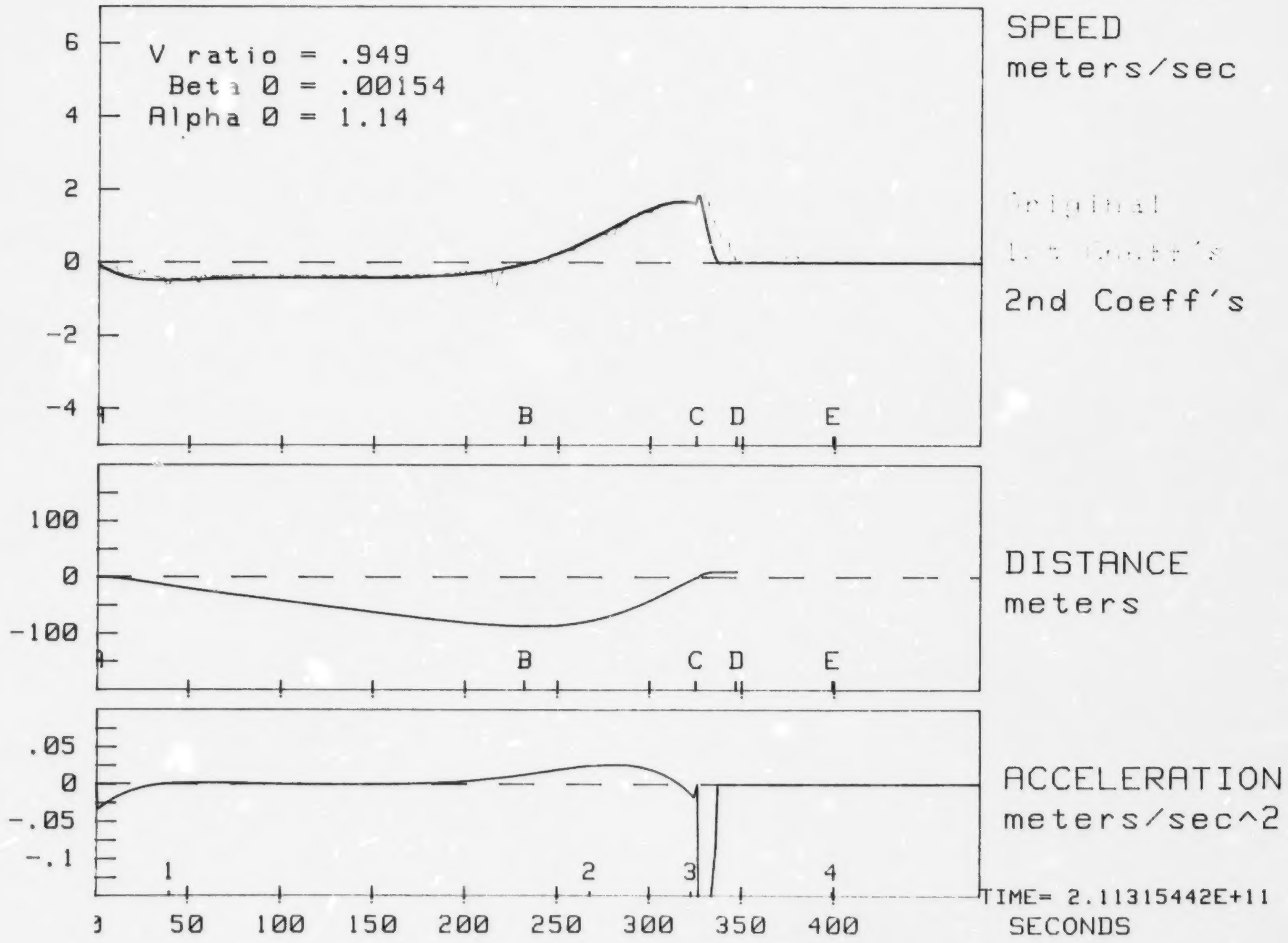

RAM # __A4 TAPE: 81-T2-2.1 07 JUL 1981 02:34:42 **FIG. #3**

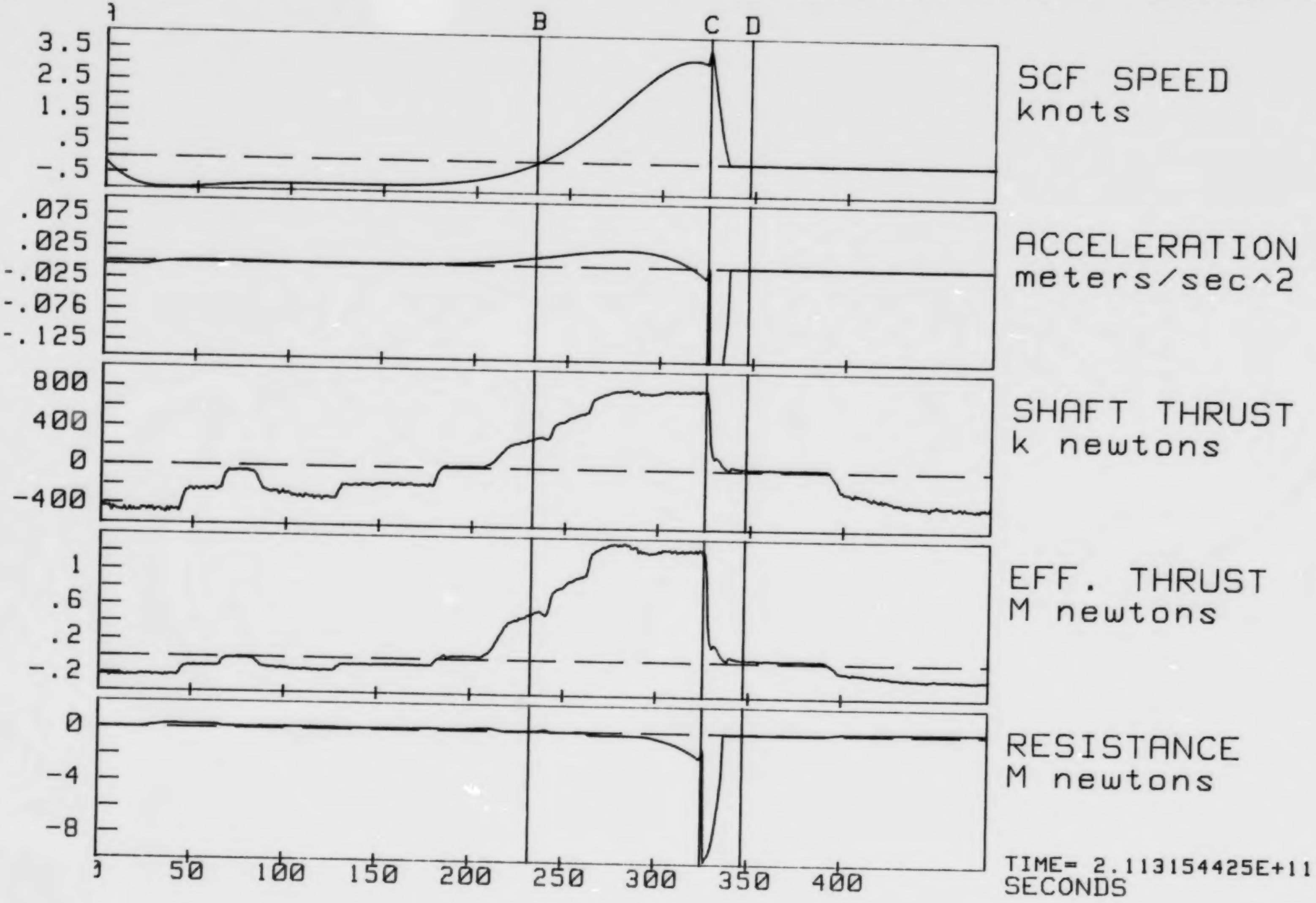

RAM # __A4   TAPE: 81-T2-2.1   07 JUL 1981 02:34:42   Fig.# 4

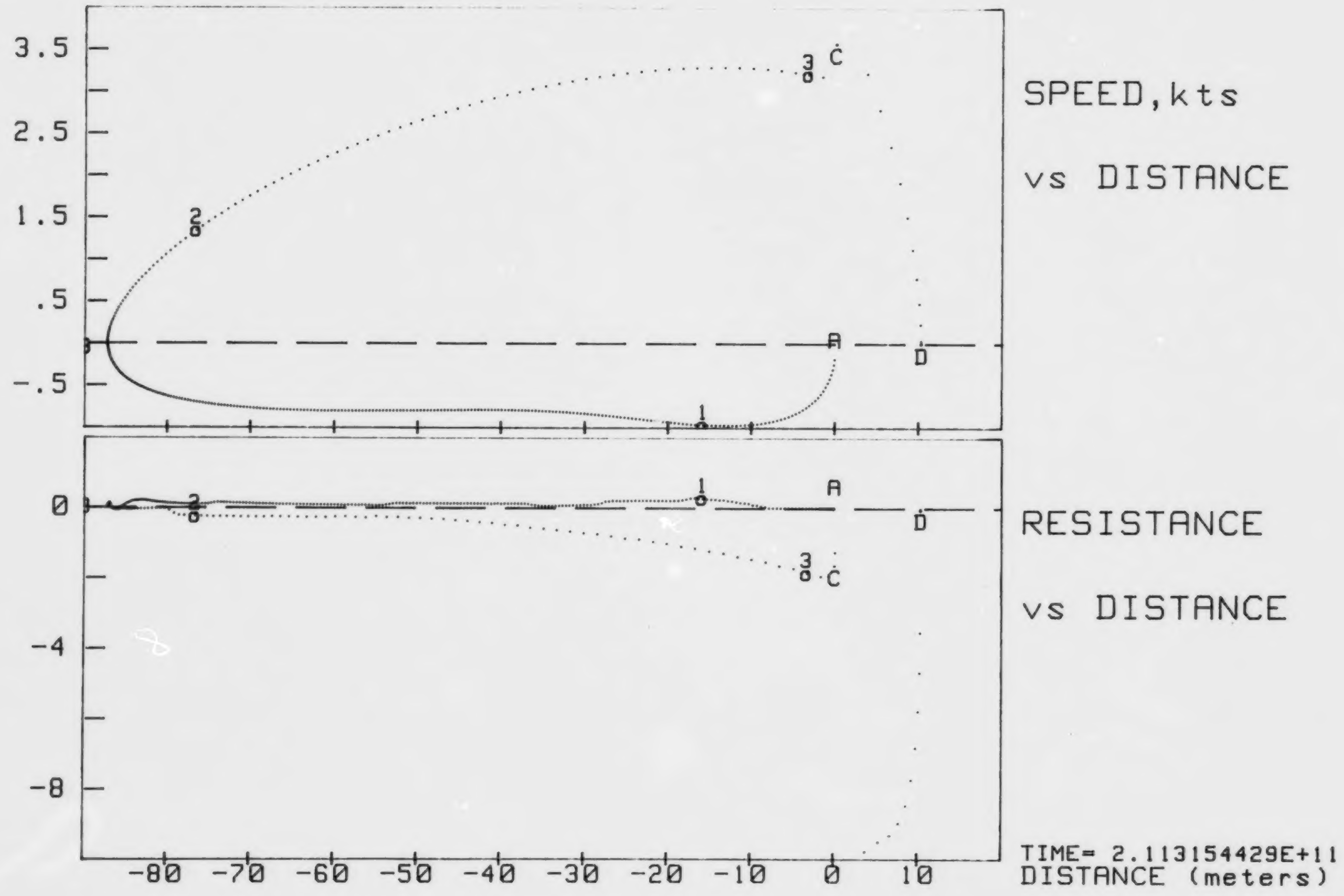

RAM # __A4   TAPE: 81-T2-2.1   07 JUL 1981 02:34:42   Fig.# 5

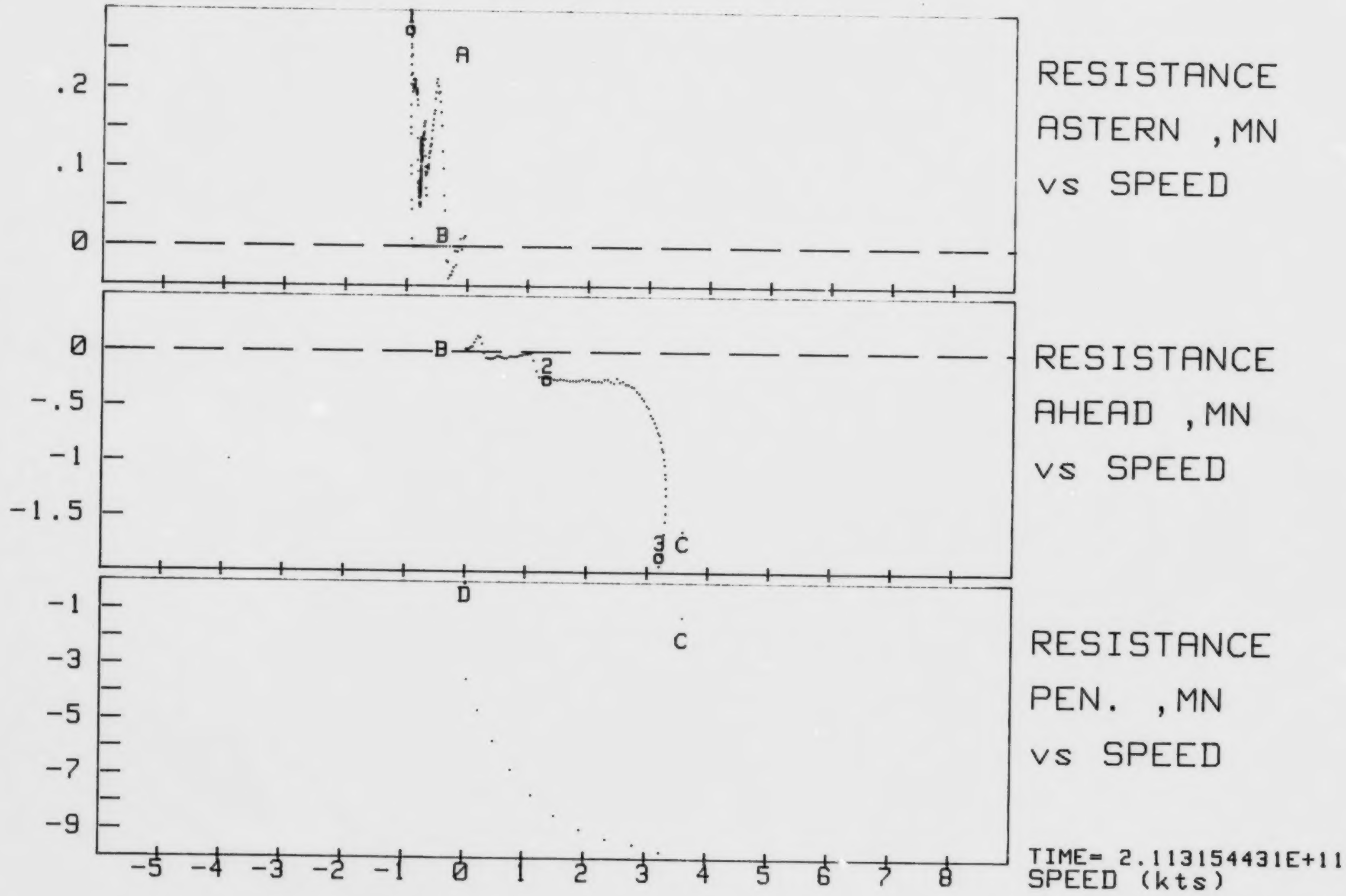

RESULTS OF RAMMING CYCLE ANALYSIS

RAM No. __A5

TAPE:	81-T2-2.1	ICE CONDITIONS:	RIDGES
CATEGORY:	R3	ICE THICKNESS:	2.68 m
QUALITY:	64AD	FLEXURAL STRENGTH:	407 kPA
TRIM:	EVEN	BUBBLER STATUS:	OFF

RAMMING CYCLE CHARACTERISTICS:

Speed of Advance	(knots)	.0602	
Speed of Impact	(knots)	4.5	(4.47)

	Duration (sec)	% Cycle Time	Distance (m)
Backing	280	53.8	-164.6
Acceleration	140	26.9	164.6
Penetration	19	3.65	9.1 (16.11)
Extraction	81	15.6	
Total Cycle	520		

Duration of Astern Mode	(sec)	180		
Duration of Reversal to Ahead	(sec)	165		
Duration of Ahead Mode	(sec)	94		
Duration of Reversal to Astern	(sec)	22		
Start of Reversal after Impact	(sec)	19		
Total Fuel Used	(mm*hr)	5	Est. kg:	-41.62
Average Fuel Rate	(mm)	34.58	Est. kg/hr:	-288.11
Backing Power	(kW)	3206		
[Est Fuel Rate	(kg/hr)]	731.52		
Acceleration Power	(kW)	8105.8		
[Est Fuel Rate	(kg/hr)]	1708.5		

RAM # __A5 TAPE: 81-T2-2.1 07 JUL 1981 02:41:42 **FIG. #1**

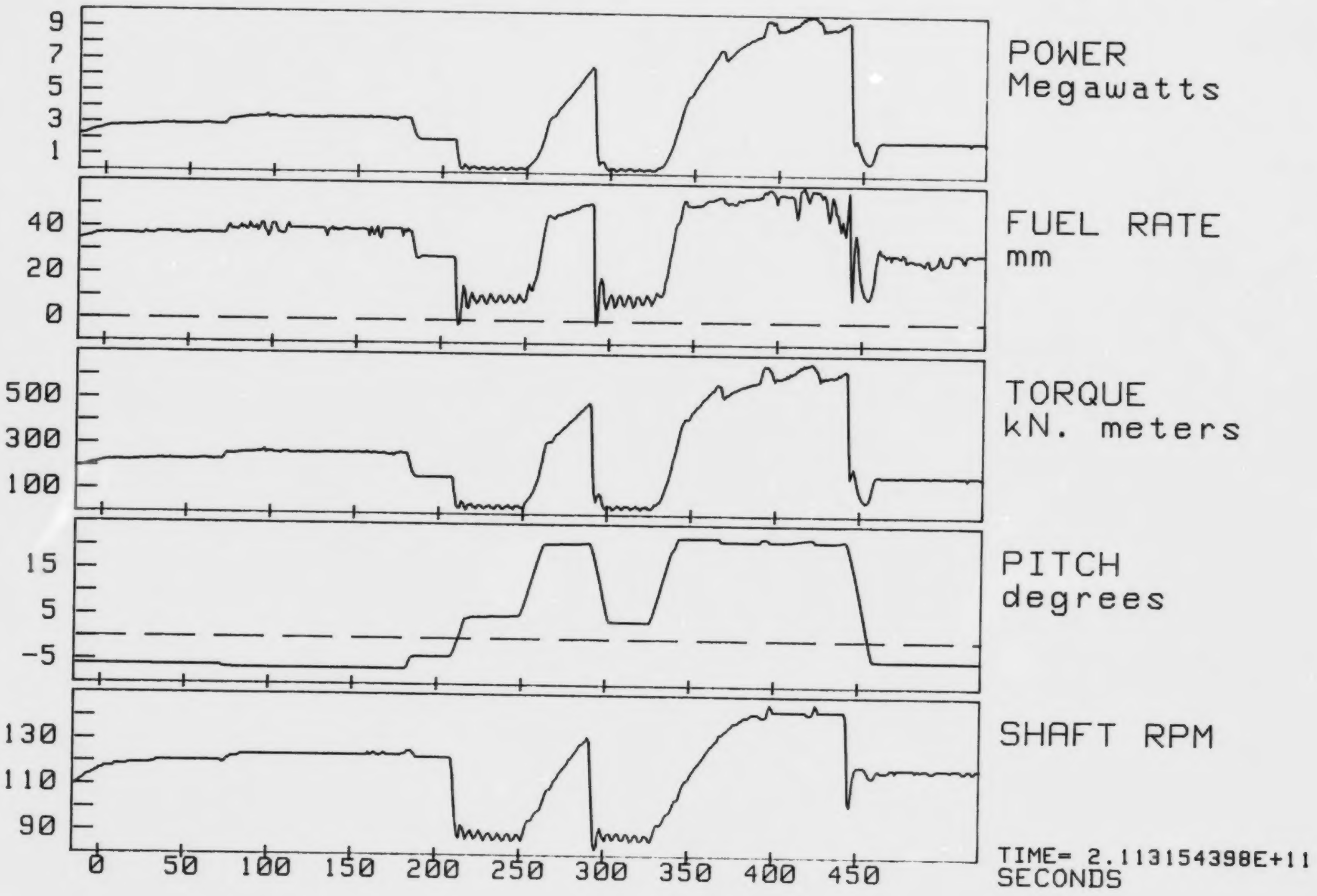

RAM # __A5 TAPE: 81-T2-2.1 07 JUL 1981 02:41:42 **FIG. #2**

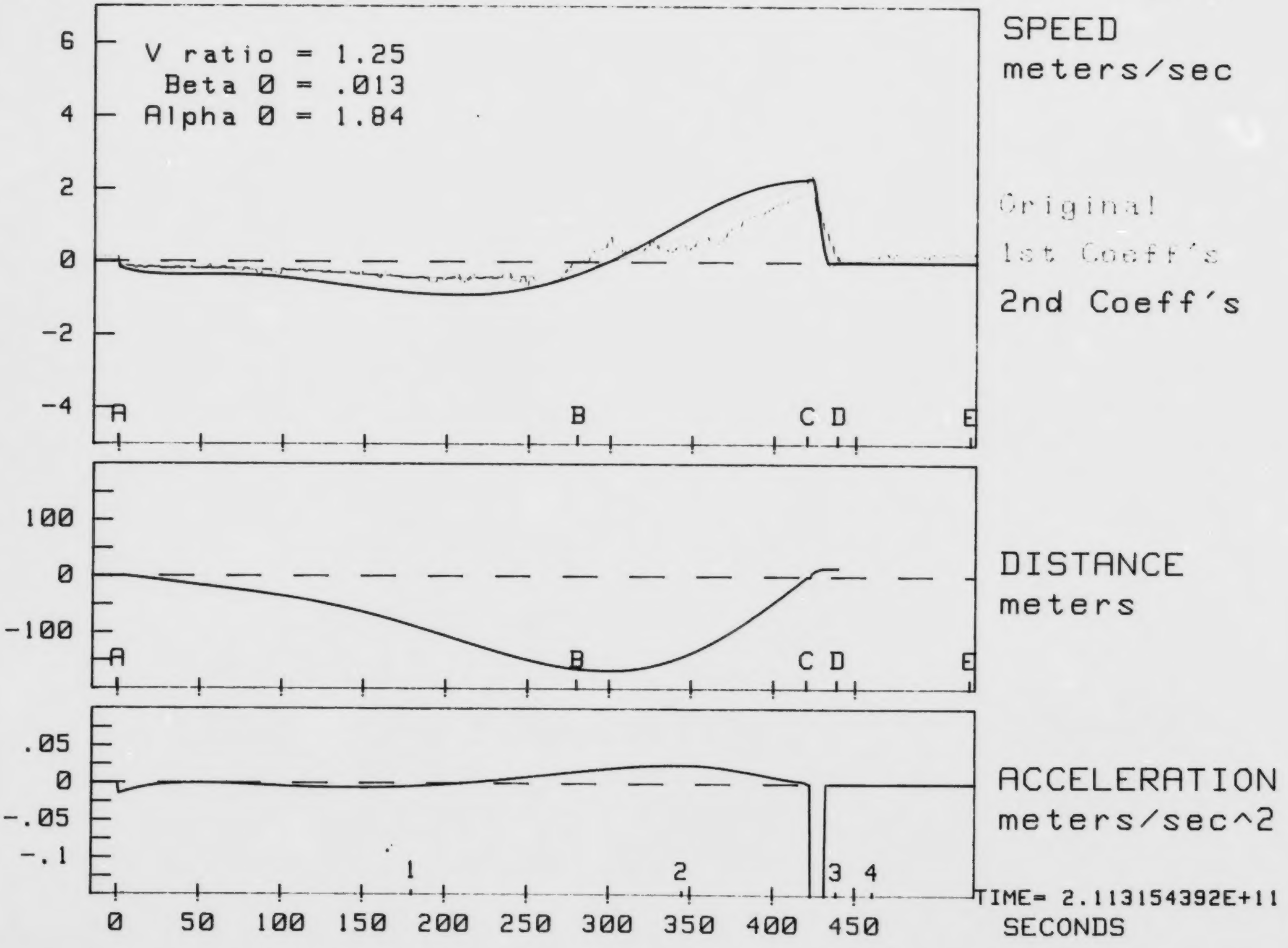

RAM # __A5 TAPE: 81-T2-2.1 07 JUL 1981 02:41:42

FIG. #3

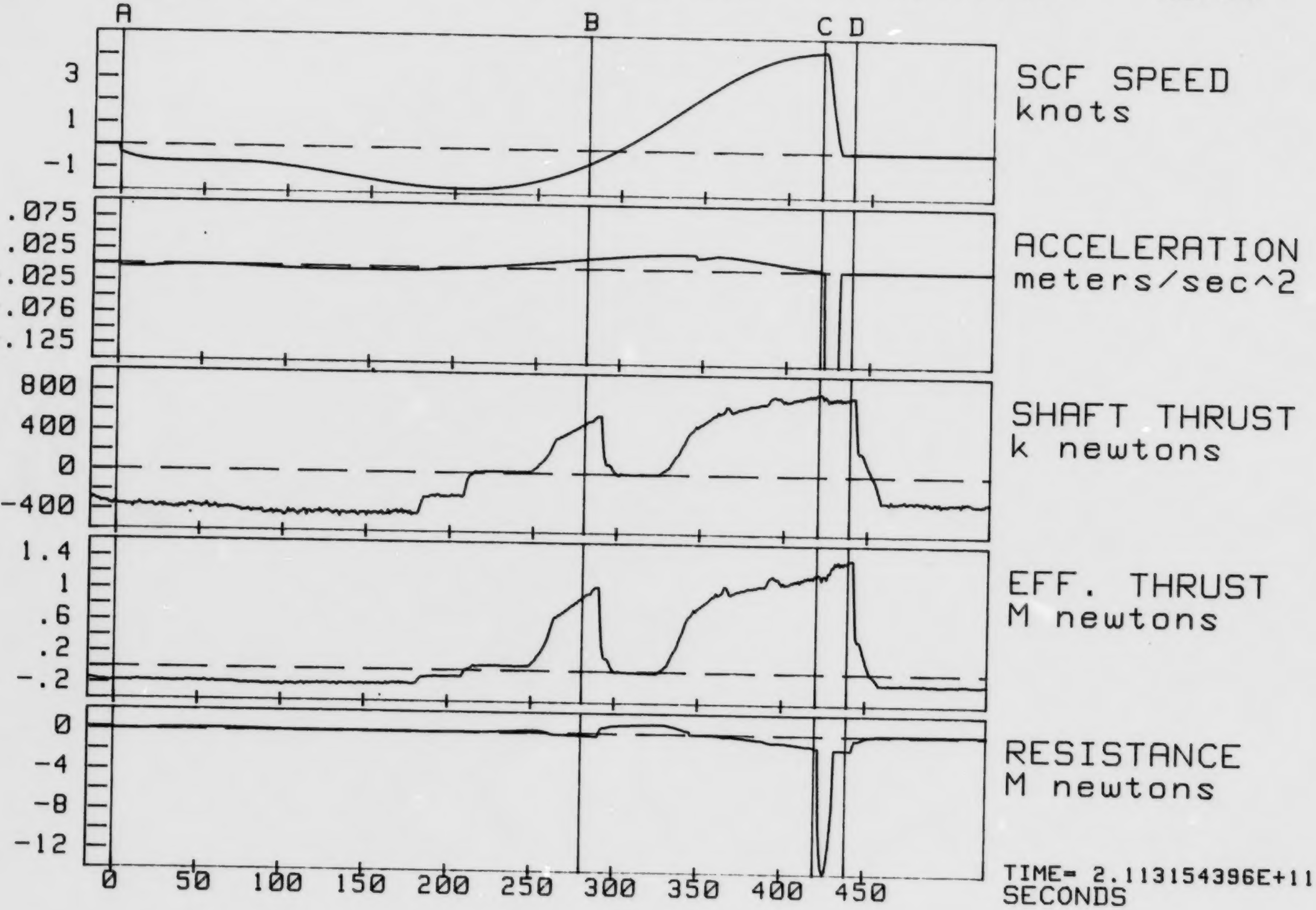

RAM # __A5 TAPE: 81-T2-2.1 07 JUL 1981 02:41:42 Fig.# 4

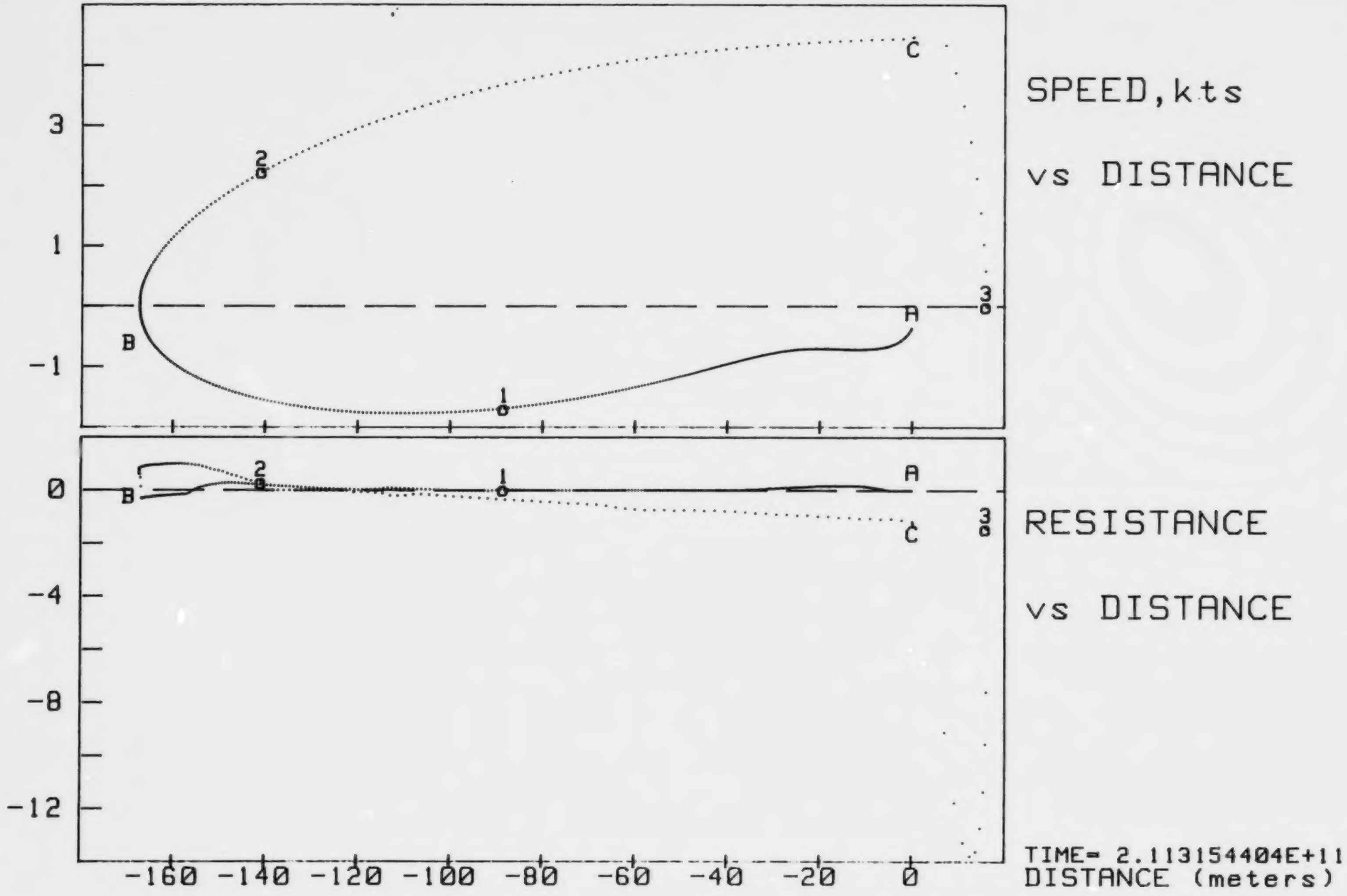

RAM # __A5 TAPE: 81-T2-2.1 07 JUL 1981 02:41:42 Fig.# 5

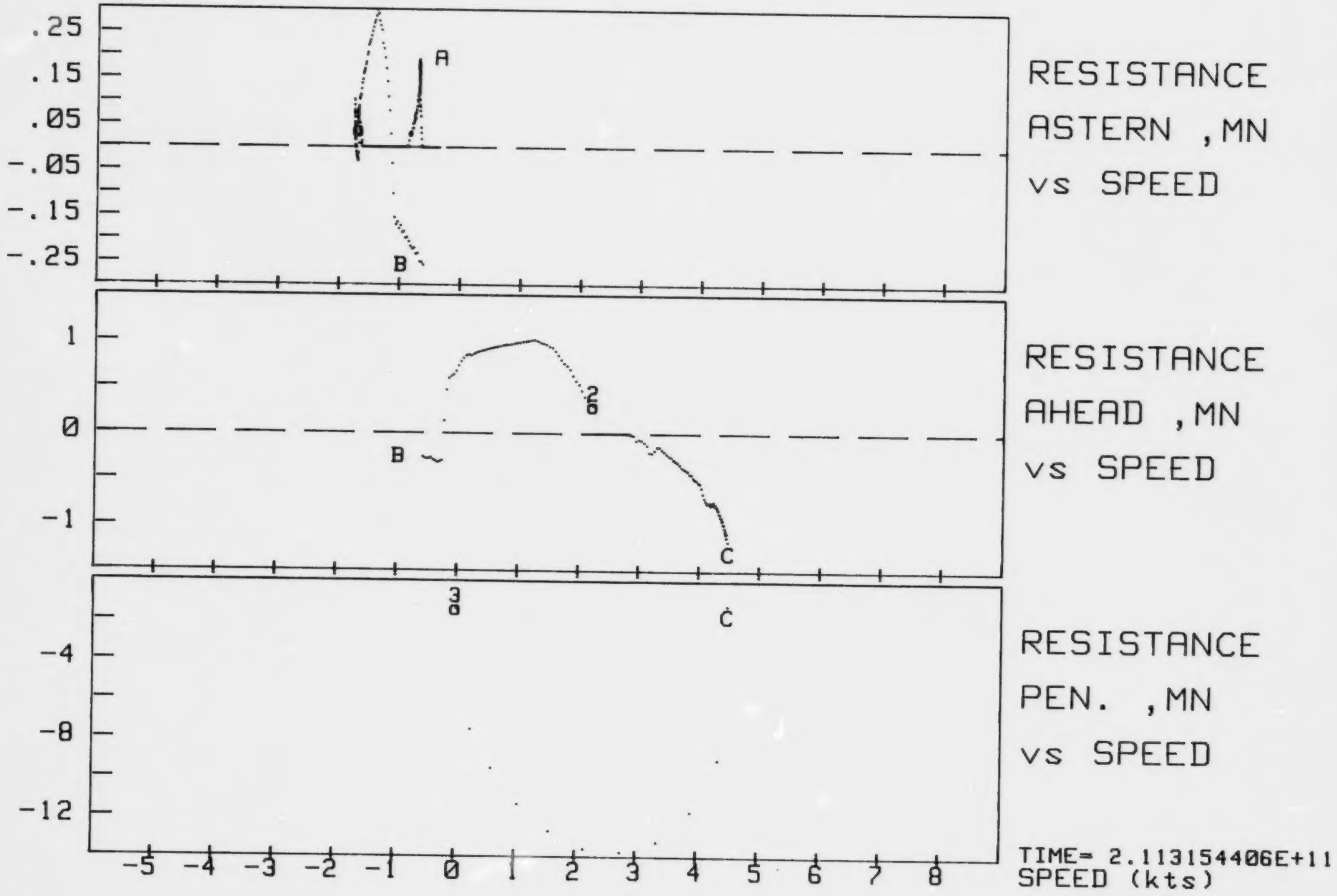

RESULTS OF RAMMING CYCLE ANALYSIS

RAM No. __A6

TAPE: 81-T2-2.1

CATEGORY: R3

QUALITY: 41AC

TRIM: EVEN

ICE CONDITIONS: RIDGES

ICE THICKNESS: 2.75 m

FLEXURAL STRENGTH: 407 kPA

BUBBLER STATUS: OFF

RAMMING CYCLE CHARACTERISTICS:

Speed of Advance	(knots)	.0691	
Speed of Impact	(knots)	4.5	(4.37)

	Duration (sec)	% Cycle Time	Distance (m)
Backing	207	56.7	-131.5
Acceleration	82	22.5	131.5
Penetration	13	3.56	6.1 (12.97)
Extraction	63	17.3	
Total Cycle	365		

Duration of Astern Mode	(sec)	158		
Duration of Reversal to Ahead	(sec)	61		
Duration of Ahead Mode	(sec)	67		
Duration of Reversal to Astern	(sec)	46		
Start of Reversal after Impact	(sec)	-3		
Total Fuel Used	(mm*hr)	3.67	Est. kg:	-17.66
Average Fuel Rate	(mm)	36.16	Est. kg/hr:	-174.13
Backing Power	(kW)	2732.6		
[Est Fuel Rate	(kg/hr)]	637.12		
Acceleration Power	(kW)	9527		
[Est Fuel Rate	(kg/hr)]	1991.9		

RAM # __A6 TAPE: 81-T2-2.1 07 JUL 1981 02:49:42 **FIG. #1**

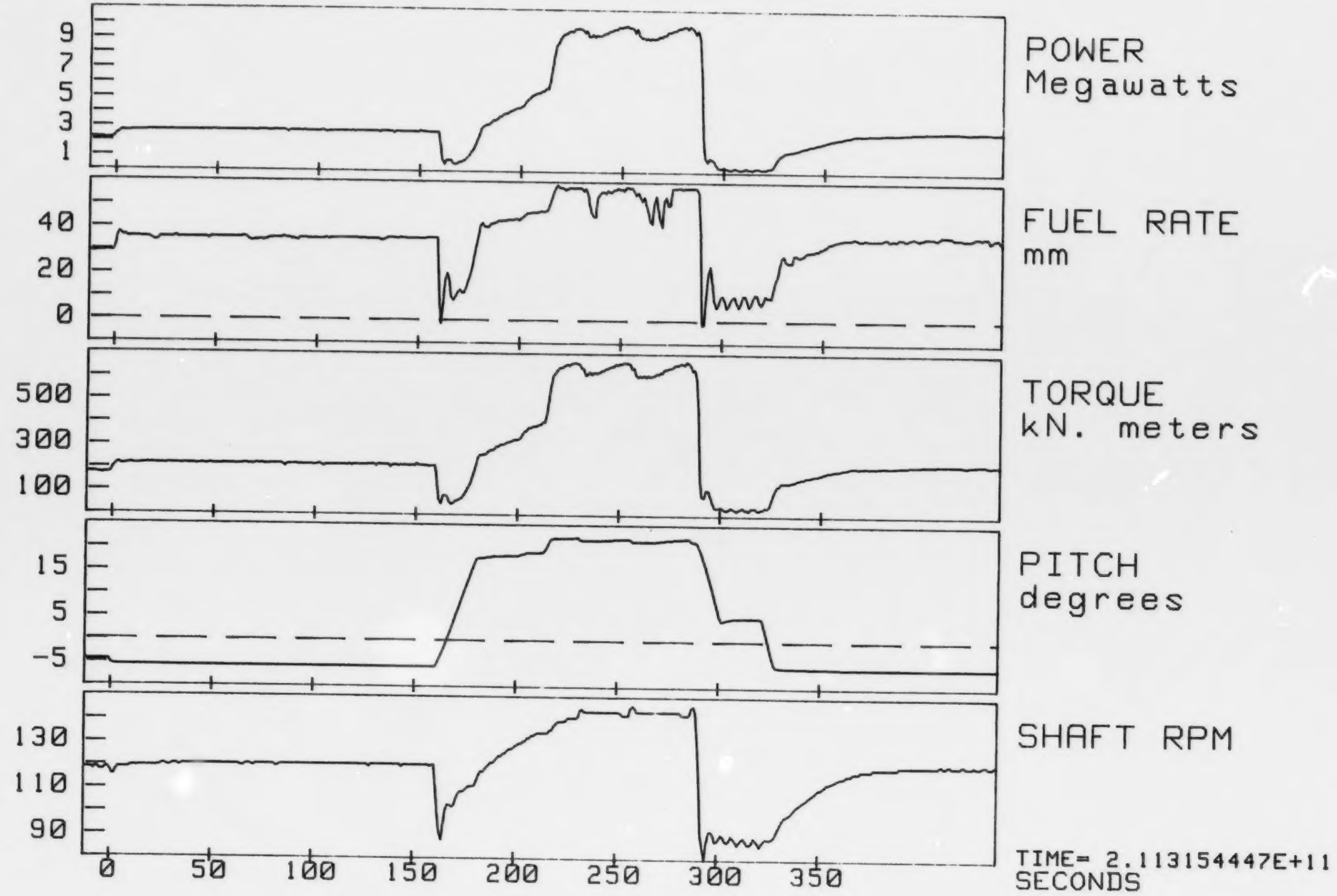

RAM # __A6 TAPE: 81-T2-2.1 07 JUL 1981 02:49:42 **FIG. #2**

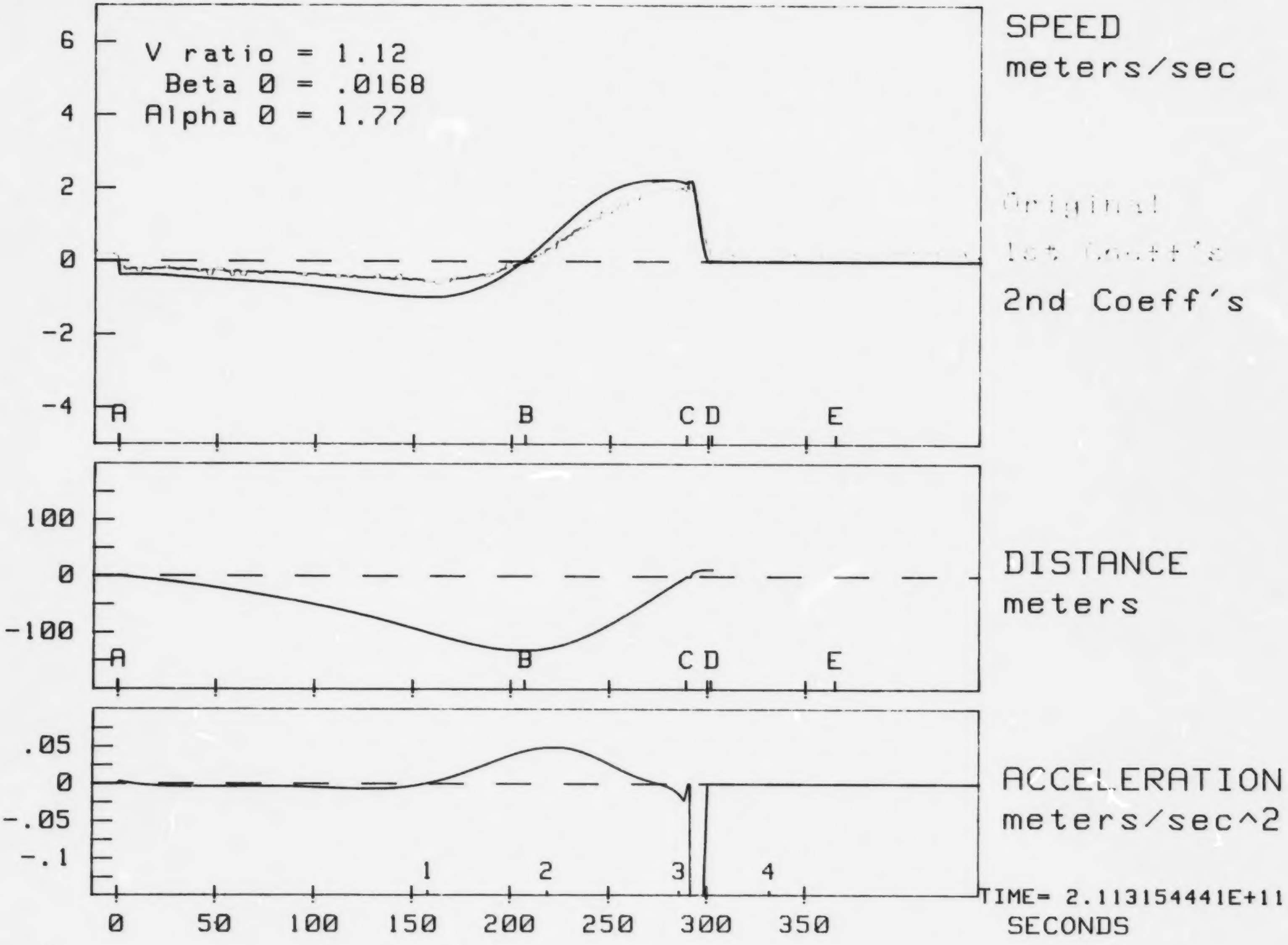

RAM # __A6 TAPE: 81-T2-2.1 07 JUL 1981 02:49:42

FIG. #3

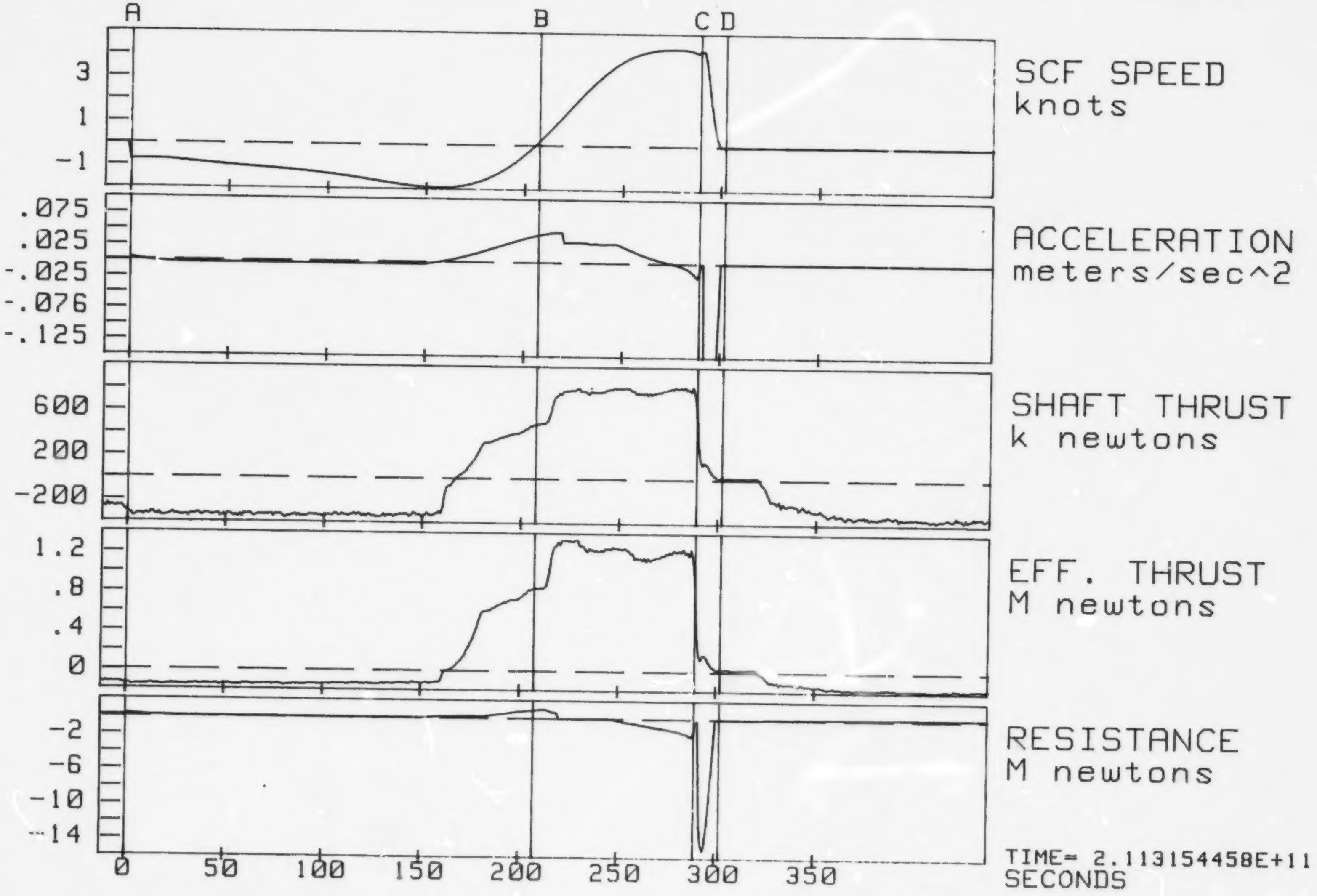

RAM # __A6   TAPE: 81-T2-2.1   07 JUL 1981 02:49:42   Fig.# 4

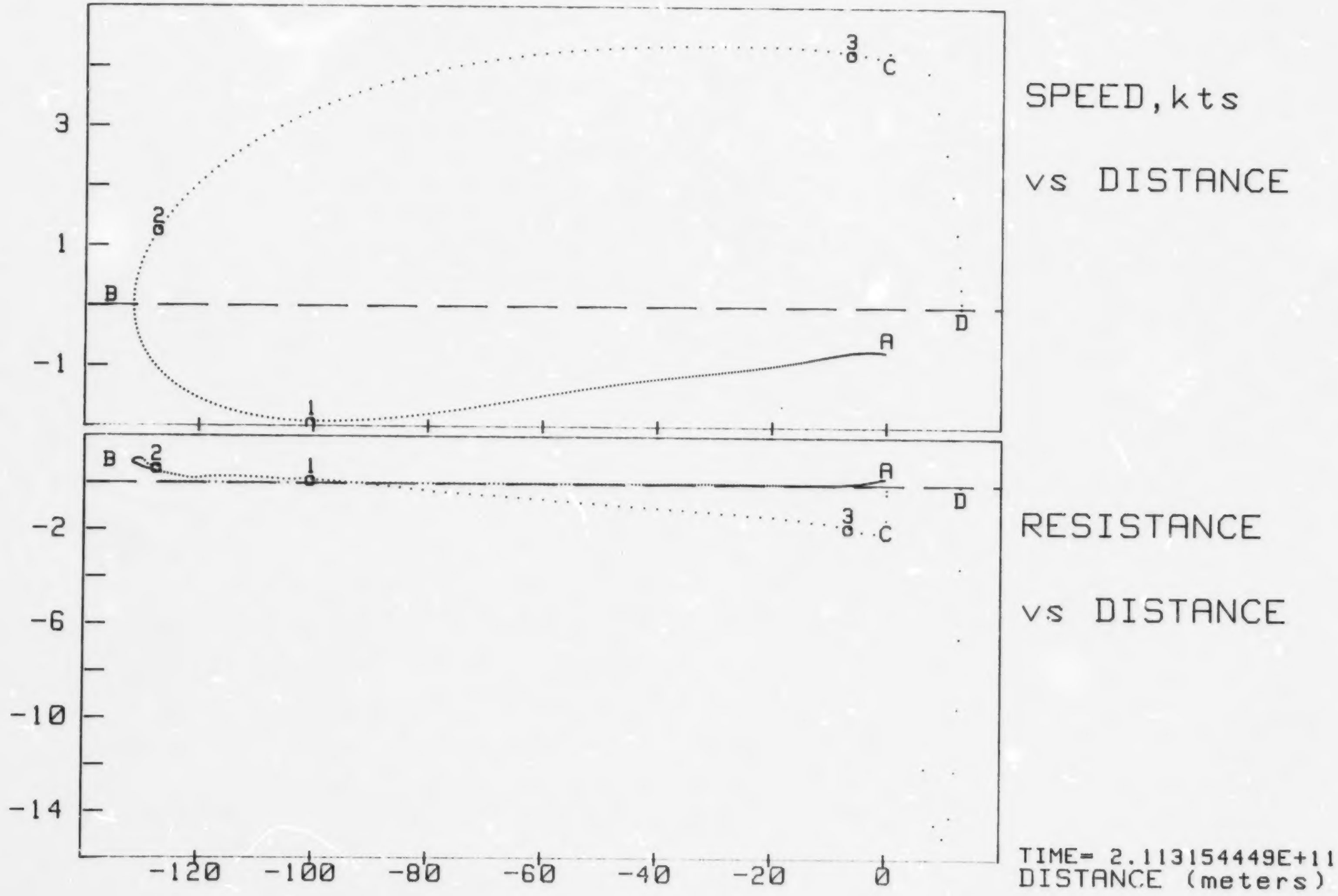

RAM # __A6 TAPE: 81-T2-2.1 07 JUL 1981 02:49:42 Fig.# 5

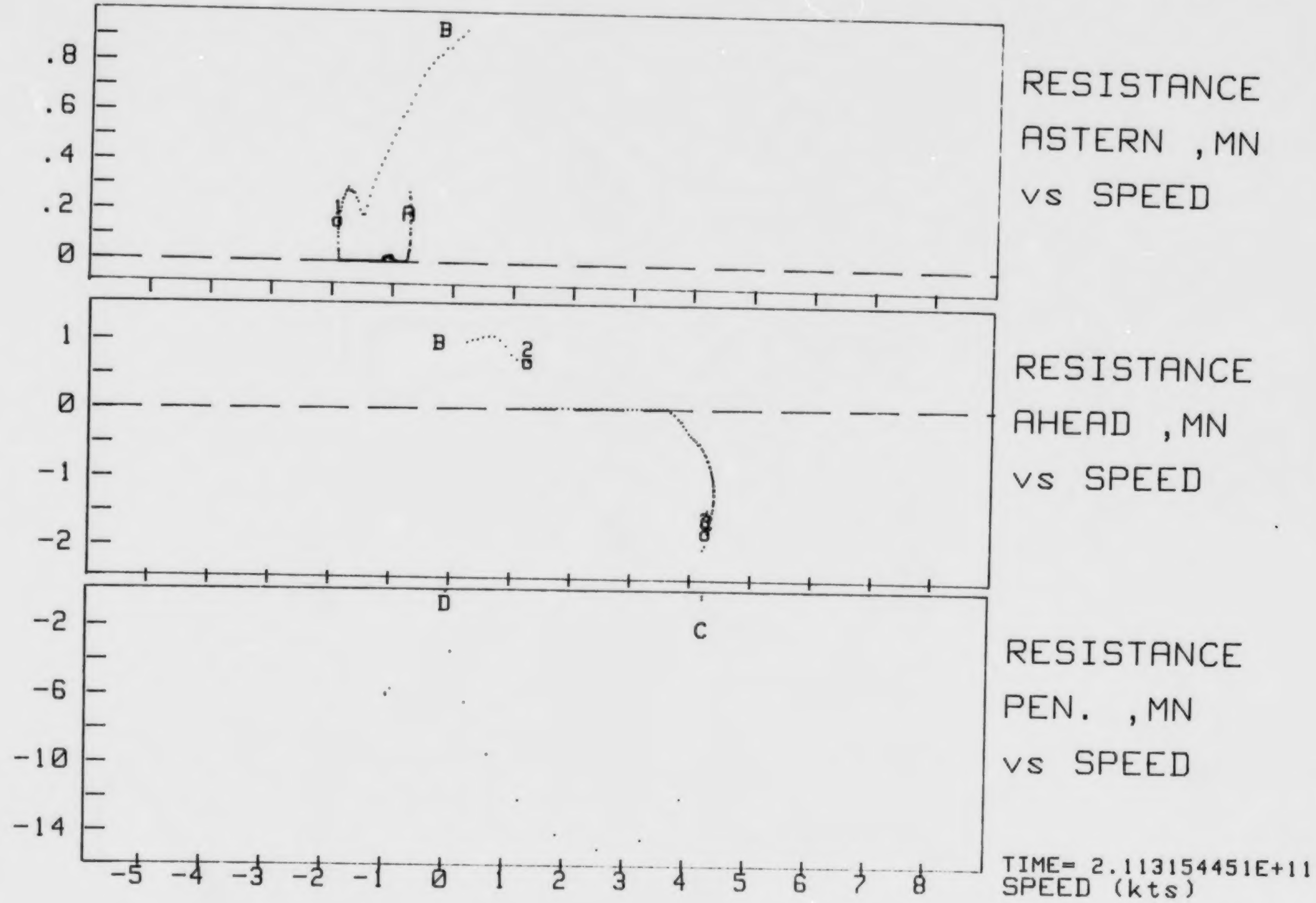

RESULTS OF RAMMING CYCLE ANALYSIS

RAM No. __A7

TAPE:	81-T2-2.1	ICE CONDITIONS:	RIDGES
CATEGORY:	R3	ICE THICKNESS:	2.74 m
QUALITY:	61AD	FLEXURAL STRENGTH:	407 kPA
TRIM:	EVEN	BUBBLER STATUS:	OFF

RAMMING CYCLE CHARACTERISTICS:

Speed of Advance	(knots)	.0583	
Speed of Impact	(knots)	4.5	(4.64)

	Duration (sec)	% Cycle Time	Distance (m)
Backing	370	61	-128.9
Acceleration	133	21.9	128.9
Penetration	25	4.12	6.1 (18.21)
Extraction	79	13	
Total Cycle	607		

Duration of Astern Mode	(sec)	269
Duration of Reversal to Ahead	(sec)	169
Duration of Ahead Mode	(sec)	90
Duration of Reversal to Astern	(sec)	72
Start of Reversal after Impact	(sec)	25

Total Fuel Used	(mm*hr)	5.91	Est. kg:	-42.91
Average Fuel Rate	(mm)	35.05	Est. kg/hr:	-254.51

Backing Power	(kW)	2448.3
[Est Fuel Rate	(kg/hr)]	580.44

Acceleration Power	(kW)	3155.4
[Est Fuel Rate	(kg/hr)]	721.44

RAM # __A7 TAPE: 81-T2-2.1 07 JUL 1981 02:57:12 **FIG. #1**

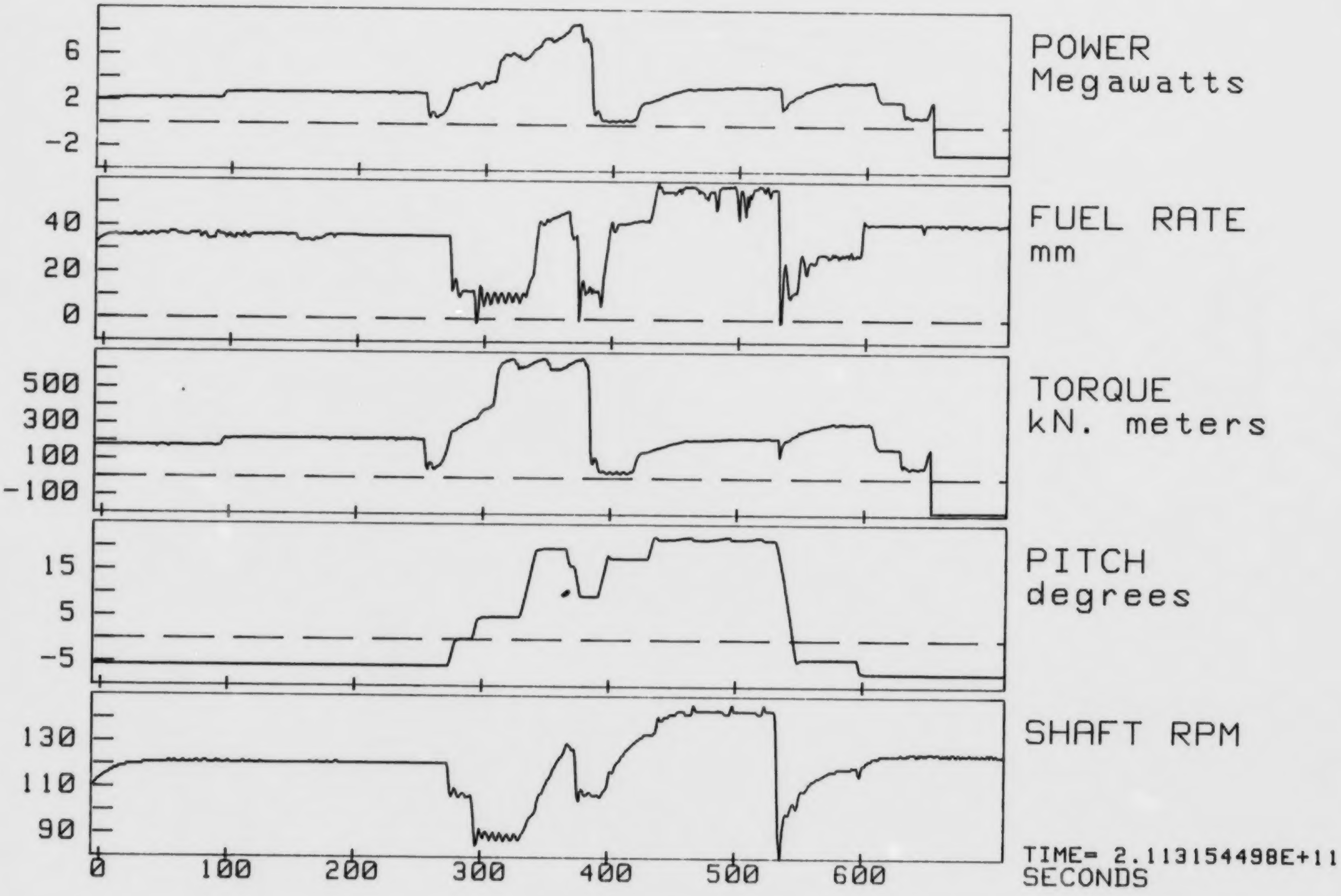

RAM # A7 TAPE: 81-T2-2.1 07 JUL 1981 02:57:12 **FIG. #2**

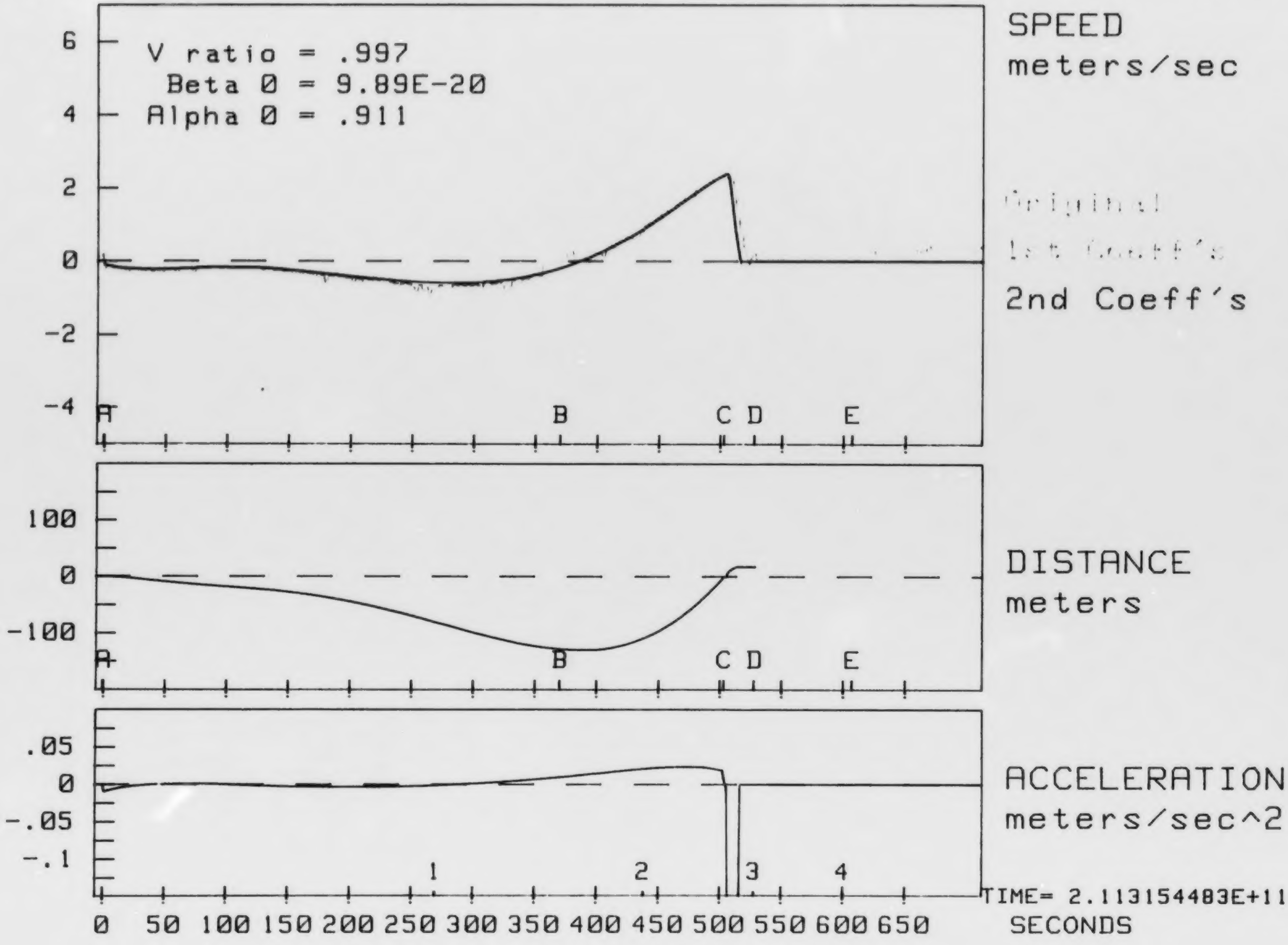

RAM # __A7 TAPE: 81-T2-2.1 07 JUL 1981 02:57:12

FIG. #3

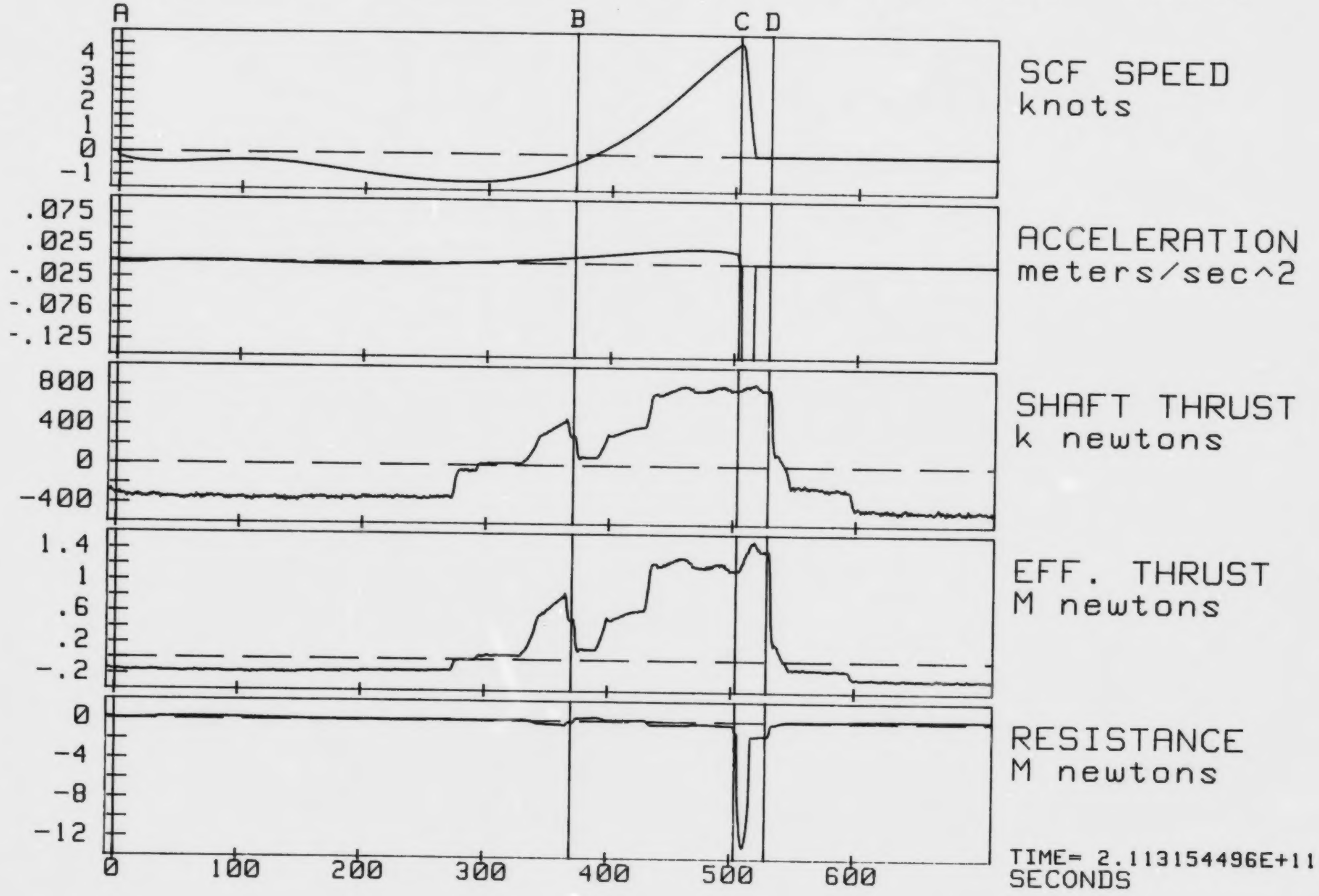

RAM # __A7 TAPE: 81-T2-2.1 07 JUL 1981 02:57:12 Fig.# 4

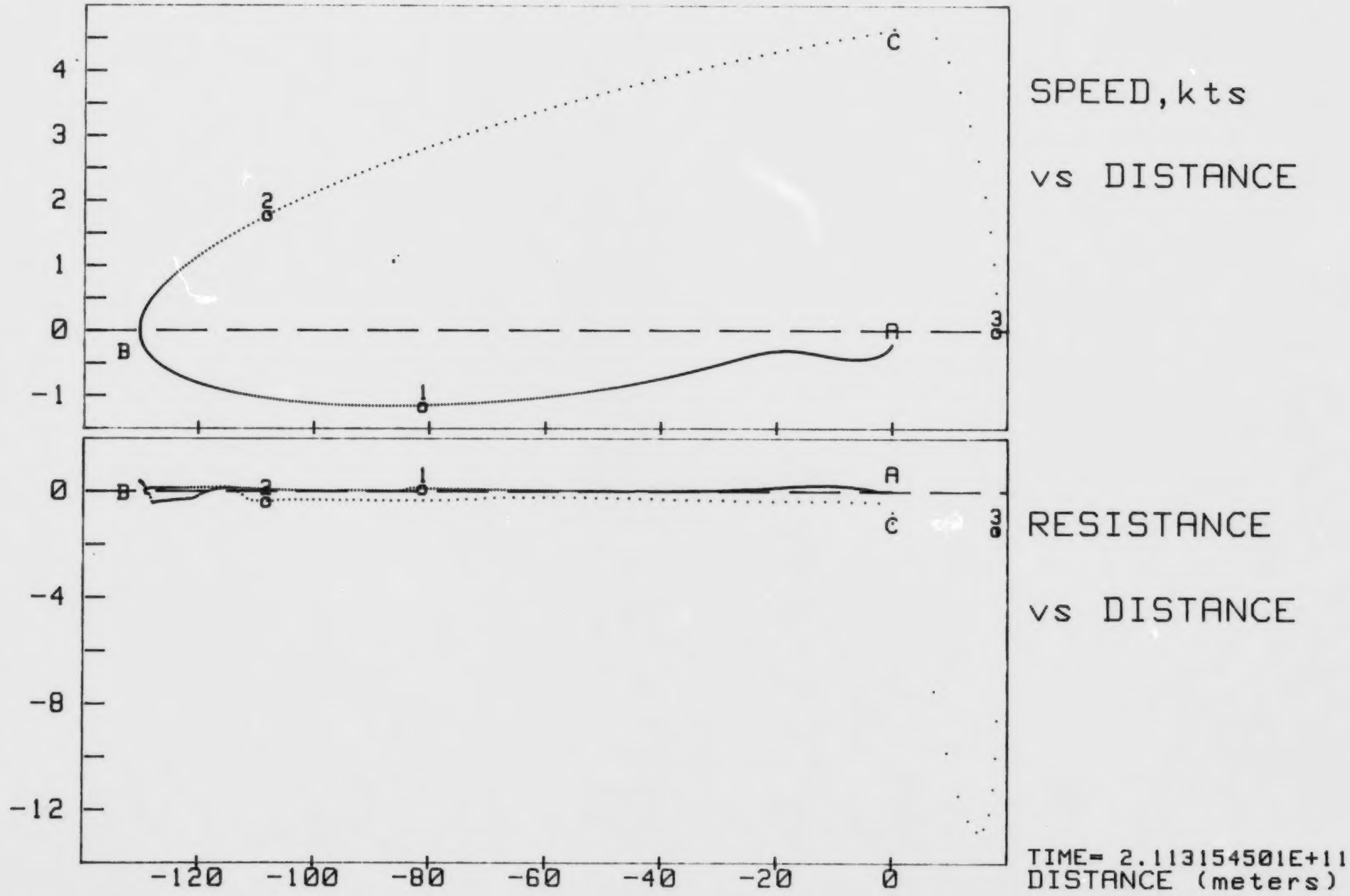

RAM # __A7 TAPE: 81-T2-2.1 07 JUL 1981 02:57:12 Fig.# 5

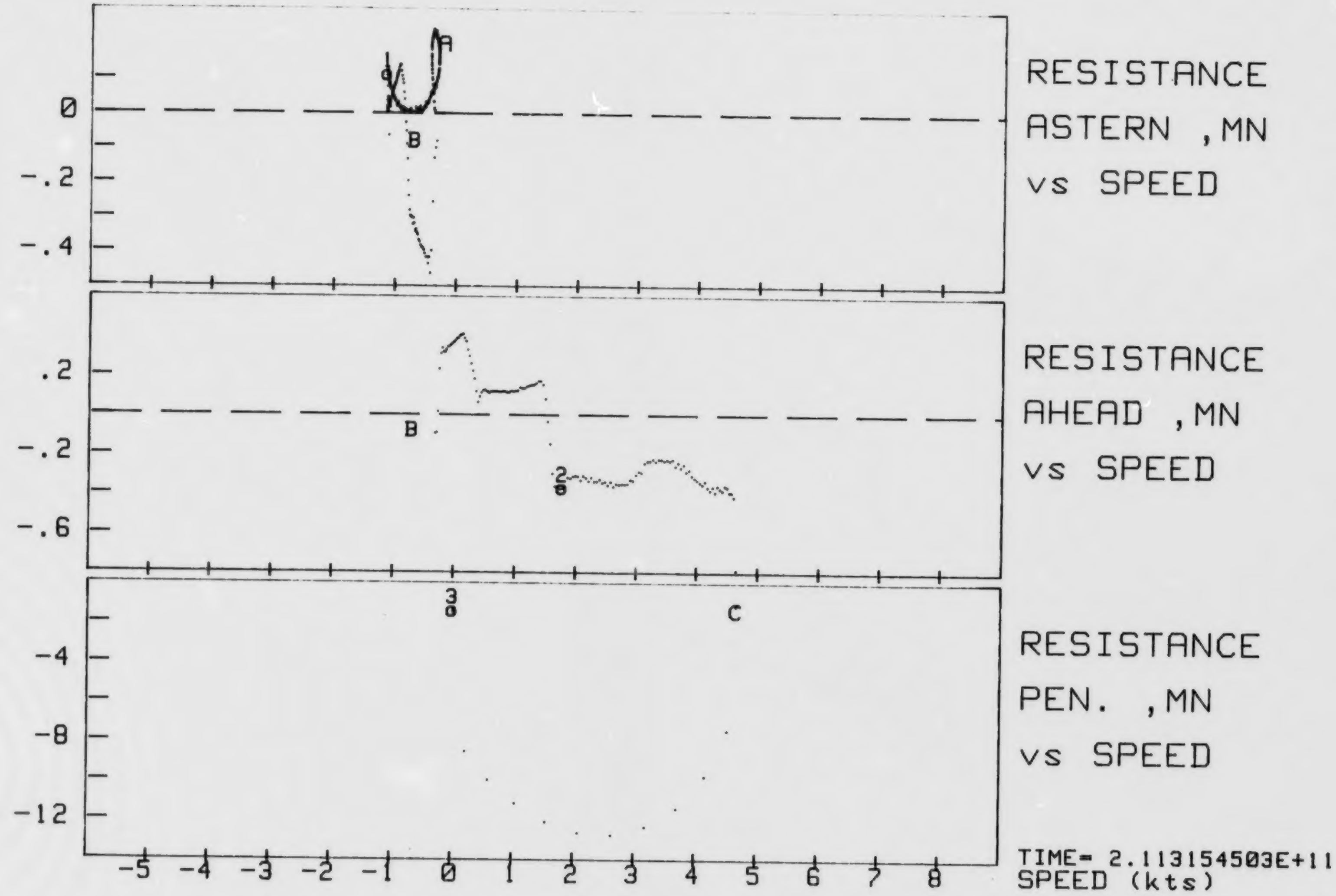
RESISTANCE ASTERN ,MN vs SPEED

RESISTANCE AHEAD ,MN vs SPEED

RESISTANCE PEN. ,MN vs SPEED

```
                    RESULTS OF RAMMING CYCLE ANALYSIS


                              RAM No.  __A8

TAPE:       81-T2-2.1                  ICE CONDITIONS:     RIDGES

CATEGORY:   R3                         ICE THICKNESS:      2.71  m

QUALITY:    61AD                       FLEXURAL STRENGTH:  407  kPA

TRIM:       EVEN
                                       BUBBLER STATUS:    OFF

RAMMING CYCLE CHARACTERISTICS:

Speed of Advance  (knots)     .0484

Speed of Impact   (knots)     4.5    ( 4.59 )


                              Duration (sec)  % Cycle Time  Distance  (m)
Backing                       431             56.4          -144.5
Acceleration                  222             29.1           144.5
Penetration                   13              1.7            12.1 (19.04)
Extraction                    98              12.8
Total Cycle                   764


Duration of Astern Mode        (sec)     192
Duration of Reversal to Ahead  (sec)     405
Duration of Ahead Mode         (sec)     60
Duration of Reversal to Astern (sec)     22
Start of Reversal after Impact (sec)     4

Total Fuel Used    (mm*hr)               6.2          Est. kg:     -143.5
Average Fuel Rate  (mm)                  29.2         Est. kg/hr: -676.31

Backing Power      (kW)                  3836.8
[Est Fuel Rate     (kg/hr)]              857.31

Acceleration Power(kW)                   9016.5
[Est Fuel Rate     (kg/hr)]              1890.1
```

RAM # __A8   TAPE: 81-T2-2.1   07 JUL 1981 03:06:12   **FIG. #1**

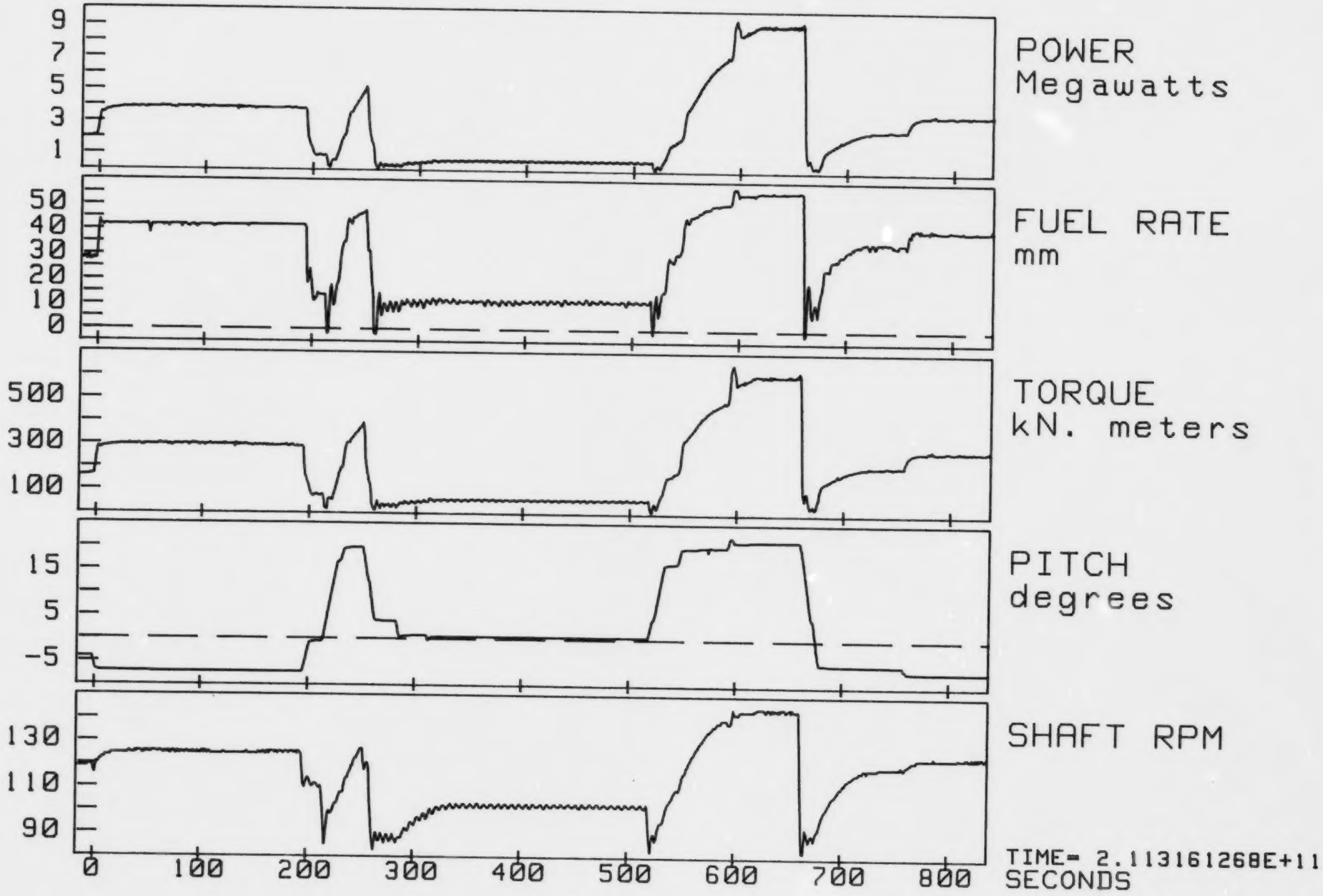

RAM # __A8 TAPE: 81-T2-2.1 07 JUL 1981 03:06:12

FIG. #2

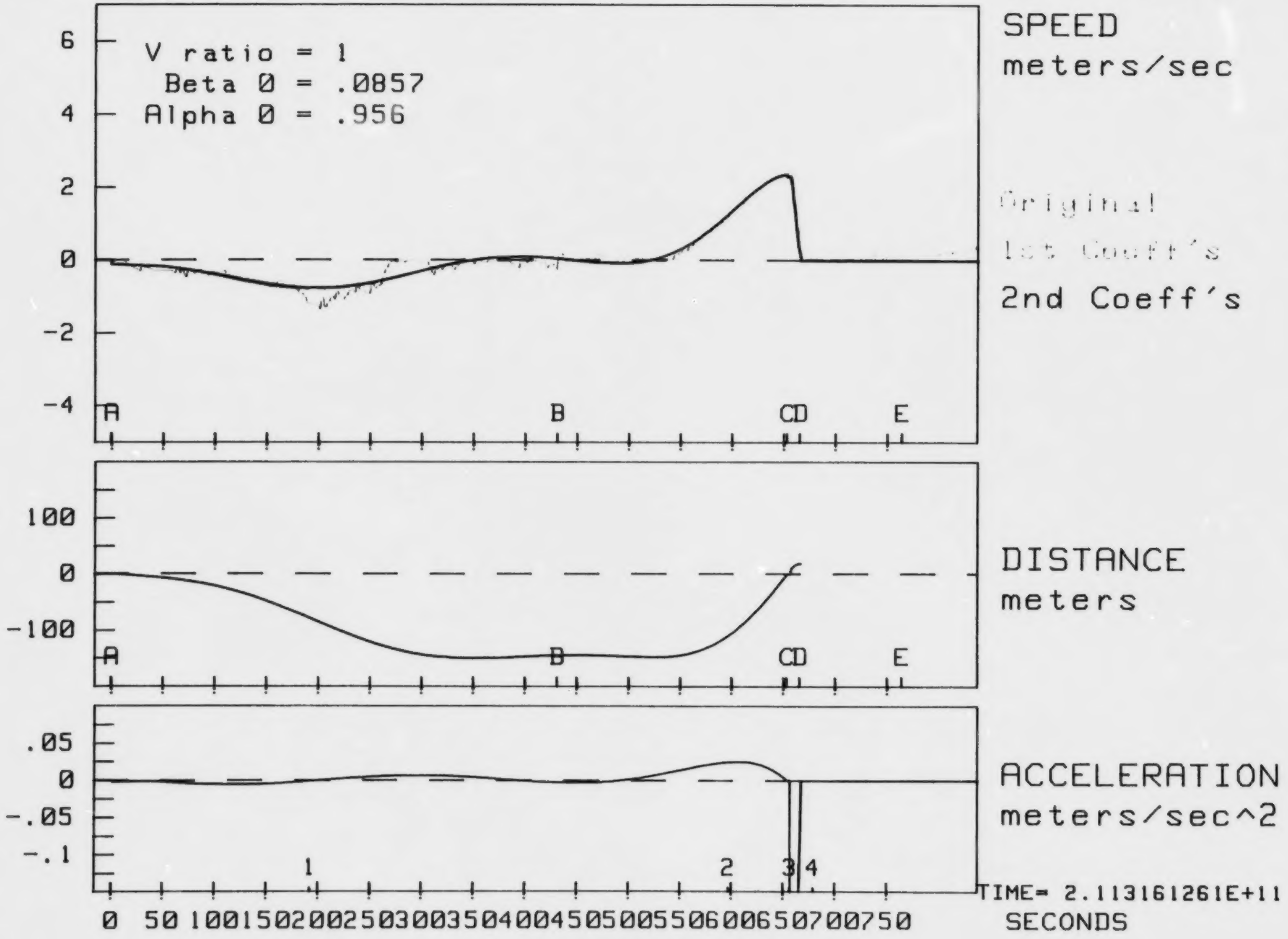

RAM # __A8 TAPE: 81-T2-2.1 07 JUL 1981 03:06:12

FIG. #3

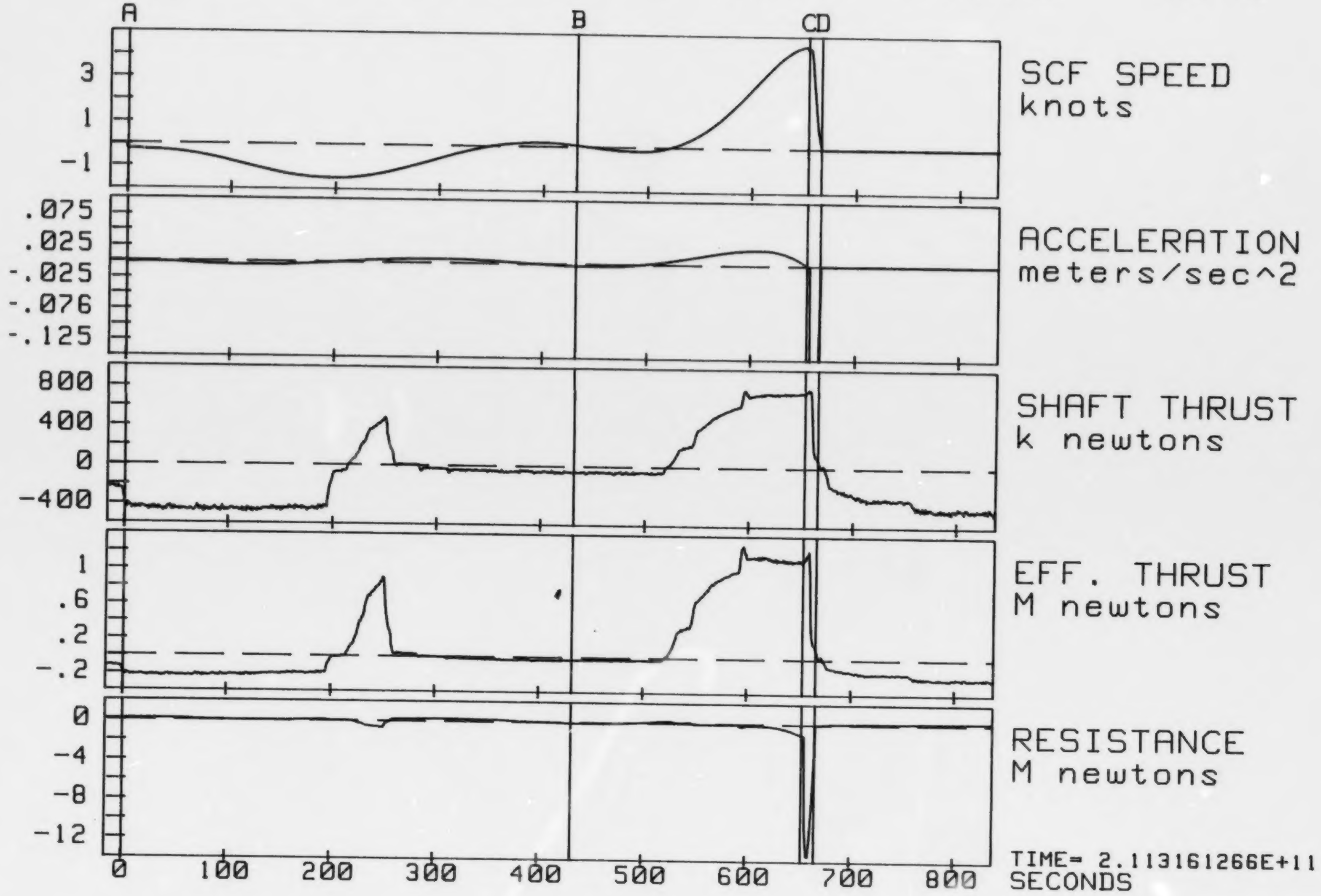

RAM # __A8 TAPE: 81-T2-2.1 07 JUL 1981 03:06:12 Fig.# 4

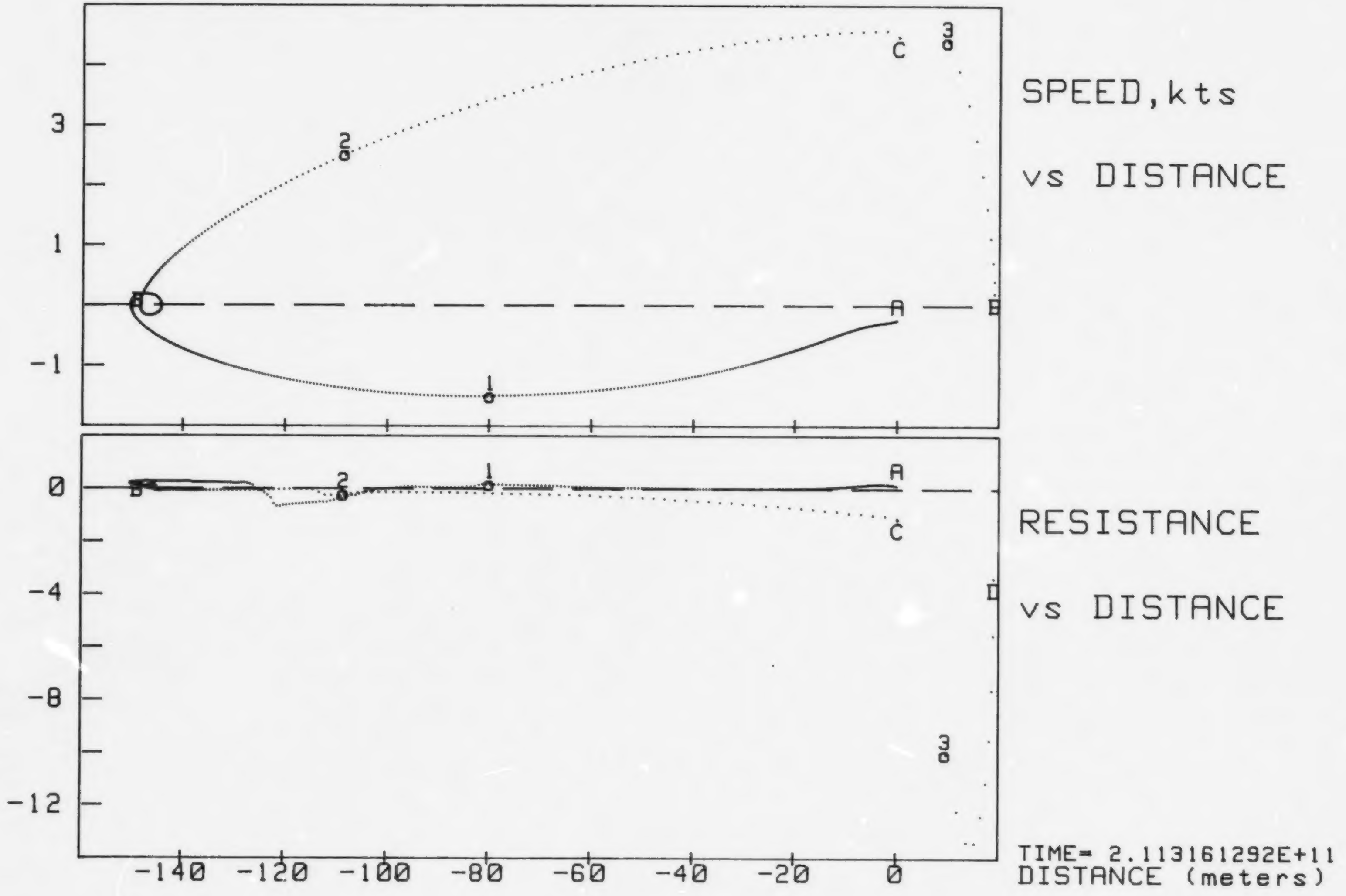

RAM # __A8   TAPE: 81-T2-2.1   07 JUL 1981 03:06:12   Fig.# 5

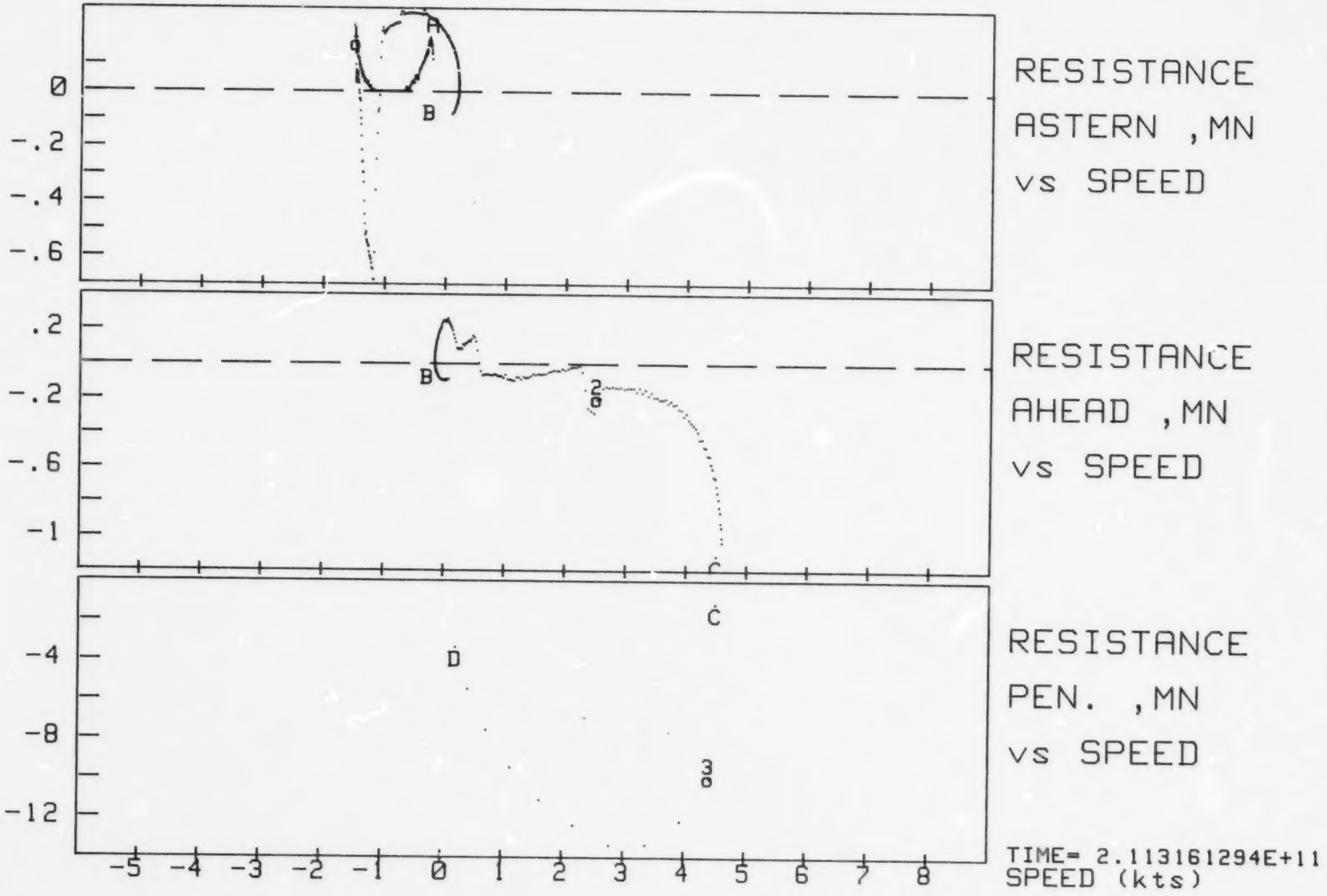

```
                    RESULTS OF RAMMING CYCLE ANALYSIS


                              RAM No.  __A9


TAPE:        81-T2-2.1                ICE CONDITIONS:      RIDGES

CATEGORY:    R3                       ICE THICKNESS:       2.67  m

QUALITY:     21AB                     FLEXURAL STRENGTH:   407  kPA

TRIM:        EVEN
                                      BUBBLER STATUS:     OFF


RAMMING CYCLE CHARACTERISTICS:

Speed of Advance  (knots)      .0685

Speed of Impact   (knots)      4.5     ( 4.48 )


                               Duration (sec)   % Cycle Time   Distance  (m)
Backing                        319              51.1           -141.3
Acceleration                   188              30.1            141.3
Penetration                    23               3.69            15.2 (21.98)
Extraction                     94               15.1
Total Cycle                    624


Duration of Astern Mode          (sec)      181
Duration of Reversal to Ahead    (sec)      255
Duration of Ahead Mode           (sec)      94
Duration of Reversal to Astern   (sec)      22
Start of Reversal after Impact   (sec)      23

Total Fuel Used    (mm*hr)                  5.79         Est. kg:     -64.99
Average Fuel Rate  (mm)                     33.38        Est. kg/hr:  -374.92

Backing Power       (kW)                    3562.4
[Est Fuel Rate      (kg/hr)]                802.59

Acceleration Power (kW)                     9615.1
[Est Fuel Rate      (kg/hr)]                2009.5
```

RAM # __A9 TAPE: 81-T2-2.1 07 JUL 1981 03:18:42 **FIG. #1**

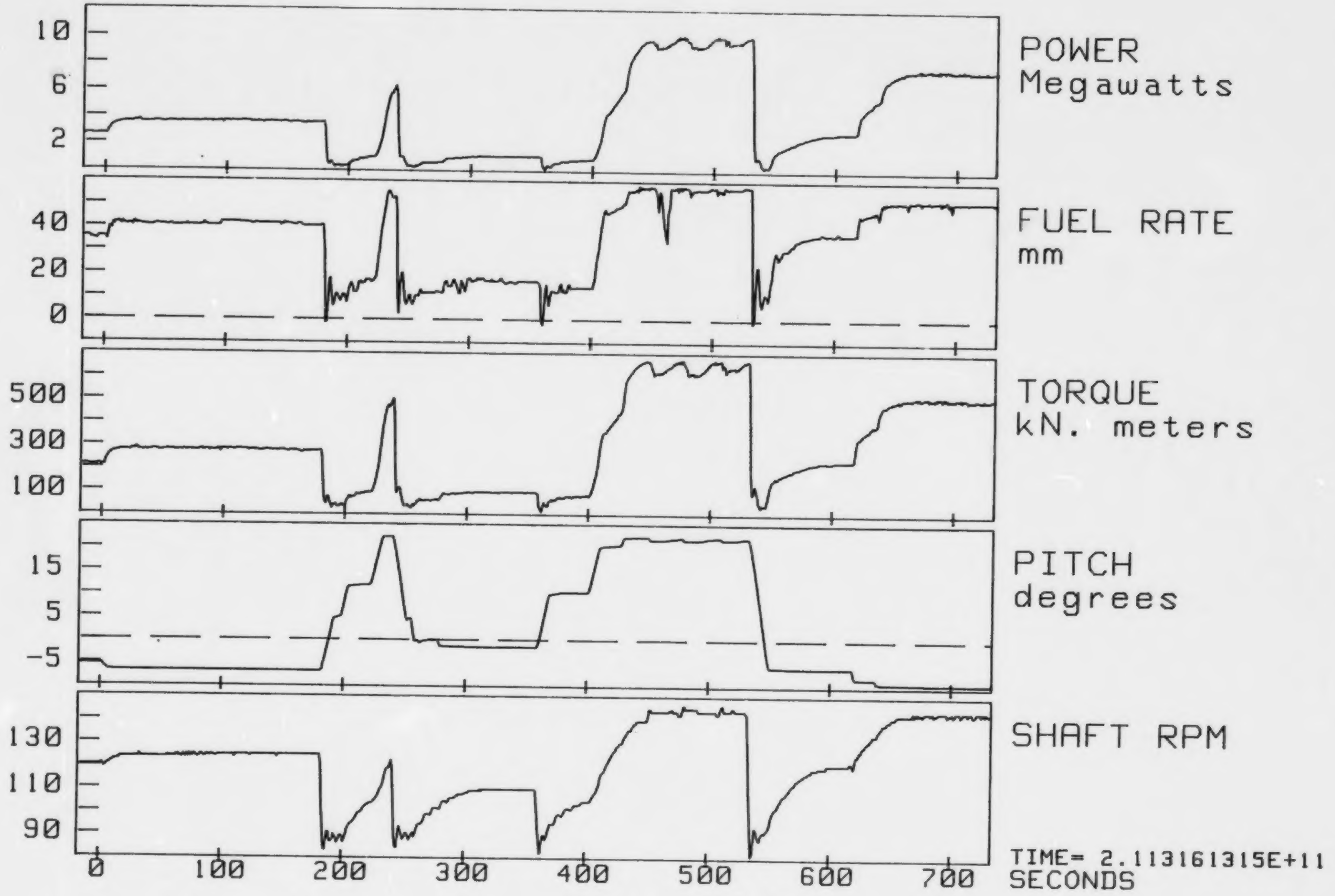

RAM # __A9 TAPE: 81-T2-2.1 07 JUL 1981 03:18:42 **FIG. #2**

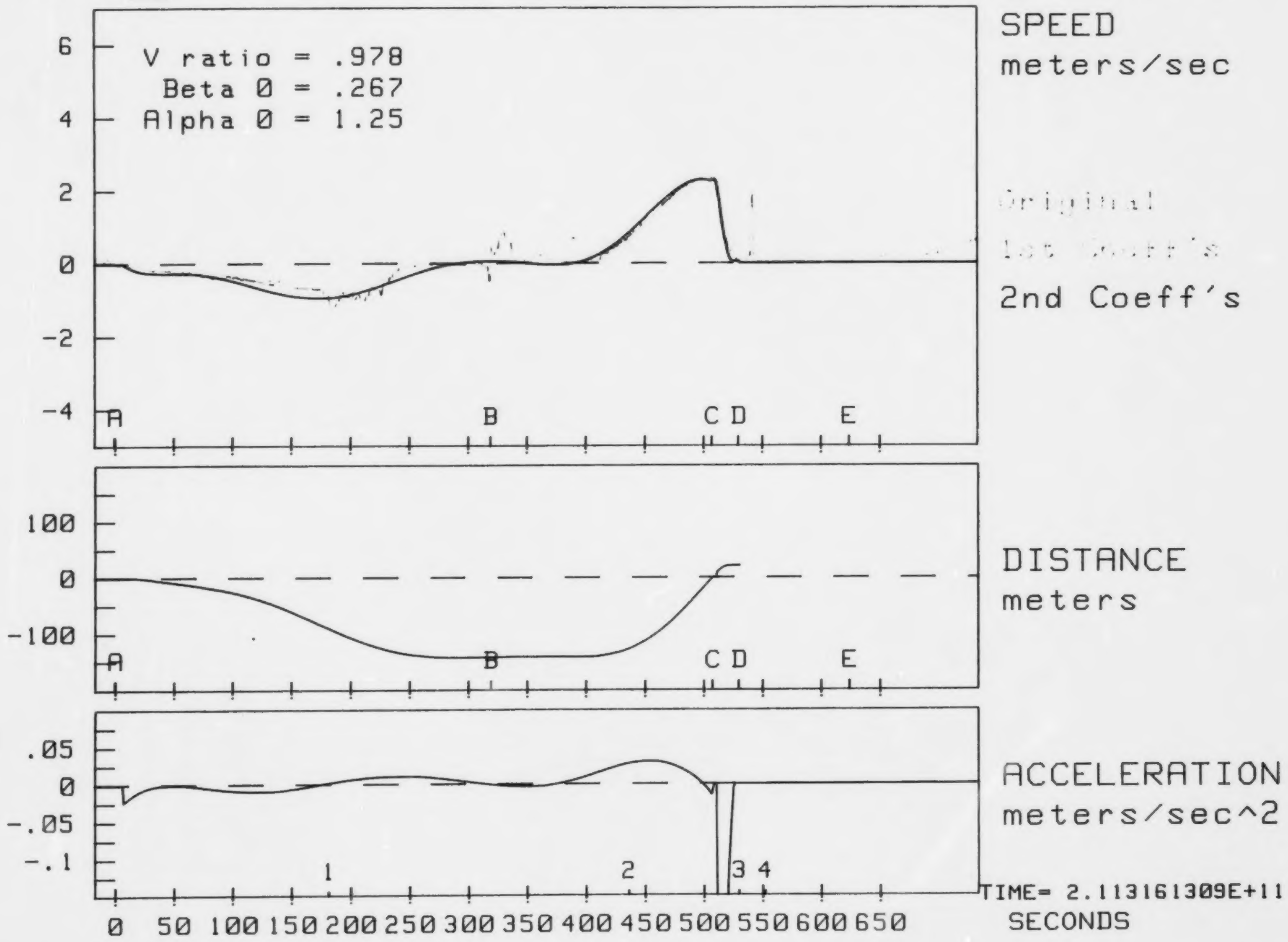

RAM # __A9 TAPE: 81-T2-2.1 07 JUL 1981 03:18:42

FIG. #3

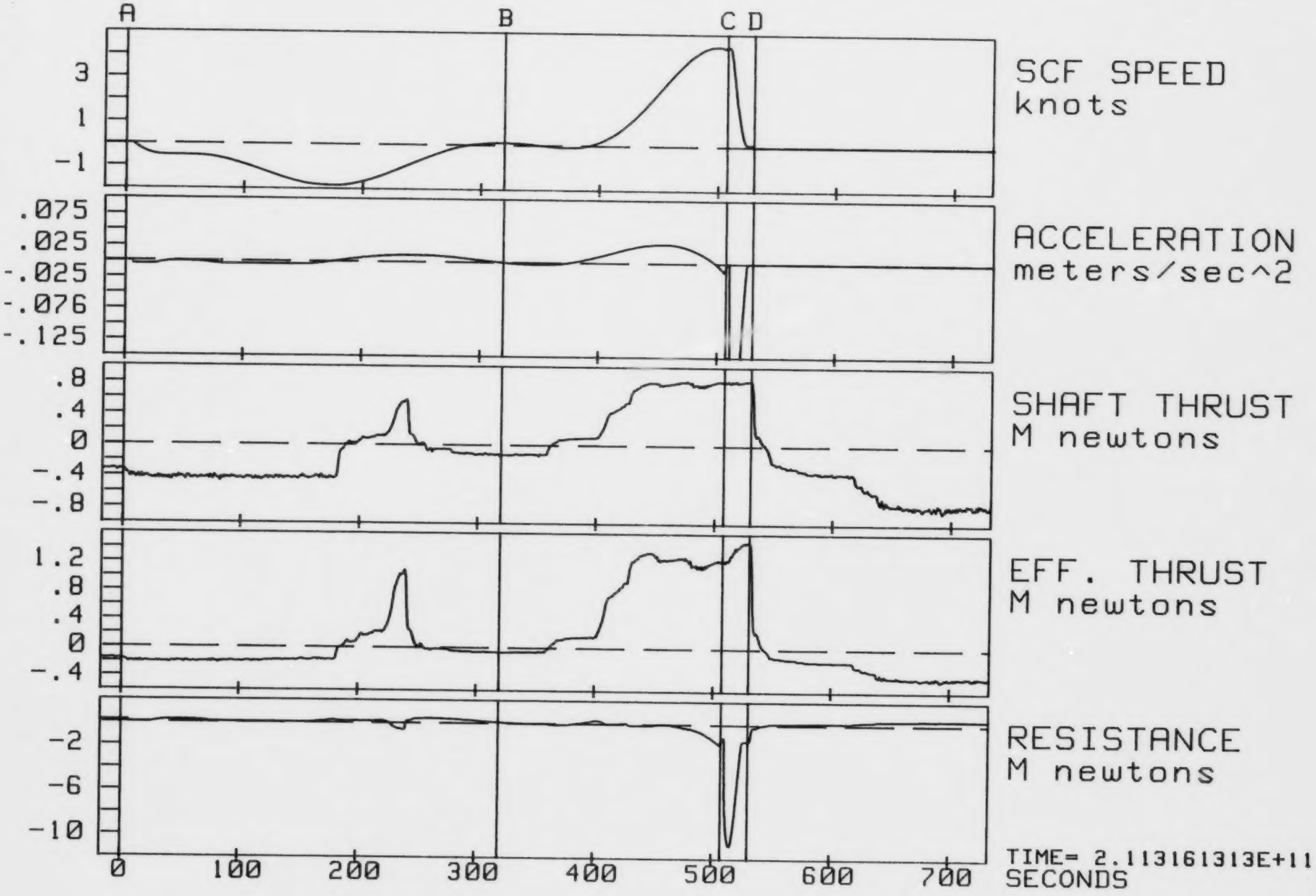

RAM # __A9 TAPE: 81-T2-2.1 07 JUL 1981 03:18:42 Fig.# 4

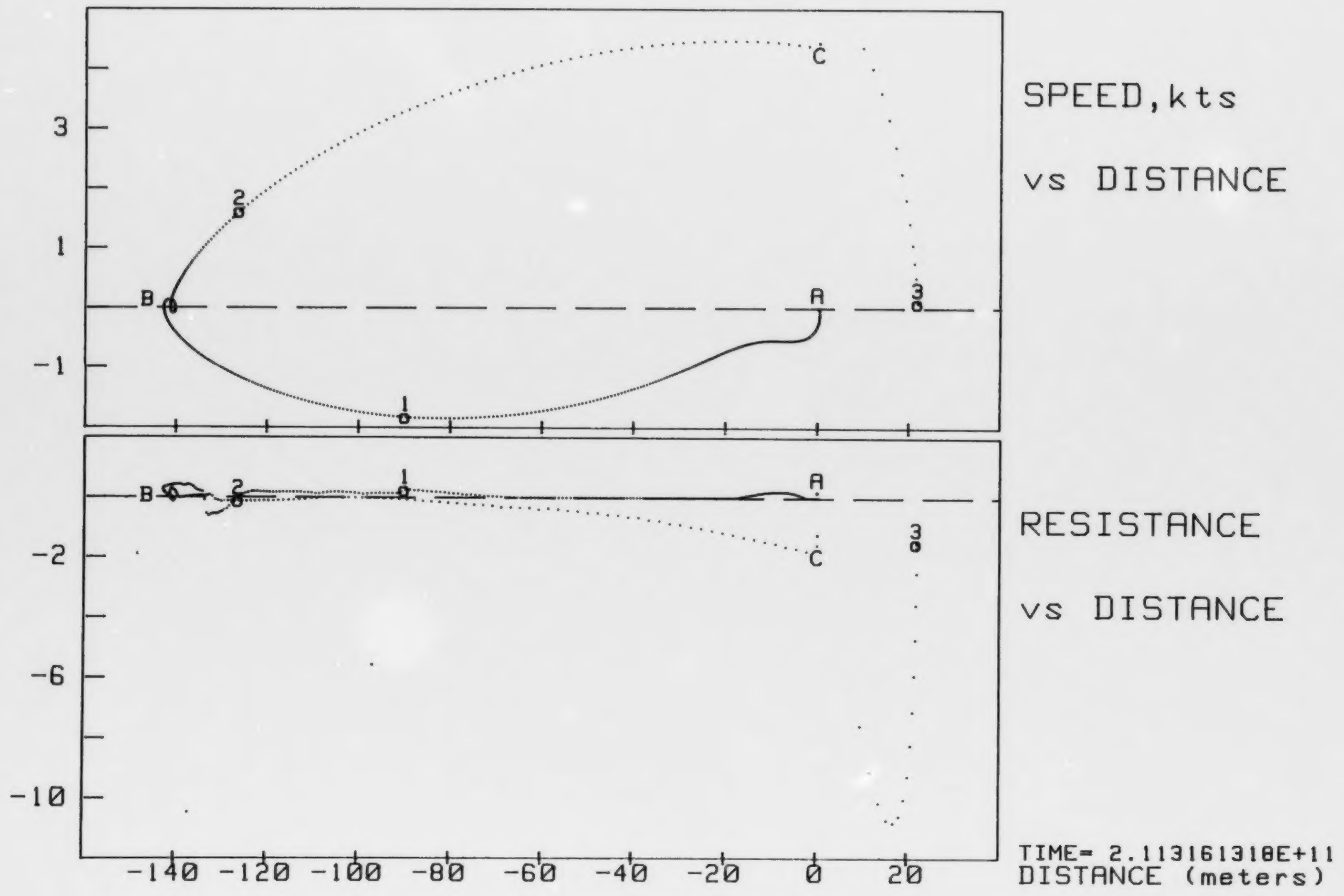

RAM # __A9 TAPE: 81-T2-2.1 07 JUL 1981 03:18:42 Fig.# 5

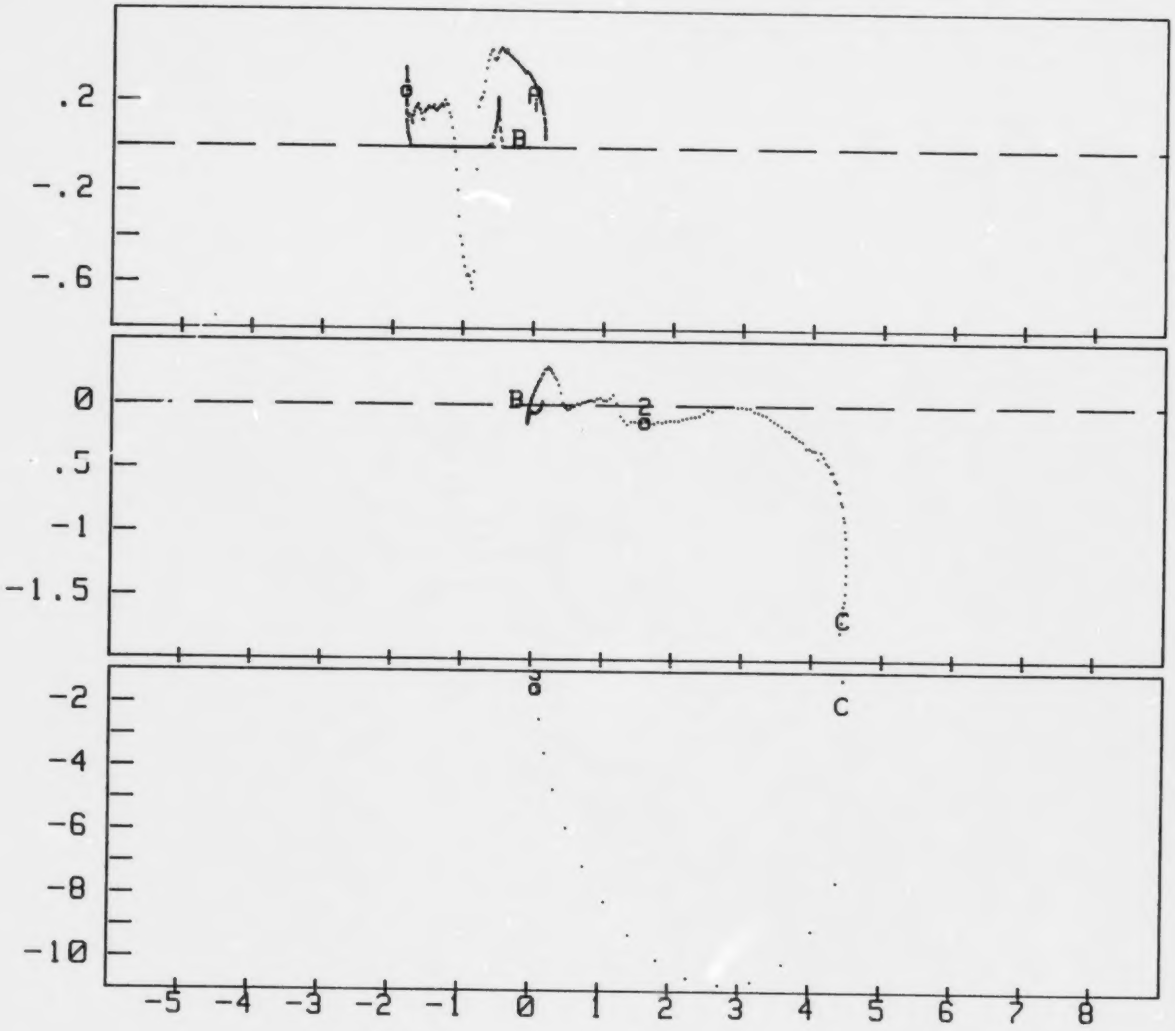

RESISTANCE ASTERN ,MN vs SPEED

RESISTANCE AHEAD ,MN vs SPEED

RESISTANCE PEN. ,MN vs SPEED

TIME= 2.11316132E+11
SPEED (kts)

RESULTS OF RAMMING CYCLE ANALYSIS

RAM No. _A10

TAPE: 81-T2-2.1
CATEGORY: R3
QUALITY: 63AD
TRIM: EVEN TRIM

ICE CONDITIONS: RIDGES
ICE THICKNESS: 2.64 m
FLEXURAL STRENGTH: 407 kPA
BUBBLER STATUS: OFF

RAMMING CYCLE CHARACTERISTICS:

Speed of Advance	(knots)	.0543	
Speed of Impact	(knots)	4.5	(4.61)

	Duration (sec)	% Cycle Time	Distance (m)
Backing	285	48.5	-159.4
Acceleration	148	25.2	159.4
Penetration	21	3.57	9.1 (16.42)
Extraction	134	22.8	
Total Cycle	588		

Duration of Astern Mode	(sec)	141		
Duration of Reversal to Ahead	(sec)	56		
Duration of Ahead Mode	(sec)	236		
Duration of Reversal to Astern	(sec)	43		
Start of Reversal after Impact	(sec)	0		
Total Fuel Used	(mm*hr)	6.38	Est. kg:	5.875
Average Fuel Rate	(mm)	39.08	Est. kg/hr:	35.971
Backing Power	(kW)	7140.8		
[Est Fuel Rate	(kg/hr)]	1516.1		
Acceleration Power	(kW)	4560.2		
[Est Fuel Rate	(kg/hr)]	1001.5		

RAM # _A10 TAPE: 81-T2-2.1 07 JUL 1981 03:29:12 **FIG. #1**

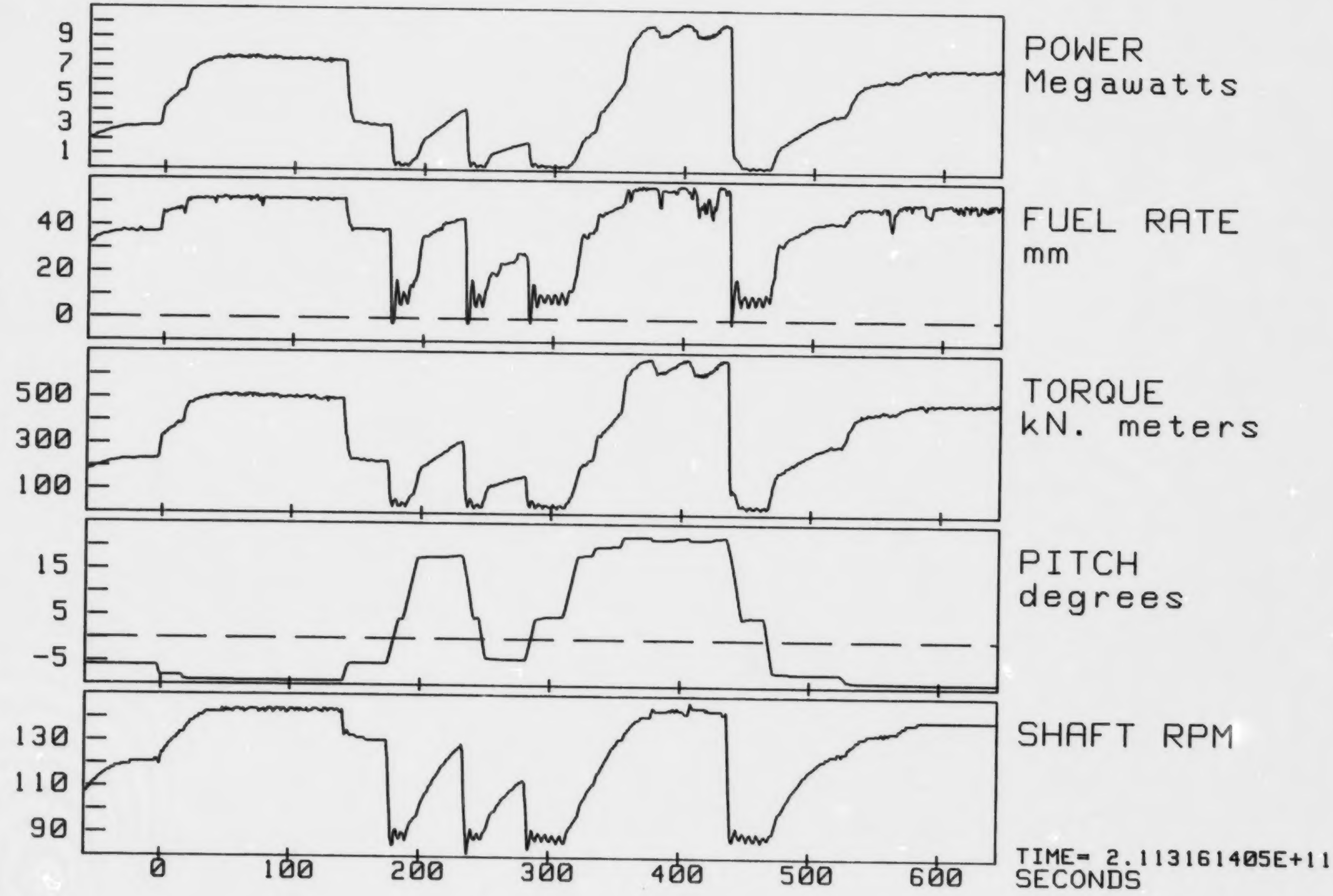

RAM # _A10   TAPE: 81-T2-2.1   07 JUL 1981 03:29:12

FIG. #2

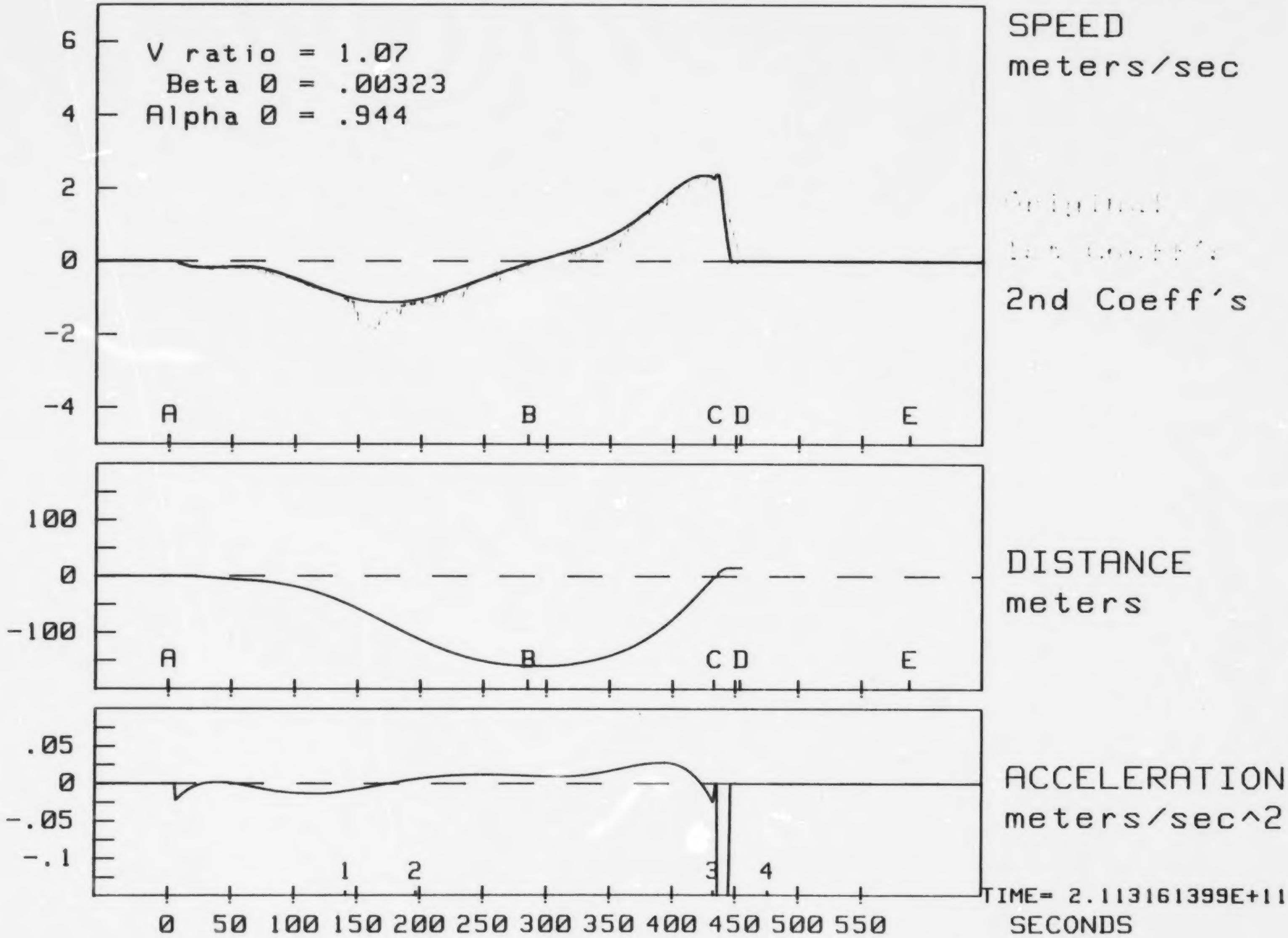

RAM # _A10 TAPE: 81-T2-2.1 07 JUL 1981 03:29:12

FIG. #3

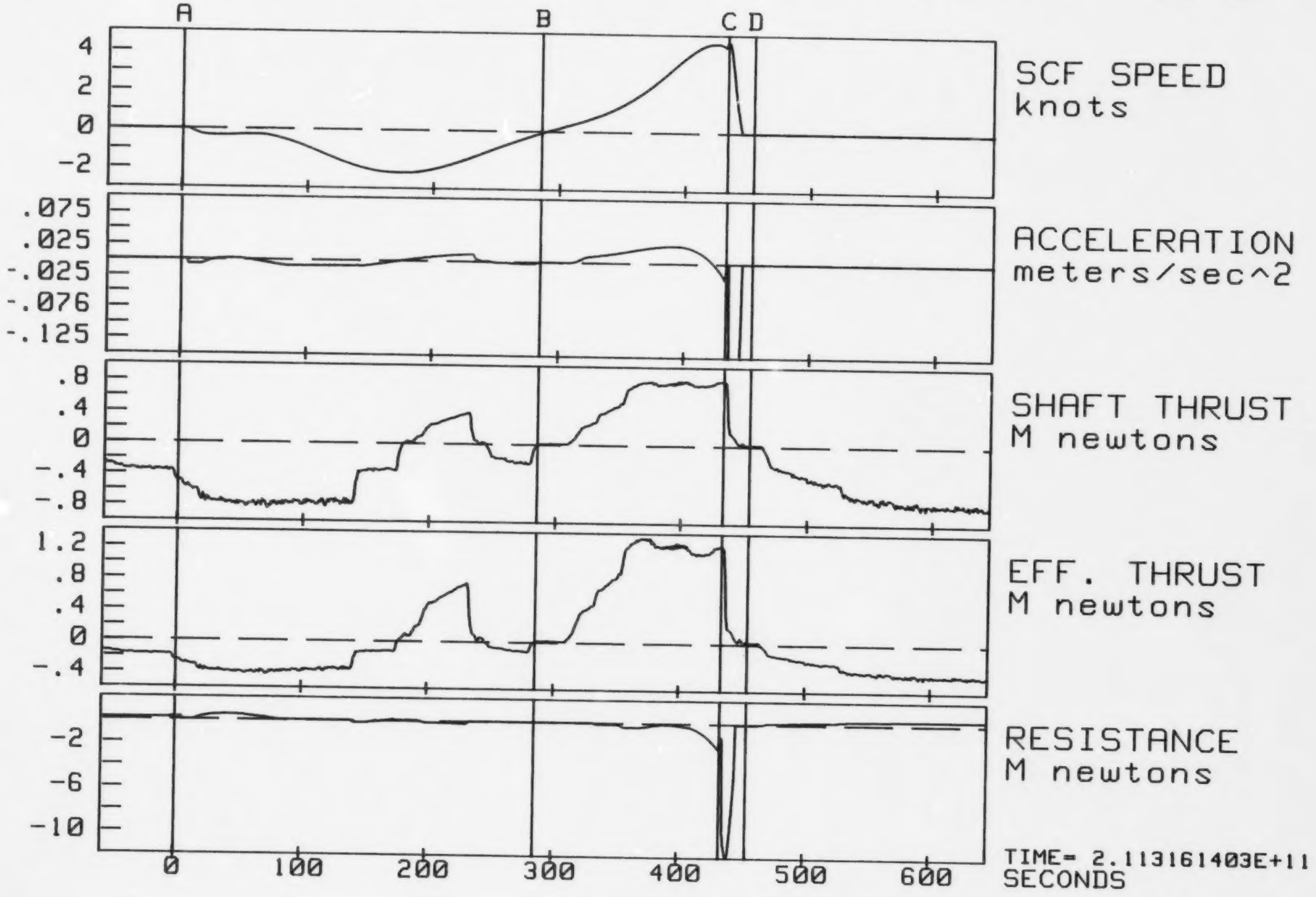

RAM # _A10 TAPE: 81-T2-2.1 07 JUL 1981 03:29:12 Fig.# 4

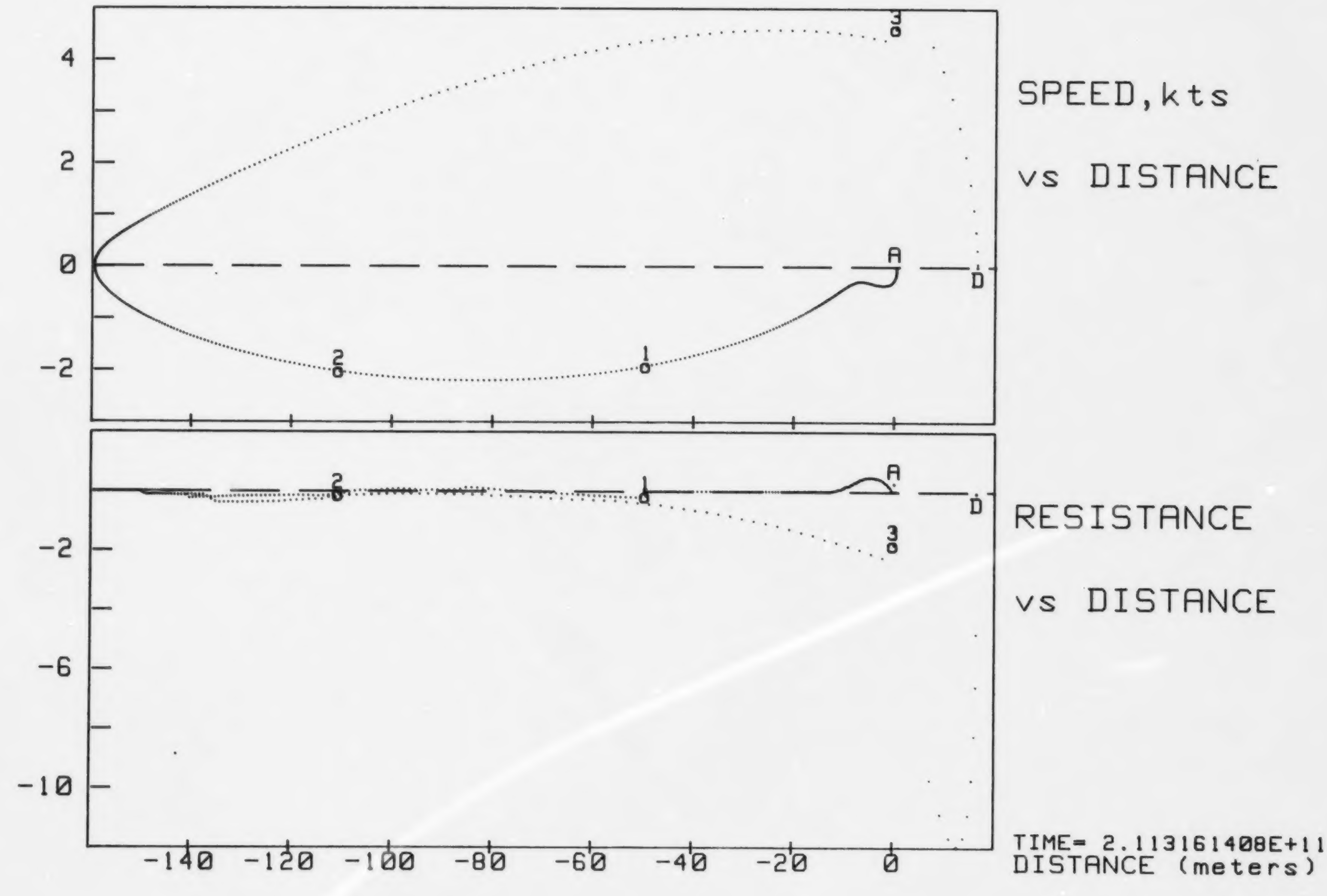

RAM # _A10   TAPE: 81-T2-2.1   07 JUL 1981 03:29:12   Fig.# 5

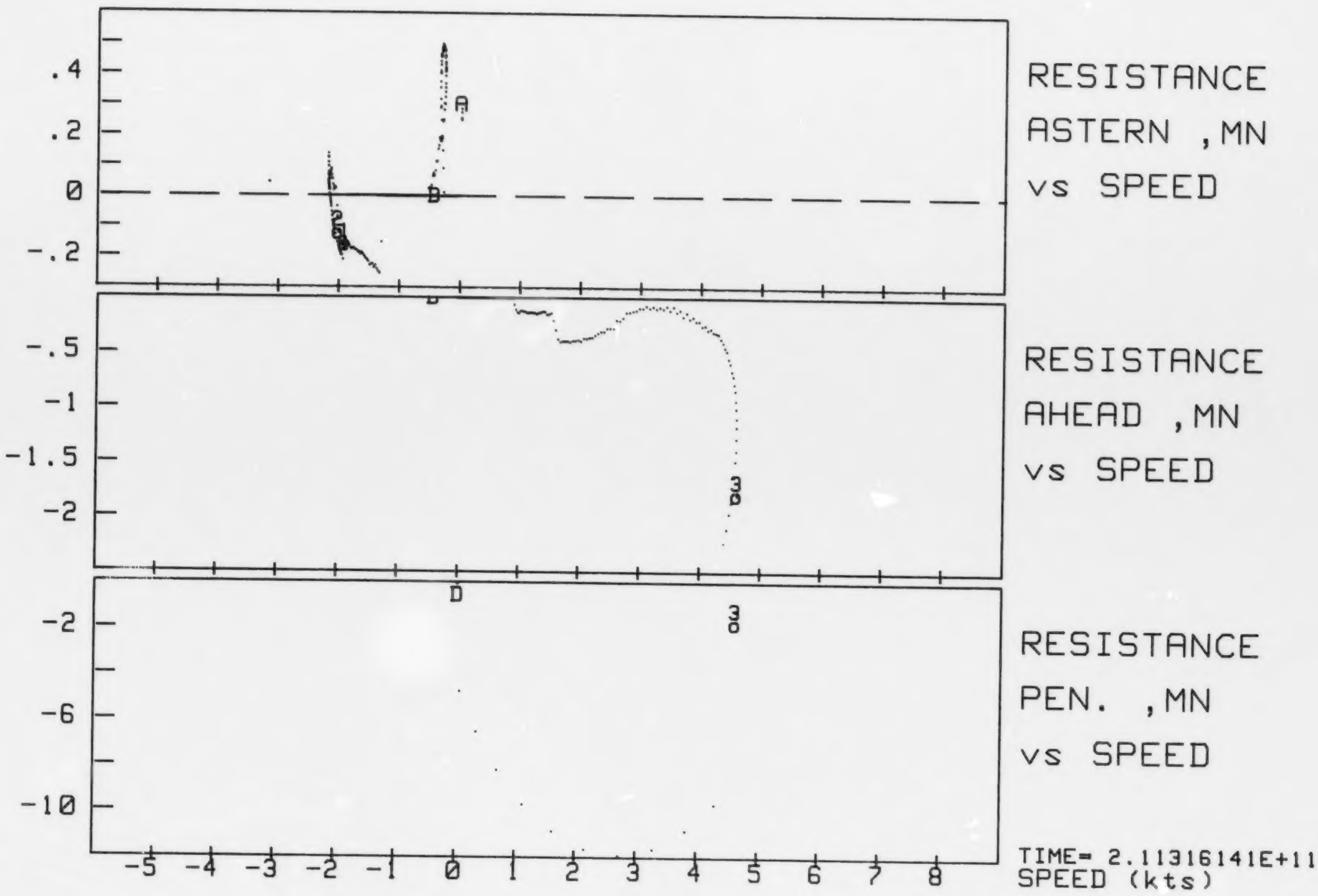

RESULTS OF RAMMING CYCLE ANALYSIS

RAM No. _A11

TAPE: 81-T2-2.1

CATEGORY: R3

QUALITY: 62AD

TRIM: EVEN

ICE CONDITIONS: RIDGES

ICE THICKNESS: 2.61 m

FLEXURAL STRENGTH: 407 kPA

BUBBLER STATUS: OFF

RAMMING CYCLE CHARACTERISTICS:

Speed of Advance	(knots)	.141	
Speed of Impact	(knots)	4.5	(4.55)

	Duration (sec)	% Cycle Time	Distance (m)
Backing	302	54.5	-122.3
Acceleration	103	18.6	122.3
Penetration	25	4.51	33 (40.08)
Extraction	124	22.4	
Total Cycle	554		

Duration of Astern Mode	(sec)	148		
Duration of Reversal to Ahead	(sec)	198		
Duration of Ahead Mode	(sec)	64		
Duration of Reversal to Astern	(sec)	55		
Start of Reversal after Impact	(sec)	5		
Total Fuel Used	(mm*hr)	5.73	Est. kg:	-15.01
Average Fuel Rate	(mm)	37.23	Est. kg/hr:	-97.548
Backing Power	(kW)	6915.7		
[Est Fuel Rate	(kg/hr)]	1471.2		
Acceleration Power	(kW)	9703.4		
[Est Fuel Rate	(kg/hr)]	2027.1		

RAM # _A11 TAPE: 81-T2-2.1 07 JUL 1981 03:38:12 **FIG. #1**

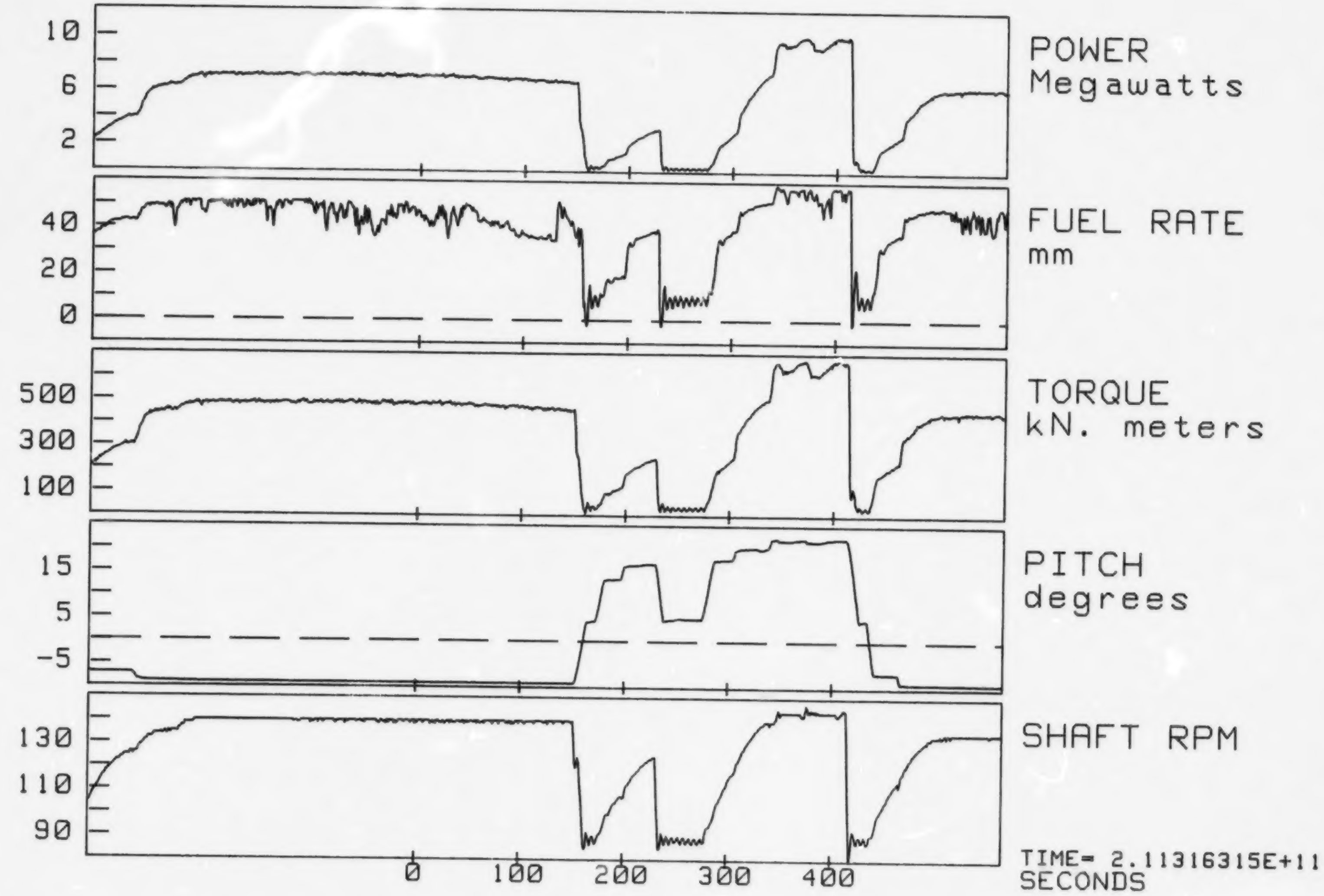

RAM # _A11 TAPE: 81-T2-2.1 07 JUL 1981 03:38:12 **FIG. #2**

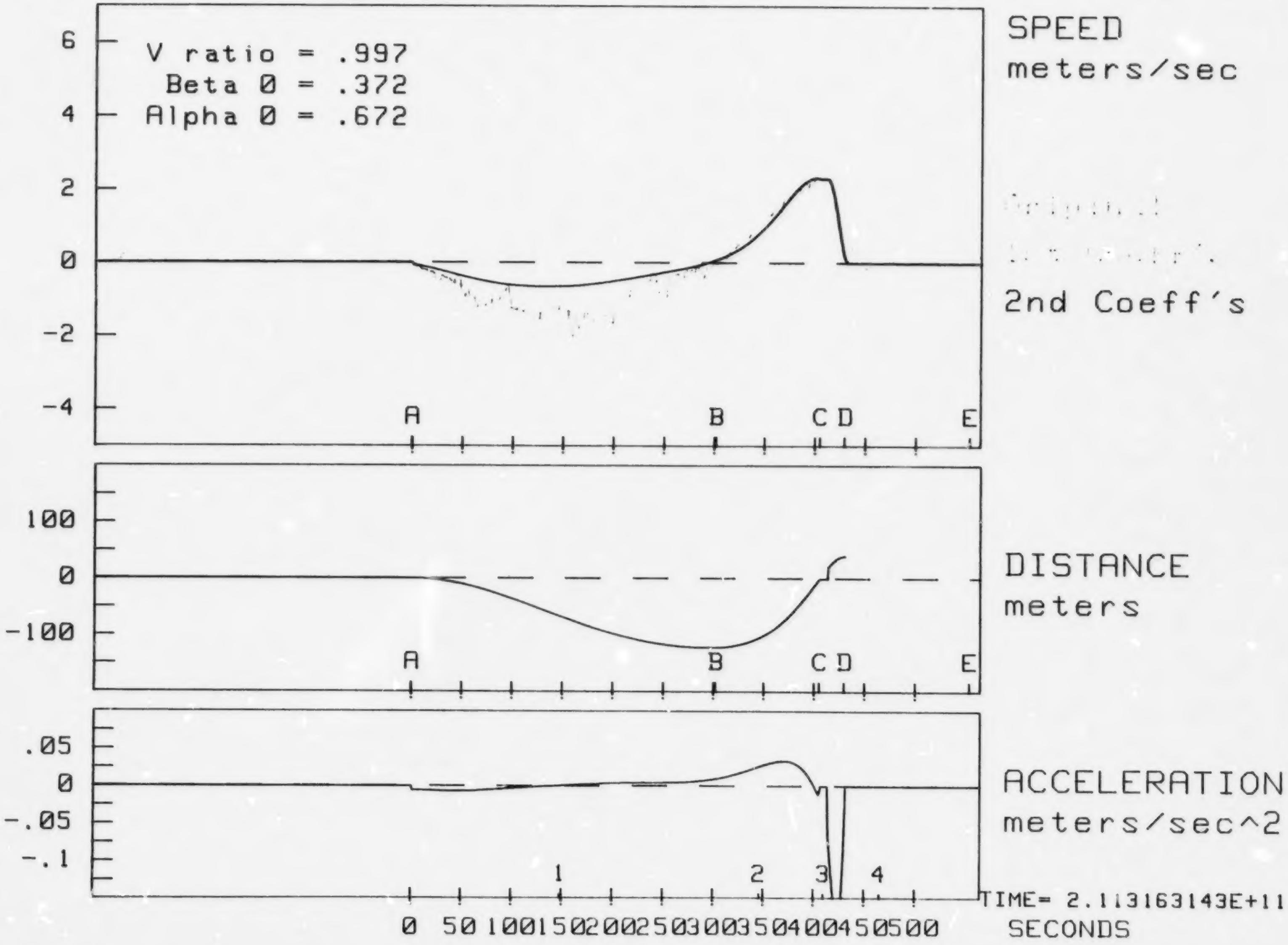

RAM # _A11 TAPE: 81-T2-2.1 07 JUL 1981 03:38:12 **FIG. #3**

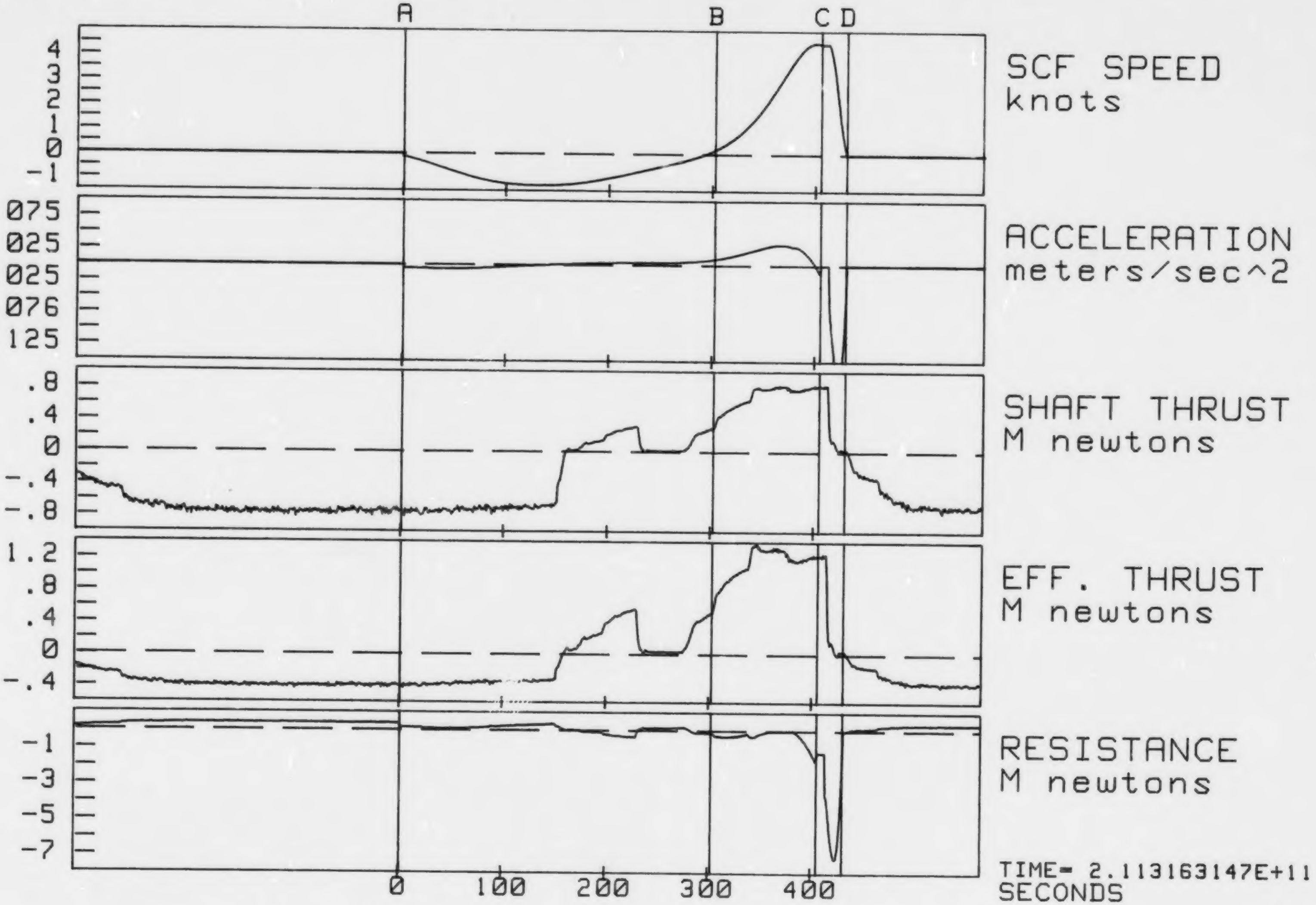

RAM # _A11 TAPE: 81-T2-2.1 07 JUL 1981 03:38:12 Fig.# 4

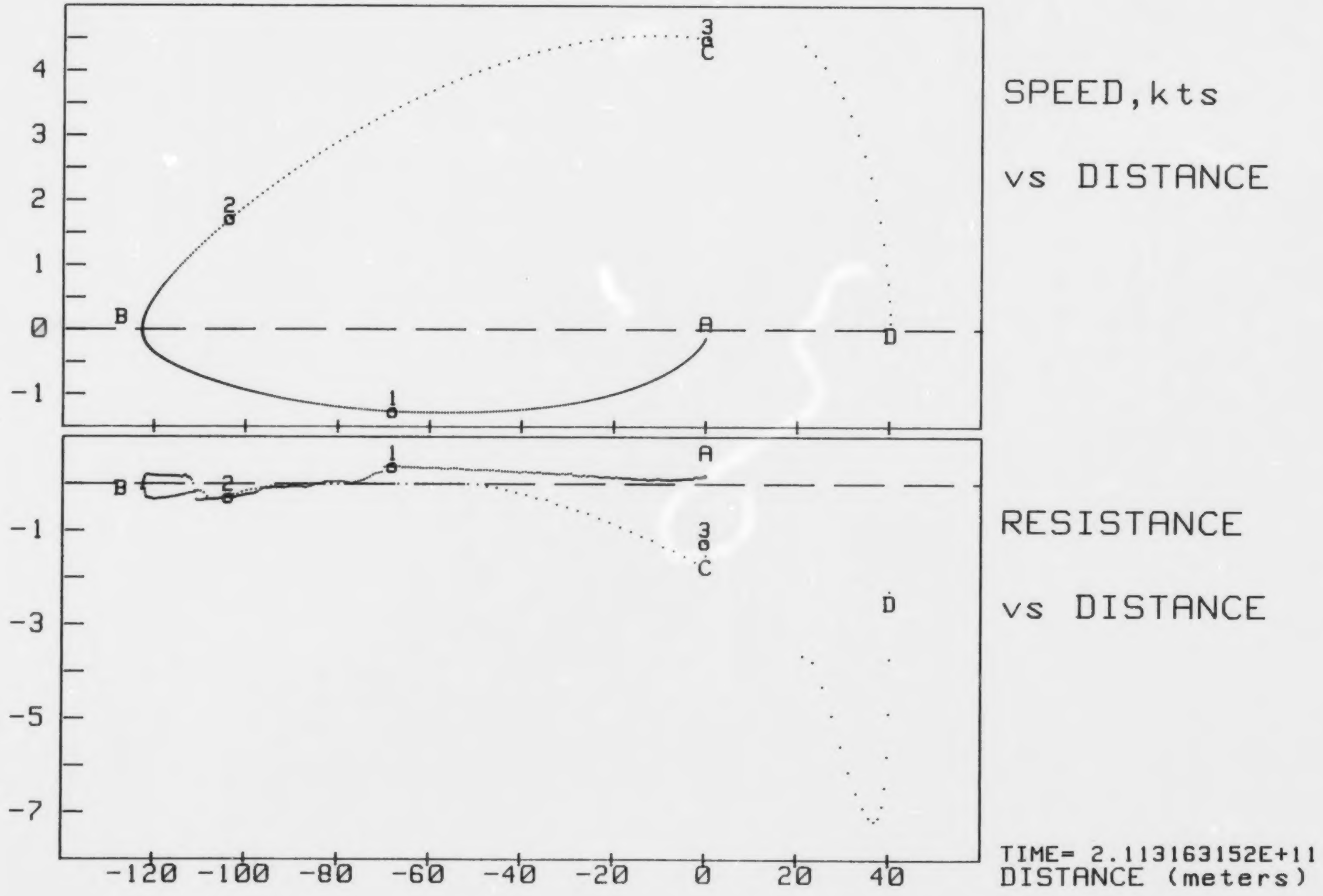

RAM # _A11   TAPE: 81-T2-2.1   07 JUL 1981 03:38:12   Fig.# 5

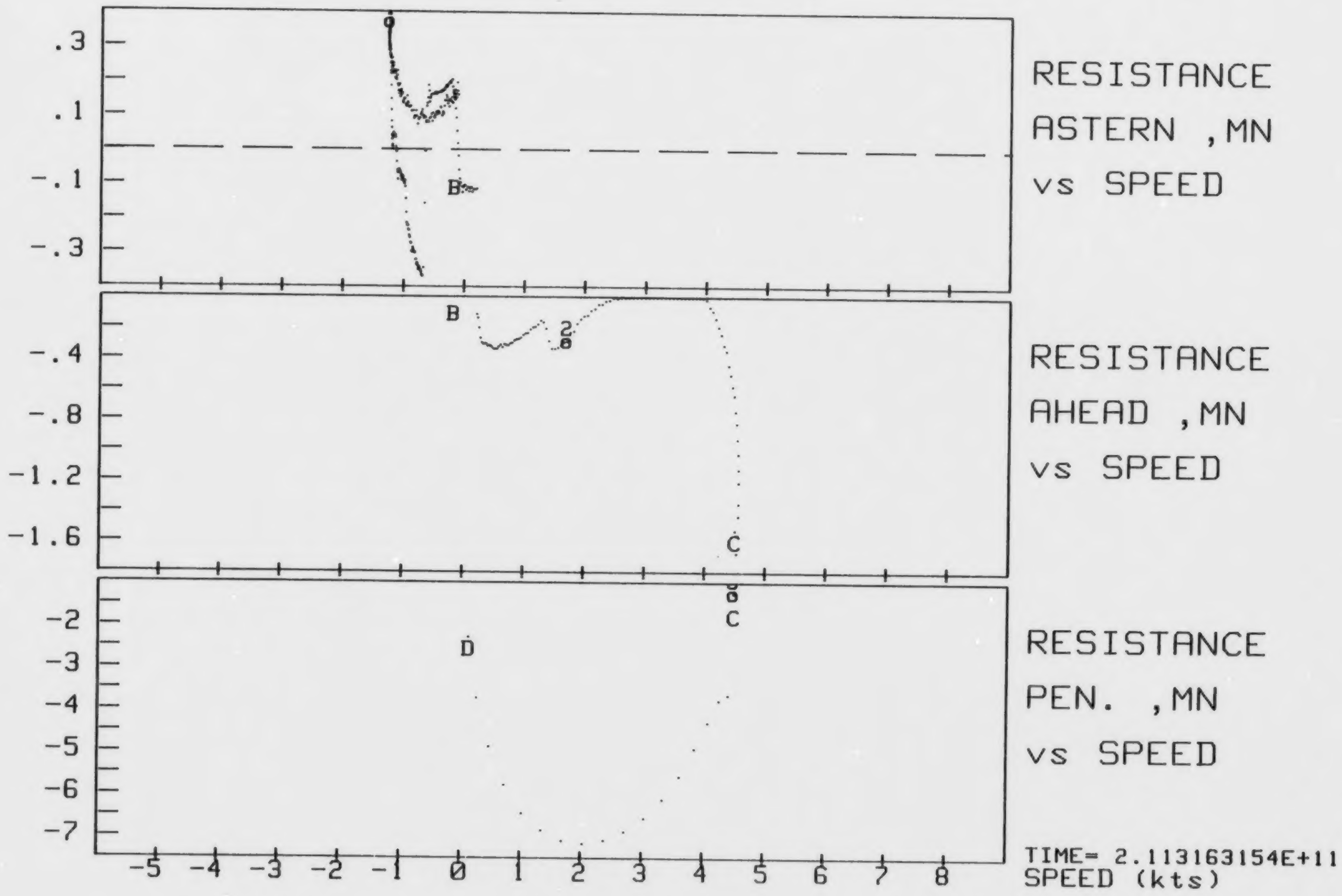

RESULTS OF RAMMING CYCLE ANALYSIS

RAM No. _A12

TAPE:	81-T2-2.1	ICE CONDITIONS:	RIDGES
CATEGORY:	R3	ICE THICKNESS:	2.56 m
QUALITY:	67BD	FLEXURAL STRENGTH:	407 kPA
TRIM:	EVEN		
		BUBBLER STATUS:	OFF

RAMMING CYCLE CHARACTERISTICS:

Speed of Advance	(knots)	.166	
Speed of Impact	(knots)	4.5	(4.15)

	Duration (sec)	% Cycle Time	Distance (m)
Backing	263	67.8	-109.7
Acceleration	89	22.9	109.7
Penetration	25	6.44	28 (33.22)
Extraction	11	2.84	
Total Cycle	388		

Duration of Astern Mode	(sec)	145		
Duration of Reversal to Ahead	(sec)	111		
Duration of Ahead Mode	(sec)	103		
Duration of Reversal to Astern	(sec)	29		
Start of Reversal after Impact	(sec)	7		
Total Fuel Used	(mm*hr)	3.7	Est. kg:	-33.37
Average Fuel Rate	(mm)	34.28	Est. kg/hr:	-309.64
Backing Power	(kW)	6818.1		
[Est Fuel Rate	(kg/hr)]	1451.8		
Acceleration Power	(kW)	6992		
[Est Fuel Rate	(kg/hr)]	1486.5		

RAM # _A12 TAPE: 81-T2-2.1 07 JUL 1981 03:51:12 **FIG. #1**

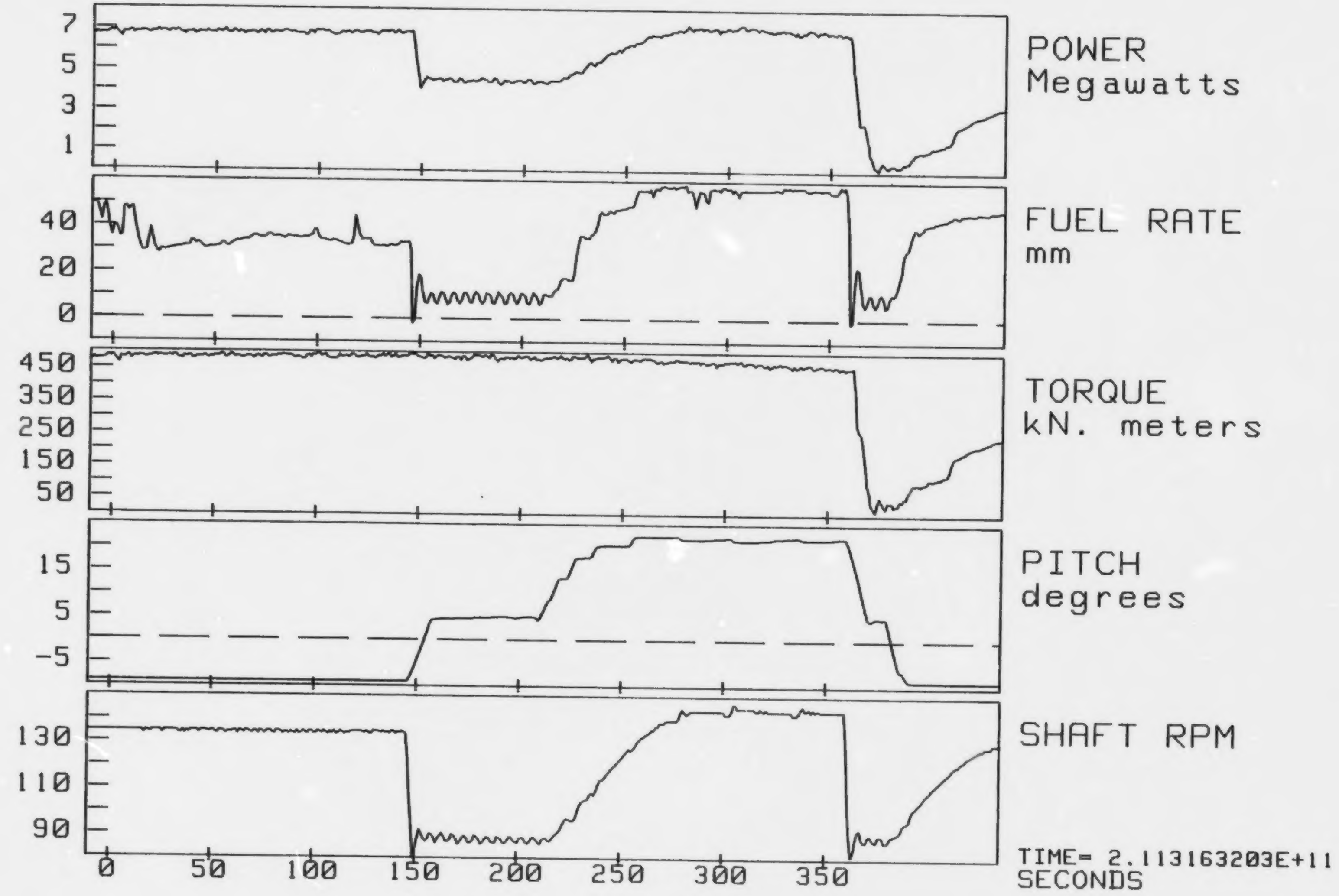

RAM # _A12 TAPE: 81-T2-2.1 07 JUL 1981 03:51:12

FIG. #2

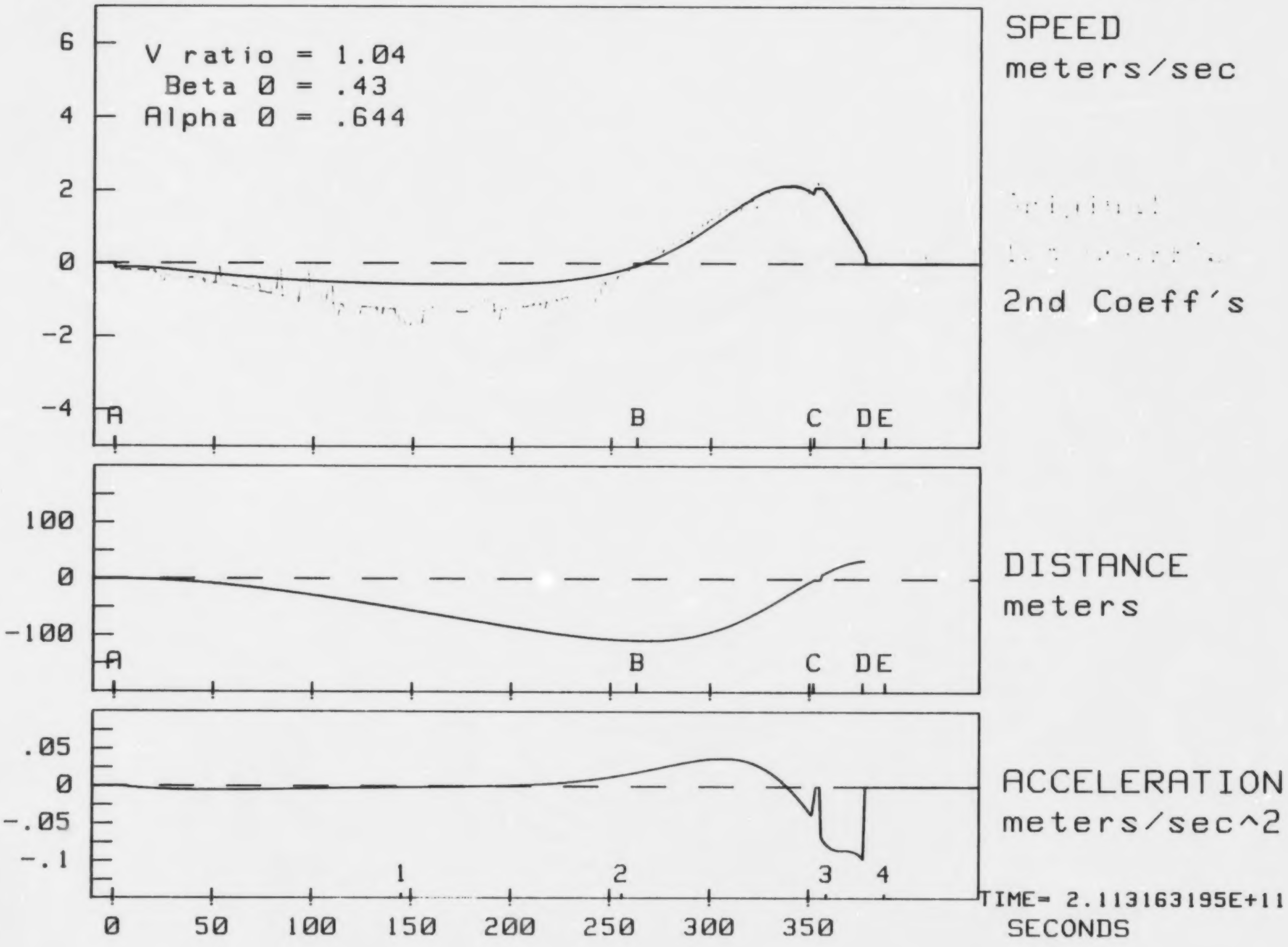

RAM # _A12 TAPE: 81-T2-2.1 07 JUL 1981 03:51:12

FIG. #3

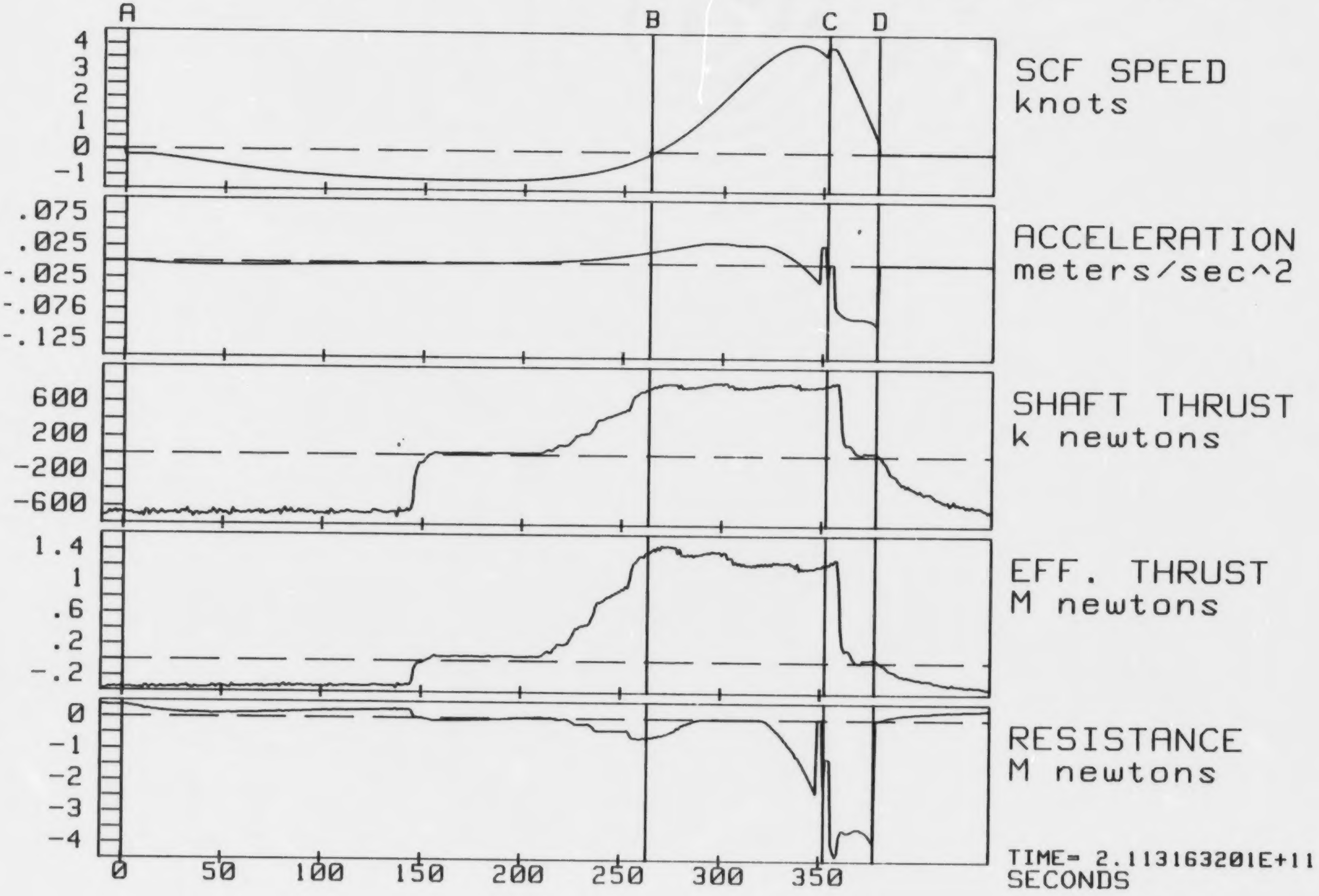

RAM # _A12 TAPE: 81-T2-2.1 07 JUL 1981 03:51:12 Fig.# 4

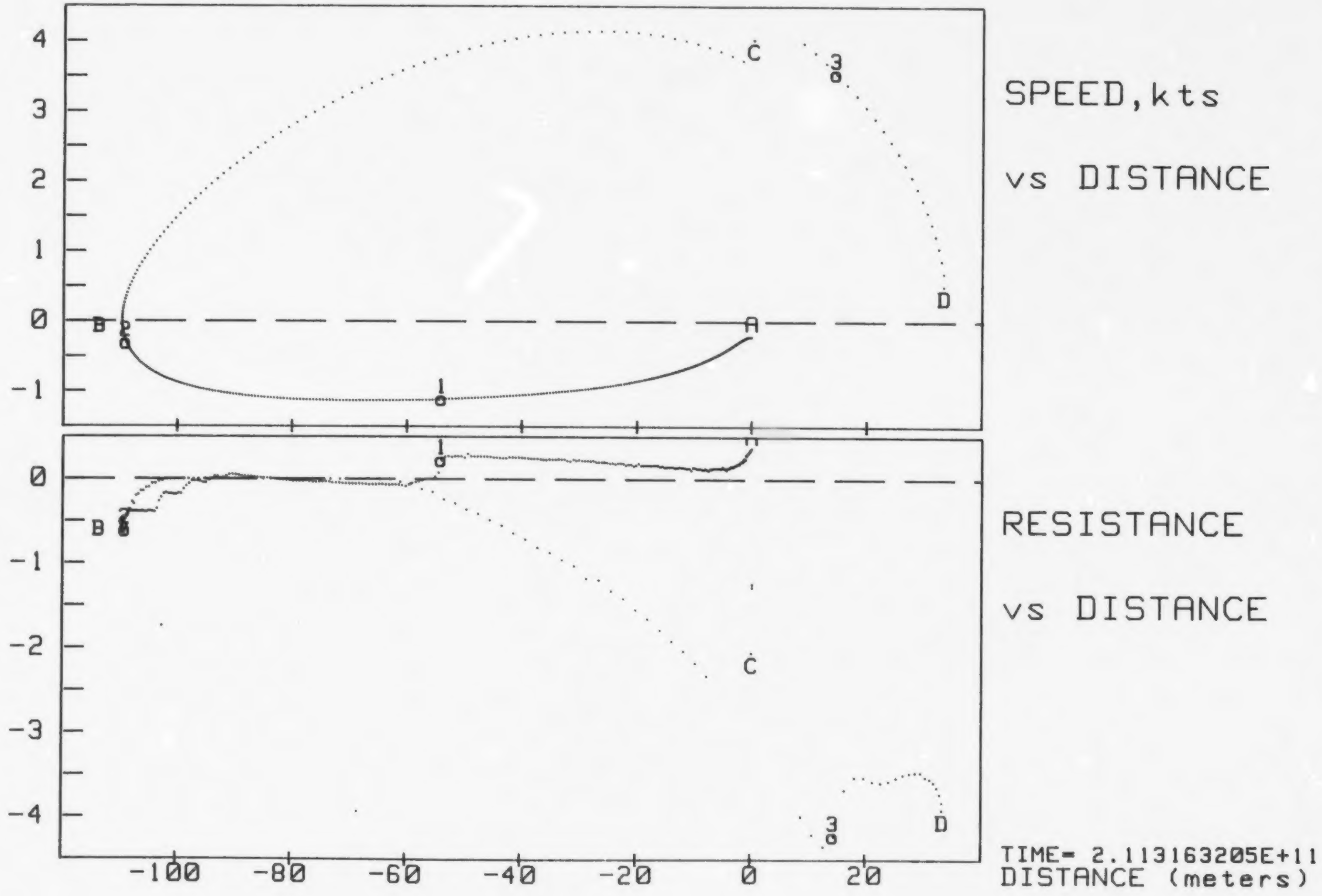

RAM # _A12 TAPE: 81-T2-2.1 07 JUL 1981 03:51:12 Fig.# 5

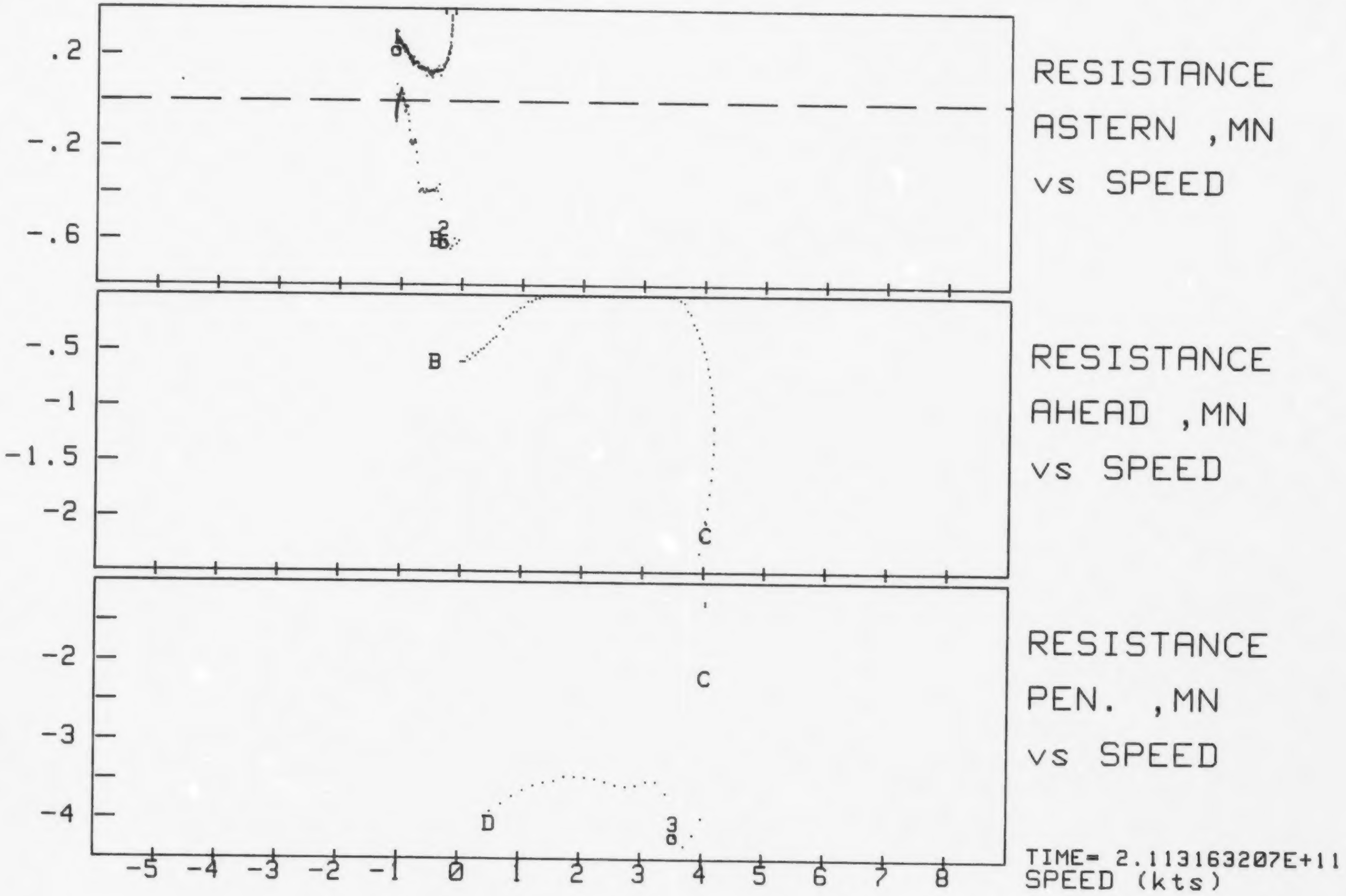

RESULTS OF RAMMING CYCLE ANALYSIS

RAM No. _A13

TAPE:	81-T2-2.1	ICE CONDITIONS:	RIDGES
CATEGORY:	R1	ICE THICKNESS:	2.52 m
QUALITY:	71BD	FLEXURAL STRENGTH:	407 kPA
TRIM:	EVEN TRIM	BUBBLER STATUS:	ON

RAMMING CYCLE CHARACTERISTICS:

Speed of Advance	(knots)	.0476
Speed of Impact	(knots)	4.5 (4.46)

	Duration (sec)	% Cycle Time	Distance (m)
Backing	367	66.8	-156.3
Acceleration	115	20.9	156.3
Penetration	18	3.28	6.1 (13.45)
Extraction	49	8.93	
Total Cycle	549		

Duration of Astern Mode	(sec)	239
Duration of Reversal to Ahead	(sec)	134
Duration of Ahead Mode	(sec)	130
Duration of Reversal to Astern	(sec)	19
Start of Reversal after Impact	(sec)	21

Total Fuel Used	(mm*hr)	6.25	Est. kg:	26.13
Average Fuel Rate	(mm)	40.96	Est. kg/hr:	171.36

Backing Power	(kW)	6218.5
[Est Fuel Rate	(kg/hr)]	1332.2

Acceleration Power	(kW)	5221.6
[Est Fuel Rate	(kg/hr)]	1133.4

RAM # _A13 TAPE: 81-T2-2.1 07 JUL 1981 03:59:42

FIG. #1

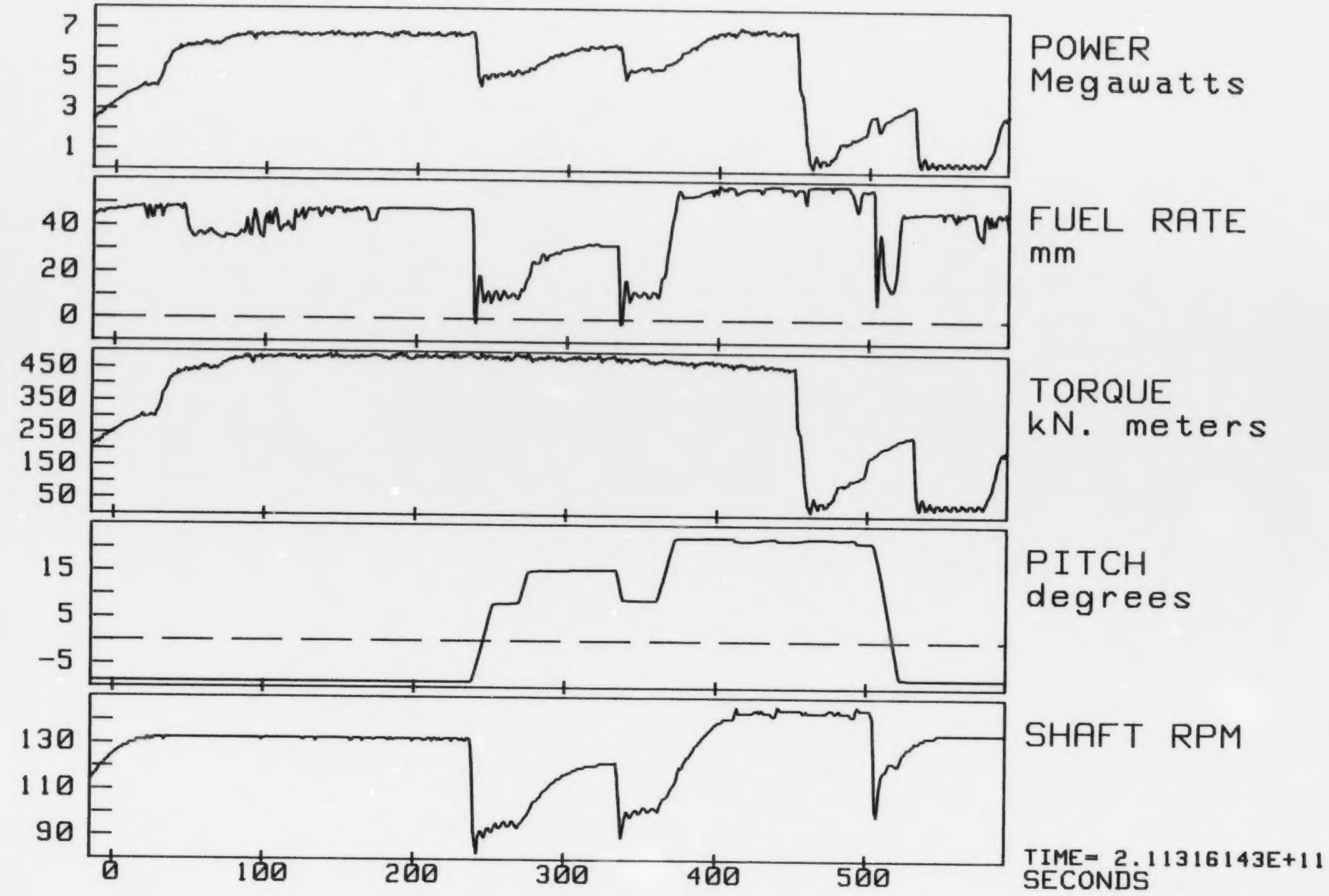

RAM # _A13 TAPE: 81-T2-2.1 07 JUL 1981 03:59:42

FIG. #2

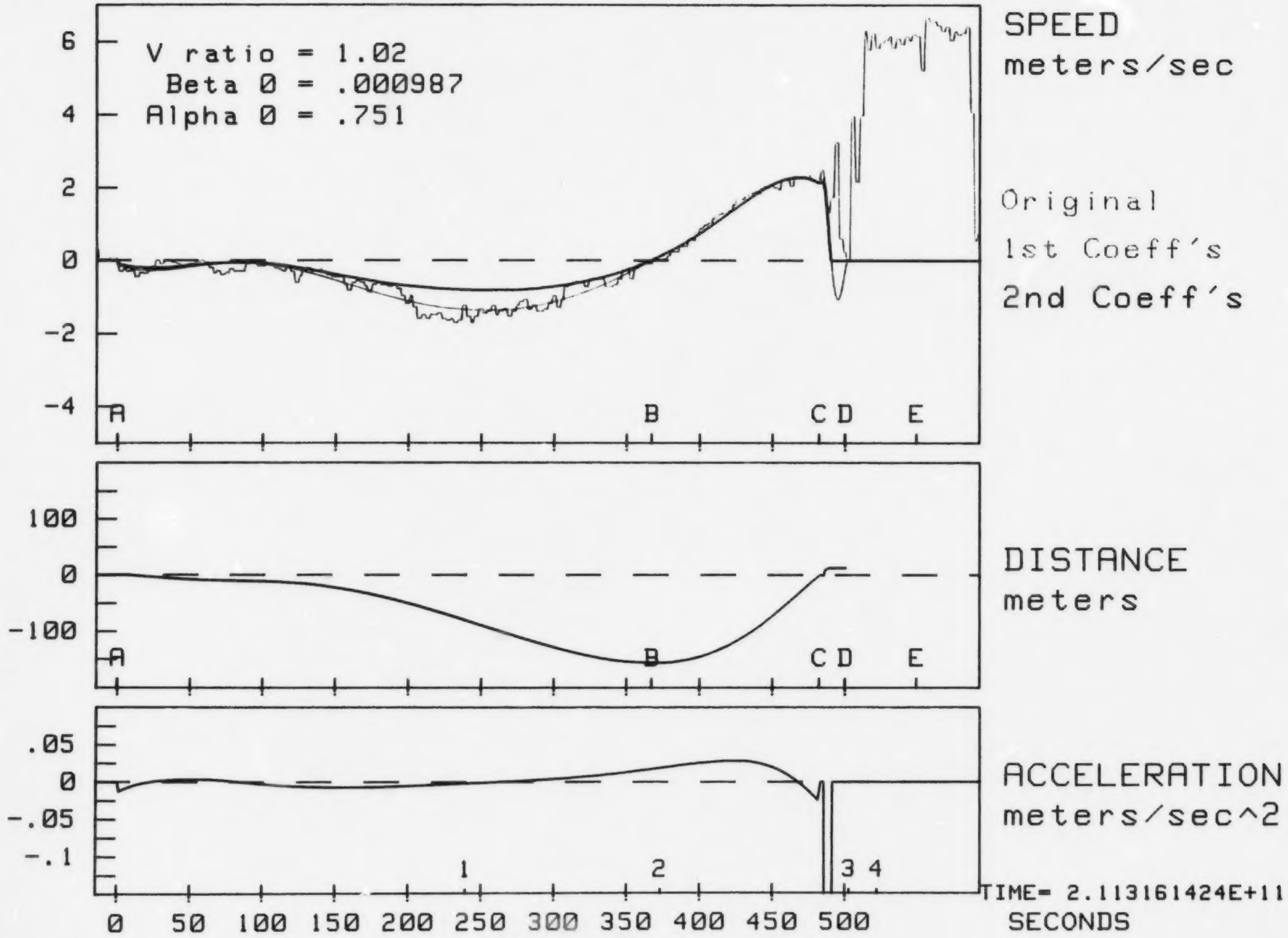

RAM # _A13   TAPE: 81-T2-2.1   07 JUL 1981 03:59:42

FIG. #3

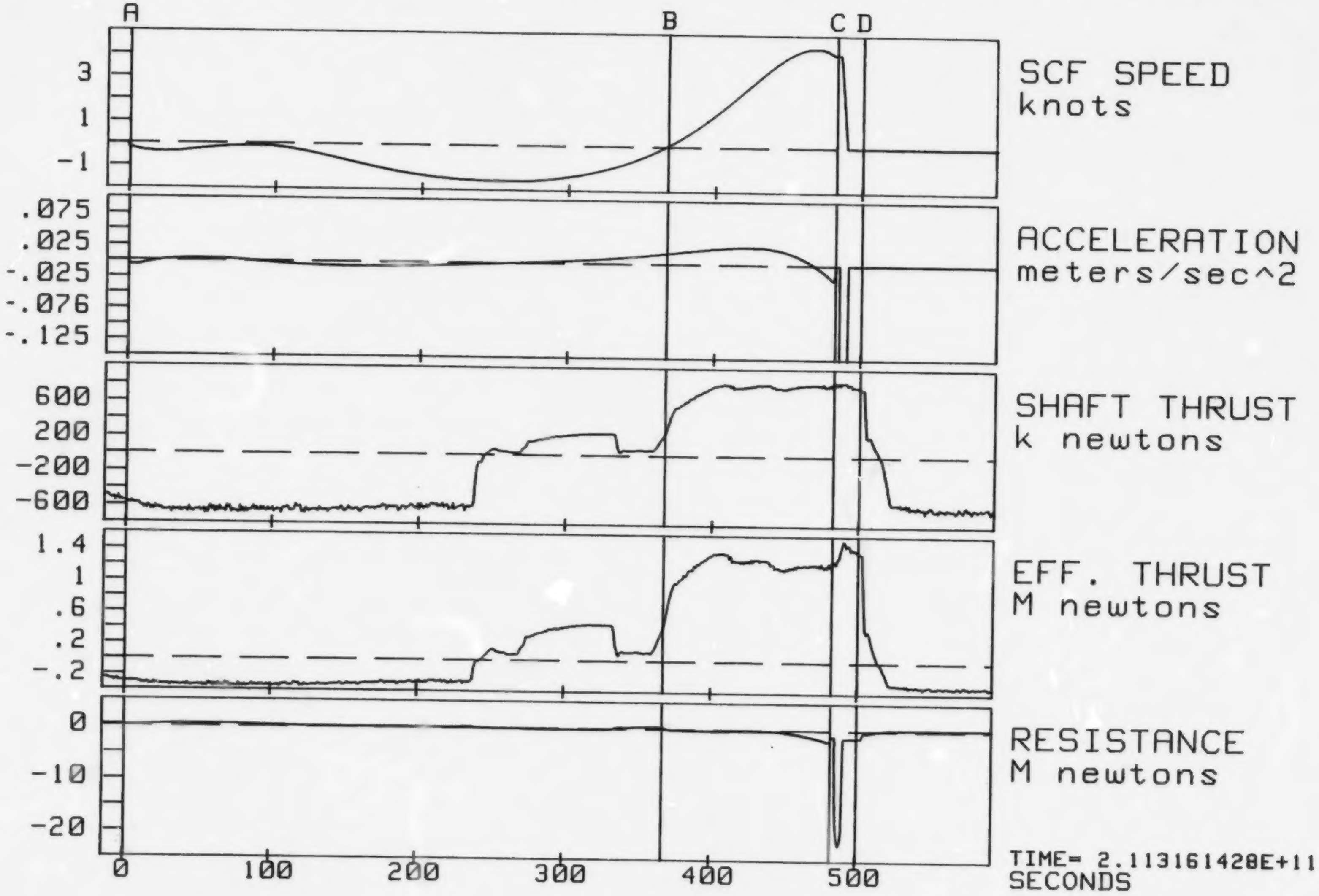

RAM # _A13 TAPE: 81-T2-2.1 07 JUL 1981 03:59:42 Fig.# 4

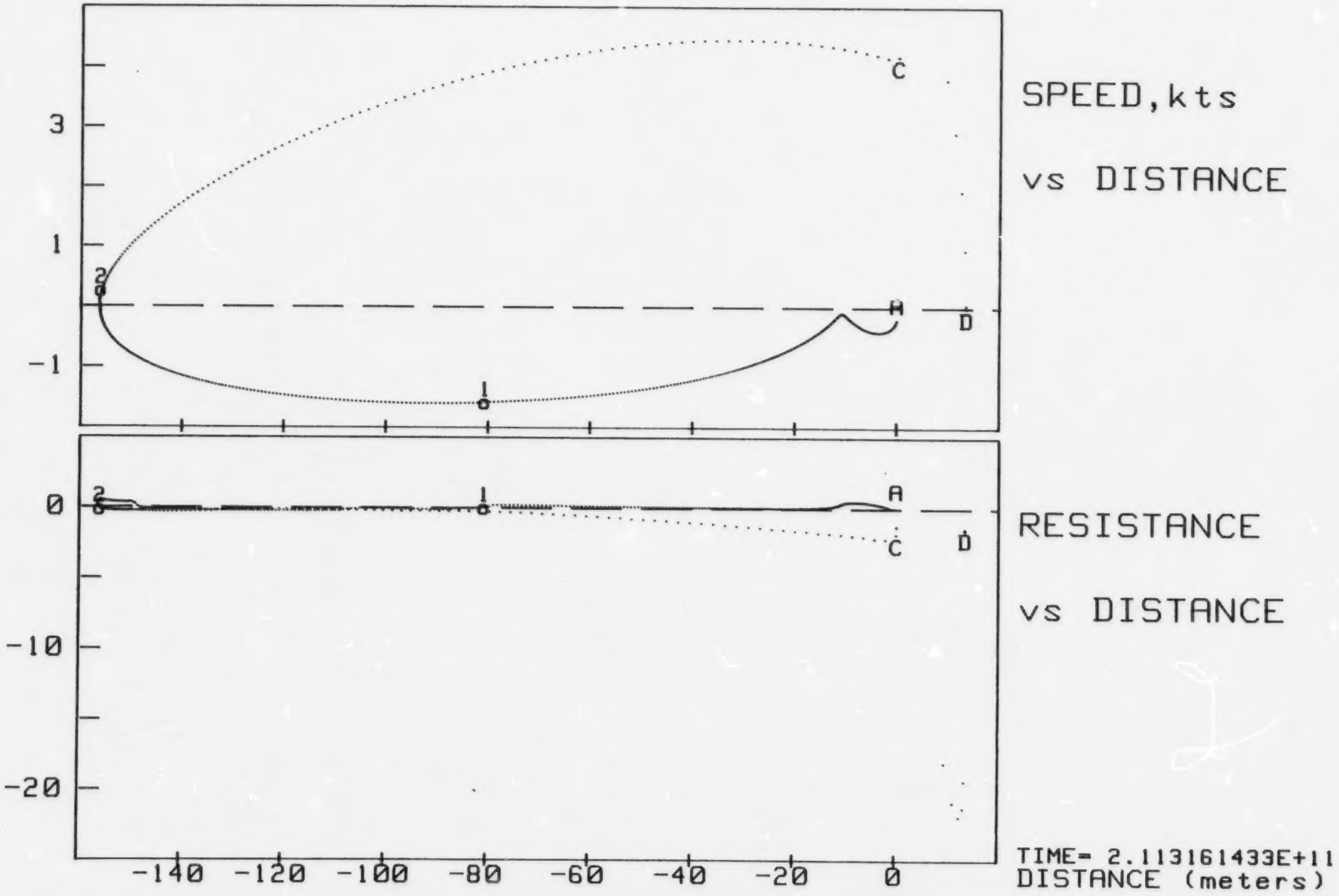

RAM # _A13   TAPE: 81-T2-2.1   07 JUL 1981 03:59:42   Fig.# 5

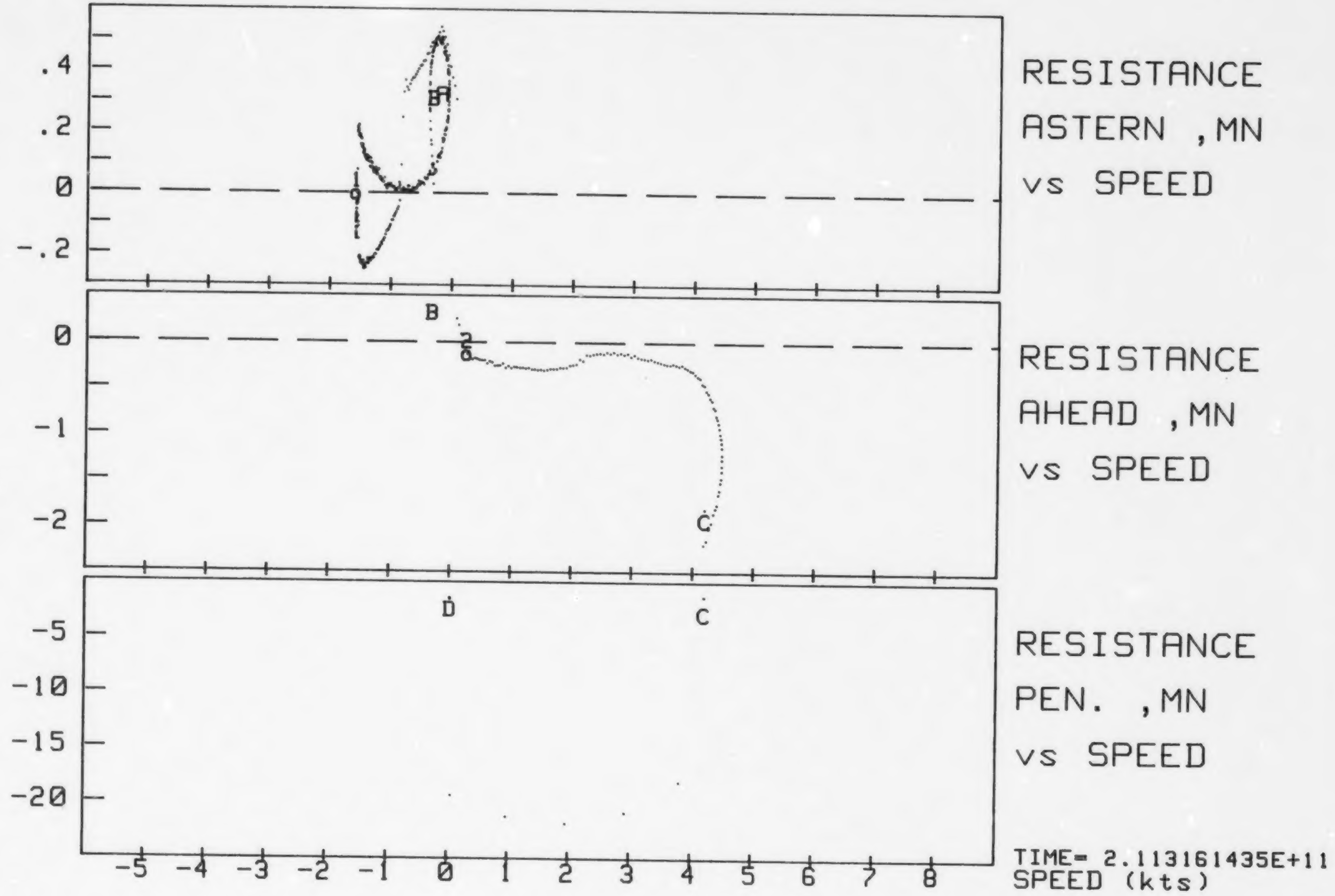

```
                  RESULTS OF RAMMING CYCLE ANALYSIS

                           RAM No.  _A14

TAPE:        81-T2-2.1                 ICE CONDITIONS:     RIDGES

CATEGORY:    R1                        ICE THICKNESS:      2.49  m

QUALITY:     68BD                      FLEXURAL STRENGTH:  407  kPA

TRIM:        EVEN TRIM                 BUBBLER STATUS:    ON

RAMMING CYCLE CHARACTERISTICS:

Speed of Advance  (knots)     .0928

Speed of Impact   (knots)     4.5    ( 4.59 )

                              Duration (sec)   % Cycle Time   Distance  (m)
Backing                       269              51.1          -138.2
Acceleration                  95               18.1           138.2
Penetration                   19               3.61           18.2 (25.12)
Extraction                    143              27.2
Total Cycle                   526

Duration of Astern Mode          (sec)     140
Duration of Reversal to Ahead    (sec)     129
Duration of Ahead Mode           (sec)     95
Duration of Reversal to Astern   (sec)     31
Start of Reversal after Impact   (sec)     0

Total Fuel Used    (mm*hr)                 5.93          Est. kg:      20.94
Average Fuel Rate  (mm)                    40.57         Est. kg/hr:   143.34

Backing Power      (kW)                    5314.1
[Est Fuel Rate     (kg/hr)]                1151.9

Acceleration Power(kW)                     9431.7
[Est Fuel Rate     (kg/hr)]                1972.9
```

RAM # _A14 TAPE: 81-T2-2.1 07 JUL 1981 04:08:12

FIG. #1

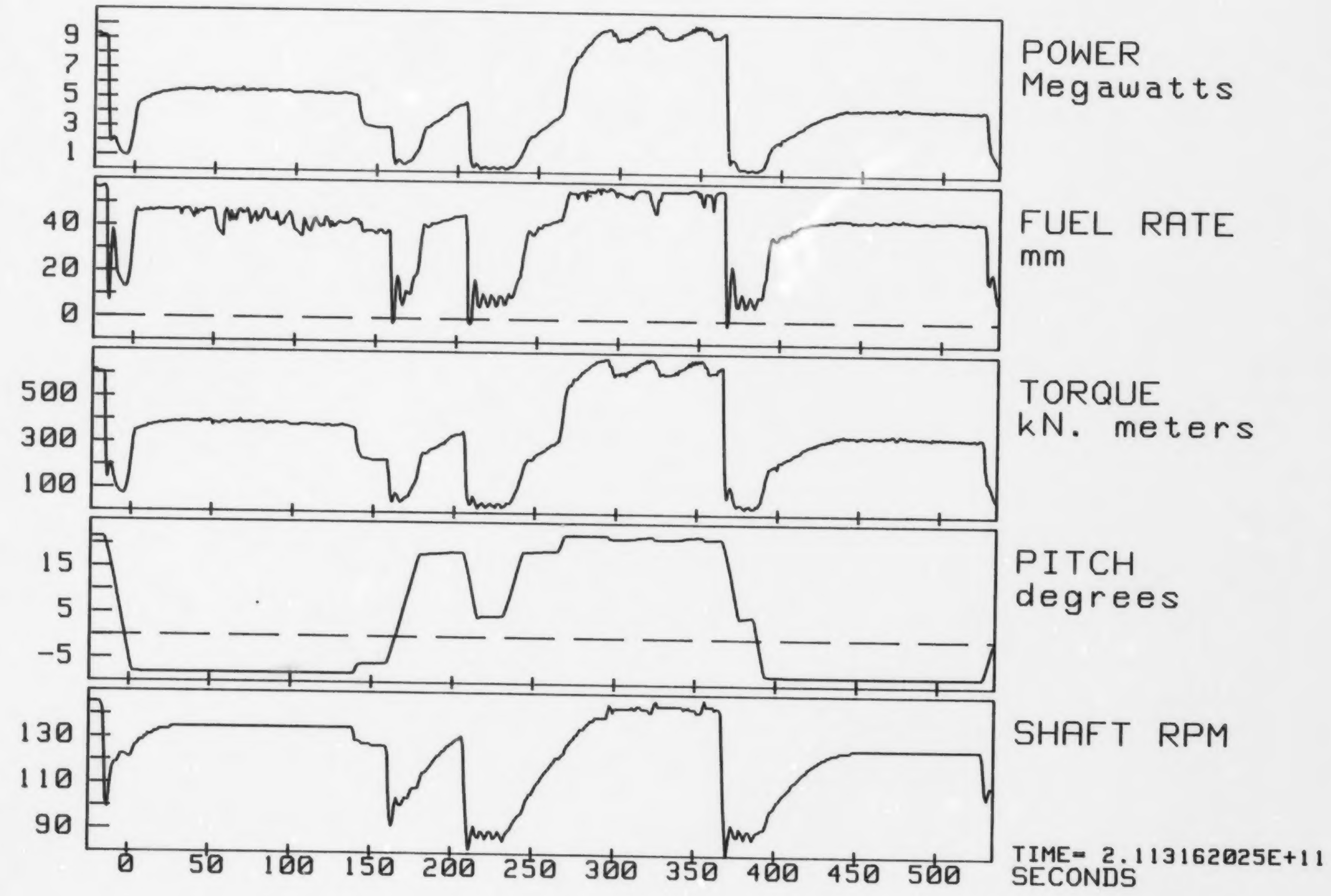

RAM # _A14 TAPE: 81-T2-2.1 07 JUL 1981 04:08:12 **FIG. #2**

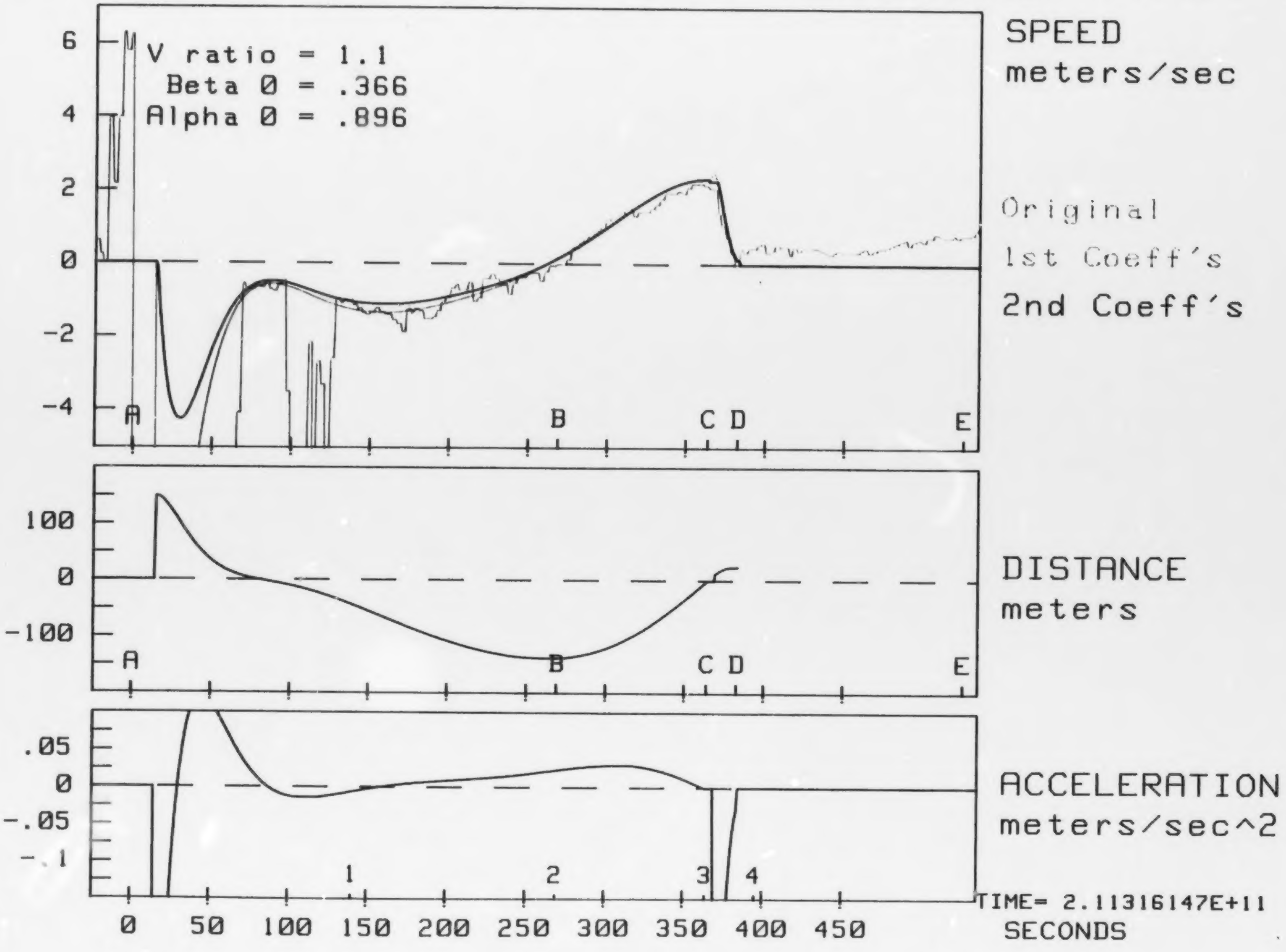

RAM # _A14 TAPE: 81-T2-2.1 07 JUL 1981 04:08:12

FIG. #3

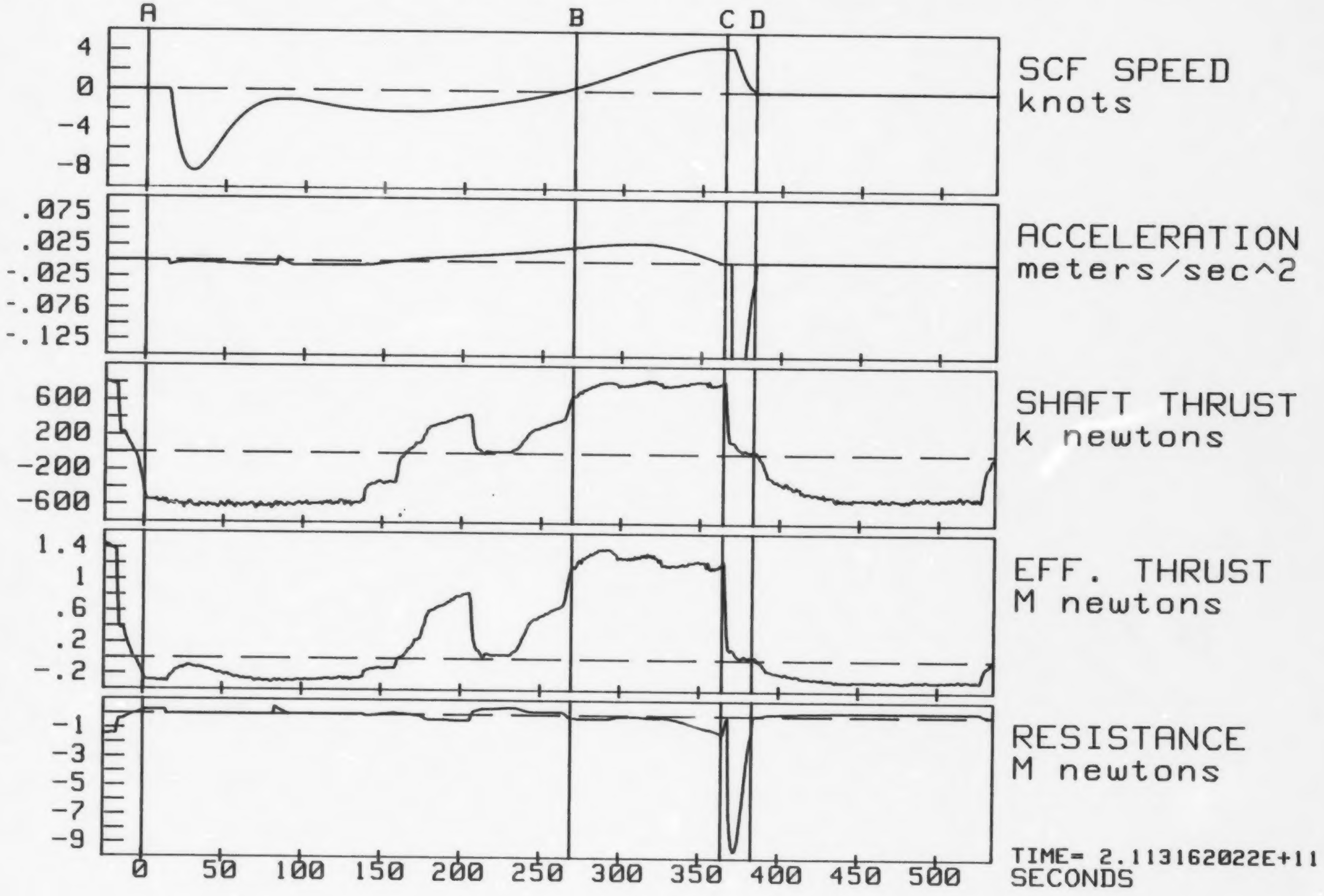

RAM # _A14 TAPE: 81-T2-2.1 07 JUL 1981 04:08:12 Fig.# 4

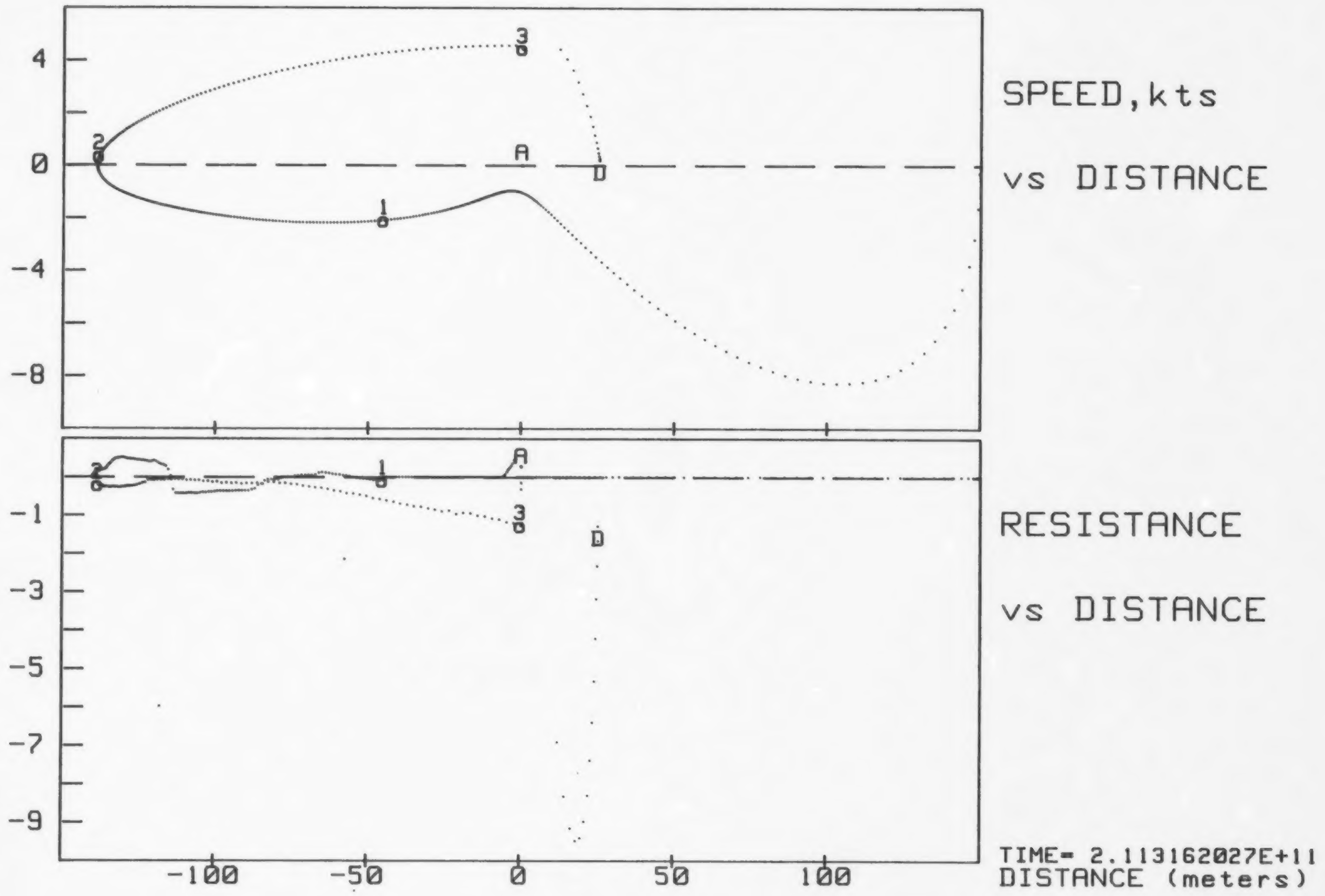

RAM # _A14 TAPE: 81-T2-2.1 07 JUL 1981 04:08:12 Fig.# 5

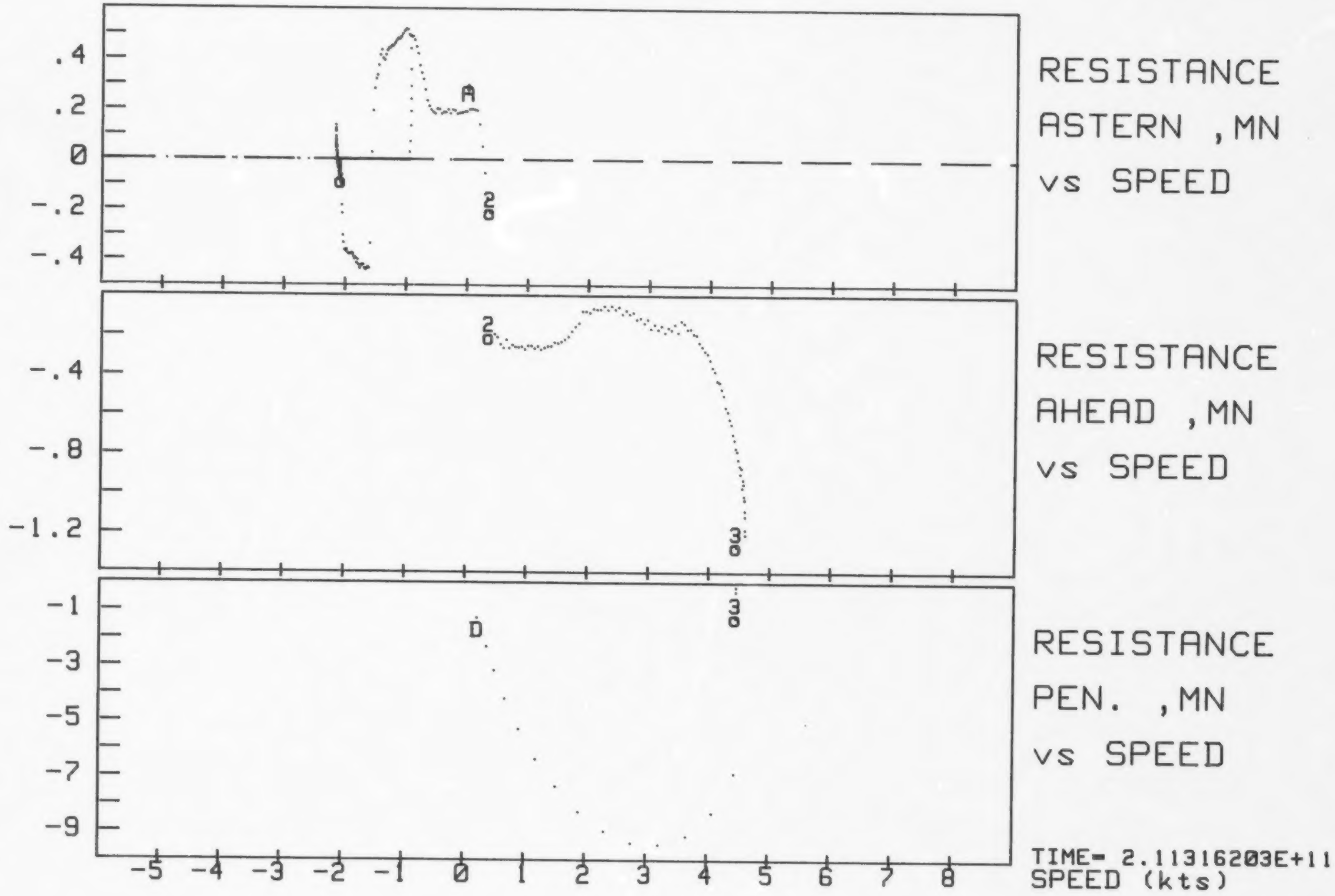

RESULTS OF RAMMING CYCLE ANALYSIS

RAM No. _A15

TAPE:	B1-T2-2.1	ICE CONDITIONS:	RIDGES
CATEGORY:	R1	ICE THICKNESS:	2.45 m
QUALITY:	67BD	FLEXURAL STRENGTH:	407 kPA
TRIM:	EVEN TRIM	BUBBLER STATUS:	ON

RAMMING CYCLE CHARACTERISTICS:

Speed of Advance	(knots)	.106	
Speed of Impact	(knots)	4.5	(4.37)

	Duration (sec)	% Cycle Time	Distance (m)
Backing	222	60.3	-127
Acceleration	96	26.1	127
Penetration	12	3.26	15.2 (20.16)
Extraction	38	10.3	
Total Cycle	368		

Duration of Astern Mode	(sec)	74
Duration of Reversal to Ahead	(sec)	134
Duration of Ahead Mode	(sec)	124
Duration of Reversal to Astern	(sec)	26
Start of Reversal after Impact	(sec)	14

Total Fuel Used	(mm*hr)	3.77	Est. kg:	-12.35
Average Fuel Rate	(mm)	36.9	Est. kg/hr:	-120.8

Backing Power	(kW)	4514.5
[Est Fuel Rate	(kg/hr)]	992.45
Acceleration Power	(kW)	9410.5
[Est Fuel Rate	(kg/hr)]	1968.7

RAM # _A15 TAPE: 81-T2-2.1 07 JUL 1981 04:15:12 **FIG. #1**

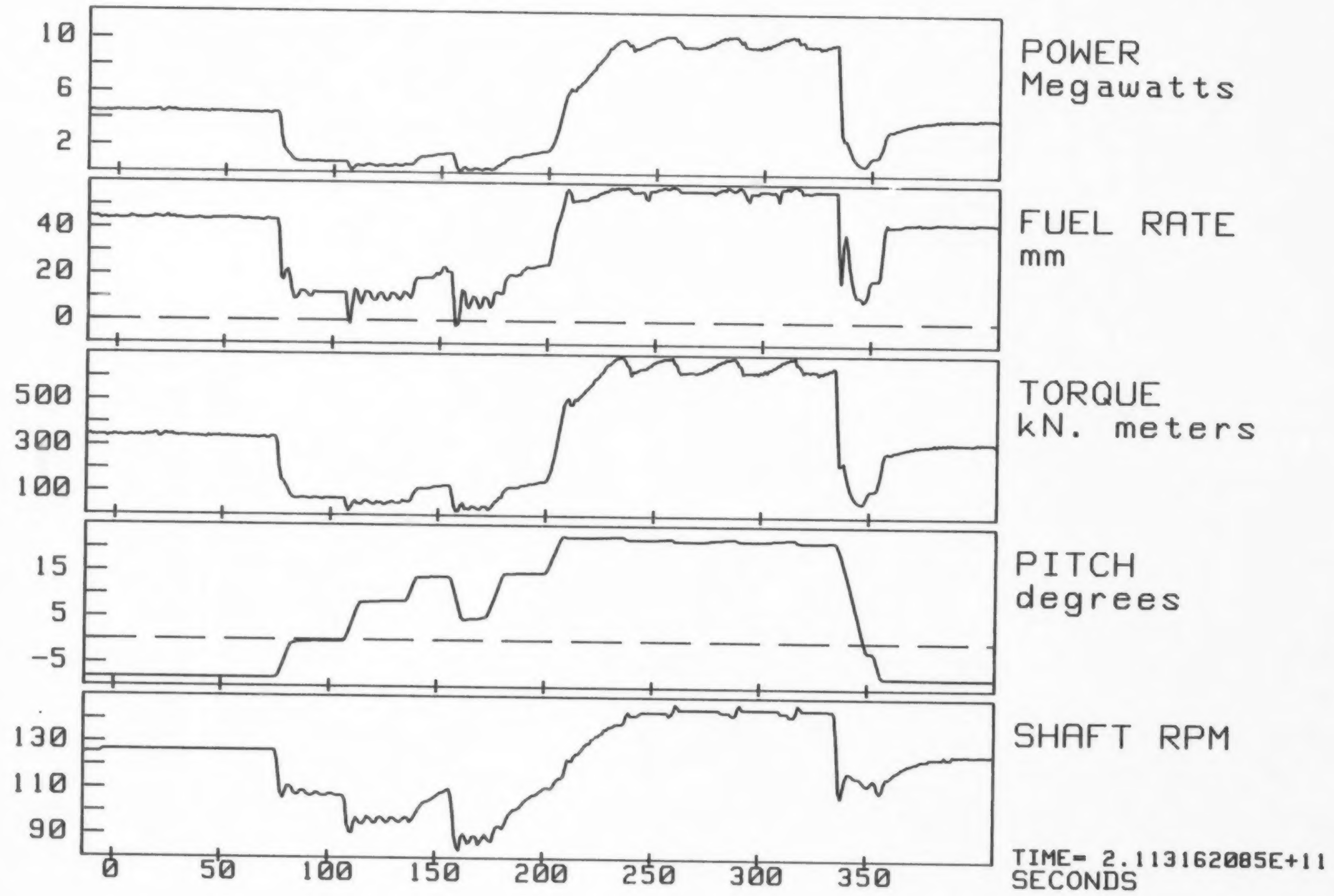

RAM # _A15 TAPE: 81-T2-2.1 07 JUL 1981 04:15:12

FIG. #2

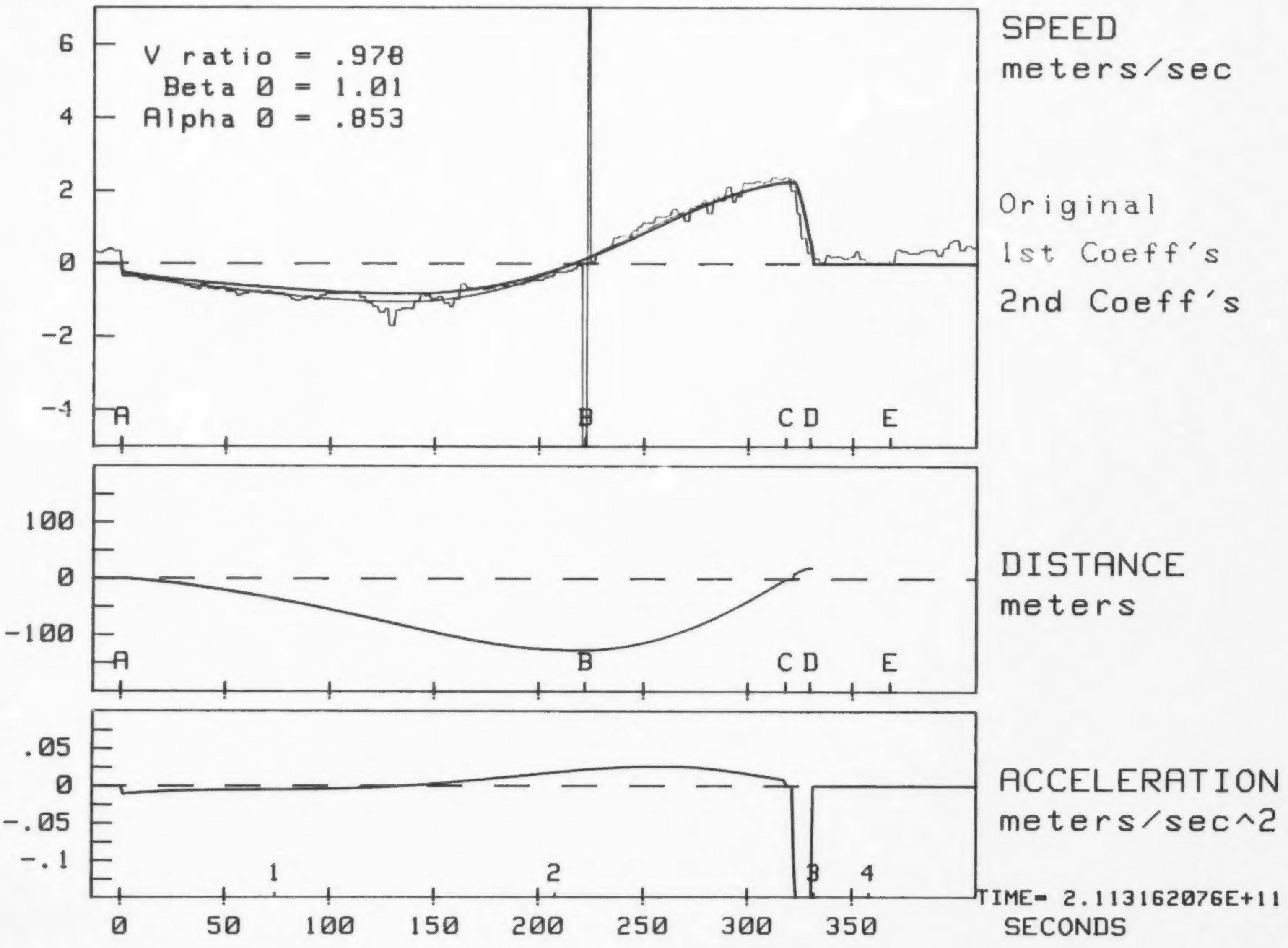

RAM # _A15 TAPE: 81-T2-2.1 07 JUL 1981 04:15:12

FIG. #3

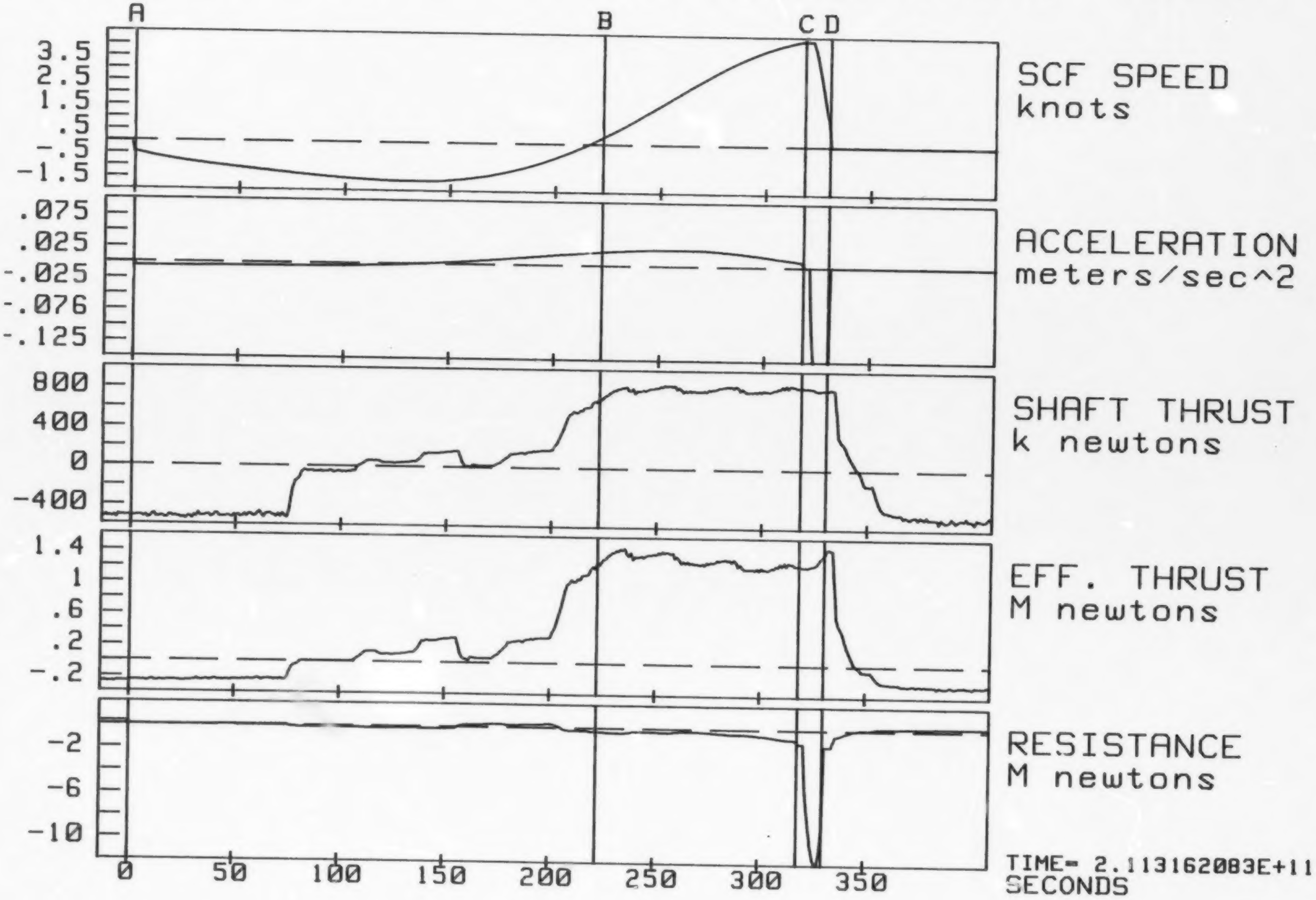

RAM # _A15 TAPE: 81-T2-2.1 07 JUL 1981 04:15:12 Fig.# 4

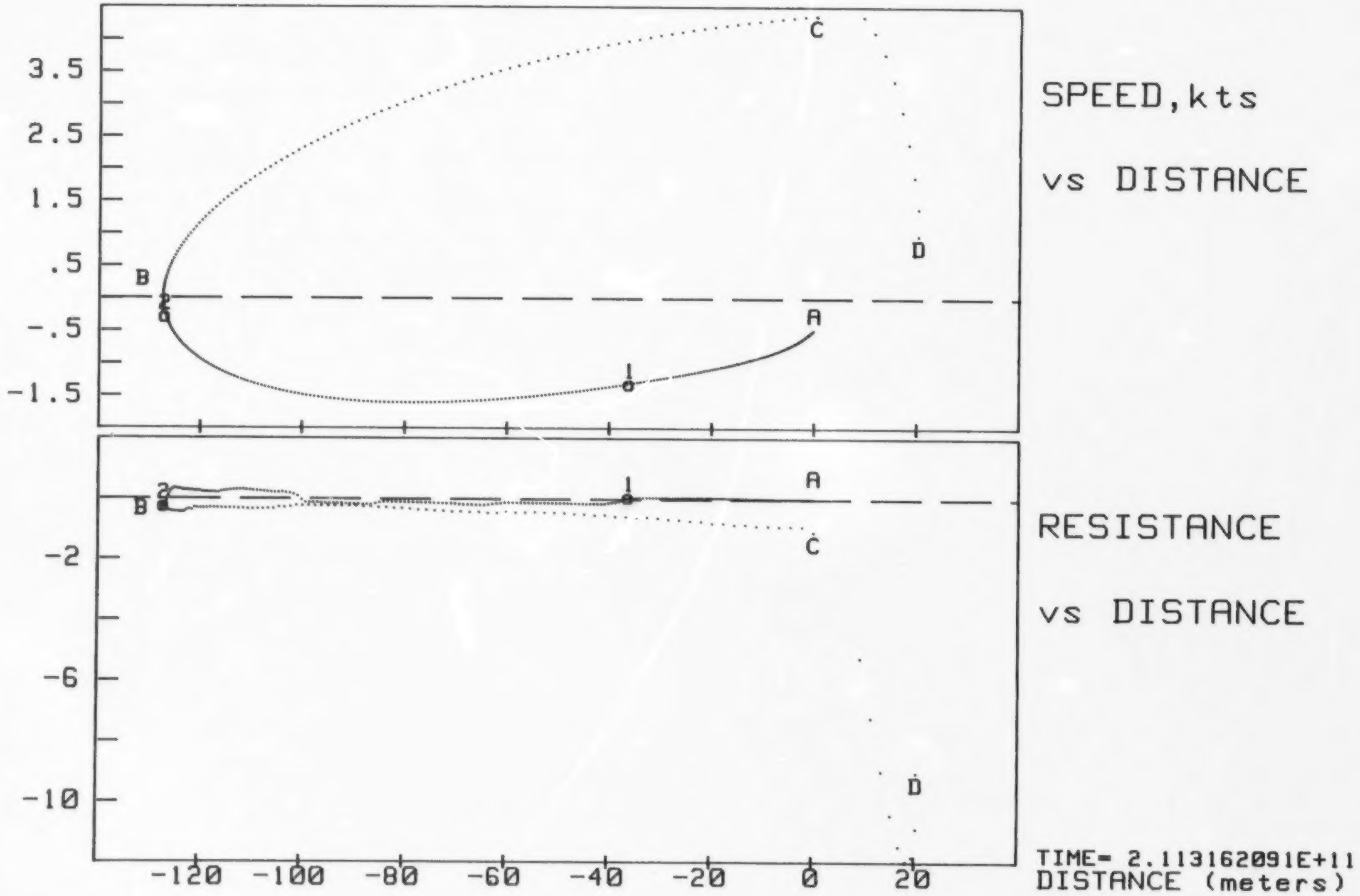

RAM # _A15 TAPE: 81-T2-2.1 07 JUL 1981 04:15:12 Fig.# 5

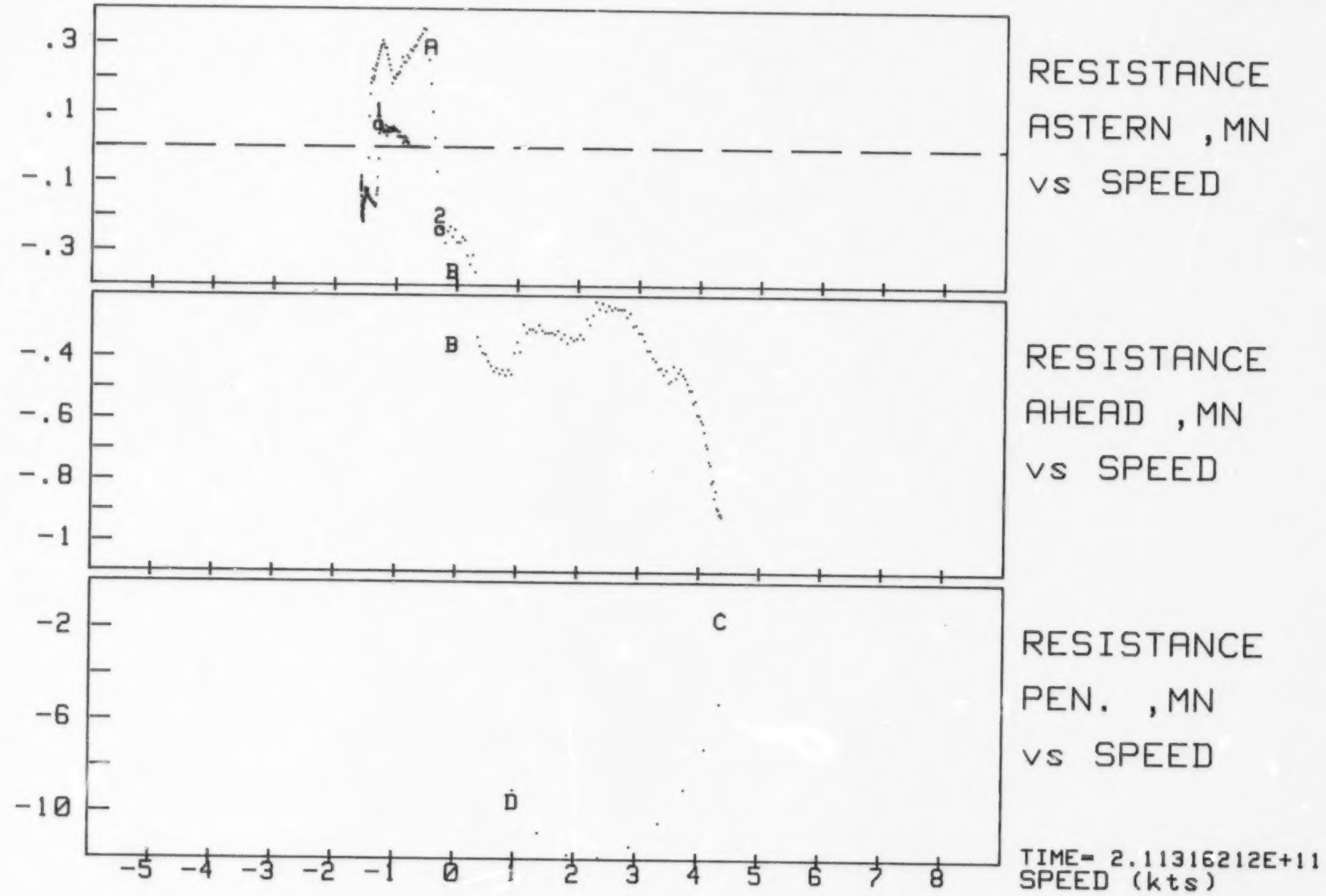

```
                RESULTS OF RAMMING CYCLE ANALYSIS


                         RAM No.  _A16

TAPE:        81-T2-2.1                 ICE CONDITIONS:     RIDGES

CATEGORY:    R1                        ICE THICKNESS:      2.4  m

QUALITY:     30BB                      FLEXURAL STRENGTH:  407  kPA

TRIM:        EVEN TRIM                 BUBBLER STATUS:    ON

RAMMING CYCLE CHARACTERISTICS:

Speed of Advance  (knots)     .0913

Speed of Impact   (knots)     4.5    ( 4.45 )


                              Duration (sec)   % Cycle Time   Distance  (m)
Backing                       256              47.8          -109.8
Acceleration                  89               16.6           109.8
Penetration                   38               7.09           21.1 (25.16)
Extraction                    153              28.5
Total Cycle                   536


Duration of Astern Mode        (sec)     173
Duration of Reversal to Ahead  (sec)     78
Duration of Ahead Mode         (sec)     97
Duration of Reversal to Astern (sec)     62
Start of Reversal after Impact (sec)     3

Total Fuel Used    (mm*hr)               6.3          Est. kg:     39.9
Average Fuel Rate (mm)                   42.3         Est. kg/hr:  268.01

Backing Power      (kW)                  4139.6
[Est Fuel Rate     (kg/hr)]              917.69

Acceleration Power(kW)                   9712
[Est Fuel Rate     (kg/hr)]              2028.8
```

RAM # _A16 TAPE: 81-T2-2.1 07 JUL 1981 04:22:12

FIG. #1

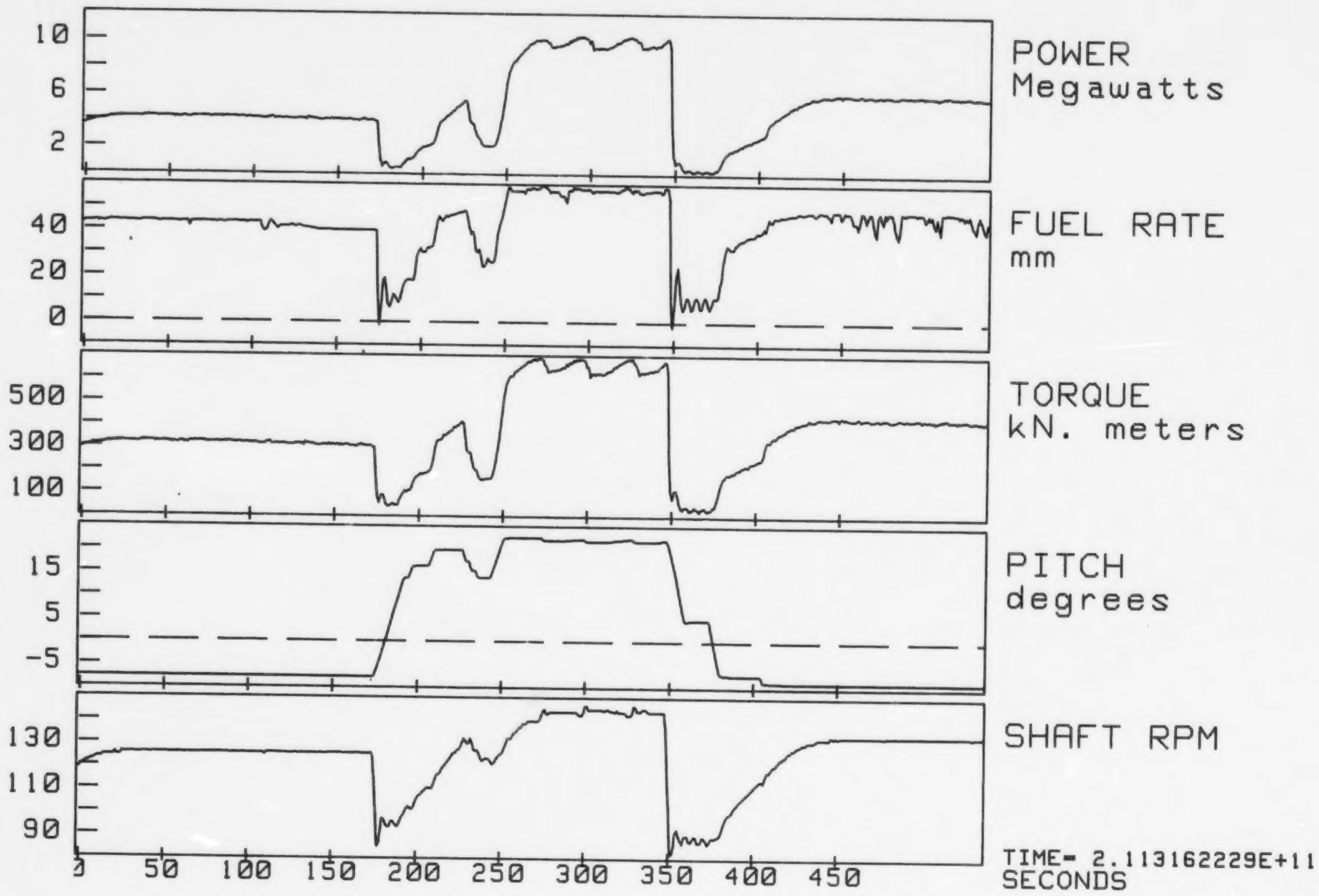

RAM # _A16 TAPE: 81-T2-2.1 07 JUL 1981 04:22:12 **FIG. #2**

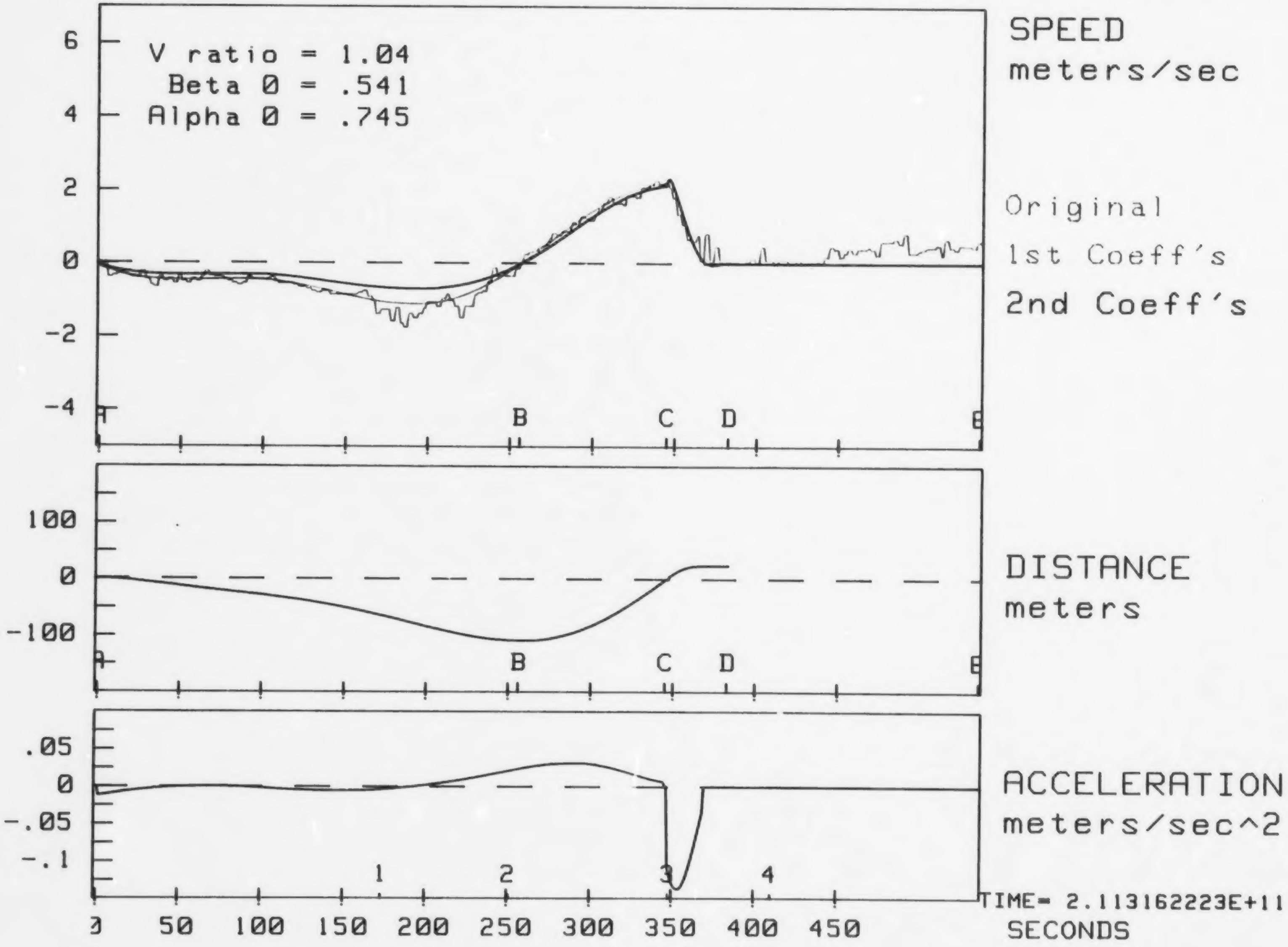

RAM # _A16 TAPE: 81-T2-2.1 07 JUL 1981 04:22:12

FIG. #3

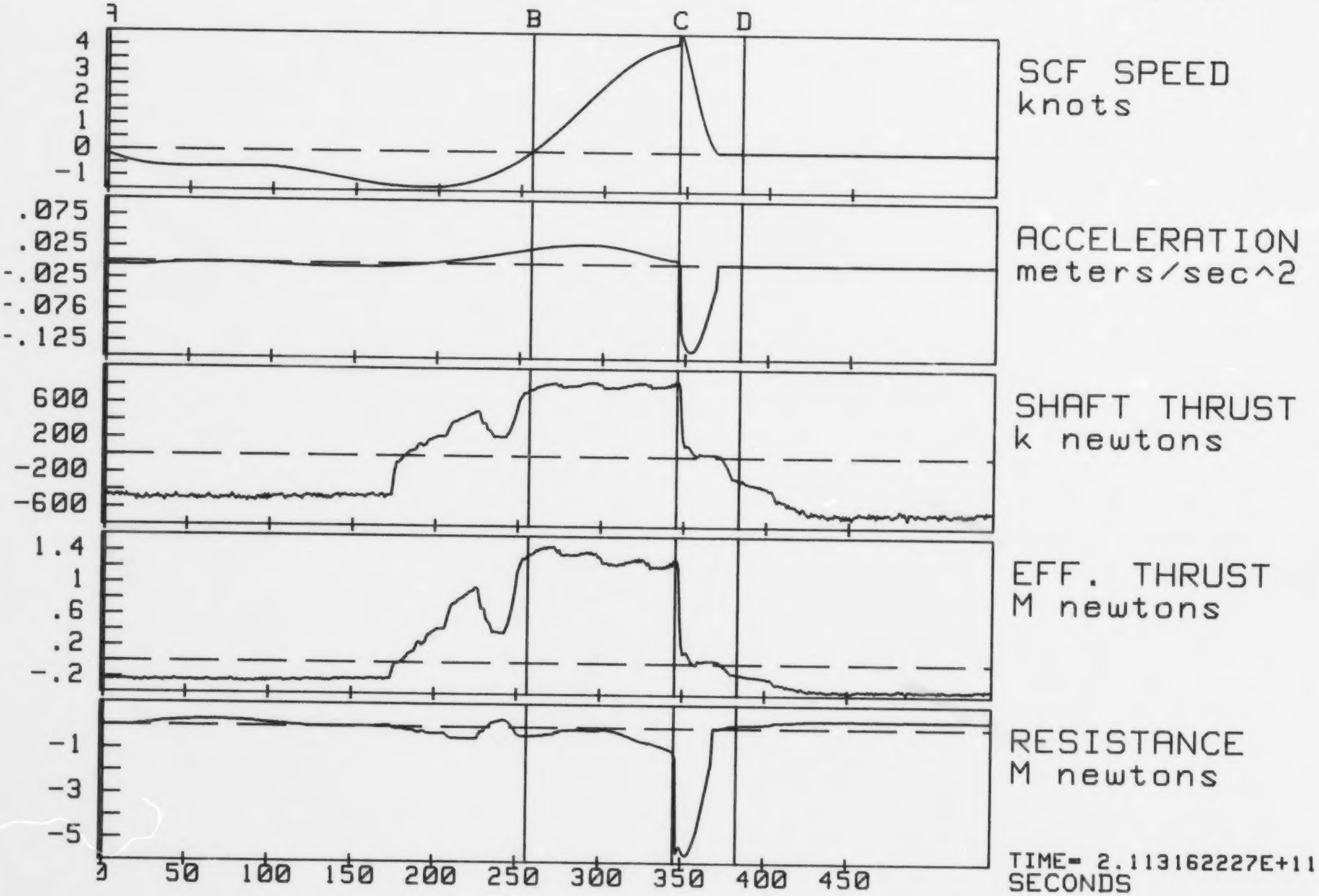

RAM # _A16 TAPE: 81-T2-2.1 07 JUL 1981 04:22:12 Fig.# 4

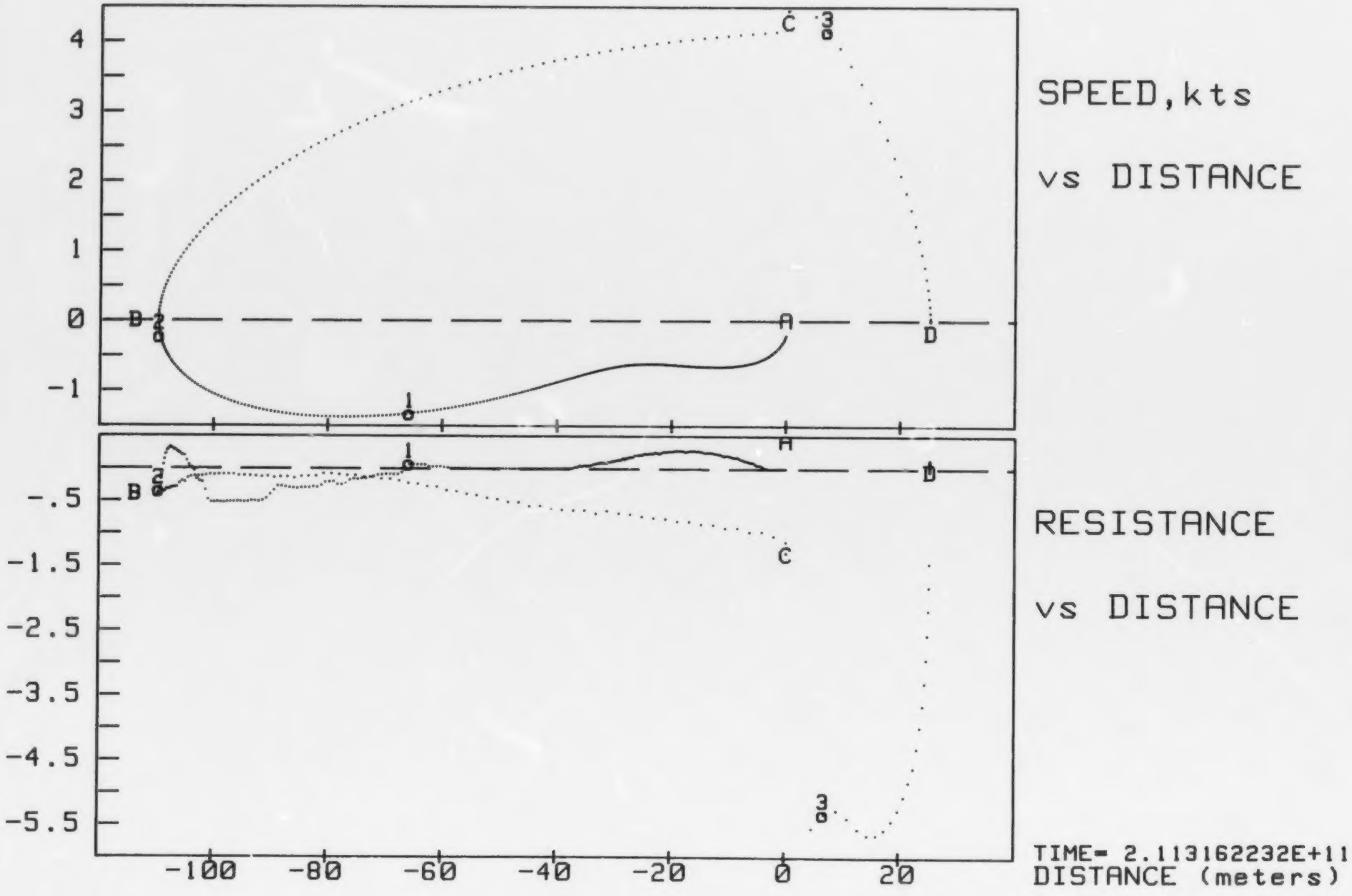

RAM # _A16 TAPE: 81-T2-2.1 07 JUL 1981 04:22:12 Fig.# 5

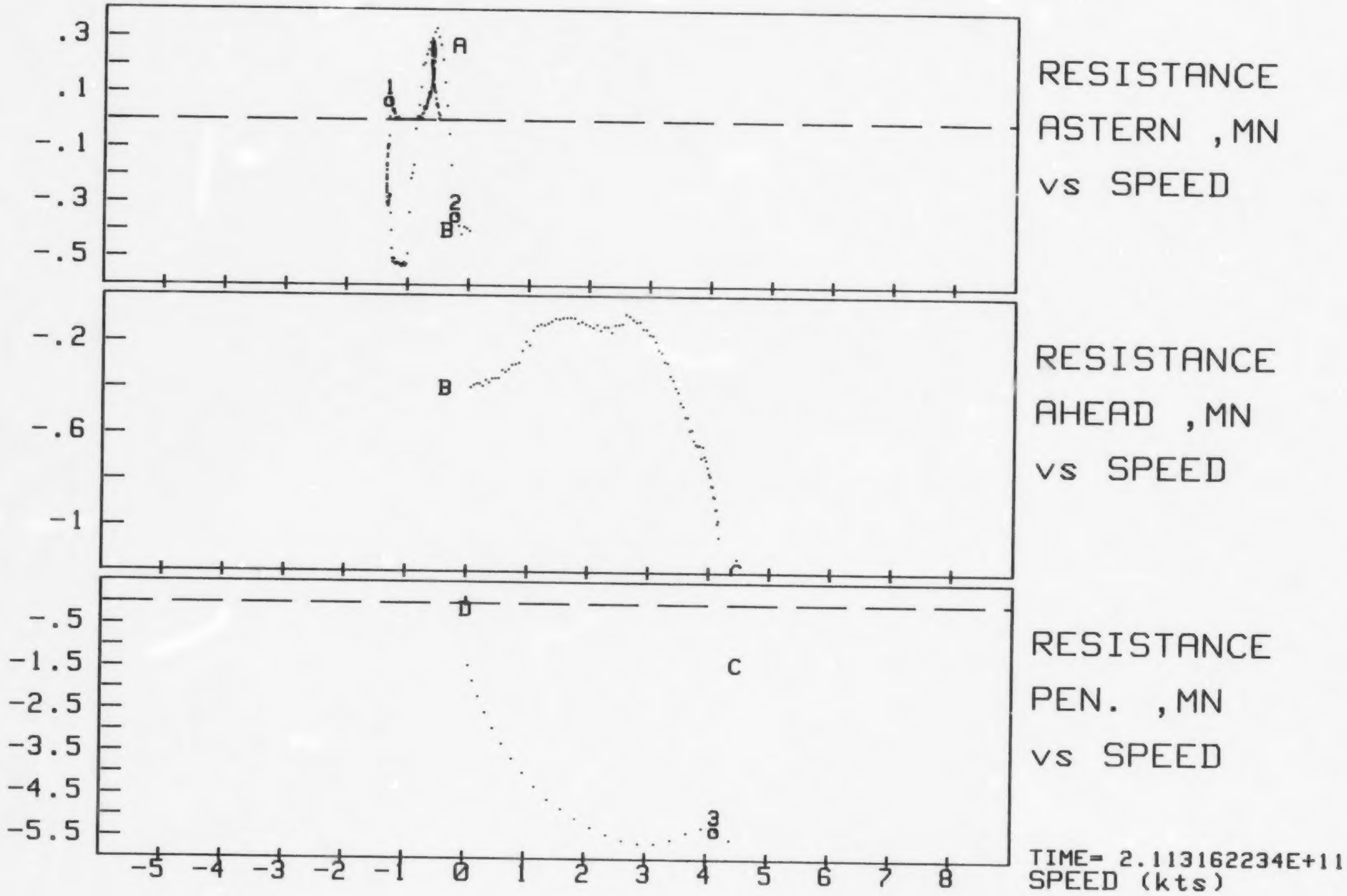

RESULTS OF RAMMING CYCLE ANALYSIS

RAM No. _A17

TAPE:	81-T2-2.1	ICE CONDITIONS:	RIDGES
CATEGORY:	R1	ICE THICKNESS:	2.11 m
QUALITY:	72BD	FLEXURAL STRENGTH:	407 kPA
TRIM:	EVEN TRIM	BUBBLER STATUS:	ON

RAMMING CYCLE CHARACTERISTICS:

Speed of Advance (knots) .147

Speed of Impact (knots) 4.5 (4.33)

	Duration (sec)	% Cycle Time	Distance (m)
Backing	239	52.8	-105.5
Acceleration	80	17.7	105.5
Penetration	36	7.95	27.3 (34.36)
Extraction	98	21.6	
Total Cycle	453		

Duration of Astern Mode	(sec)	137
Duration of Reversal to Ahead	(sec)	93
Duration of Ahead Mode	(sec)	122
Duration of Reversal to Astern	(sec)	95
Start of Reversal after Impact	(sec)	33

Total Fuel Used	(mm*hr)	5.22	Est. kg:	26.11
Average Fuel Rate	(mm)	41.46	Est. kg/hr:	207.5

Backing Power	(kW)	5902.8
[Est Fuel Rate	(kg/hr)]	1269.3
Acceleration Power	(kW)	9881.8
[Est Fuel Rate	(kg/hr)]	2062.7

RAM # _A17   TAPE: 81-T2-2.1 07 JUL 1981 04:28:42   **FIG. #1**

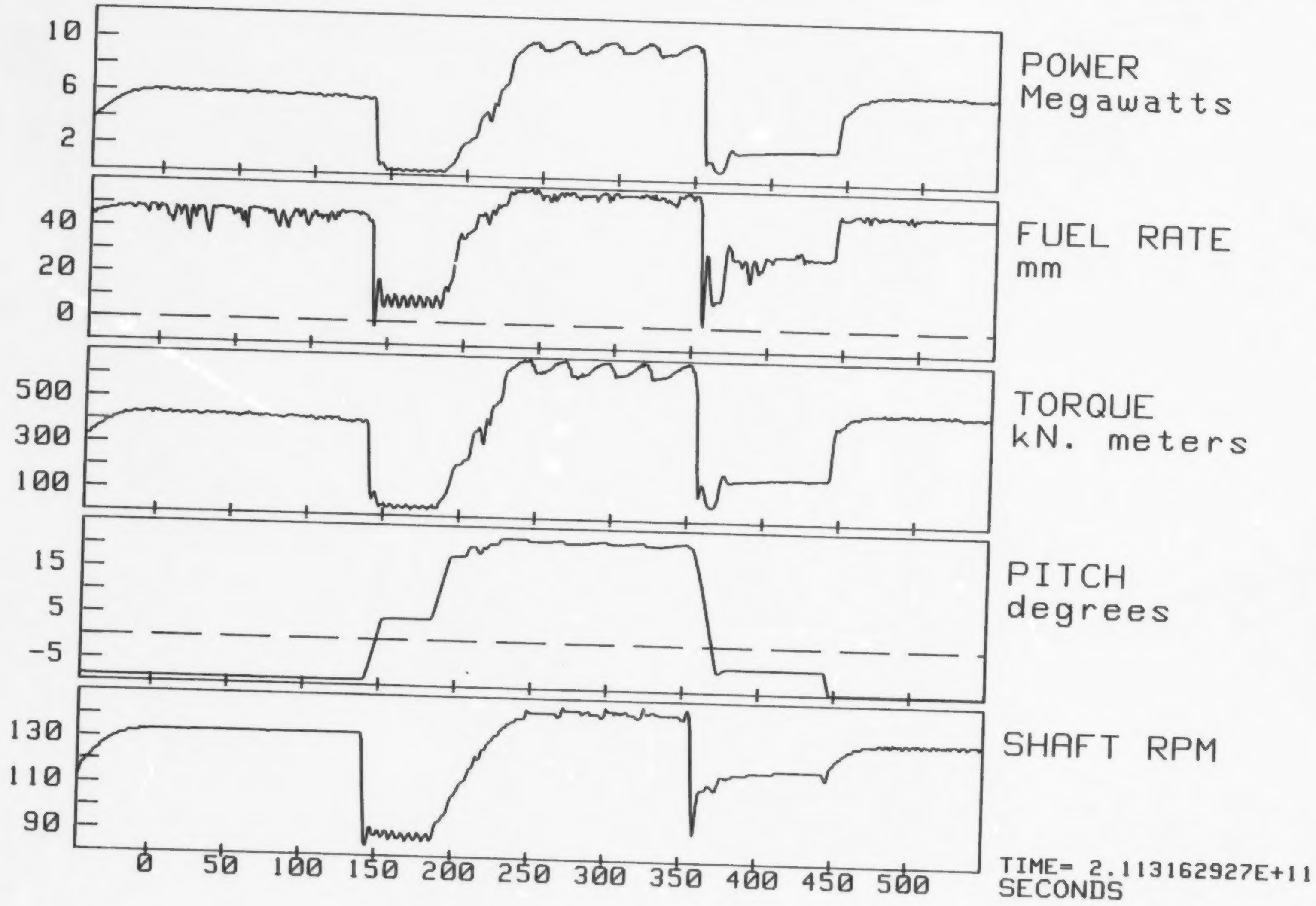

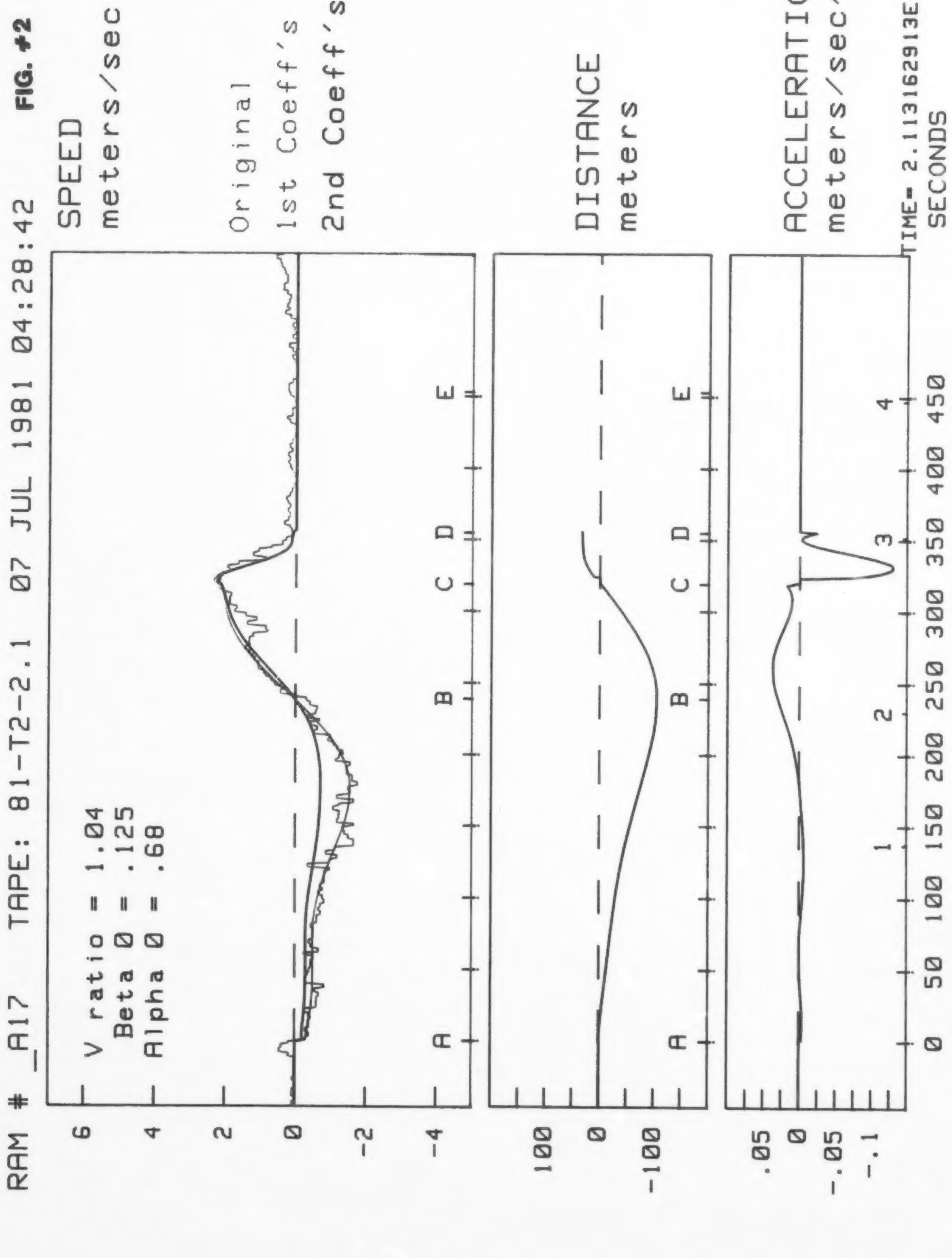
RAM # _A17 TAPE: 81-T2-2.1 07 JUL 1981 04:28:42
SPEED
meters/sec
Original
1st Coeff's
2nd Coeff's
V ratio = 1.04
Beta 0 = .125
Alpha 0 = .68
6
4
2
0
-2
-4
A
B
C
D
E
DISTANCE
meters
100
0
-100
ACCELERATION
meters/sec^2
.05
0
-.05
-.1
0
50
100
150
200
250
300
350
400
450
1
2
3
4
TIME= 2.11316291 3E+11
SECONDS

FIG. #2

RAM # _A17 TAPE: 81-T2-2.1 07 JUL 1981 04:28:42

FIG. #3

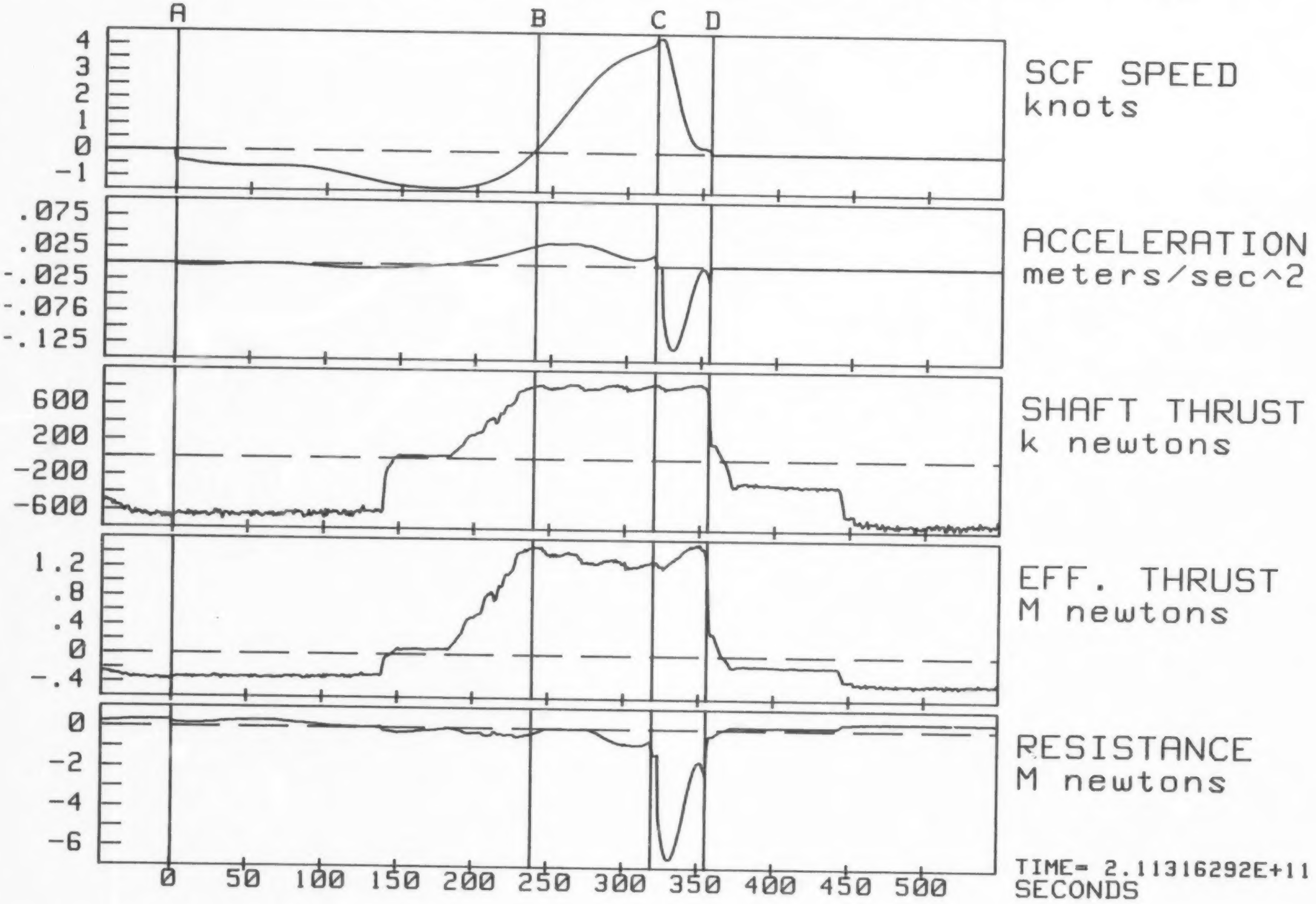

RAM # _A17   TAPE: 81-T2-2.1   07 JUL 1981 04:28:42   Fig.# 4

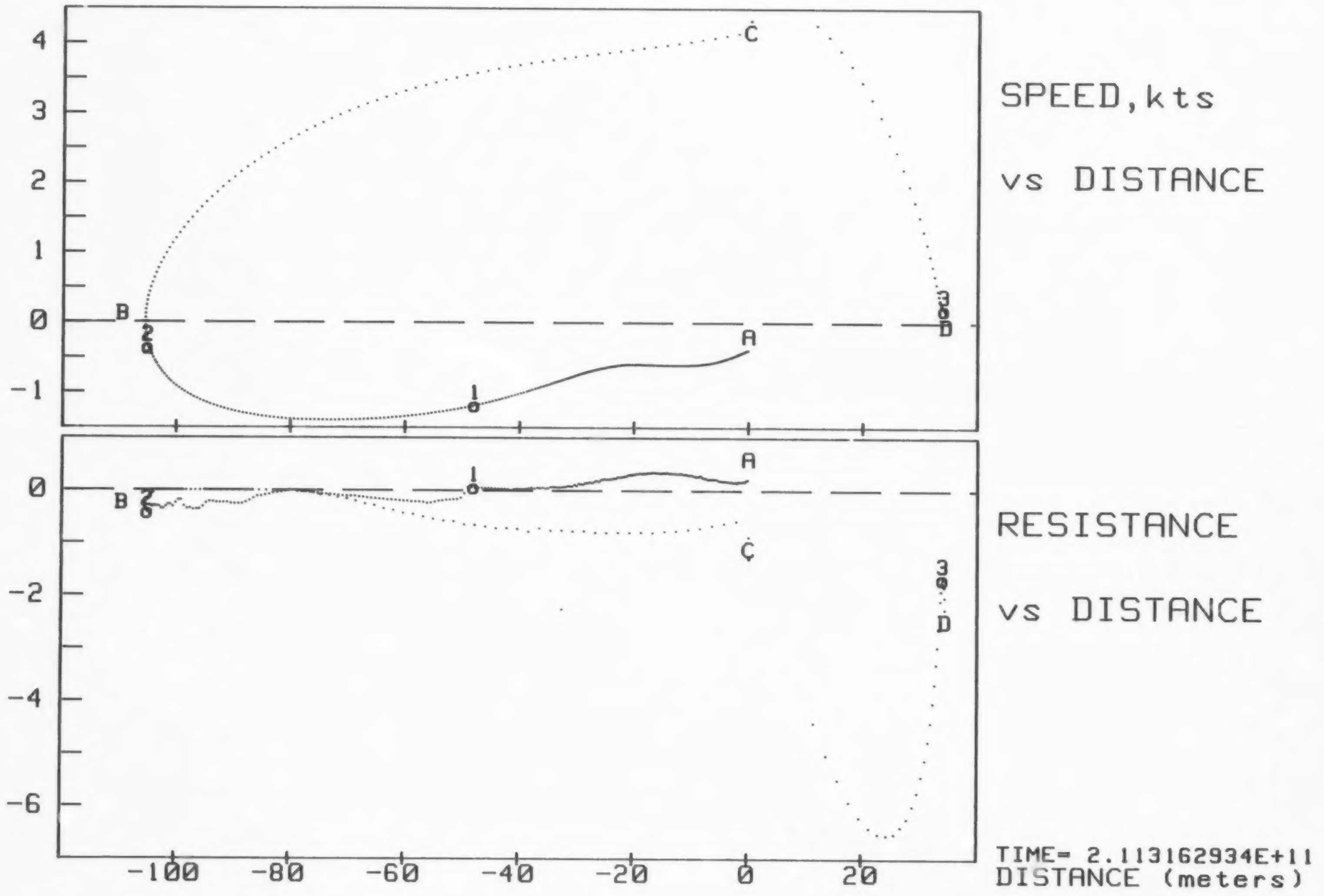

RAM # _A17 TAPE: 81-T2-2.1 07 JUL 1981 04:28:42 Fig.# 5

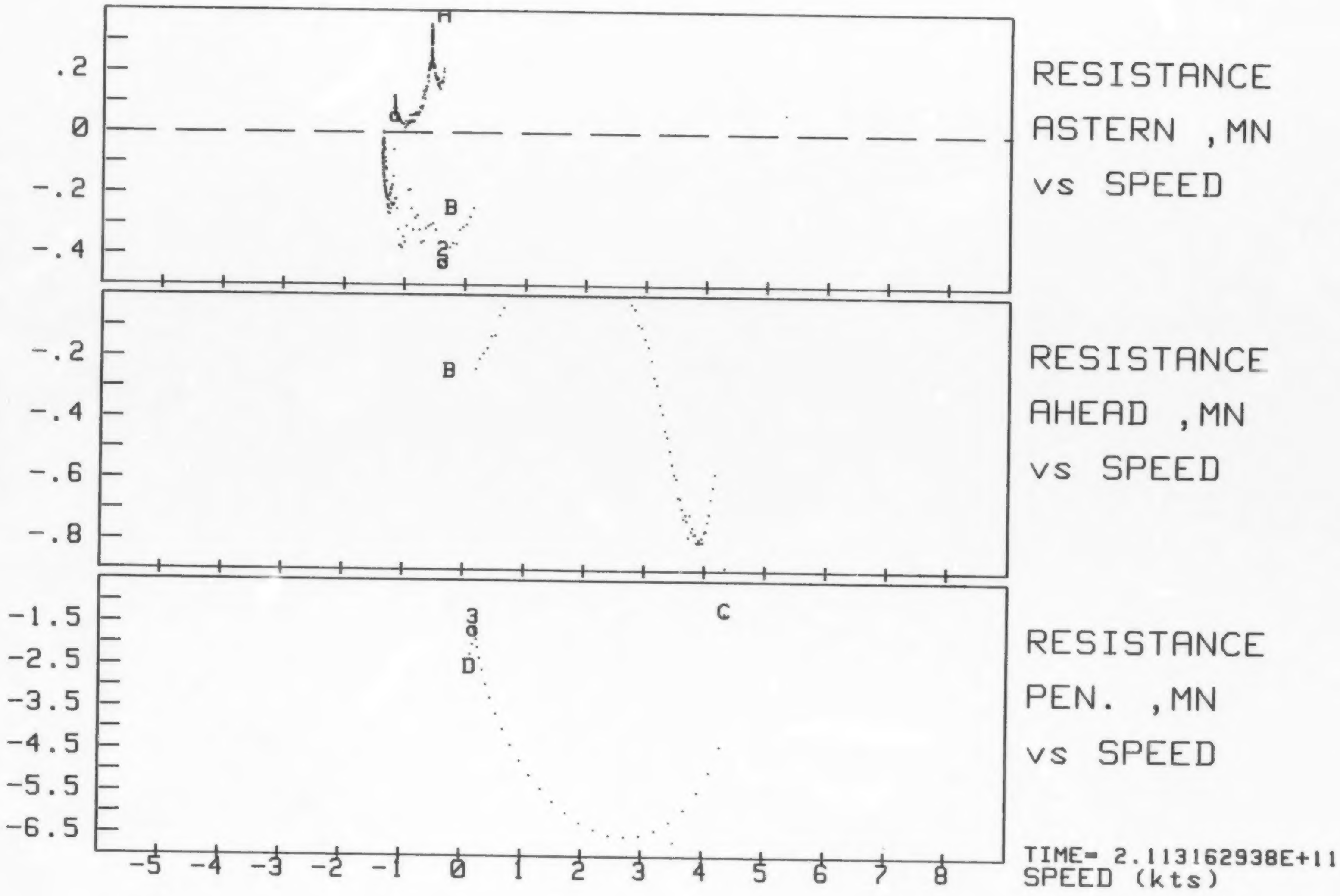

RESULTS OF RAMMING CYCLE ANALYSIS

```
                         RAM No.  _A18

TAPE:       81-T2-2.1                 ICE CONDITIONS:      RIDGES

CATEGORY:   R1                        ICE THICKNESS:       .0182  m

QUALITY:    65AD                      FLEXURAL STRENGTH:   407   kPA

TRIM:       EVEN TRIM                 BUBBLER STATUS:    ON

RAMMING CYCLE CHARACTERISTICS:

Speed of Advance   (knots)     .107

Speed of Impact    (knots)     4.5     ( 4.3 )


                               Duration (sec)    % Cycle Time   Distance  (m)
Backing                        334               58.8           -117.8
Acceleration                   97                17.1            117.8
Penetration                    83                14.6            27.3 (31.32)
Extraction                     54                9.51
Total Cycle                    568


Duration of Astern Mode        (sec)     0
Duration of Reversal to Ahead  (sec)     331
Duration of Ahead Mode         (sec)     97
Duration of Reversal to Astern (sec)     136
Start of Reversal after Impact (sec)    -3

Total Fuel Used    (mm*hr)               5.12          Est. kg:     -69.77
Average Fuel Rate (mm)                   32.45         Est. kg/hr: -442.19

Backing Power      (kW)                  5855.3
[Est Fuel Rate     (kg/hr)]              1259.8

Acceleration Power(kW)                   3226.1
[Est Fuel Rate     (kg/hr)]              735.53
```

RAM # _A18 TAPE: 81-T2-2.1 07 JUL 1981 04:36:12

FIG. #1

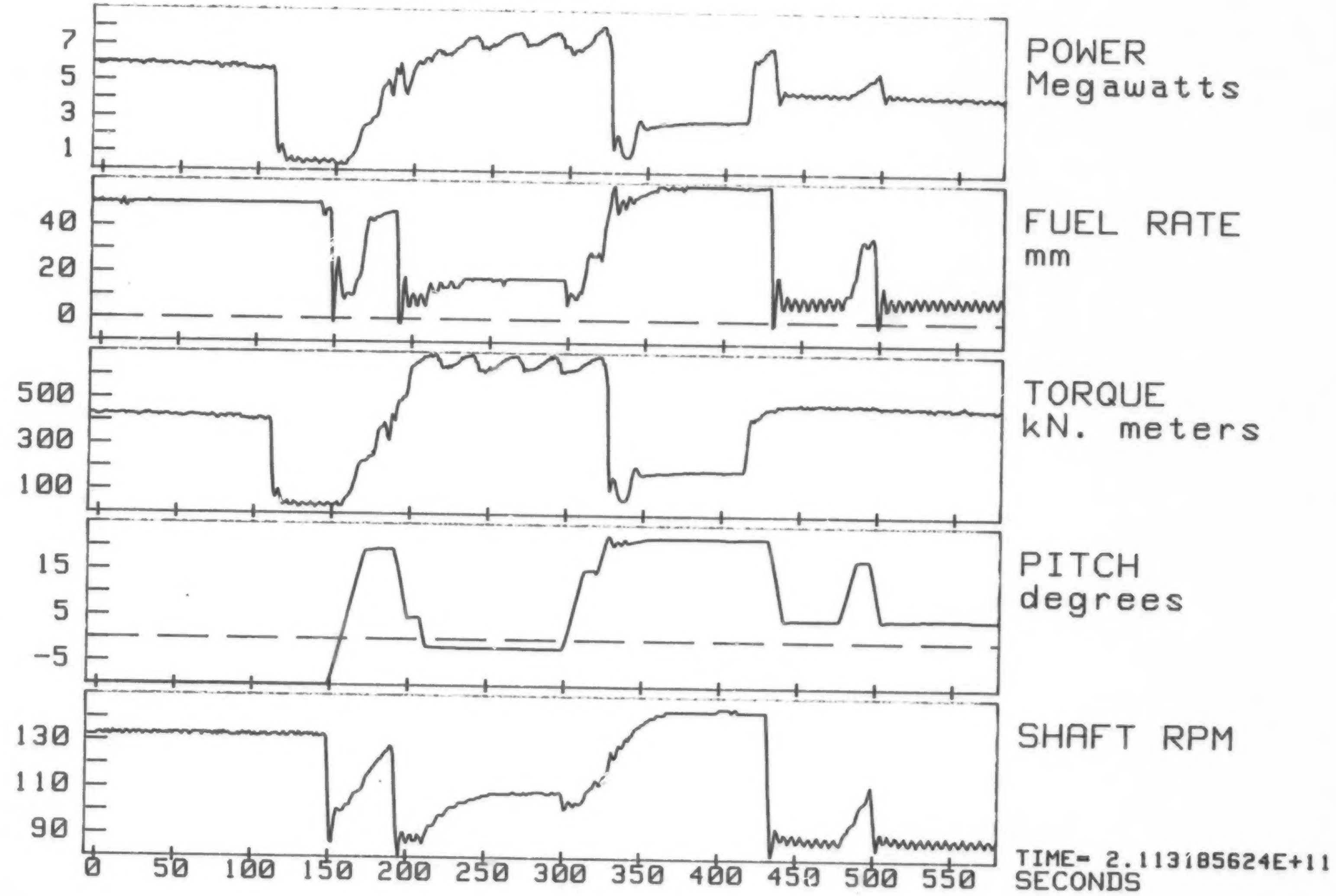

RAM # _A18 TAPE: 81-T2-2.1 07 JUL 1981 04:36:12

FIG. #2

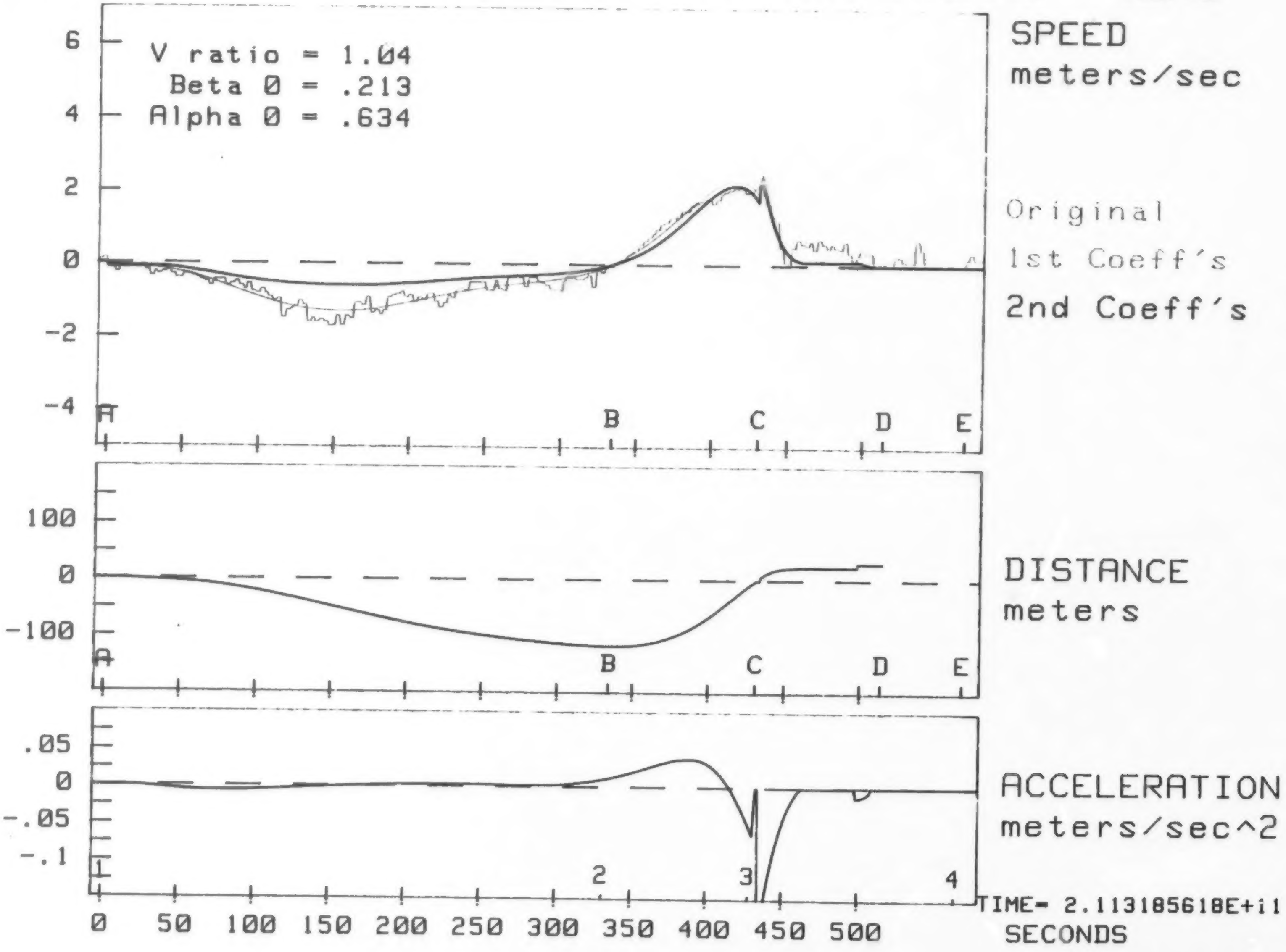

RAM # _A18 TAPE: 81-T2-2.1 07 JUL 1981 04:36:12

FIG. #3

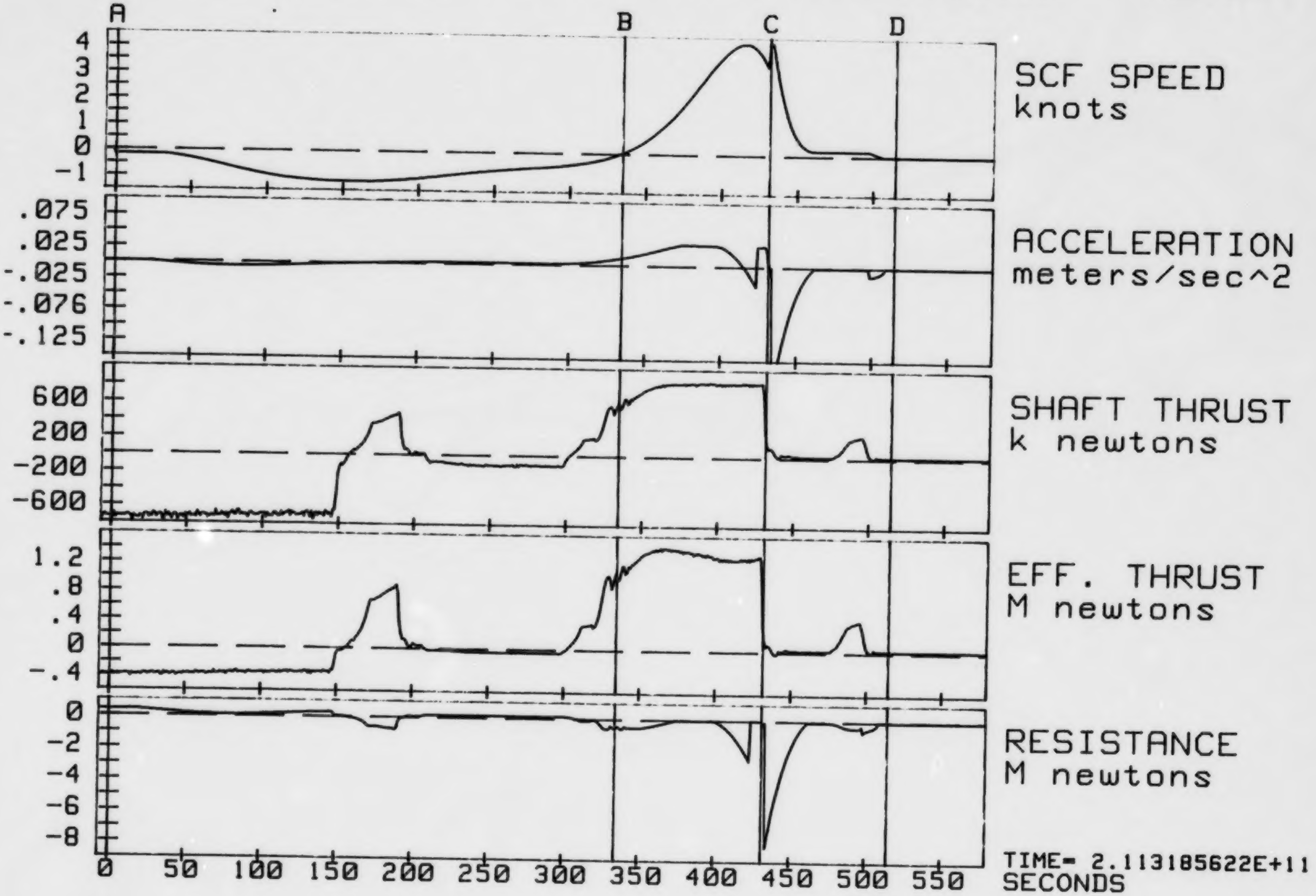

RAM # _A18   TAPE: 81-T2-2.1   07 JUL 1981 04:36:12   Fig.# 4

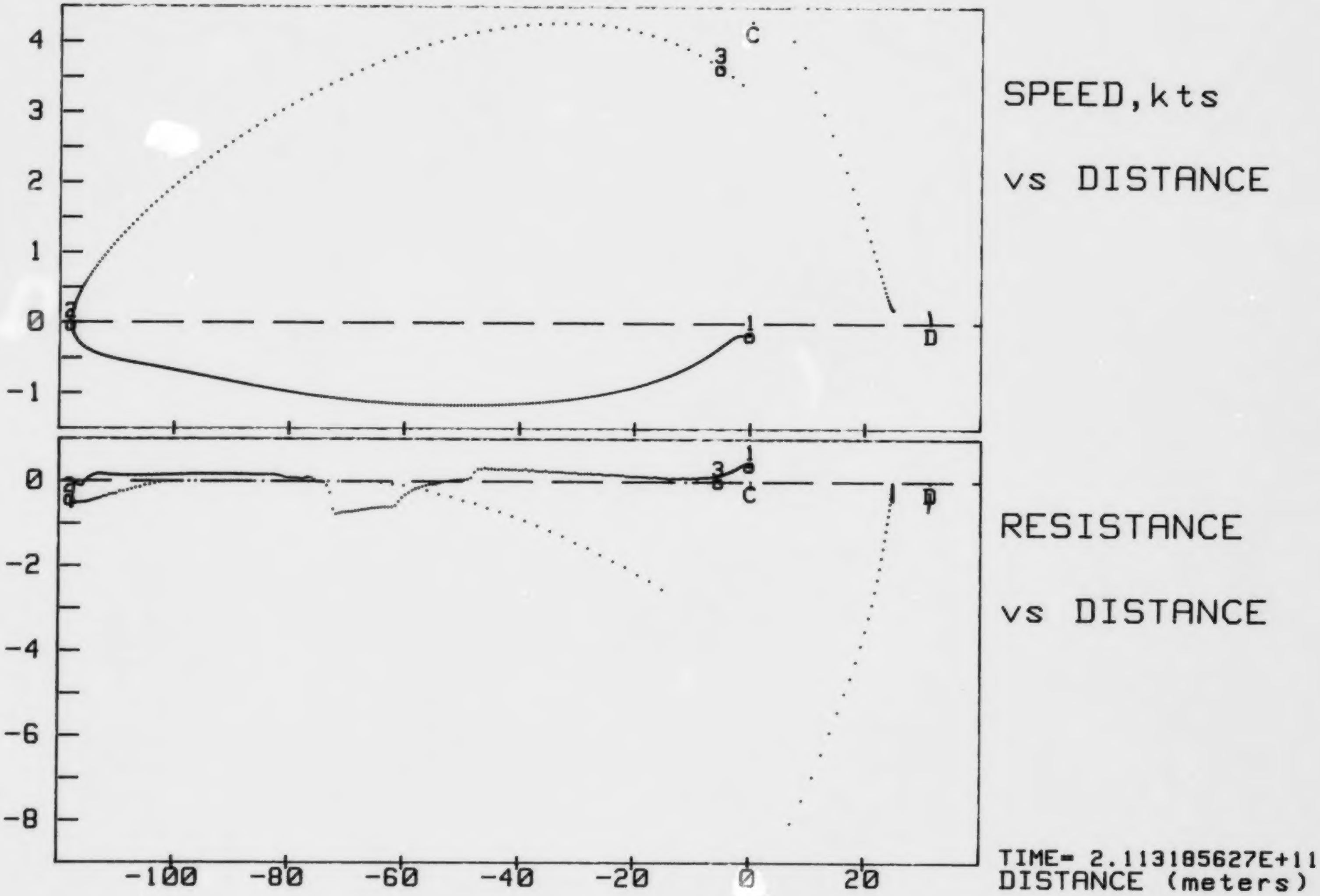

RAM # _A18 TAPE: 81-T2-2.1 07 JUL 1981 04:36:12 Fig.# 5

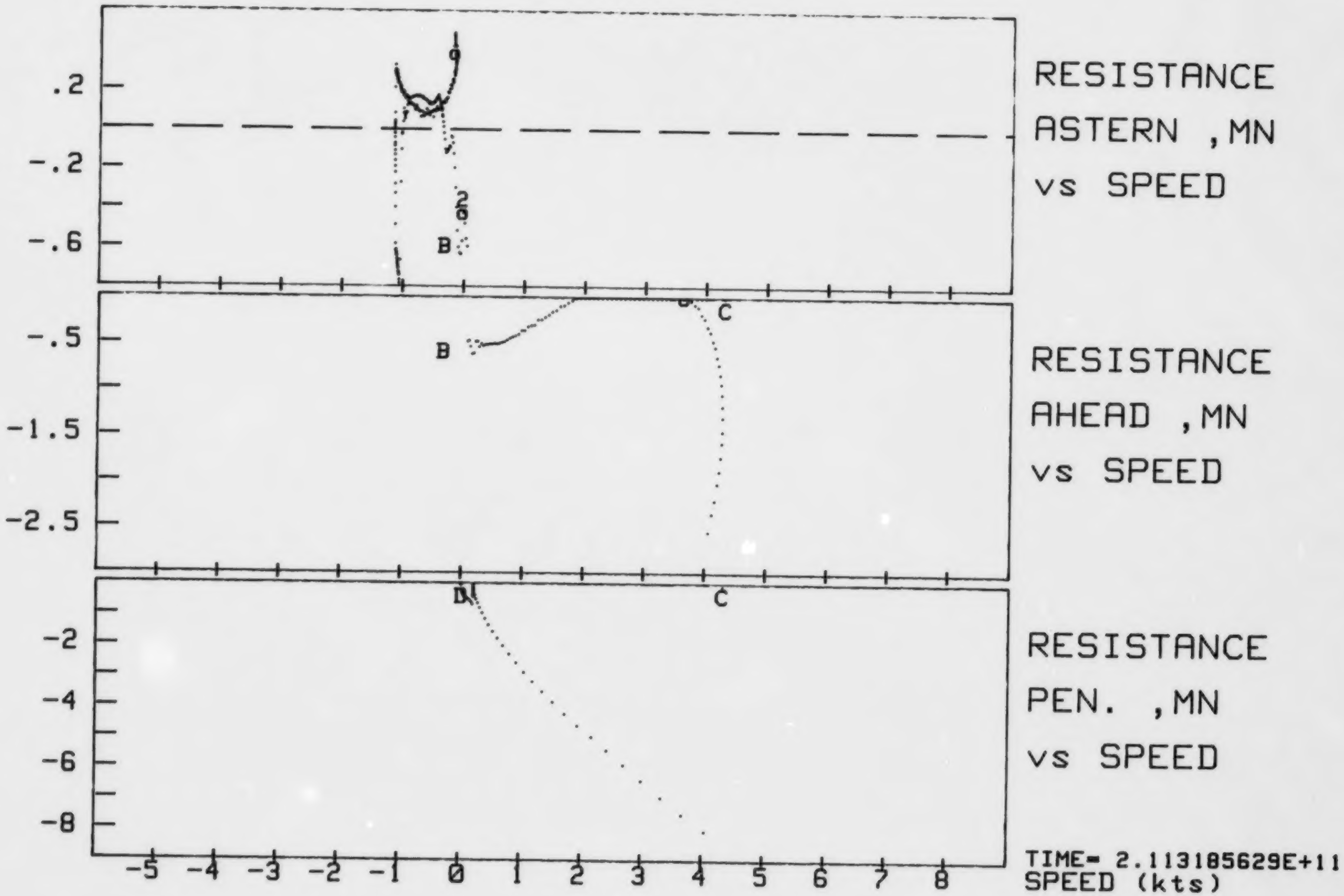

ADMIRALTY INLET TRIALS, 1981

SERIES B

RESULTS OF RAMMING CYCLE ANALYSIS

RAM No. __81

TAPE:	81-T2-3.1	ICE CONDITIONS:	LEVEL ICE
CATEGORY:	L1	ICE THICKNESS:	1.51 m
QUALITY:	26AB	FLEXURAL STRENGTH:	163 kPA
TRIM:	EVEN TRIM	BUBBLER STATUS:	ON

RAMMING CYCLE CHARACTERISTICS:

Speed of Advance (knots) .601

Speed of Impact (knots) 5 (4.95)

	Duration (sec)	% Cycle Time	Distance (m)
Backing	269	44.5	-138.8
Acceleration	101	16.7	138.8
Penetration	218	36.1	178.8 (186.6)
Extraction	16	2.65	
Total Cycle	604		

Duration of Astern Mode	(sec)	146
Duration of Reversal to Ahead	(sec)	63
Duration of Ahead Mode	(sec)	357
Duration of Reversal to Astern	(sec)	19
Start of Reversal after Impact	(sec)	196

Total Fuel Used	(mm*hr)	7.76	Est. kg:	93.11
Average Fuel Rate	(mm)	46.28	Est. kg/hr:	554.97

Backing Power	(kW)	-2504.7
[Est Fuel Rate	(kg/hr)]	-407.2
Acceleration Power	(kW)	-2498.6
[Est Fuel Rate	(kg/hr)]	-405.96

RAM # __B1 TAPE: 81-T2-3.1 07 JUL 1981 13:58:52 **FIG. #1**

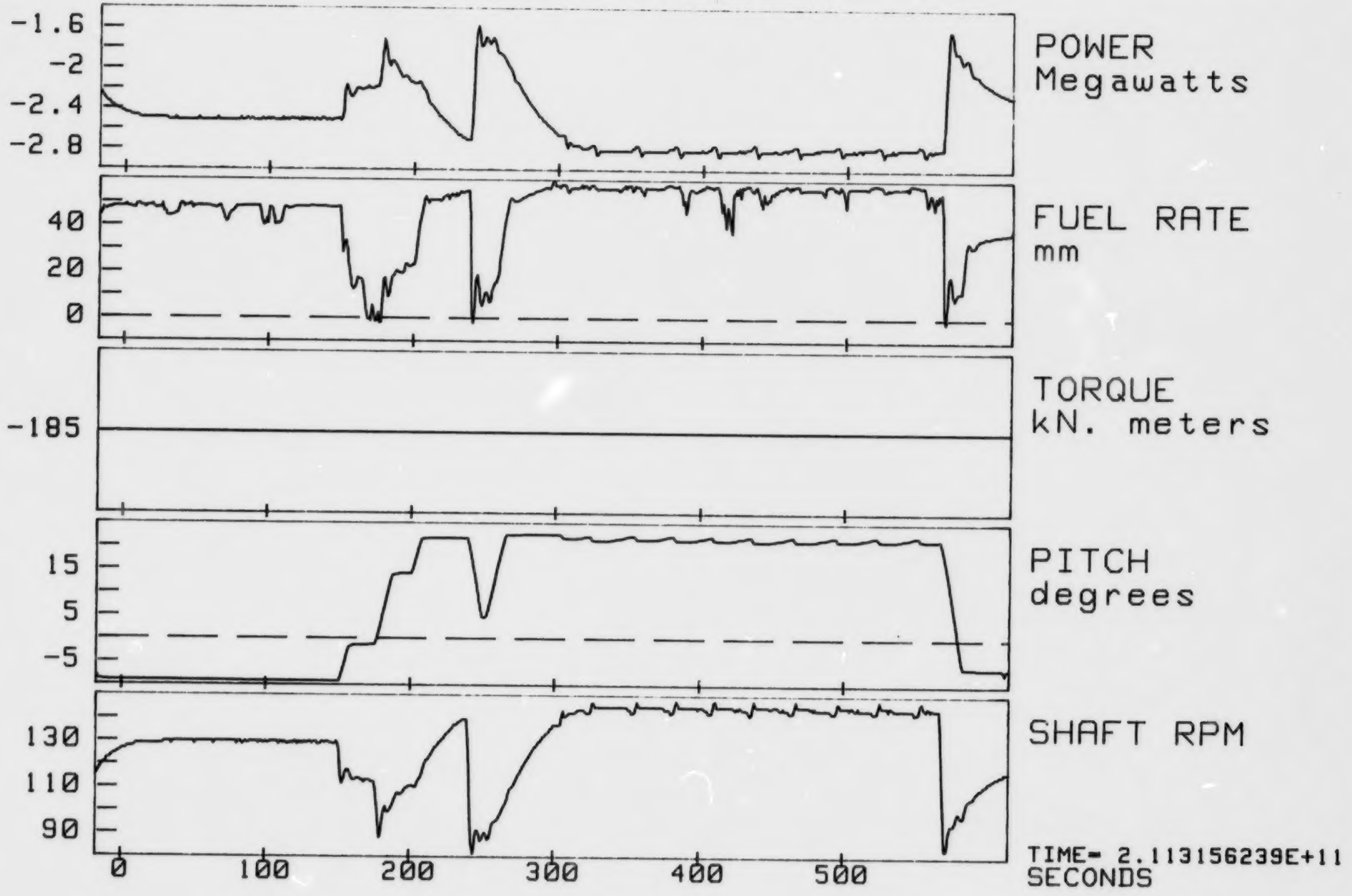

FIG. #2

RAM # __B1 TAPE: 81-T2-3.1 07 JUL 1981 13:58:52

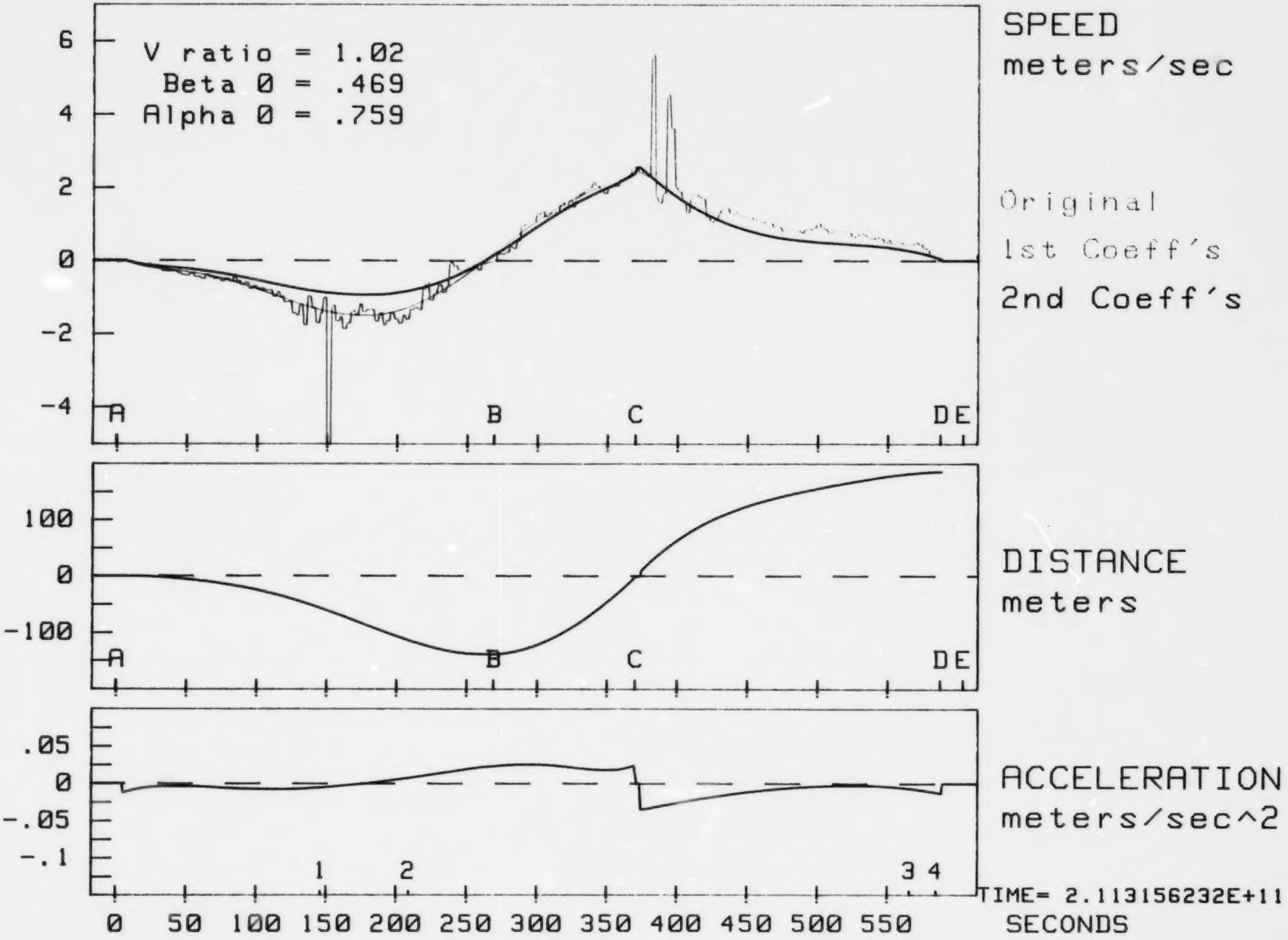

RAM # B1 TAPE: 81-T2-3.1 07 JUL 1981 13:58:52

FIG. #3

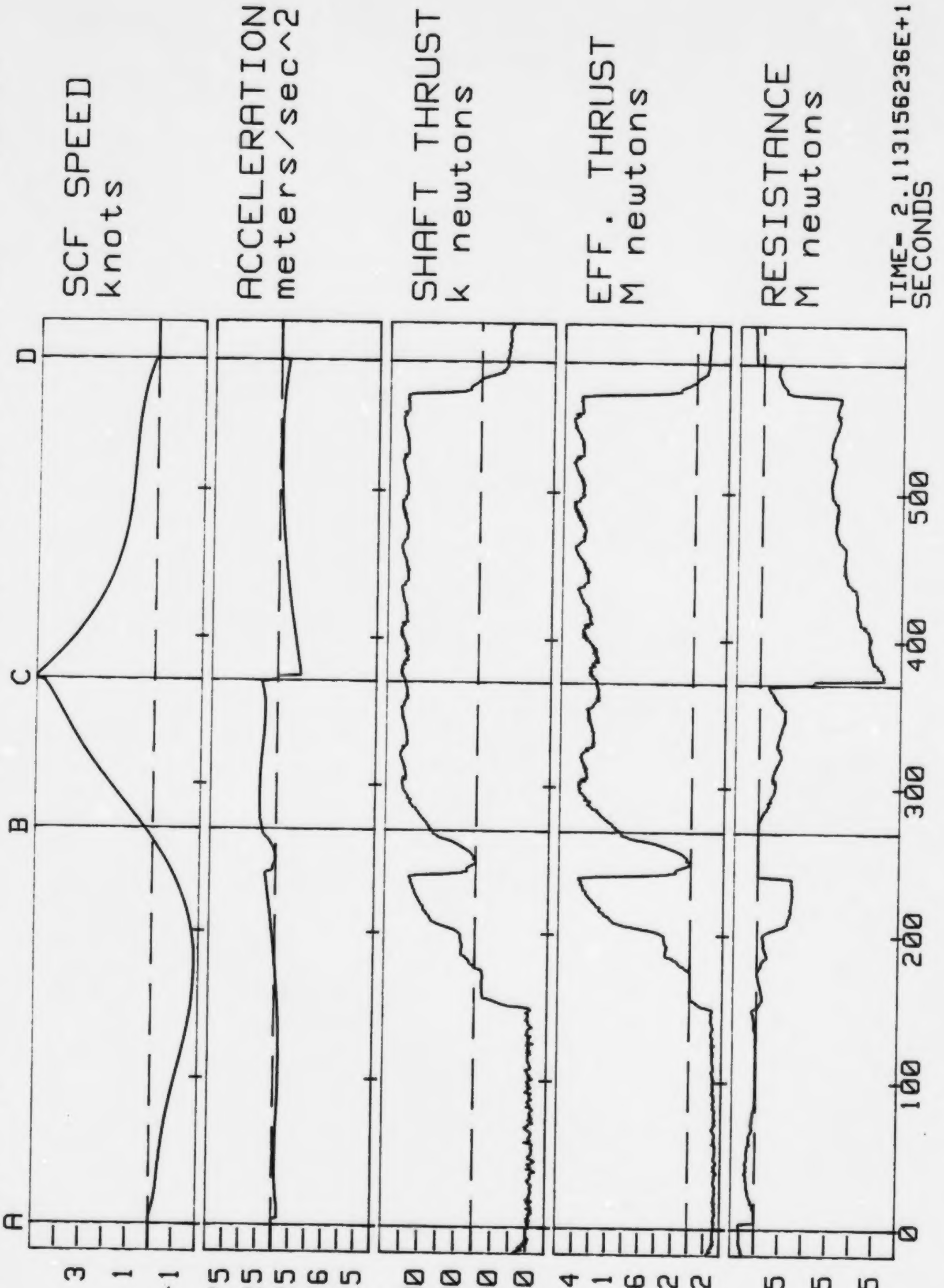

RAM # __B1 TAPE: 81-T2-3.1 07 JUL 1981 13:58:52 Fig.# 4

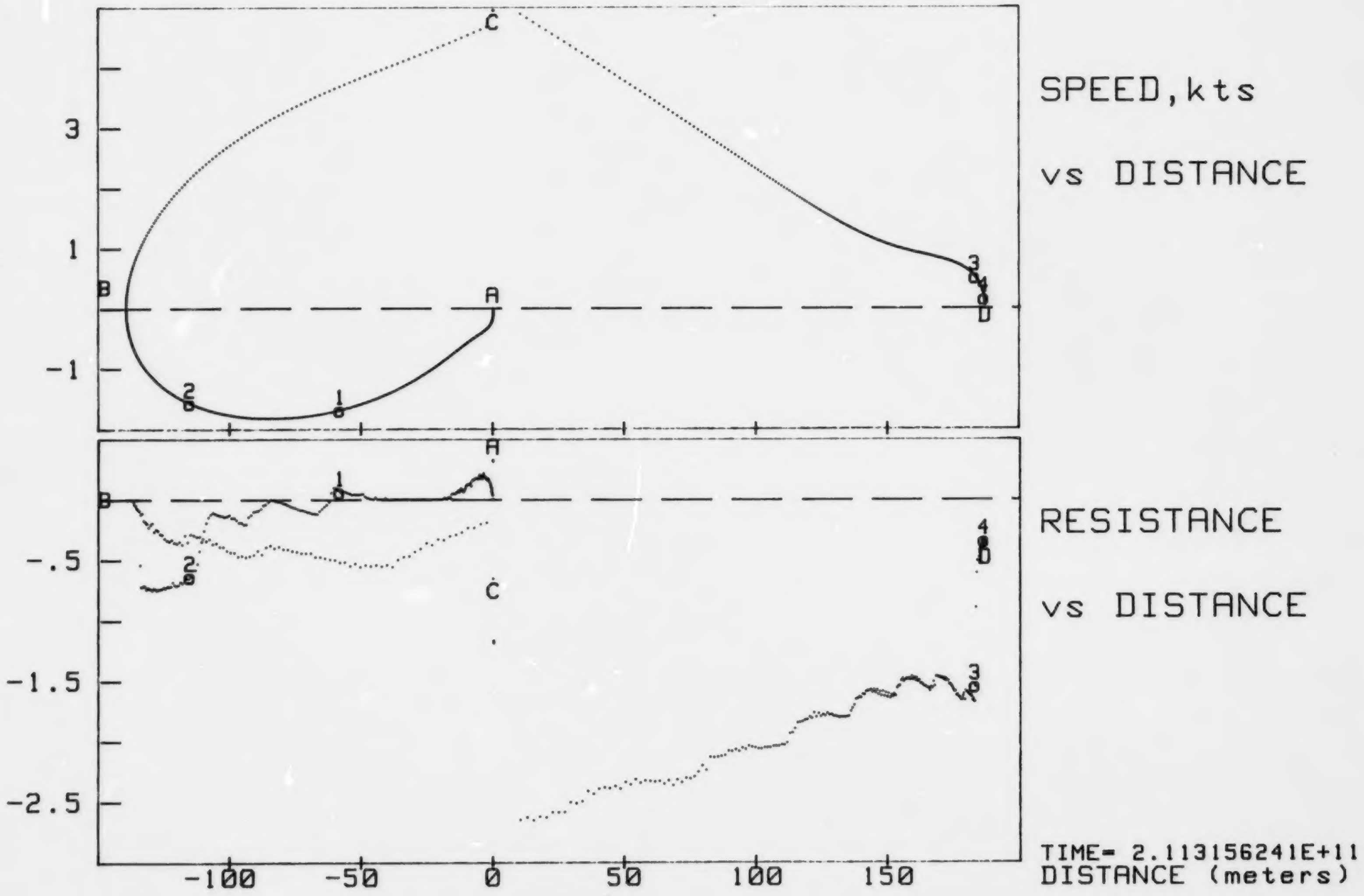

RAM # __B1 TAPE: 81-T2-3.1 07 JUL 1981 13:58:52 Fig.# 5

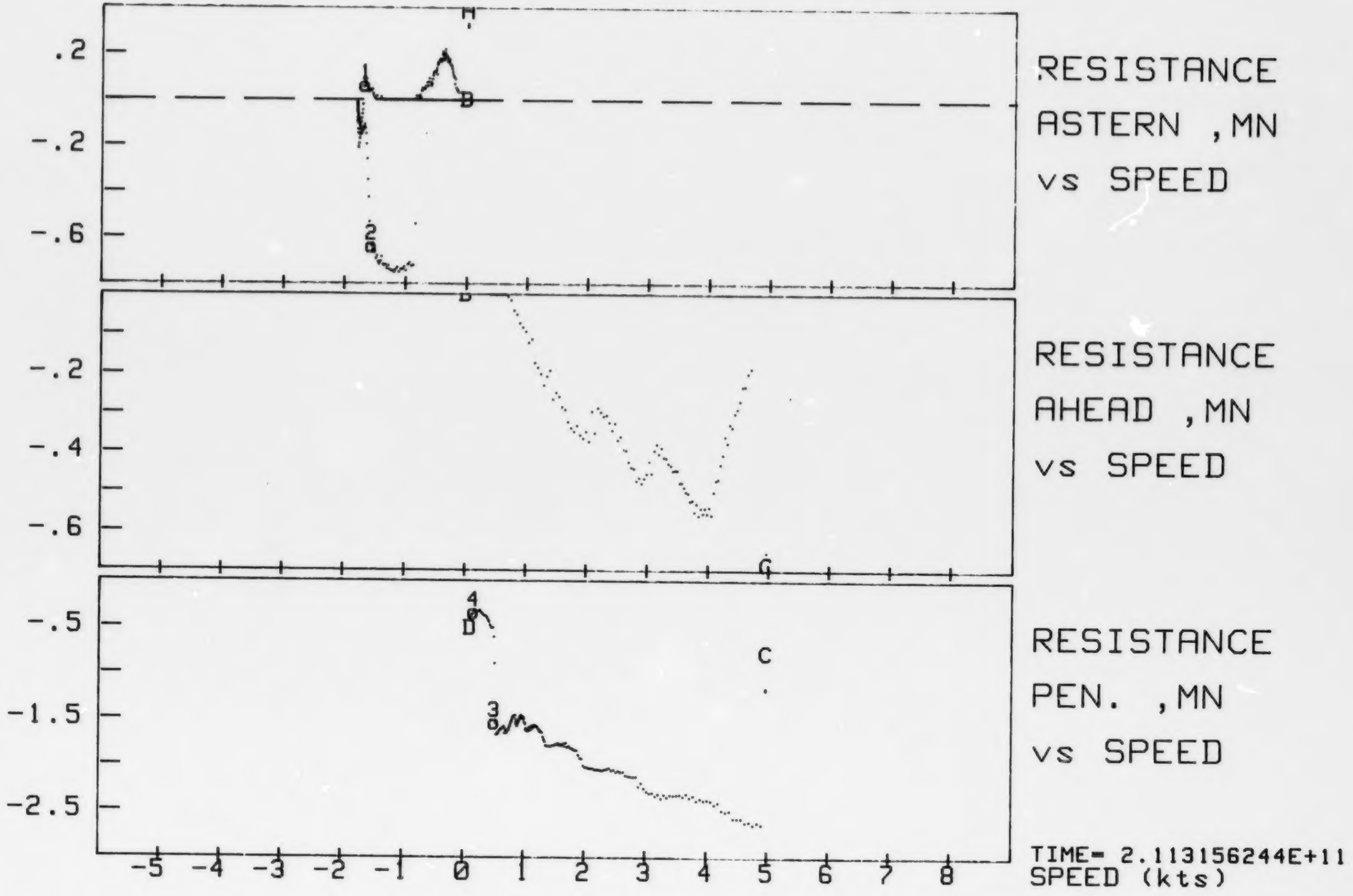

RESULTS OF RAMMING CYCLE ANALYSIS

RAM No. __B3

TAPE:	81-T2-3.1	ICE CONDITIONS:	RIDGES
CATEGORY:	R1	ICE THICKNESS:	2 m
QUALITY:	29BB	FLEXURAL STRENGTH:	163 kPA
TRIM:	EVEN TRIM	BUBBLER STATUS:	ON

RAMMING CYCLE CHARACTERISTICS:

Speed of Advance	(knots)	.241
Speed of Impact	(knots)	5.5 (5.67)

	Duration (sec)	% Cycle Time	Distance (m)
Backing	271	62.4	-161.5
Acceleration	90	20.7	161.5
Penetration	53	12.2	30.3 (53.82)
Extraction	20	4.61	
Total Cycle	434		

Duration of Astern Mode	(sec)	177
Duration of Reversal to Ahead	(sec)	63
Duration of Ahead Mode	(sec)	162
Duration of Reversal to Astern	(sec)	22
Start of Reversal after Impact	(sec)	41

Total Fuel Used	(mm*hr)	4.99	Est. kg:	24.36
Average Fuel Rate	(mm)	41.38	Est. kg/hr:	202.09

Backing Power	(kW)	3154
[Est Fuel Rate	(kg/hr)]	721.15
Acceleration Power	(kW)	9387.7
[Est Fuel Rate	(kg/hr)]	1964.2

RAM # __B3 TAPE: 81-T2-3.1 07 JUL 1981 14:18:16

FIG. #1

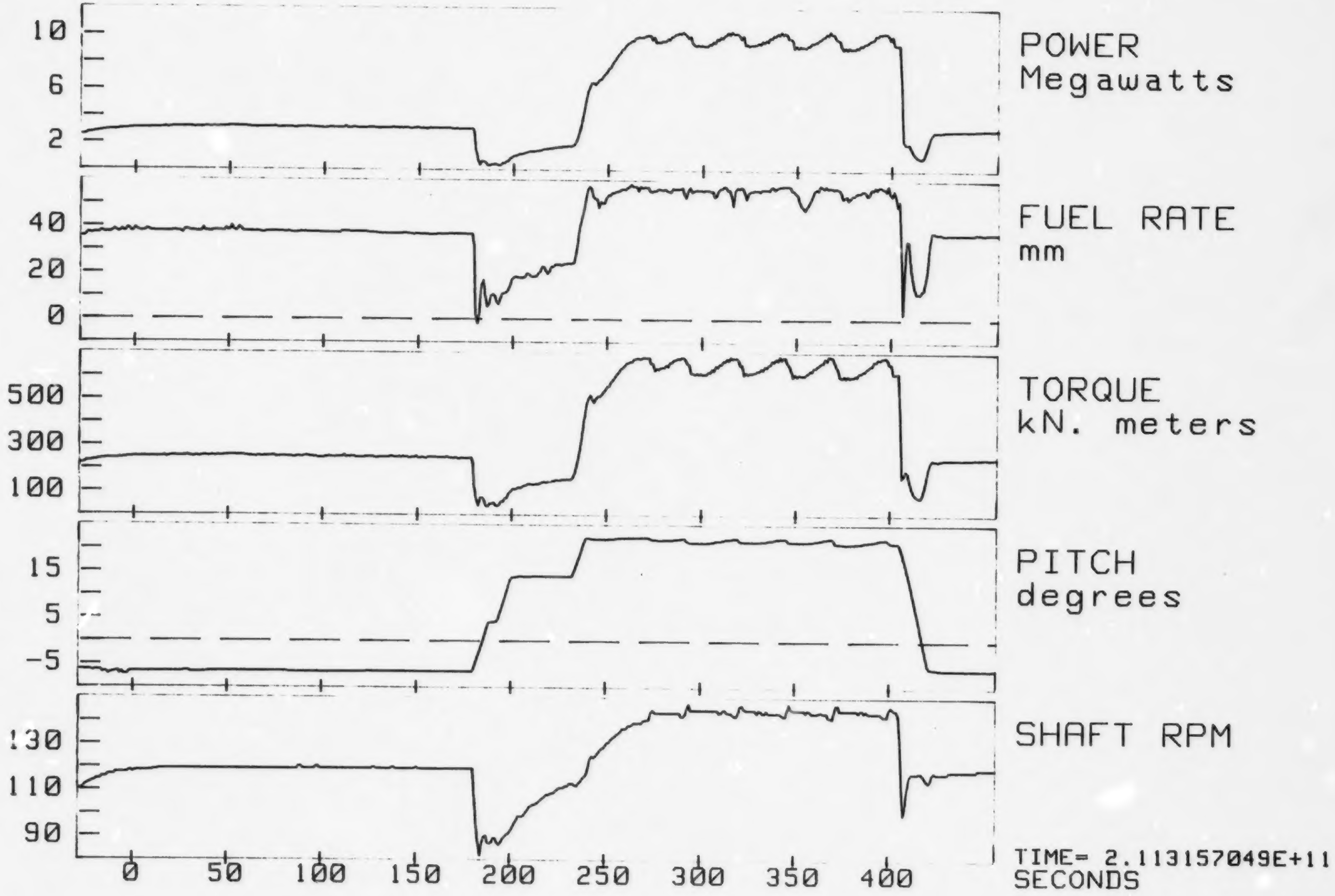

RAM # __B3   TAPE: 81-T2-3.1   07 JUL 1981 14:18:16

FIG. #2

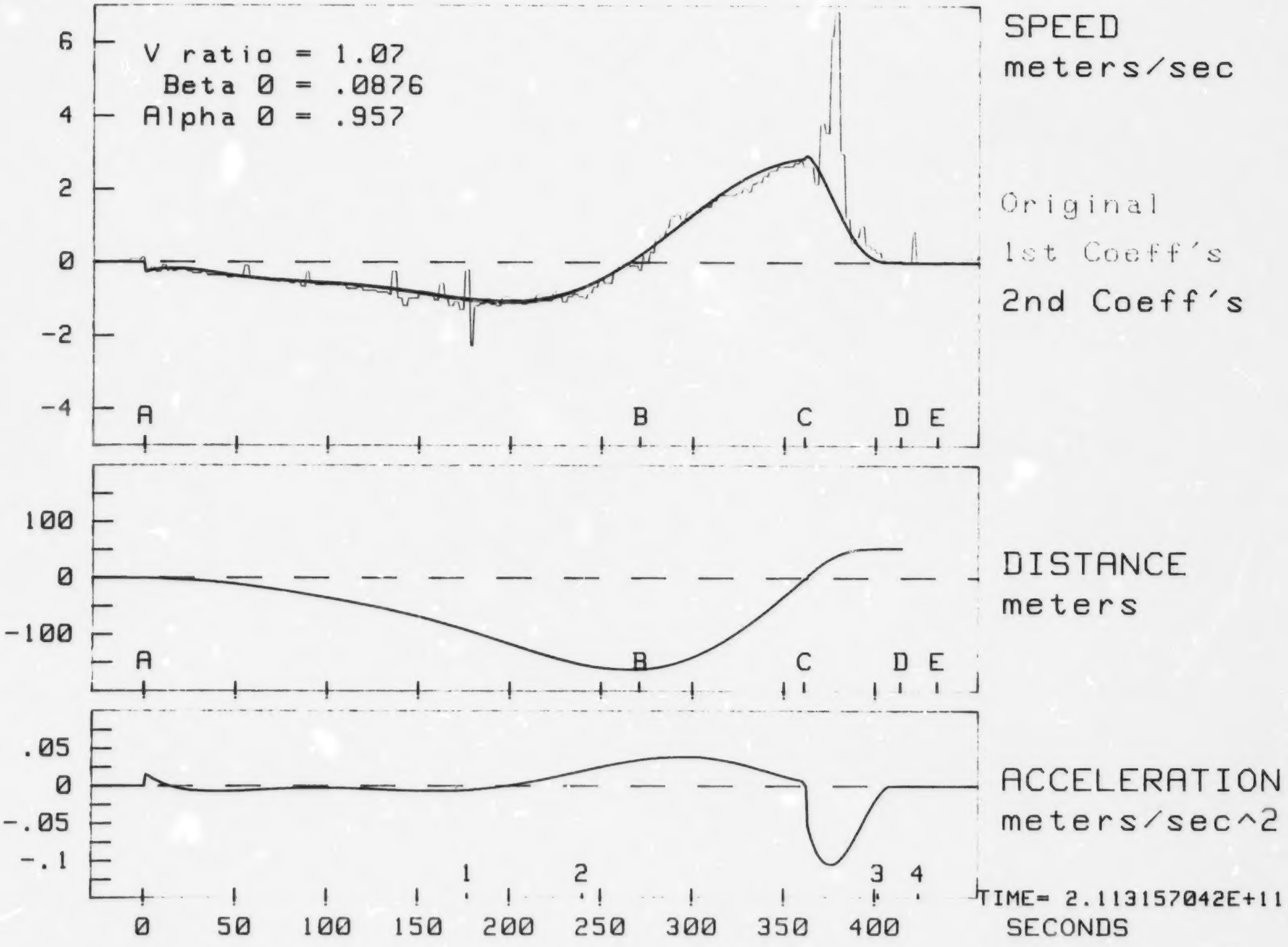

RAM # __B3 TAPE: 81-T2-3.1 07 JUL 1981 14:18:16

FIG. #3

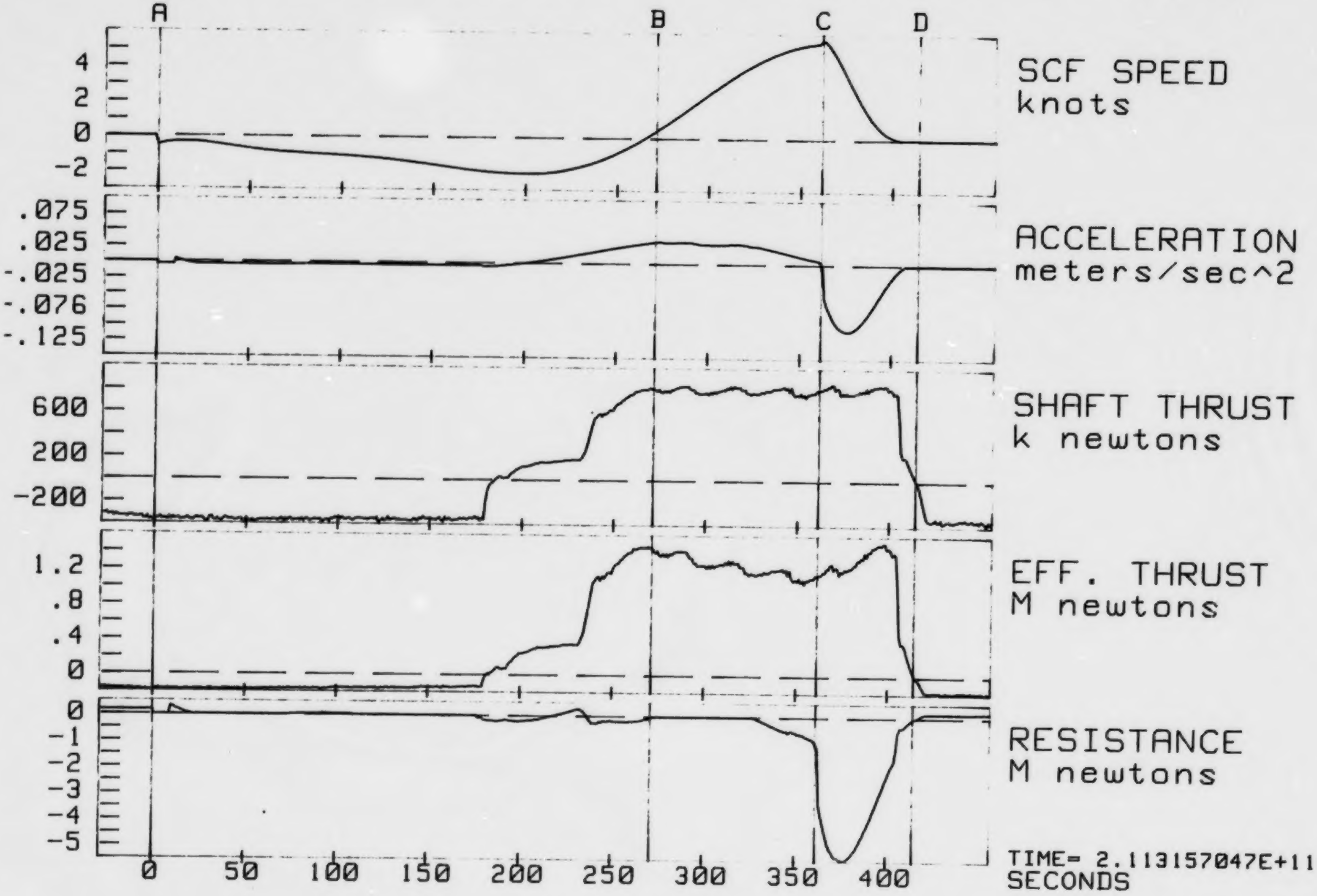

RAM # __B3 TAPE: 81-T2-3.1 07 JUL 1981 14:18:16 Fig.# 4

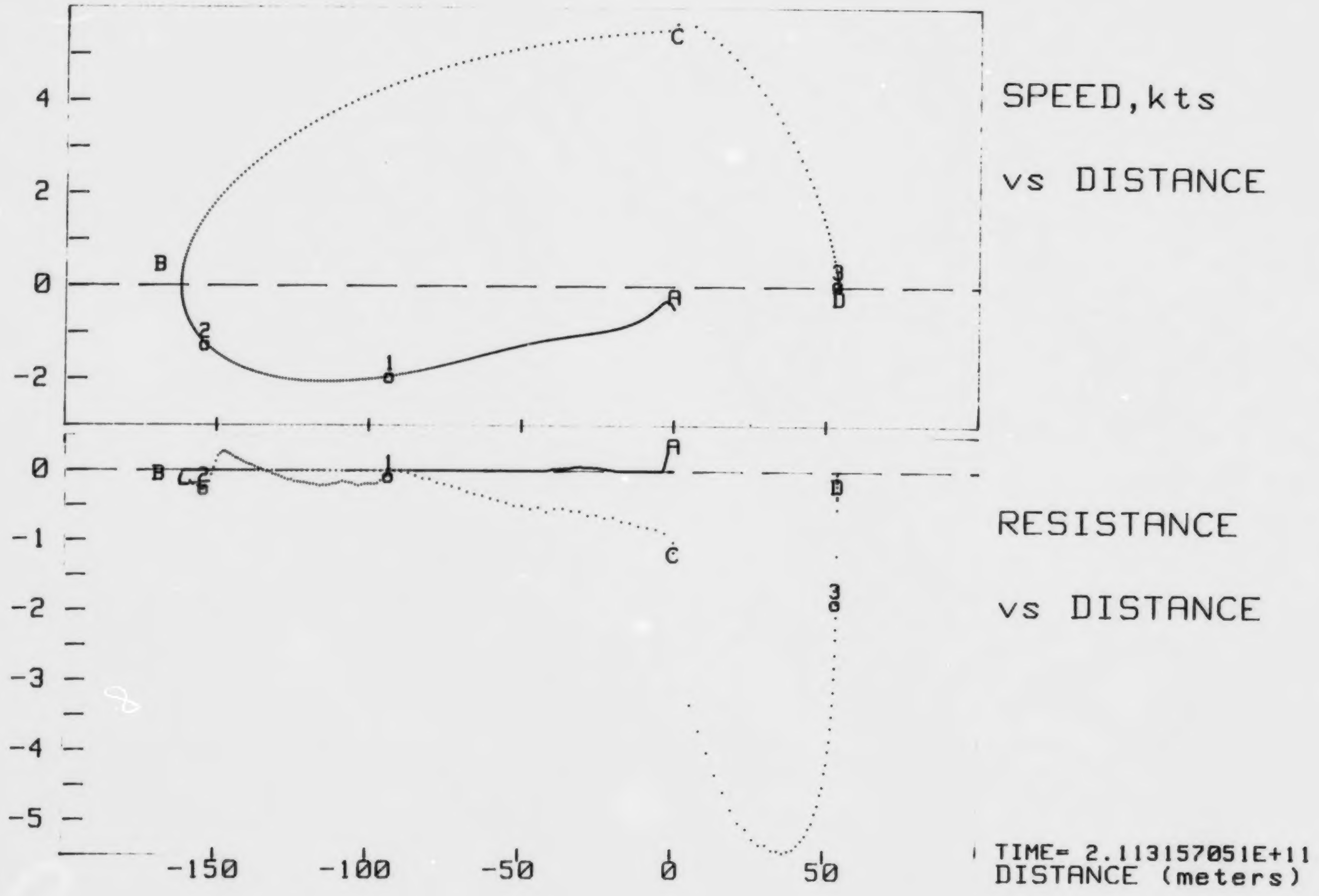

RAM # __B3   TAPE: 81-T2-3.1   07 JUL 1981 14:18:16   Fig.# 5

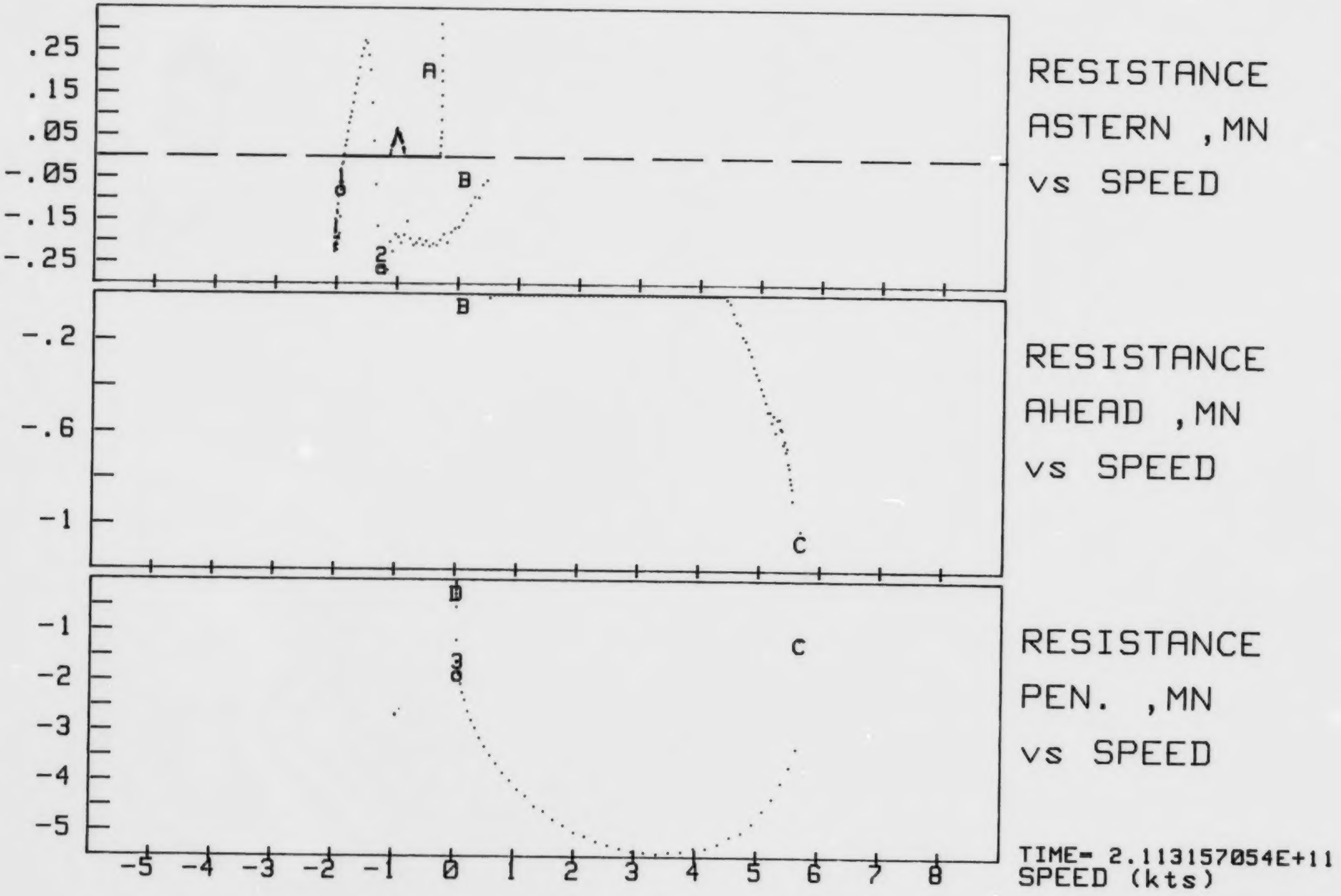

RESULTS OF RAMMING CYCLE ANALYSIS

RAM No. __B4

TAPE:	81-T2-3.1	ICE CONDITIONS:	LEVEL ICE
CATEGORY:	L1	ICE THICKNESS:	1.4 m
QUALITY:	45AC	FLEXURAL STRENGTH:	163 kPA
TRIM: EVEN ~~BOW DOWN~~		BUBBLER STATUS:	ON

RAMMING CYCLE CHARACTERISTICS:

Speed of Advance (knots)	.436	
Speed of Impact (knots)	5.5	(5.39)

	Duration (sec)	% Cycle Time	Distance (m)
Backing	261	46.8	-186.6
Acceleration	112	20.1	186.6
Penetration	176	31.5	113.6 (125.2)
Extraction	9	1.61	
Total Cycle	558		

Duration of Astern Mode (sec)	156		
Duration of Reversal to Ahead (sec)	94		
Duration of Ahead Mode (sec)	287		
Duration of Reversal to Astern (sec)	21		
Start of Reversal after Impact (sec)	164		
Total Fuel Used (mm*hr)	6.61	Est. kg:	45.5
Average Fuel Rate (mm)	42.65	Est. kg/hr:	293.57
Backing Power (kW)	3045.3		
[Est Fuel Rate (kg/hr)]	699.49		
Acceleration Power (kW)	9499.7		
[Est Fuel Rate (kg/hr)]	1986.5		

RAM # __B4 TAPE: 81-T2-3.1 07 JUL 1981 14:25:52 **FIG. #1**

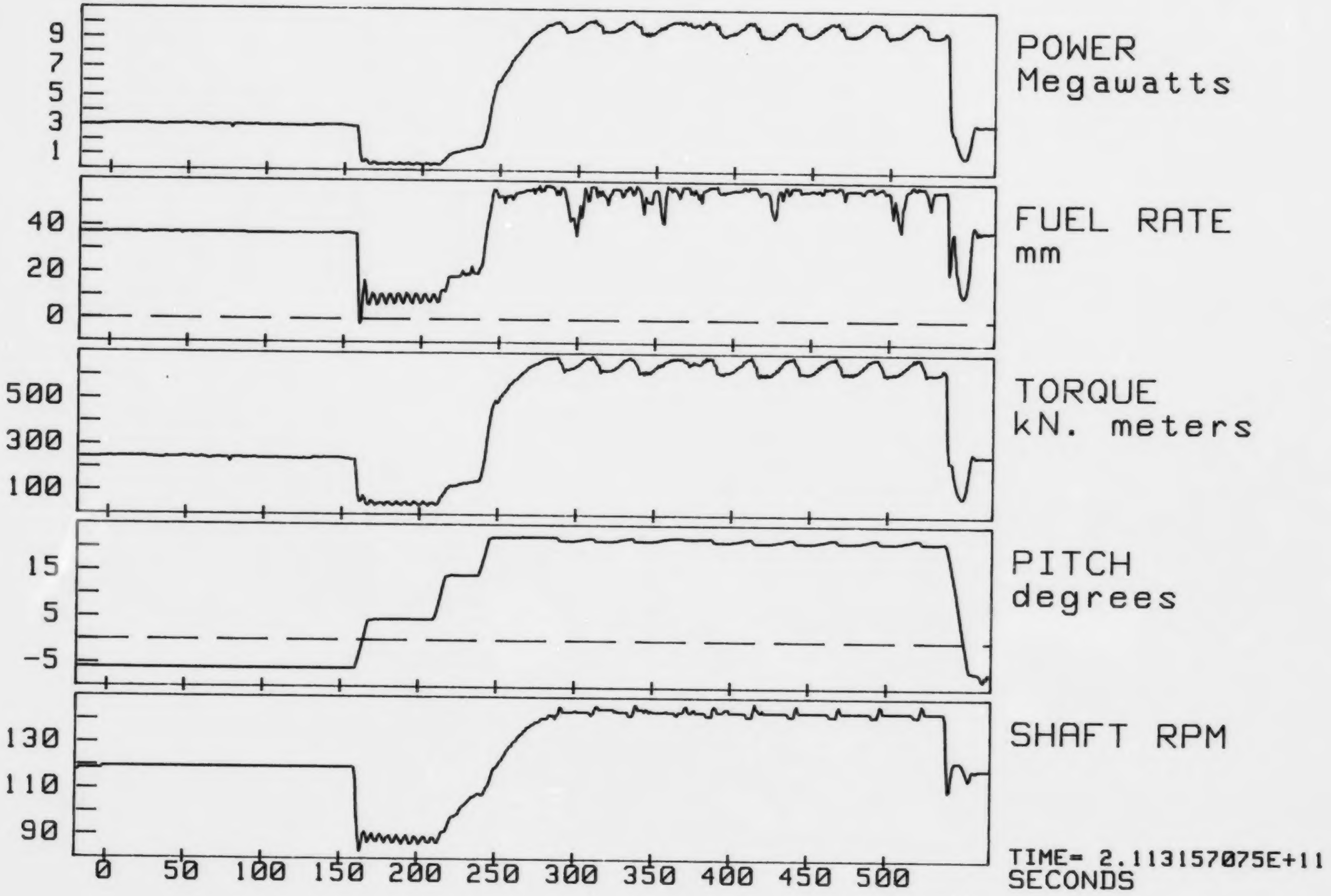

RAM # B4 TAPE: 81-T2-3.1 07 JUL 1981 14:25:52

FIG. #2

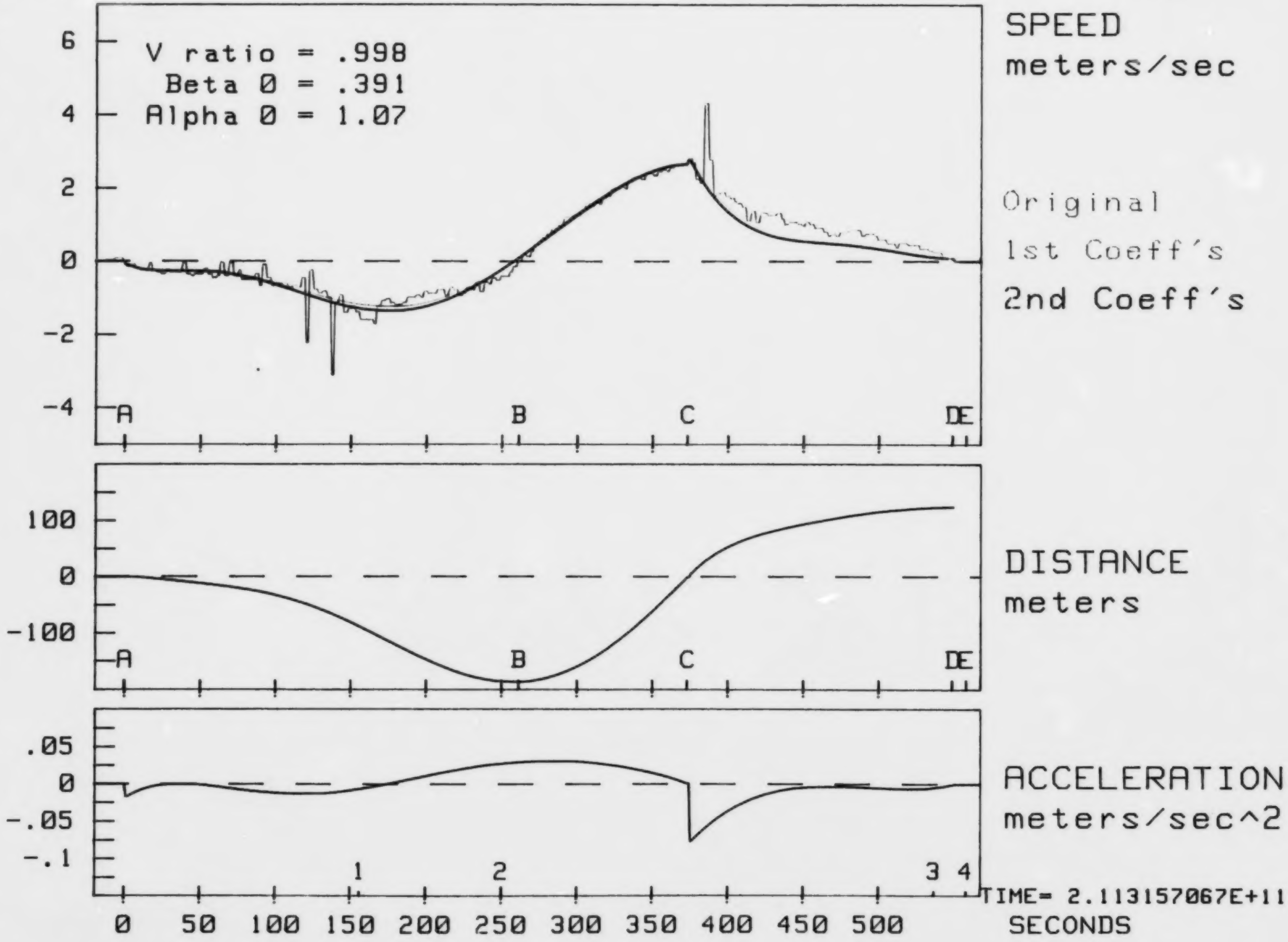

RAM # __B4 TAPE: 81-T2-3.1 07 JUL 1981 14:25:52 **FIG. #3**

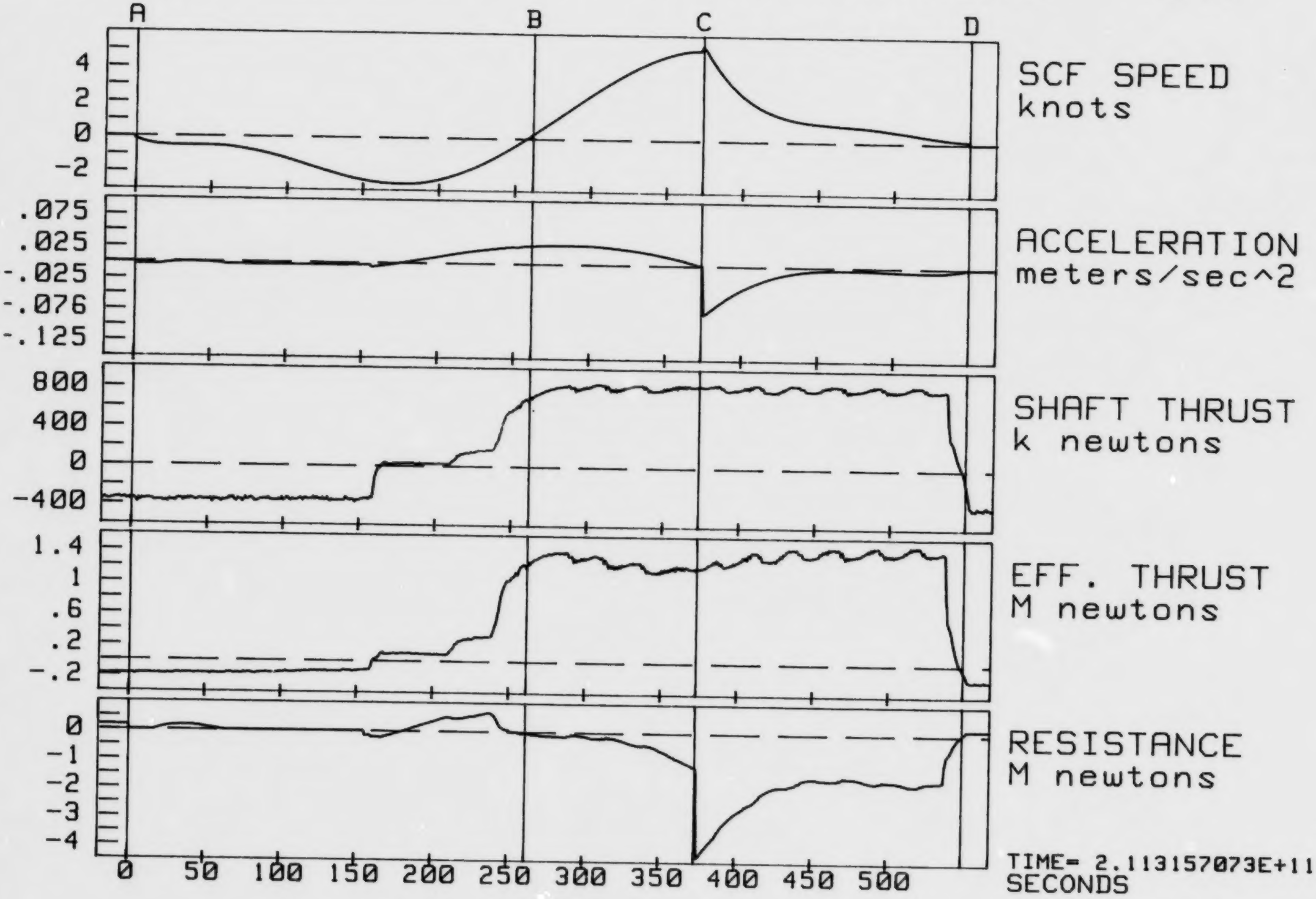

RAM # __B4   TAPE: 81-T2-3.1   07 JUL 1981 14:25:52   Fig.# 4

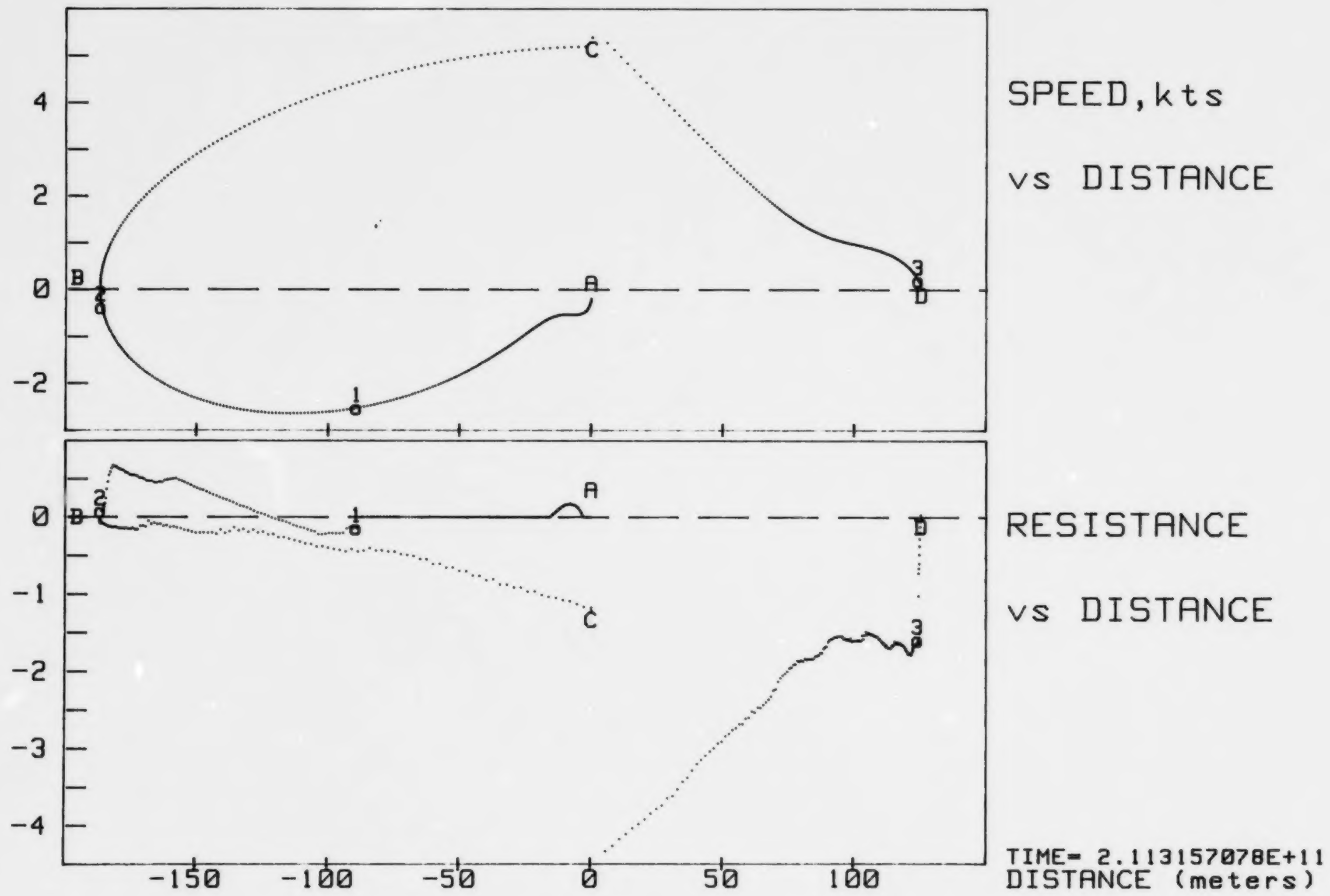

RAM # __B4 TAPE: 81-T2-3.1 07 JUL 1981 14:25:52 Fig.# 5

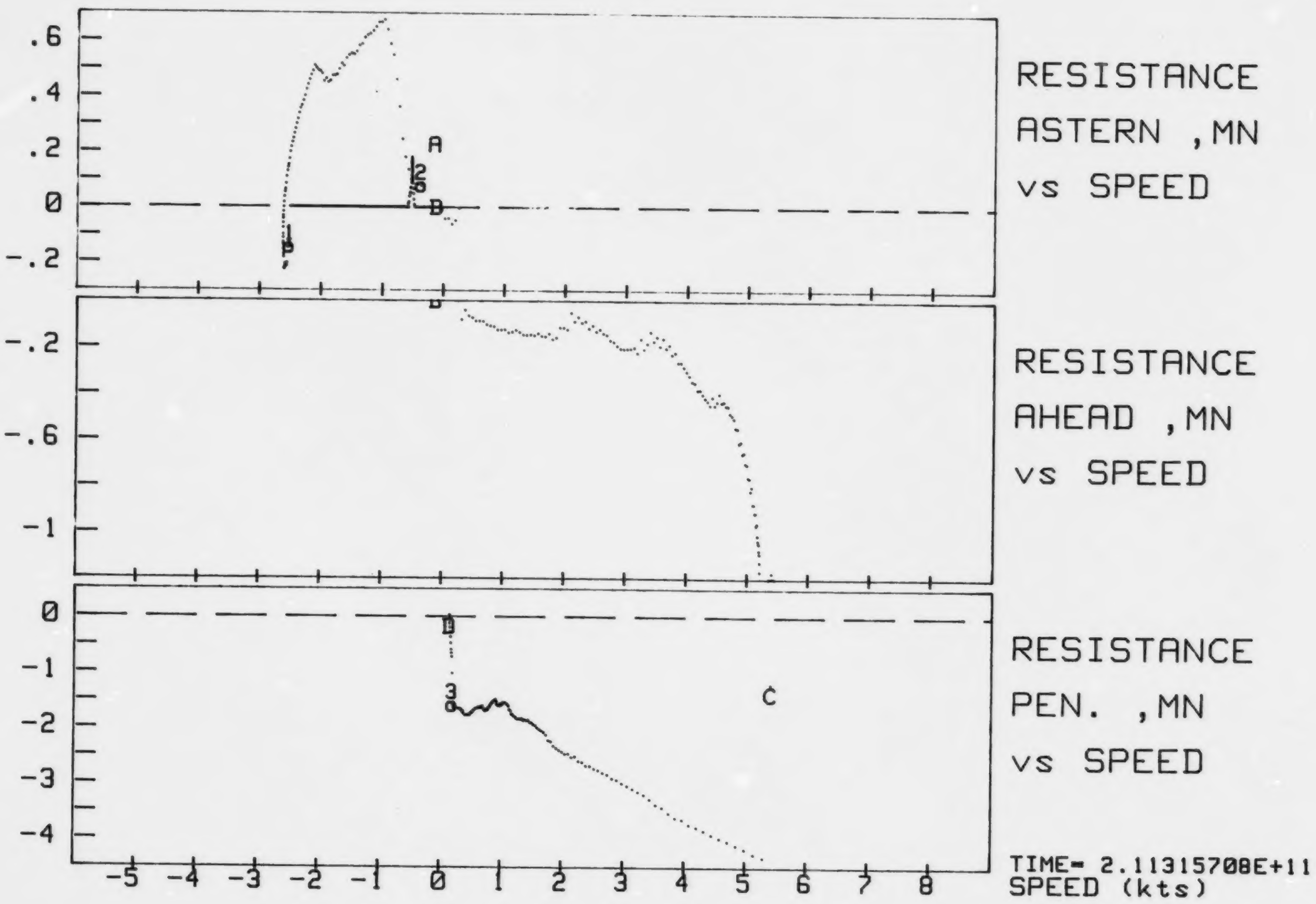

RESULTS OF RAMMING CYCLE ANALYSIS

RAM No. __B5

TAPE: 81-T2-3.1 ICE CONDITIONS: LEVEL ICE

CATEGORY: L1 ICE THICKNESS: 1.62 m

QUALITY: 28BB FLEXURAL STRENGTH: 163 kPA

TRIM: EVEN TRIM BUBBLER STATUS: ON

RAMMING CYCLE CHARACTERISTICS:

Speed of Advance (knots) .421

Speed of Impact (knots) 5.5 (5.41)

	Duration (sec)	% Cycle Time	Distance (m)
Backing	348	53.8	-152.8
Acceleration	101	15.6	152.8
Penetration	187	28.9	136.4 (140)
Extraction	11	1.7	
Total Cycle	647		

Duration of Astern Mode	(sec)	266
Duration of Reversal to Ahead	(sec)	68
Duration of Ahead Mode	(sec)	273
Duration of Reversal to Astern	(sec)	25
Start of Reversal after Impact	(sec)	158

Total Fuel Used	(mm*hr)	7.74	Est. kg:	58.28
Average Fuel Rate	(mm)	43.08	Est. kg/hr:	324.26

Backing Power	(kW)	2487.6
[Est Fuel Rate	(kg/hr)]	588.28

Acceleration Power	(kW)	9435.7
[Est Fuel Rate	(kg/hr)]	1973.7

RAM # __B5 TAPE: 81-T2-3.1 07 JUL 1981 14:35:31 **FIG. #1**

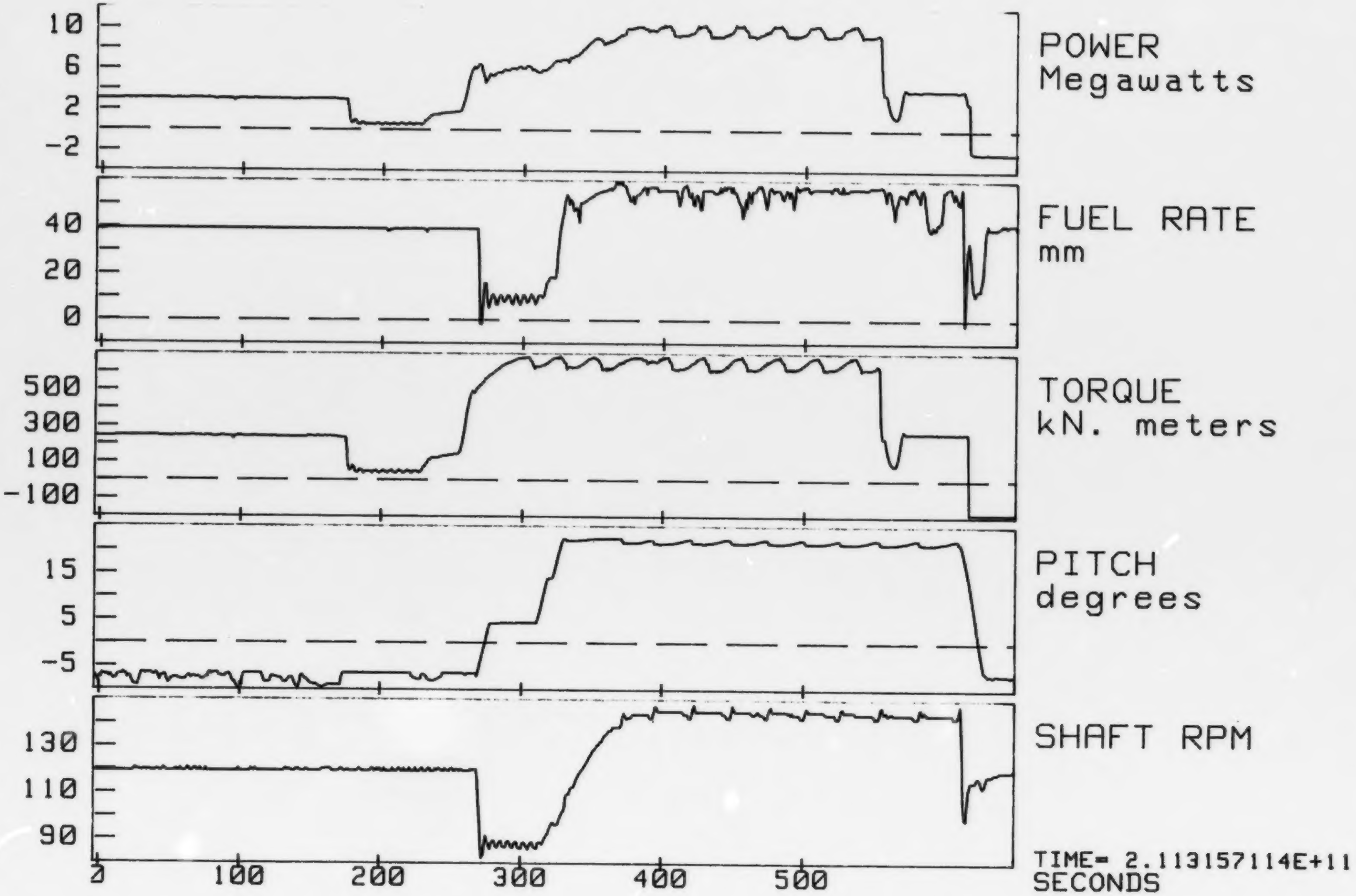

RAM # __B5 TAPE: 81-T2-3.1 07 JUL 1981 14:35:31 **FIG. #2**

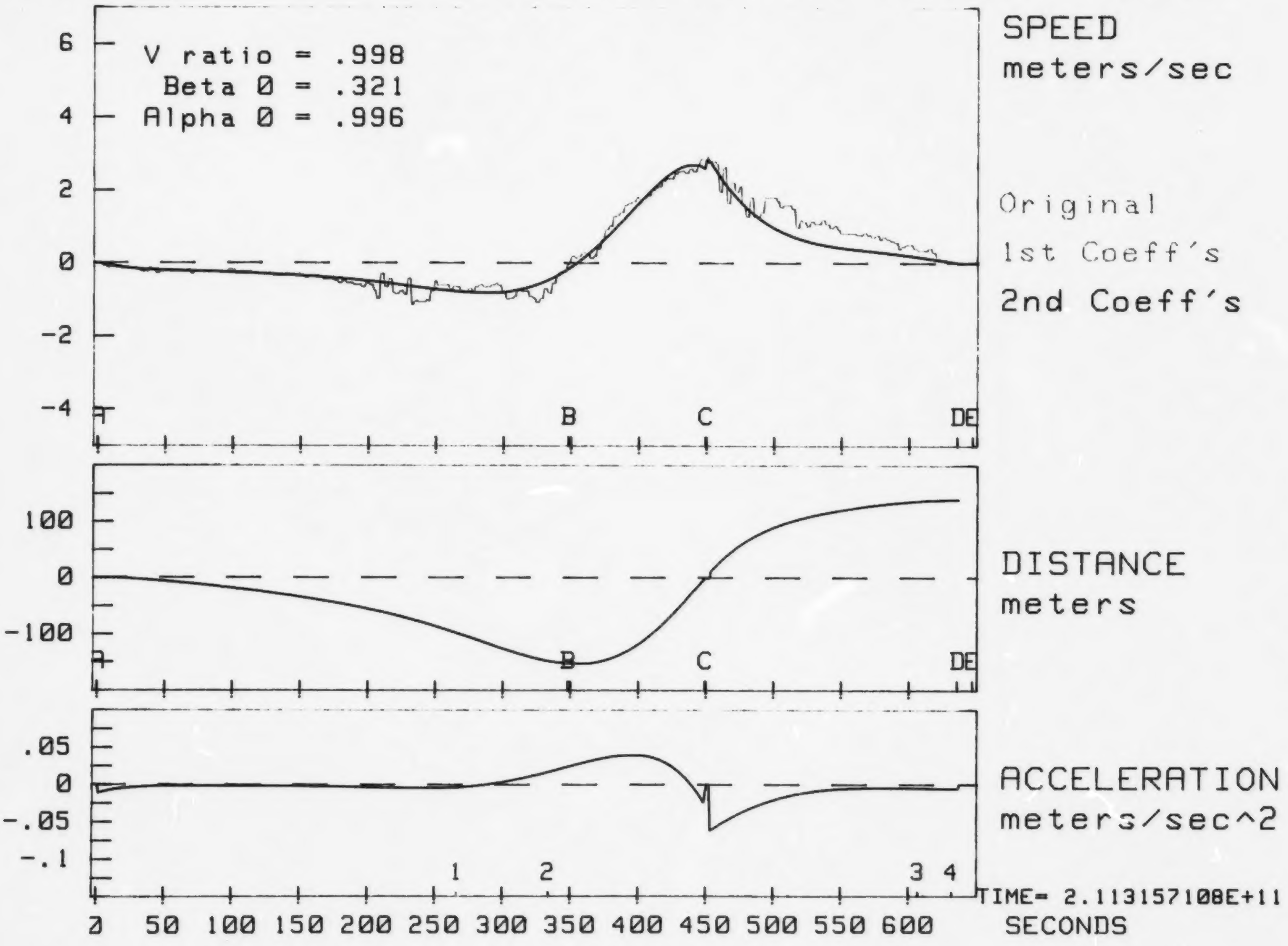

RAM # __B5 TAPE: 81-T2-3.1 07 JUL 1981 14:35:31

FIG. #3

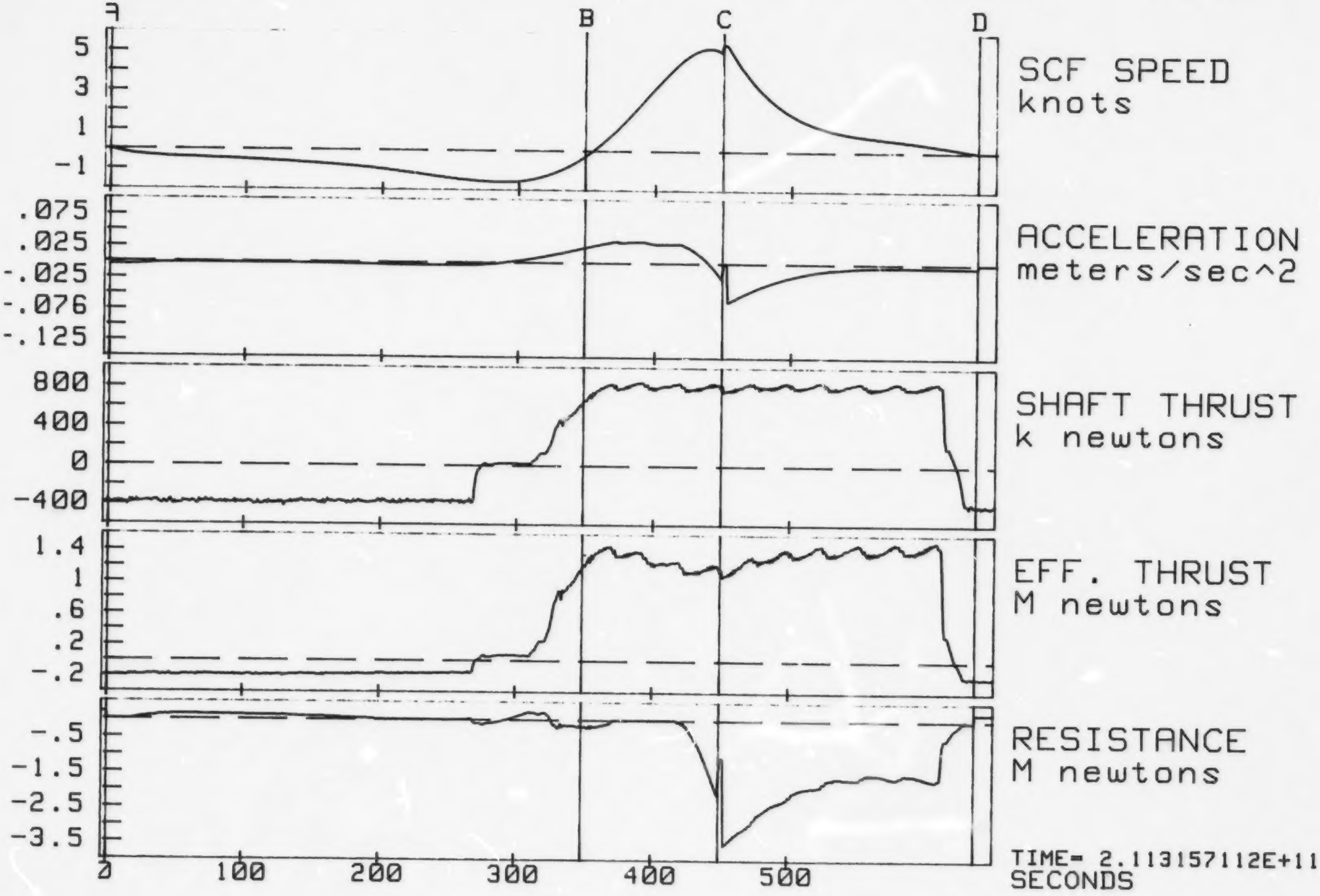

RAM # __B5 TAPE: 81-T2-3.1 07 JUL 1981 14:35:31 Fig.# 4

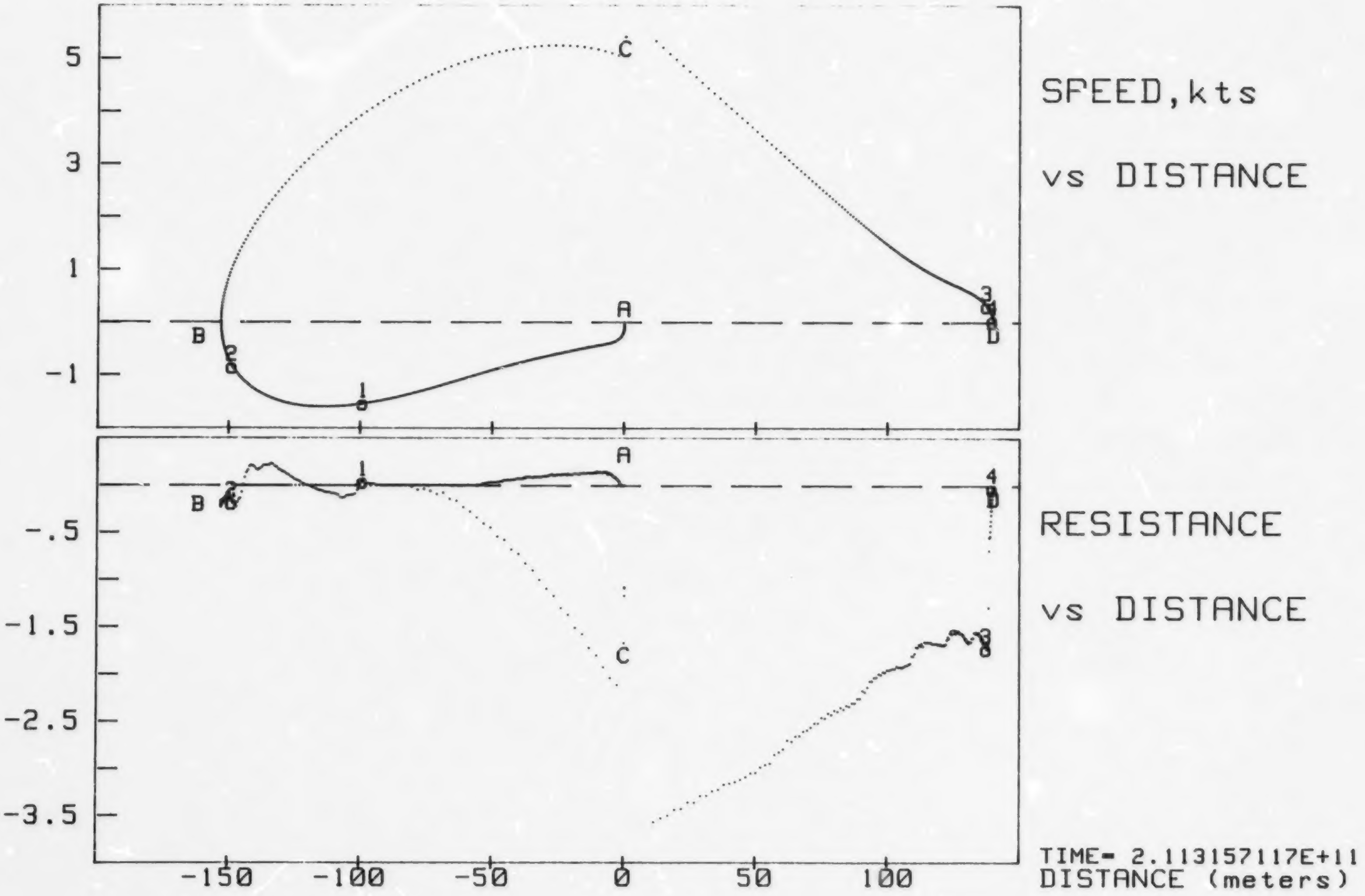

RAM # __B5 TAPE: 81-T2-3.1 07 JUL 1981 14:35:31 Fig.# 5

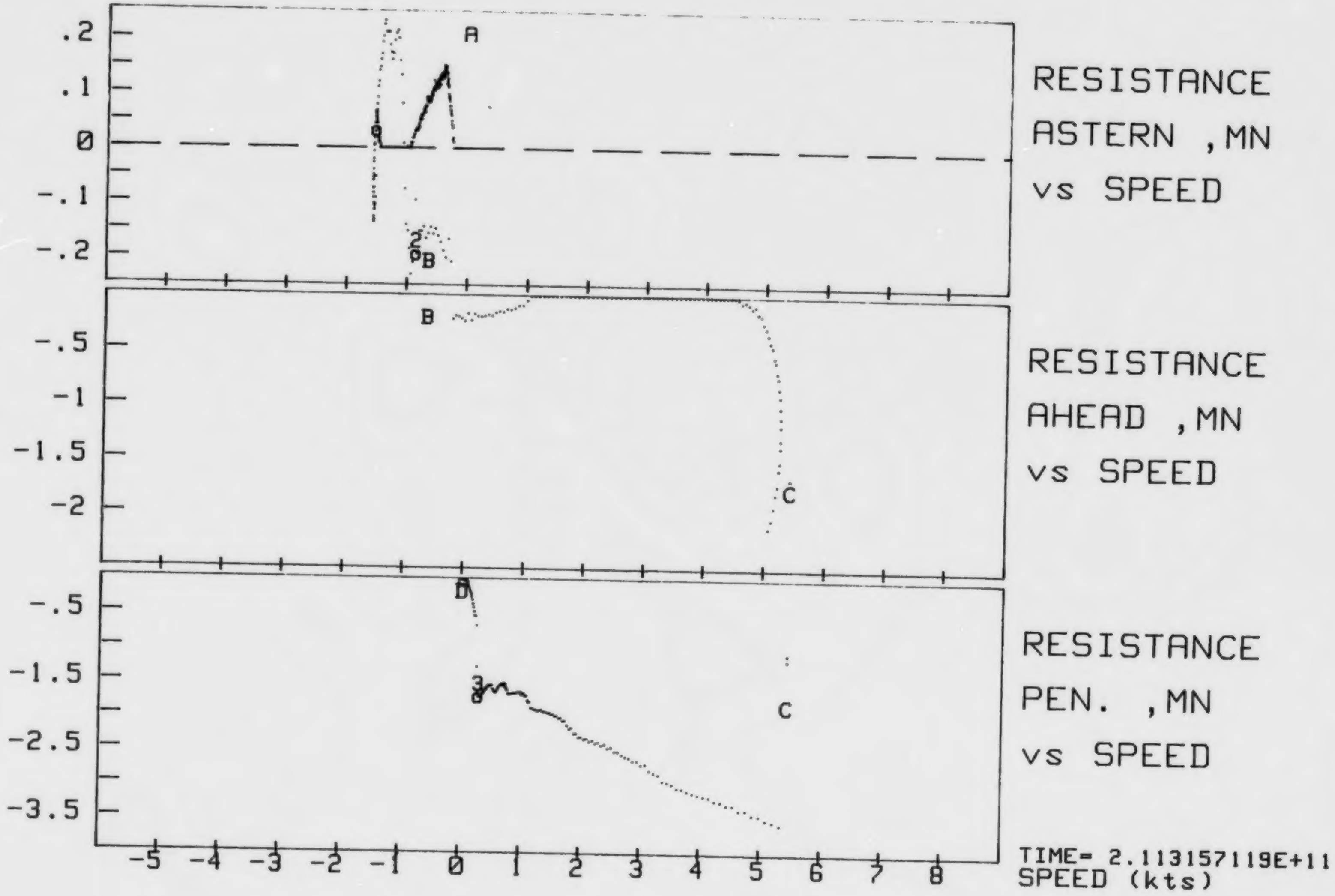

RESISTANCE ASTERN ,MN vs SPEED

RESISTANCE AHEAD ,MN vs SPEED

RESISTANCE PEN. ,MN vs SPEED

TIME= 2.113157119E+11

RESULTS OF RAMMING CYCLE ANALYSIS

RAM No. __B6

TAPE:	81-T2-3.1	ICE CONDITIONS:	LEVEL ICE
CATEGORY:	L1	ICE THICKNESS:	1.66 m
QUALITY:	31BB	FLEXURAL STRENGTH:	163 kPA
TRIM:	EVEN TRIM	BUBBLER STATUS:	ON

RAMMING CYCLE CHARACTERISTICS:

Speed of Advance	(knots)	.526
Speed of Impact	(knots)	5.5 (5.76)

	Duration (sec)	% Cycle Time	Distance (m)
Backing	254	54.4	-178.9
Acceleration	115	24.6	178.9
Penetration	98	21	121.2 (126.3)
Extraction	0	0	
Total Cycle	467		

Duration of Astern Mode	(sec)	181
Duration of Reversal to Ahead	(sec)	37
Duration of Ahead Mode	(sec)	249
Duration of Reversal to Astern	(sec)	0
Start of Reversal after Impact	(sec)	98

Total Fuel Used	(mm*hr)	6.05	Est. kg:	75.58
Average Fuel Rate	(mm)	46.66	Est. kg/hr:	582.6
Backing Power	(kW)	3557.8		
[Est Fuel Rate	(kg/hr)]	801.67		
Acceleration Power	(kW)	8990.1		
[Est Fuel Rate	(kg/hr)]	1884.9		

RAM # __B6 TAPE: 81-T2-3.1 07 JUL 1981 14:44:52 **FIG. #1**

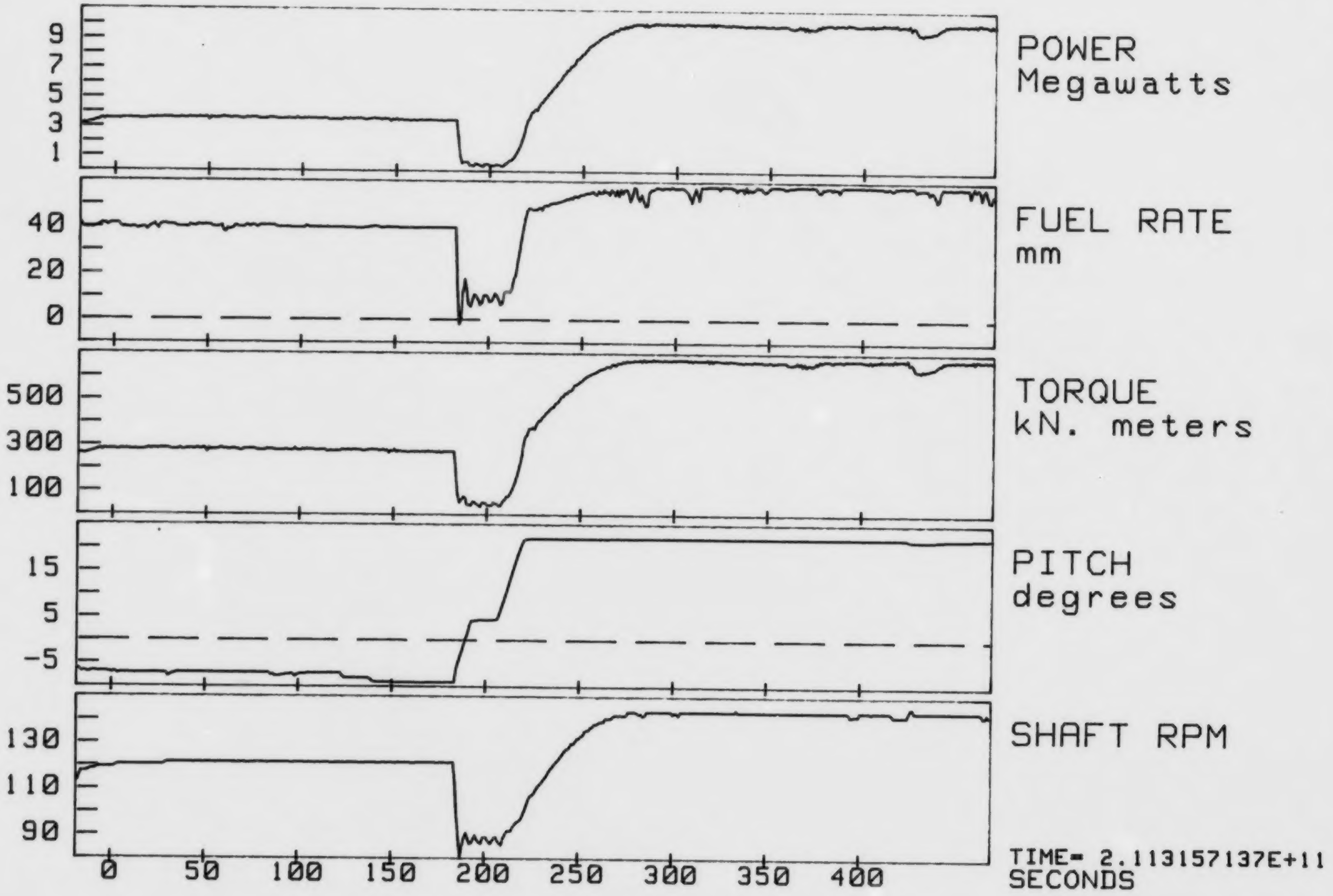

RAM # __B6   TAPE: 81-T2-3.1   07 JUL 1981 14:44:52

FIG. #2

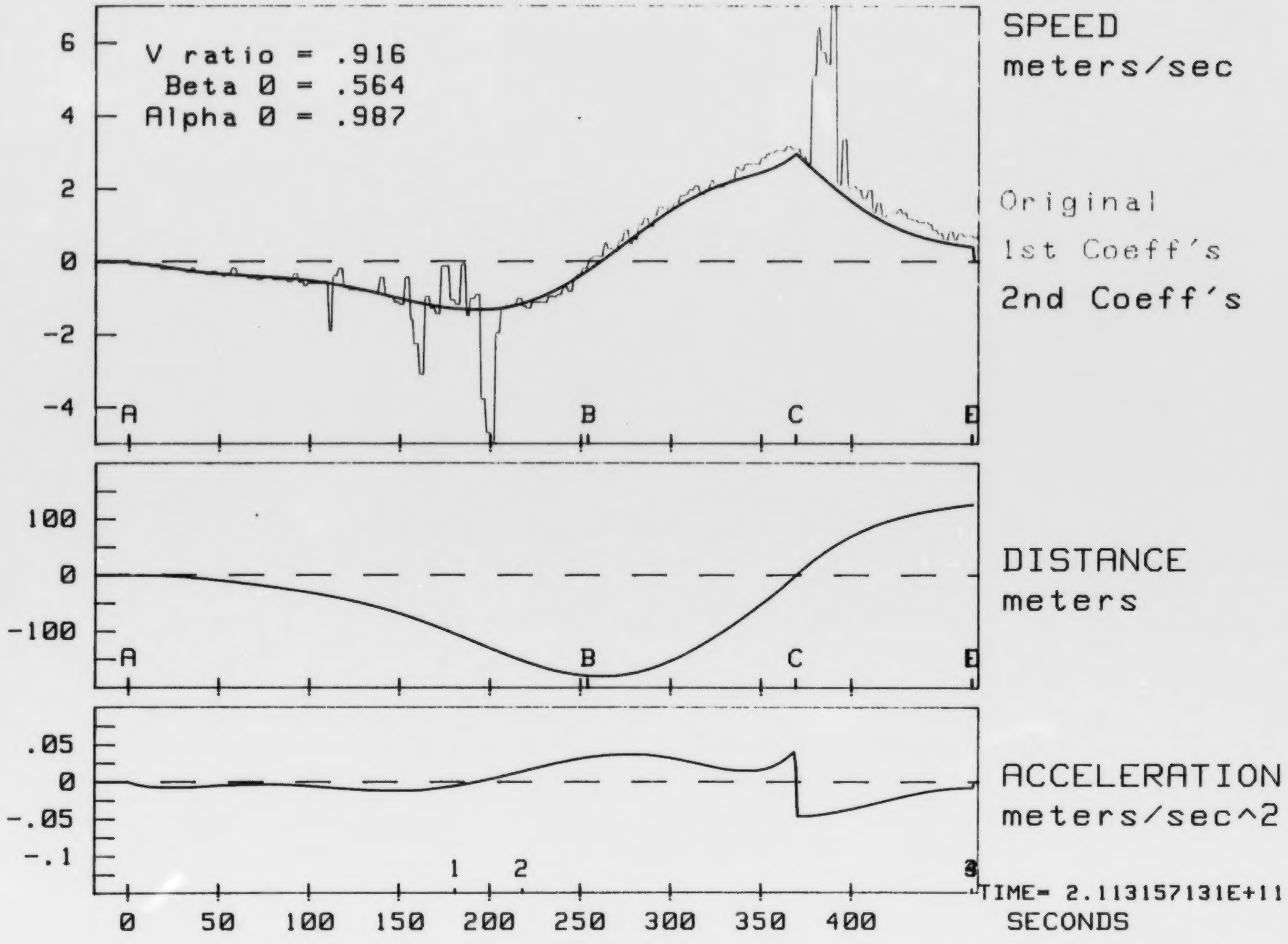

RAM # __B6 TAPE: 81-T2-3.1 07 JUL 1981 14:44:52

FIG. #3

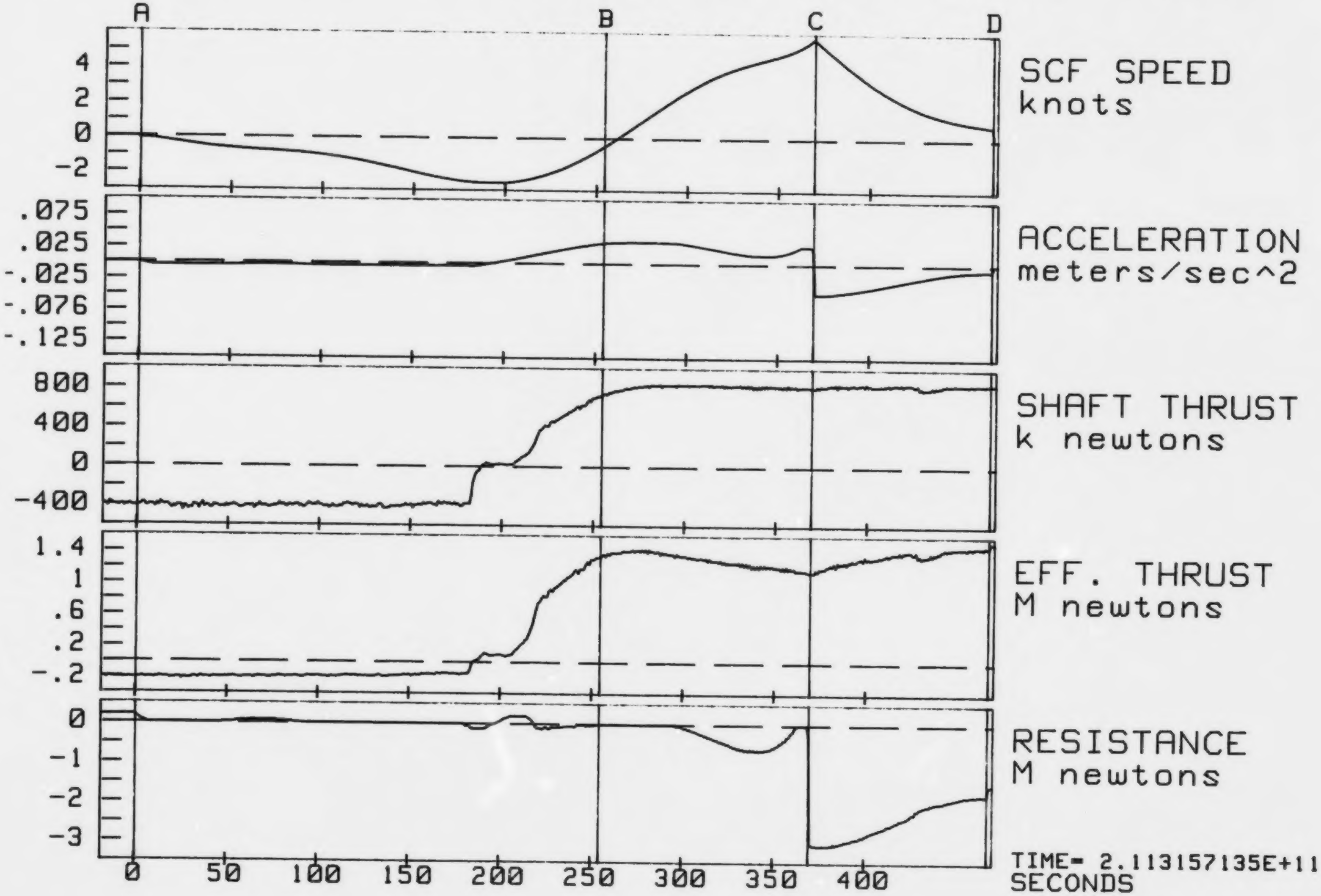

RAM # __B6 TAPE: 81-T2-3.1 07 JUL 1981 14:44:52 Fig.# 4

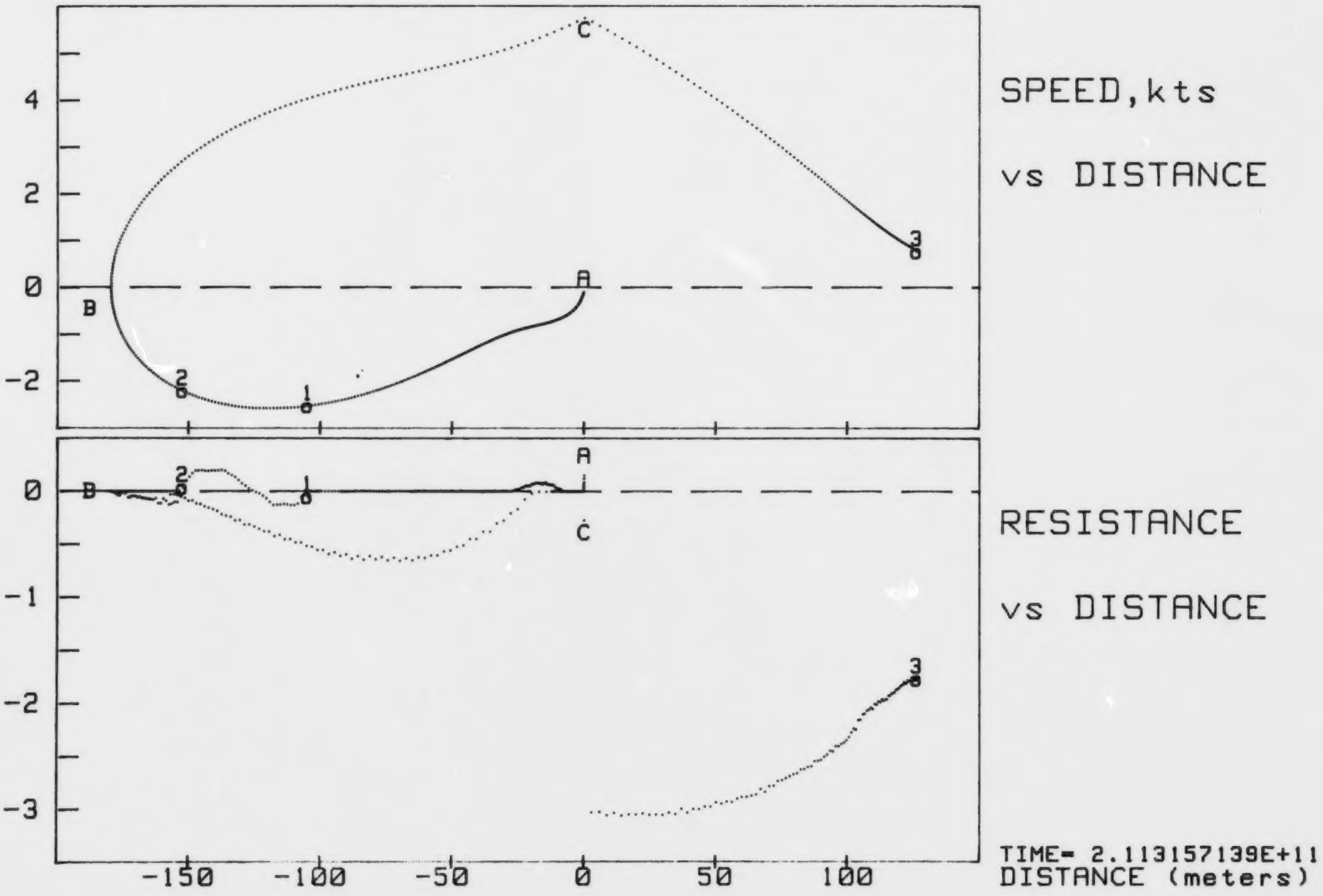

RAM # __B6 TAPE: 81-T2-3.1 07 JUL 1981 14:44:52 Fig.# 5

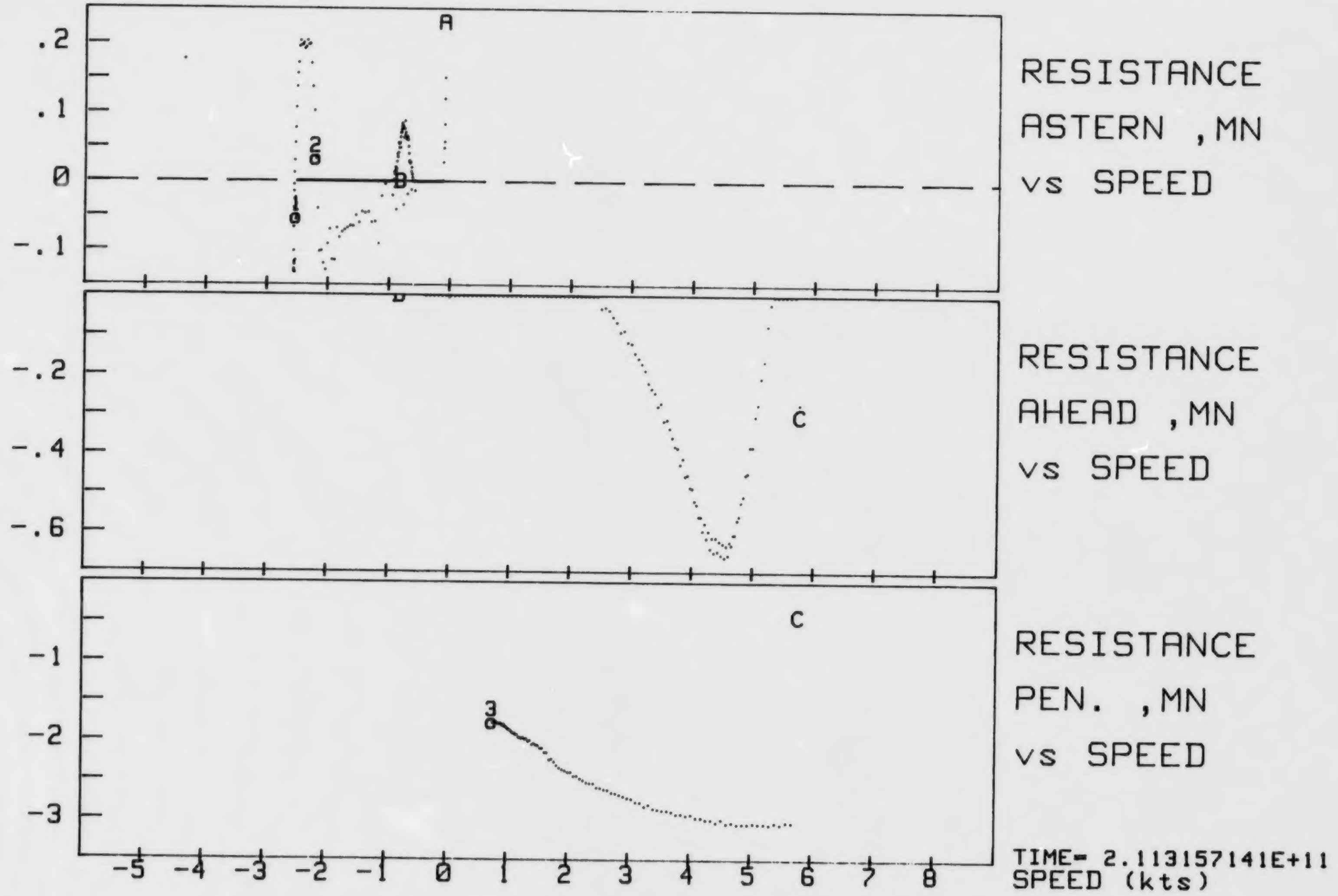

RESULTS OF RAMMING CYCLE ANALYSIS

RAM No. __B7

TAPE:	81-T2-3.1	ICE CONDITIONS:	LEVEL ICE
CATEGORY:	L1	ICE THICKNESS:	1.56 m
QUALITY:	31BB	FLEXURAL STRENGTH:	163 kPA
TRIM:	EVEN TRIM	BUBBLER STATUS:	ON

RAMMING CYCLE CHARACTERISTICS:

Speed of Advance	(knots)	.504
Speed of Impact	(knots)	5.5 (5.79)

	Duration (sec)	% Cycle Time	Distance (m)
Backing	255	48.5	-168
Acceleration	107	20.3	168
Penetration	156	29.7	128.8 (136.4)
Extraction	8	1.52	
Total Cycle	526		

Duration of Astern Mode	(sec)	172		
Duration of Reversal to Ahead	(sec)	59		
Duration of Ahead Mode	(sec)	263		
Duration of Reversal to Astern	(sec)	21		
Start of Reversal after Impact	(sec)	132		
Total Fuel Used	(mm*hr)	6.64	Est. kg:	72.59
Average Fuel Rate	(mm)	45.47	Est. kg/hr:	496.81
Backing Power	(kW)	3248.9		
[Est Fuel Rate	(kg/hr)]	740.08		
Acceleration Power	(kW)	9444.9		
[Est Fuel Rate	(kg/hr)]	1975.6		

RAM # __B7 TAPE: 81-T2-3.1 07 JUL 1981 14:54:52

FIG. #1

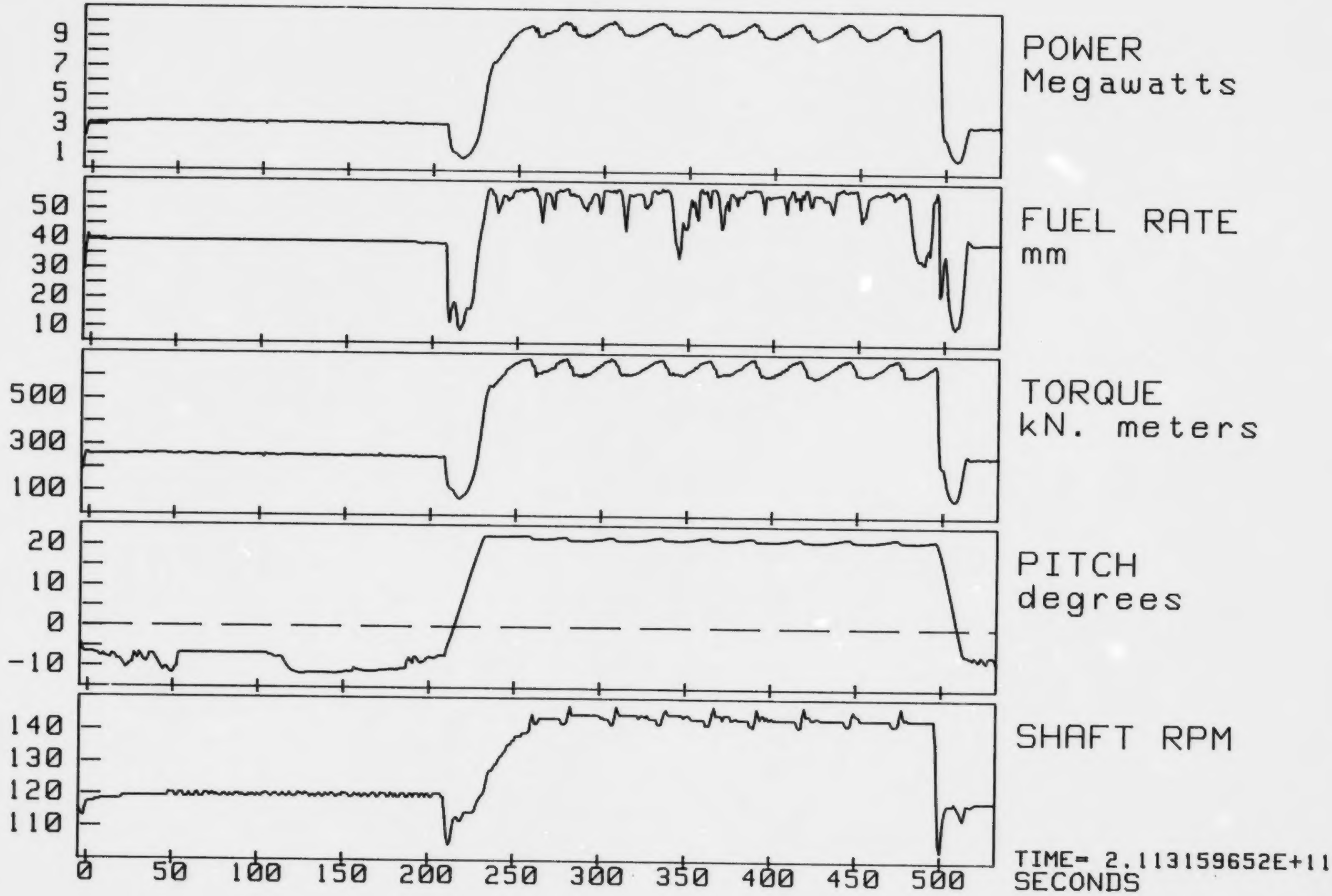

RAM # __B7 TAPE: 81-T2-3.1 07 JUL 1981 14:54:52

FIG. #2

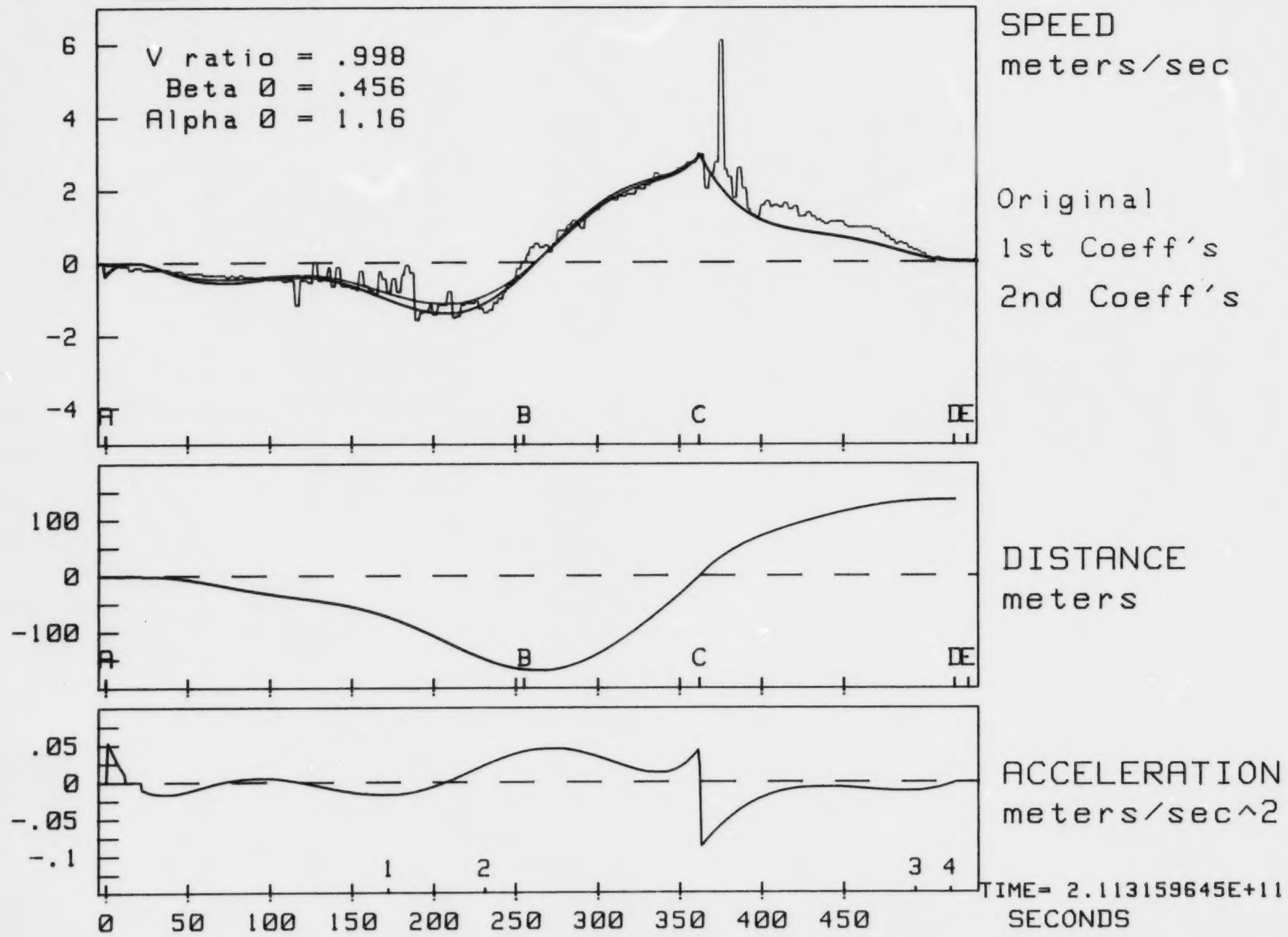

RAM # __B7   TAPE: 81-T2-3.1   07 JUL 1981 14:54:52

FIG. #3

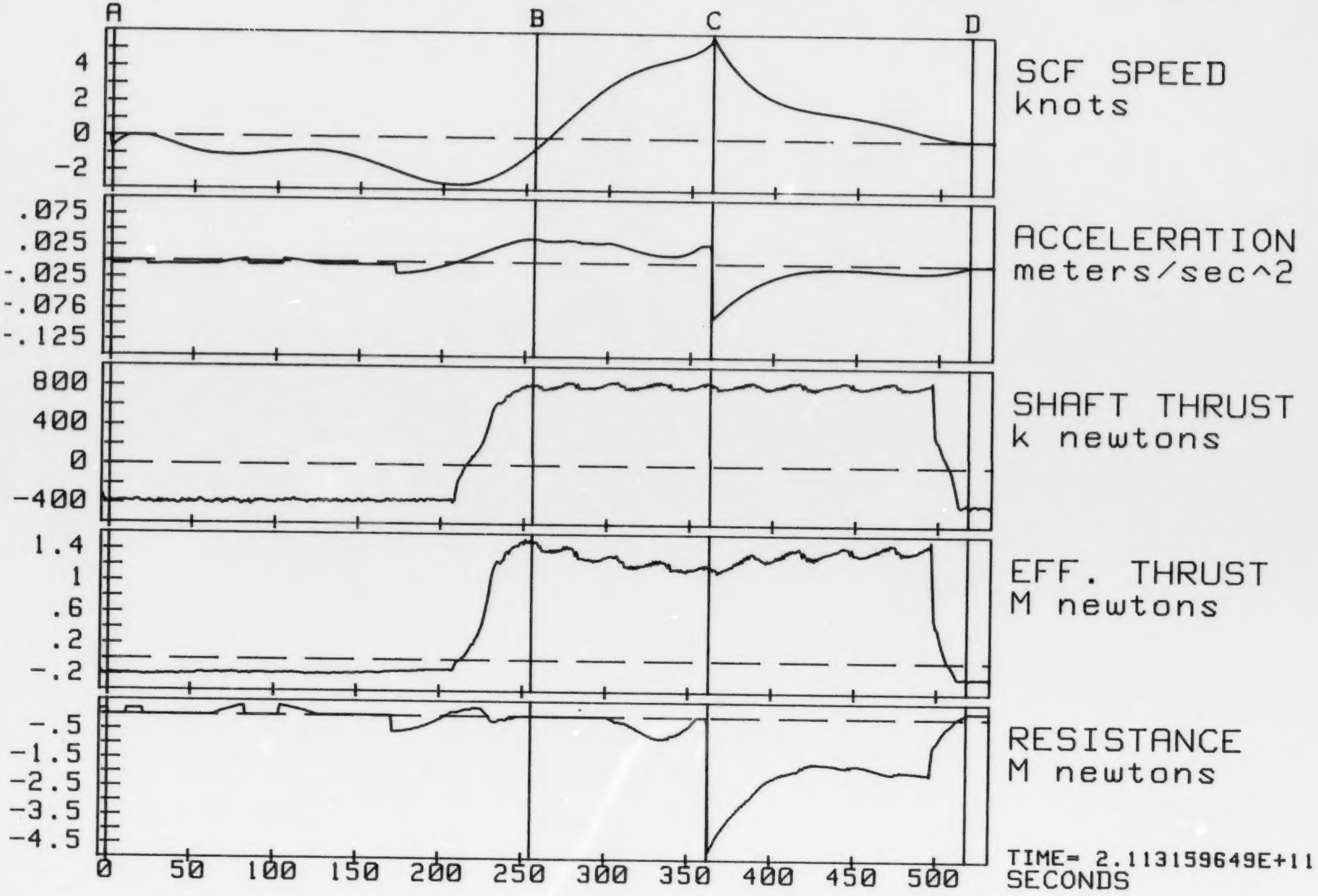

RAM # __B7   TAPE: 81-T2-3.1   07 JUL 1981 14:54:52   Fig.# 4

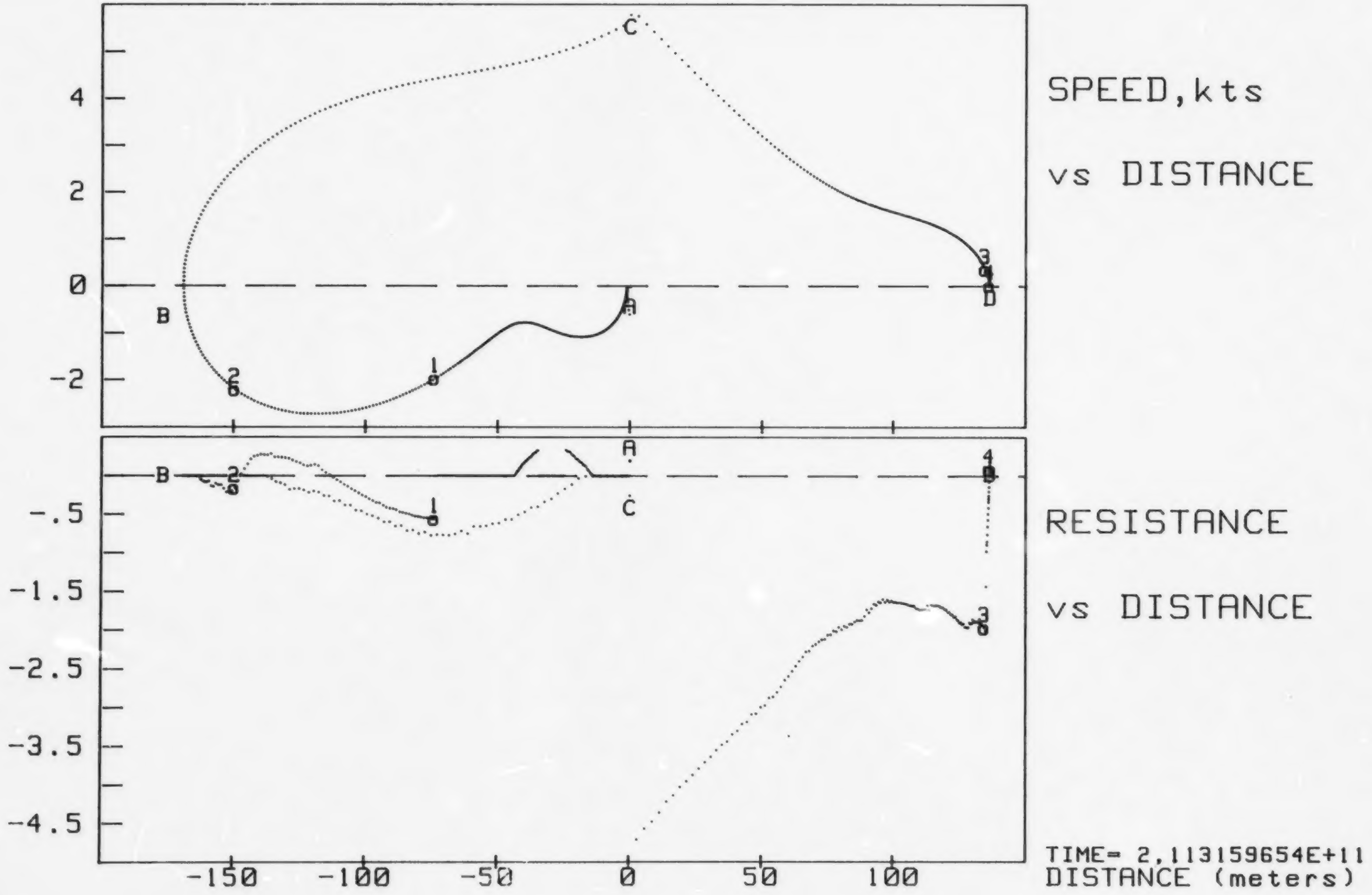

RAM # __B7 TAPE: 81-T2-3.1 07 JUL 1981 14:54:52 Fig.# 5

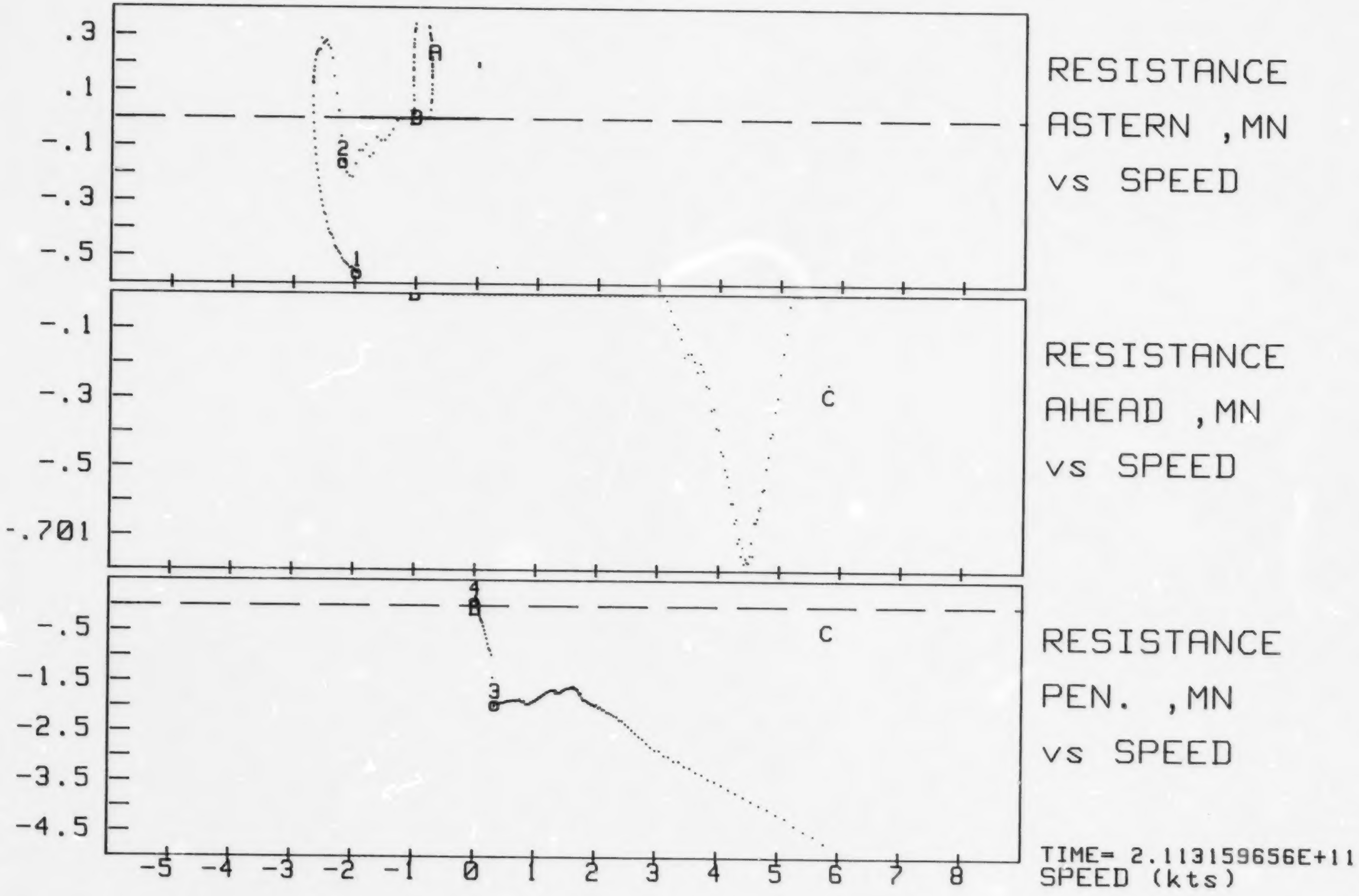

RESULTS OF RAMMING CYCLE ANALYSIS

RAM No. __B8

TAPE: 81-T2-3.1
CATEGORY: R1
QUALITY: 47BC
TRIM: EVEN TRIM

ICE CONDITIONS: RIDGES
ICE THICKNESS: 1.67 m
FLEXURAL STRENGTH: 163 kPA
BUBBLER STATUS: ON

RAMMING CYCLE CHARACTERISTICS:

Speed of Advance	(knots)	.144	
Speed of Impact	(knots)	5.5	(6.09)

	Duration (sec)	% Cycle Time	Distance (m)
Backing	263	58.6	-176.6
Acceleration	106	23.6	176.6
Penetration	46	10.2	15.2 (33.16)
Extraction	34	7.57	
Total Cycle	449		

Duration of Astern Mode	(sec)	169
Duration of Reversal to Ahead	(sec)	77
Duration of Ahead Mode	(sec)	157
Duration of Reversal to Astern	(sec)	17
Start of Reversal after Impact	(sec)	34

Total Fuel Used	(mm*hr)	5.05	Est. kg:	17.02
Average Fuel Rate	(mm)	40.47	Est. kg/hr:	136.5

Backing Power	(kW)	3250.6
[Est Fuel Rate	(kg/hr)]	740.42
Acceleration Power	(kW)	9388.3
[Est Fuel Rate	(kg/hr)]	1964.3

RAM # __B8 TAPE: 81-T2-3.1 07 JUL 1981 15:03:52 **FIG. #1**

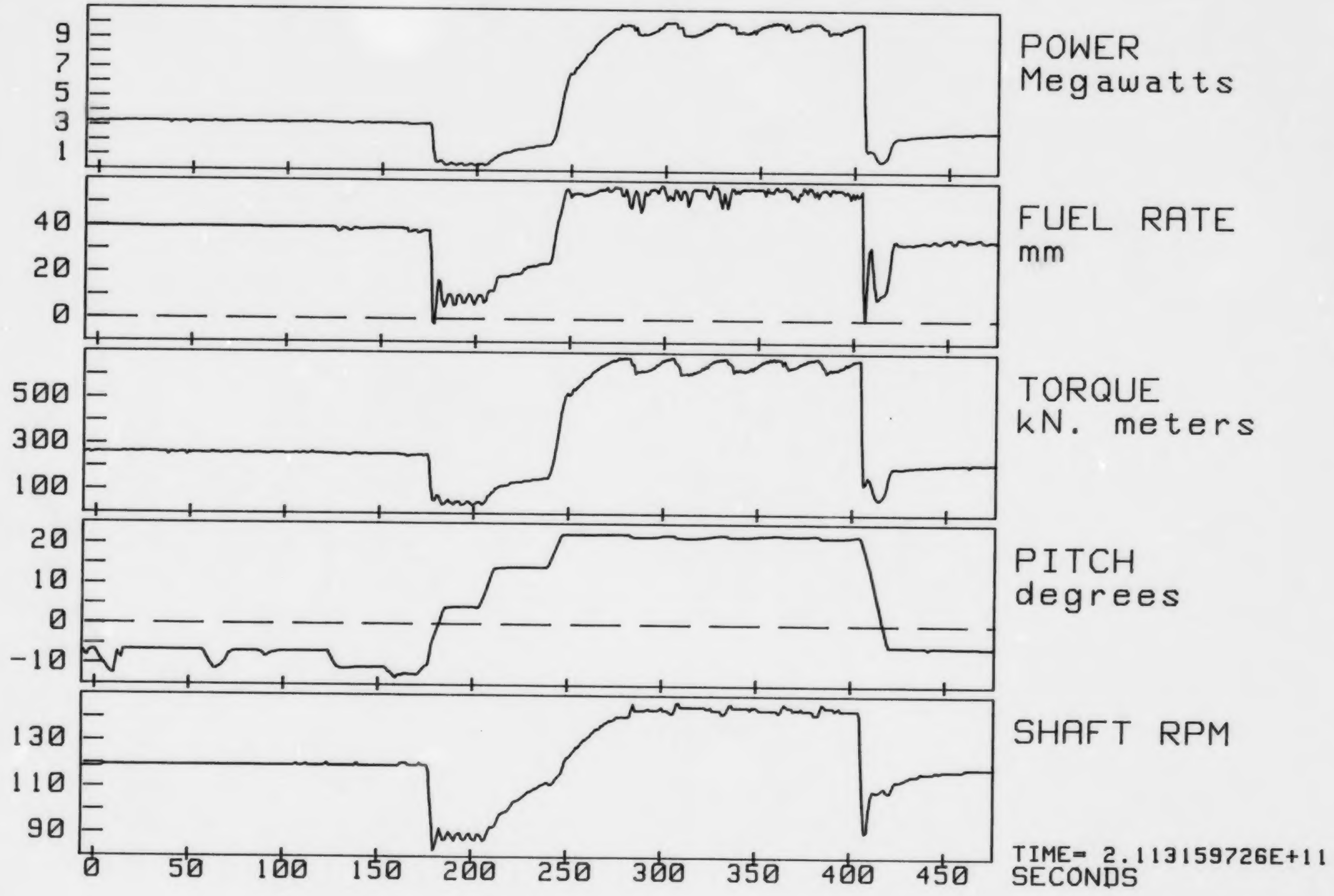

FIG. #2

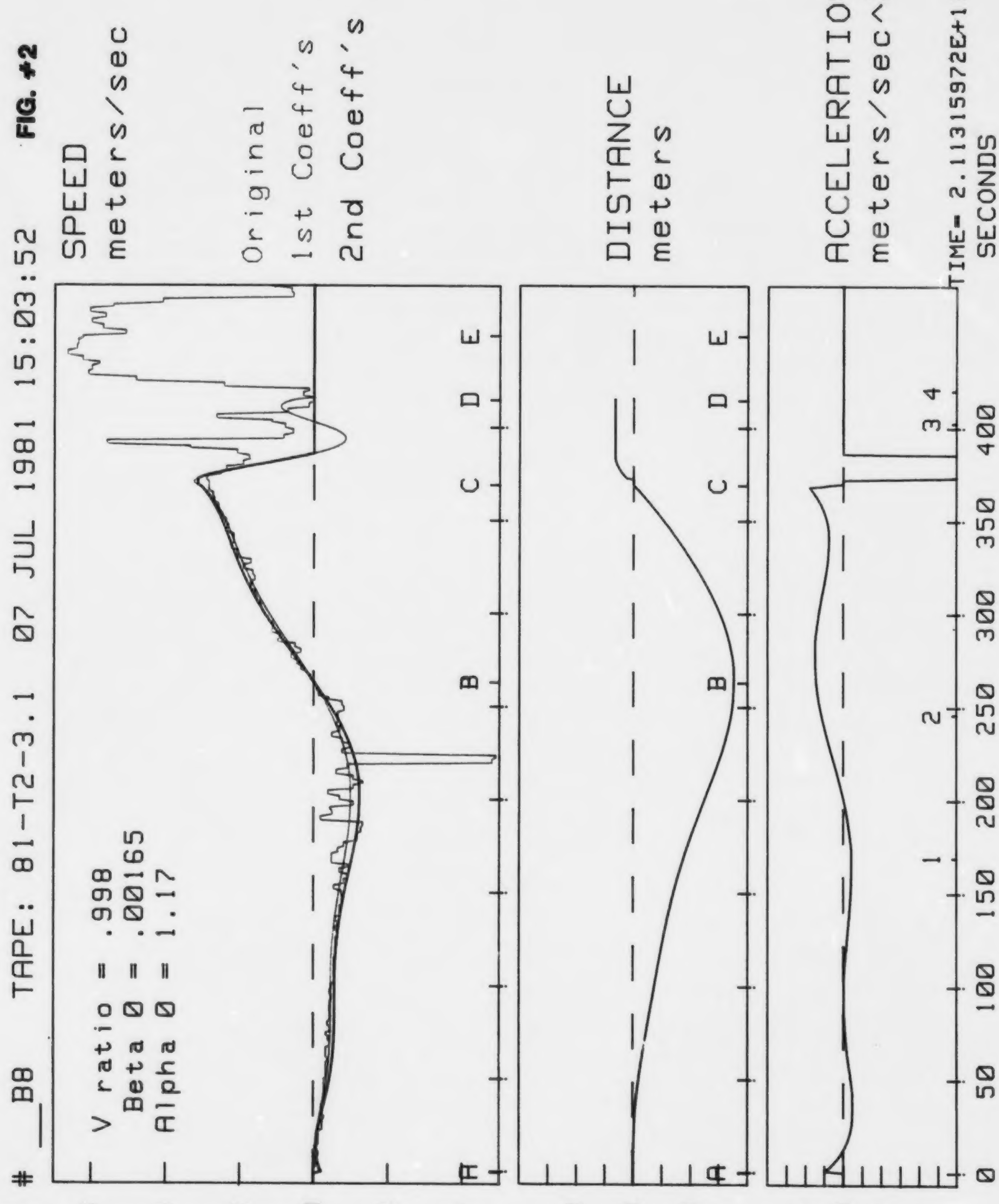
RAM # BB TAPE: 81-T2-3.1 07 JUL 1981 15:03:52
V ratio = .998
Beta 0 = .00165
Alpha 0 = 1.17
SPEED
meters/sec
Original
1st Coeff's
2nd Coeff's
6
4
2
0
-2
-4
A
B
C
D
E
DISTANCE
meters
100
0
-100
ACCELERATION
meters/sec^2
.05
0
-.05
-.1
1
2
3 4
0
50
100
150
200
250
300
350
400
TIME= 2.11315972E+11
SECONDS

RAM # __B8 TAPE: 81-T2-3.1 07 JUL 1981 15:03:52

FIG. #3

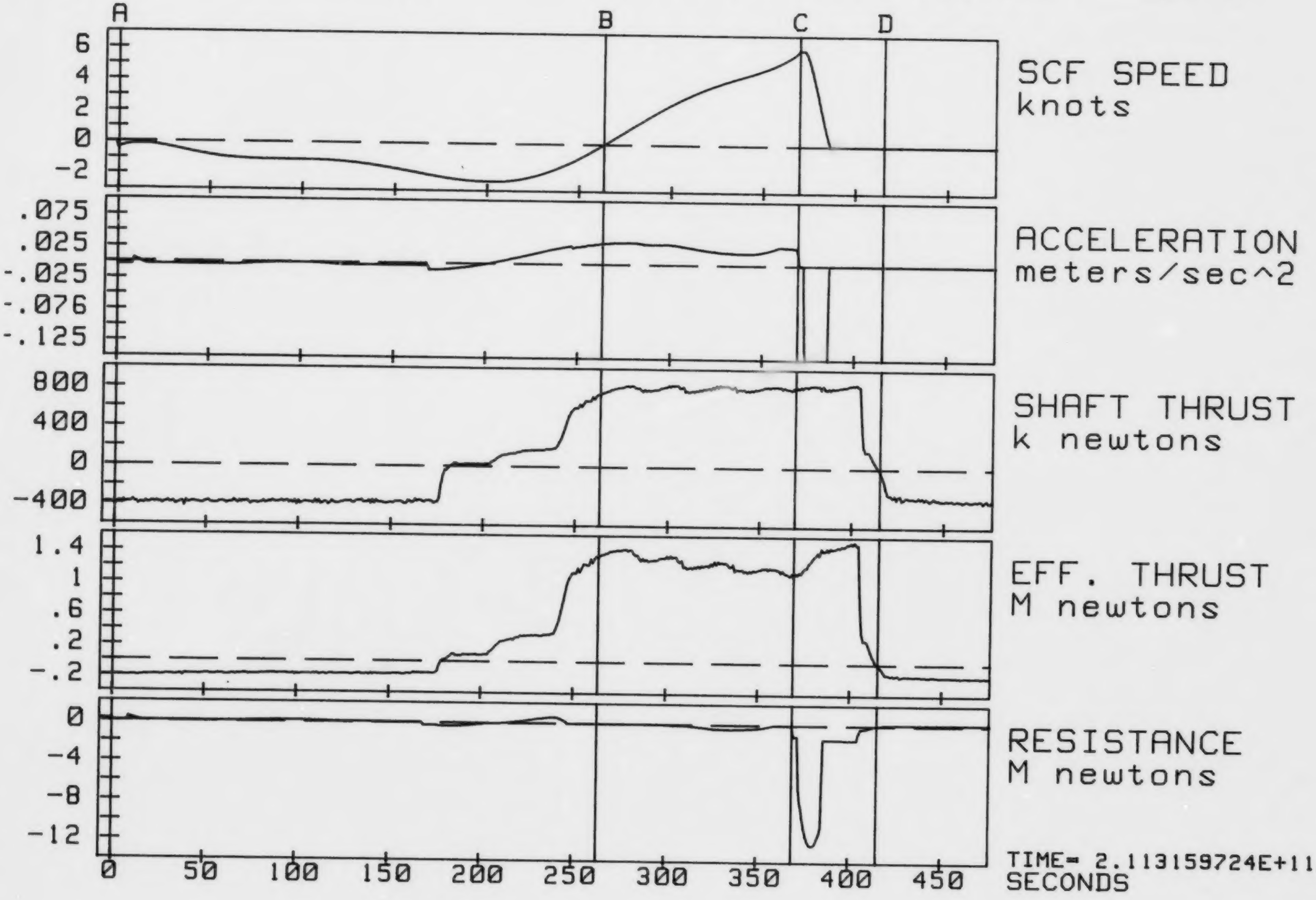

RAM # __B8 TAPE: 81-T2-3.1 07 JUL 1981 15:03:52 Fig.# 4

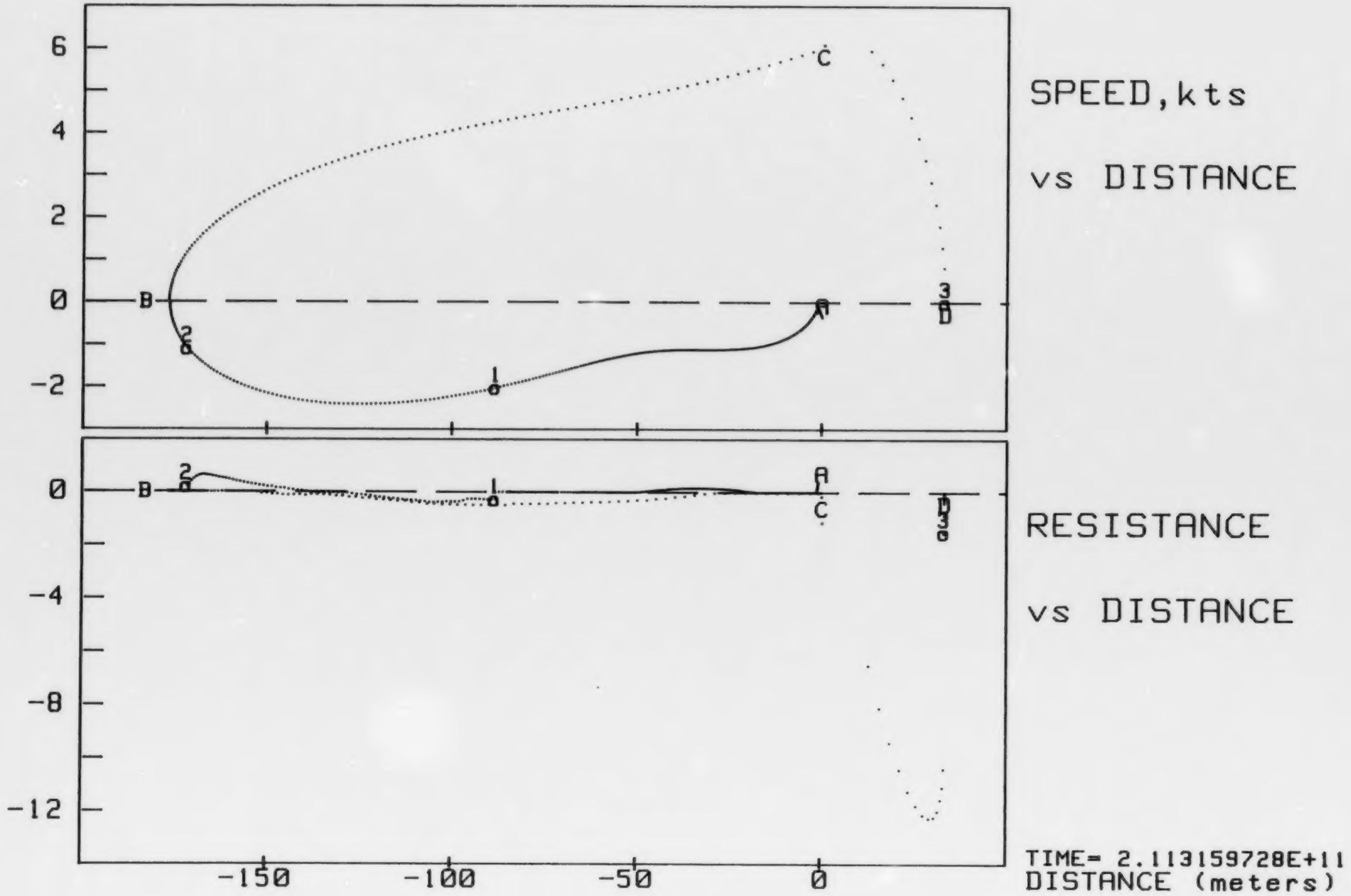

RAM # __B8   TAPE: 81-T2-3.1   07 JUL 1981 15:03:52   Fig.# 5

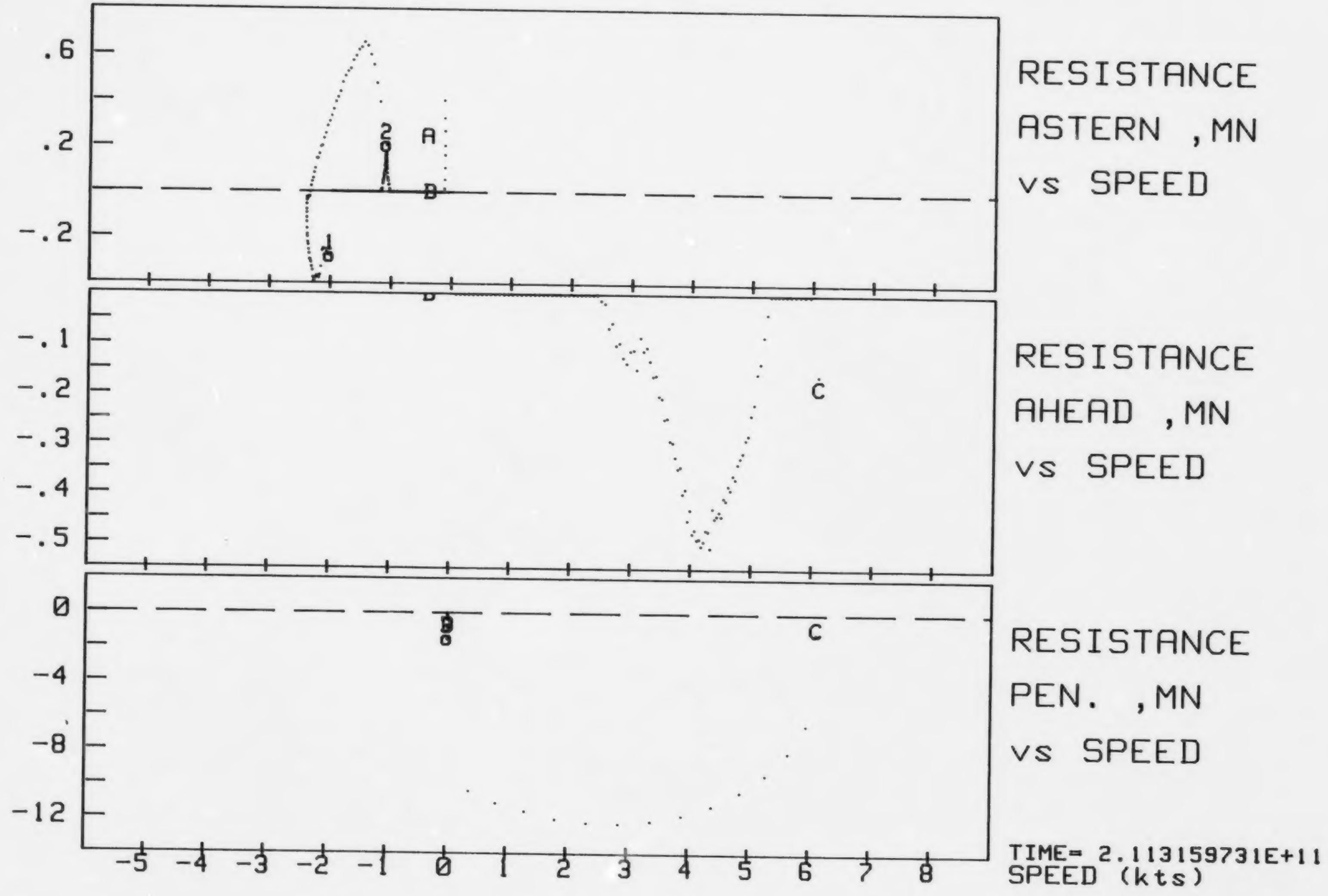

RESISTANCE ASTERN ,MN vs SPEED

RESISTANCE AHEAD ,MN vs SPEED

RESISTANCE PEN. ,MN vs SPEED

TIME= 2.113159731E+11

RESULTS OF RAMMING CYCLE ANALYSIS

RAM No. _B18

TAPE:	81-T2-4	ICE CONDITIONS:	LEVEL ICE
CATEGORY:	L1	ICE THICKNESS:	1.55 m
QUALITY:	54BD	FLEXURAL STRENGTH:	163 kPA
TRIM:	EVEN TRIM	BUBBLER STATUS:	ON

RAMMING CYCLE CHARACTERISTICS:

Speed of Advance	(knots)	.487
Speed of Impact	(knots)	5 (5.17)

	Duration (sec)	% Cycle Time	Distance (m)
Backing	248	45.8	-149.9
Acceleration	111	20.5	149.9
Penetration	157	29	142.4 (135.7)
Extraction	26	4.8	
Total Cycle	542		

Duration of Astern Mode	(sec)	177
Duration of Reversal to Ahead	(sec)	71
Duration of Ahead Mode	(sec)	271
Duration of Reversal to Astern	(sec)	23
Start of Reversal after Impact	(sec)	160

Total Fuel Used	(mm*hr)	7.43	Est. kg:	116.6
Average Fuel Rate	(mm)	49.32	Est. kg/hr:	774.17

Backing Power	(kW)	4669.6
[Est Fuel Rate	(kg/hr)]	1023.4

Acceleration Power	(kW)	9564.9
[Est Fuel Rate	(kg/hr)]	1999.5

RAM # _B18   TAPE: 81-T2-4   07 JUL 1981 18:18:36   **FIG. #1**

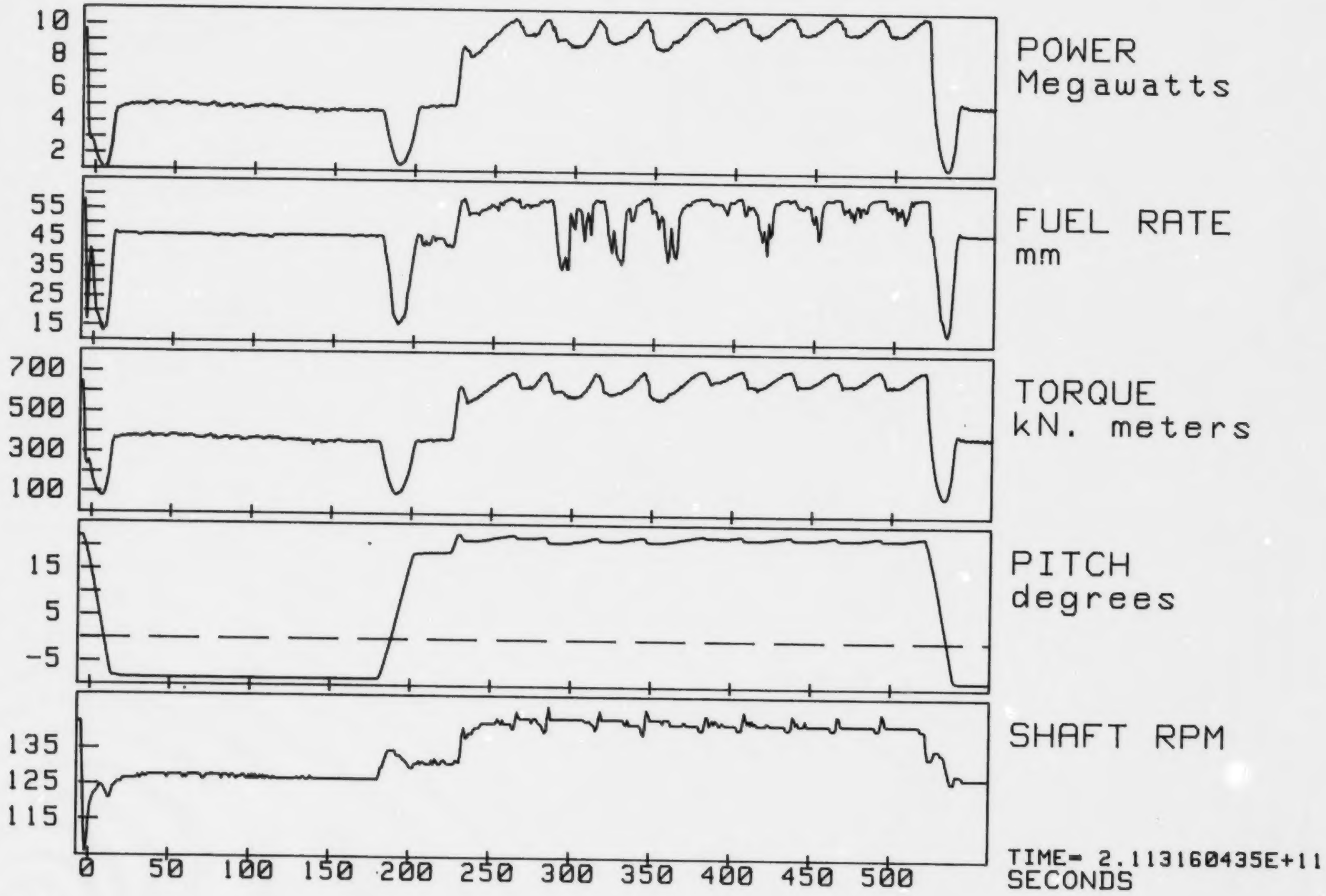

RAM # _B18 TAPE: 81-T2-4 07 JUL 1981 18:18:36

FIG. #2

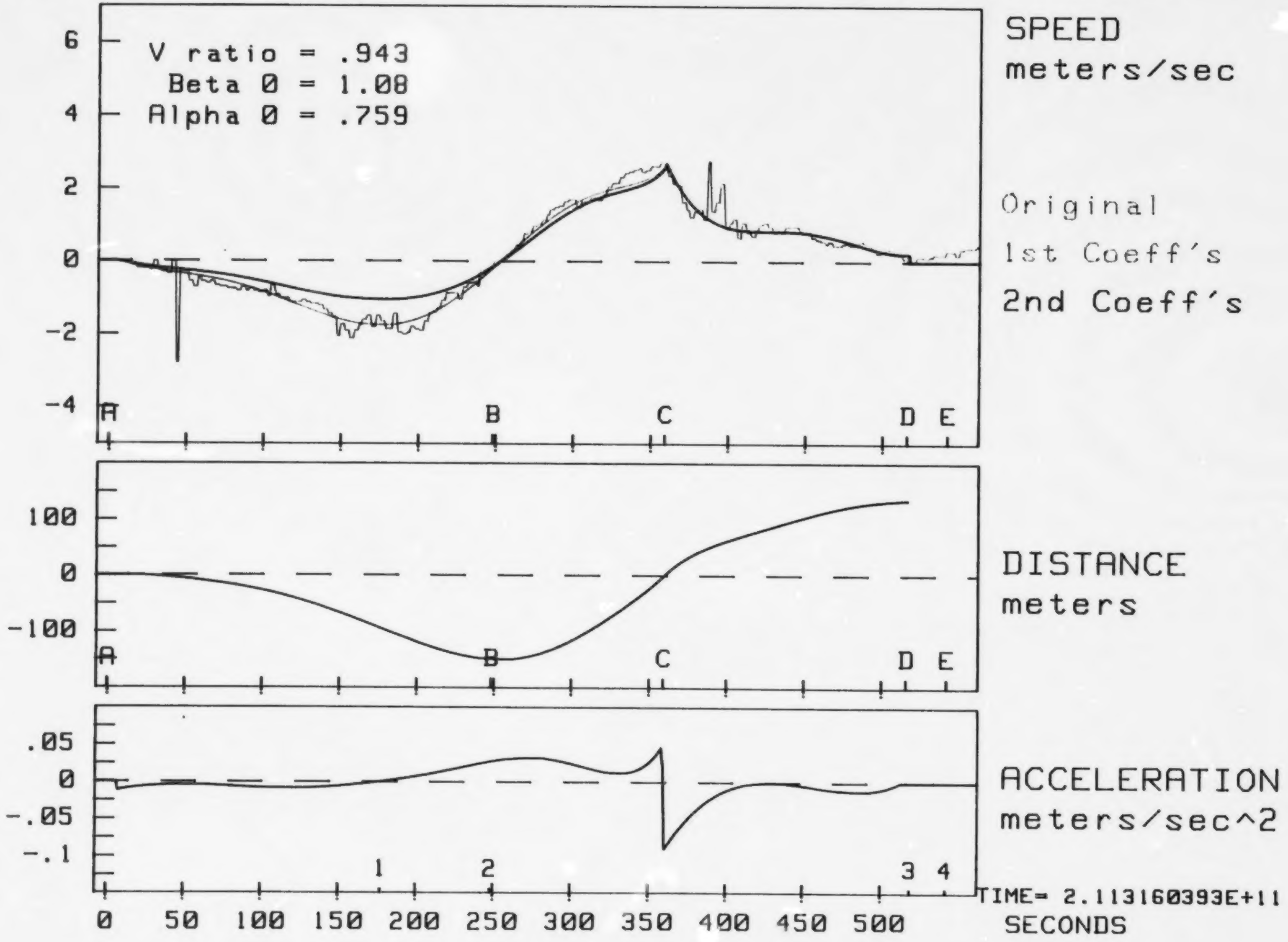

RAM # _B18 TAPE: 81-T2-4 07 JUL 1981 18:18:36

FIG. #3

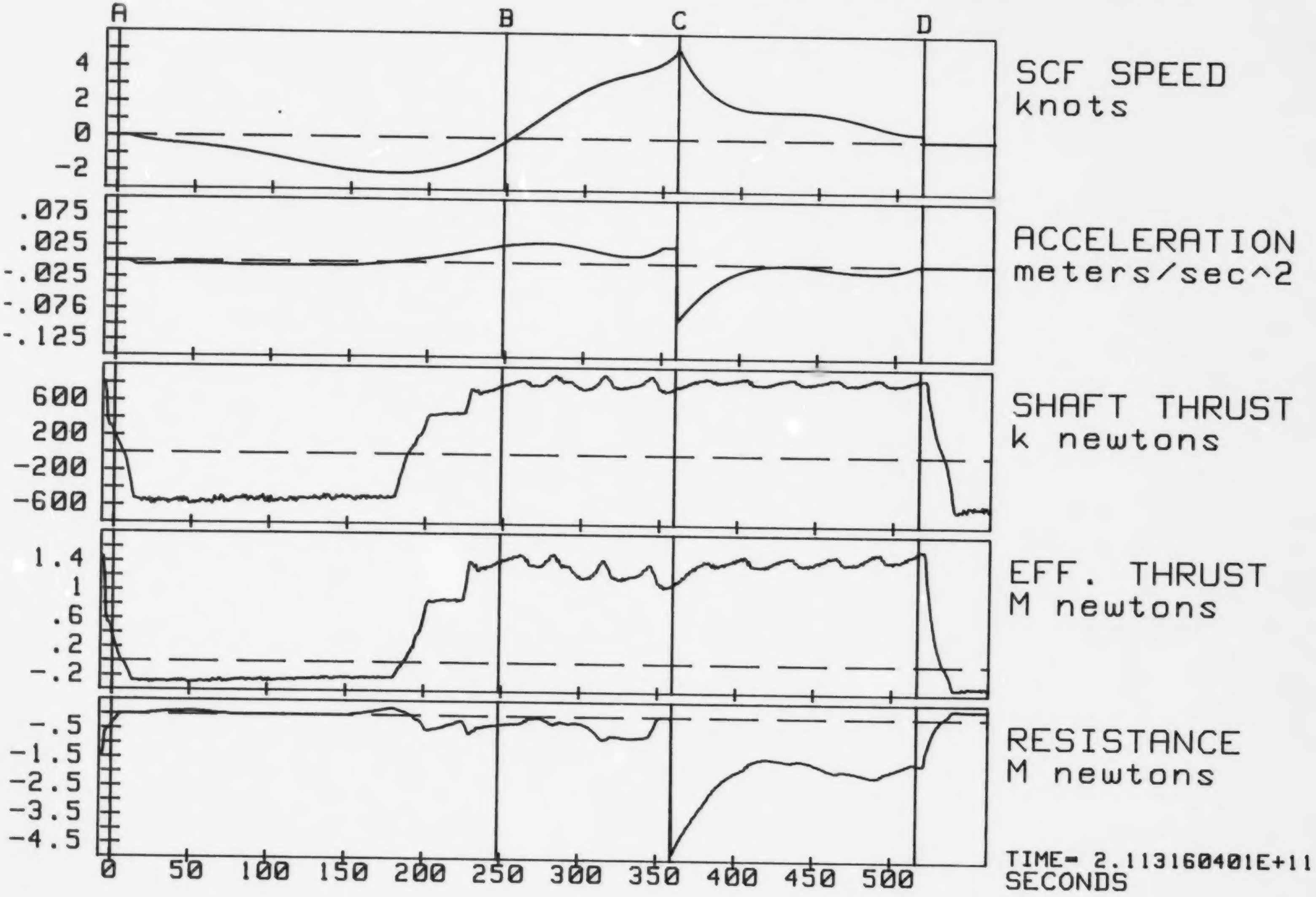

RAM # _B18   TAPE: 81-T2-4   07 JUL 1981 18:18:36   Fig.# 4

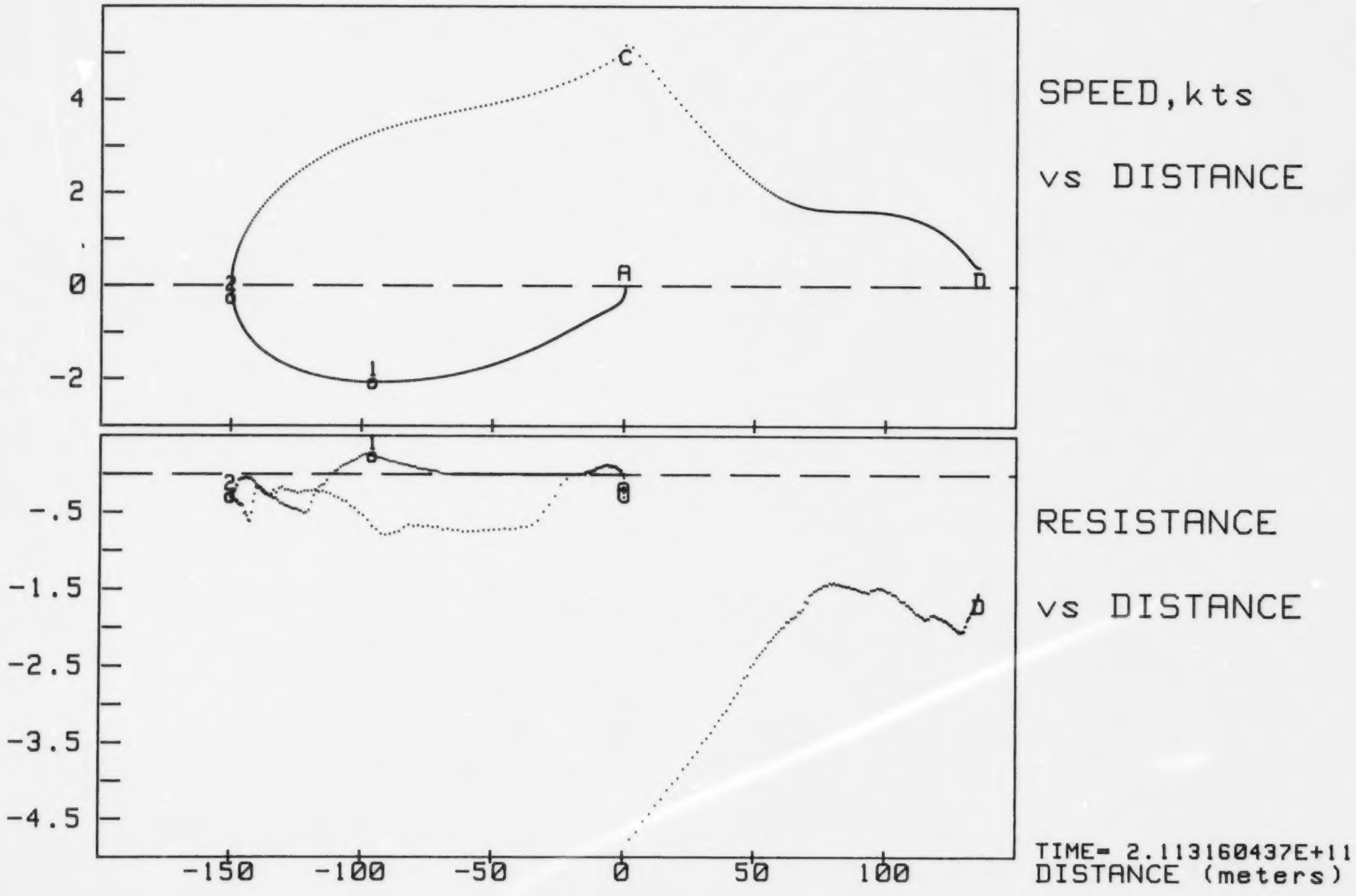

RAM # _B18   TAPE: 81-T2-4   07 JUL 1981 18:18:36   Fig.# 5

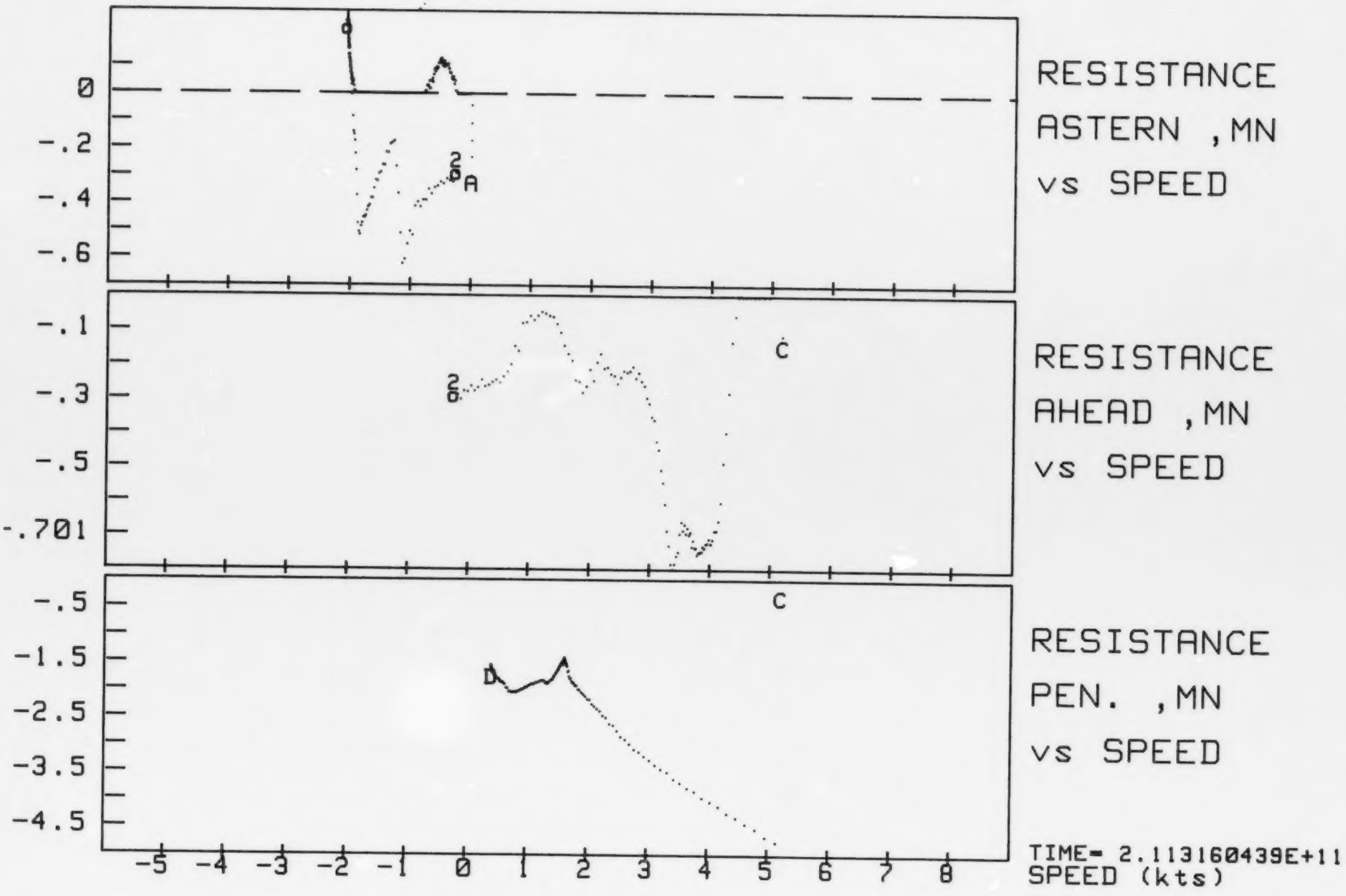

RESULTS OF RAMMING CYCLE ANALYSIS

RAM No. _B19

TAPE:	81-T2-4	ICE CONDITIONS:	LEVEL ICE
CATEGORY:	L1	ICE THICKNESS:	1.4 m
QUALITY:	31BB	FLEXURAL STRENGTH:	163 kPA
TRIM:	EVEN TRIM	BUBBLER STATUS:	ON

RAMMING CYCLE CHARACTERISTICS:

Speed of Advance (knots) .414

Speed of Impact (knots) 5 (5.21)

	Duration (sec)	% Cycle Time	Distance (m)
Backing	241	51.1	-125.4
Acceleration	100	21.2	125.4
Penetration	115	24.4	93.9 (100.6)
Extraction	16	3.39	
Total Cycle	472		

Duration of Astern Mode	(sec)	181
Duration of Reversal to Ahead	(sec)	23
Duration of Ahead Mode	(sec)	250
Duration of Reversal to Astern	(sec)	15
Start of Reversal after Impact	(sec)	113

Total Fuel Used	(mm*hr)	6.47	Est. kg:	102.1
Average Fuel Rate	(mm)	49.38	Est. kg/hr:	778.76

Backing Power	(kW)	4950.6
[Est Fuel Rate	(kg/hr)]	1079.4
Acceleration Power	(kW)	8700.3
[Est Fuel Rate	(kg/hr)]	1827.1

RAM # _B19 TAPE: 81-T2-4 07 JUL 1981 18:27:06

FIG. #1

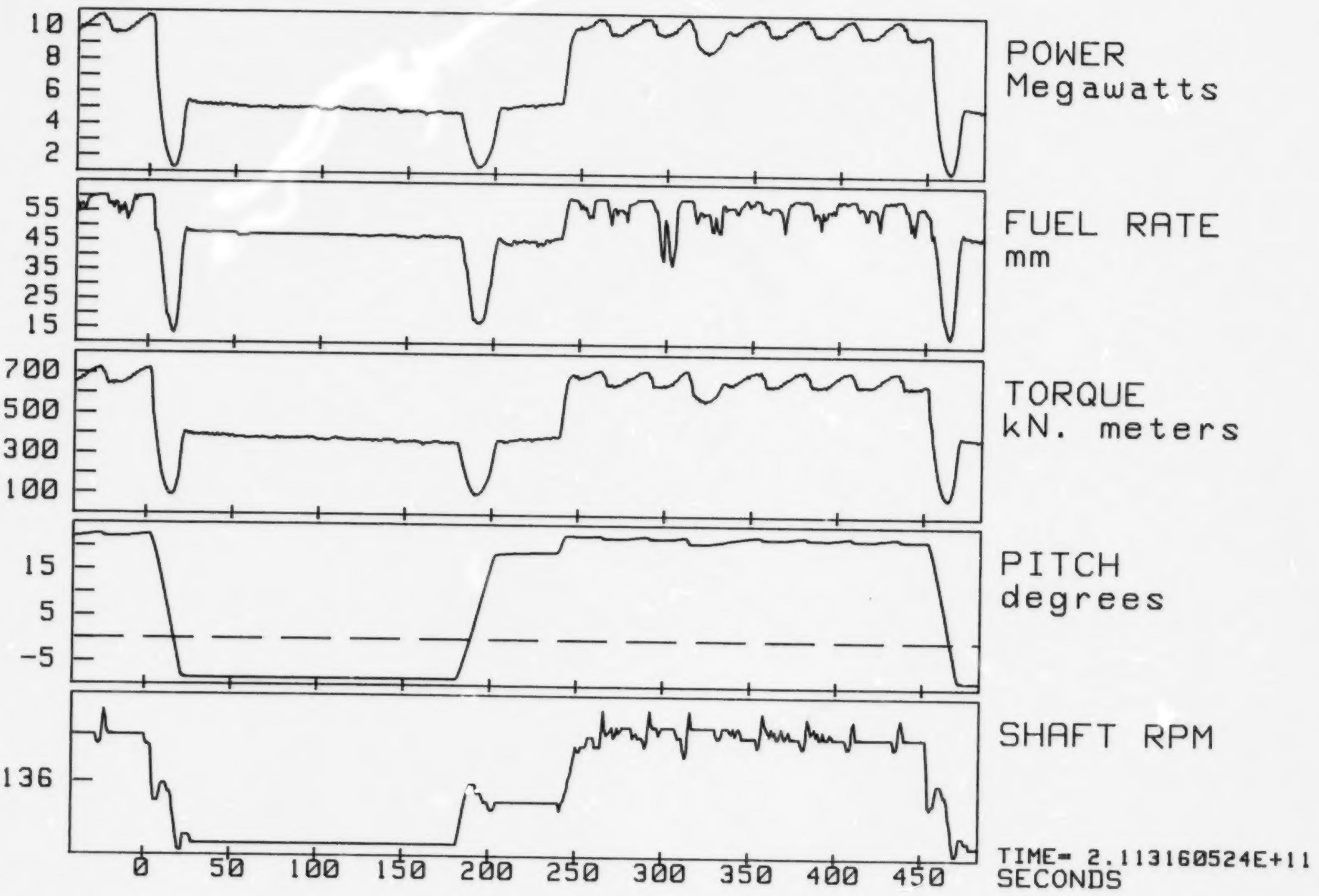

RAM # _B19 TAPE: 81-T2-4 07 JUL 1981 18:27:06

FIG. #2

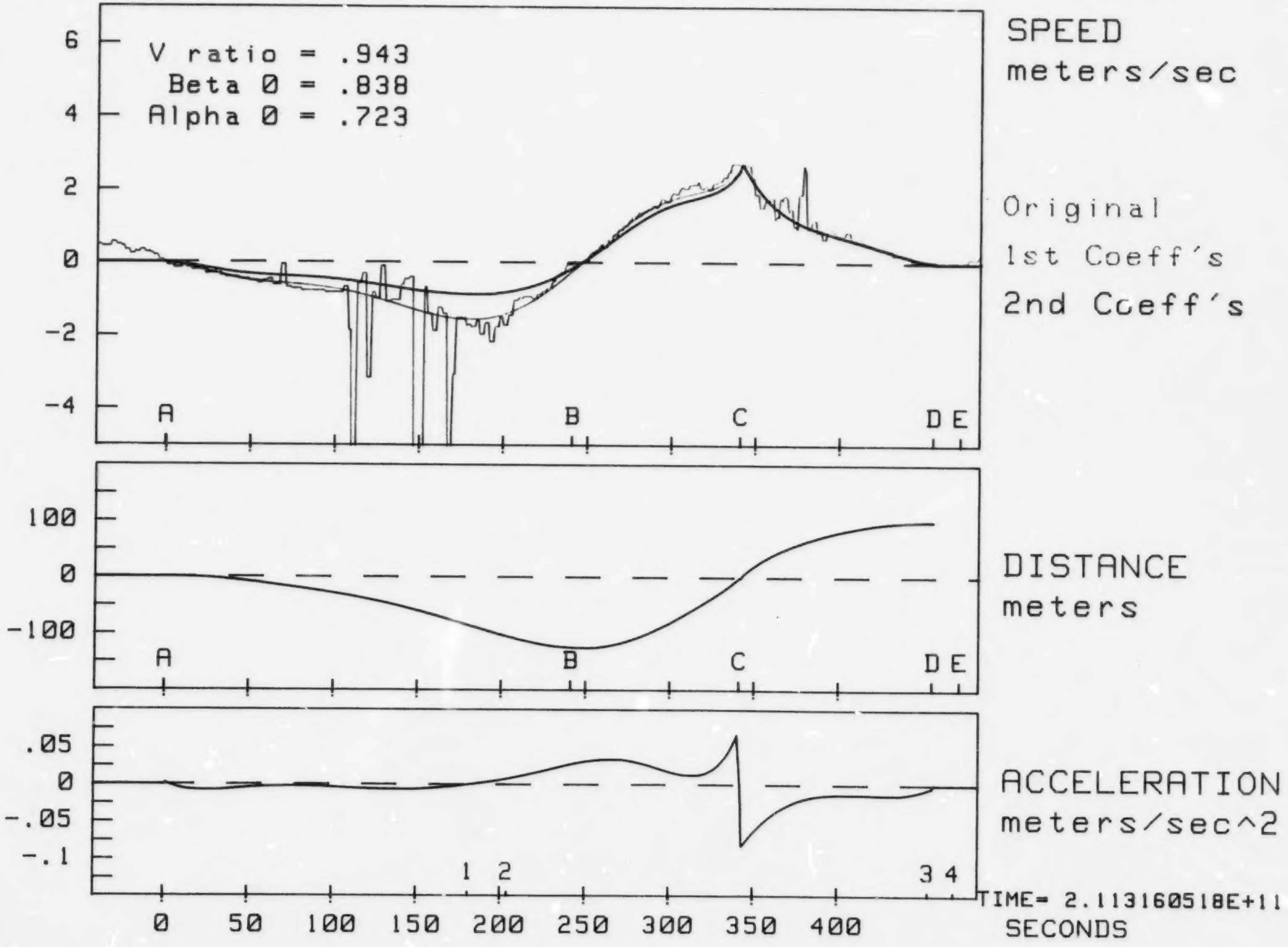

RAM # _B19 TAPE: 81-T2-4 07 JUL 1981 18:27:06

FIG. #3

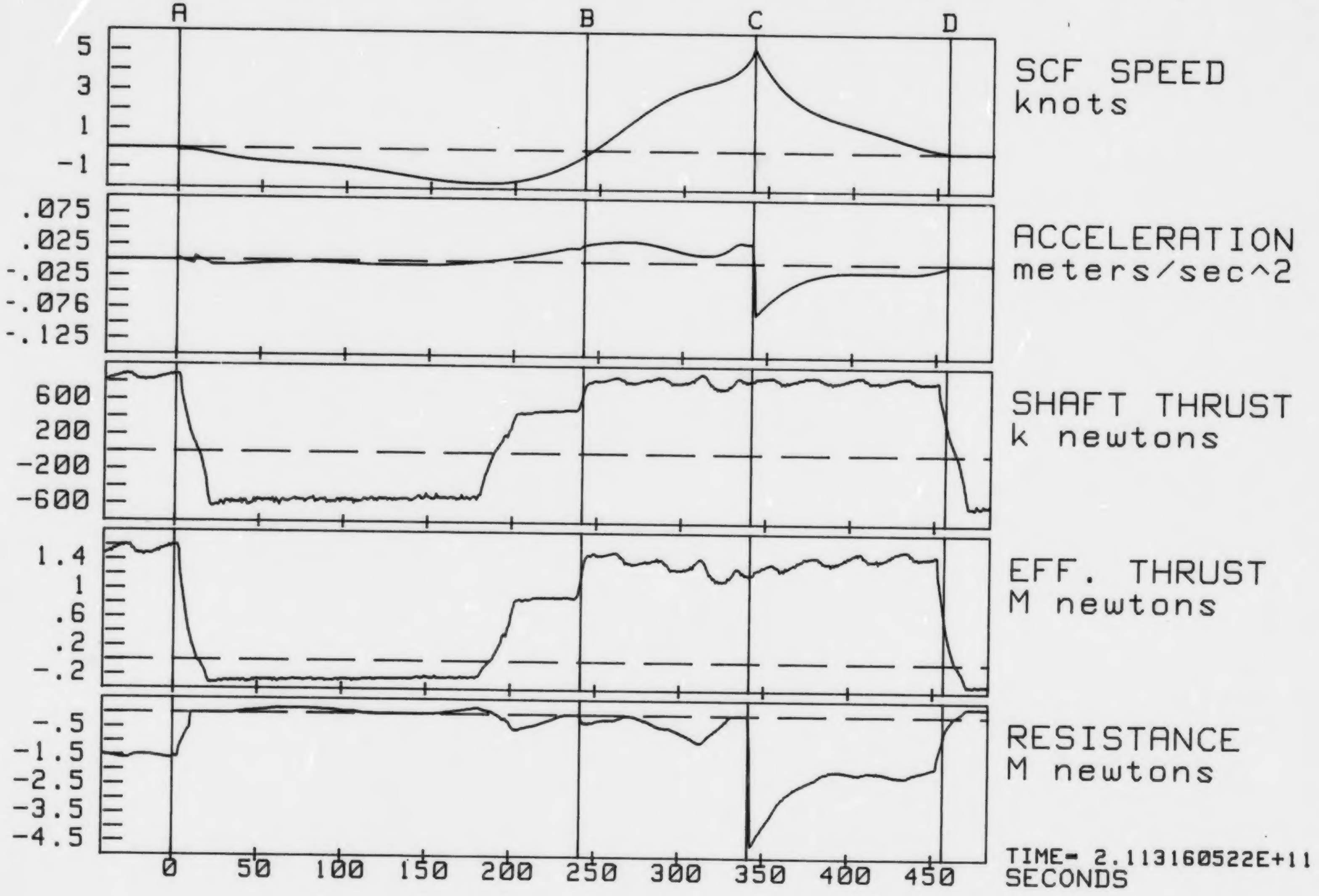

RAM # _B19   TAPE: 81-T2-4   07 JUL 1981 18:27:06   Fig.# 4

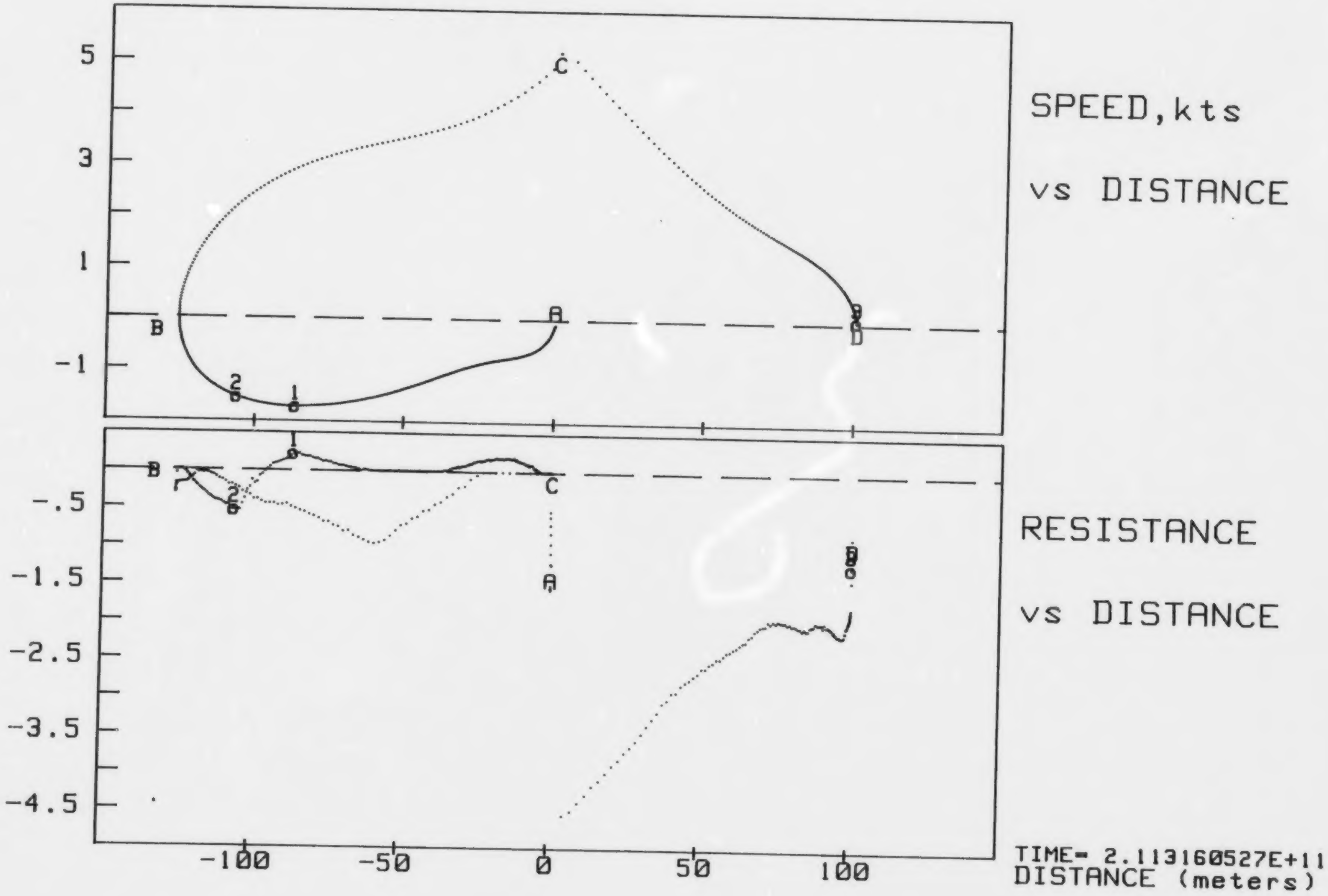

RAM # _B19 TAPE: 81-T2-4 07 JUL 1981 18:27:06 Fig.# 5

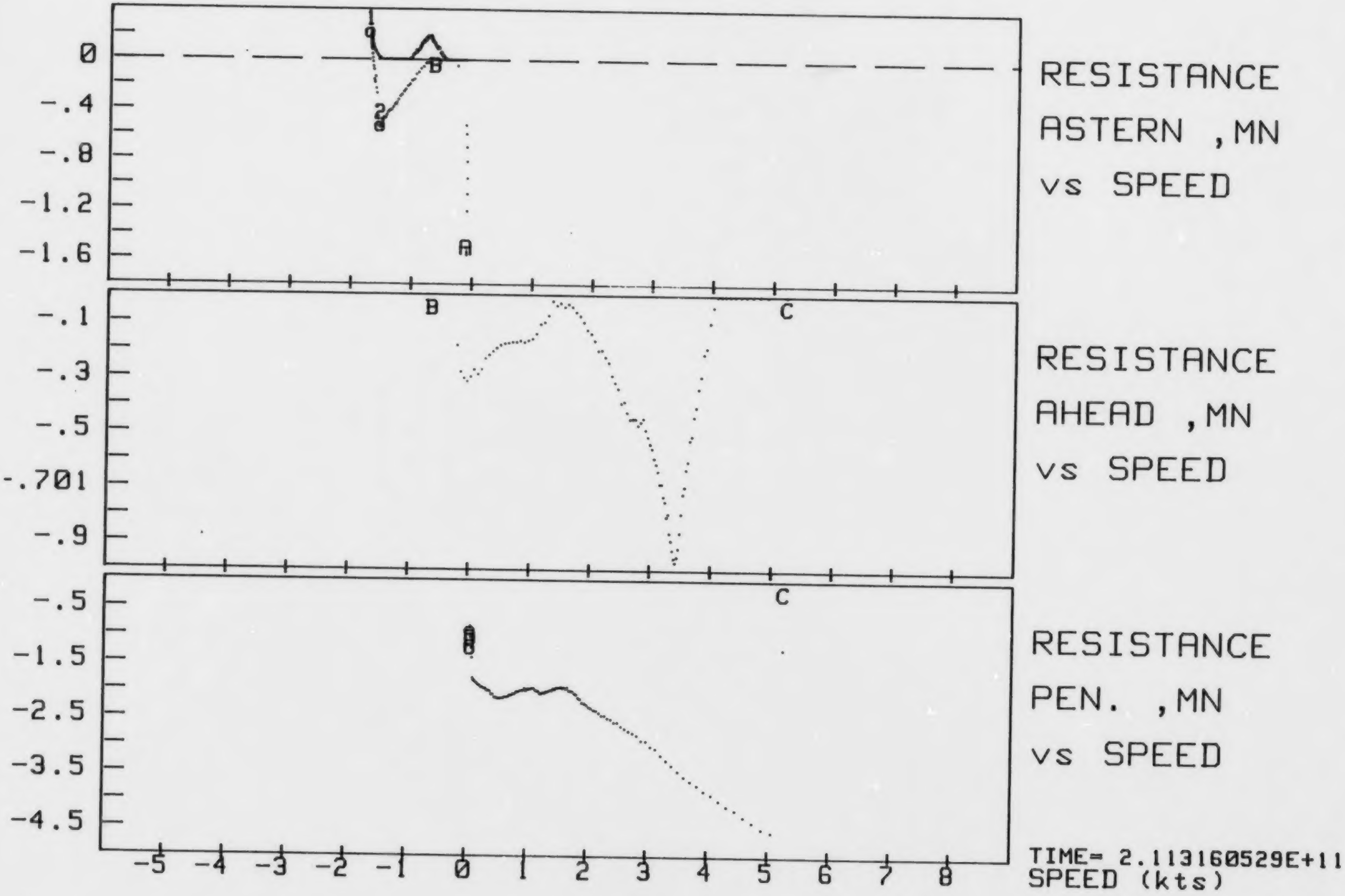

RESULTS OF RAMMING CYCLE ANALYSIS

RAM No. _B20

TAPE:	81-T2-4	ICE CONDITIONS:	LEVEL ICE
CATEGORY:	L1	ICE THICKNESS:	1.5 m
QUALITY:	68BD	FLEXURAL STRENGTH:	163 kPA
TRIM:	EVEN TRIM	BUBBLER STATUS:	ON

RAMMING CYCLE CHARACTERISTICS:

Speed of Advance	(knots)	.391	
Speed of Impact	(knots)	5.8	(5.94)

	Duration (sec)	% Cycle Time	Distance (m)
Backing	157	49.1	-161.9
Acceleration	100	31.3	161.9
Penetration	57	17.8	51.5 (64.44)
Extraction	6	1.88	
Total Cycle	320		

Duration of Astern Mode	(sec)	90
Duration of Reversal to Ahead	(sec)	51
Duration of Ahead Mode	(sec)	116
Duration of Reversal to Astern	(sec)	62
Start of Reversal after Impact	(sec)	0

Total Fuel Used	(mm*hr)	3.73	Est. kg:	21.37
Average Fuel Rate	(mm)	41.92	Est. kg/hr:	240.46

Backing Power	(kW)	4901.2
[Est Fuel Rate	(kg/hr)]	1069.6

Acceleration Power	(kW)	10091
[Est Fuel Rate	(kg/hr)]	2104.3

RAM # _B20 TAPE: 81-T2-4 07 JUL 1981 18:36:35

FIG. #1

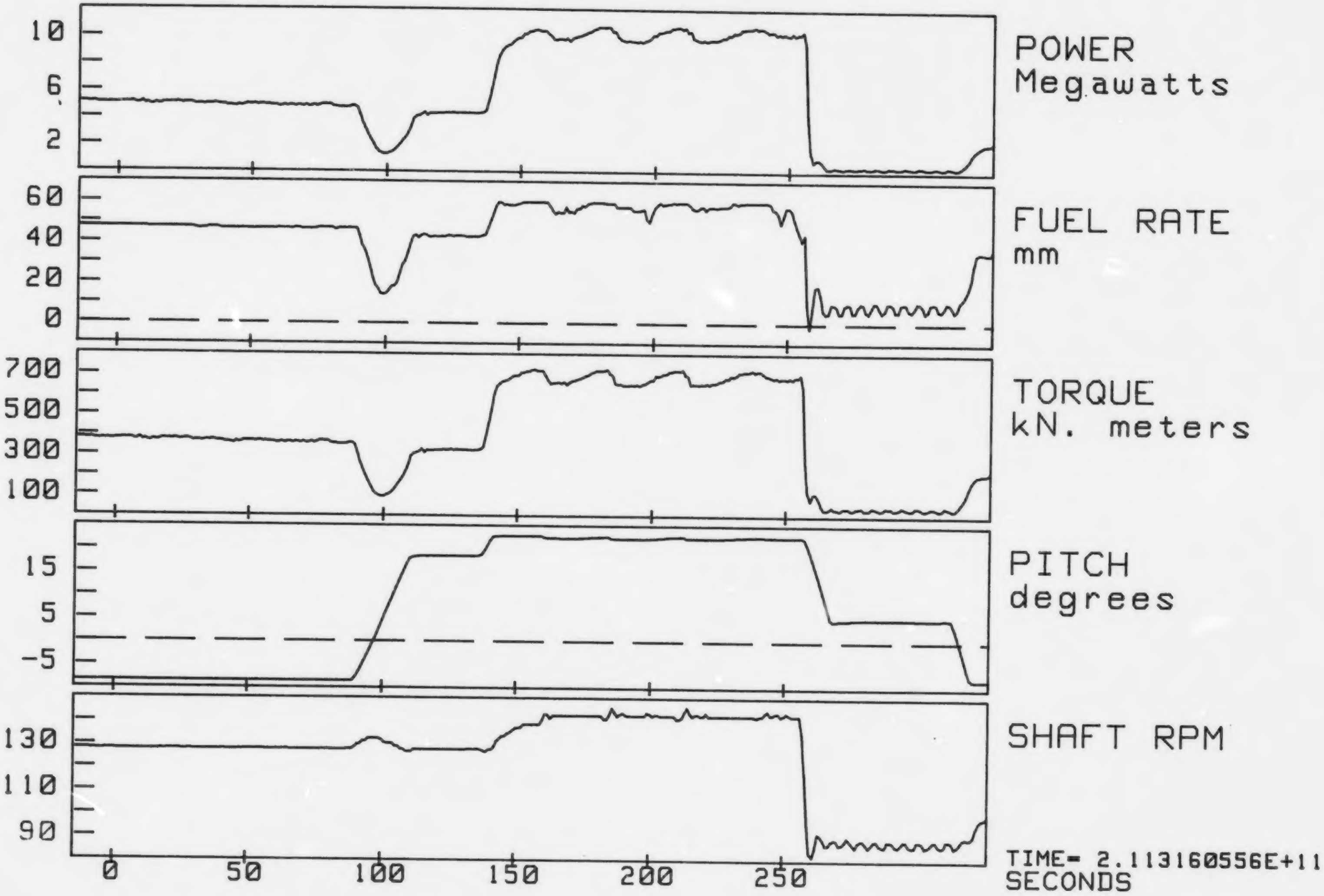

RAM # _B20 TAPE: 81-T2-4 07 JUL 1981 18:36:35

FIG. #2

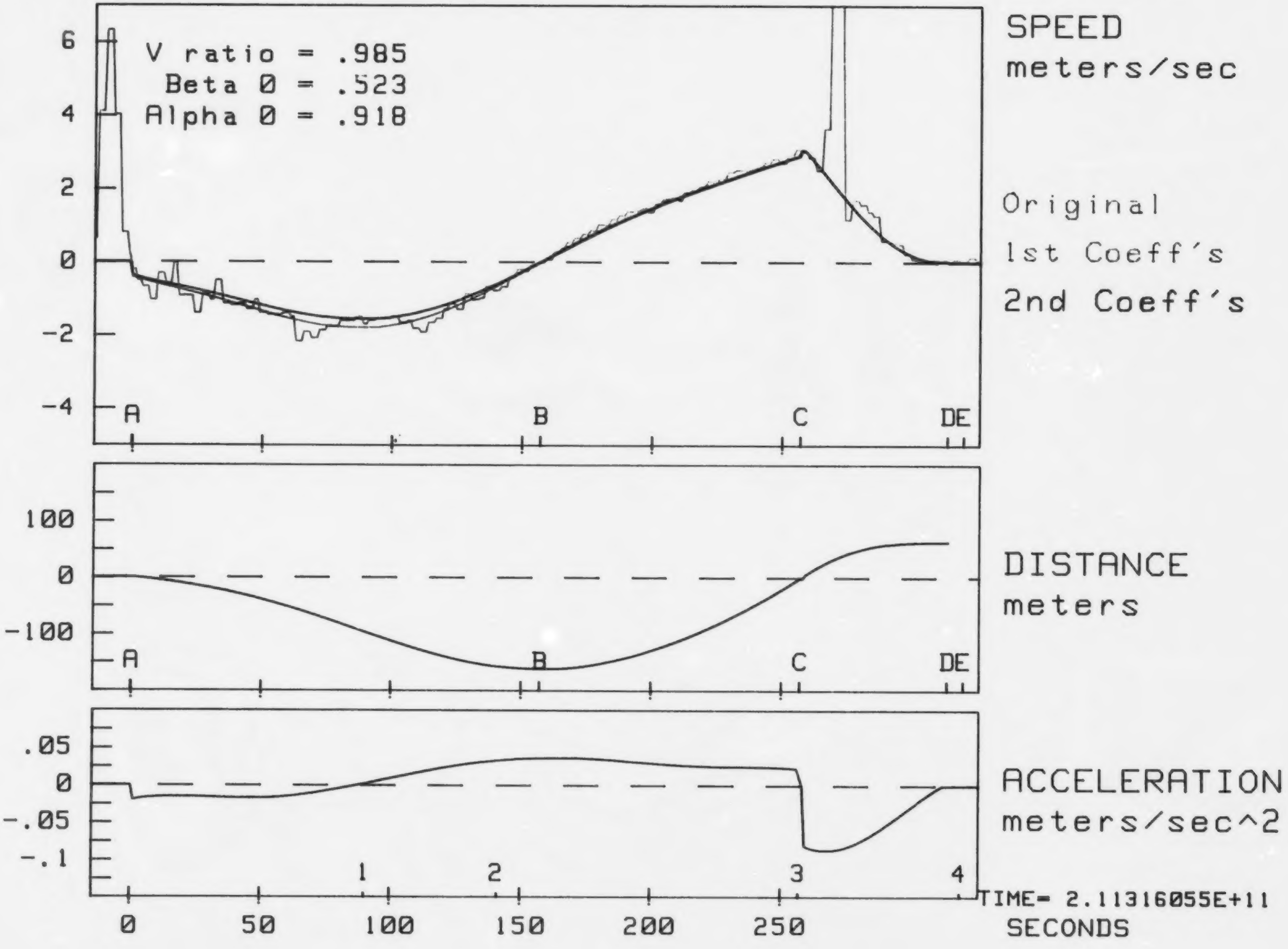

RAM # _B20 TAPE: 81-T2-4 07 JUL 1981 18:36:35

FIG. #3

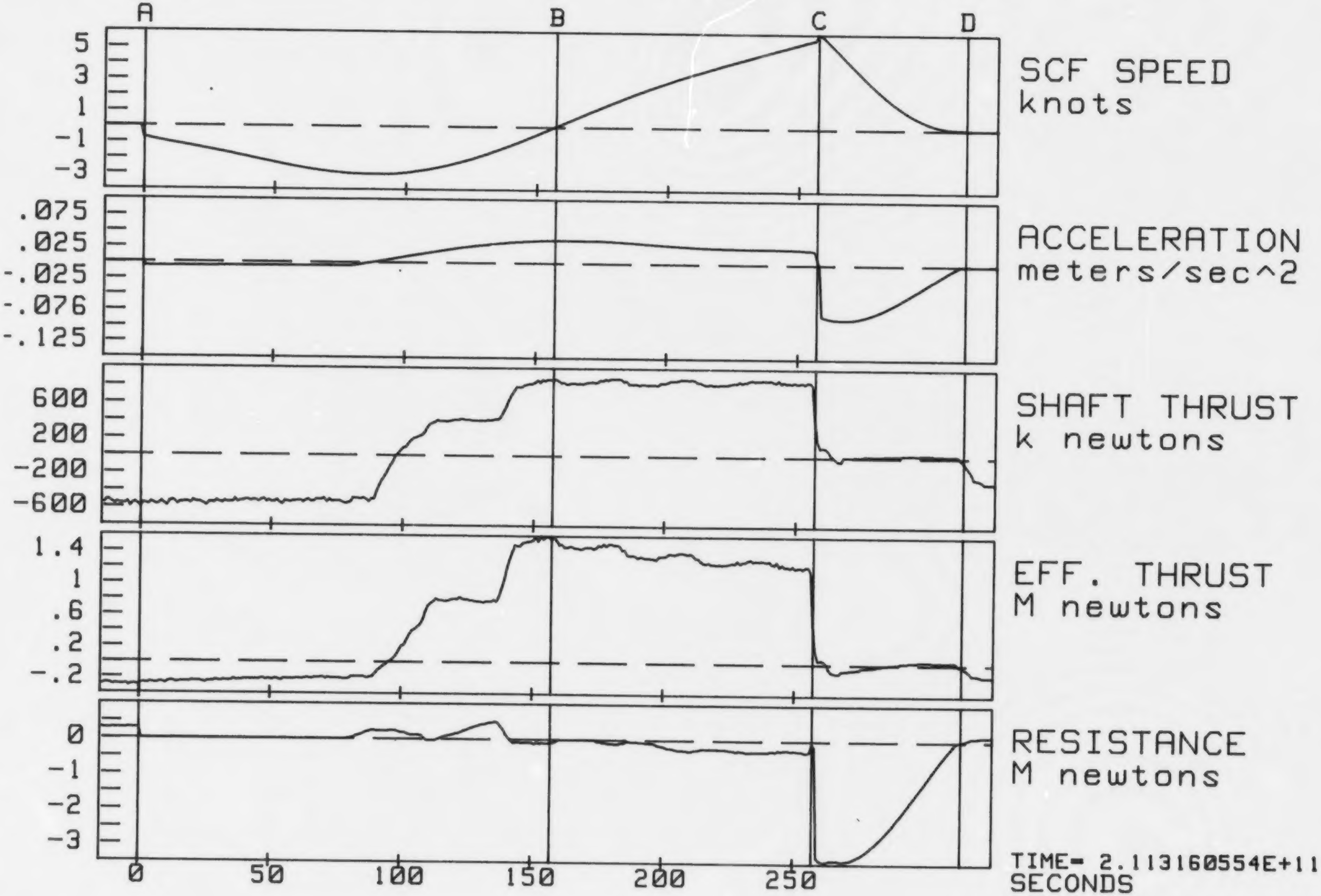

RAM # _B20 TAPE: 81-T2-4 07 JUL 1981 18:36:35 Fig.# 4

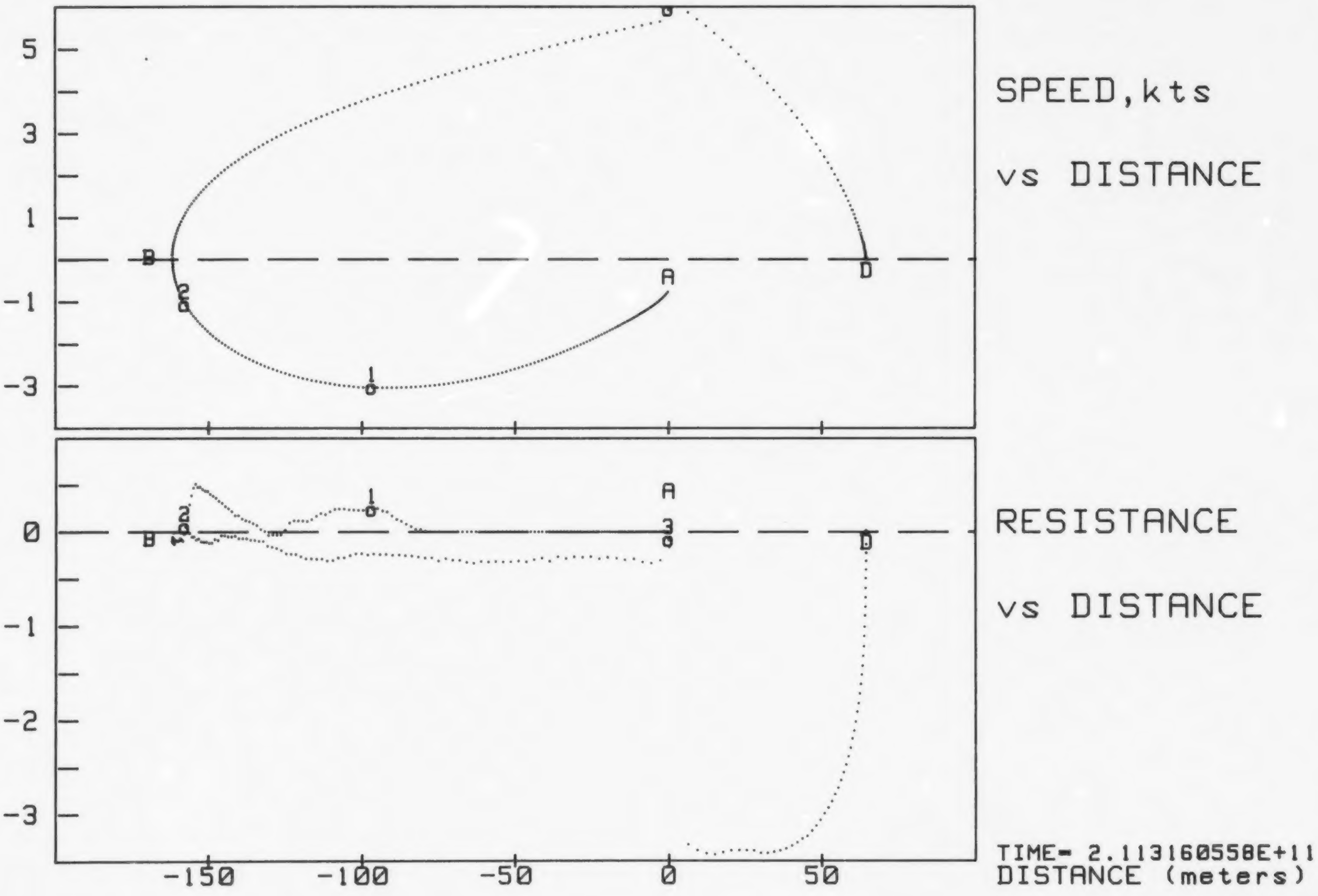

RAM # _B20 TAPE: 81-T2-4 07 JUL 1981 18:36:35 Fig.# 5

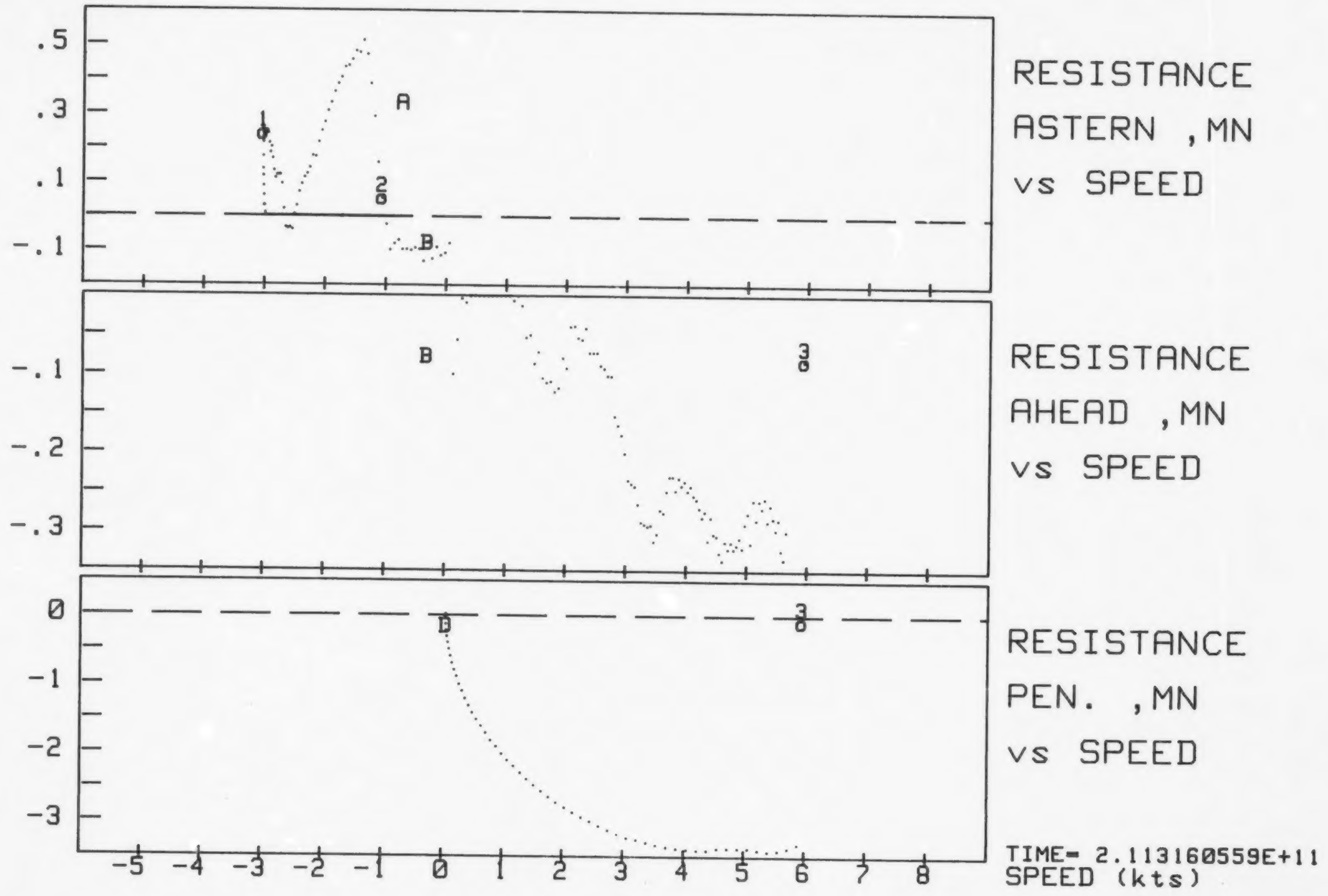

RESULTS OF RAMMING CYCLE ANALYSIS

RAM No. _B21

TAPE:	81-T2-4	ICE CONDITIONS:	LEVEL ICE
CATEGORY:	L1	ICE THICKNESS:	1.65 m
QUALITY:	47BC	FLEXURAL STRENGTH:	163 kPA
TRIM:	EVEN TRIM	BUBBLER STATUS:	ON

RAMMING CYCLE CHARACTERISTICS:

Speed of Advance	(knots)	.656	
Speed of Impact	(knots)	5.5	(5.67)

	Duration (sec)	% Cycle Time	Distance (m)
Backing	258	47.3	-152.3
Acceleration	111	20.3	152.3
Penetration	156	28.6	175.8 (184.2)
Extraction	21	3.85	
Total Cycle	546		

Duration of Astern Mode	(sec)	192		
Duration of Reversal to Ahead	(sec)	58		
Duration of Ahead Mode	(sec)	290		
Duration of Reversal to Astern	(sec)	6		
Start of Reversal after Impact	(sec)	171		
Total Fuel Used	(mm*hr)	7.59	Est. kg:	125.2
Average Fuel Rate	(mm)	50.04	Est. kg/hr:	825.78
Backing Power	(kW)	4187.7		
[Est Fuel Rate	(kg/hr)]	927.28		
Acceleration Power	(kW)	9940.6		
[Est Fuel Rate	(kg/hr)]	2074.4		

RAM # _B21 TAPE: 81-T2-4 07 JUL 1981 18:40:00 **FIG. #1**

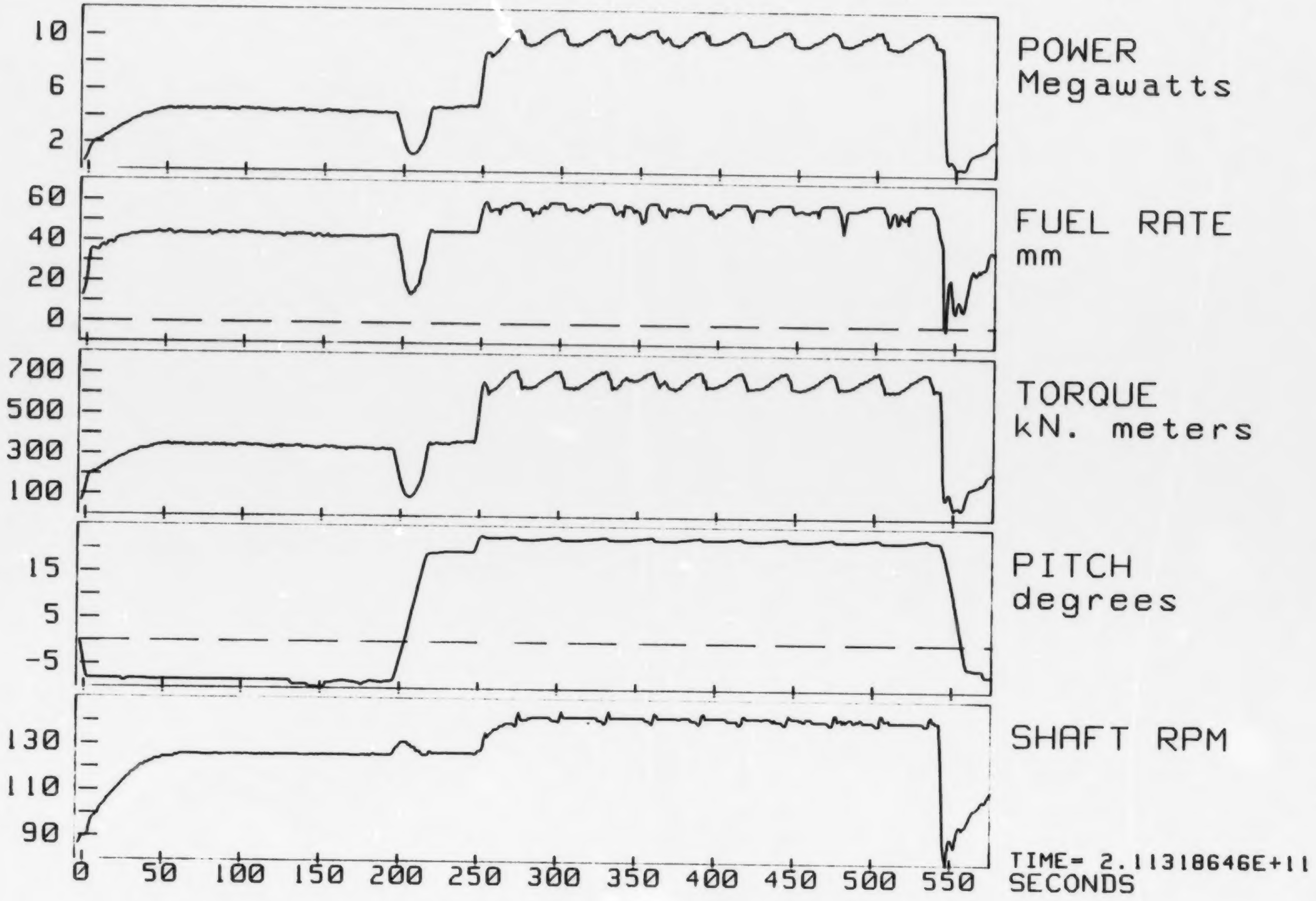

RAM # _B21   TAPE: 81-T2-4   07 JUL 1981 18:40:00   **FIG. #2**

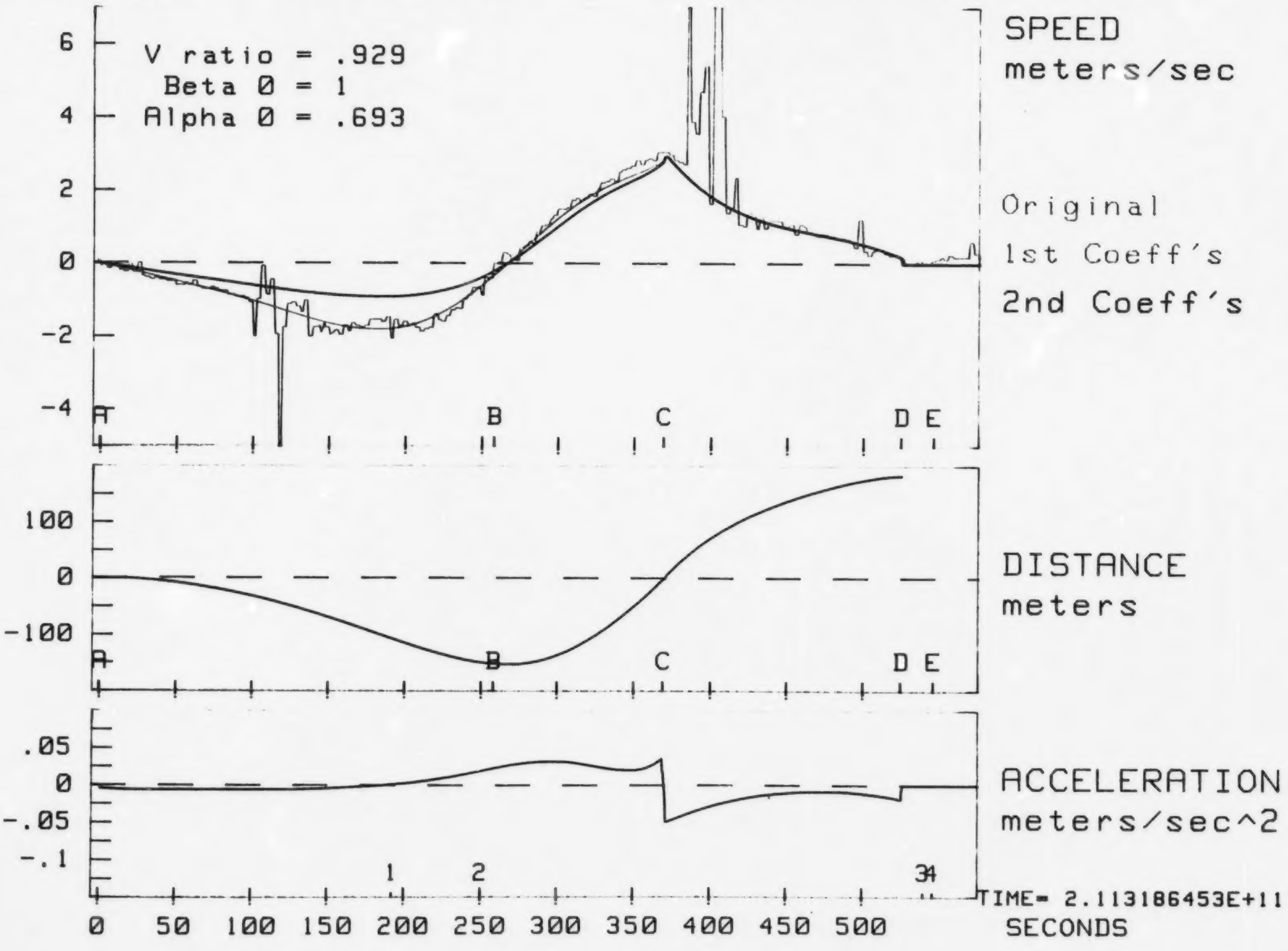

RAM # _B21 TAPE: 81-T2-4 07 JUL 1981 18:40:00

FIG. #3

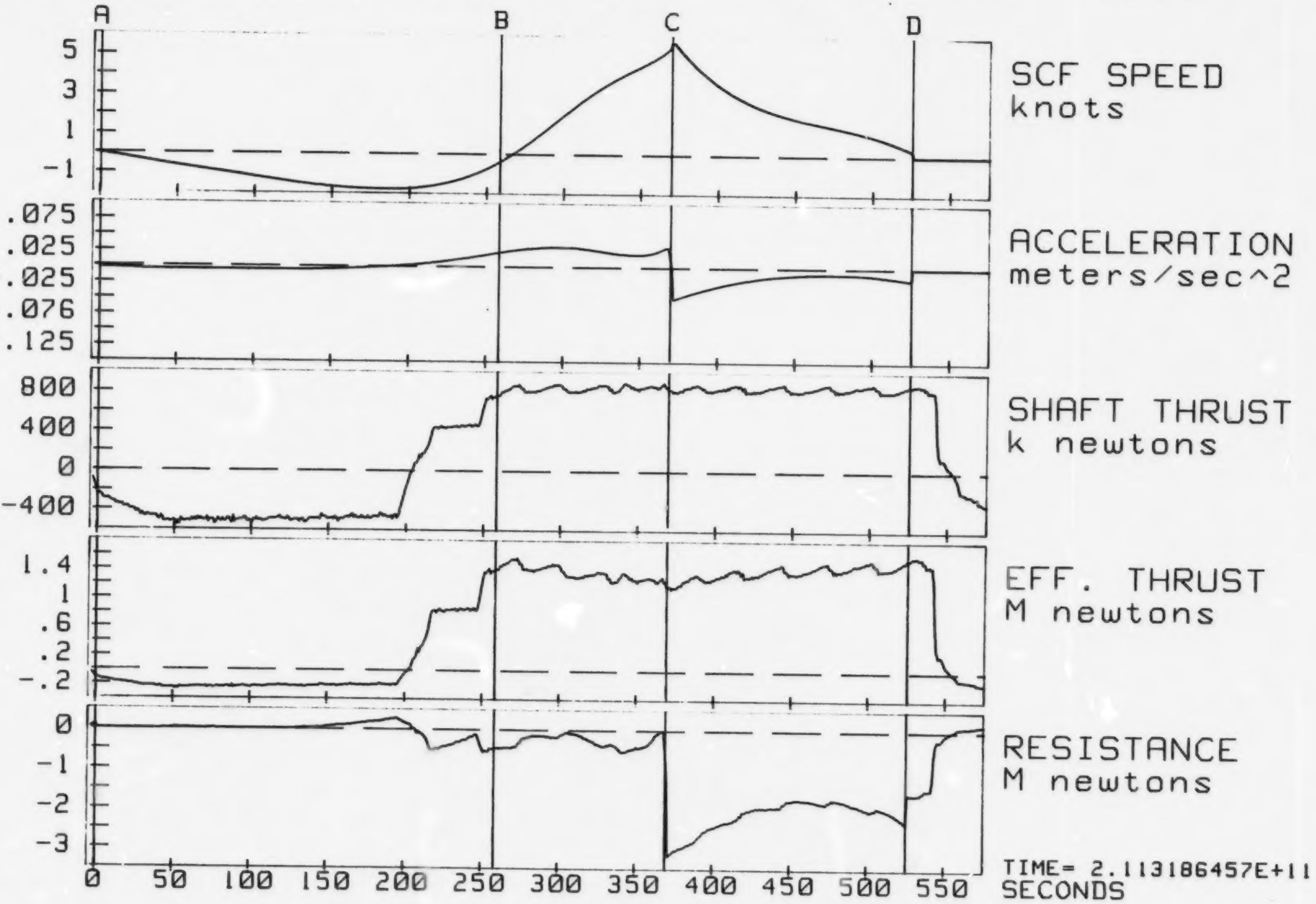

RAM # _B21   TAPE: 81-T2-4   07 JUL 1981 18:40:00   Fig.# 4

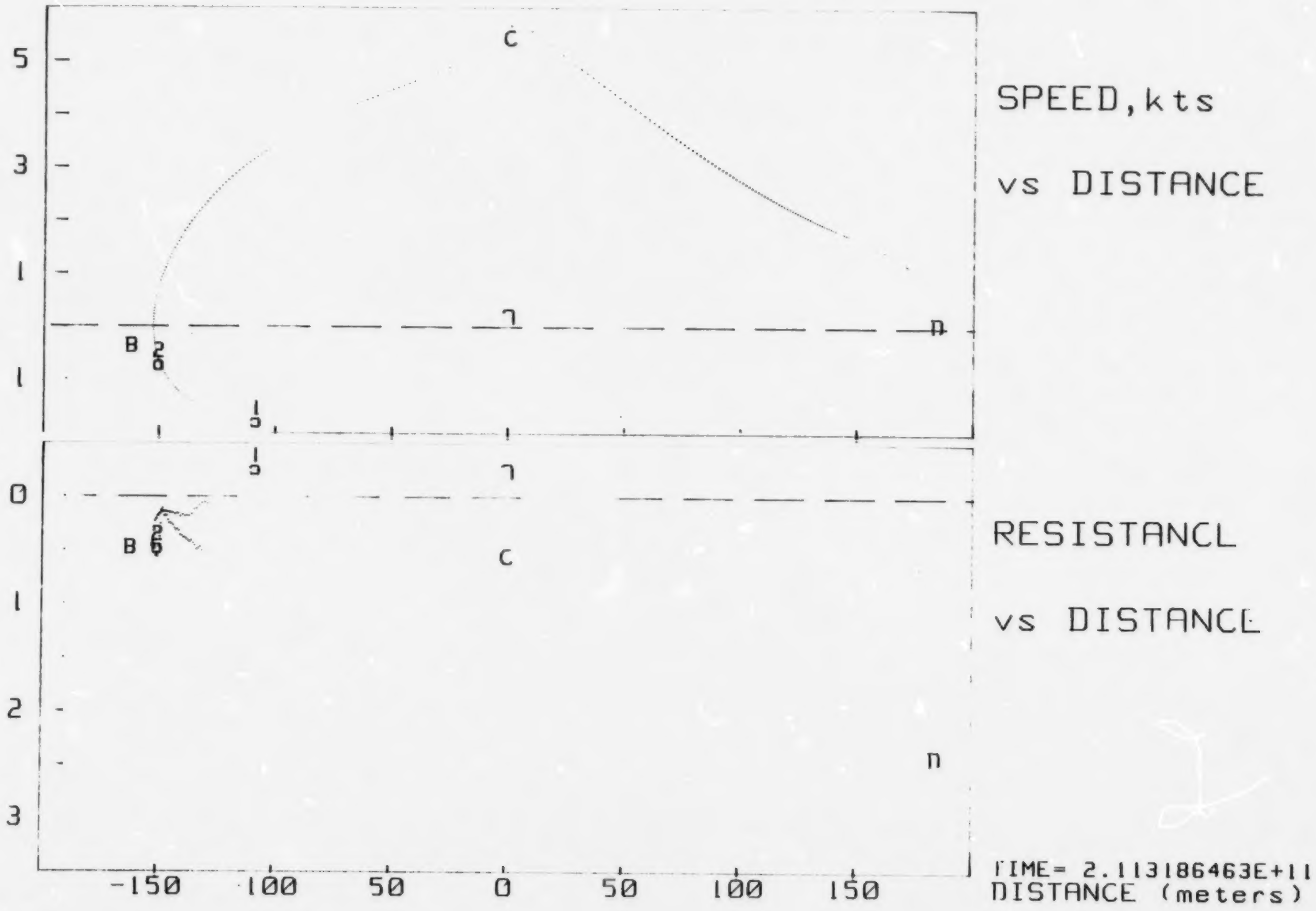

RAM # _B21 TAPE: 81-T2-4 07 JUL 1981 18:40:00 Fig.# 5

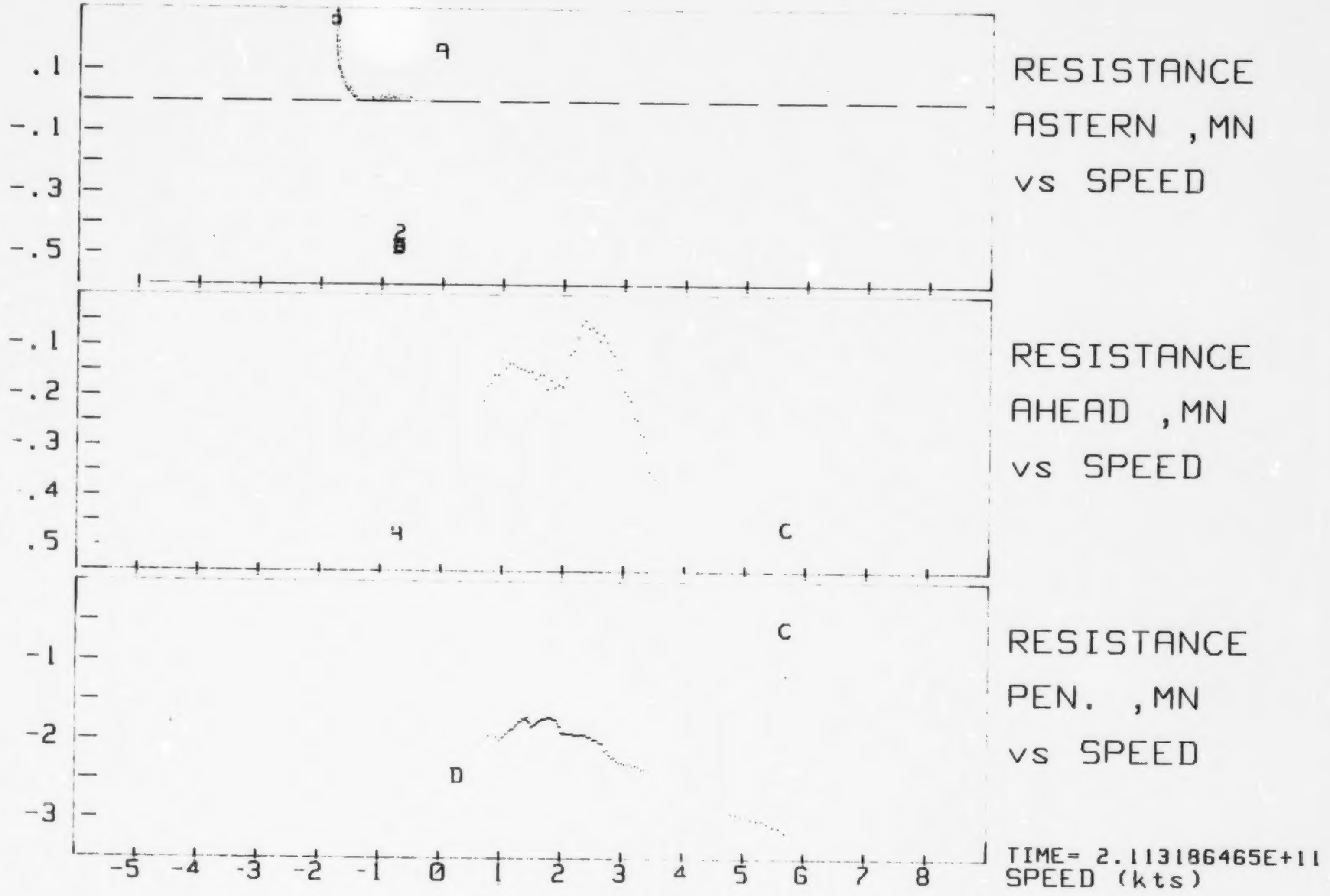

RESULTS OF RAMMING CYCLE ANALYSIS

RAM No. _B22

TAPE:	81-T2-4	ICE CONDITIONS:	LEVEL ICE
CATEGORY:	L1	ICE THICKNESS:	1.45 m
QUALITY:	51BC	FLEXURAL STRENGTH:	163 kPA
TRIM:	EVEN TRIM	BUBBLER STATUS:	ON

RAMMING CYCLE CHARACTERISTICS:

Speed of Advance	(knots)	.556	
Speed of Impact	(knots)	5.2	(5.26)

	Duration (sec)	% Cycle Time	Distance (m)
Backing	331	40.3	-193.6
Acceleration	184	22.4	193.6
Penetration	282	34.3	242.4 (235.2)
Extraction	25	3.04	
Total Cycle	822		

Duration of Astern Mode	(sec)	163		
Duration of Reversal to Ahead	(sec)	302		
Duration of Ahead Mode	(sec)	336		
Duration of Reversal to Astern	(sec)	21		
Start of Reversal after Impact	(sec)	286		
Total Fuel Used	(mm*hr)	9.8	Est. kg:	71.42
Average Fuel Rate	(mm)	42.92	Est. kg/hr:	312.79
Backing Power	(kW)	3806.7		
[Est Fuel Rate	(kg/hr)]	851.3		
Acceleration Power	(kW)	9901.1		
[Est Fuel Rate	(kg/hr)]	2066.5		

RAM # _B22 TAPE: 81-T2-4 07 JUL 1981 18:52:44

FIG. #1

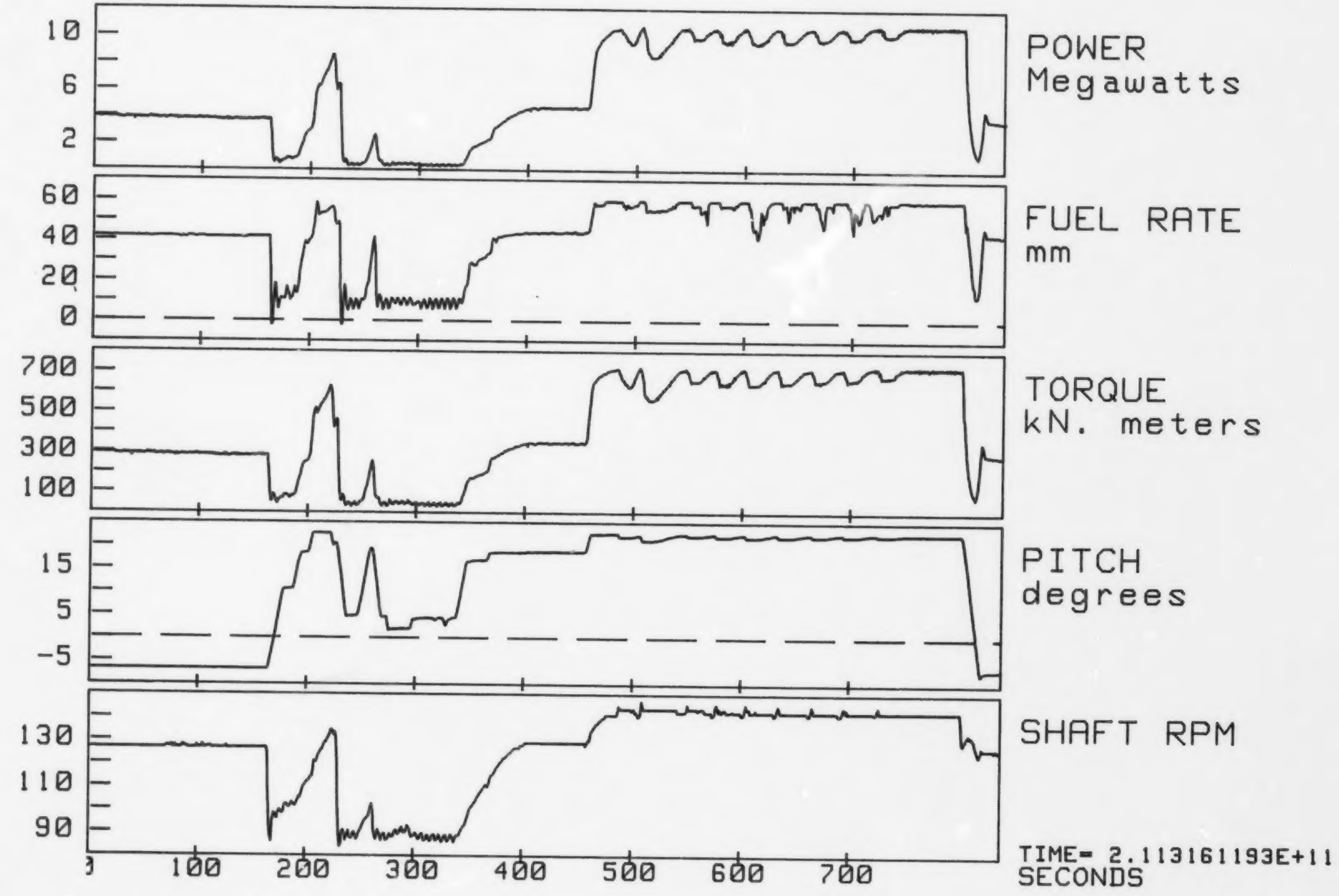

RAM # _B22 TAPE: 81-T2-4 07 JUL 1981 18:52:44

FIG. #2

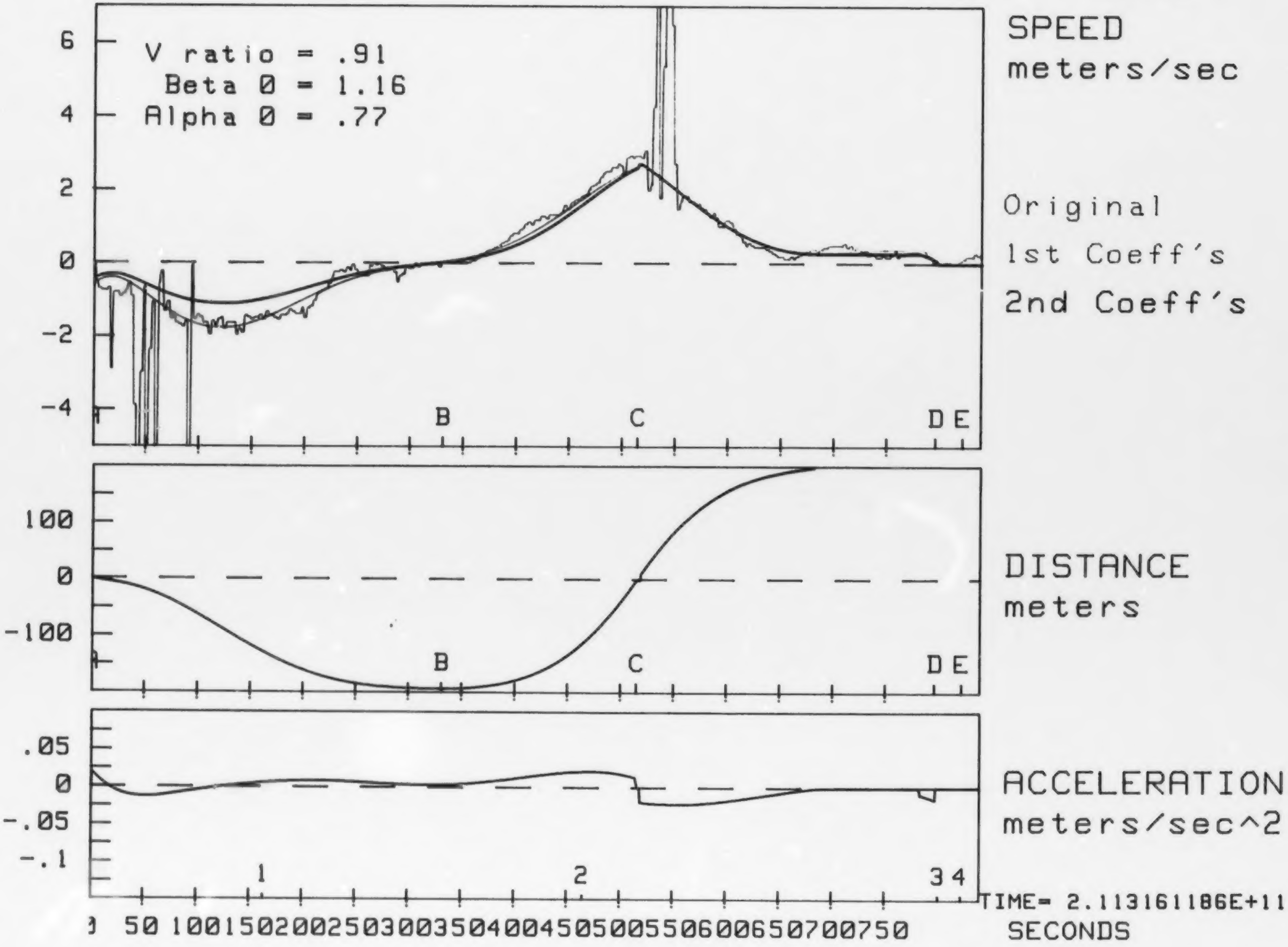

RAM # _B22 TAPE: 81-T2-4 07 JUL 1981 18:52:44

FIG. #3

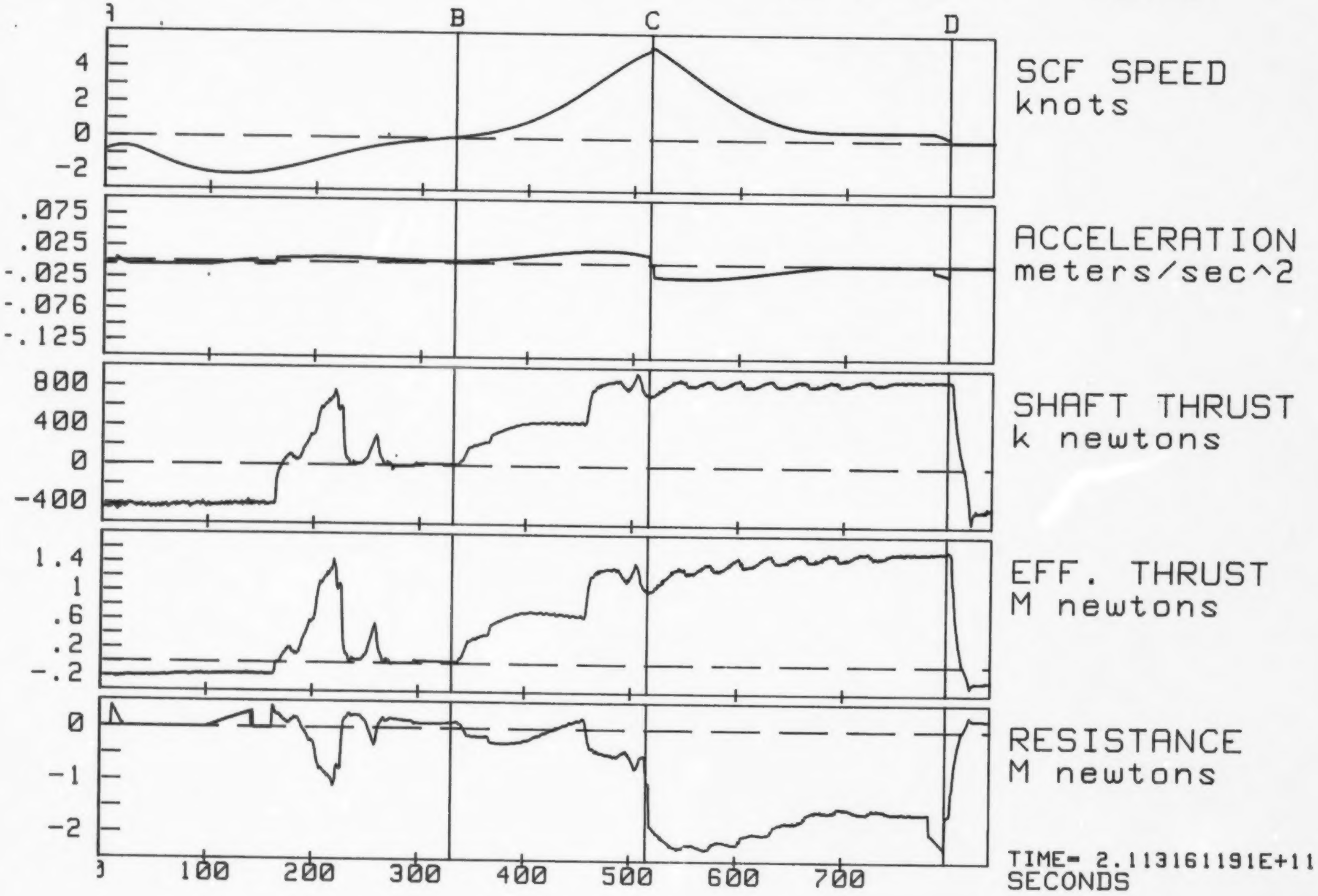

RAM # _B22   TAPE: 81-T2-4   07 JUL 1981 18:52:44   Fig.# 4

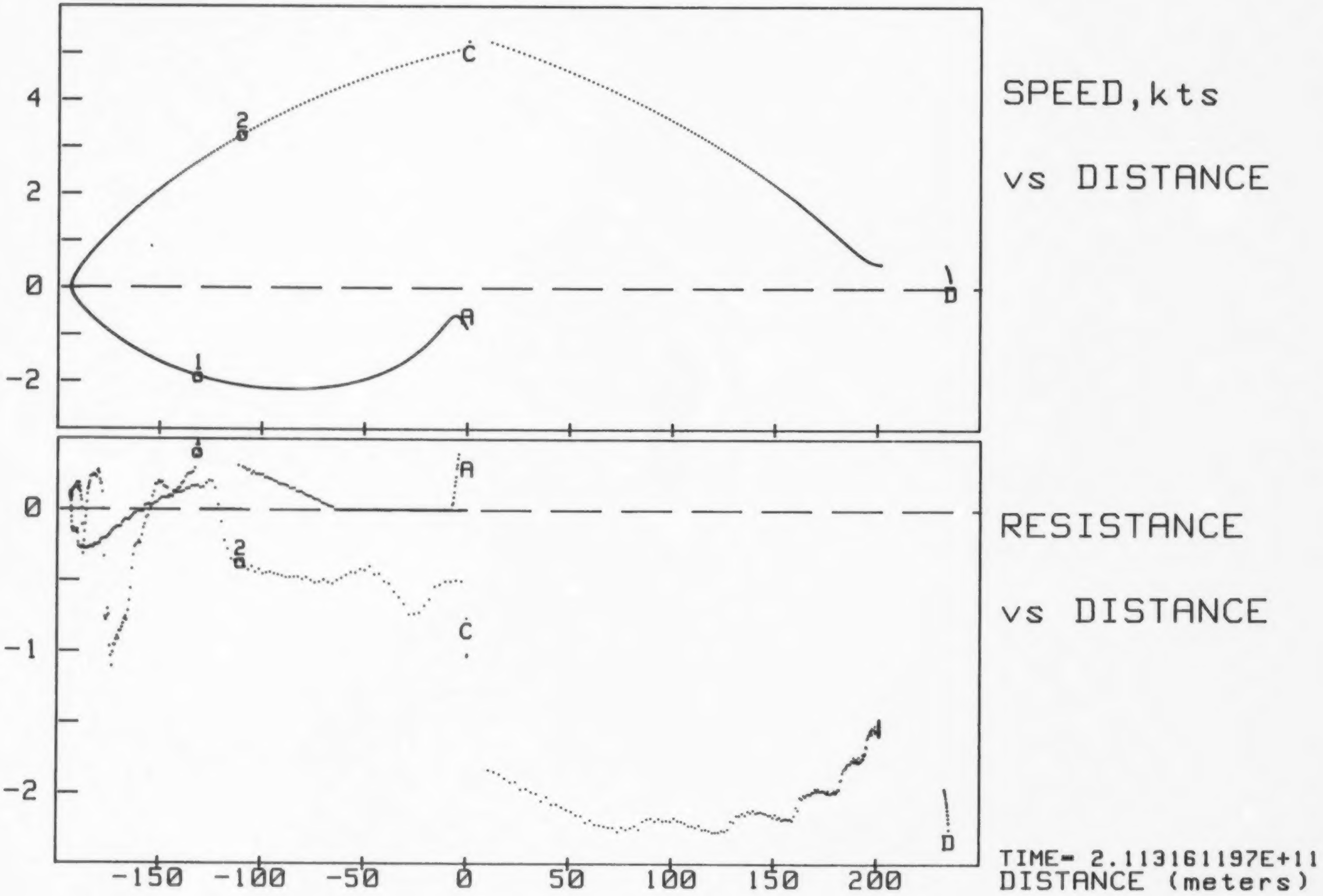

RAM # _B22 TAPE: 81-T2-4 07 JUL 1981 18:52:44 Fig.# 5

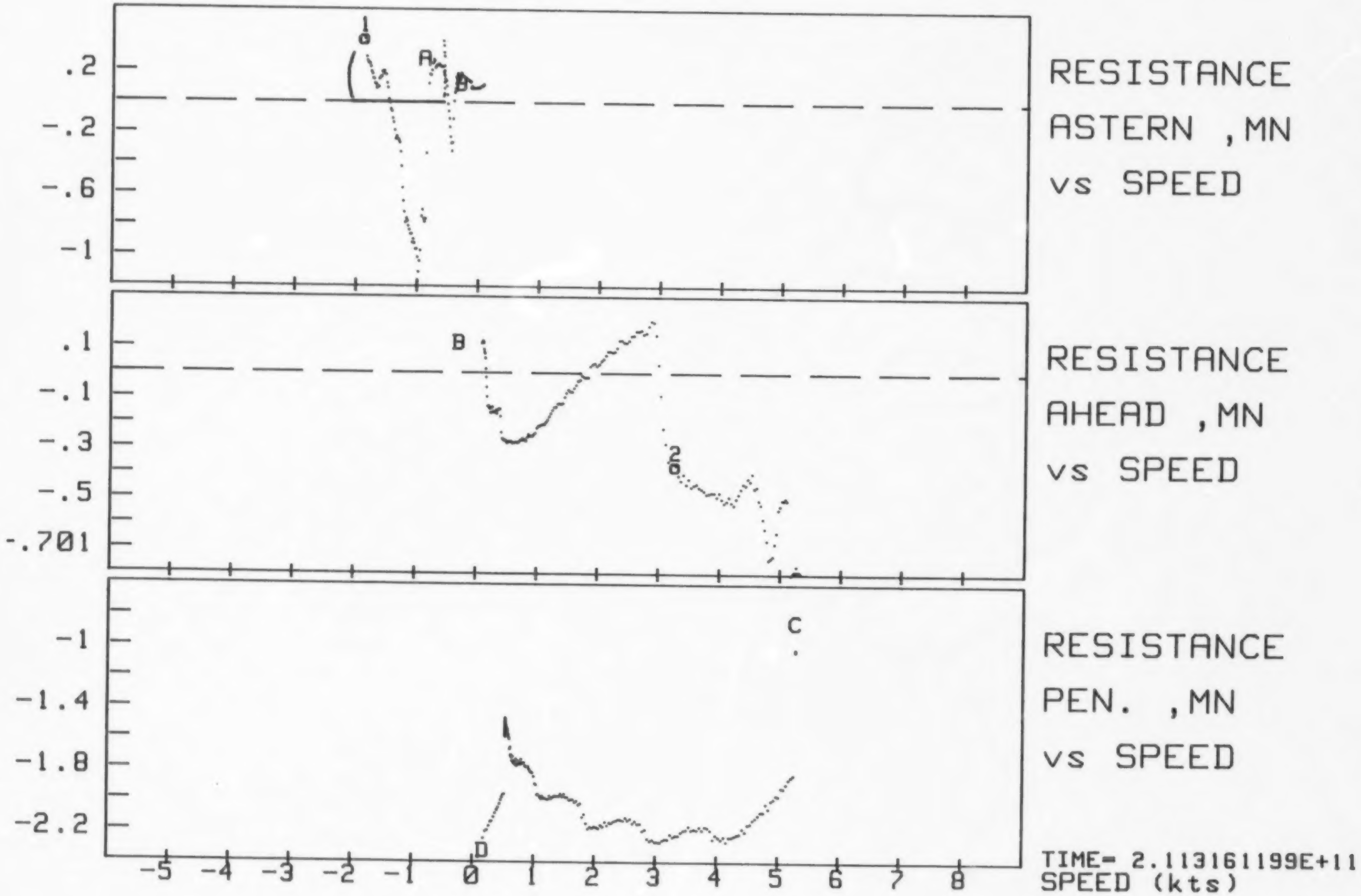

RESULTS OF RAMMING CYCLE ANALYSIS

RAM No. _B23

TAPE:	81-T2-4	ICE CONDITIONS:	LEVEL ICE
CATEGORY:	L1	ICE THICKNESS:	1.4 m
QUALITY:	32BB	FLEXURAL STRENGTH:	163 kPA
TRIM:	EVEN TRIM	BUBBLER STATUS:	ON

RAMMING CYCLE CHARACTERISTICS:

Speed of Advance	(knots)	.442
Speed of Impact	(knots)	5.6 (5.92)

	Duration (sec)	% Cycle Time	Distance (m)
Backing	253	59.3	-136.5
Acceleration	95	22.2	136.5
Penetration	70	16.4	81.8 (97.03)
Extraction	9	2.11	
Total Cycle	427		

Duration of Astern Mode	(sec)	198
Duration of Reversal to Ahead	(sec)	35
Duration of Ahead Mode	(sec)	113
Duration of Reversal to Astern	(sec)	81
Start of Reversal after Impact	(sec)	-2

Total Fuel Used	(mm*hr)	4.63	Est. kg:	3.97
Average Fuel Rate	(mm)	39.04	Est. kg/hr:	33.469

Backing Power	(kW)	3525.8
[Est Fuel Rate	(kg/hr)]	795.29
Acceleration Power	(kW)	10312
[Est Fuel Rate	(kg/hr)]	2148.4

RAM # _B23 TAPE: 81-T2-4 07 JUL 1981 19:04:31

FIG. #1

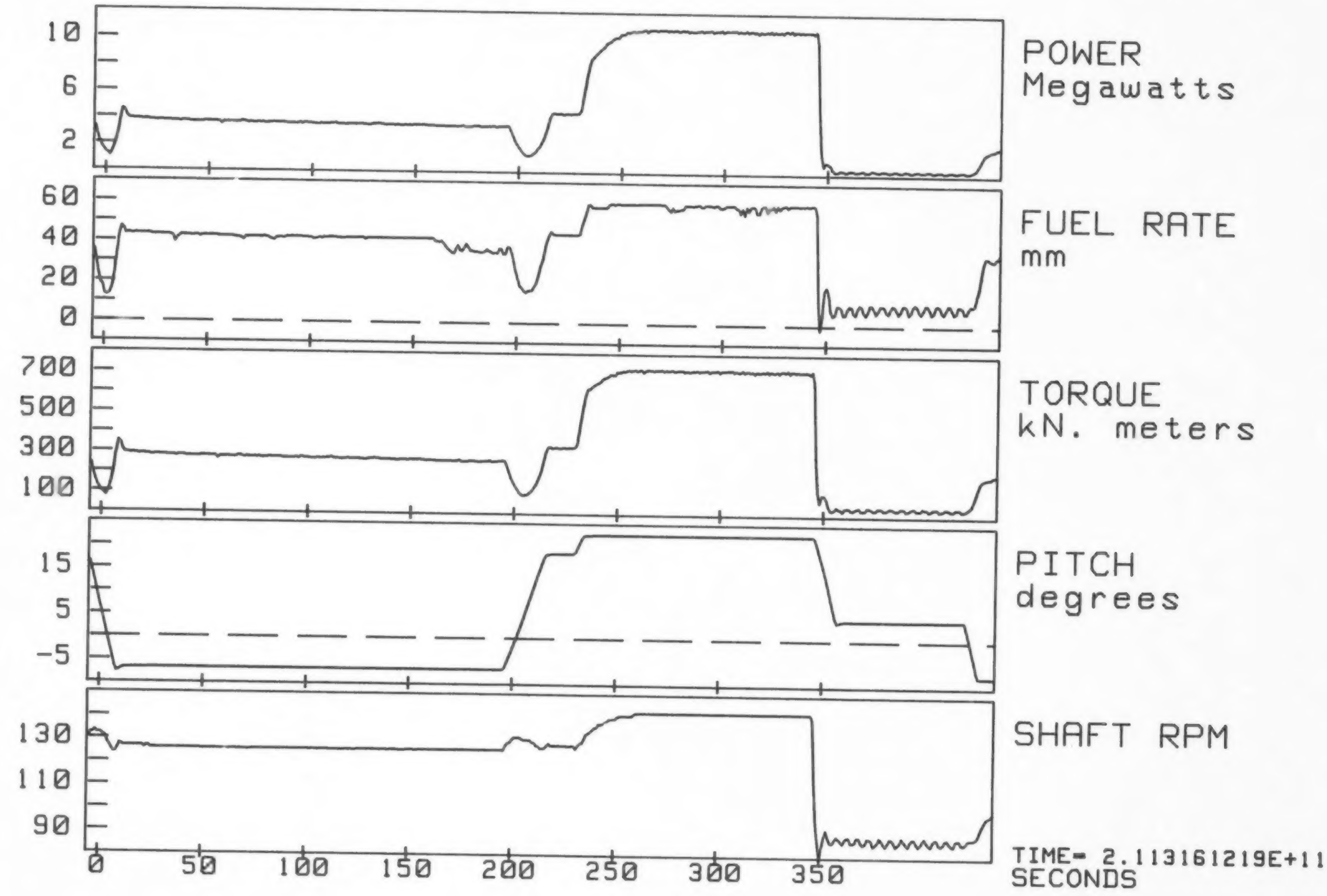

RAM # _B23 TAPE: 81-T2-4 07 JUL 1981 19:04:31

FIG. #2

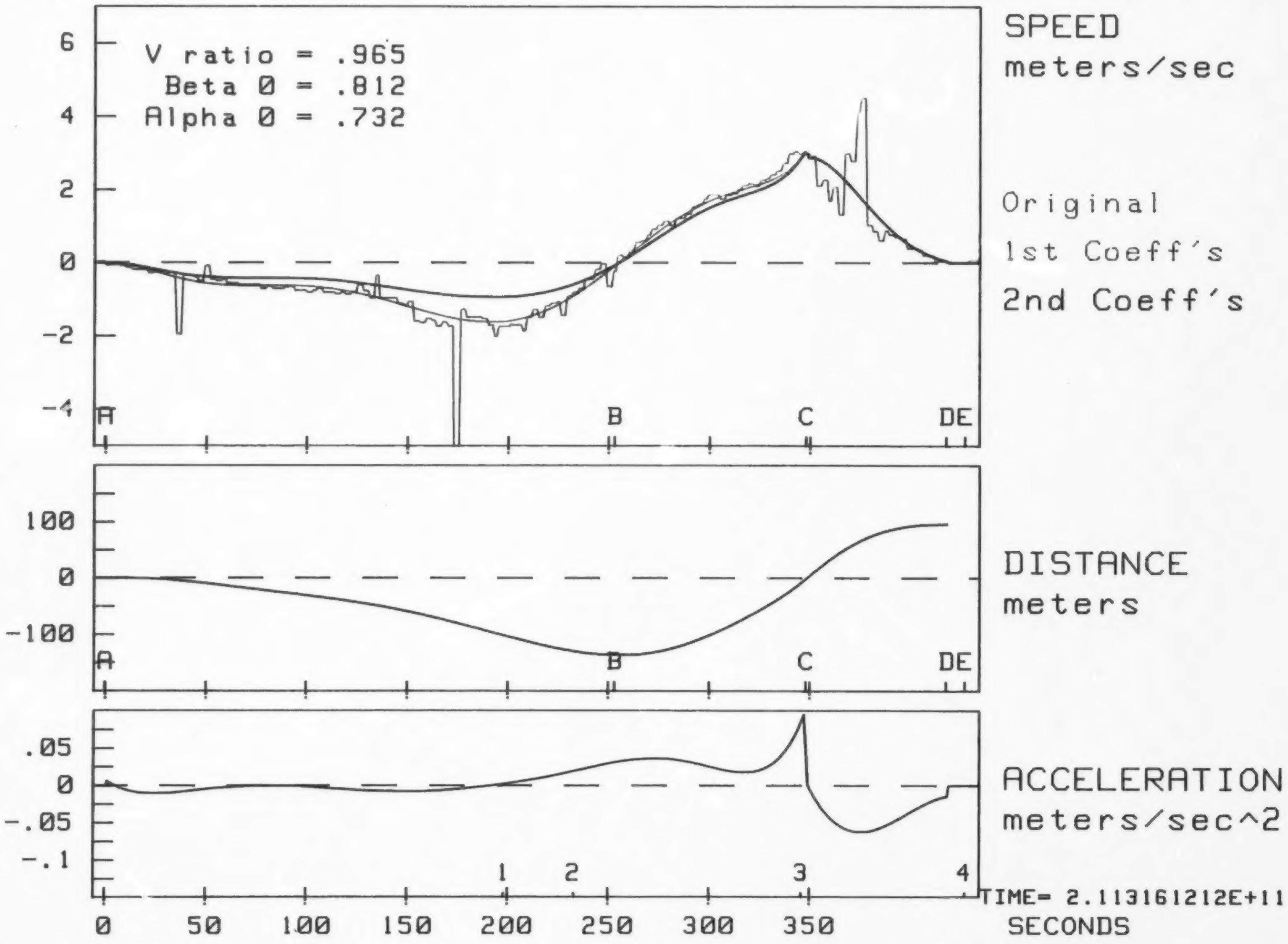

RAM # _B23 TAPE: 81-T2-4 07 JUL 1981 19:04:31

FIG. #3

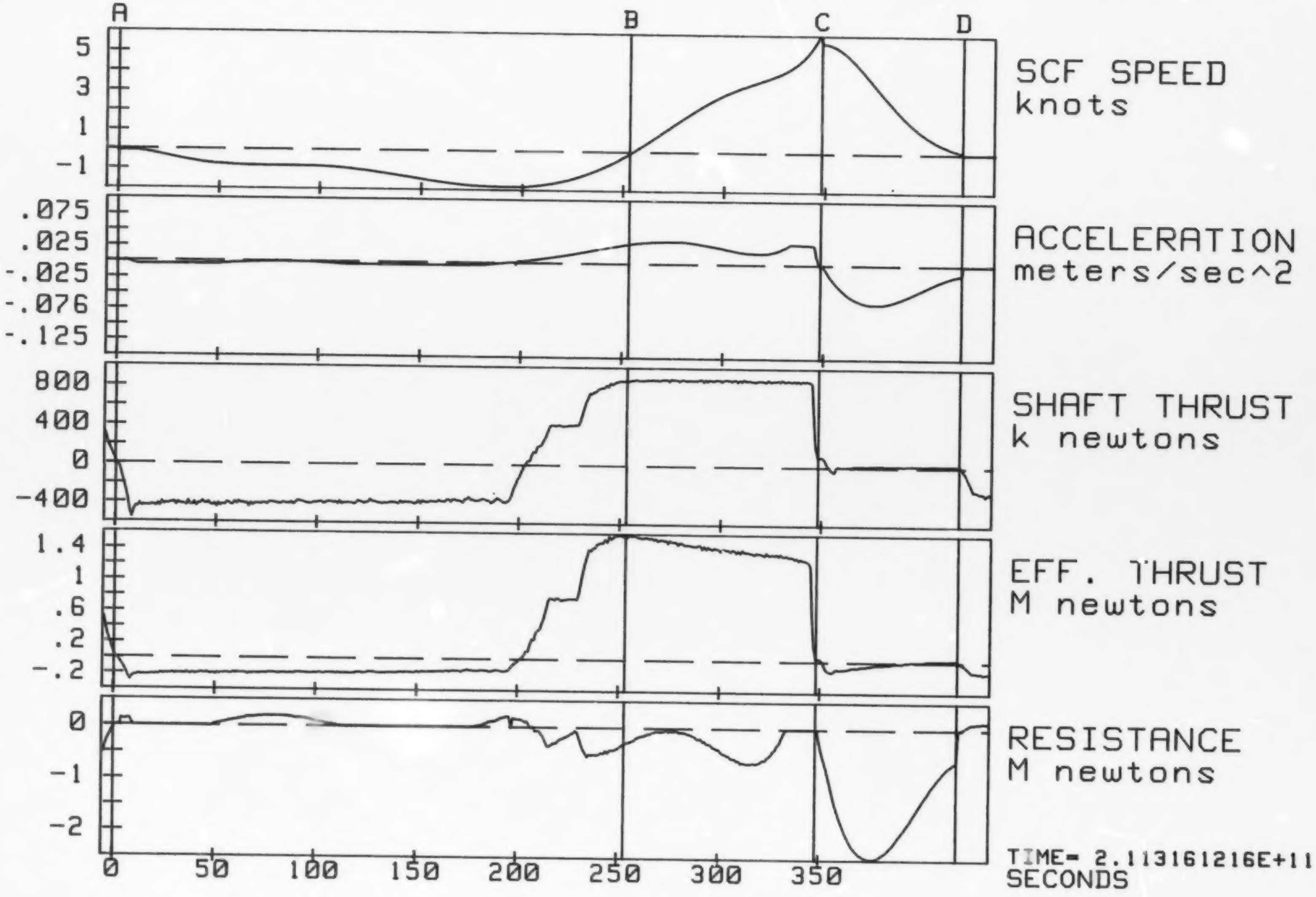

RAM # _B23   TAPE: 81-T2-4   07 JUL 1981 19:04:31   Fig.# 4

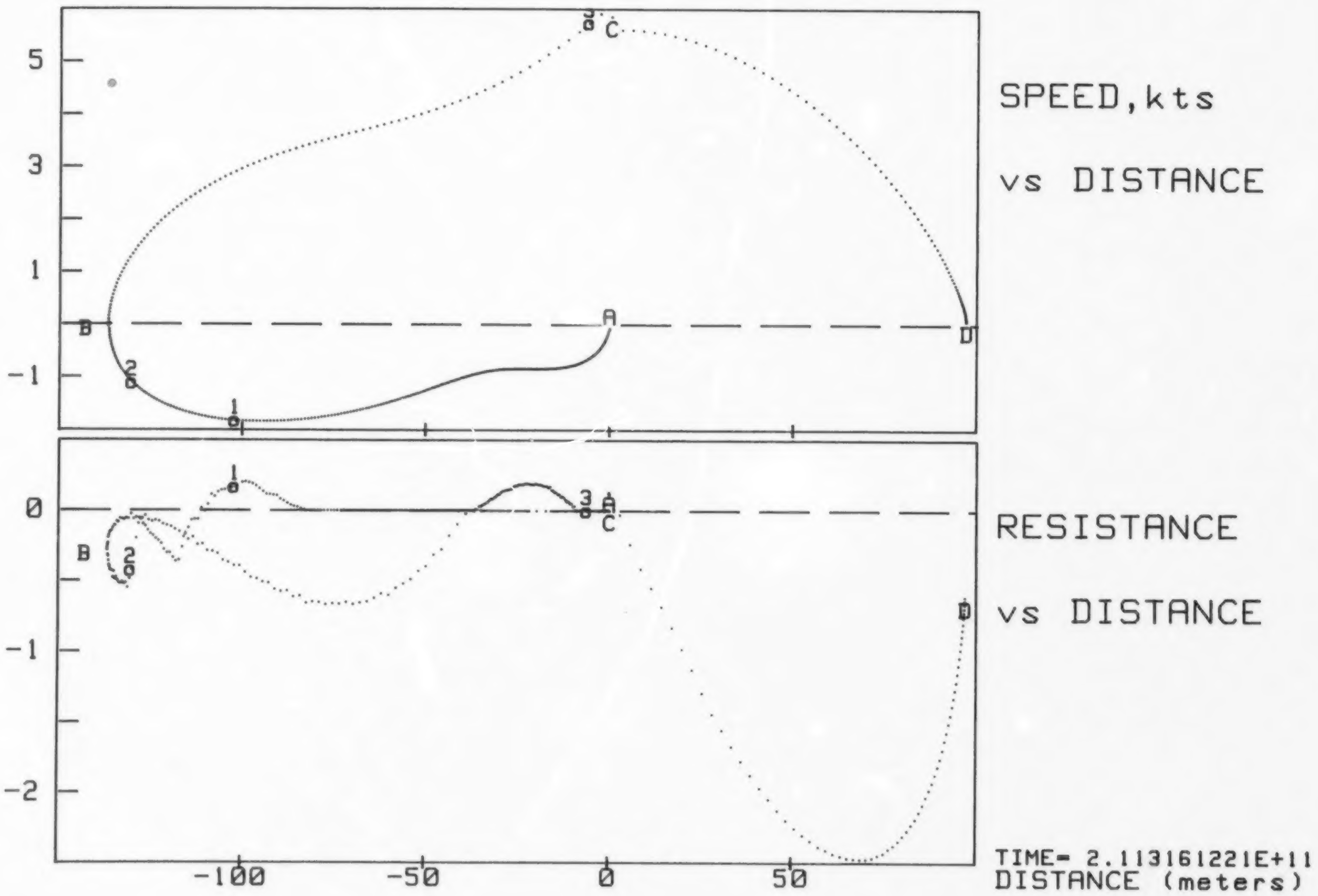

RAM # _B23 TAPE: 81-T2-4 07 JUL 1981 19:04:31 Fig.# 5

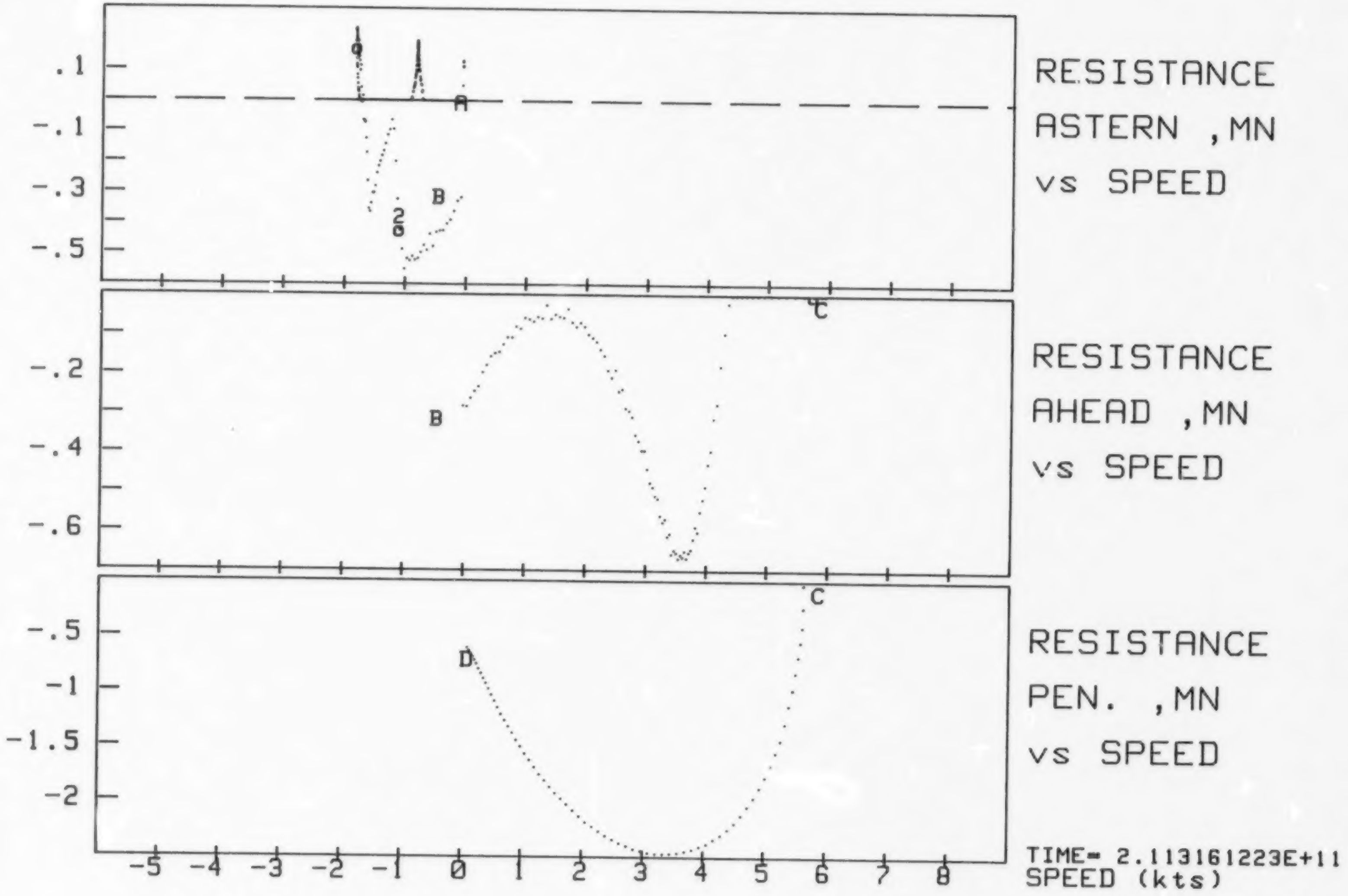

ADMIRALTY INLET TRIALS, 1981

SERIES C

RESULTS OF RAMMING CYCLE ANALYSIS

RAM No. __C6

TAPE:	81-T2-5.1	ICE CONDITIONS:	LEVEL ICE
CATEGORY:	L4	ICE THICKNESS:	1.56 m
QUALITY:	26AB	FLEXURAL STRENGTH:	104 kPA
TRIM:	BOW UP	BUBBLER STATUS:	OFF

RAMMING CYCLE CHARACTERISTICS:

Speed of Advance	(knots)	.389	
Speed of Impact	(knots)	6	(6.25)

	Duration (sec)	% Cycle Time	Distance (m)
Backing	246	52.6	-158
Acceleration	102	21.8	158
Penetration	102	21.8	97 (93.55)
Extraction	18	3.85	
Total Cycle	468		

Duration of Astern Mode	(sec)	146
Duration of Reversal to Ahead	(sec)	47
Duration of Ahead Mode	(sec)	247
Duration of Reversal to Astern	(sec)	21
Start of Reversal after Impact	(sec)	92

Total Fuel Used	(mm*hr)	6.52	Est. kg:	108.1
Average Fuel Rate	(mm)	50.12	Est. kg/hr:	831.76

Backing Power	(kW)	7163.9
[Est Fuel Rate	(kg/hr)]	1520.7

Acceleration Power	(kW)	9680.6
[Est Fuel Rate	(kg/hr)]	2022.6

RAM # __C6 TAPE: 81-T2-5.1 08 JUL 1981 14:12:39

FIG. #1

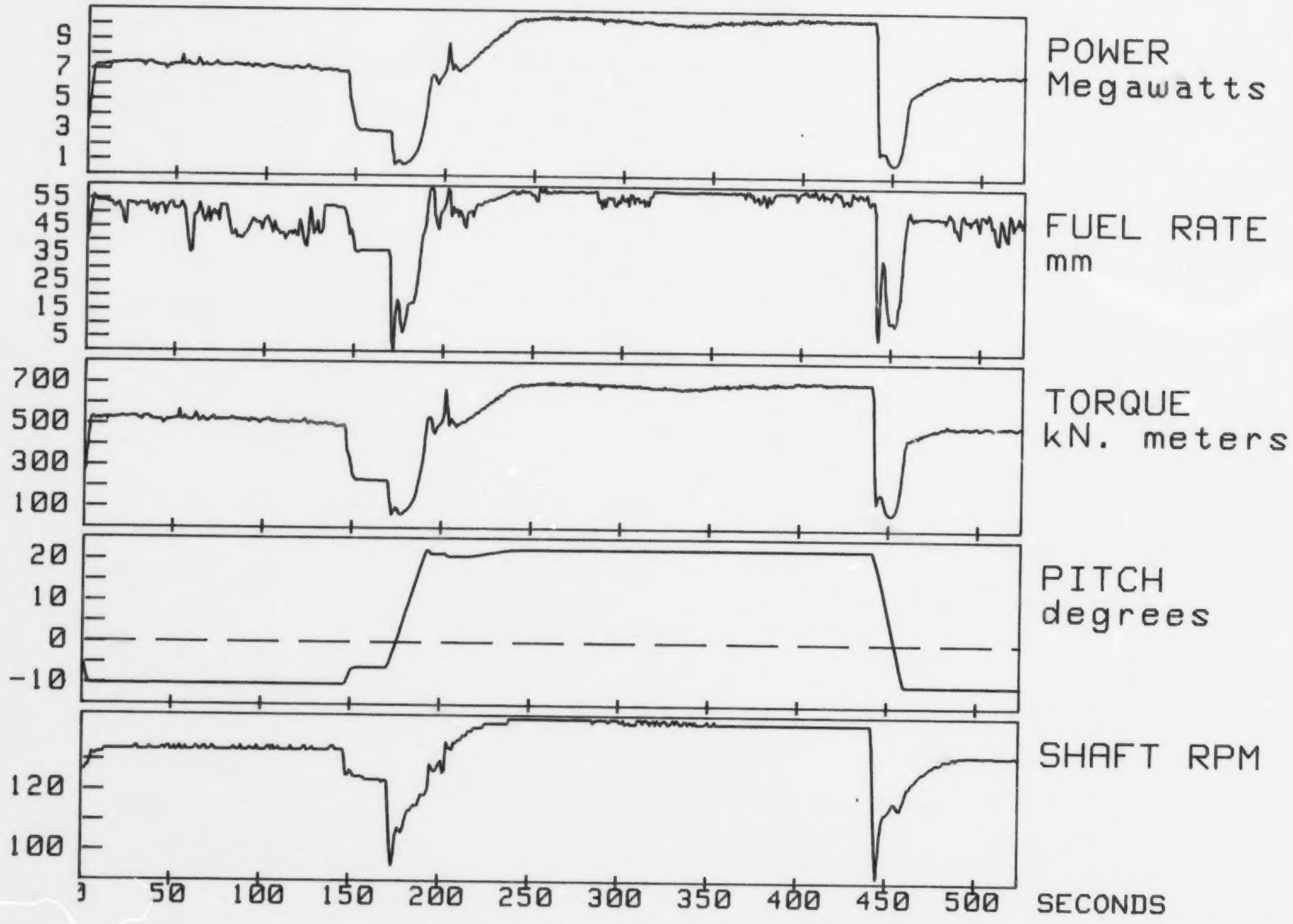

RAM # __C6 TAPE: 81-T2-5.1 08 JUL 1981 14:12:39 **FIG. #2**

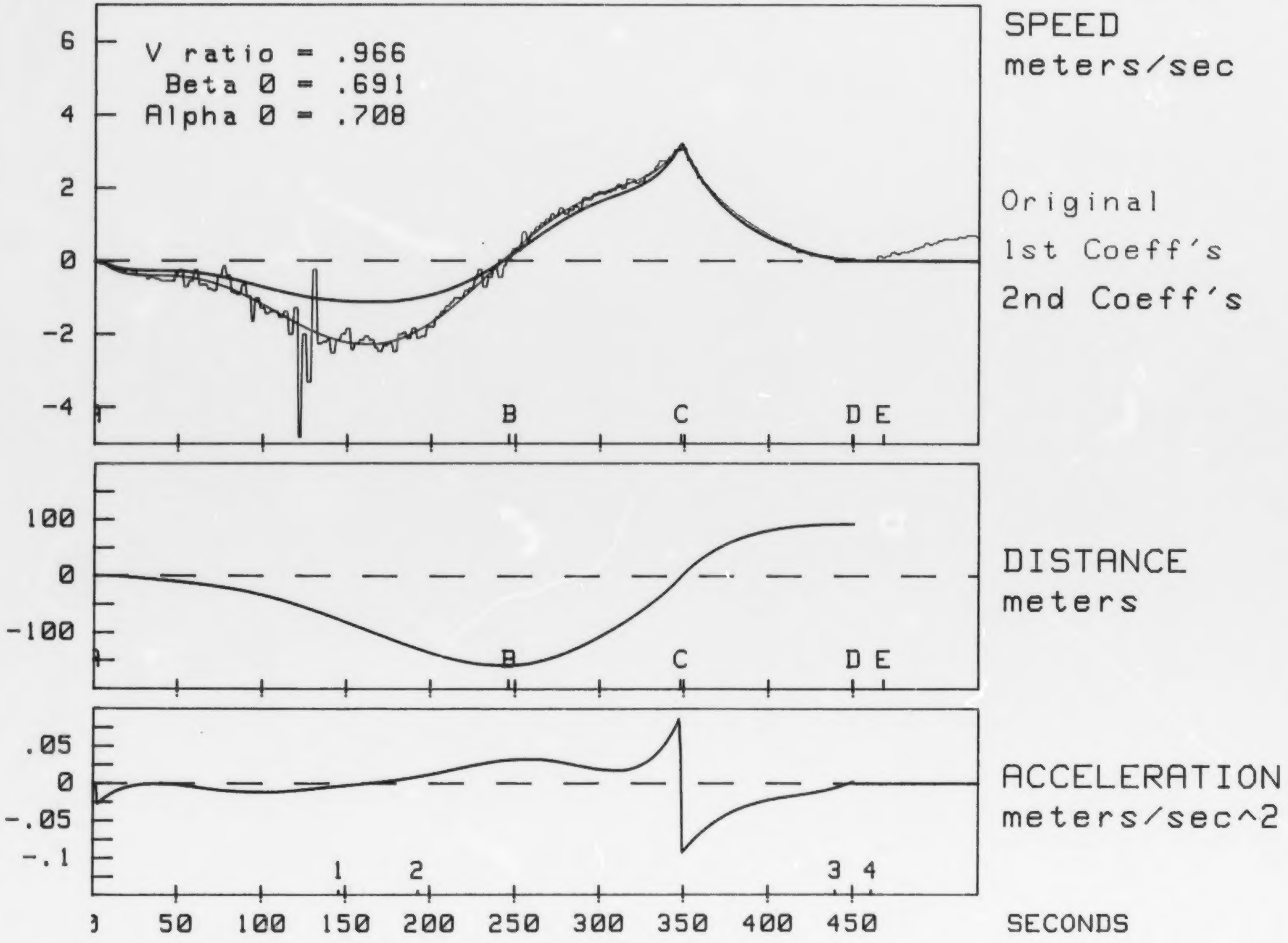

RAM # __C6 TAPE: 81-T2-5.1 08 JUL 1981 14:12:39

FIG. #3

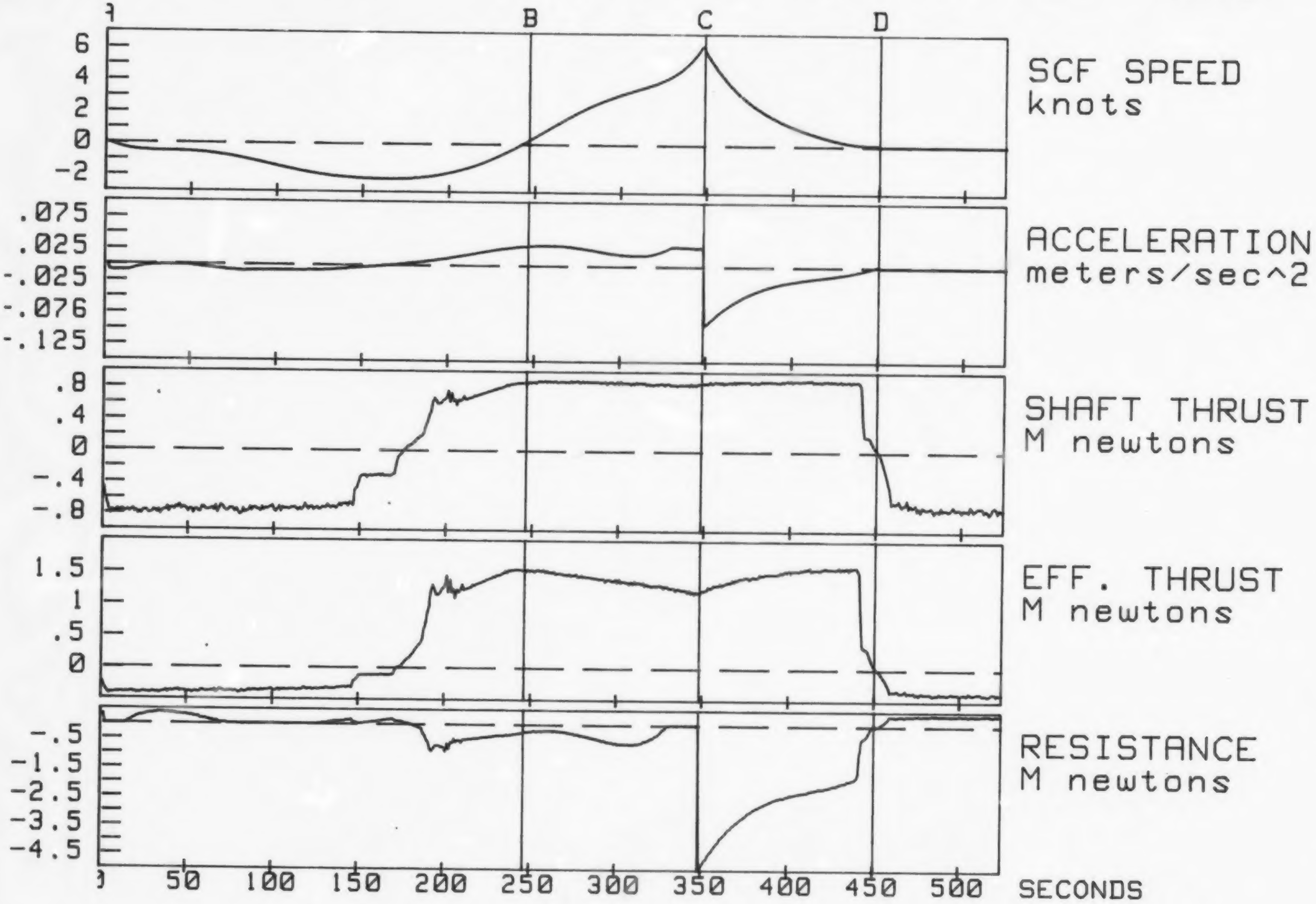

RAM # __C6 TAPE: 81-T2-5.1 08 JUL 1981 14:12:39 Fig.# 4

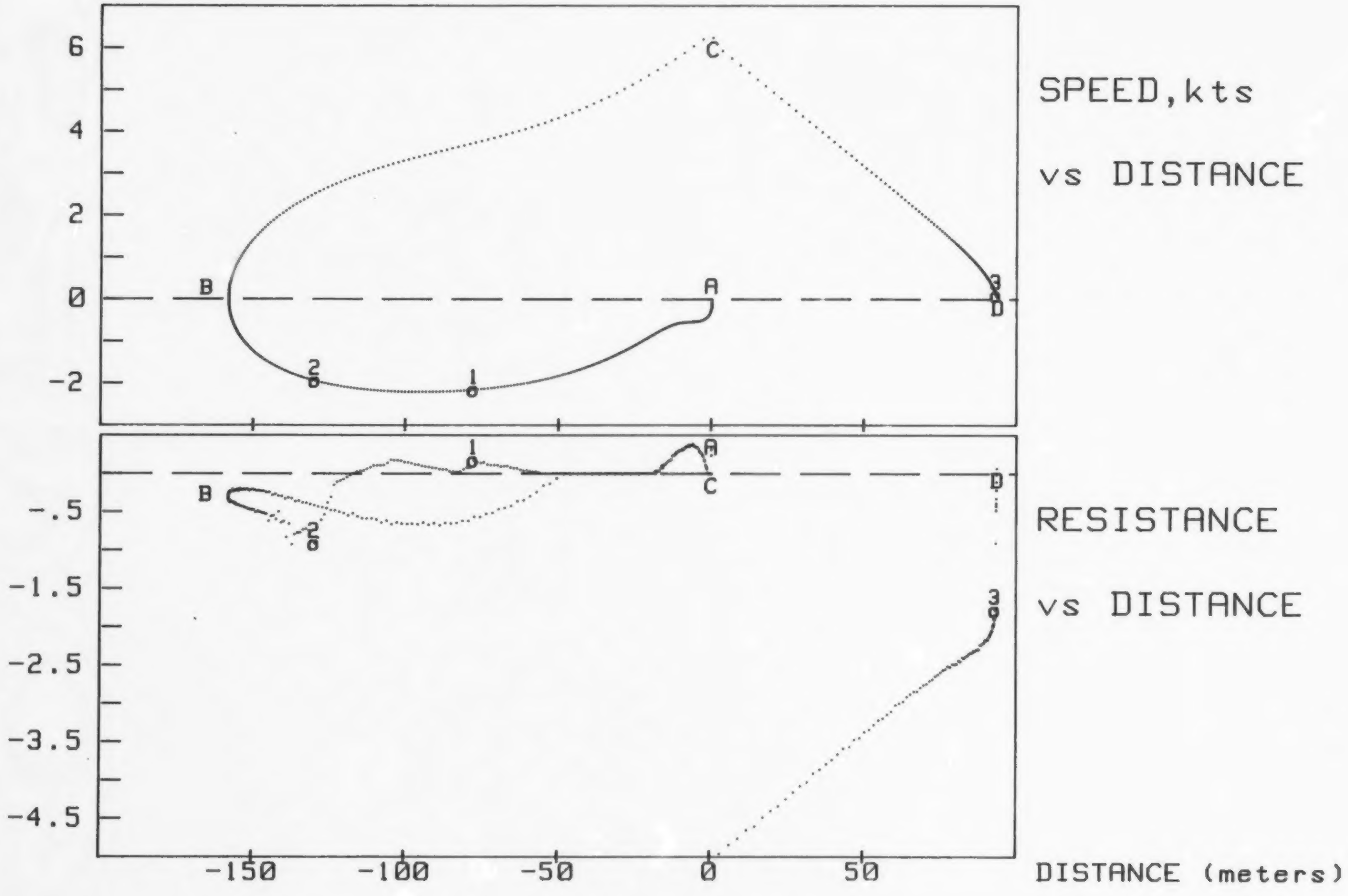

RAM # __C6 TAPE: 81-T2-5.1 08 JUL 1981 14:12:39 Fig.# 5

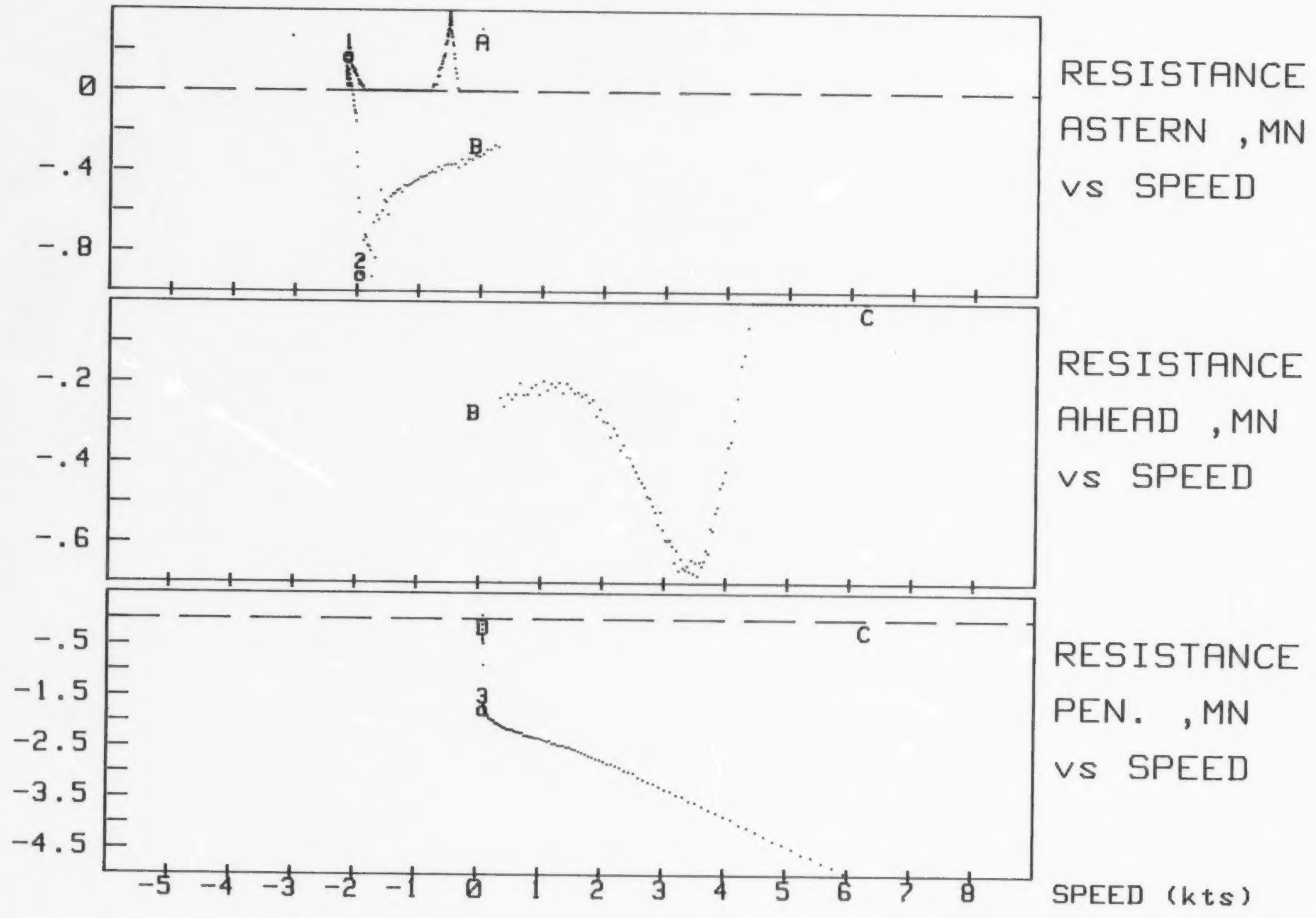

RESULTS OF RAMMING CYCLE ANALYSIS

RAM No. __C7

TAPE:	81-T2-5.1	ICE CONDITIONS:	LEVEL ICE
CATEGORY:	L2	ICE THICKNESS:	1.8 m
QUALITY:	55CC	FLEXURAL STRENGTH:	104 kPA
TRIM:	BOW UP	BUBBLER STATUS:	ON

RAMMING CYCLE CHARACTERISTICS:

Speed of Advance (knots) .53

Speed of Impact (knots) 5.5 (5.9)

	Duration (sec)	% Cycle Time	Distance (m)
Backing	233	43.5	-130.7
Acceleration	95	17.7	130.7
Penetration	194	36.2	157.6 (146.1)
Extraction	14	2.61	
Total Cycle	536		

Duration of Astern Mode	(sec)	135		
Duration of Reversal to Ahead	(sec)	56		
Duration of Ahead Mode	(sec)	323		
Duration of Reversal to Astern	(sec)	22		
Start of Reversal after Impact	(sec)	186		
Total Fuel Used	(mm*hr)	7.49	Est. kg:	126
Average Fuel Rate	(mm)	50.32	Est. kg/hr:	846.25
Backing Power	(kW)	6641.4		
[Est Fuel Rate	(kg/hr)]	1416.5		
Acceleration Power	(kW)	10259		
[Est Fuel Rate	(kg/hr)]	2137.8		

RAM # __C7 TAPE: .81-T2-5.1 08 JUL 1981 14:22:02 **FIG. #1**

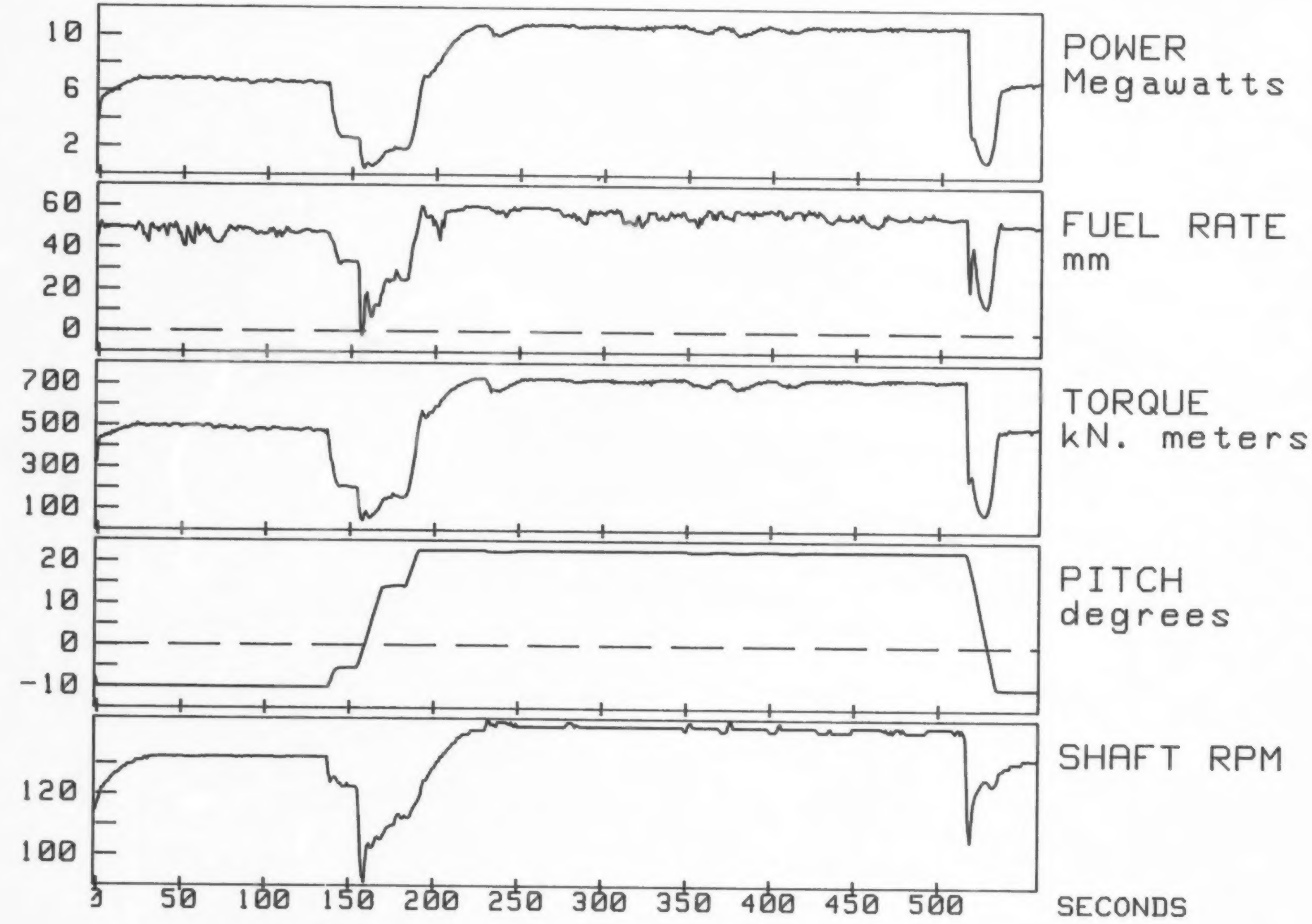

RAM # · C7 TAPE: 81-T2-5.1 08 JUL 1981 14:22:02

FIG. #2

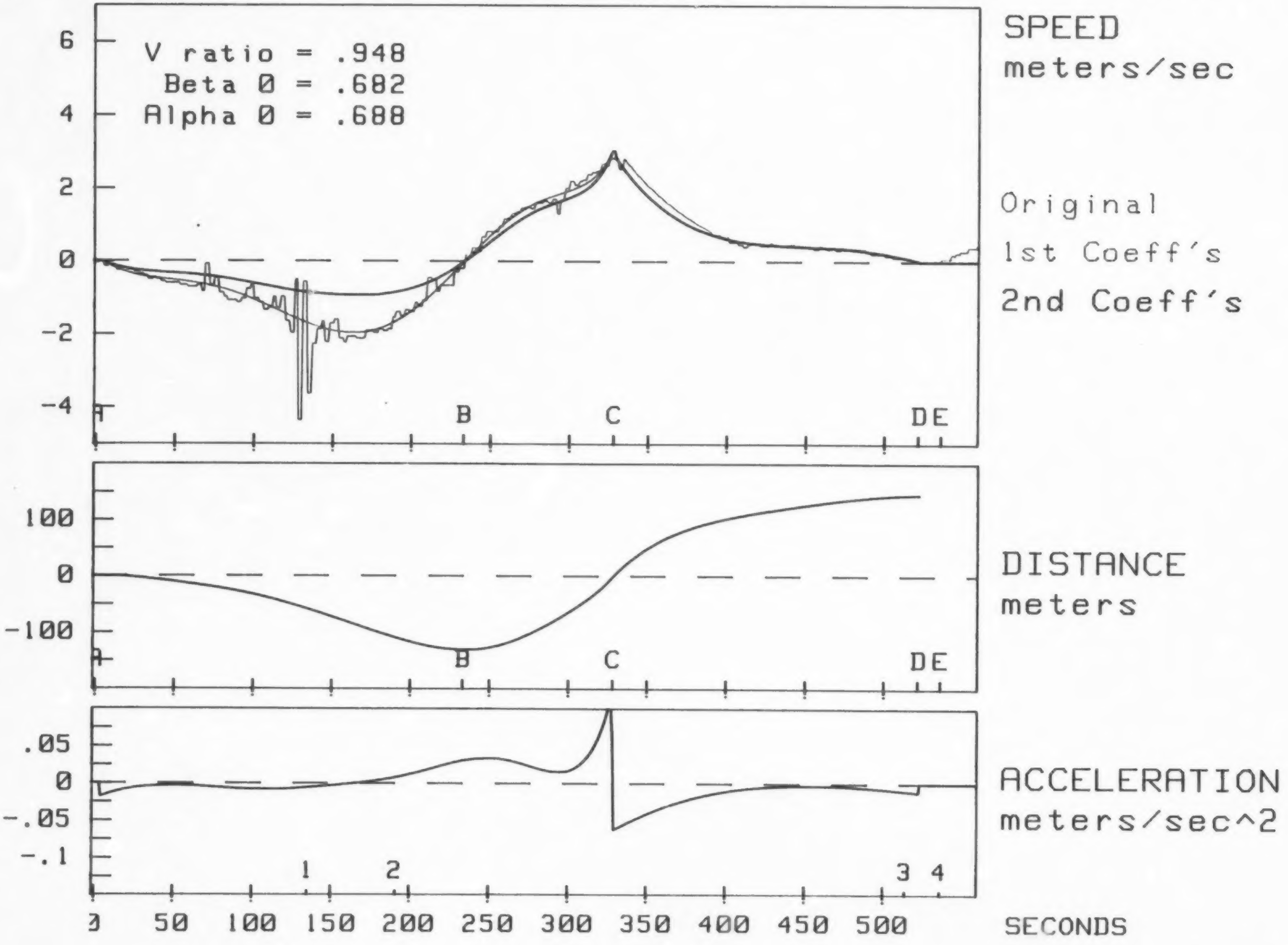

RAM # __C7 TAPE: 81-T2-5.1 08 JUL 1981 14:22:02

FIG. #3

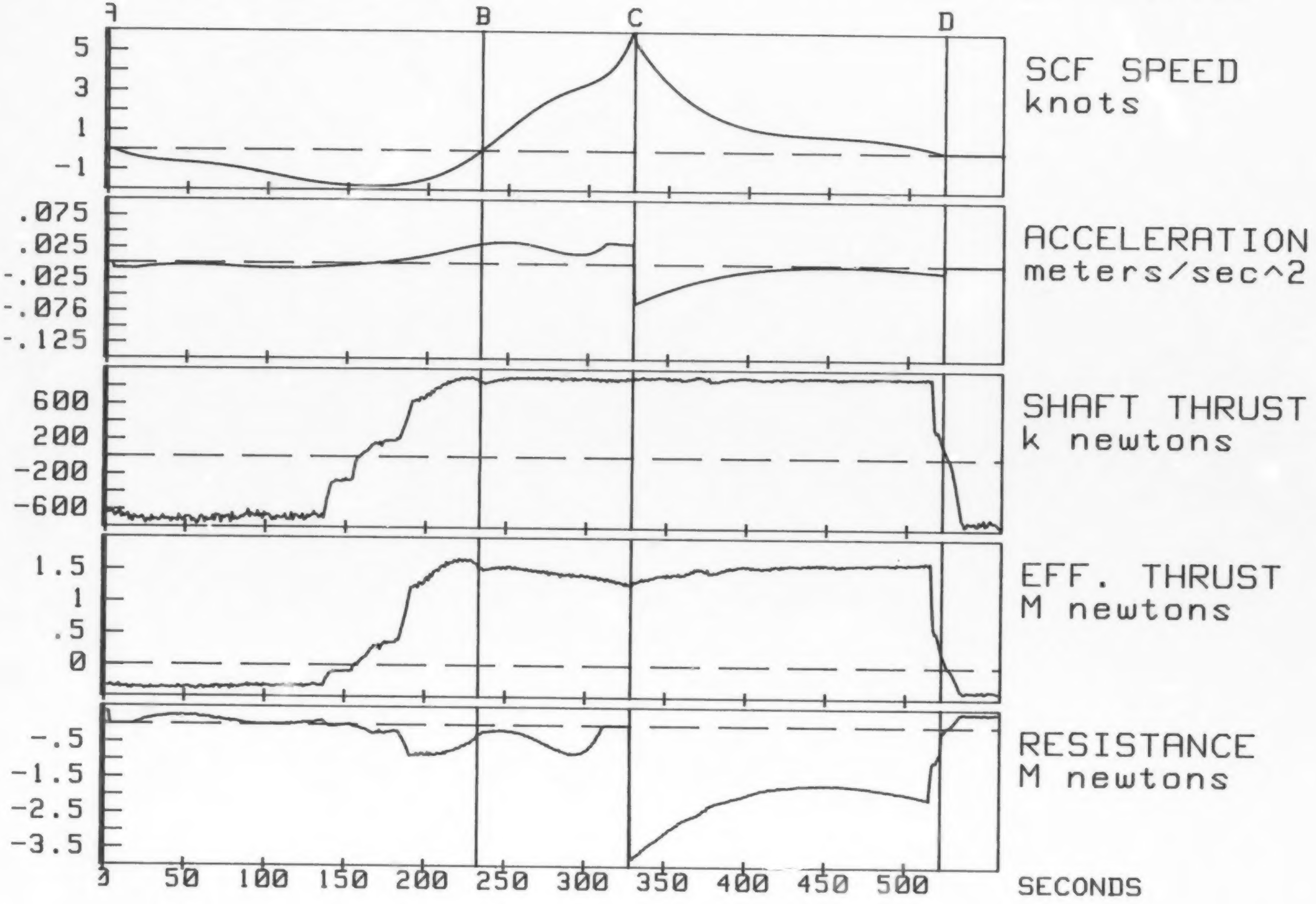

RAM # __C7 TAPE: 81-T2-5.1 08 JUL 1981 14:22:02 Fig.# 4

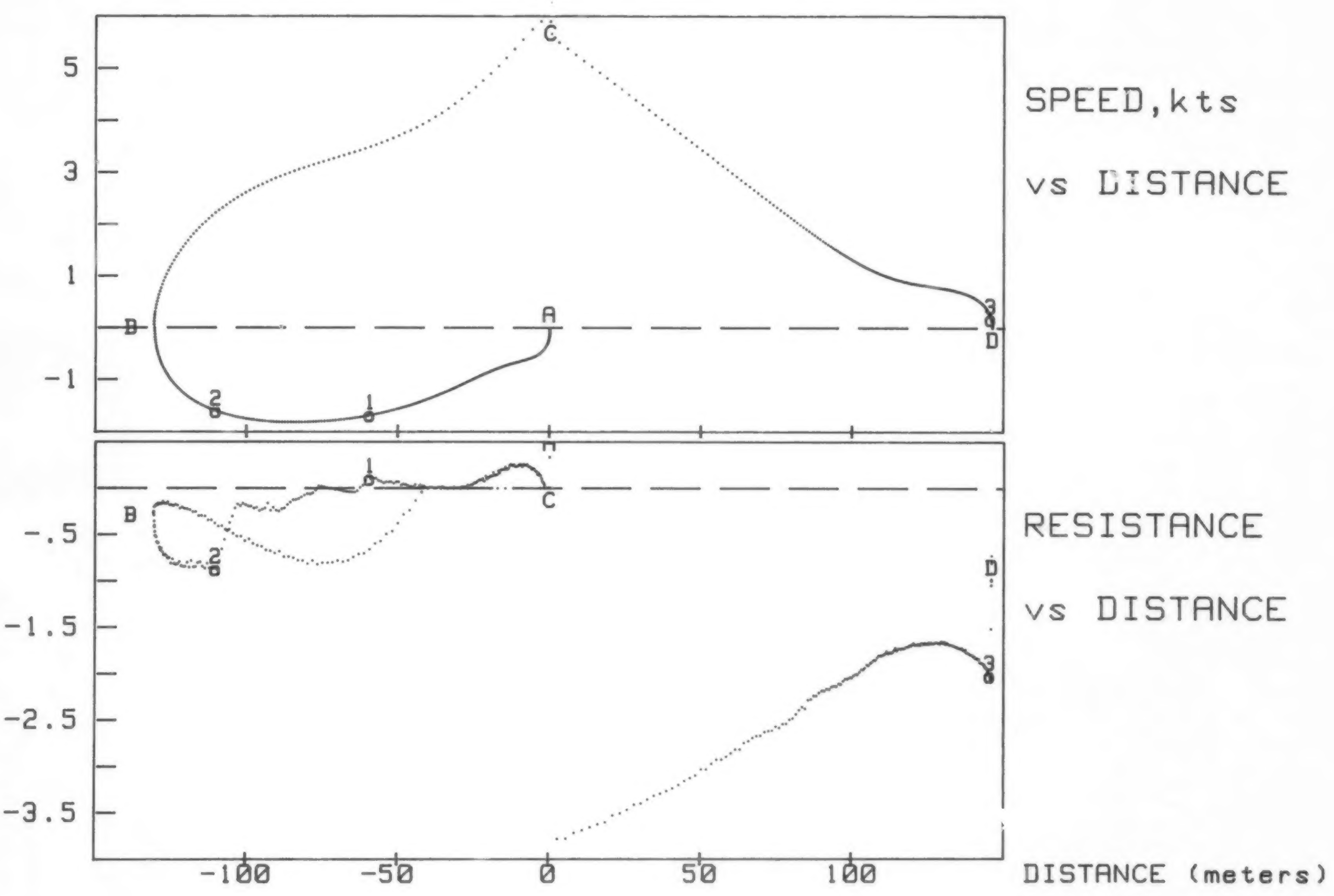

RAM # __C7   TAPE: 81-T2-5.1   08 JUL 1981 14:22:02   Fig.# 5

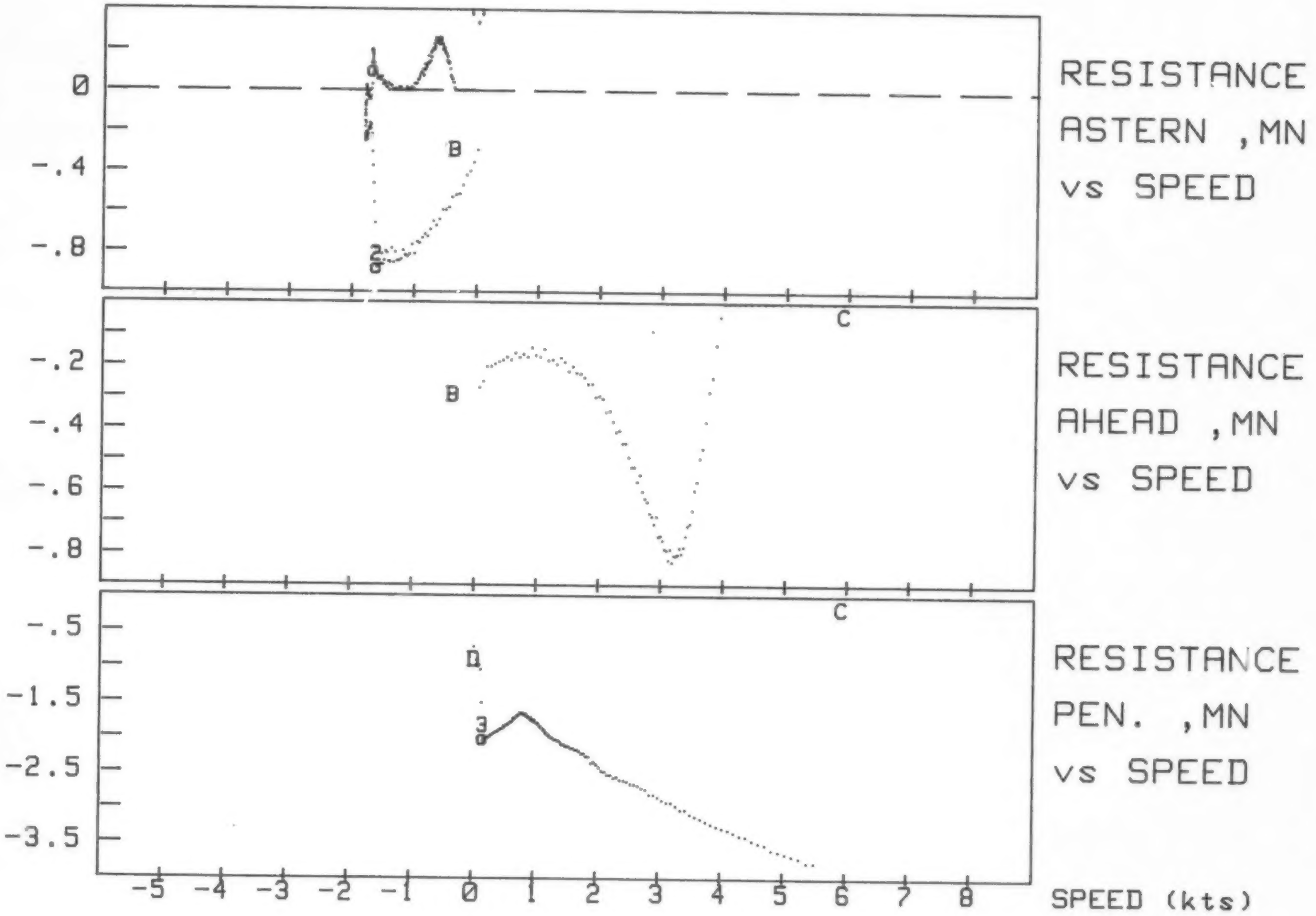

RESULTS OF RAMMING CYCLE ANALYSIS

RAM No. __C8

TAPE:	81-T2-5.1	ICE CONDITIONS:	LEVEL ICE
CATEGORY:	L2	ICE THICKNESS:	1.6 m
QUALITY:	47BC	FLEXURAL STRENGTH:	104 kPA
TRIM:	BOW UP	BUBBLER STATUS:	ON

RAMMING CYCLE CHARACTERISTICS:

Speed of Advance	(knots)	.491	
Speed of Impact	(knots)	5.5	(5.75)

	Duration (sec)	% Cycle Time	Distance (m)
Backing	225	45.8	-149.6
Acceleration	111	22.6	149.5
Penetration	144	29.3	121.2 (124.1)
Extraction	11	2.24	
Total Cycle	491		

Duration of Astern Mode	(sec)	133		
Duration of Reversal to Ahead	(sec)	84		
Duration of Ahead Mode	(sec)	252		
Duration of Reversal to Astern	(sec)	22		
Start of Reversal after Impact	(sec)	133		
Total Fuel Used	(mm*hr)	6.95	Est. kg:	121.8
Average Fuel Rate	(mm)	50.97	Est. kg/hr:	893.34
Backing Power	(kW)	6665.8		
[Est Fuel Rate	(kg/hr)]	1421.4		
Acceleration Power	(kW)	10287		
[Est Fuel Rate	(kg/hr)]	2143.5		

RAM # __C8   TAPE: 81-T2-5.1   08 JUL 1981 14:30:40   **FIG. #1**

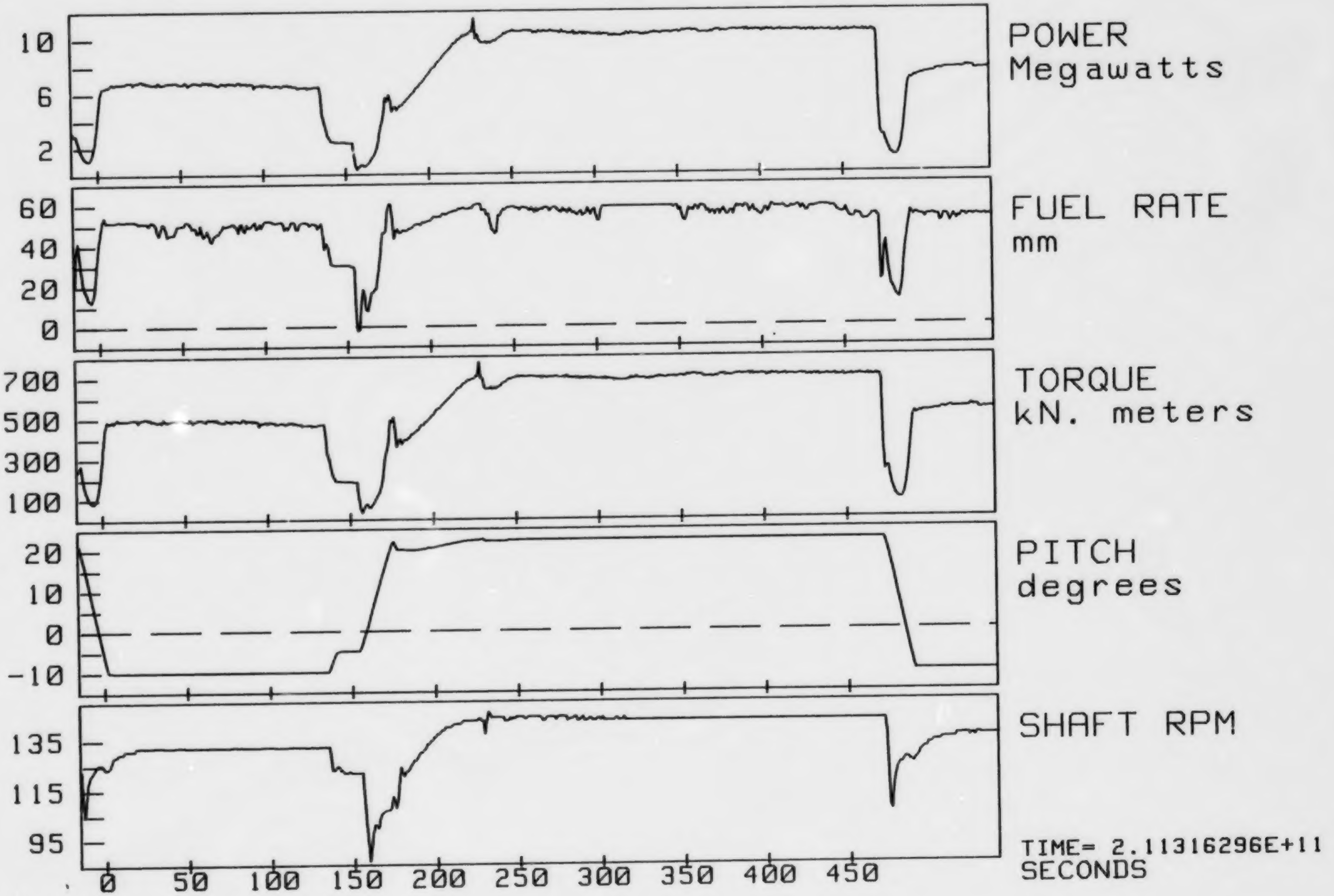

RAM # __C8 TAPE: 81-T2-5.1 08 JUL 1981 14:30:40

FIG. #2

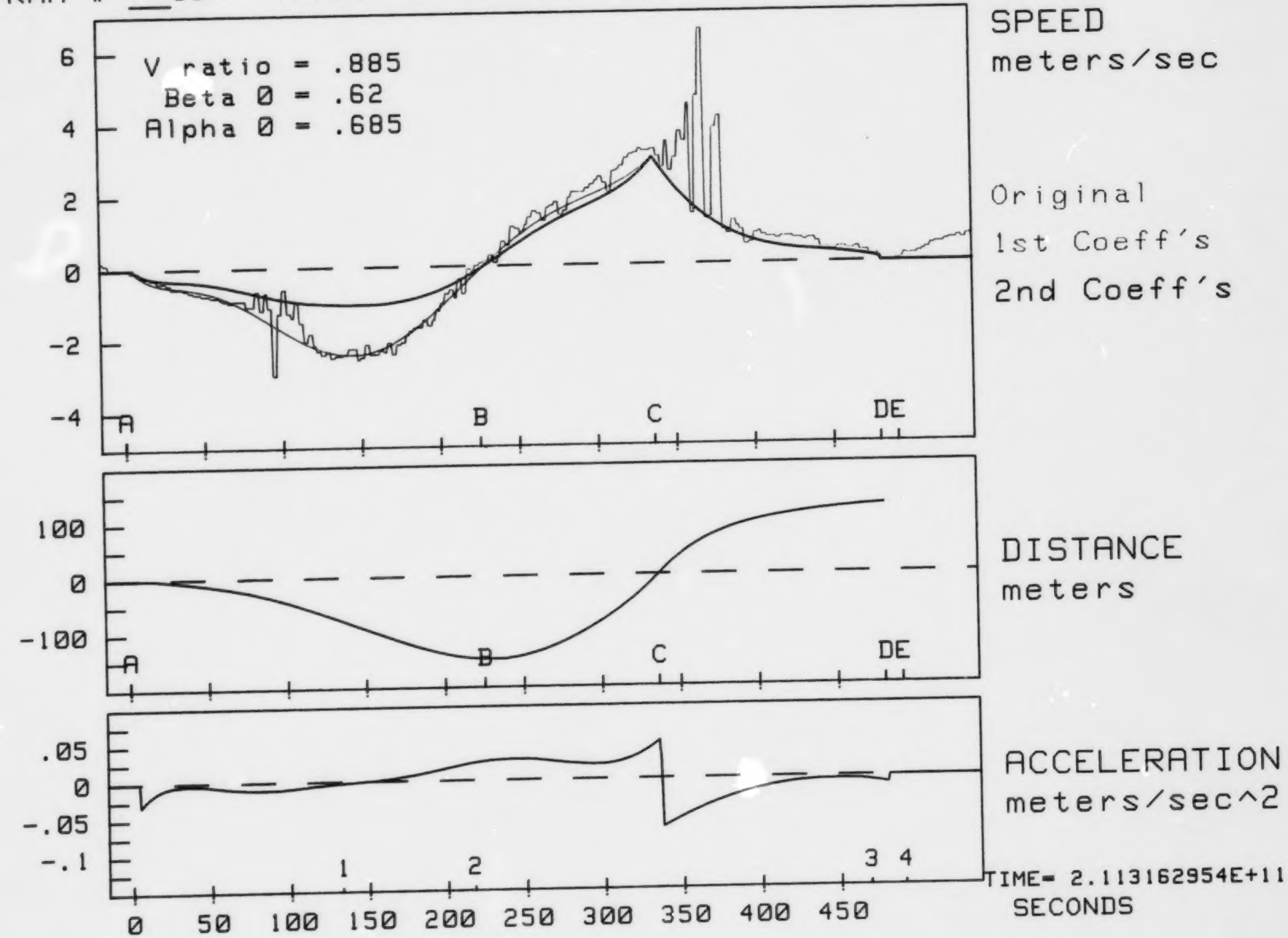

RAM # __C8 TAPE: 81-T2-5.1 08 JUL 1981 14:30:40 **FIG. #3**

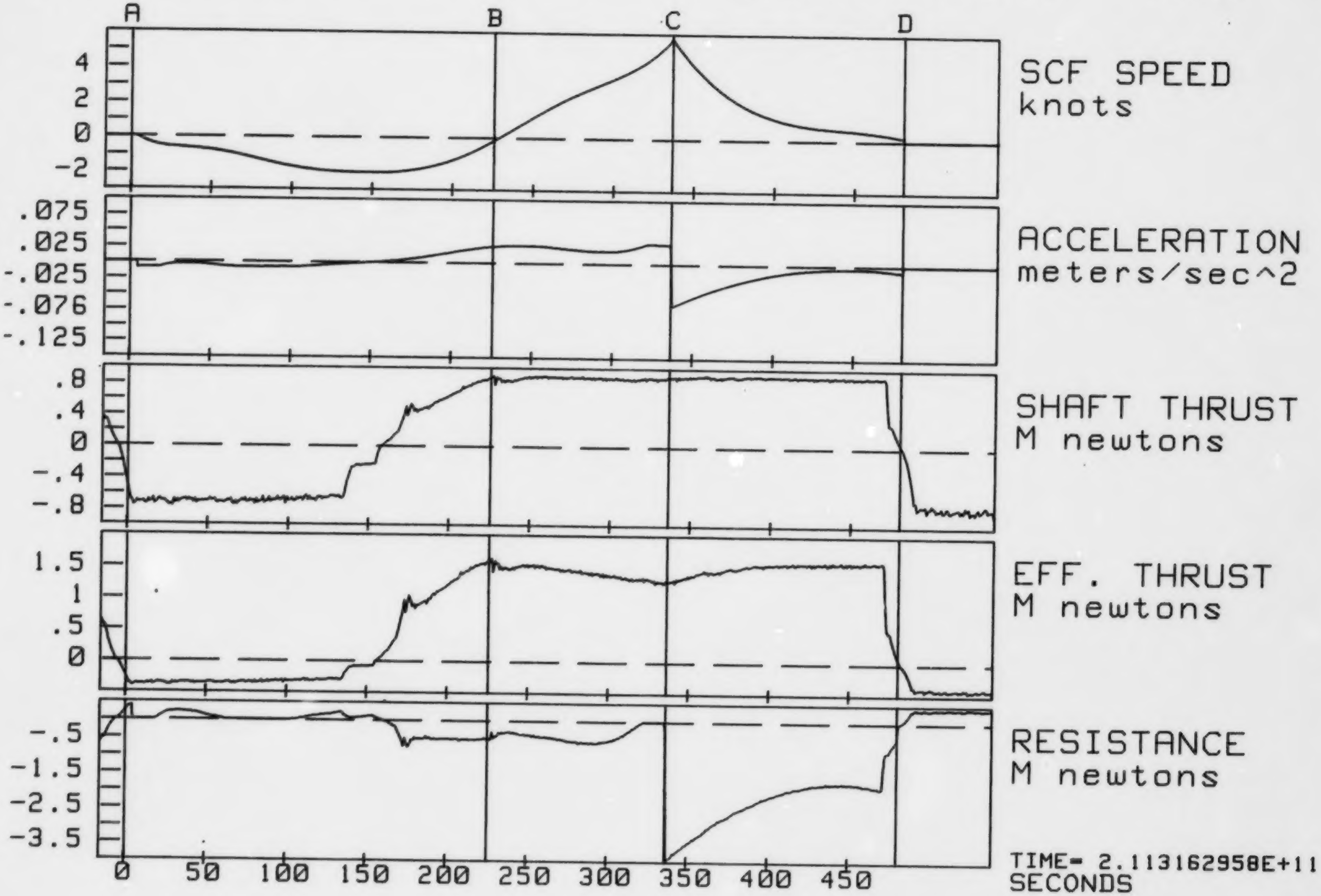

RAM # __C8 TAPE: 81-T2-5.1 08 JUL 1981 14:30:40 Fig.# 4

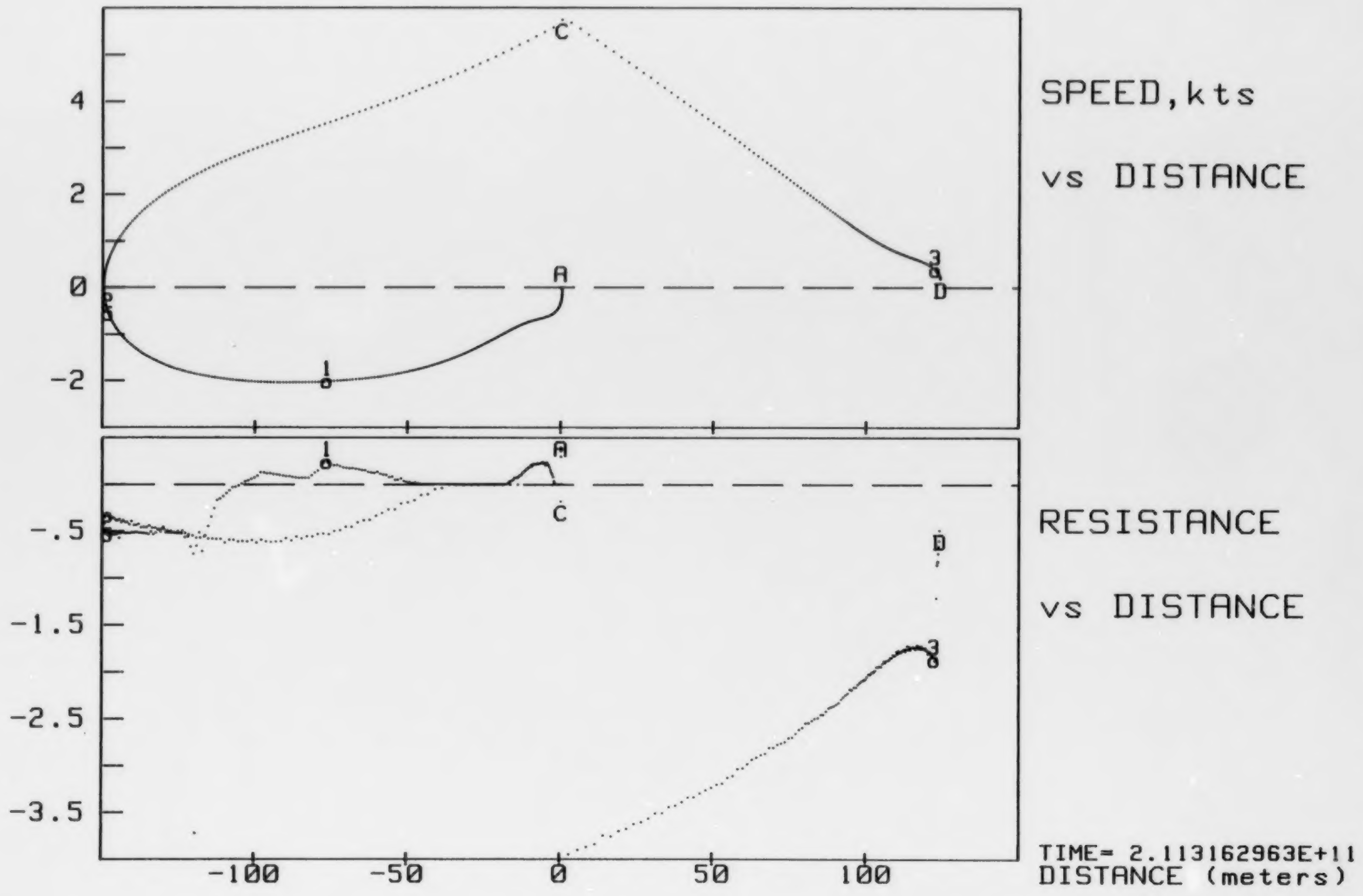

RAM # __C8 TAPE: 81-T2-5.1 08 JUL 1981 14:30:40 Fig.# 5

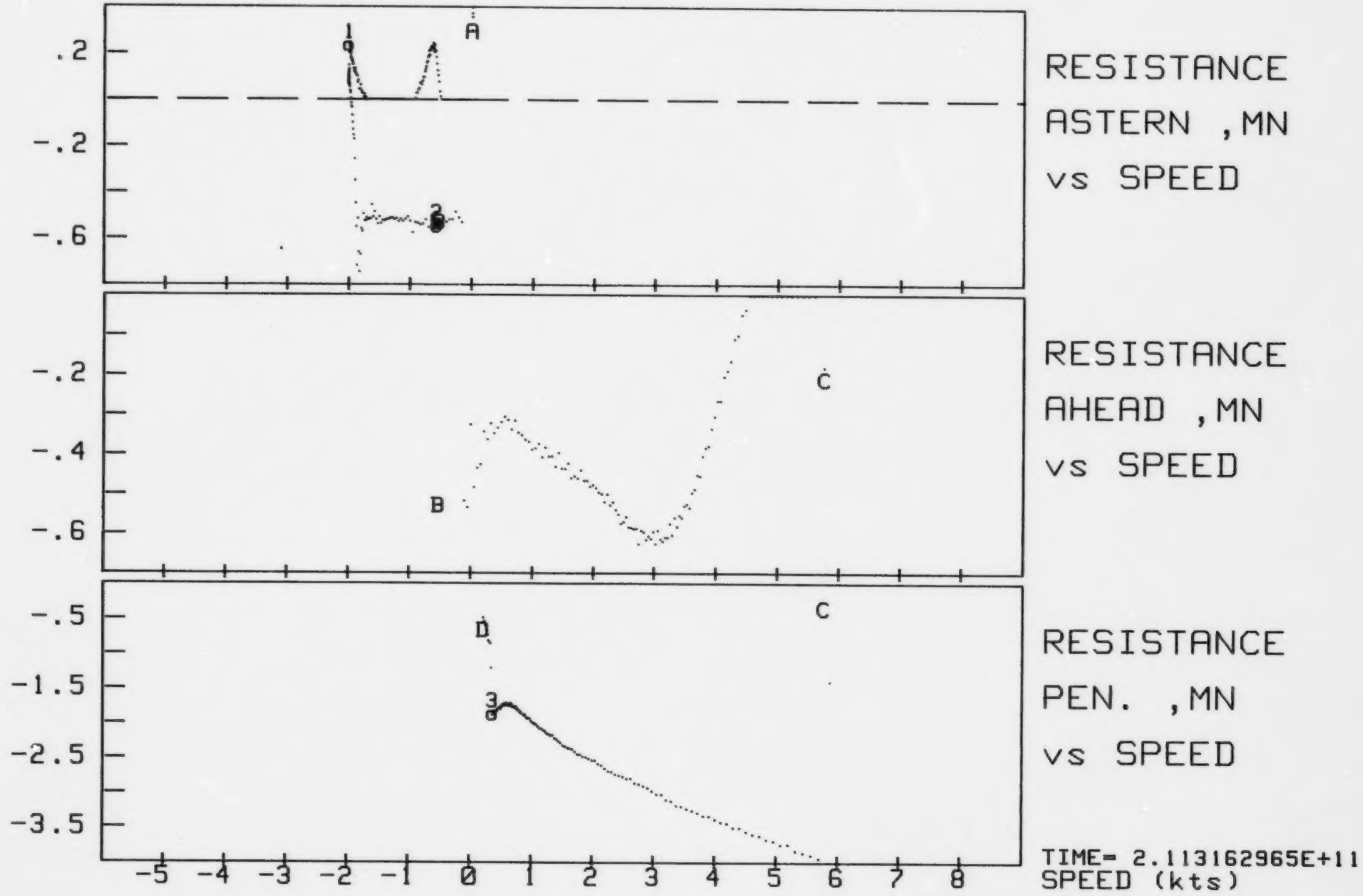

RESULTS OF RAMMING CYCLE ANALYSIS

RAM No. _C24

TAPE:	81-T2-6.3	ICE CONDITIONS:	LEVEL ICE
CATEGORY:	L4	ICE THICKNESS:	1.65 m
QUALITY:	61AD	FLEXURAL STRENGTH:	104 kPA
TRIM:	BOW UP	BUBBLER STATUS:	OFF

RAMMING CYCLE CHARACTERISTICS:

Speed of Advance	(knots)	.231	
Speed of Impact	(knots)	2.5	(2.37)

	Duration (sec)	% Cycle Time	Distance (m)
Backing	80	41.2	-25.86
Acceleration	43	22.2	25.86
Penetration	32	16.5	6.1 (23.09)
Extraction	39	20.1	
Total Cycle	194		

Duration of Astern Mode	(sec)	27
Duration of Reversal to Ahead	(sec)	25
Duration of Ahead Mode	(sec)	105
Duration of Reversal to Astern	(sec)	18
Start of Reversal after Impact	(sec)	34

Total Fuel Used	(mm*hr)	2.59	Est. kg:	37.14
Average Fuel Rate	(mm)	48.14	Est. kg/hr:	689.15

Backing Power	(kW)	8238.5
[Est Fuel Rate	(kg/hr)]	1735

Acceleration Power	(kW)	9883.6
[Est Fuel Rate	(kg/hr)]	2063

RAM # _C24 TAPE: 81-T2-6.3 08 JUL 1981 19:16:46 **FIG. #1**

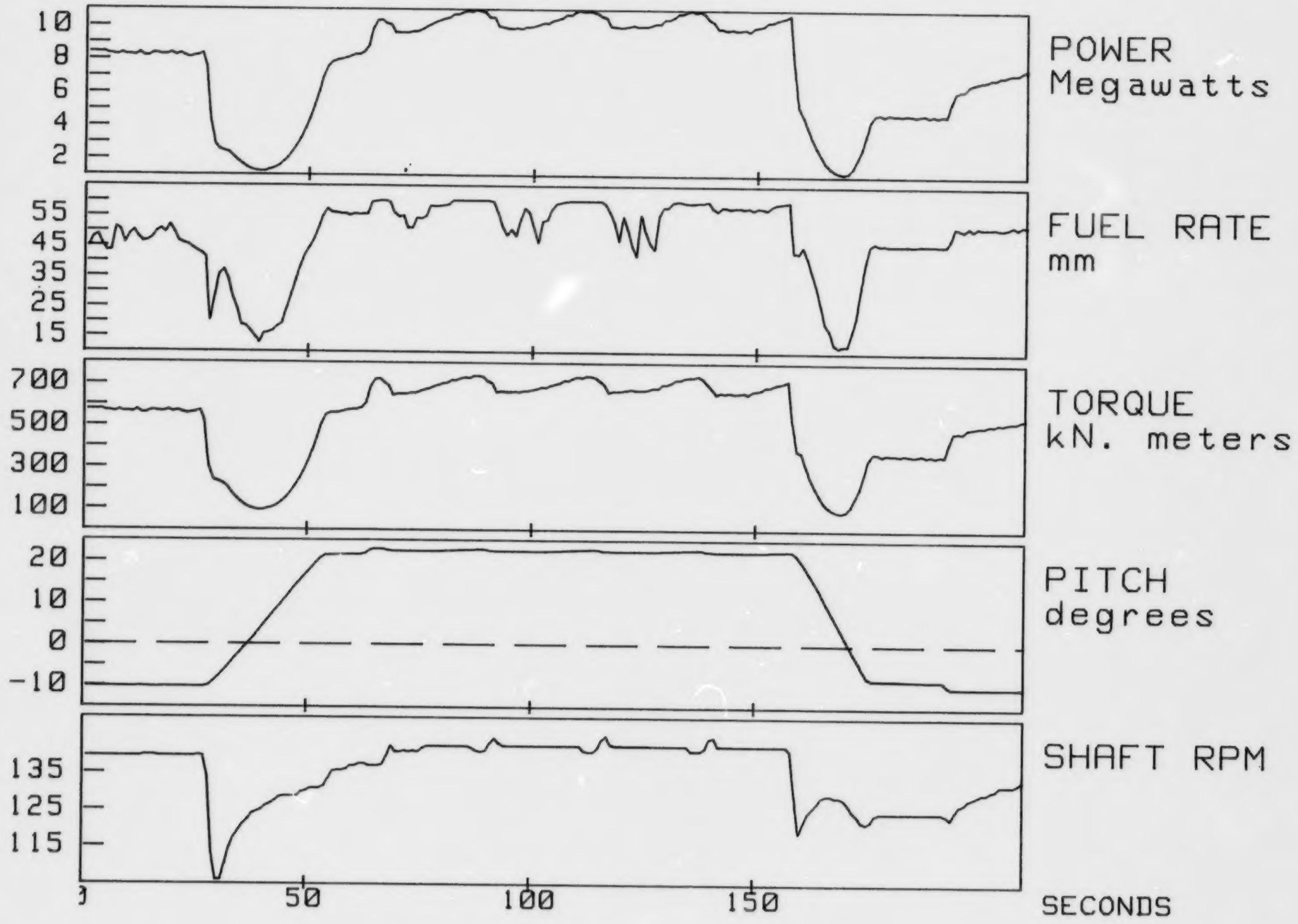

FIG. #2

RAM # _C24   TAPE: 81-T2-6.3   08 JUL 1981 19:16:46

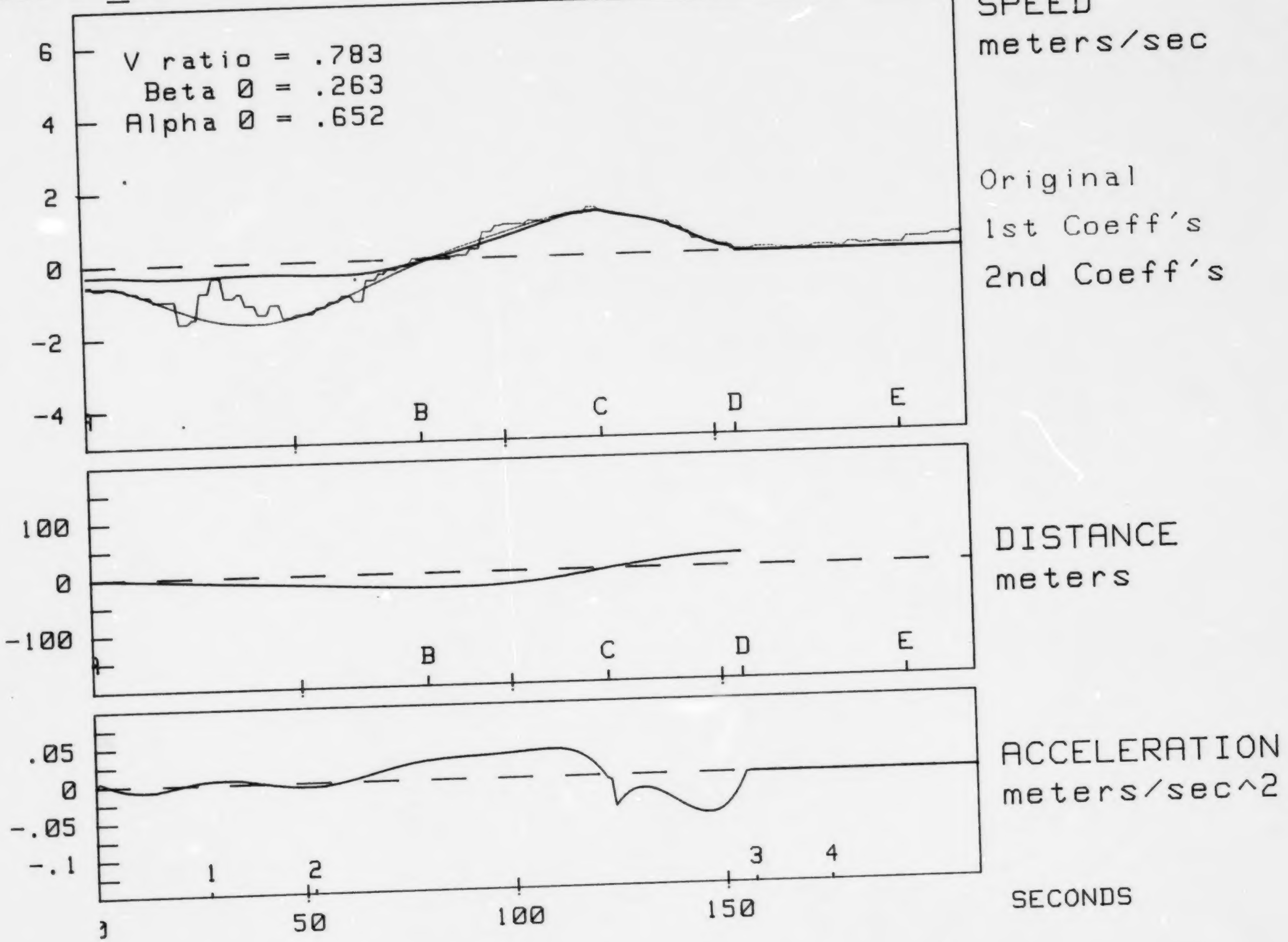

RAM # _C24 TAPE: 81-T2-6.3 08 JUL 1981 19:16:46 **FIG. #3**

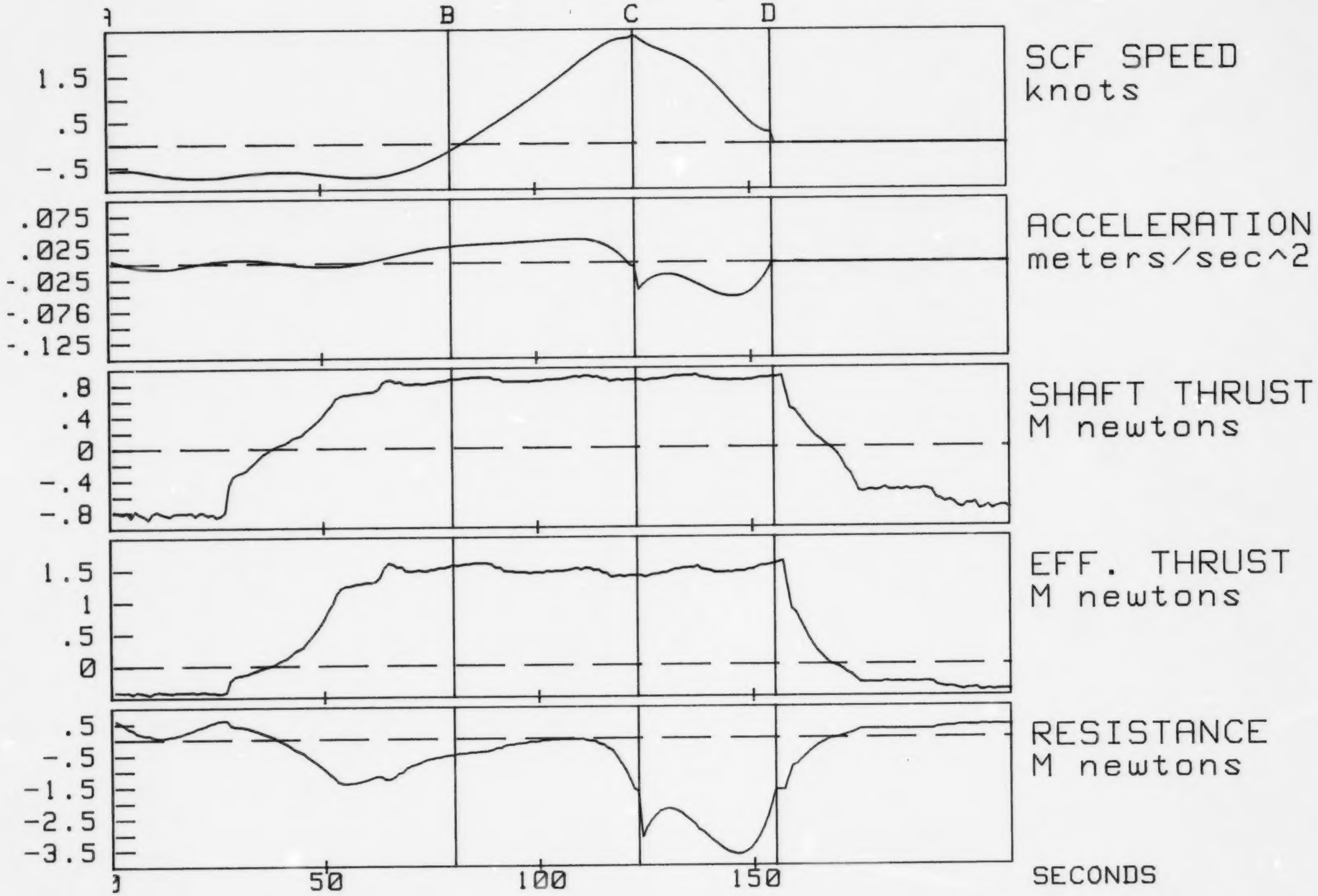

RAM # _C24 TAPE: 81-T2-6.3 08 JUL 1981 19:16:46 Fig.# 4

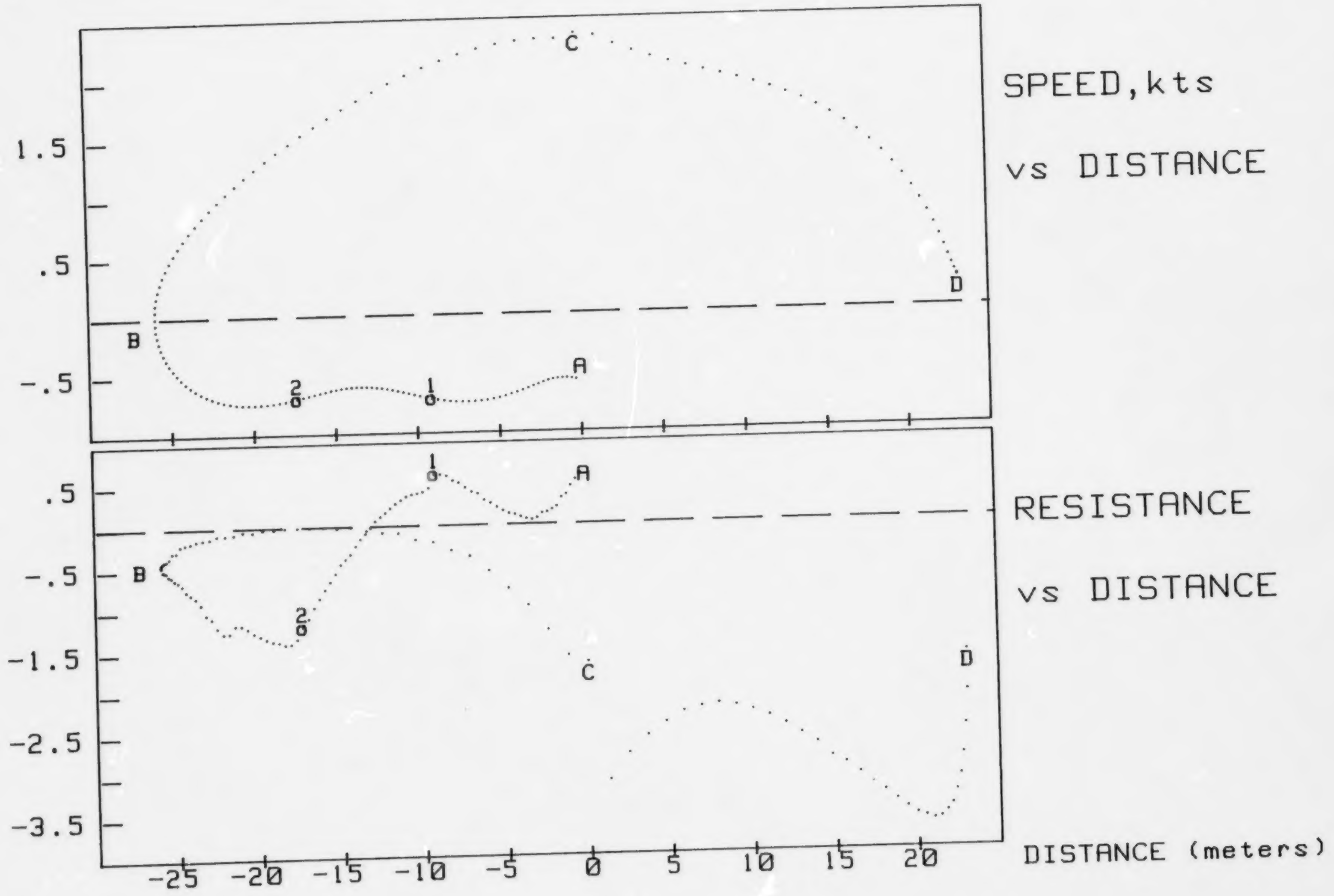
SPEED,kts vs DISTANCE

RESISTANCE vs DISTANCE

RAM # _C24   TAPE: 81-T2-6.3   08 JUL 1981 19:16:46   Fig.# 5

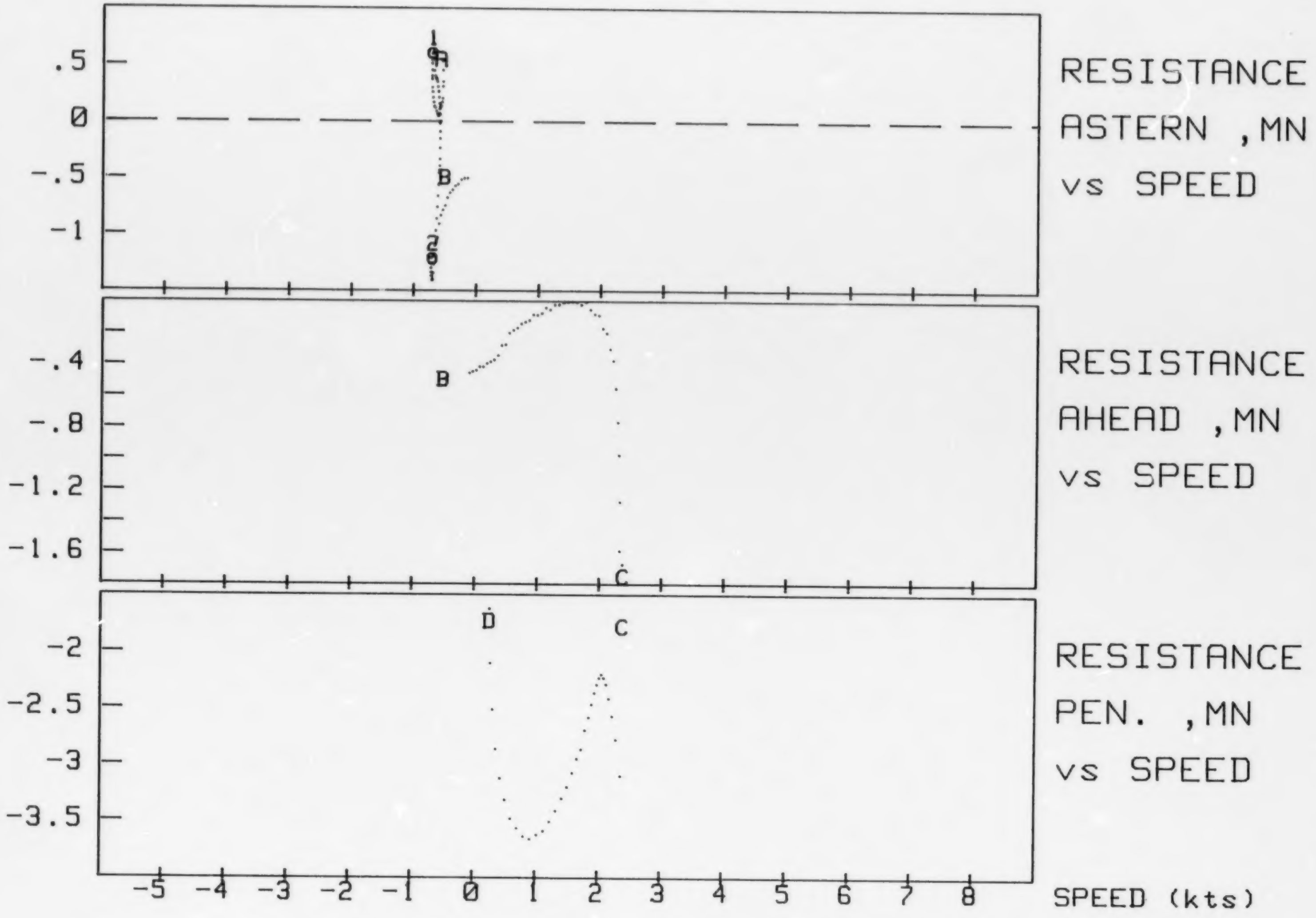

```
                    RESULTS OF RAMMING CYCLE ANALYSIS


                              RAM No.  _C25

TAPE:       81-T2-6.3                    ICE CONDITIONS:     LEVEL ICE

CATEGORY:   L4                           ICE THICKNESS:      1.6  m

QUALITY:    21AB                         FLEXURAL STRENGTH:  104  kPA

TRIM:       BOW UP                       BUBBLER STATUS:    OFF

RAMMING CYCLE CHARACTERISTICS:

Speed of Advance  (knots)     .192

Speed of Impact   (knots)     2.5    ( 2.22 )

                              Duration (sec)   % Cycle Time   Distance  (m)
Backing                       182              65.7          -33.48
Acceleration                  47               17             33.48
Penetration                   48               17.3           27.3 (27.31)
Extraction                    0                0
Total Cycle                   277


Duration of Astern Mode         (sec)      73
Duration of Reversal to Ahead   (sec)      94
Duration of Ahead Mode          (sec)      110
Duration of Reversal to Astern  (sec)      0
Start of Reversal after Impact  (sec)      48

Total Fuel Used    (mm*hr)                 3.44          Est. kg:     33.78
Average Fuel Rate (mm)                     44.67         Est. kg/hr:  439

Backing Power      (kW)                    6327.3
[Est Fuel Rate     (kg/hr)]                1353.9

Acceleration Power(kW)                     9727
[Est Fuel Rate     (kg/hr)]                2031.8
```

RAM # _C25 TAPE: 81-T2-6.3 08 JUL 1981 19:19:15

FIG. #1

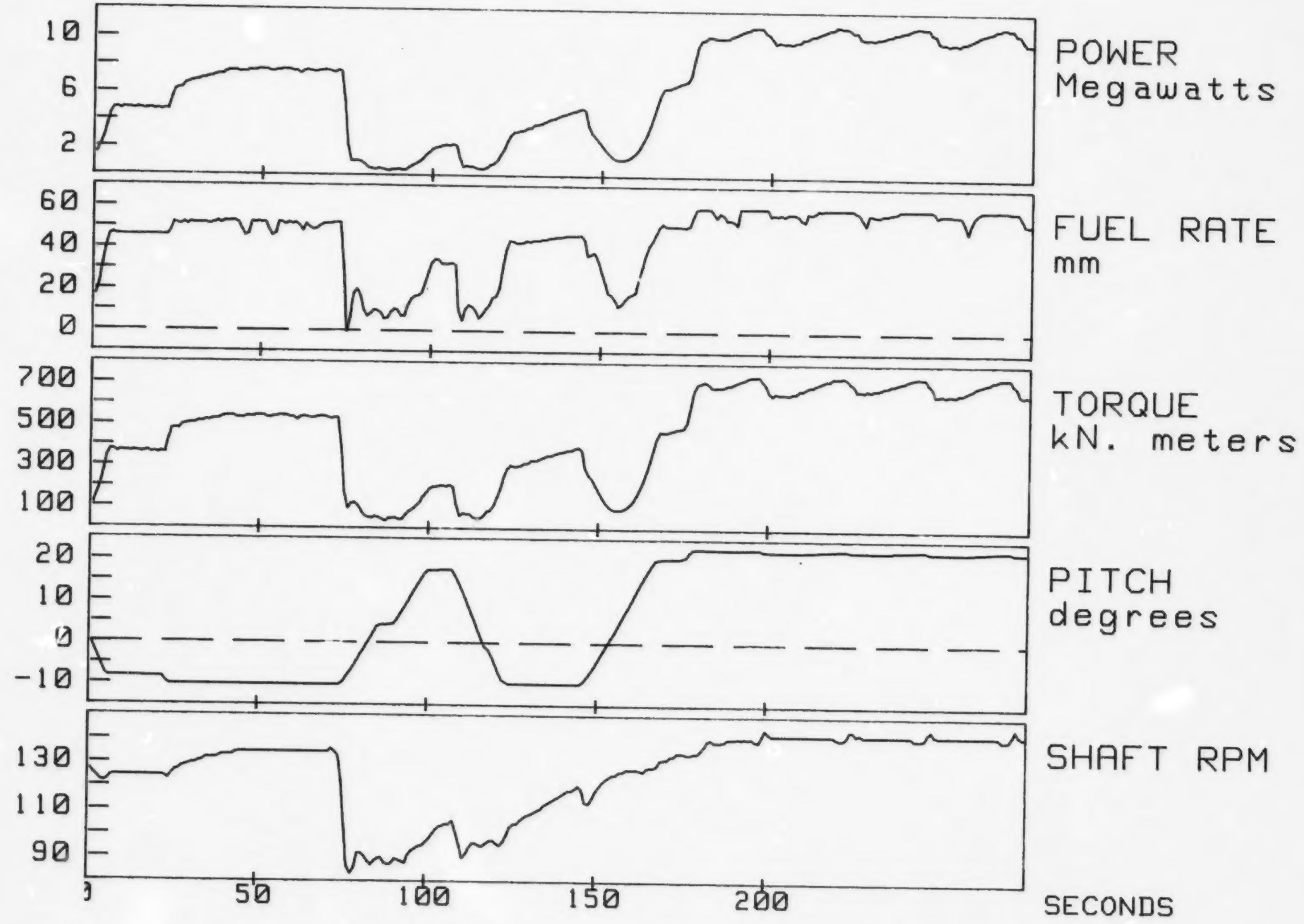

RAM # _C25 TAPE: 81-T2-6.3 08 JUL 1981 19:19:15 **FIG. #2**

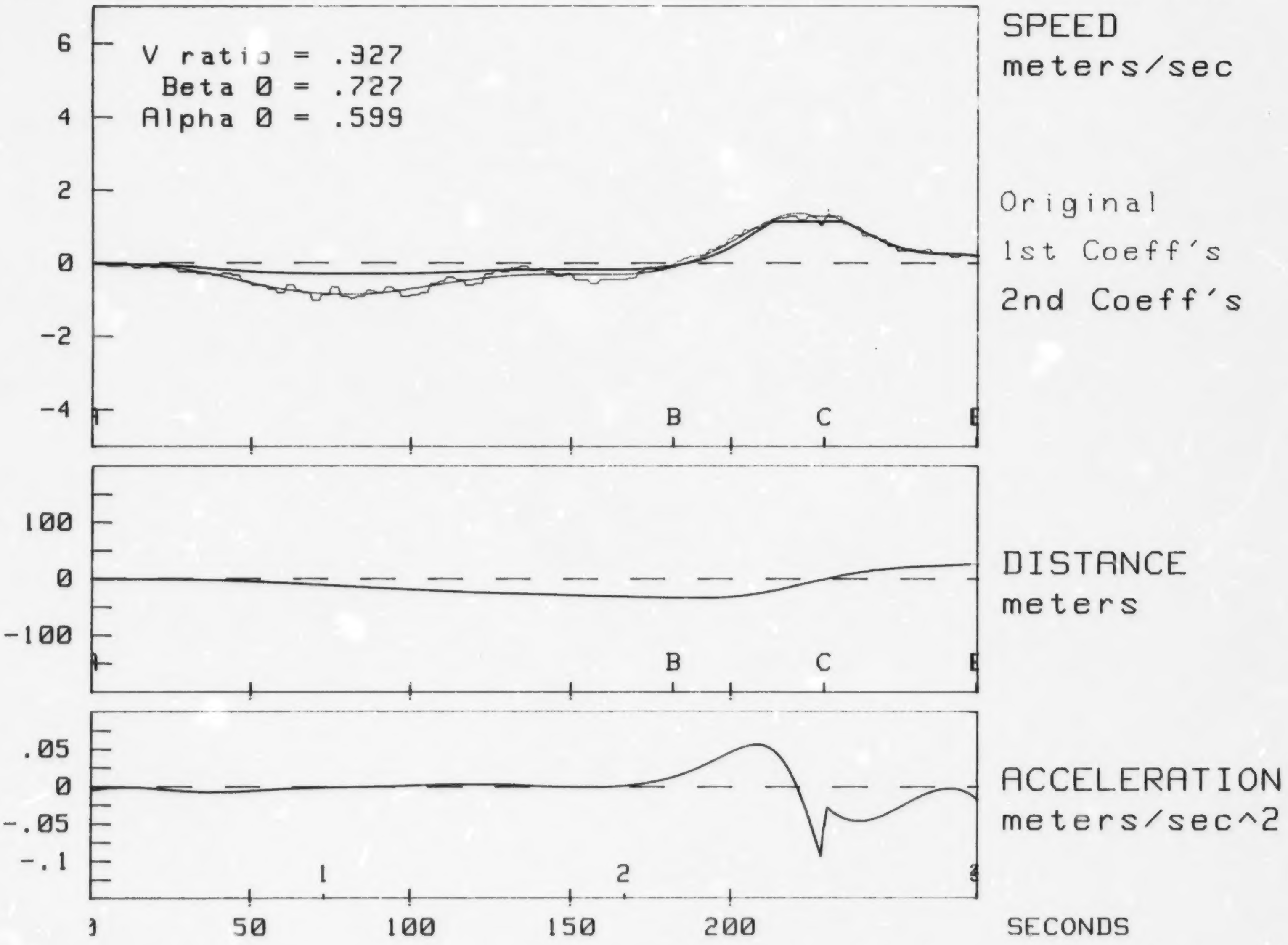

RAM # _C25 TAPE: 81-T2-6.3 08 JUL 1981 19:19:15 **FIG. #3**

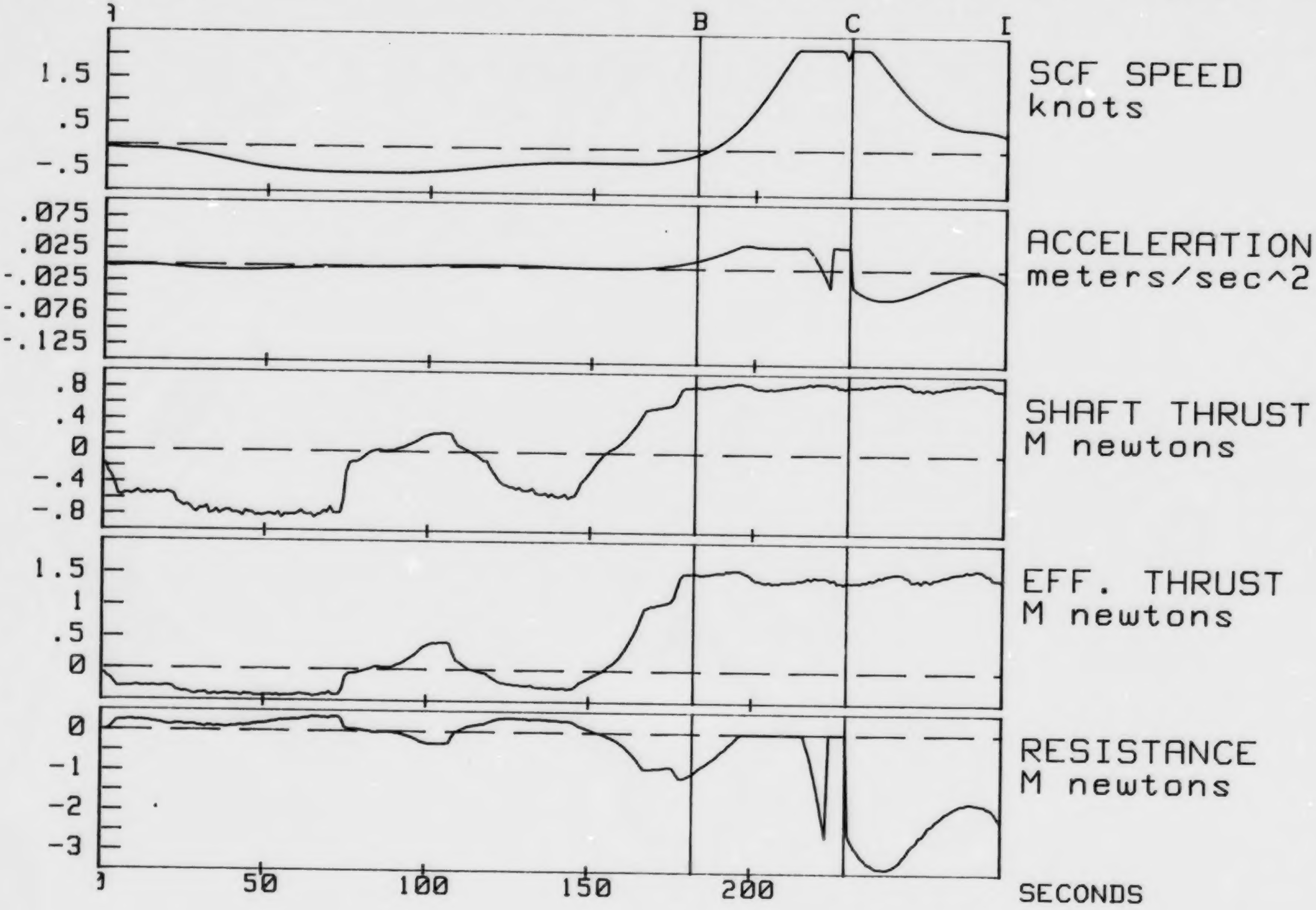

RAM # _C25 TAPE: 81-T2-6.3 08 JUL 1981 19:19:15 Fig.# 4

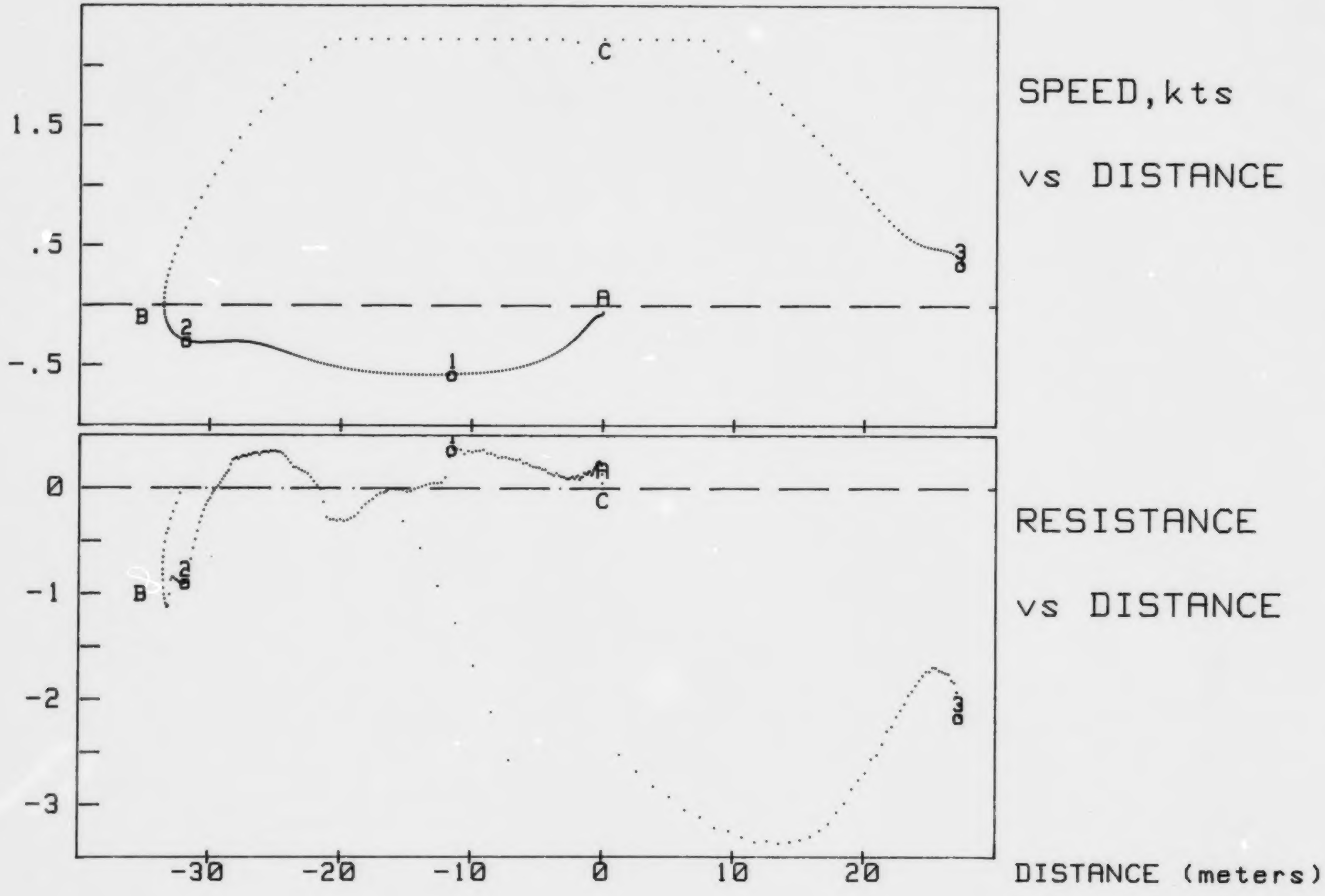

RAM # _C25 TAPE: 81-T2-6.3 08 JUL 1981 19:19:15 Fig.# 5

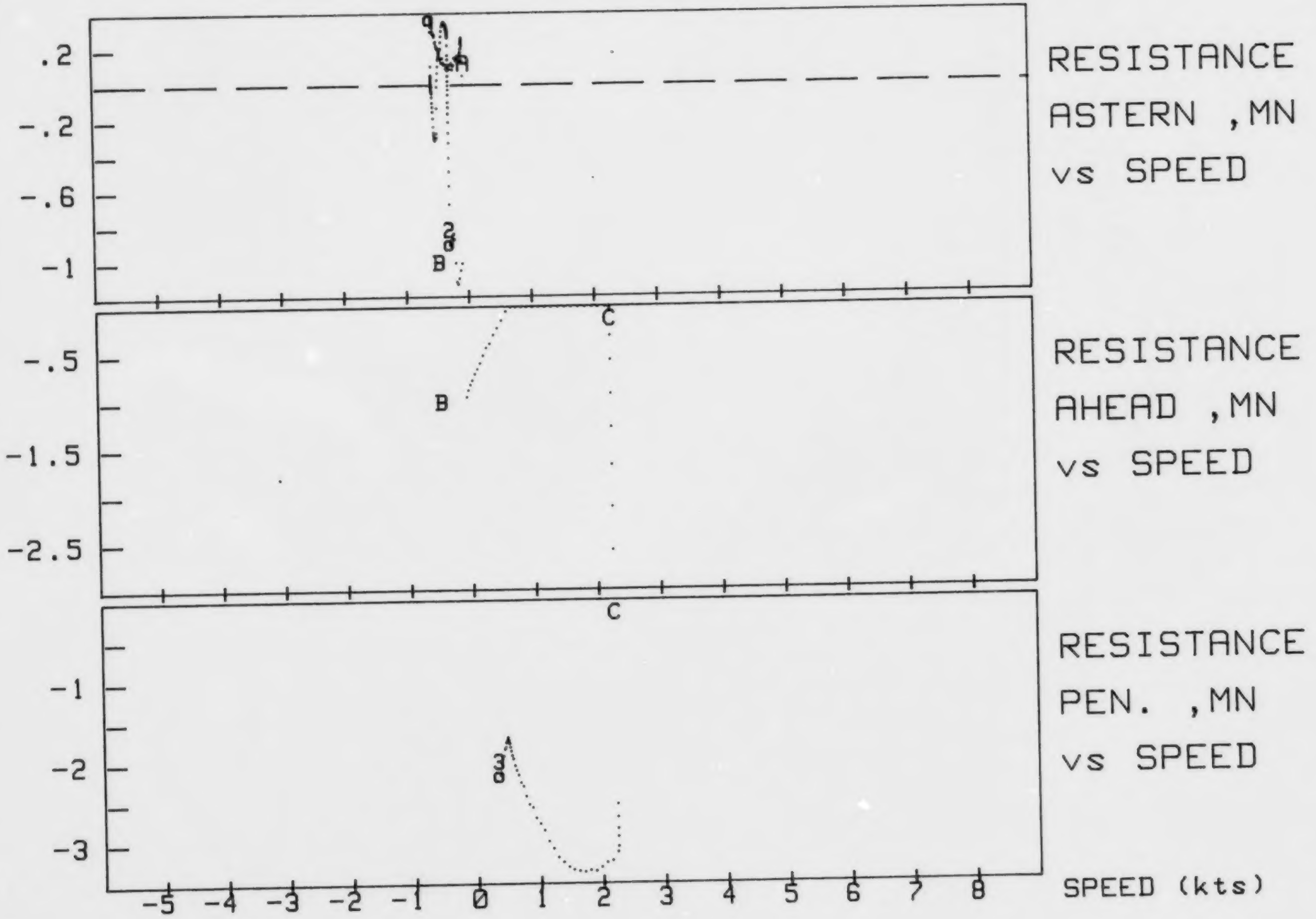

```
                    RESULTS OF RAMMING CYCLE ANALYSIS


                              RAM No.  _C27


TAPE:        81-T2-6.3                ICE CONDITIONS:      LEVEL ICE

CATEGORY:    L4                       ICE THICKNESS:       1.68  m

QUALITY:     53AB                     FLEXURAL STRENGTH:  104   kPA

TRIM:        BOW UP                   BUBBLER STATUS:     OFF


RAMMING CYCLE CHARACTERISTICS:

Speed of Advance  (knots)      .629

Speed of Impact   (knots)      2.5     ( 2.27 )


                               Duration (sec)   % Cycle Time   Distance  (m)
Backing                        77               23             -18.73
Acceleration                   32               9.55            18.72
Penetration                    215              64.2            27.3 (108.4)
Extraction                     11               3.28
Total Cycle                    335


Duration of Astern Mode           (sec)       25
Duration of Reversal to Ahead     (sec)       31
Duration of Ahead Mode            (sec)       270
Duration of Reversal to Astern    (sec)       9
Start of Reversal after Impact    (sec)       217

Total Fuel Used     (mm*hr)                   4.9        Est. kg:      94.68
Average Fuel Rate   (mm)                      52.7       Est. kg/hr:   1017.5

Backing Power       (kW)                      6167.8
[Est Fuel Rate      (kg/hr)]                  1322.1

Acceleration Power  (kW)                      9979.8
[Est Fuel Rate      (kg/hr)]                  2082.2
```

RAM # _C27   TAPE: 81-T2-6.3 08 JUL 1981 19:31:16   **FIG. #1**

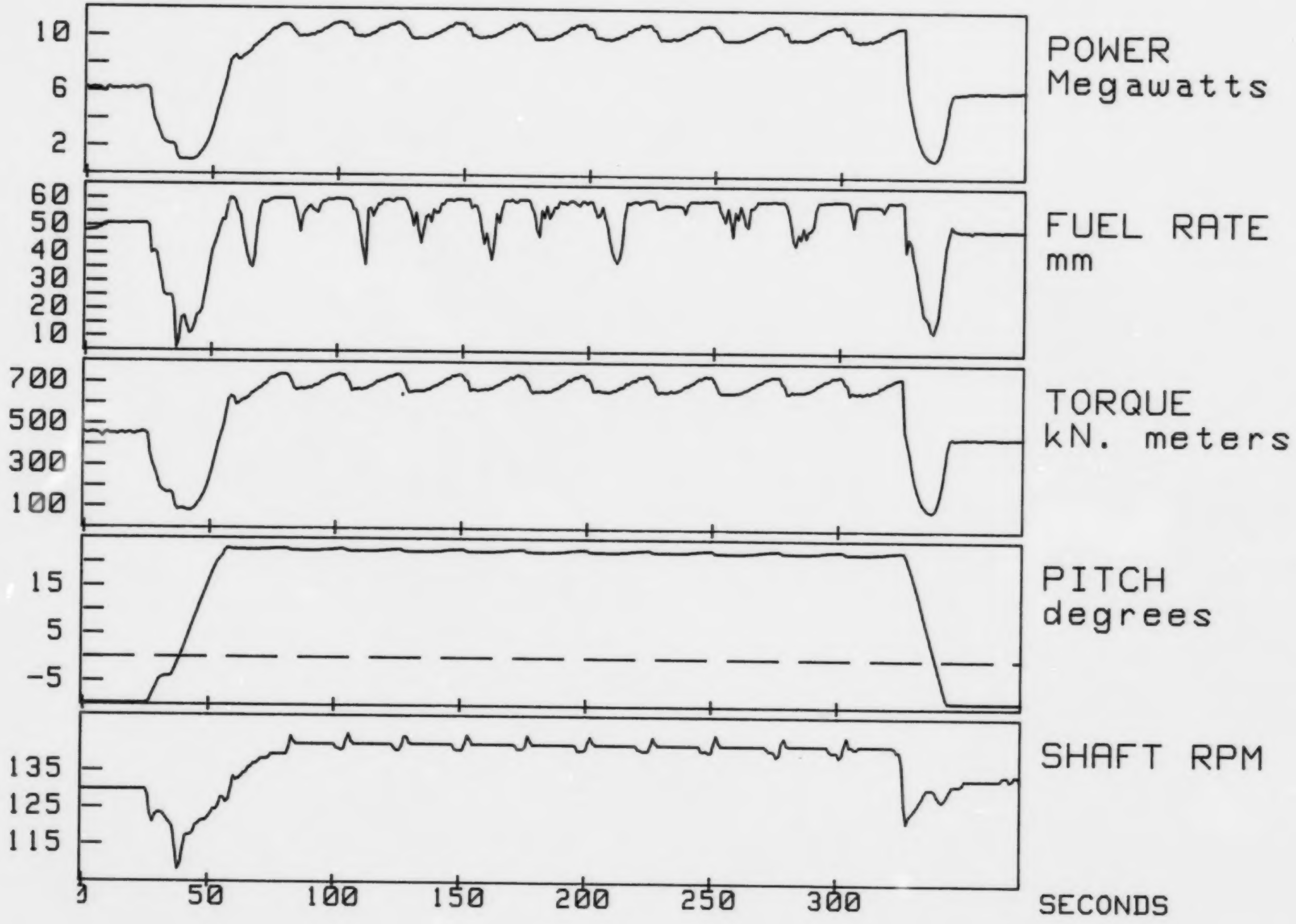

RAM # _C27 TAPE: 81-T2-6.3 08 JUL 1981 19:31:16 **FIG. #2**

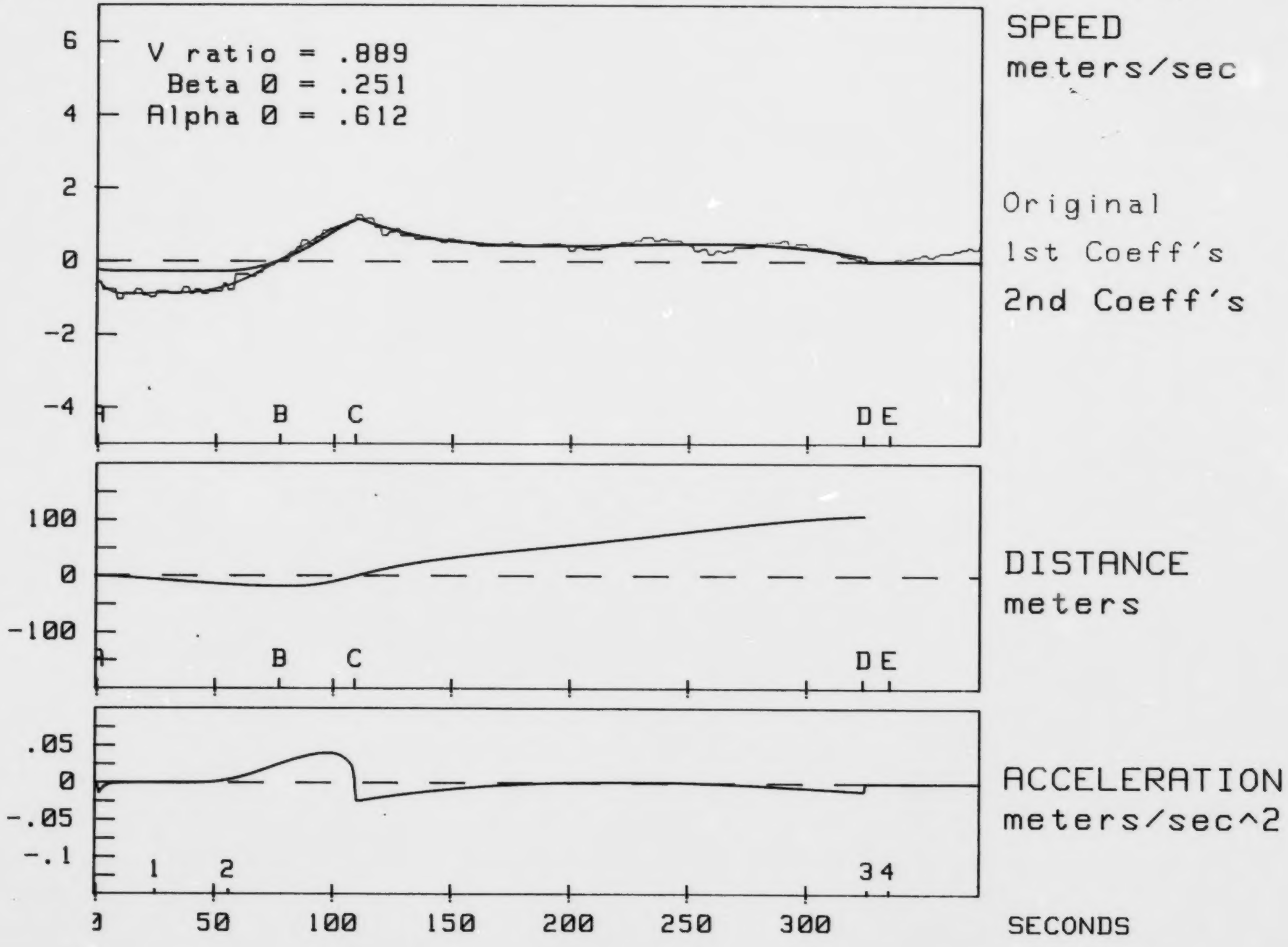

RAM # _C27 TAPE: 81-T2-6.3 08 JUL 1981 19:31:16 **FIG. #3**

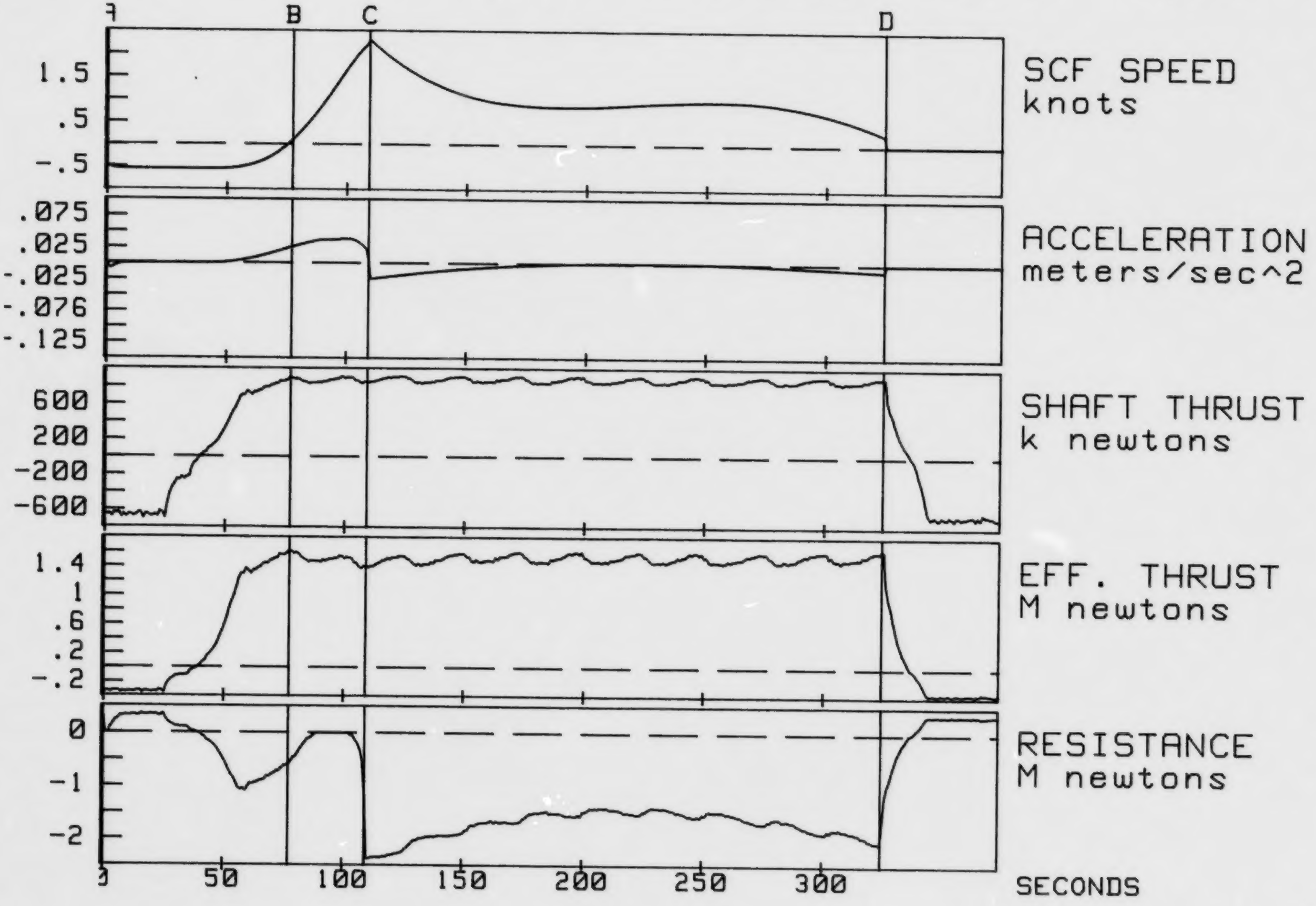

RAM # _C27   TAPE: 81-T2-6.3   08 JUL 1981 19:31:16   Fig.# 4

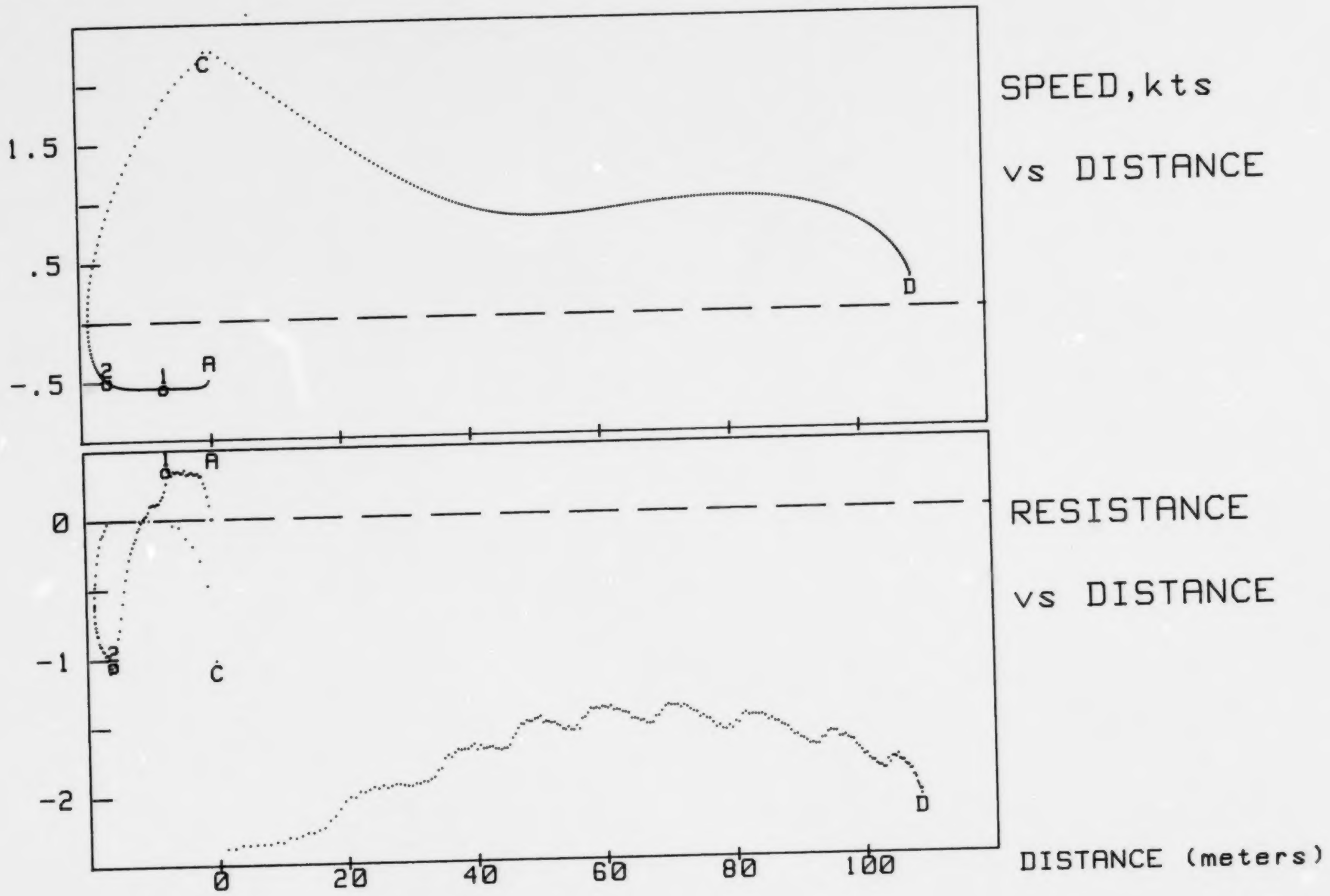

RAM # _C27 TAPE: 81-T2-6.3 08 JUL 1981 19:31:16 Fig.# 5

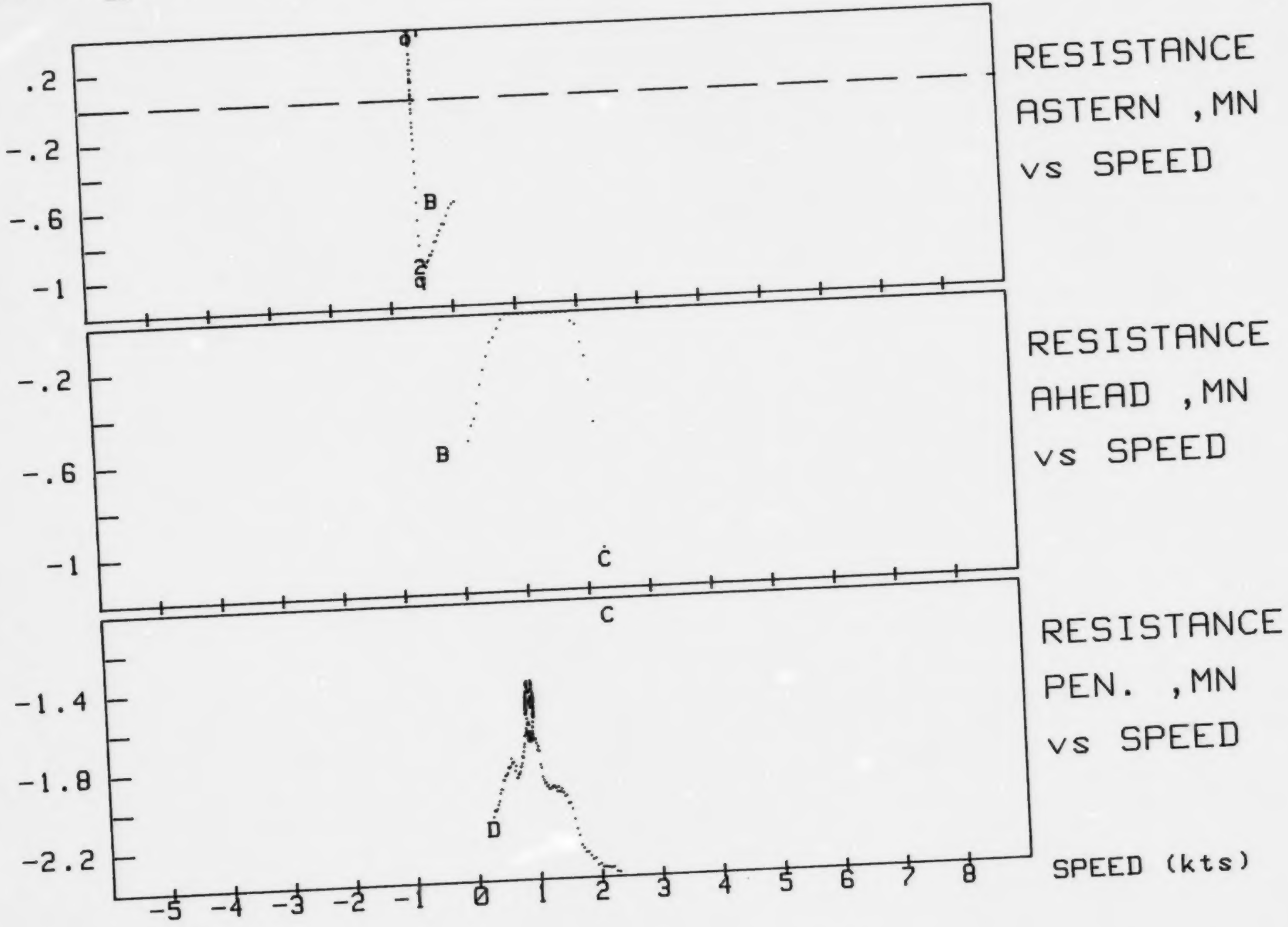

RESULTS OF RAMMING CYCLE ANALYSIS

RAM No. _C29

TAPE:	81-T2-6.3	ICE CONDITIONS:	LEVEL ICE
CATEGORY:	L4	ICE THICKNESS:	1.52 m
QUALITY:	26AB	FLEXURAL STRENGTH:	104 kPA
TRIM:	BOW UP	BUBBLER STATUS:	OFF

RAMMING CYCLE CHARACTERISTICS:

Speed of Advance	(knots)	.424	
Speed of Impact	(knots)	3.7	(3.93)

	Duration (sec)	% Cycle Time	Distance (m)
Backing	229	51.2	-88.94
Acceleration	85	19	88.94
Penetration	114	25.5	97 (97.49)
Extraction	19	4.25	
Total Cycle	447		

Duration of Astern Mode	(sec)	177		
Duration of Reversal to Ahead	(sec)	28		
Duration of Ahead Mode	(sec)	226		
Duration of Reversal to Astern	(sec)	16		
Start of Reversal after Impact	(sec)	117		
Total Fuel Used	(mm*hr)	6.25	Est. kg:	105.1
Average Fuel Rate	(mm)	50.33	Est. kg/hr:	846.65
Backing Power	(kW)	6354.4		
[Est Fuel Rate	(kg/hr)]	1359.3		
Acceleration Power	(kW)	9056.3		
[Est Fuel Rate	(kg/hr)]	1898.1		

RAM # _C29 TAPE: 81-T2-6.3 08 JUL 1981 19:50:25 **FIG. #1**

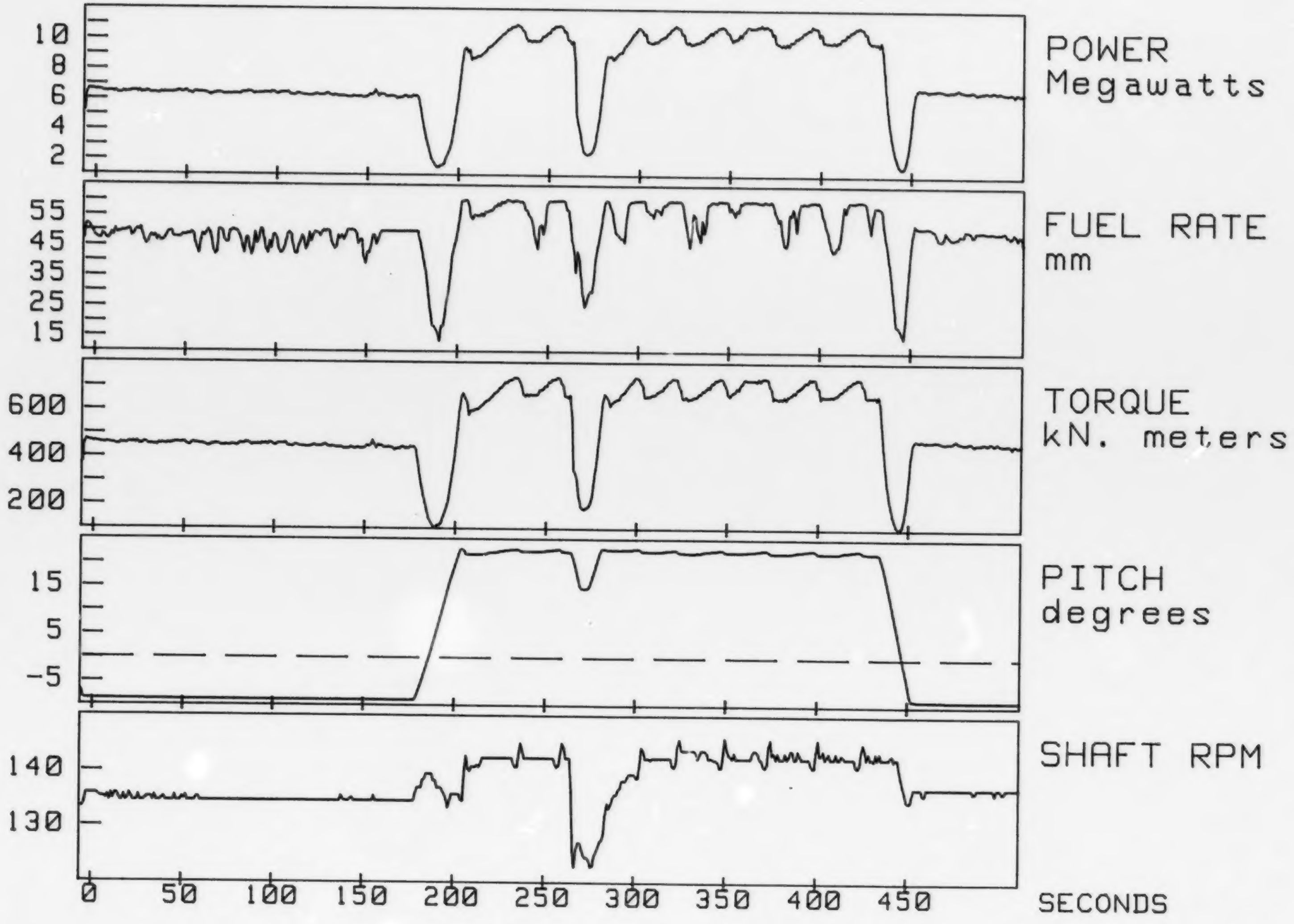

RAM # _C29 TAPE: 81-T2-6.3 08 JUL 1981 19:50:25

FIG. #2

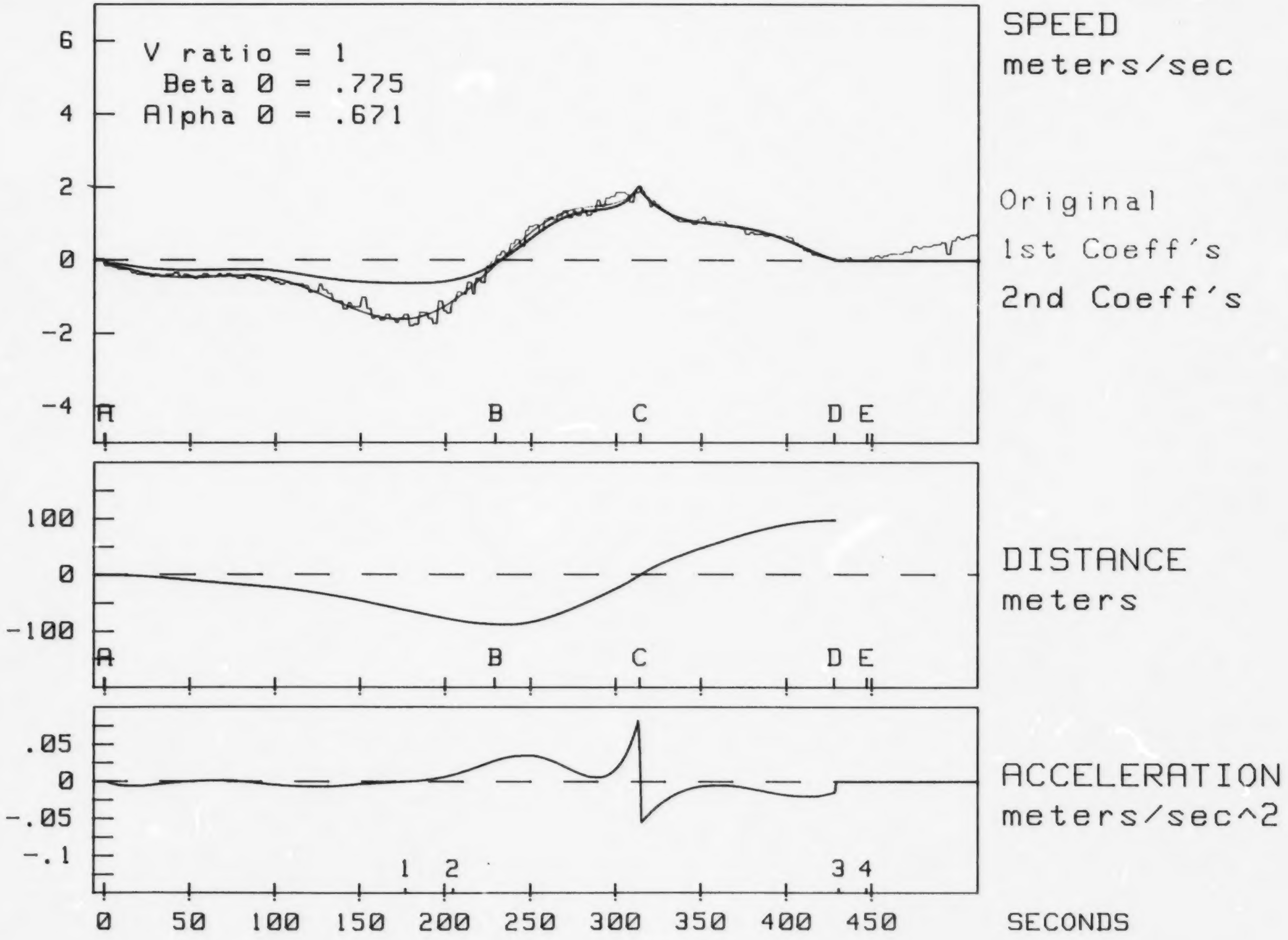

RAM # _C29 TAPE: 81-T2-6.3 08 JUL 1981 19:50:25

FIG. #3

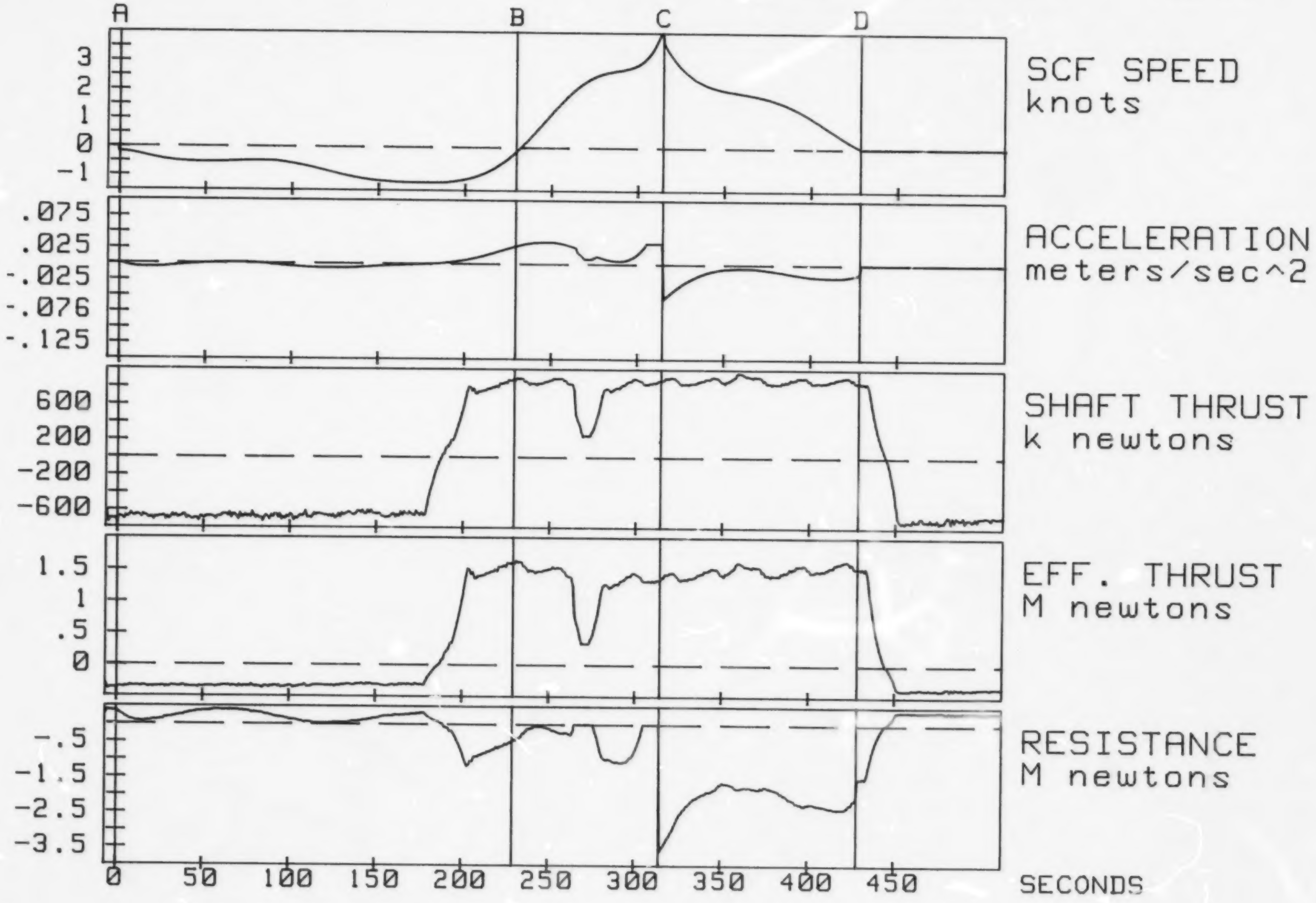

RAM # _C2S TAPE: 81-T2-6.3 08 JUL 1981 19:50:25 Fig.# 4

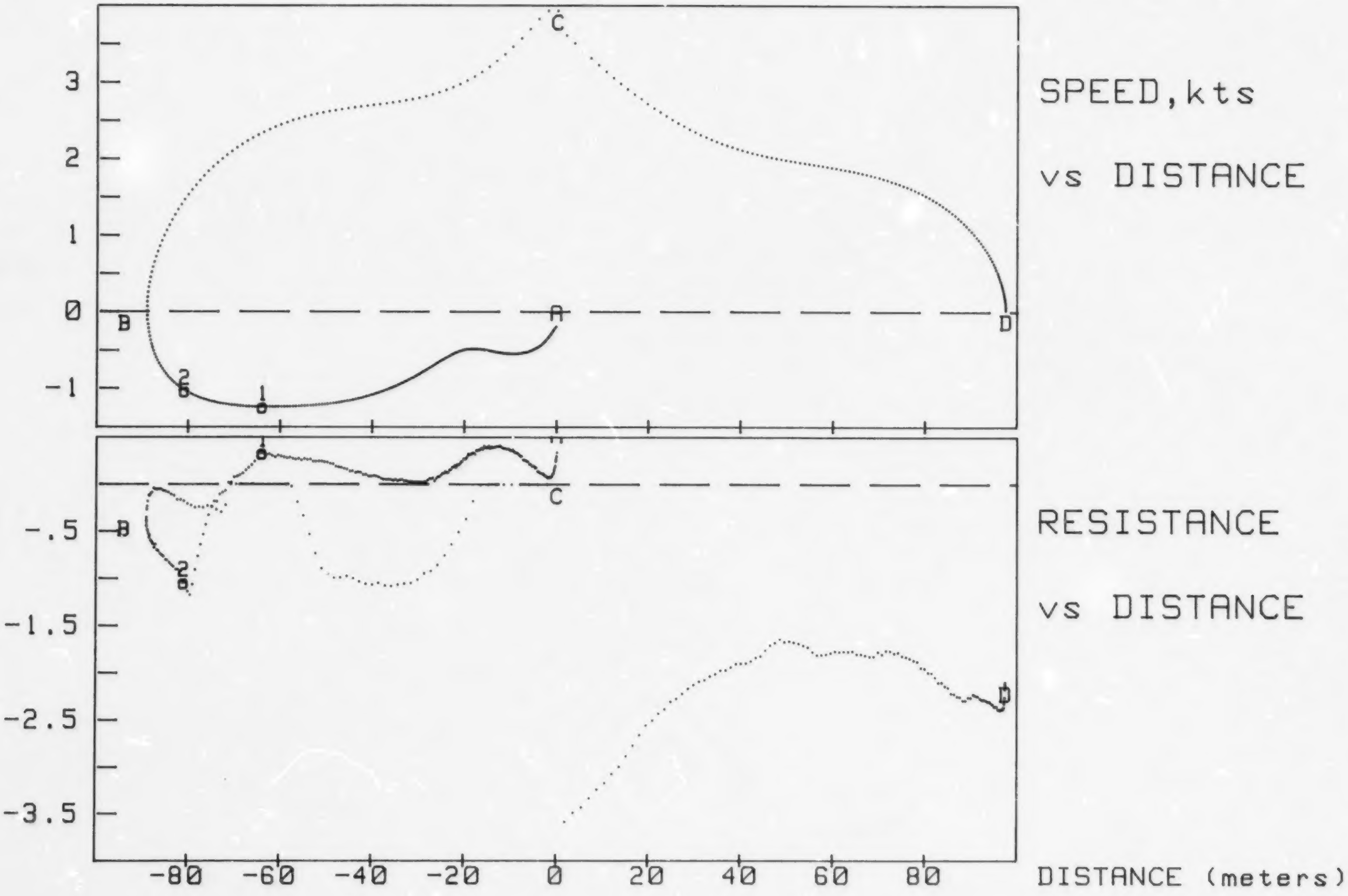

SPEED, kts vs DISTANCE

RESISTANCE vs DISTANCE

RAM # _C29   TAPE: 81-T2-6.3   08 JUL 1981 19:50:25   Fig.# 5

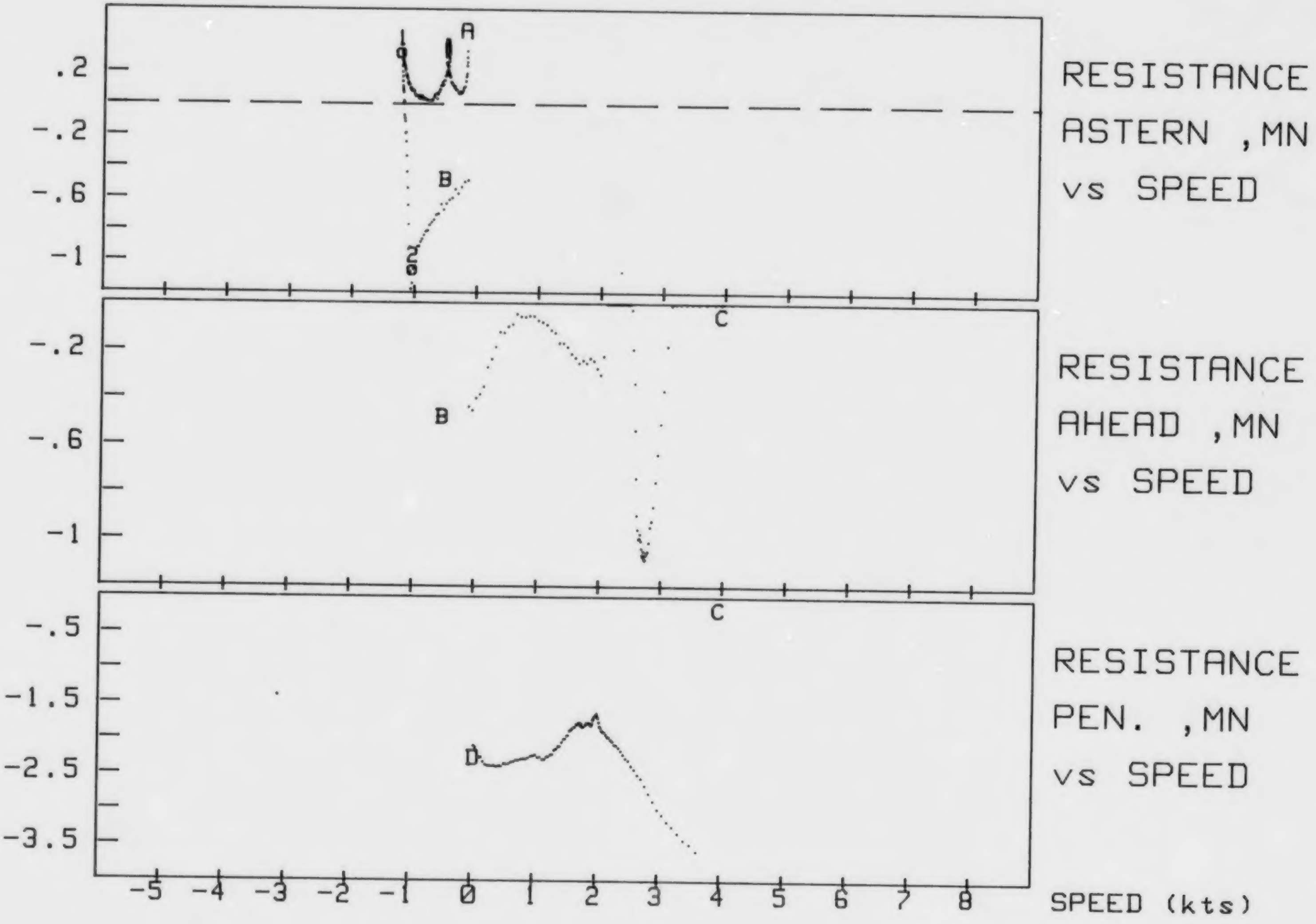

RESULTS OF RAMMING CYCLE ANALYSIS

RAM No. _C31

TAPE:	81-T2-6.3	ICE CONDITIONS:	LEVEL ICE
CATEGORY:	L4	ICE THICKNESS:	1.42 m
QUALITY:	23AB	FLEXURAL STRENGTH:	104 kPA
TRIM:	BOW UP	BUBBLER STATUS:	OFF

RAMMING CYCLE CHARACTERISTICS:

Speed of Advance	(knots)	.47	
Speed of Impact	(knots)	3.7	(3.87)

	Duration (sec)	% Cycle Time	Distance (m)
Backing	170	35.5	-62.43
Acceleration	65	13.6	62.43
Penetration	159	33.2	115.1 (115.8)
Extraction	85	17.7	
Total Cycle	479		

Duration of Astern Mode	(sec)	87
Duration of Reversal to Ahead	(sec)	53
Duration of Ahead Mode	(sec)	317
Duration of Reversal to Astern	(sec)	20
Start of Reversal after Impact	(sec)	222

Total Fuel Used	(mm*hr)	6.89	Est. kg:	127
Average Fuel Rate	(mm)	51.82	Est. kg/hr:	954.33

Backing Power	(kW)	6587.2
[Est Fuel Rate	(kg/hr)]	1405.7
Acceleration Power	(kW)	10078
[Est Fuel Rate	(kg/hr)]	2101.8

RAM # _C31 TAPE: 81-T2-6.3 08 JUL 1981 20:02:24 **FIG. #1**

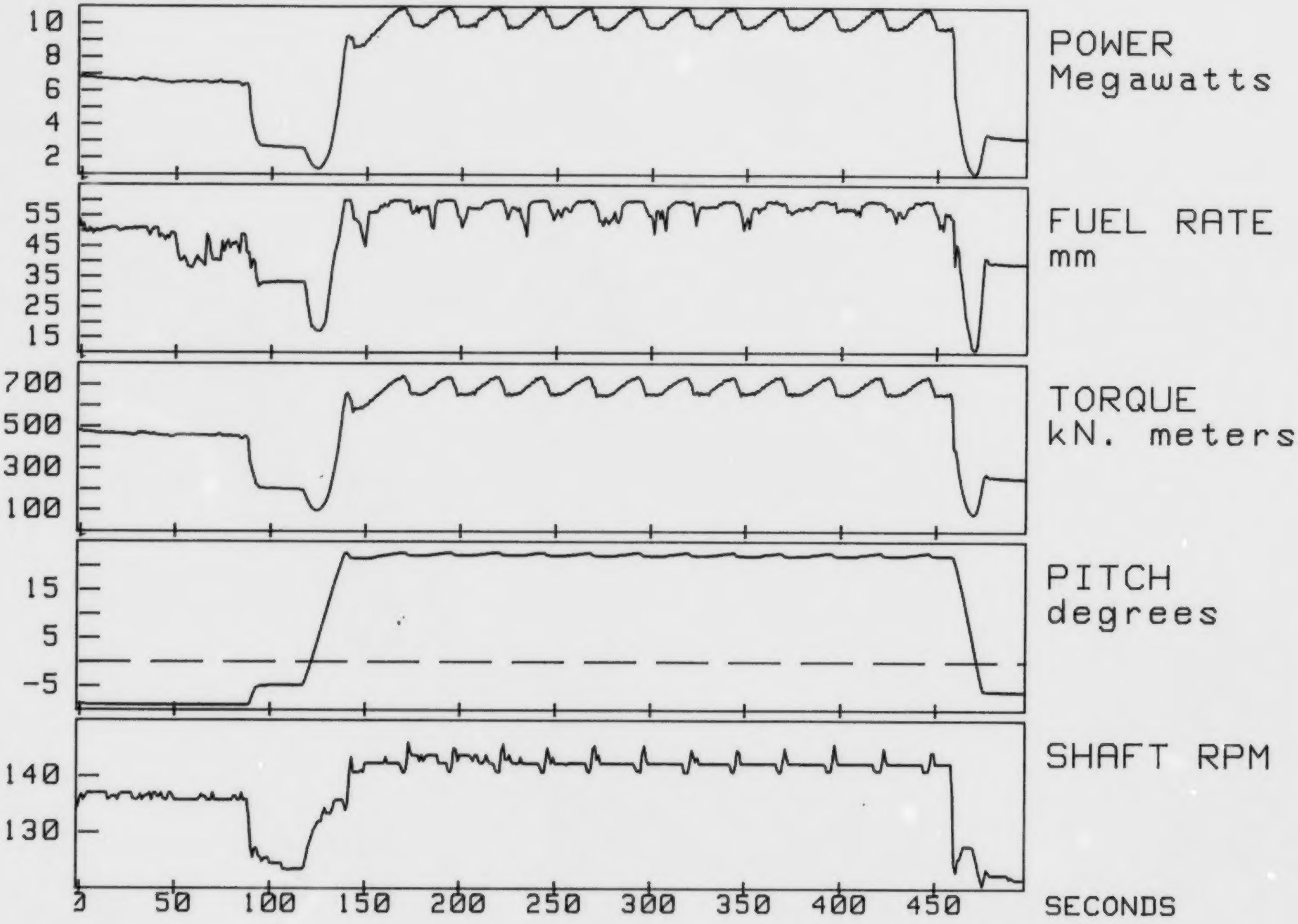

FIG. #2

RAM # _C31 TAPE: 81-T2-6.3 08 JUL 1981 20:02:24

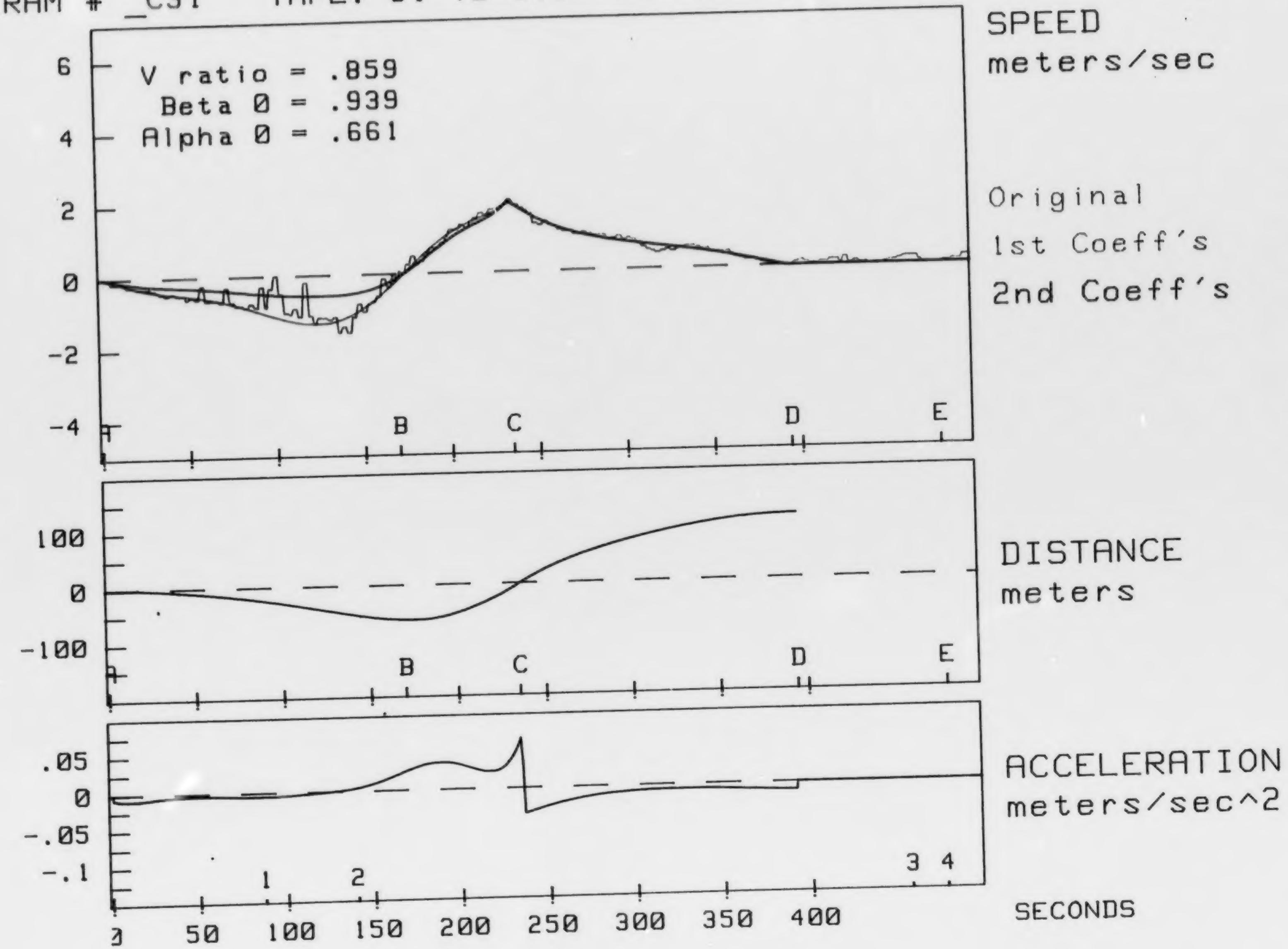

RAM # _C31 TAPE: 81-T2-6.3 08 JUL 1981 20:02:24 **FIG. #3**

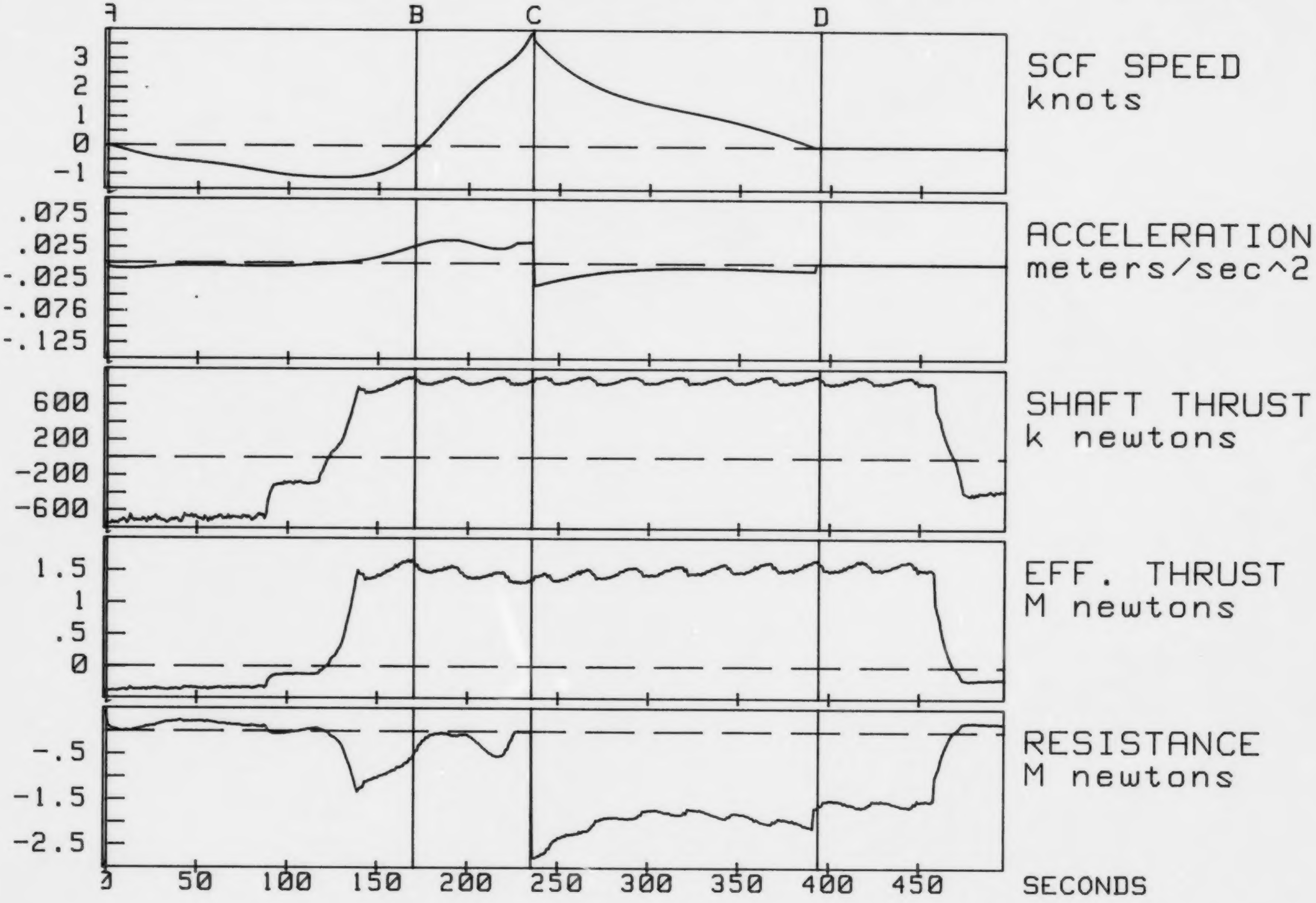

RAM # _C31   TAPE: 81-T2-6.3 08 JUL 1981 20:02:24   Fig.# 4

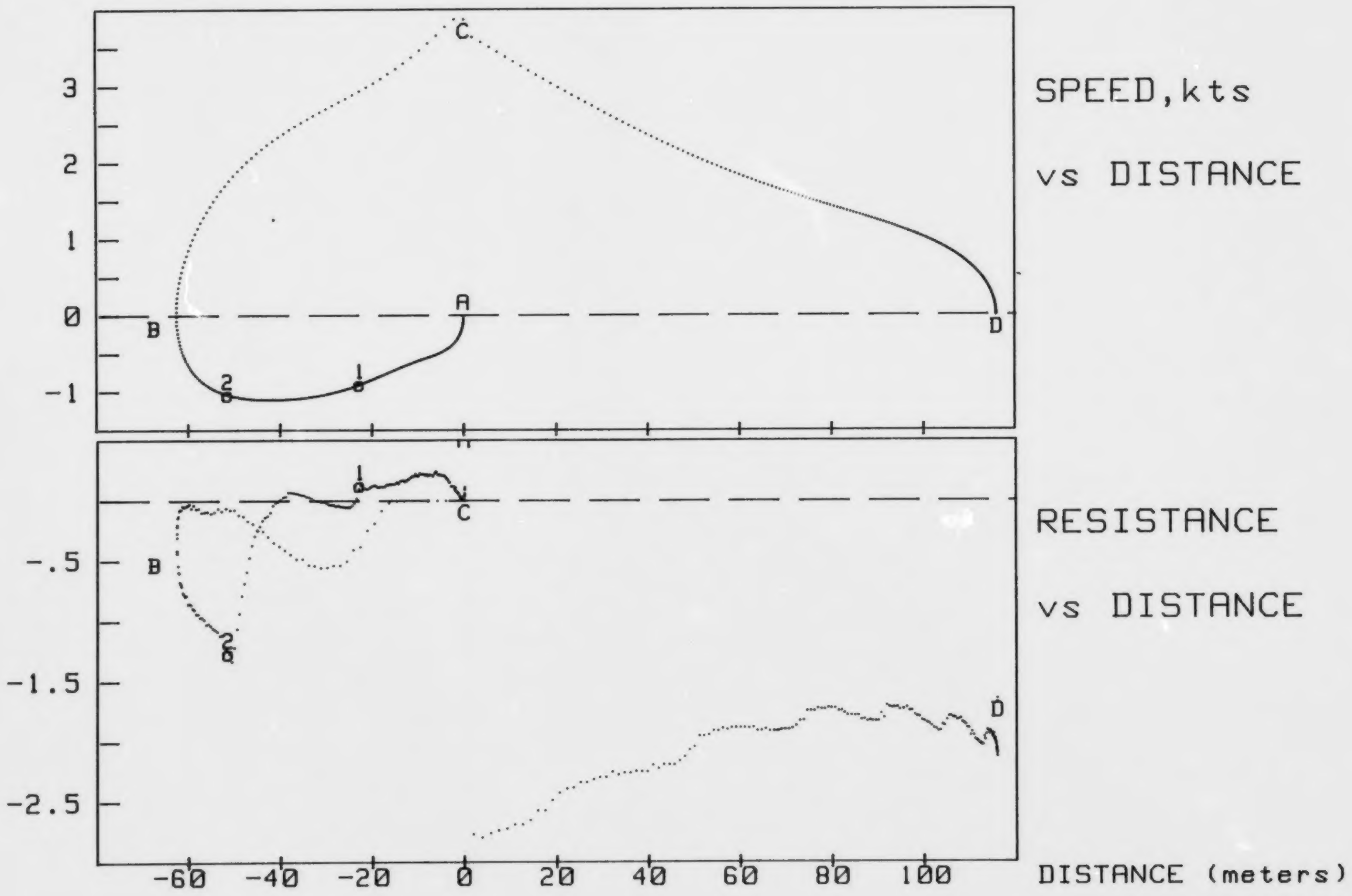

RAM # _C31   TAPE: 81-T2-6.3   08 JUL 1981 20:02:24   Fig.# 5

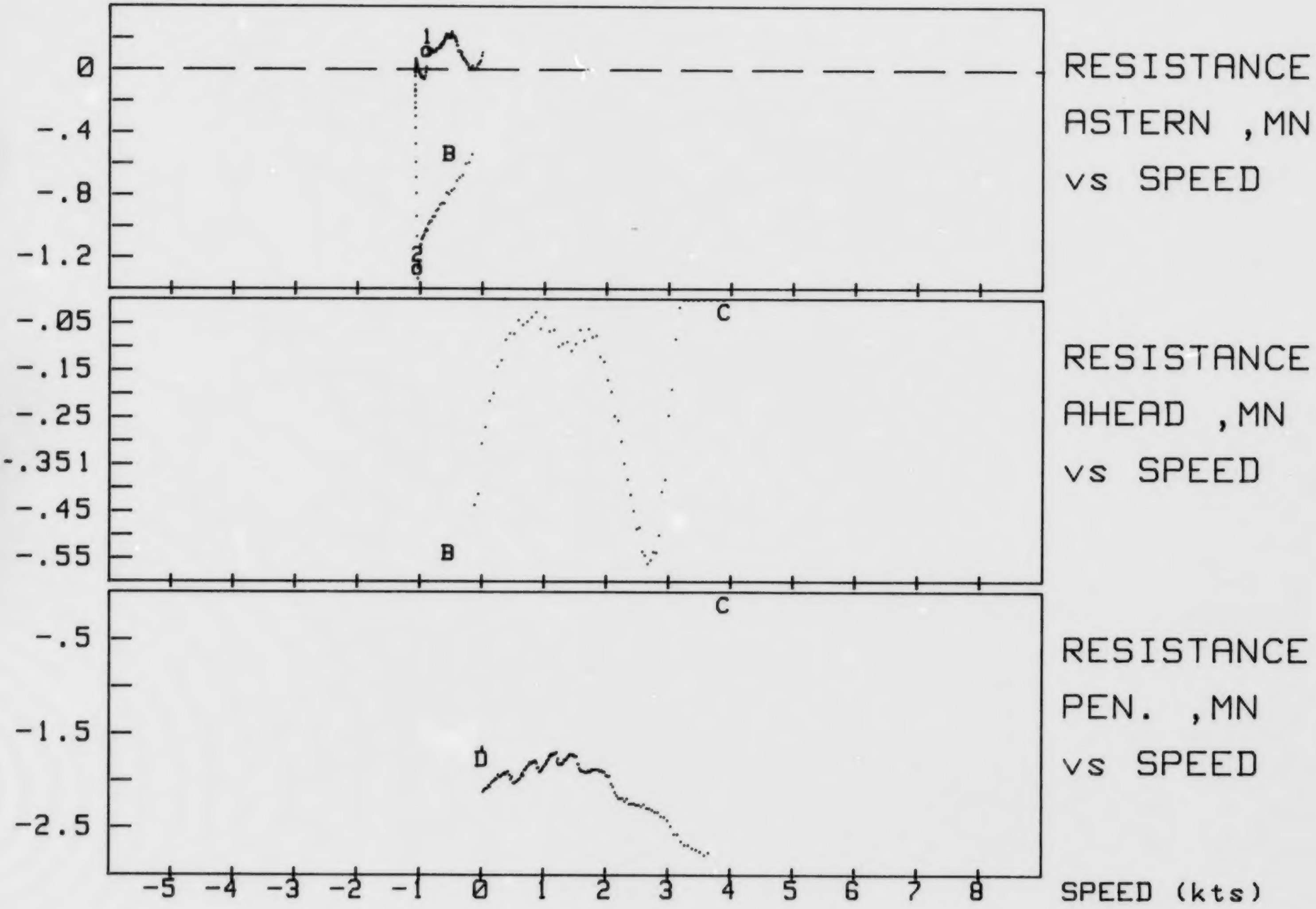

RESULTS OF RAMMING CYCLE ANALYSIS

RAM No. _C32

TAPE:	81-T2-6.3	ICE CONDITIONS:	RIDGES
CATEGORY:	R4	ICE THICKNESS:	1.75 m
QUALITY:	32BC	FLEXURAL STRENGTH:	104 kPA
TRIM:	BOW UP	BUBBLER STATUS:	OFF

RAMMING CYCLE CHARACTERISTICS:

Speed of Advance	(knots)	.153	
Speed of Impact	(knots)	3.7	(3.61)

	Duration (sec)	% Cycle Time	Distance (m)
Backing	205	53.5	-67.78
Acceleration	76	19.8	67.78
Penetration	30	7.83	30.3 (30.07)
Extraction	72	18.8	
Total Cycle	383		

Duration of Astern Mode	(sec)	151		
Duration of Reversal to Ahead	(sec)	31		
Duration of Ahead Mode	(sec)	185		
Duration of Reversal to Astern	(sec)	16		
Start of Reversal after Impact	(sec)	86		
Total Fuel Used	(mm*hr)	5.29	Est. kg:	85.57
Average Fuel Rate	(mm)	49.74	Est. kg/hr:	804.3
Backing Power	(kW)	7042.1		
[Est Fuel Rate	(kg/hr)]	1496.4		
Acceleration Power	(kW)	10221		
[Est Fuel Rate	(kg/hr)]	2130.3		

RAM # _C32 TAPE: 81-T2-6.3 08 JUL 1981 20:16:40 **FIG. #1**

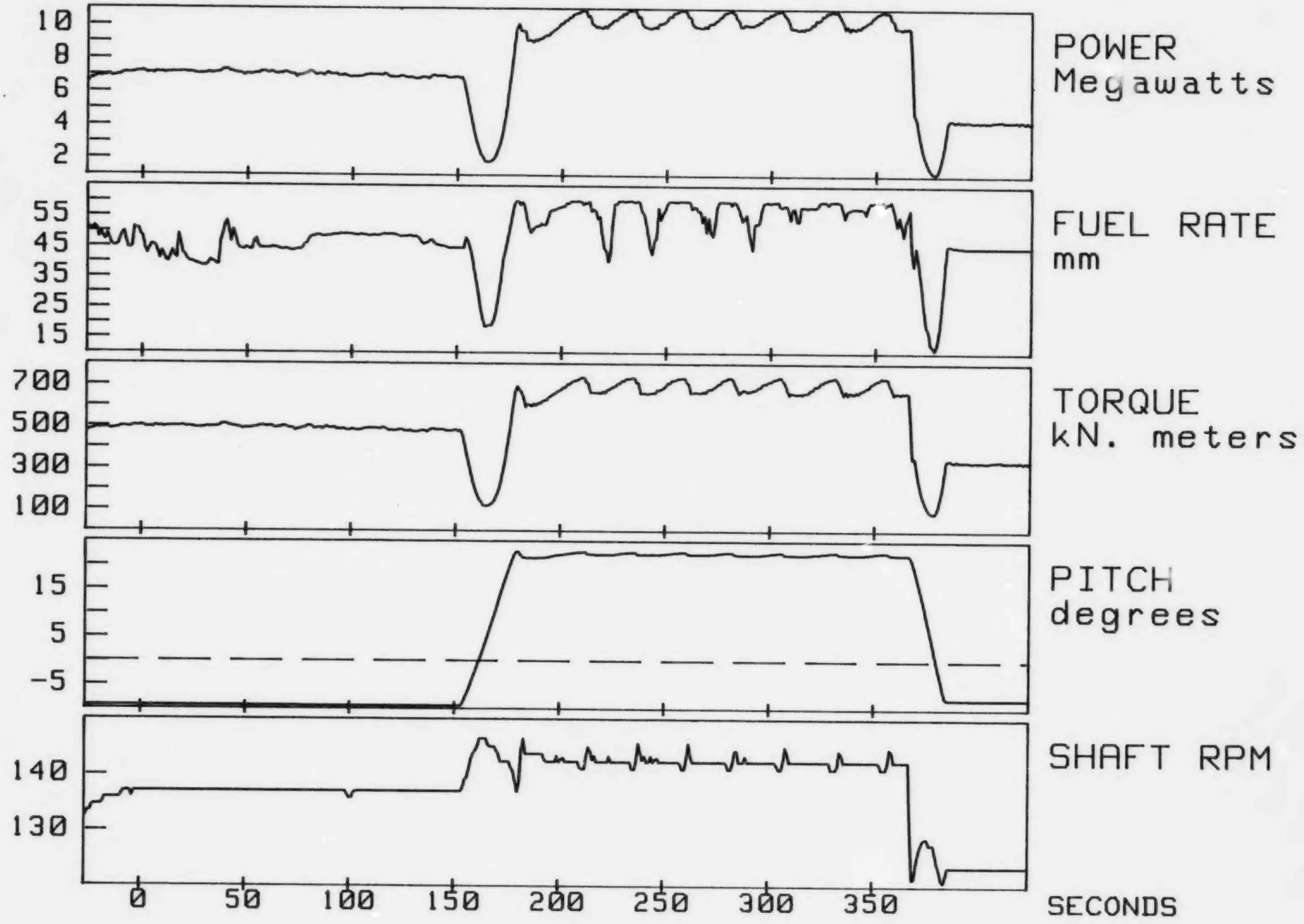

RAM # _C32 TAPE: 81-T2-6.3 08 JUL 1981 20:16:40

FIG. #2

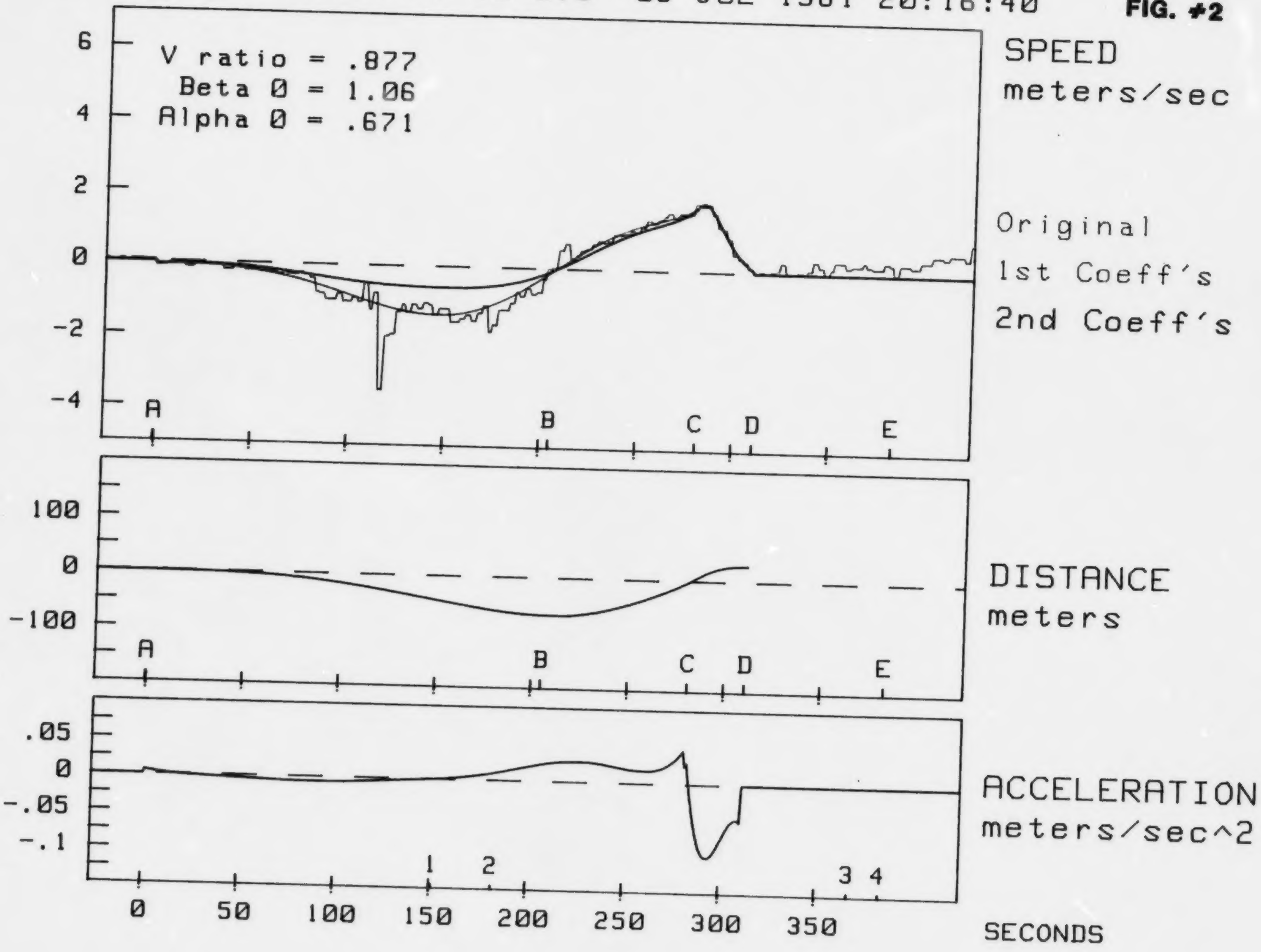

RAM # _C32 TAPE: 81-T2-6.3 08 JUL 1981 20:16:40

FIG. #3

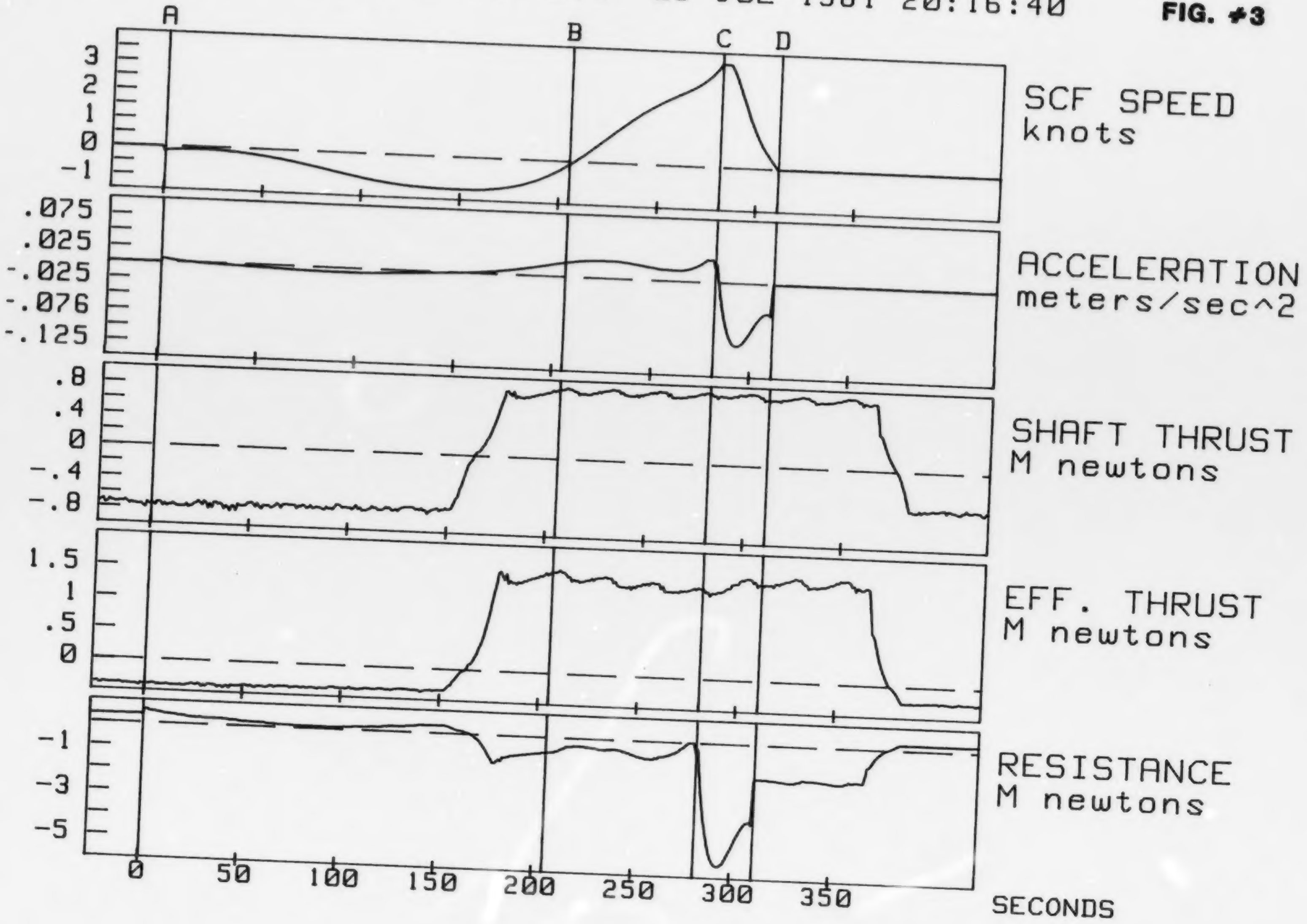

RAM # _C32 TAPE: 81-T2-6.3 08 JUL 1981 20:16:40 Fig.# 4

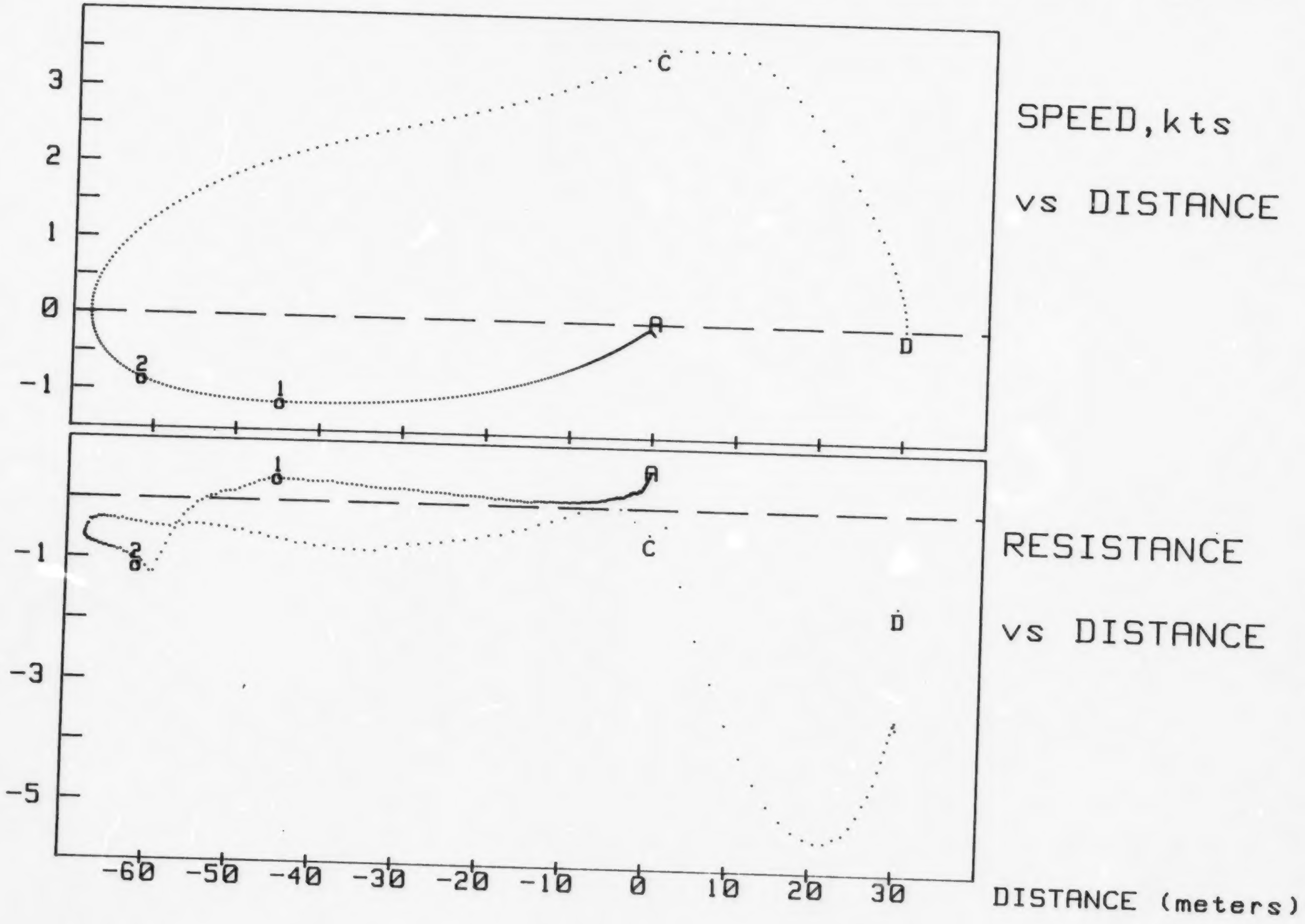

SPEED,kts

vs DISTANCE

RESISTANCE

vs DISTANCE

RAM # _C32 TAPE: 81-T2-6.3 08 JUL 1981 20:16:40 Fig.# 5

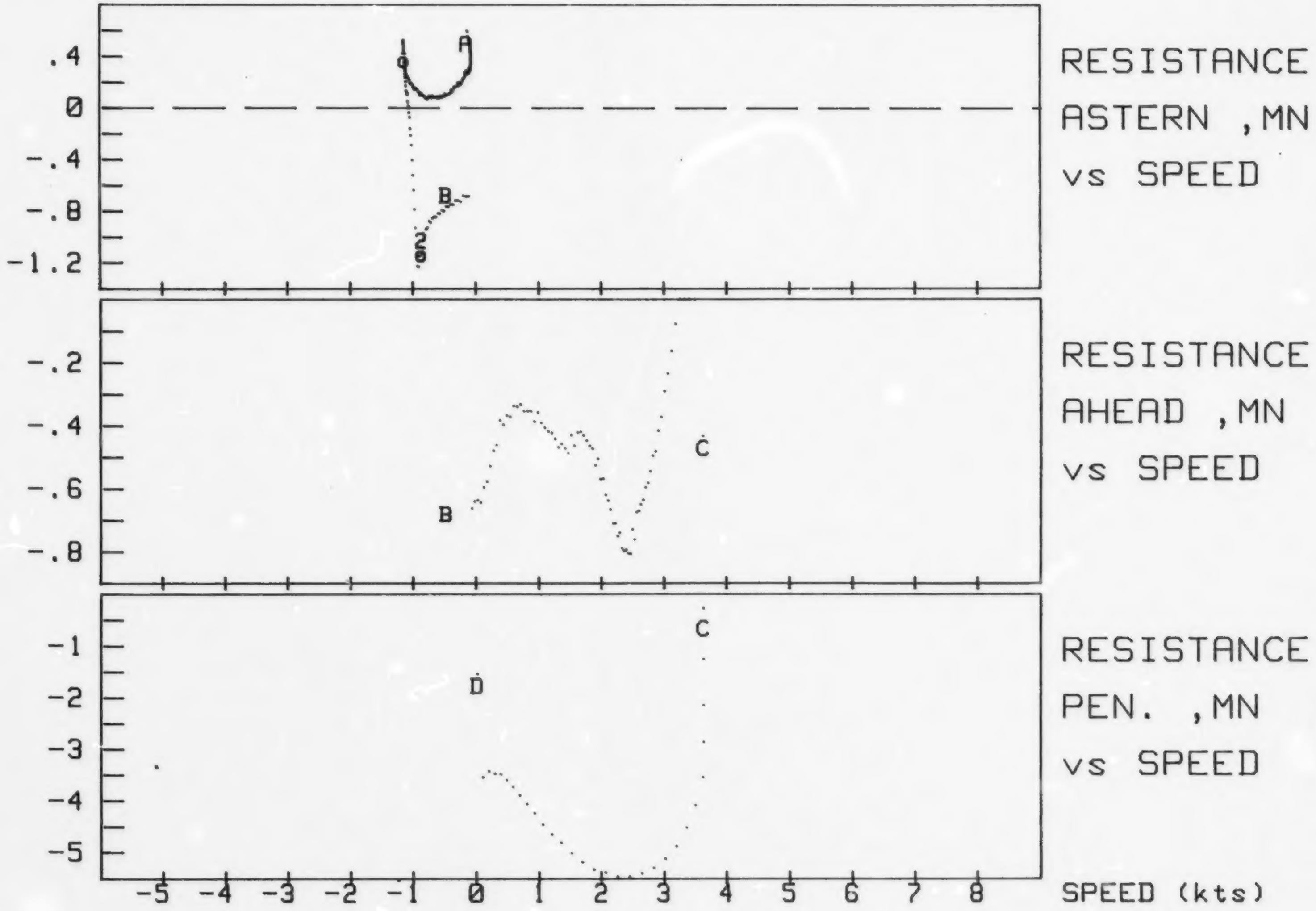

Table C.1 is a summary of the runs.

As detailed in Chapter 3, the following ten rams were incomplete and, thus, were not analyzed in the standard format:

Series A: A1
Series B: B10, B11, B12, B16
Series C: C18, C27, C33, C34, and C35

TABLE C.1 SUMMARY OF RESULTS

RAM NO.	TAPE NO.	CATEGORY	QUALITY	TRIM	ICE CONDITIONS (m)	ICE THICKNESS (kPa)	FLEXURAL STRENGTH	BUBBLER STATUS	MEASURED IMPACT SPEED (kts)	MEASURED PENETRATION DISTANCE (m)	COMMENTS
A1	D2	R3	80AB	LK	R	2.00 MC	407	OFF	3.5	53	Incomplete
A2		R3	61AD	LK	R	2.36 E	407	OFF	3.7	15.2	
A3		R3	62AD	LK	R	2.52 E	407	OFF	3.7	9.1	
A4		R3	67BD	LK	R	2.60 E	407	OFF	3.7	4.5	
A5		R3	64AD	LK	R	2.68 E	407	OFF	4.5	9.1	
A6		R3	41AC	LK	R	2.75 M	407	OFF	4.5	6.1	
A7		R3	61AD	LK	R	2.74 E	407	OFF	4.5	6.1	
A8		R3	61AD	LK	R	2.71 E	407	OFF	4.5	12.1	
A9		R3	21AB	LK	R	2.67 MC	407	OFF	4.5	15.2	
A10		R3	63AD	LK	R	2.64 E	407	OFF	4.5	9.1	
A11		R3	62AD	LK	R	2.61 E	407	OFF	4.5	33	
A12		R3	67BD	LK	R	2.56 E	407	OFF	4.5	28	
A13		R1	71BD	LK	R	2.52 E	407	ON	4.5	6.1	
A14		R1	68BD	LK	R	2.49 E	407	ON	4.5	18.2	
A15		R1	67BD	LK	R	2.45 E	407	ON	4.5	15.2	
A16		R1	30BB	LK	R	2.40 MC	407	ON	4.5	21.2	
A17		R1	72BD	LK	R	2.11 E	407	ON	4.5	27.3	
A18		R1	65AD	LK	R	1.82 E	407	ON	4.5	27.3	

TABLE C.1 (continued)

RAM NO.	TAPE NO.	CATEGORY	QUALITY	TRIM	ICE CONDITIONS (m)	ICE THICKNESS (kPa)	FLEXURAL STRENGTH	BUBBLER STATUS	MEASURED IMPACT SPEED (kts)	MEASURED PENETRATION DISTANCE (m)	COMMENTS
B1	D3	L1	26AB	LK	L	1.51 M	163	ON	5.0	178.8	
B2		L1	30BB	LK	L	1.60 M	163	ON	5.0	90.0	
B3		R1	29BB	LK	R	2.0 M	163	ON	5.5	30.3	
B4		L1	45AC	LK	L	1.4 M	163	ON	5.5	113.6	
B5		L1	28BB	LK	L	1.62 M	163	ON	5.5	136.4	
B6		L1	31BB	LK	L	1.66 M	163	ON	5.5	121.2	
B7		L1	31BB	LK	L	1.56 M	163	ON	5.5	128.8	
B8		R1	47BC	LK	R	1.67 M	163	ON	5.5	15.2	
B9		R1	48BC	LK	R	4.9 M	163	ON	5.0	4.5	
B10		R1	87BC1	LK	R	1.67 M	163	ON	5.0	12.1	INCOMPLETE
B11		R1	104CC2	LK	R	1.6 M	163	ON	5.0	15.2	INCOMPLETE
B12		R1	104CC3	LK	R	1.56 M	163	ON	5.0	33.3	INCOMPLETE
B17	D4	L1	15BA	LK	L	1.70 MC	163	ON	5.0	121.2	
B18		L1	54BD	LK	L	1.55 E	163	ON	5.0	142.4	
B19		L1	31BB	LK	L	1.40 MC	163	ON	5.0	93.9	
B20	D4	L1	68BD	LK	L	1.50 E	163	ON	5.8	51.5	
B21		L1	47BC	LK	L	1.65 M	163	ON	5.5	175.8	
B22		L1	51BC	LK	L	1.45 M	163	ON	5.2	242.4	
B23		L1	32BB	LK	L	1.40 MC	163	ON	5.6	81.8	
B24		L1	30BB	LK	L	1.48 MC	163	ON	5.5	227.3	
C6	D5	L4	26AB	BU	L	1.56 MC	104	OFF	6.0	97.0	
C7		L2	55CC	BU	L	1.80 M	104	ON	5.5	157.6	
C8		L2	47BC	BU	L	1.60 M	104	ON	5.5	121.2	
C9		L2	27BB	BU	L	1.35 M	104	ON	5.5	175.8	
C10		L2	24AB	BU	L	1.82 MC	104	ON	6.0	127.3	
C18		R2	76AC1	BU	R	1.68 M	104	ON	2.0	3.0	INCOMPLETE
C24	D6	L4	61AD	BU	L	1.65 E	104	OFF	2.5	6.1	
C25		L4	21AB	BU	L	1.60 MC	104	OFF	2.5	27.3	
C26		L4	20AB	BU	L	1.65 MC	104	OFF	2.5	78.8	INCOMPLETE
C27		L4	53AB1	BU	L	1.68 MC	104	OFF	2.5	27.3	
C29		L4	26AB	BU	L	1.52 MC	104	OFF	3.7	97.0	
C30		L4	23AB	BU	L	1.68 MC	104	OFF	3.7	112.1	
C31		L4	23AB	BU	L	1.42 MC	104	OFF	3.7	115.1	
C32		R4	32CB	BU	R	1.75 M	104	OFF	3.7	30.3	
C33		R4	77AB2	BU	R	1.84 MC	104	OFF	3.7	45.5	INCOMPLETE

APPENDIX D

SPEED LOG CORRECTIONS

Preliminary analyses have shown that the doppler speed-log was not accurate nor consistent. This was clearly identified by examination and data reduction of several rams. There were absolute as well as relative indicators of the poor quality and error. These indicators were:

a) The one second averages would often change suddenly either up or down. The change in speed or acceleration is governed by the inertial characteristics of the ship. While high and constant deceleration rates can be expected in heavy ice, the limit on acceleration was determined by the ship propulsive capabilities and mass. Considering the maximum effective thrust at full power (1.558MN), ignoring the broken channel resistance at low speed, and considering the mass of the ship to be 38.104 Mkg with zero added mass, the maximum forward acceleration the ship can produce is of the order of $0.04\ m/s^2$. Therefore, the upper limit on speed change in a one second time interval would be 0.04 m/s. This limit was exceeded when large excursions occurred and hence these excursions had to be averaged out or eliminated from the records. Figure D.1 illustrates this type of problem.

To rectify these errors two measures were built-in the software. The first was the interactive clean-up routine in which the operator will have the option of blanking out the data in a set range where it was found obviously erroneous. The second measure was using a polynomial curve fitting procedure to eliminiate the "noise" in the speed log. By doing so, the best fitting polynomial would be used again to regenerate the speed record but without the noise or erratic jumps.

b) When the speed record was used to determine the breakpoints and various time cycle components, the results were compared to those reported in the trials report [21]. Generally, good agreement was observed between the durations of the various stages as obtained from tape to those determined from video analysis. However, the impact speed and penetration distance were generally greater than the reported values.

Table D.1 gives a comparison of impact speed, penetration time and distance for a selected number of rams. While the duration of penetration varied slightly with an average of 1.8% above the field measurement on video, the corresponding difference in impact speed and penetration distance were 6.3% and 33.1% higher than video. It should be noted that with a standard deviation not exceeding 7.8% of the mean the data was quite consistent. However, the observed trends indicate the following.

° The time base as determined by breakpoints on the tape compares very closely to that obtained from video, and it was believed to be correct and sufficiently accurate.

° The impact speed was consistently higher but by only a small percentage. In consultation with TDC it was felt that the measured speeds of impact as reported in [21] should be

FIGURE D.1

TYPICAL LARGE EXCURSIONS
IN SPEED RECORD - RAM B9

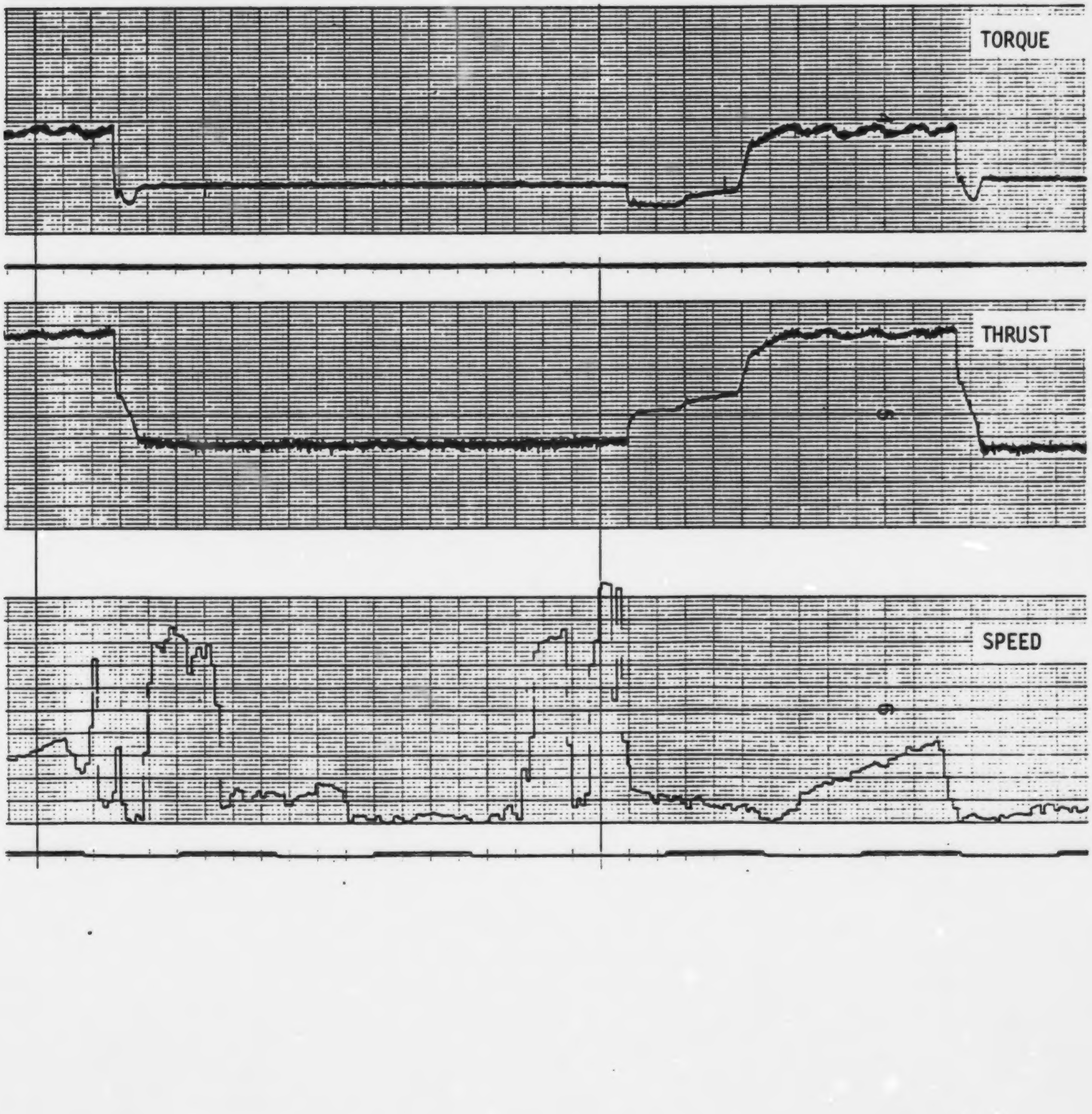

TABLE D.1

COMPARISON OF TAPE AND VIDEO ANALYSIS RESULTS

RAM NO.	IMPACT SPEED (knots)		PENETRATION TIME (sec)		PENETRATION DISTANCE (m)	
	TAPE	VIDEO	TAPE	VIDEO	TAPE	VIDEO
C6	6.3	6.0	97	100	133	97
C9	6.7	5.5	179	175	216	176
B1	5.0	5.0	216	210	220	179
B4	5.6	5.5	174	165	174	114
B5	5.6	5.5	176	170	176	136
B6	6.0	5.5	134	140	165	121
B7	5.7	5.5	143	135	168	129
MEAN RATIO TAPE/VIDEO	1.062		1.018		1.331	
STANDARD DEVIATION AS % OF MEAN	7.06%		3.90%		7.77%	

used as reference since the doppler log was in question. Since there was no absolute measurement calibration of the doppler device in the field, it was not possible for us to develop any credible method to correct or validate the impact speeds as obtained from tapes. Despite some questioning of the accuracy of the reported values (appears to be rounded to 0.5 knots most of the time) an agreement was reached to use the impact speeds reported in [21] and the best estimate of impact speed.

° The differences in impact speed and duration do not correspond to the observed difference in penetration distance. There are only two explanations. If the speed log was always overstated and showed a declining accuracy at decreasing speeds, the shape of the speed-time curve would be distorted and could account for the differences. The other possibility is that of error in measuring the penetration distance. It was indicated in the report [21] that the reported values were taken from side-looking video. This method is very undesirable for measurement of distance since it is susceptible to various sources of error. We are inclined to question the accuracy of this method particularly with reference to the method of calibration of the screen and the fact that the camera was not fixed and had tilt and zoom capabilities. The last two features are highly undesirable in cases where a screen calibration and accurate measurements are needed. However, we were told by TDC that the penetration distances as reported were actually measured on the ice. Although the method of measurement was not documented in the trip report [21] or relevant documents which were made available to us it was agreed that these reported penetration distances should be used as best estimates of reference values to enable the correction of the speed log.

Subsequently, additional corrections of the penetration profile were developed to accommodate the foregoing requirements and details of such corrections will be discussed in Section 4.4.4.

c) When integration of the speed record was conducted to determine the distances travelled, it was found that the backing distance was not equal to the acceleration distance. In some cases, the backing distance was 60% greater than the acceleration distance. Possible explanations of this discrepancy were:

° Errors in doppler speed log readings,
° The ship yaws, changes course and penetrates the ice somewhere halfway in the broken channel track,
° The ship slows down in the clogged channel and the impact in fact does not occur at the same position where the backing started,
° Improper setting of breakpoints

In evaluating the above possibilities a number of ramming incidents were briefly reviewed and various characteristics were estimated from the charts. From comparison of the results it was concluded that the measured and video data agreed well with respect to the time components and, hence the setting of the breakpoints was correct. The fact that the data was obtained during dedicated trials and event markers were used to indicate the moment of ice impact which coincided with the setting of the breakpoints, and that no unusual incidents have been reported from analysis of the video recordings, rule out the possibilities of the MV ARCTIC changing course in a short ram or of slowing down in the clogged channel.

The only remaining explanation was that the errors in the speed log readings were the cause of discrepancies in the results of the analysis. It appeared that the readings around 5 to 6 knots were more reliable. This would mean that the doppler log indicated higher values at lower speeds. The effect of speeds astern on the reliability of the log readings was not known, but from comparison of the backing and penetration distance, the readings seemed to be also high, and indicative of large errors,particularly in the astern mode.

Again due to the lack of any absolute reference measurements of speed of backing distance, we developed a self-correction method to correct the doppler log records for further use in the data reduction and analysis. Details of this methodology may be found in Section 4.4.5 of this report.

It should be noted that we have made an attempt to validate/calibrate speed records using the available video tape. Apart from the poor tape quality, no credible calibration was found on tape. Thus it was not possible for us to calibrate the screen. Using the sketchy calibrations which were found on the video tape, it was found that the width of the screen covered only approximately 16.5 meters. Therefore, we looked at several rams with a total penetration of 5.1 meters. We have been able to develop a nonlinear calibration curve which used the reported distances [21] as reference values. The scatter was high and the reliability of the calibration curve could not be verified. Further work would be required to verify and extend this type of calibration to longer penetration distances. Our initial attempt was not successful because of unexplicable problems. For instance, while Ram No.C18 should have had a reported penetration distance of 3m the video observation indicated a penetration distance greater than the screen width. In Ram No.B9, the video tape log indicated continuous backing where penetration was expected. These problems were attributed to incorrect video tape logging which would require validation prior to any future video work.

It is worthy of mention that Arctec has conducted several studies where the video technique was used as the main source of velocity data in continuous and ramming mode operation. Examples are the CCGS J.A. MACDONALD and CCGS LOUIS S. ST. LAURENT. The results obtained in either case were highly reliable and could be entered into digital computer for standard analysis to obtain speed, acceleration, penetration, resistance and penetration energy. The technique appears to be tedious, but eventually it can be a very fast, efficient and cost effective means of data acquisition provided that proper planning, conduct and precautions are made. The accuracy of the technique is goverened by the field calibration, quality of the tape and ice features, and finally the thoroughness and training of personnel conducting the data reduction from the screen.

Another possible technique which can be used to validate and correct the doppler speed-log is the accelerations technique. The measured ship accelerations and angular motions can be used to determine the forward ship speed. The solution can be based on the rigid-body equations (summarized in Section 2.3) and it could be explored in the future.

D.1 Correction of Penetration Profile

The correction of the penetration profile was developed to perform two functions:

a) To correct the impact speed at the point of impact to that of the video measurement.

b) To correct the penetration speed profile such that the calculated penetration distance converges to the measured penetration distance.

The penetration distance was considered correct and required no change.

In order to accomplish the above corrective measures, a special algorithm had to be written and incorporated in the original software. To eliminate the requirements for major changes in the software, a simple algorithm was written to do the following:

a) The first step was to correct the forward speed so that the speed of impact equals the video speed of impact. This was done by simply calculating the speed ratio:

$$V\ \text{ratio} = \frac{V\ \text{video}}{V\ \text{tape}} \qquad (D.1)$$

This ratio is then used to permanently correct the speed record in the range from the beginning of acceleration until the end of penetration.

b) The second step was to integrate the speed-log to determine the penetration distance as calculated from tape data, P_c, compare P_c to the measured penetration distance, P_m. If they are not within 1 percent, calculate a correction parameter β_o from:

$$\beta_o = \sqrt{P_m/P_c} \qquad (D.2)$$

c) Apply the correction parameter β_o to the speed using the following linear correction method:

$$v = v \; . \; \{\frac{v}{v_o} \; (1 - \beta_o) + \beta_o\} \qquad (D.3)$$

d) Therefore, if P_m was lower than P_c, the velocity will be reduced and vice versa. The new speed record can then be integrated, to obtain a second estimate of penetration and repeat (b) and (c) above until either β_o tends to zero or a close correction within 1% was achieved.

e) The cummulative value of β_o is the cummulative product of all values during the iteration steps.

If P_c is about one third greater than P_m, the corresponding starting value of β_o is 0.866. However, depending on the number of iteration steps the value of β_o can be lower.

By examination of Equation (D.3) and by integration it can be shown that for an approximately linear speed record, and for $\beta_o = 0$, the maximum expected reduction in penetration distance would be approximately one third. This means cutting the speed in mid-range by 50% and at the lower 10 percent of the range by 90%. In our opinion, these are drastic corrections and have to be viewed as such. Theoretically, the speed can be corrected to any level to match the penetration distance, but from a realistic point of view, the original data looses its value and meaning if one has to correct it by large factors especially when these factors are not based on any rigorous experimental evaluation. One might as well forget about the original data and assume a shape for the speed descent during penetration, then evaluate the shape parameters knowing the time duration, the impact speed and the penetration distance (area under the speed-time curve).

Therefore, our philosophy in applying any further correction to the data in such cases where β_o was close to zero, was that of just reporting both the target penetration and the corrected penetration distances side-by-side.

We have also examined the resistance during penetration stage as obtained before and after applying this correction. Figure D.2 illustrates the results of such examination in comparison to predictor models for Ram No.C6. The curves illustrated represent the following:

1. The resistance vs. speed for Ram C6 before applying the present correction.
2. The resistance vs. speed for Ram C6 after applying the correction.
3. Full scale predictor equation based on Lake Melville trials.
4. Nawwar and Edwards equation (dimensional form).

FIGURE D.2

COMPARISON of RESISTANCE ESTIMATES DURING PENETRATION - RAM No. C-6

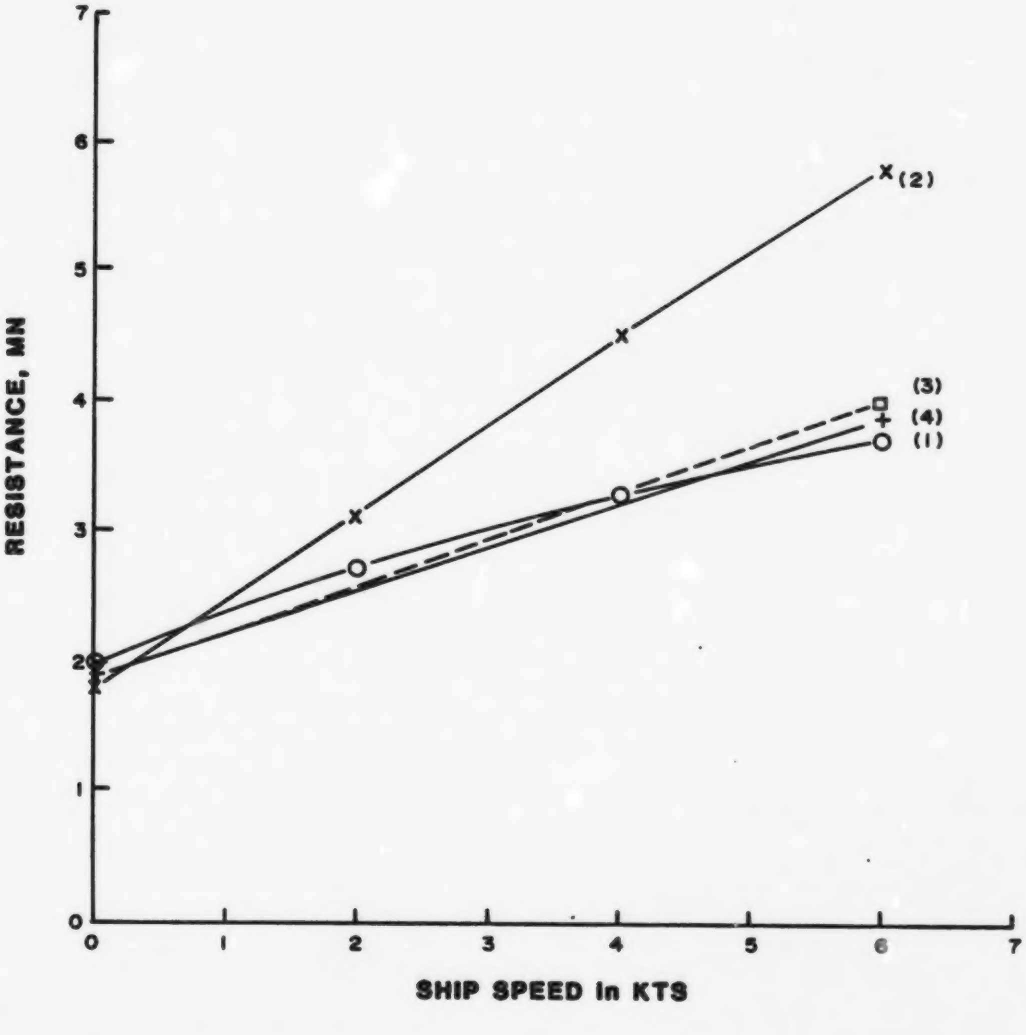

The comparison shows clearly that the original results before correction agree very well with both full scale data in level ice (based on Pozn and Ionov model) and Nawwar and Edward's model which was based entirely on model scale data (not including the MV ARCTIC data). The result is puzzling because it is contrary to expectation. While one would expect greater conformity of the corrected data with model and full scale observations, the opposite occurs. This raises two questions:

- ° the first concerns the validity of β_o correction which is based on the premise that video impact speed and penetration distance are correct.

- ° the second question concerns the validity of level ice continuous transit resistance models in transient conditions.

At the present, we can offer no conclusive answer to any of the above questions and further investigation will be necessary to evaluate the validity of either argument. For the time being, the correction methodology described in this section will be implemented on all data reduction runs.

D.2 Self-Correction of Acceleration Distance

This method was based on the premise that if the speed record was correct, the backing distance and acceleration distance must be equal. The second major assumption was that concerning the error in speed. Figure D.3 illustrates that at some high speed, v_o, there is no correction required and hence the correction factor is equal to unity. At very low speed it is assumed that the correction factor is α_o. While the shape of the correction factor as a function of speed is unknown, we will assume in this analysis that it is linear. The value of α_o can be either greather or smaller than unity depending on the observed characteristics of the response (speed) signal. Therefore, the correction factor at any speed, α, is given by:

$$\alpha = \alpha_o + \frac{v}{v_o}(1 - \alpha_o) \qquad (D.4)$$

The correction is valid for either positive (ahead) or negative (astern) speeds. When $v < 0$, α will be less than α_o.

FIGURE D.3

ASSUMED CORRECTION FACTOR-SPEED RELATIONSHIP

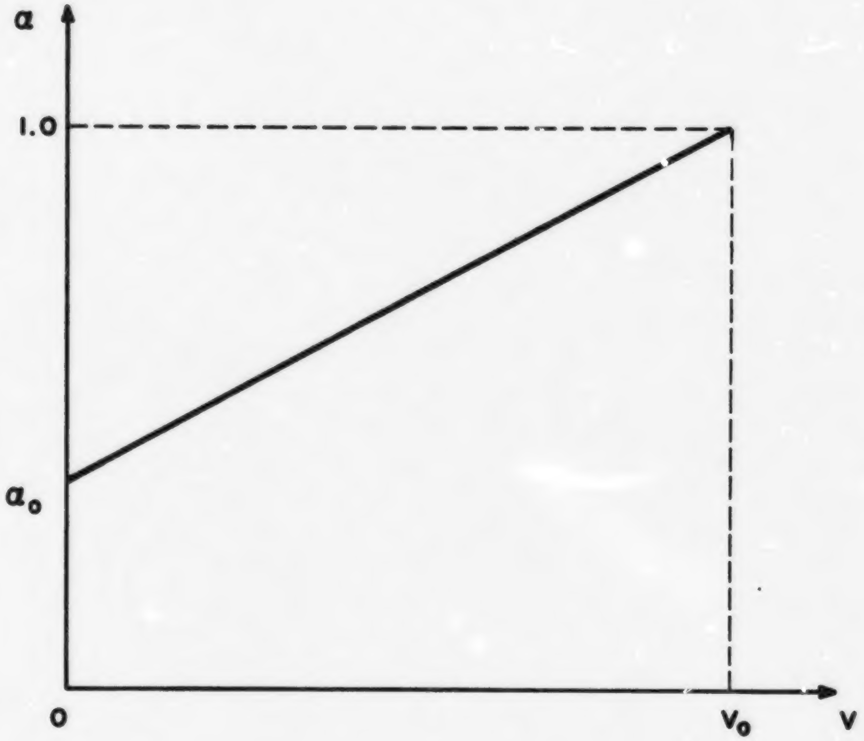

Since the ship speed, v, is expressed in terms of an nth degree polynomial we may write:

$$v = \sum_{k=0}^{n} a_k\, t^k \tag{D.5}$$

where t is the time at any point within the cycle. Integrating the velocity, obtain the penetration:

$$x = \sum_{k=0}^{n} \frac{1}{(k+1)} \cdot a_k\, t^{k+1} \tag{D.6}$$

At the end of backing period, t_b, the penetration should be negative (astern) and is given by:

$$x_b = \sum_{k=0}^{n} \frac{1}{(k+1)} \cdot a_k\, (t_b)^{k+1} \tag{D.7}$$

At this time the direction of motion is reversed and the ship accelerates forward at the end of acceleration period and after a total elapsed time, t_c, the total distance travelled, x_c, should vanish. In reality, if there is an error in speed, x_c, will not vanish and will have a value equal to the difference between the acceleration and backing distances. Therefore,

$$x_c = \sum_{k=0}^{n} \frac{1}{(k+1)}\, a_k\, (t_c)^{k+1} \tag{D.8}$$

The value of x_c can be either positive or negative. In order to eliminate x_c we correct the velocity such that $x_c = 0$. The correction required will be determined from this condition. Now let the corrected speed, v' be expressed in a new polynomial:

$$v' = \sum_{k=0}^{n} b_k \cdot t^k \tag{D.9}$$

where b_k are the coefficients of the polynomial. Also obtain the corrected speed from Equations (D.4) and (D.5) and reduce the resulting expression to the following form:

$$v' = \sum_{k=0}^{n} \left\{ \alpha_0\, a_k + \left(\frac{1 - \alpha_0}{v_0}\right) \sum_{i=0}^{k} a_i \cdot a_{k-i} \right\} t^k \tag{D.10}$$

From Equation (D.9) and (D.10)obtain the relationship between the corrected polynomial coefficients and the values calculated from the original data:

$$b_k = \alpha_o a_k + \left(\frac{1 - \alpha_o}{v_o}\right) \sum_{i=0}^{k} a_i \cdot a_{k-i}, \quad \text{for } 0<k<n \qquad \text{(D.11a)}$$

$$b_k = \left(\frac{1 - \alpha_o}{v_o}\right) \sum_{i=k-n}^{n} a_i \cdot a_{k-i}, \quad \text{for } n<k<2n \qquad \text{(D.11b)}$$

Now the corrected distance can be obtained by replacing a_k in Equation (D.8) with b_k and in this case x'_c should vanish. Thus,

$$x'_c = \sum_{k=0}^{n} \frac{1}{(k+1)} \cdot b_k \cdot t_c^{k+1} = 0 \qquad \text{(D.12)}$$

Substituting Equation (D.11) into (D.12)and solving for the unknown α_o obtain:

$$\boxed{\alpha_o = \frac{1}{1 - \frac{x_c}{Z}}} \qquad \text{(D.13)}$$

where x_c = the error in penetration calculation given by Equation (D.8)

$$\boxed{Z = \frac{1}{v_o} \sum_{k=0}^{n} \frac{1}{k+1} \left\{ \sum_{i=k-n>0}^{k<n} a_i \cdot a_{k-i} \right\} t_c^{k+1}} \qquad \text{(D.14)}$$

If $x_c < 0$, i.e. the backing distance is greater than the acceleration distance the speed correction factor $\alpha_o < 0$ and vice versa.

Therefore, the method of correction can be defined as follows:

a) Calculate, x_c, the net difference between the backing and acceleration distances. If not close or equal to zero a correction will be required.

b) Use the polynomial regression coefficients, a_k, and t_c, to compute Z according to Equation (D.14). In this calculation v_o is an arbitrary base speed and may be taken equal to the speed of impact at the end of acceleration stage or other values which may be justified.

c) Determine the basic speed correction factor, α_o, from Equation (D.13).

d) Correct the polynomial coefficients using Equation (D.11) to obtain b_k and replace the original coefficients.

e) Recalculate the velocity, acceleration and penetration time series using the corrected coefficients.

f) The same correction factor and steps (d) and (e) should be applied also to be penetration stage.

The foregoing procedure fulfills the basic requirements of a ramming cycle and is expected to produce reasonable overall results. Verification will be provided in the final report.

APPENDIX E

TREND ANALYSIS and PERFORMANCE PREDICTIONS

APPENDIX E

TREND ANALYSIS AND PERFORMANCE PREDICTIONS

E.1 Ramming Components Trend Analysis

This appendix presents the results of a detailed evaluation of the components of the ramming process. This process, previously described by the action cycle and the response cycle, has now been divided into independent components, which can be combined to give the entire ramming cycle. These components, illustrated in Figure E.1, are:

- penetration
- acceleration
- astern mode
- stopping

As will become clear later, this is the sequence in which the ramming cycle is put together in determining the ramming procedure.

The data for each component of most of the ramming incidents have been evaluated on the basis of:

- ice thickness
- ahead power level
- astern power level
- bubbler status
- trim
- thrust cut-off
- execution of ramming procedure

The evaluation is illustrated in a large number of graphs for the various conditions of ice thickness and power levels. Each data point has been identified in the graphs. Every component has three variables, which have been cross plotted in three ways:

- penetration:	distance	vs	impact speed	(Figure E2, A & B)
	time	vs	impact speed	(Figure E3, A & B)
	time	vs	distance	(Figure E4, A & B)
- acceleration:	distance	vs	impact speed	(Figure E5, A & B)
	time	vs	impact speed	(Figure E6, A & B)
	time	vs	distance	(Figure E7, A & B)
- astern mode:	distance	vs	backing speed	(Figure E8, A & B)
	time	vs	backing speed	(Figure E9, A & B)
	time	vs	distance	(Figure E10, A & B)
- stopping:	distance	vs	backing speed	(Figure E11, A & B)
	time	vs	backing speed	(Figure E12, A & B)
	time	vs	distance	(Figure E13, A & B)

The next step in the evaluation was to determine the trends of the best achievable performance for each component, which would result in the highest speed of advance. Using the results presented in Appendix C, the trend lines were developed by trial and error, keeping in mind the physical constraints and limitations of the ship (e.g. maximum accelerations, speed limitations in the broken channel). The trends were determined for the following operational conditions:

- ice thickness of 1.6 m and 2.5 m
- full power ahead, 10.5 MW
- astern power levels of 5.0 MW and 7.5 MW
- fast reversal to ahead pitch
- fast reversal to astern pitch

The trend analysis for the penetration component was carried out mainly concentrating on the situation of bubbler on with level keel. However, the case of bubbler off with bow up showed no noticeable difference from these trends. Evaluation of other categories were not conclusive.

The trends of other components were found to be the same for all categories, since no systematic effect could be detected.

The reversal to ahead pitch is included in the stopping maneuver which runs from the end of the astern mode (backing up with selected astern power) to the start of the acceleration (continuation of full power applied during stopping). The reversal to astern pitch is not covered in the graphs but is assumed to be started at the end of the penetration phase and completed during the extraction time.

The idealised ramming procedure shown on Figure E1, has been derived from actual well executed cycle components. Therefore this procedure can be executed and the predicted performance should be achieved under similar prevailing conditions.

The trends of each component as plotted on the three graphs corresponds with each other so that now it can be seen, which rams have been well executed and which ones appear to be reliable. The deviation of data points from the trends can in most cases be explained when reviewing the results of the data analysis presented in Appendix C.

A clear example of explicable deviation from the trends is the stopping data of Series A, shown in Figure E12. Reviewing Appendix C will learn that the stopping maneuvers in that series have been executed with hesitation and delay of action.

In order to eliminate the backing speed, which in fact is not relevant to the ramming process, the stopping distance can be plotted against the astern mode distance or the astern mode time, as demonstrated for ice thickness 1.6m in Figures E14 and E15. This relationship is useful in assembling the components to obtain the entire ramming cycle, since the backing distance, which should equal the acceleration distance, is a composite of astern mode and stopping distance.

E.2 Ramming Components Synthesis

The synthesis of a ramming cycle and the required operational procedure is carried out as follows:

- selected impact speed,
- determine penetration distance and time on a basis of impact speed,
- determine acceleration distance and time on a basis of impact speed,
- backing distance equals acceleration distance,
- determine the composite of astern mode distance and stopping distance to match the total backing distance,
- determine the required astern mode time on a basis of astern mode distance,
- determine the achievable stopping time on a basis of stopping distance,
- standard minimum extraction time losses taken at 10 seconds.

Figures E16 and E17 are diagrams which can be used to determine the ramming cycle components and the operational procedure for an ice thickness of 1.6m. Figure E16 shows the penetration and acceleration characteristics all conveniently in one diagram on a basis of the impact speed. The characteristics for 2.5m ice are indicated as well.

Figure E17, produced for 1.6m ice only shows the backing characteristics in a plot of time versus distance. The backing distance is the sum of stopping and astern mode distances.

After determination of the various components from these two diagrams, the speed of advance can be computed.

This graphical method to determine the ramming performance and the operational ramming procedure is illustrated by two examples, which have been indicated in Figures E16 and E17:

Conditions

Ice thickness	1.6m
Ahead power	10.5 MW
Astern power	7.5 MW

Bubbler : on
Trim : level keel

Operational Procedures

Pitch reversal from astern to ahead in 35 seconds.
Full power (10.5 MW) assumed during final 10 seconds of the stopping phase.
Pitch reversal from ahead to astern in 20 seconds, starting the final 10 seconds of the penetration phase.
Standard mnimum extraction time losses of 10 seconds, in which pitch reversal is completed.
Fuel consumption is based on:

Fuel Rate (kg/hr) = 199.4 P (in MW) + 92.25

Average power levels for calculation of fuel consumption:
Astern Mode : astern power (7.5 MW).
Stopping : final 10 seconds full power (10.5 MW), remainder of the time half of average of ahead and astern power (4.5 MW).
Acceleration : ahead power (10.5 MW).
Penetration : ahead power (10.5 MW) except final 10 seconds.
Reversal : 5 seconds half of ahead power (5.25 MW).
10 seconds idle power (1.05MW).
5 seconds half of astern power (3.75 MW).

Ramming Components

Selection of impact speed	5 kt	6 kt
From Figure E16:		
Penetration : Distance	123 m	173 m
Time	139 sec	195 sec
Acceleration : Distance	100 m	160 m
Time	76 sec	96 sec
From Figure E17:		
Up to Backing Distance	100 m	160 m
Left to Astern Mode : Down to Distance	58 m	96 m
Left to Time	111 sec	150 sec
Left to Stopping Dist. : Down to Distance	42 m	64 m
Down to Stopping Time : Left to Time	57 sec	68 sec

Speed of Advance

Penetration Distance	123 m	173 m
Total Cycle Time	393 sec	519 sec
Speed of Advance : m/sec	0.3130	0.3333
m/hr	1127	1200
knots	0.608	0.648

Fuel Consumption and Mileage

Astern Mode : 1588 kg/hr	48.96 kg	66.17 kg
Stopping : 990 and 2186 kg/hr	19.00 kg	22.02 kg
Acceleration : 2186 kg/hr	46.15 kg	58.29 kg
Penetration : 2186 kg/hr (minus 10 sec)	78.33 kg	112.34 kg
Reversal : 1139, 302 and 840 kg/hr	3.59 kg	3.59 kg
Total fuel used	196.03 kg	262.41 kg
Average fuel consumption	1796 kg/hr	1820 kg/hr
Fuel Mileage	0.339 NM/tonne	0.356 NM/tonne

This method has been used to determine the remaining performance and optimum ramming strategy as presented in Section 6.4. In addition to the analysis presented in this appendix, the effects of different power levels and ice thicknesses have been investigated to expand the performance predictions. This was achieved through a regression type of analysis of each component, followed by the previously described synthesis and computations of performance. It would be worthwhile to further develop this methodology and to confirm the performance predictions on the basis of additional ramming data points or other available sources.

Although the power levels have been used in the performance predictions, it is actually the effective thrust that dictates the performance. Since the relationships between power and thrust had been determined, the power was used as a more practical variable. For the sake of the ramming operation from the bridge of the ship, it may be desirable to express this power in an other variable. In case of the MV ARCTIC's machinery control system where power is controlled through pitch setting, the latter may become the operational variable in the ramming procedure.

FIGURE E.1 IDEALIZED RAMMING PROCEDURE

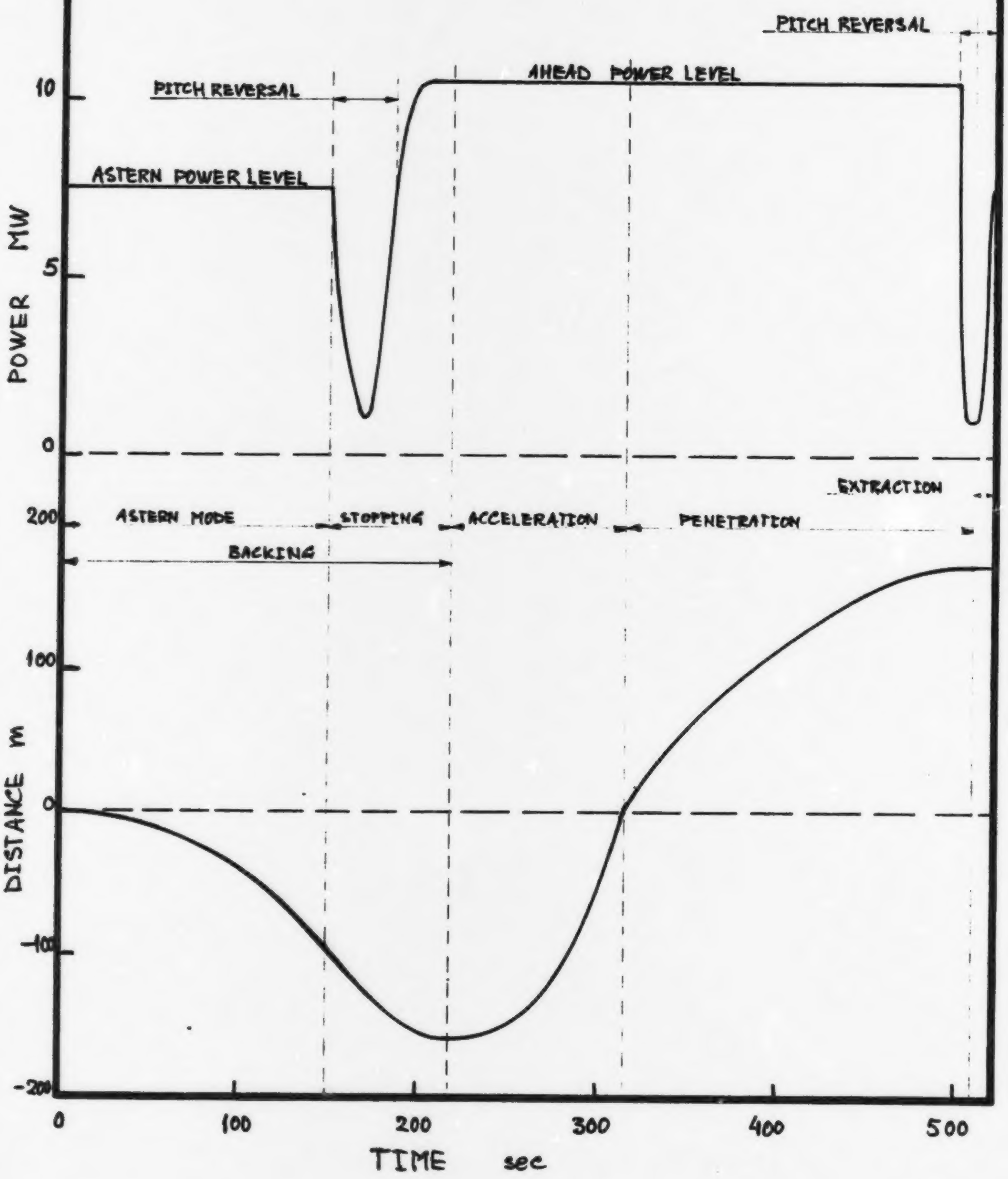

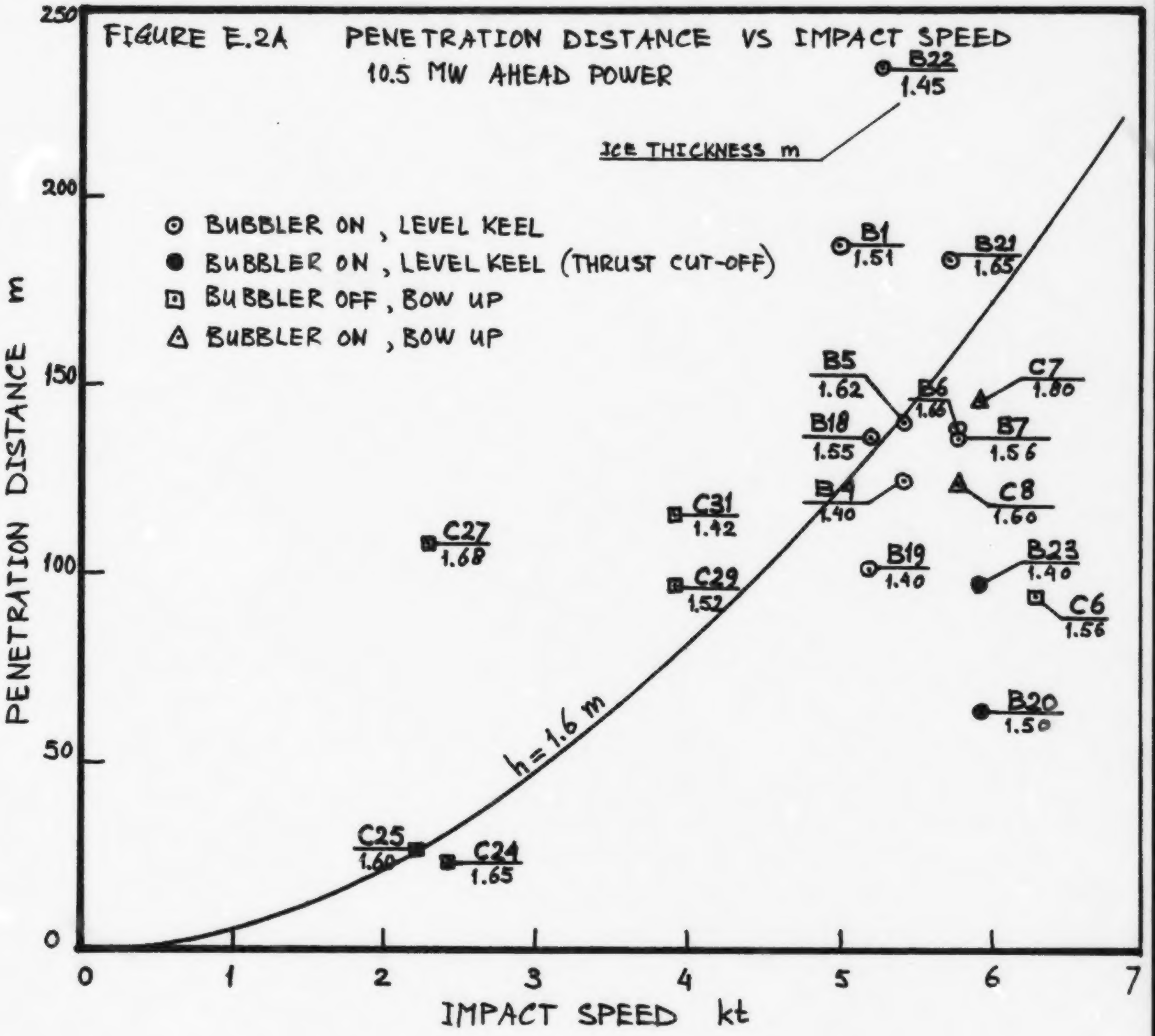

FIGURE E.2A PENETRATION DISTANCE VS IMPACT SPEED
10.5 MW AHEAD POWER

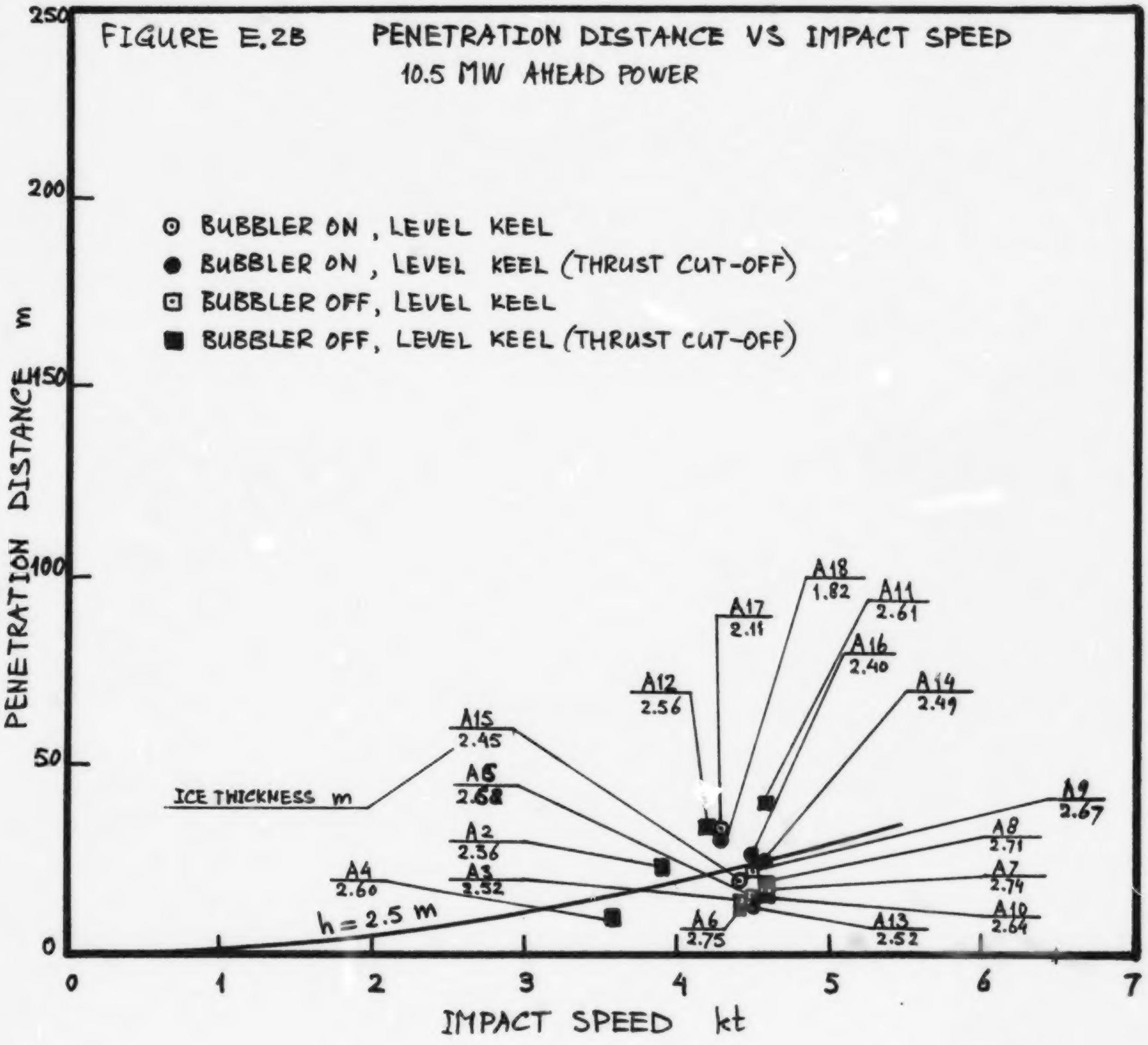

FIGURE E.2B PENETRATION DISTANCE VS IMPACT SPEED
10.5 MW AHEAD POWER

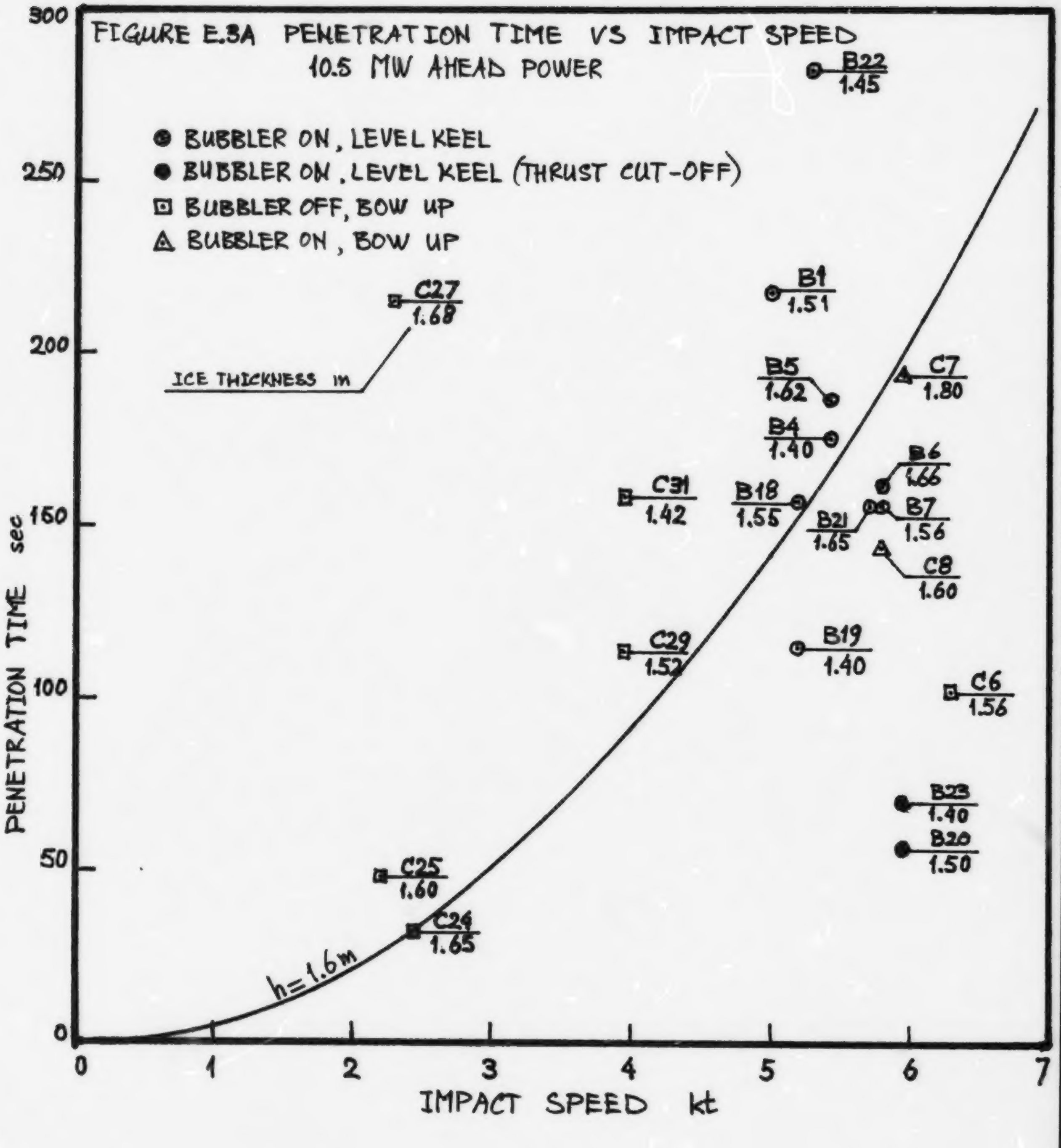

FIGURE E.3A PENETRATION TIME VS IMPACT SPEED
10.5 MW AHEAD POWER

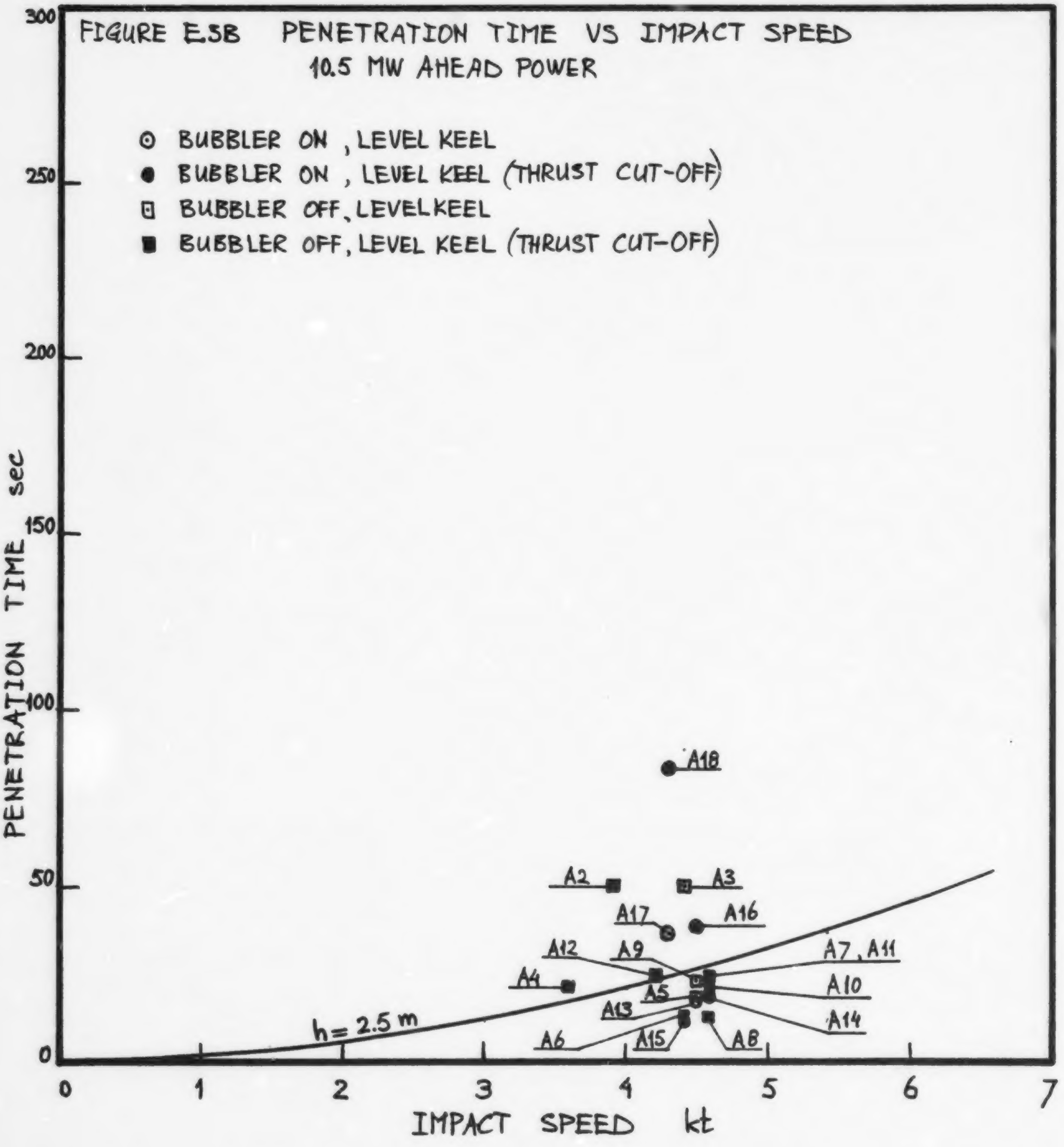

FIGURE E.5B PENETRATION TIME VS IMPACT SPEED
10.5 MW AHEAD POWER

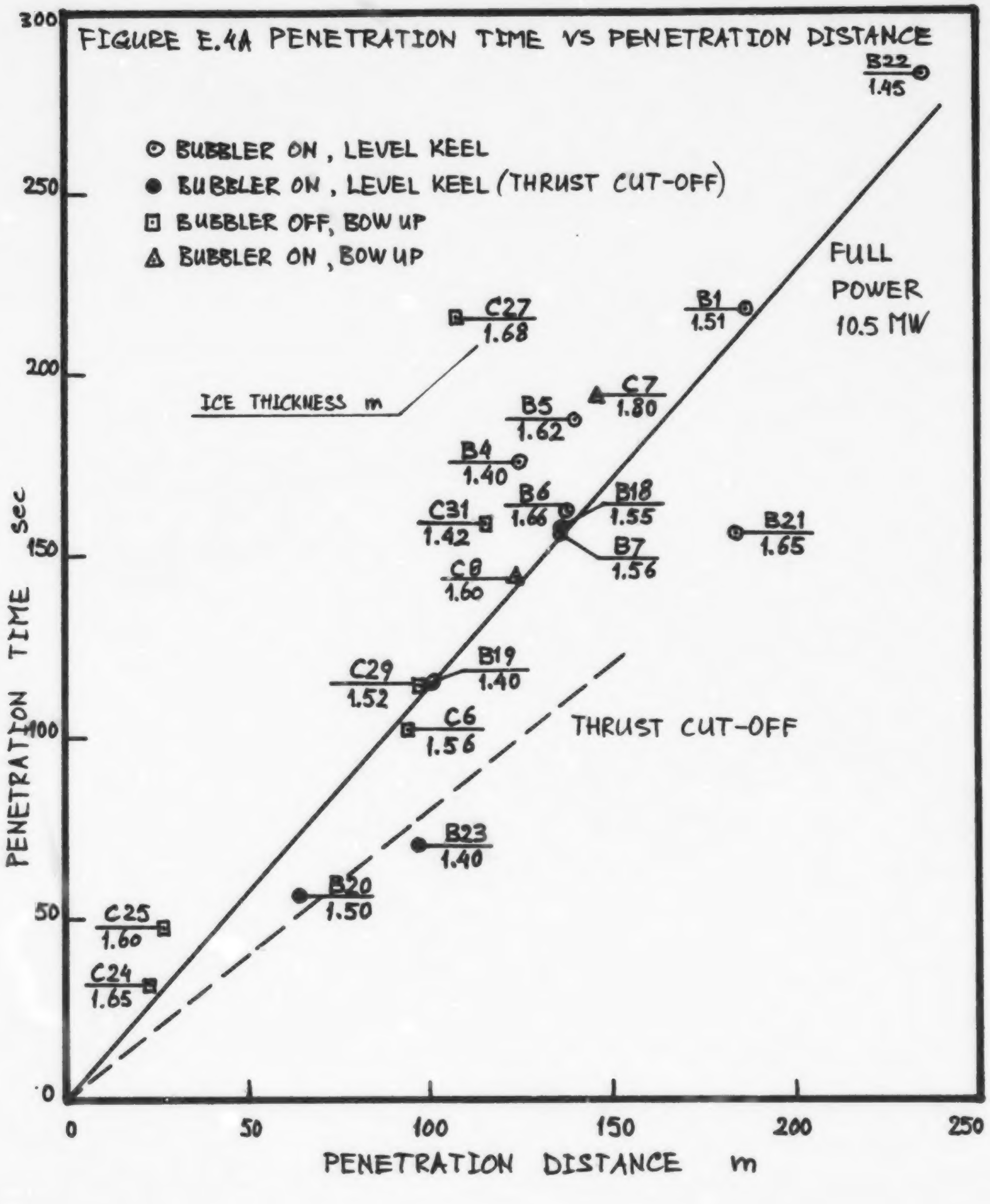

FIGURE E.4A PENETRATION TIME VS PENETRATION DISTANCE

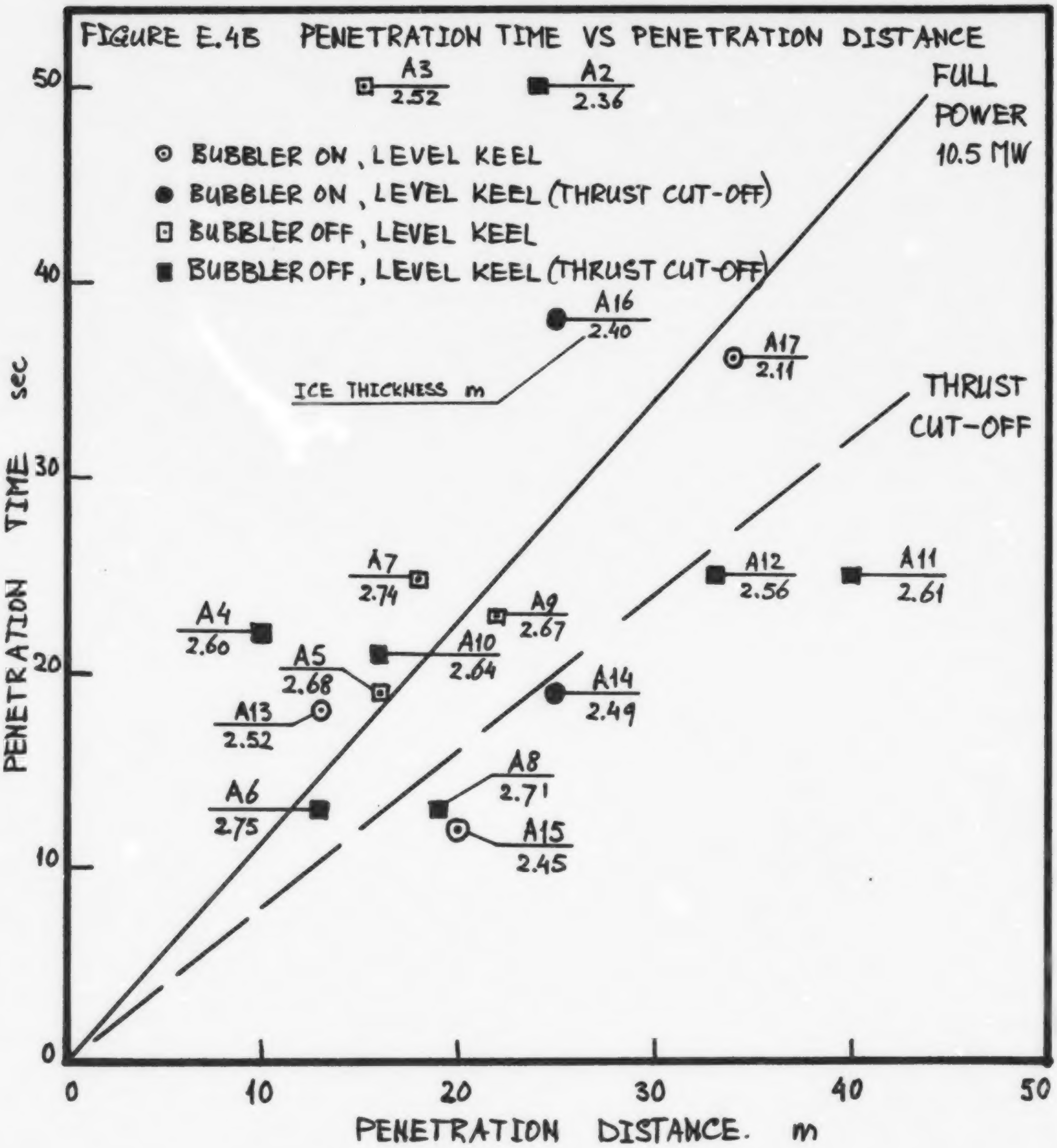

FIGURE E.4B PENETRATION TIME VS PENETRATION DISTANCE

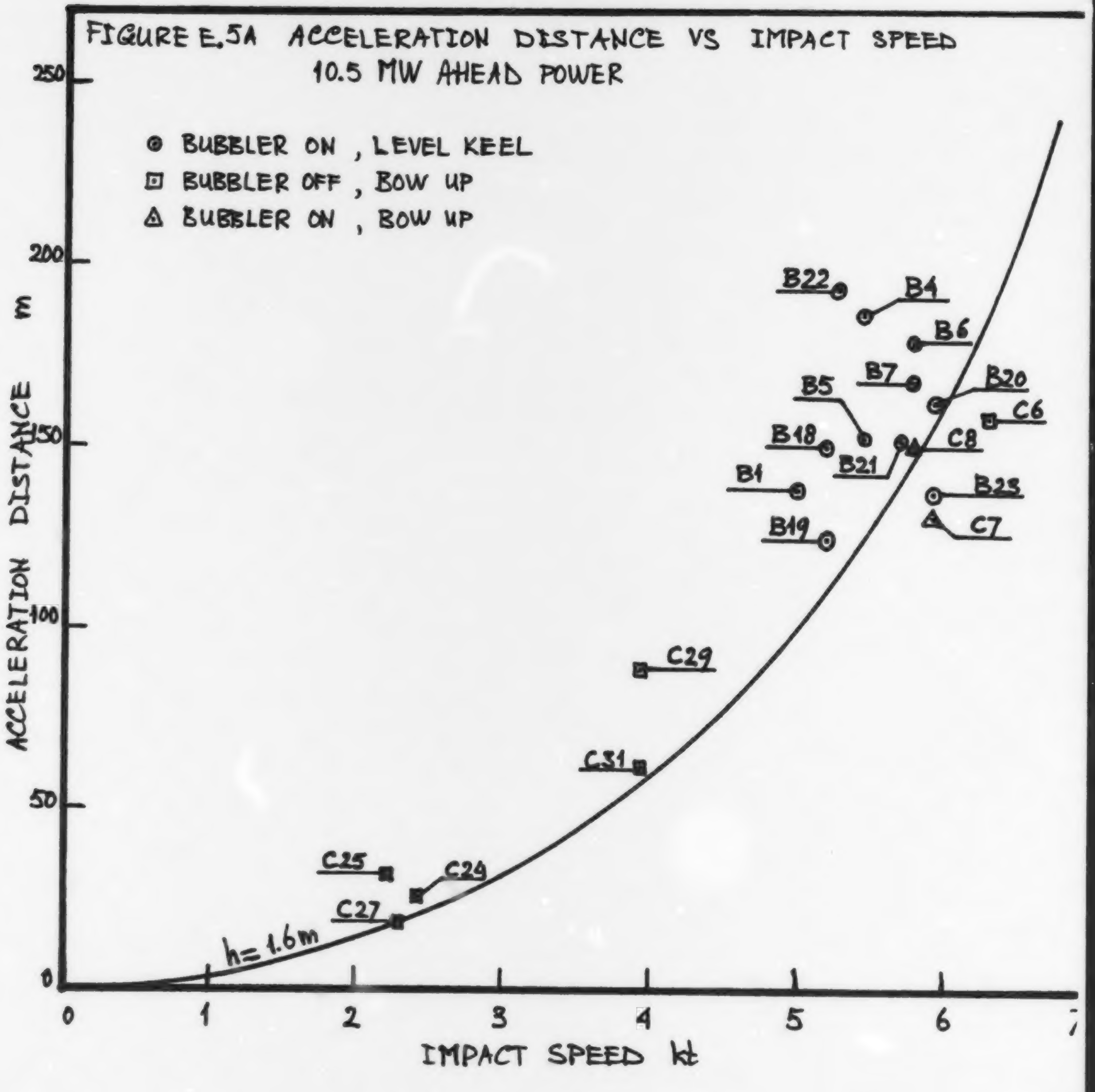

FIGURE E.5A ACCELERATION DISTANCE VS IMPACT SPEED
10.5 MW AHEAD POWER

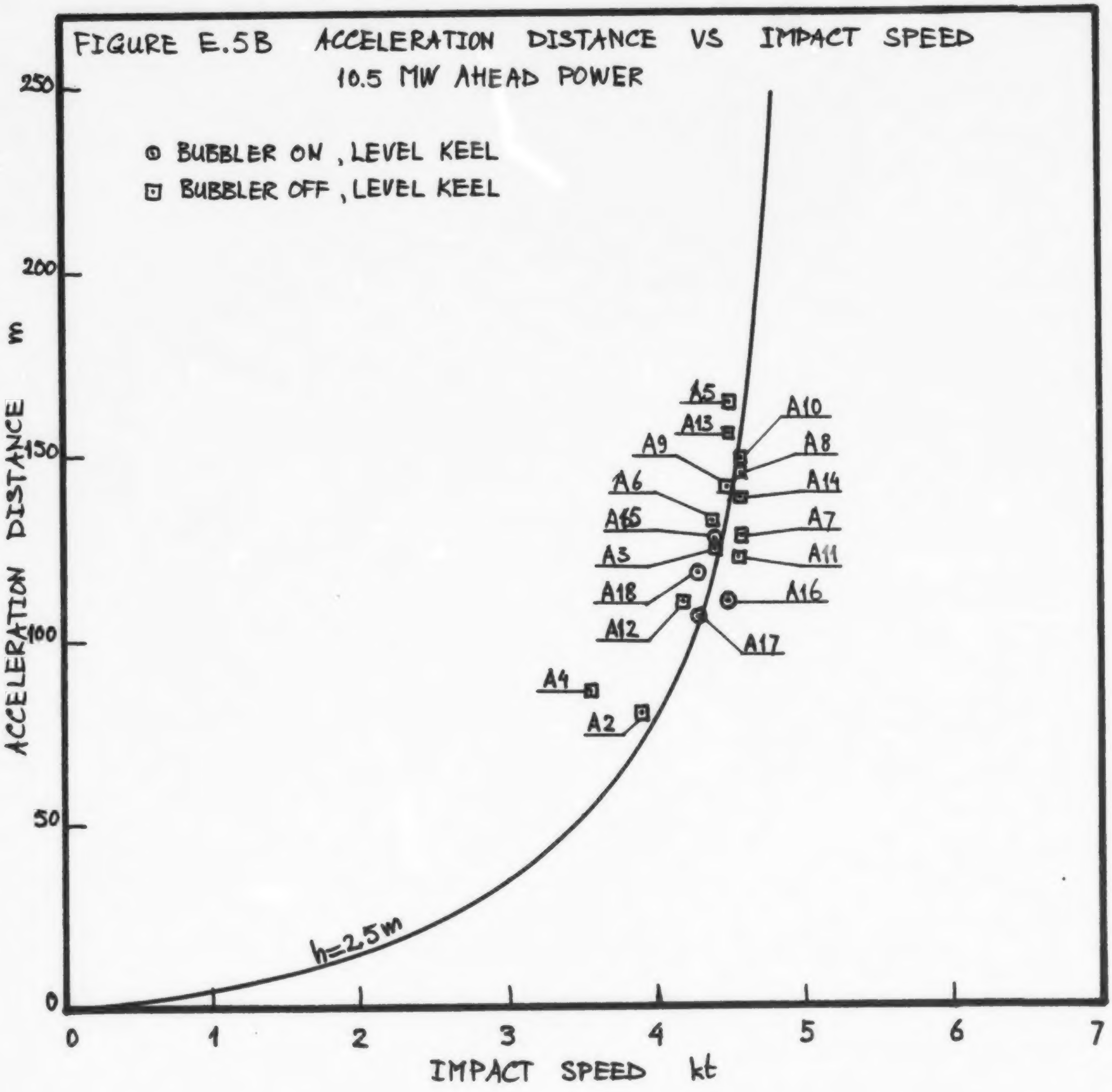
FIGURE E.5B ACCELERATION DISTANCE VS IMPACT SPEED
10.5 MW AHEAD POWER

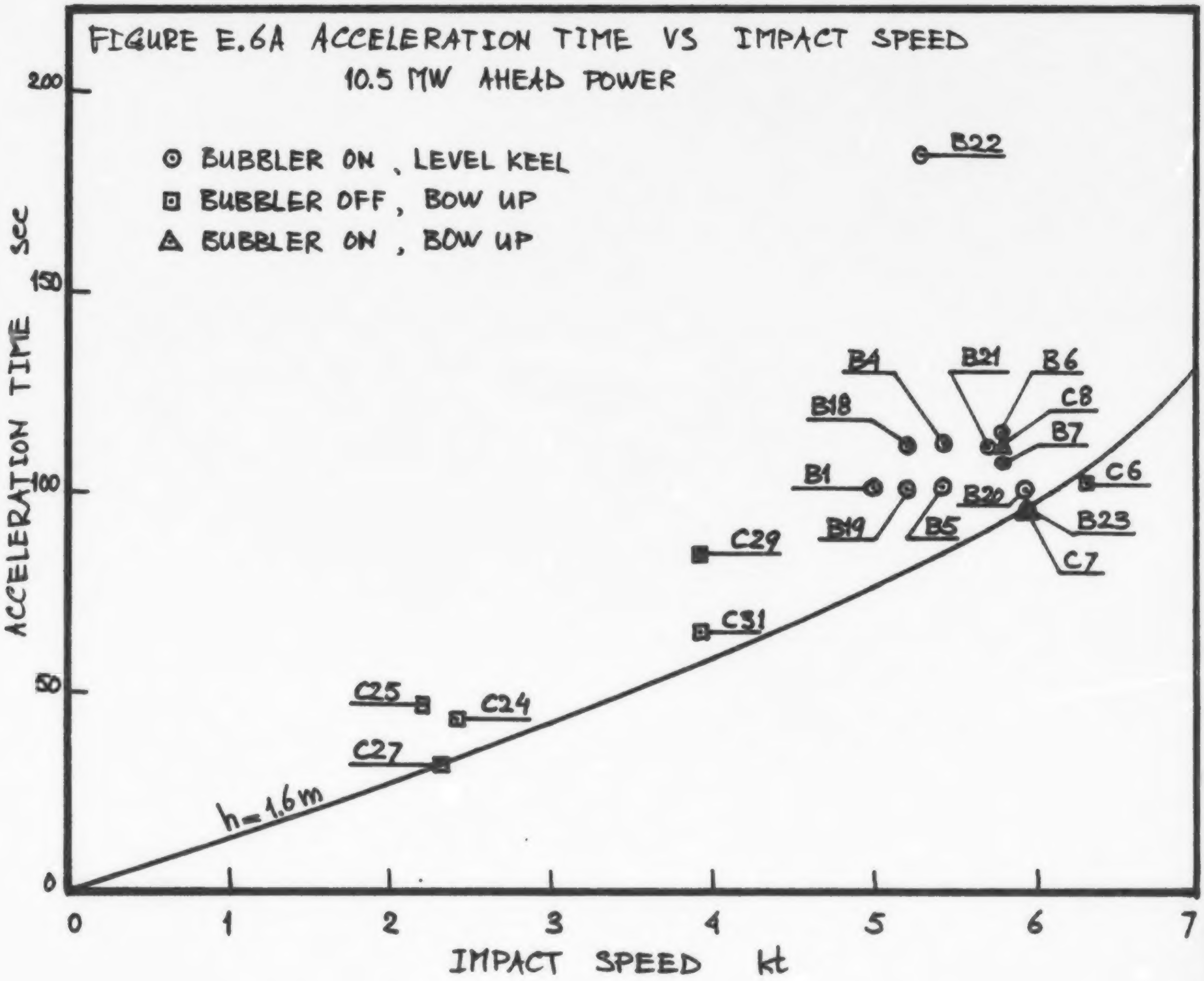

FIGURE E.6A ACCELERATION TIME VS IMPACT SPEED
10.5 MW AHEAD POWER

FIGURE E.6B ACCELERATION TIME VS IMPACT SPEED
10.5 MW AHEAD POWER

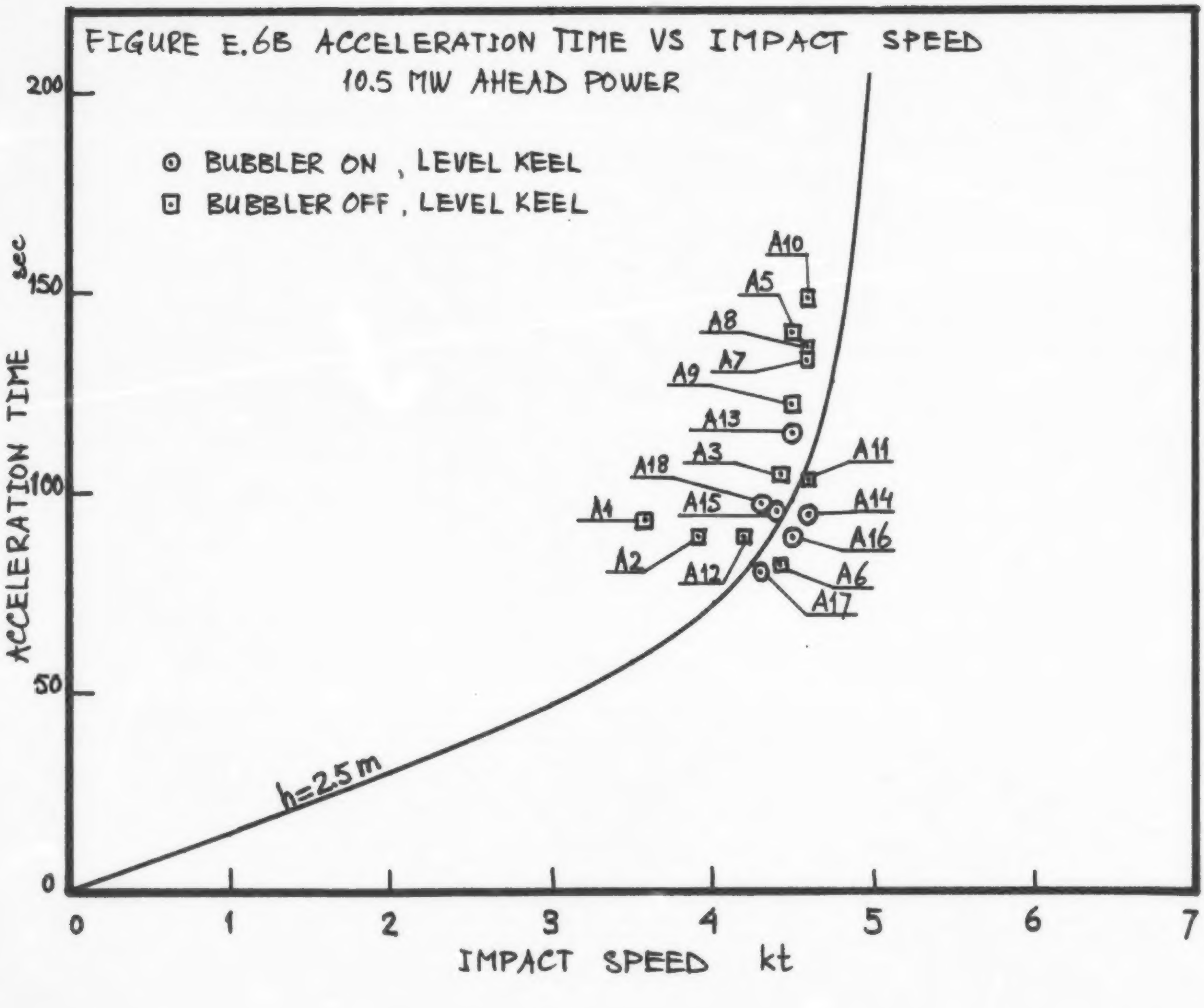

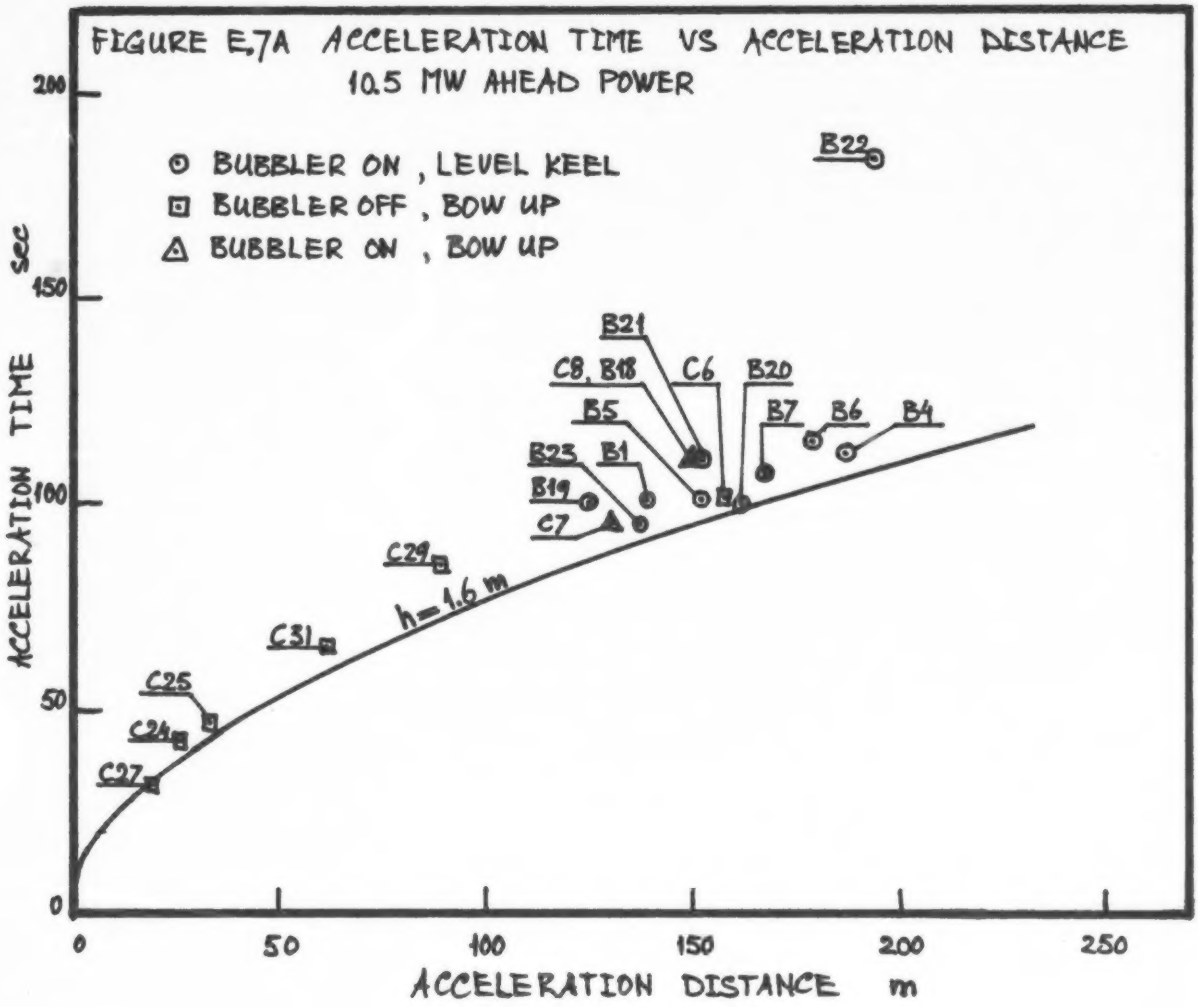

FIGURE E.7A ACCELERATION TIME VS ACCELERATION DISTANCE
10.5 MW AHEAD POWER

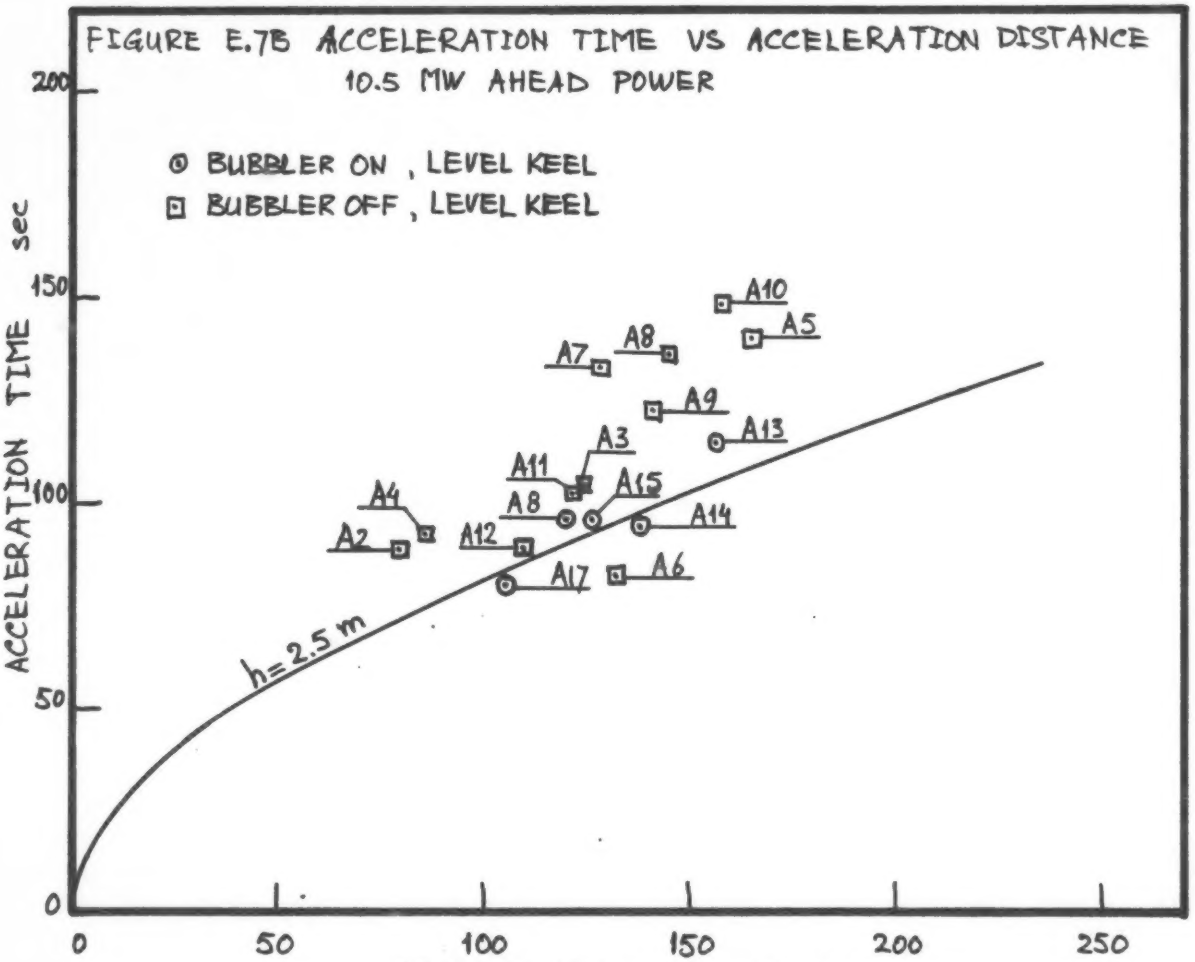

FIGURE E.7B ACCELERATION TIME VS ACCELERATION DISTANCE
10.5 MW AHEAD POWER

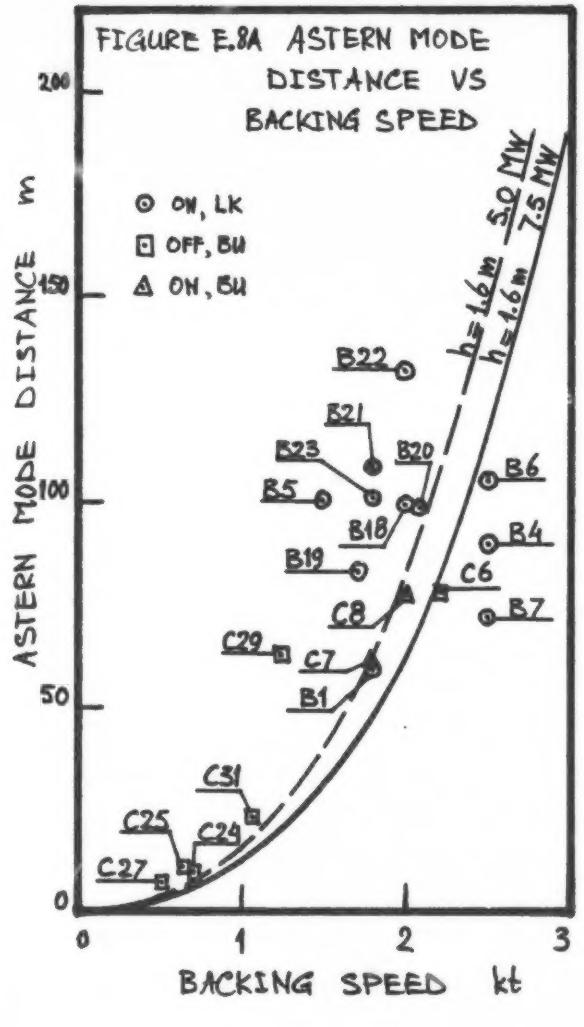

FIGURE E.8A ASTERN MODE DISTANCE VS BACKING SPEED

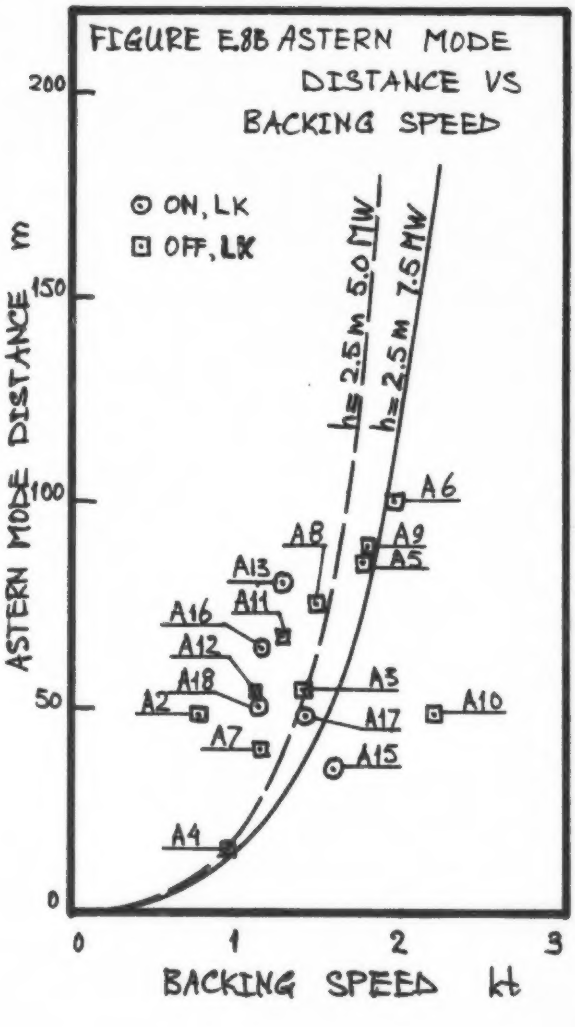

FIGURE E.8B ASTERN MODE DISTANCE VS BACKING SPEED

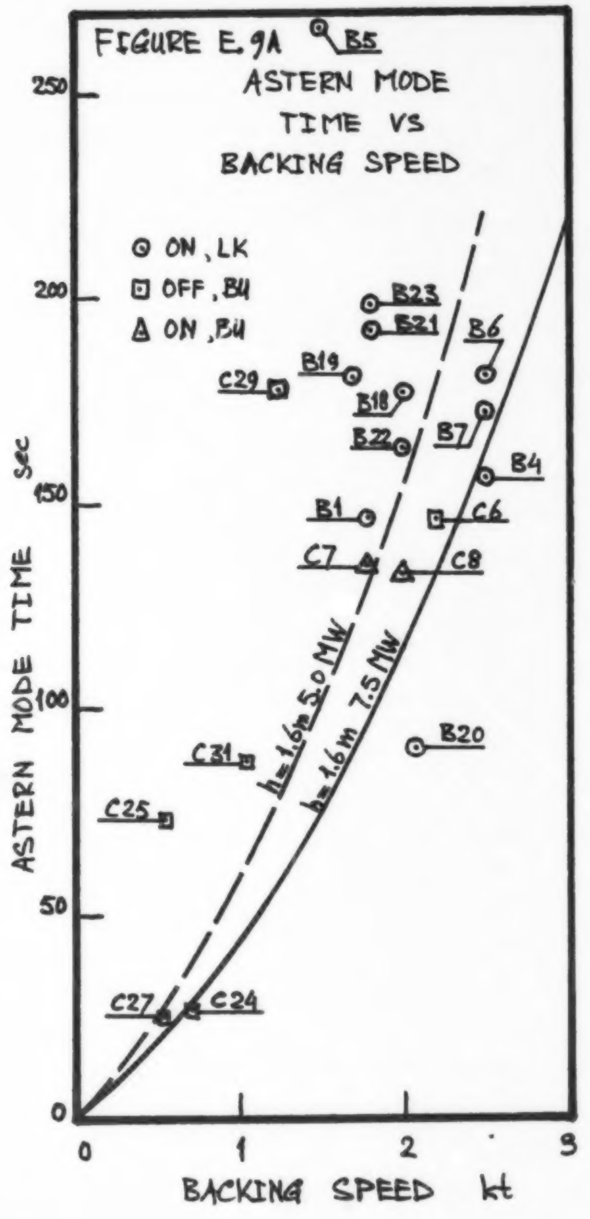

FIGURE E.9A
ASTERN MODE TIME VS BACKING SPEED

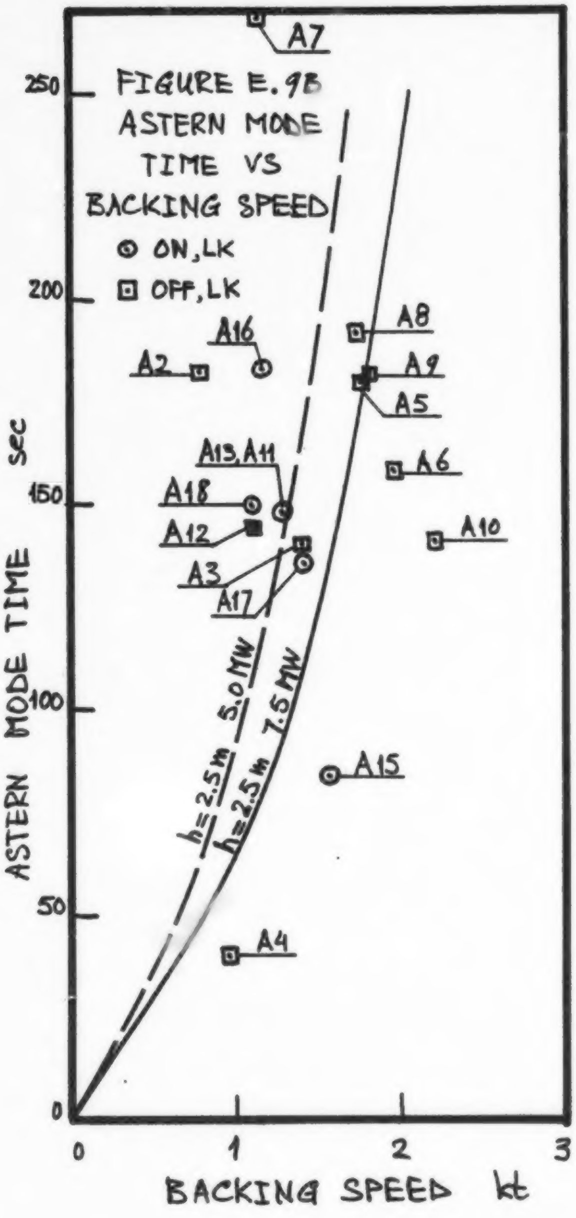

FIGURE E.9B
ASTERN MODE TIME VS BACKING SPEED

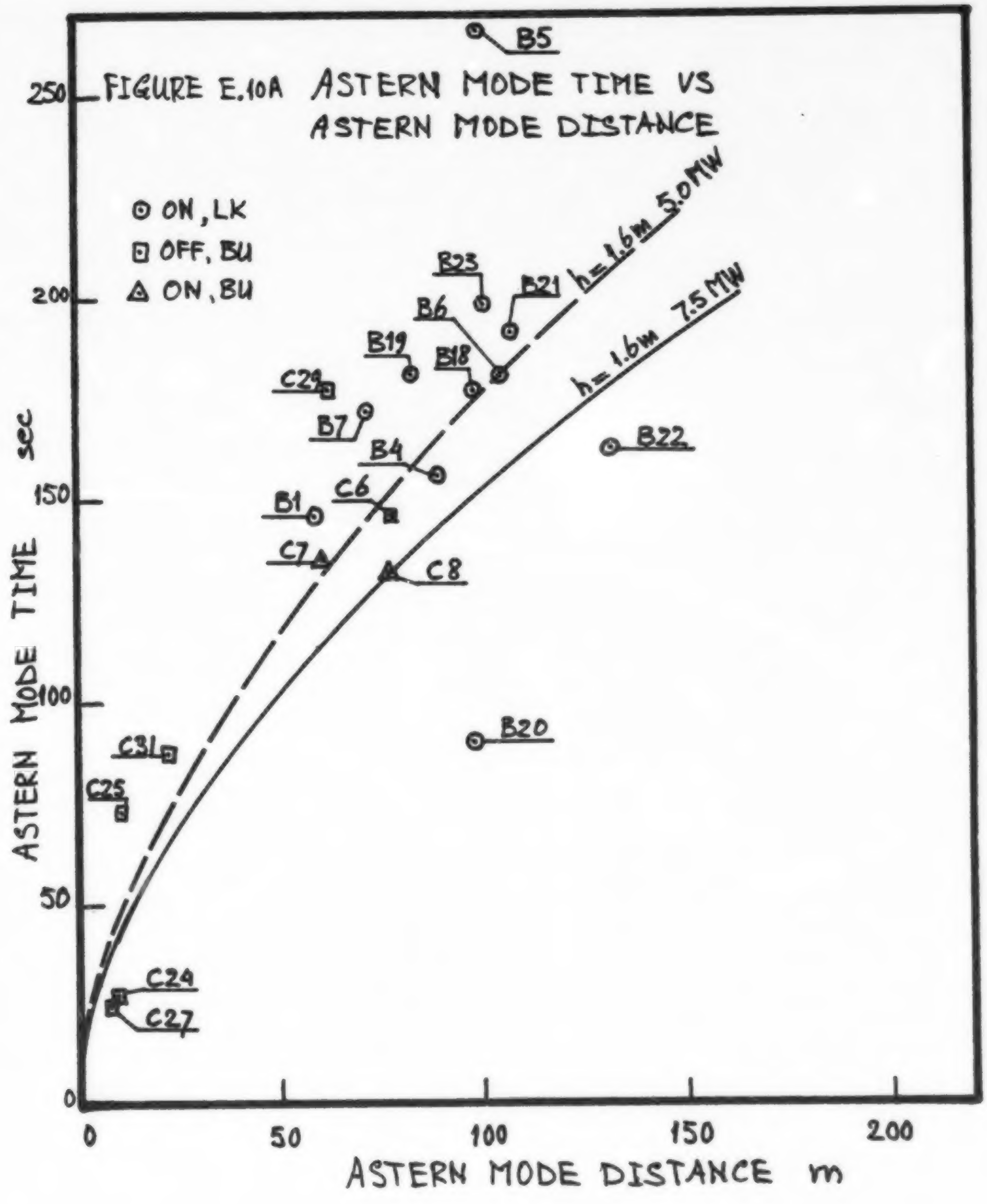

FIGURE E.10A ASTERN MODE TIME VS ASTERN MODE DISTANCE

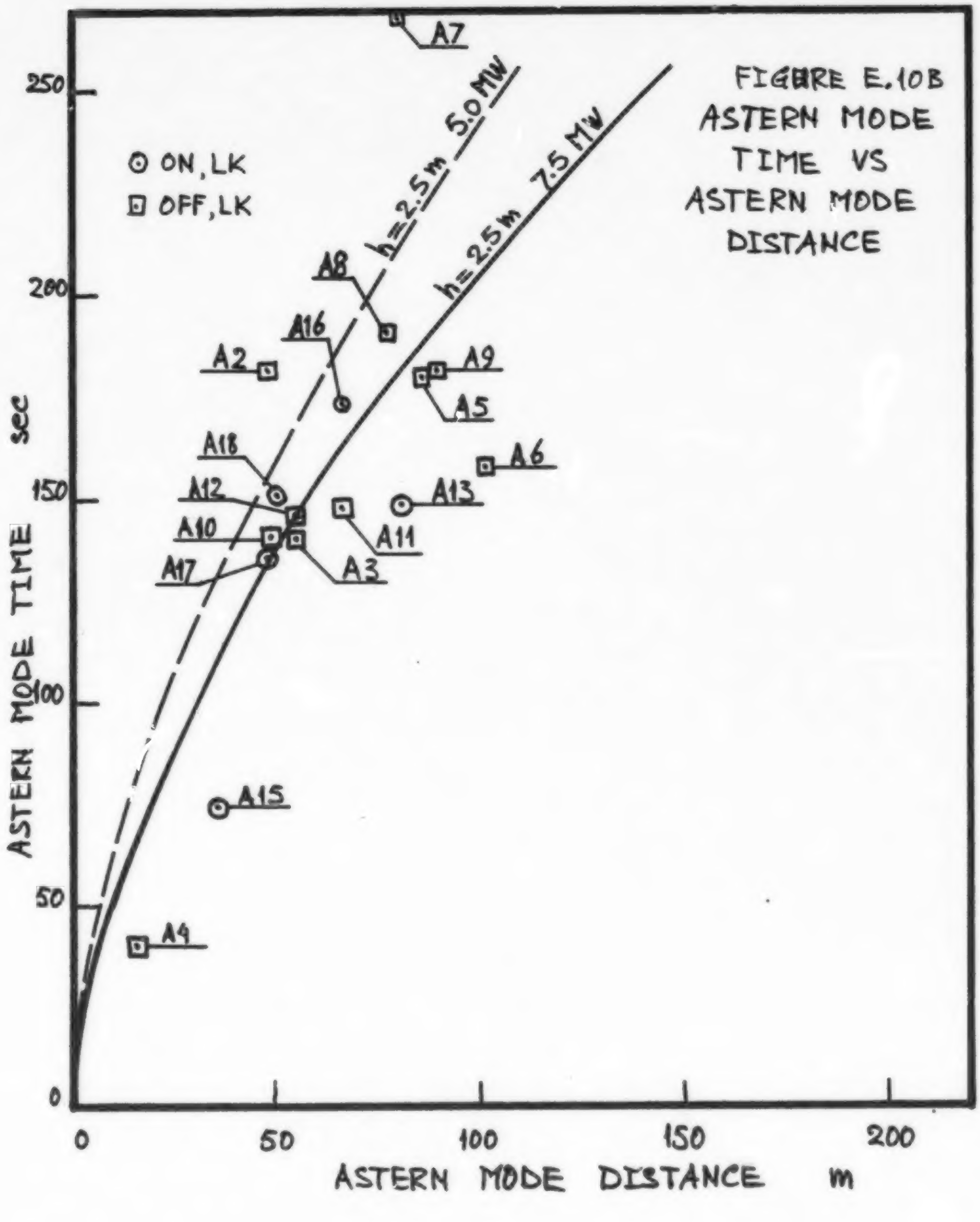

FIGURE E.10B ASTERN MODE TIME VS ASTERN MODE DISTANCE

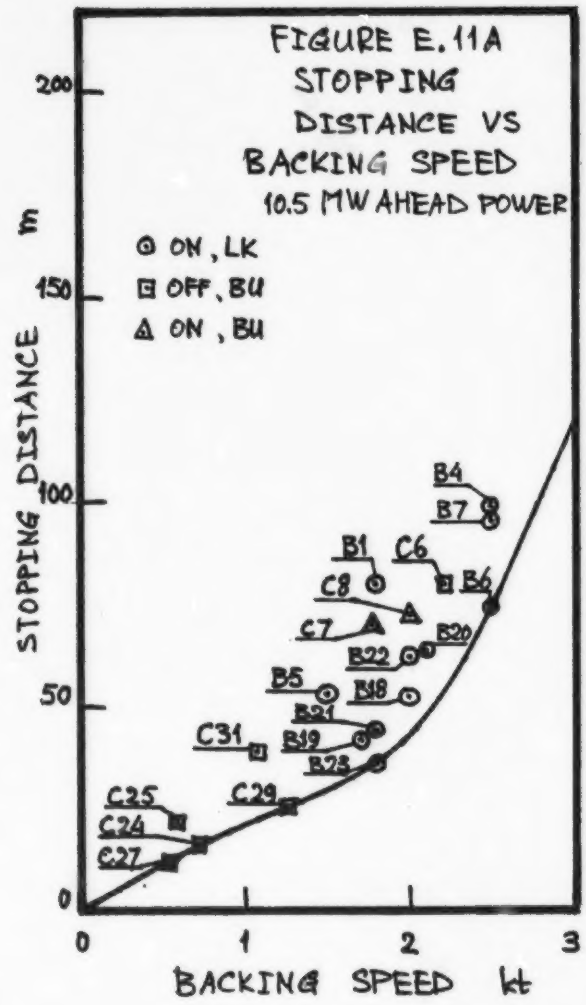

FIGURE E.11A STOPPING DISTANCE VS BACKING SPEED

10.5 MW AHEAD POWER

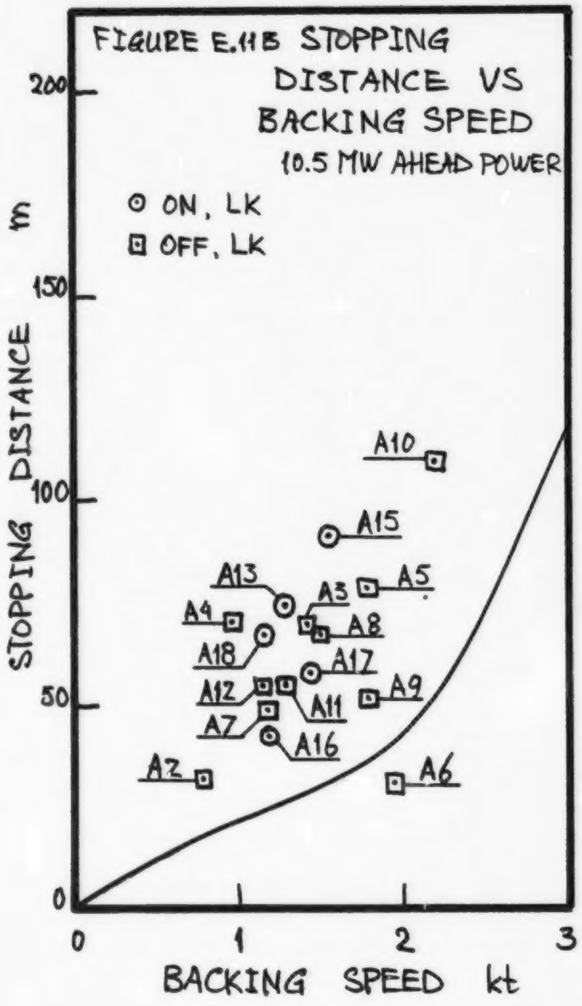

FIGURE E.11B STOPPING DISTANCE VS BACKING SPEED

10.5 MW AHEAD POWER

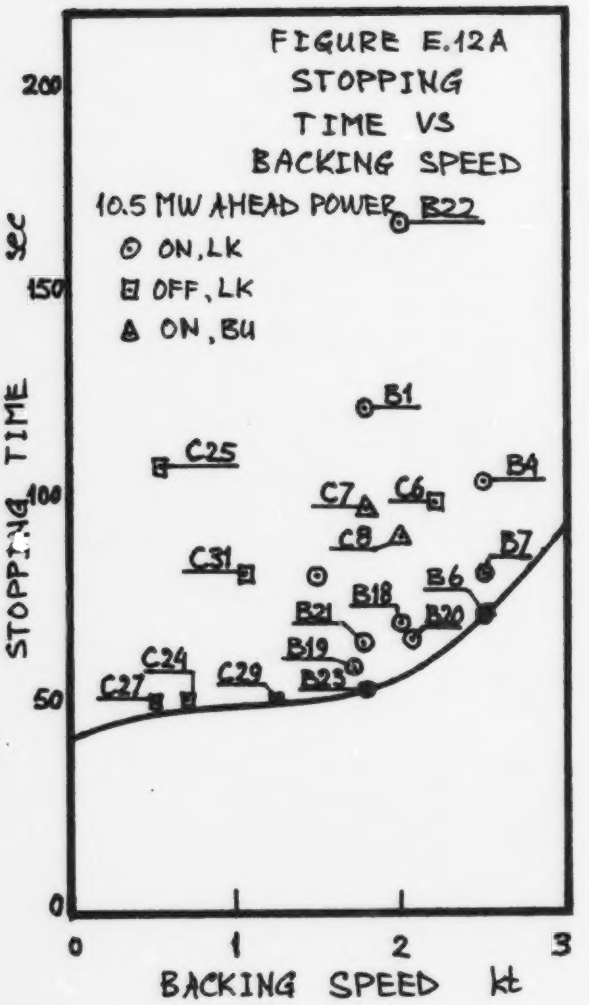
FIGURE E.12A STOPPING TIME VS BACKING SPEED

10.5 MW AHEAD POWER

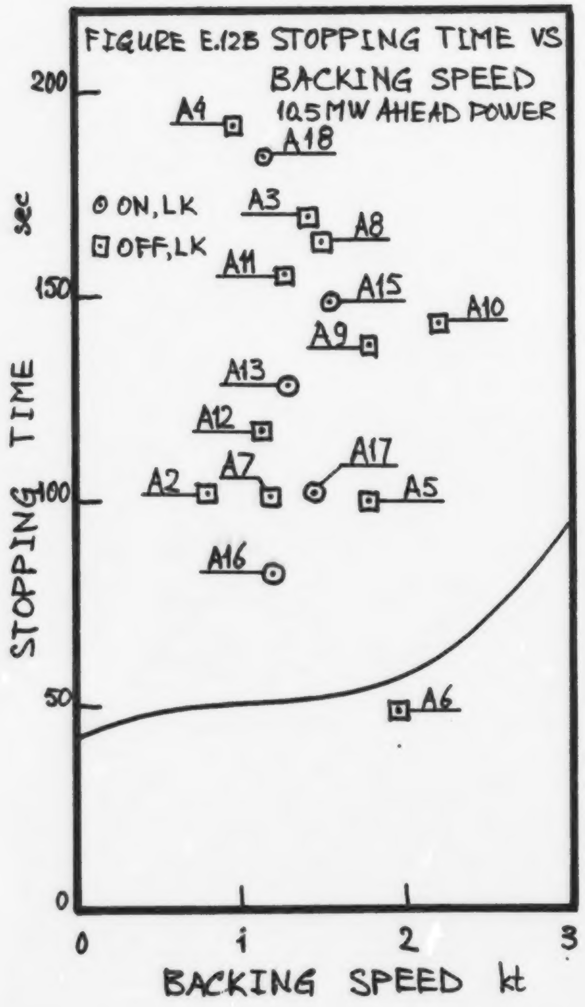
FIGURE E.12B STOPPING TIME VS BACKING SPEED

10.5 MW AHEAD POWER

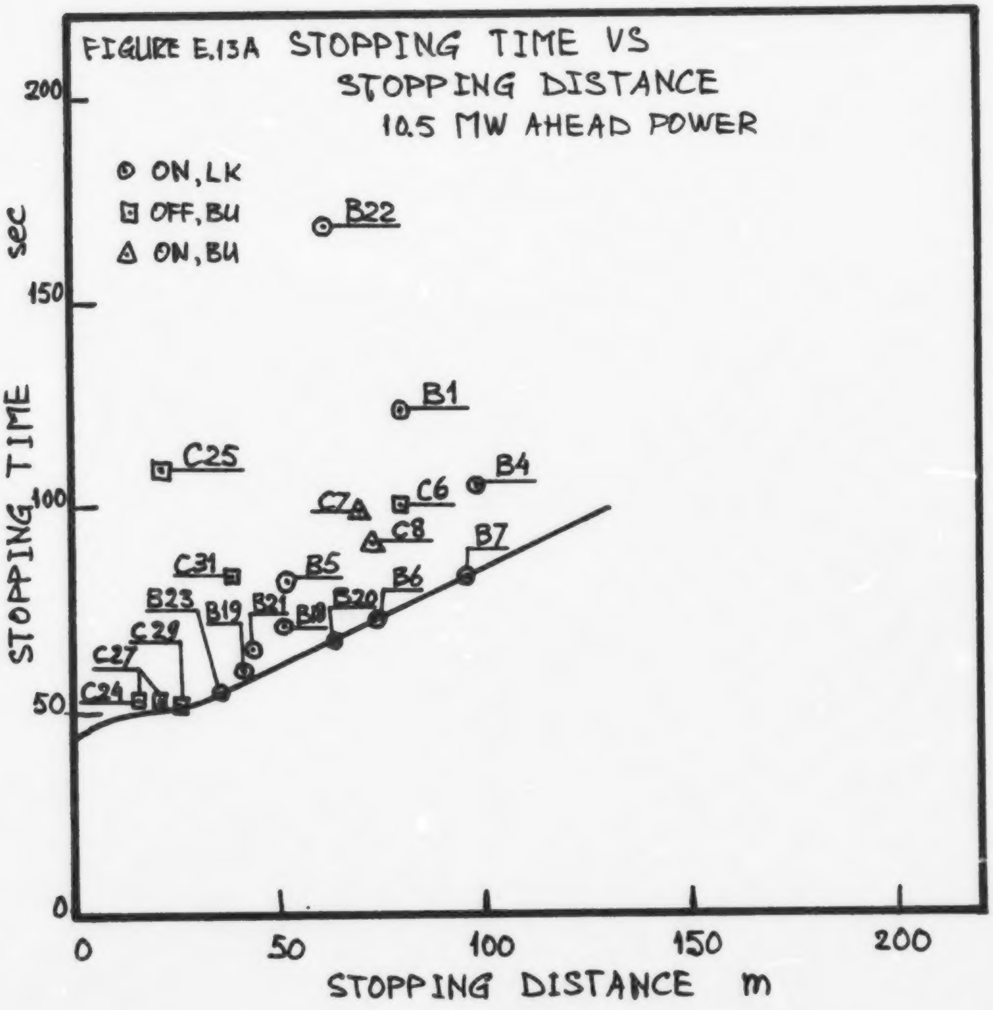

FIGURE E.13A STOPPING TIME VS STOPPING DISTANCE

10.5 MW AHEAD POWER

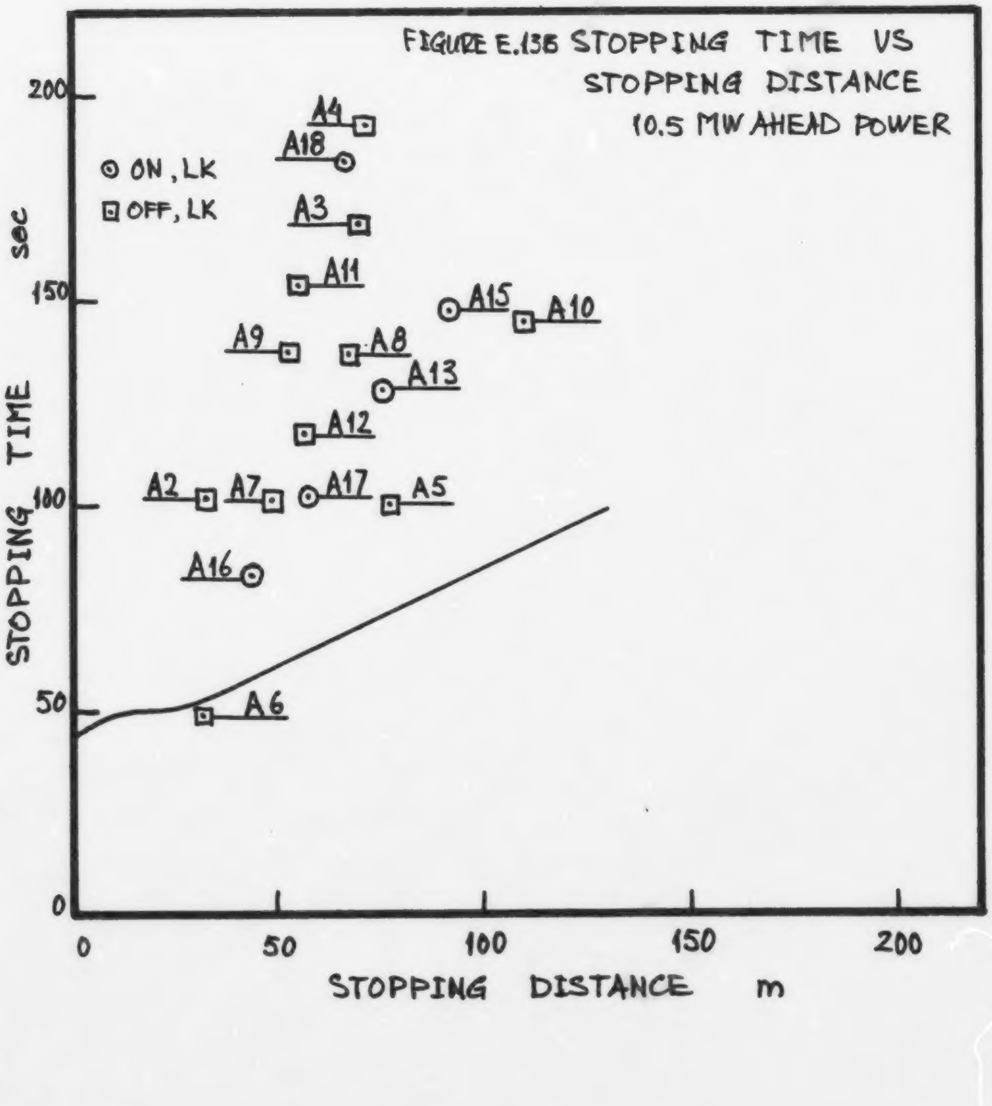

FIGURE E.13B STOPPING TIME VS STOPPING DISTANCE 10.5 MW AHEAD POWER

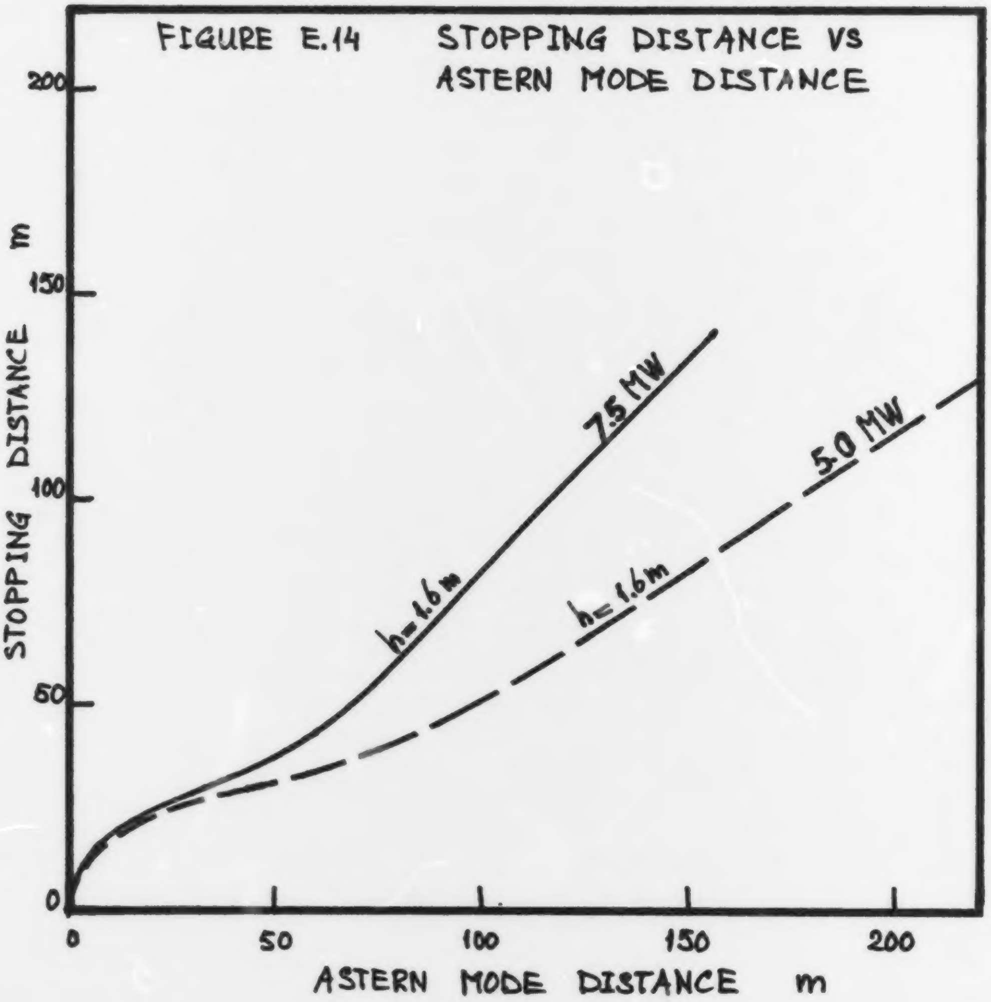

FIGURE E.14 STOPPING DISTANCE VS ASTERN MODE DISTANCE

FIGURE E.15 STOPPING DISTANCE VS ASTERN MODE TIME

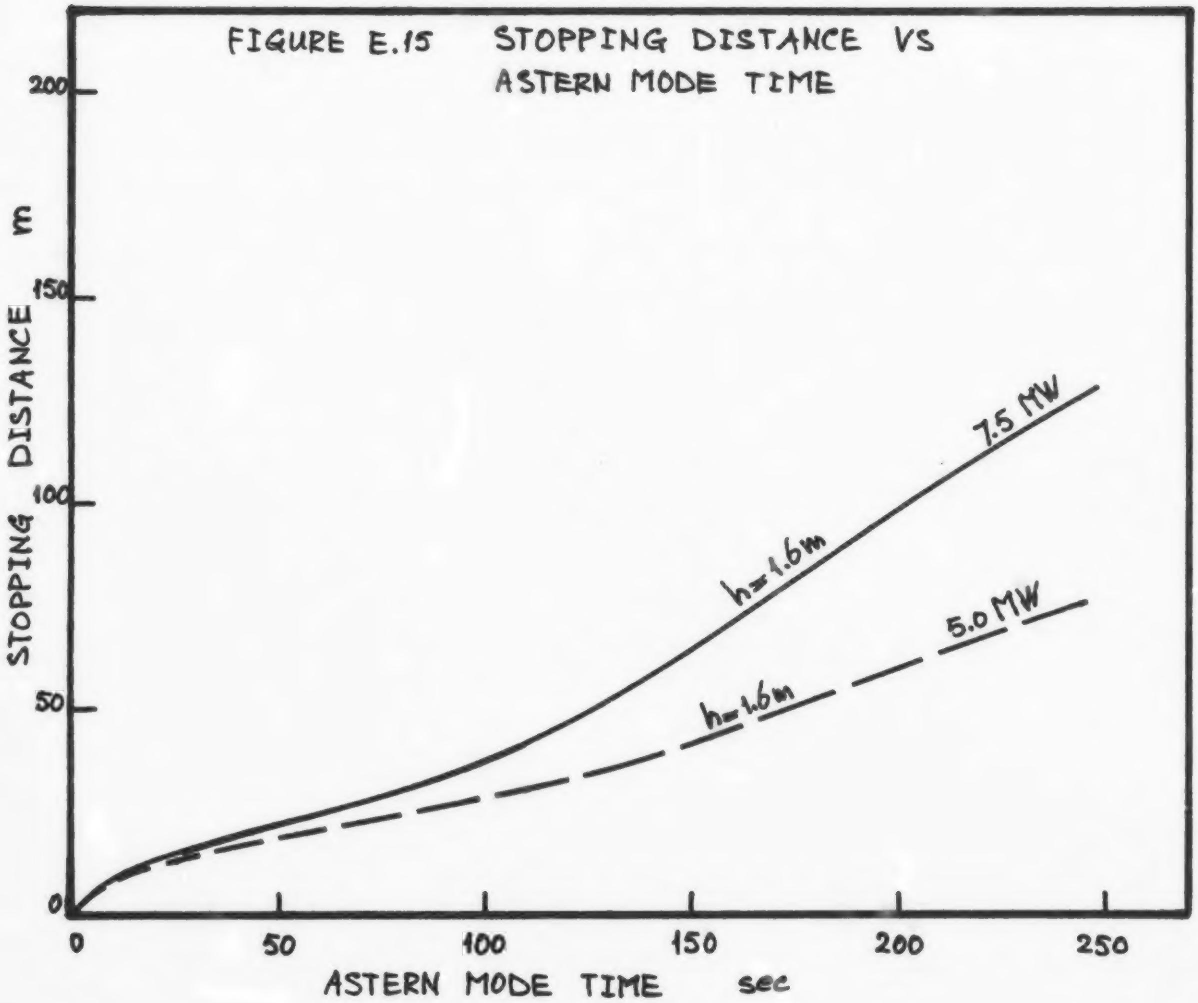

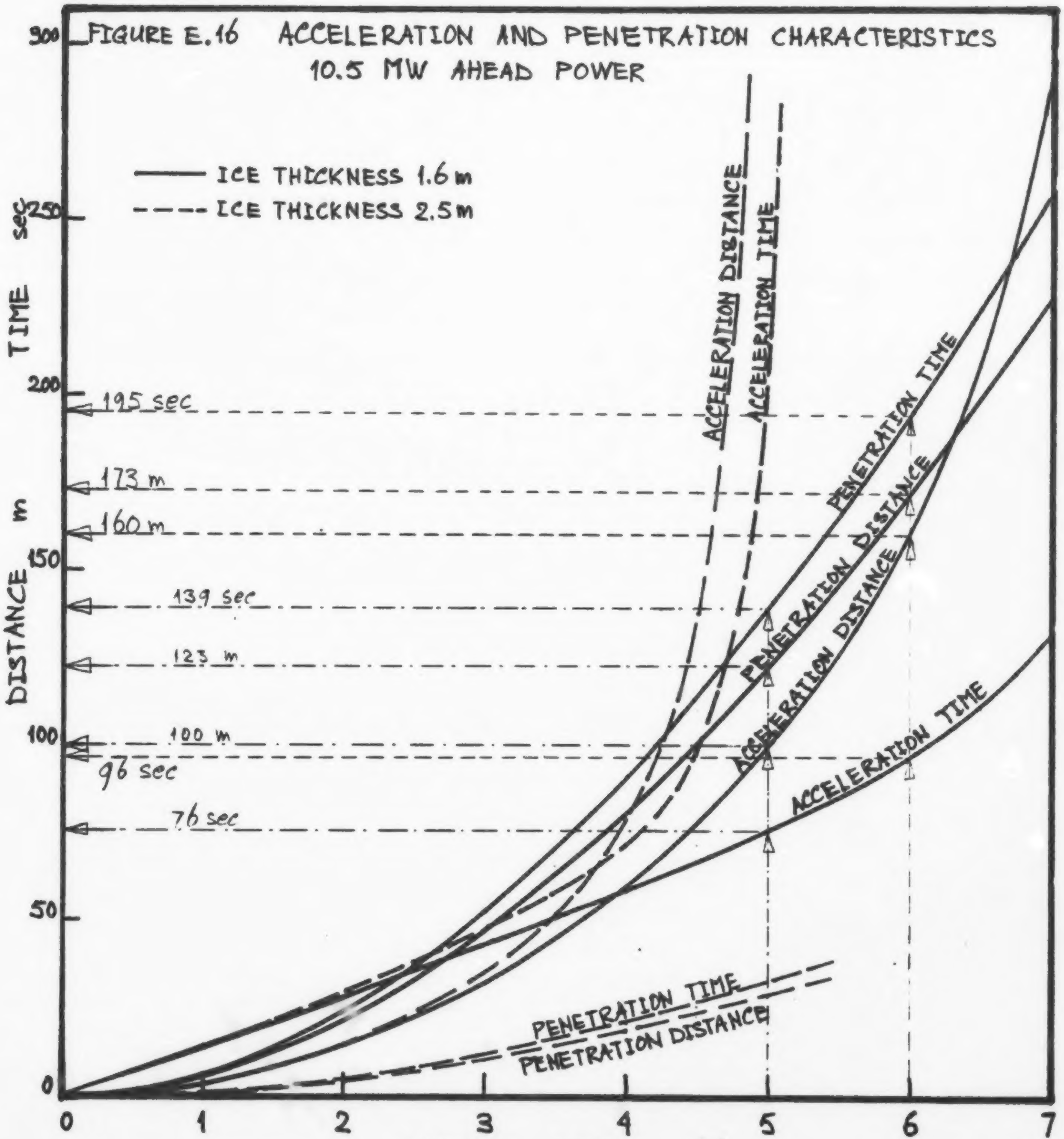

FIGURE E.16 ACCELERATION AND PENETRATION CHARACTERISTICS
10.5 MW AHEAD POWER

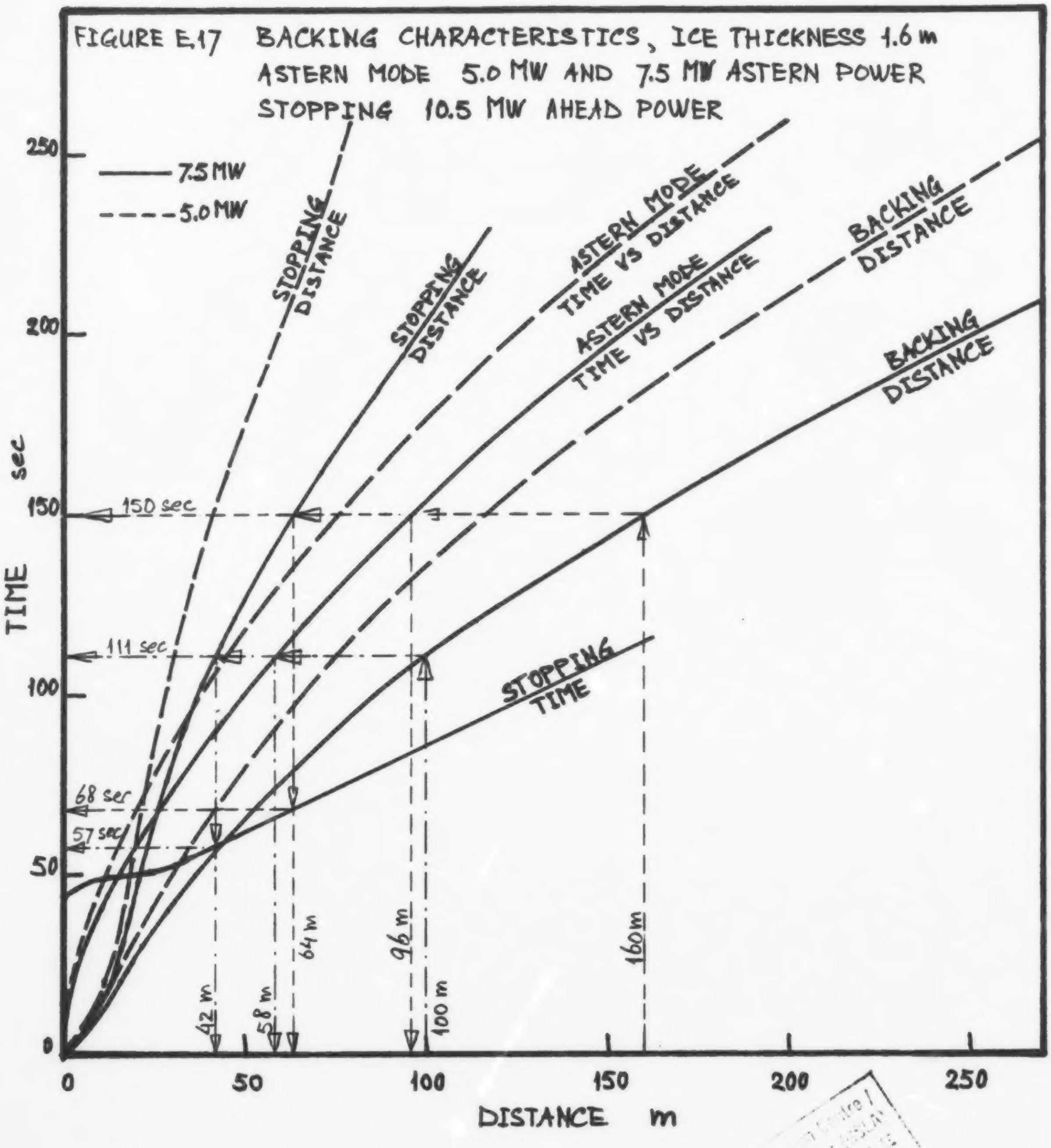

FIGURE E.17 BACKING CHARACTERISTICS, ICE THICKNESS 1.6 m
ASTERN MODE 5.0 MW AND 7.5 MW ASTERN POWER
STOPPING 10.5 MW AHEAD POWER

Library ... Centre /
... FEB 26 1996
Transport Canada